CHARACTERISATION OF INPUT AND OUTPUT MECHANISMS IN THE ZEBRA FINCH CIRCADIAN SYSTEM

by

CATHERINE LINDA JONES

A thesis submitted to The University of Birmingham for the degree of

DOCTOR OF PHILOSOPHY

School of Biosciences

College of Life and Environmental Sciences

The University of Birmingham

September 2011

Abstract

Circadian rhythms are biochemical, physiological, or behavioural over 24 hours. The avian circadian system is complex, involving numerous oscillators in the brain. I characterised two hypothalamic input mechanism (melatonin receptors and light) and one output mechanism (vasotocin) in the zebra finch. Melatonin receptors were cloned and expression levels investigated in the brain and in peripheral tissues. Receptors were found in all tissues, with some pronounced rhythmic mRNA expression. Tissue-specific differences in temporal distribution, peak expression and amplitude suggests melatonin have varied roles in different tissues and different receptors control/influence these roles. Effect of light in the hypothalamus was investigated by exposing light into the dark phase of an LD cycle and studying the difference in C-FOS expression. C-FOS was found in hypothalamic nuclei associated with photic transduction. C-FOS-IR cells were also found in the two known avian hypothalamic oscillators, the LHN and SCN. Arginine-Vasotocin is a neuropeptide involved in numerous bodily and nervous tissue functions, secreted within the hypothalamus and pituitary gland. Immunofluorescent experiments showed marked differences in expression, as different zeitgeber times and between species. This study has improved our understanding of avian circadian systems, providing new insights into the hypothalamic oscillator of a complex circadian organisation.

Dedication

This thesis is dedicated to my mother, father, brother (Caroline, Roger and David) and Grandma (Betty) who have shown me continued love and support in whatever I choose to do, and for that I am truly grateful.

Zebra Finches from the breeding aviary.

Acknowledgements

I am very grateful to my supervisor Roland Brandstaetter for wonderful opportunity of doing this thesis, all your help, advice and direction he gave me throughout the course of this study. This project would not exist without your invaluable patience, encouragement and support throughout the past four years. Thanks to Dr. Gisela Helfer; for introducing me to the wonderful world molecular biology. Your help, advice and encouragement along the way were greatly appreciated and will not be forgotten.

I am thankful to my colleagues at the University of Birmingham; particularly Laine Wallace and Anthony Jones for their advice and help in the genomics laboratory. Thanks go to Pete Jones and Phil Archer in the BMSU; for taking care of the birds for my experiments. I would also like to thank my PhD colleagues from the school of bioscience for keeping me sane and supporting me throughout my PhD, the laughs and drinks along the way were greatly appreciated.

My deepest thanks go to my family Caroline, Roger, David, Linda and Betty and the Burgess's; your love and support is always there when I need it most and is always greatly received. To Richard Tudor, thanks go to you for your love and support throughout my PhD, writing of this thesis and molecular advice along the way. For keeping me smiling and going, it is all very much appreciated. And to all my friends who have been there for me when I needed them most and kept me going.

Finally, thanks are due to the School of Biosciences, University of Birmingham and the Biotechnology and Biological Sciences Research Council (BBSRC) for the funding of this project.

Contents

List of Figures

CHAPTER THREE – MOLECULAR METHODOLOGY VALIDATION

CHAPTER FOUR – MELATONIN RECEPTOR EXPRESSION IN THE ZEBRA FINCH BRAIN AND PERIPHERAL TISSUES

CHAPTER FIVE – MELATONIN MEMBRANE RECEPTOR LOCALISATION IN TWO AVIAN CIRCADIAN OSCILLATORY REGIONS

CHAPTER SIX – LIGHT INDUCED C-FOS EXPRESSION IN THE ZEBRA FINCH HYPOTHALAMUS

CHAPTER SEVEN – ARGININE-VASOTOCIN (AVT) EXPRESSION IN THE ZEBRA FINCH HYPOTHALAMUS

List of Tables

List of Abbreviations

AVP or VP	Arginine-vasopressin
AVT or VT	Arginine-vasotocin
BMAL	Brain and muscle aryl hydrocarbon receptor nuclear translocator (ARNT)-like
CLOCK	Circadian locomotor output cycles kaput
CRY	Cryptochrome
CT	Circadian Time
DD/dimLL	Constant darkness or constant dim light
FSH	Follicle-stimulating hormone
GLv	Lateral geniculate nucleus *pars ventralis*
GnRH	Gonadotropin-releasing hormone
LD	Light-dark cycle
LH	Luteinizing hormone
LHN	Lateral hypothalamic nucleus
MEL	Melatonin
Mel-1A	Melatonin receptor 1 A
Mel-1B	Melatonin receptor 1 B
Mel-1C	Melatonin receptor 1 C
PAS	Per-ARNT-Sim
PER	Period gene
PON	Preoptic nucleus
PVN	Paraventricular nucleus
PPN	Periventricular Preoptic nucleus
RT-PCR	Reverse transcription polymerase chain reaction
RHT	Retino-hypothalamic tract
SCN	Suprachiasmatic nucleus
– mSCN	– medial SCN
– vSCN	– visual SCN
SON	Supraoptic nucleus
TIM	Timeless
ZT	Zeitgeber time

CHAPTER 1

General Introduction

CHAPTER 1 – GENERAL INTRODUCTION

1.1 Circadian system

1.1.1 Introduction

In 1929, a French astronomer called Jean Jaques d'Ortous de Mairan noticed that the opening and closing of the leaves of a *Mimosa pudica* plant still occurred when placed into constant darkness; this gave the first noted demonstration of independent intrinsic biological rhythms created by endogenous gene expression and enhanced by photoperiods (light/dark cycles) (de Mairan, 1929). In 1946, Franz Halberg was the first person who coined the term "Circadia" from the Latin *circa* meaning "around" and *diem* or *dies* meaning "day"; the circadian rhythm is therefore roughly a 24 hour (h) cycle of physiological processes (Halberg, 1946), such as with the mimosa plant, the opening and closing of its leaves. Circadian rhythms are generated endogenously, although they are affected, or entrained, by external cues, e.g. light, temperature, etc. True circadian rhythms persist when the external cues are removed, i.e. the Mimosa plant in constant darkness, for a period of about 24 hours.

Endogenous circadian rhythms are found in a large number of organisms from prokaryotes to mammals; created by the geophysical rotation of the earth around the sun, most rhythms oscillate around a period of 24 hours (Circadian) and some rhythms run close to a 12 month period (Circannual). These cycles are synchronized by external cues that are known as

zeitgeber; under laboratory conditions, the time a cue starts (e.g. lights on) is designated zeitgeber time zero (ZT0; Figure 1.1.1.a.; Brandstaetter, *et al.*, 2000; Gwinner and Brandstaetter, 2001).

Circadian rhythmicity regulates the production of hormones (e.g. melatonin), the organism's physiology (homeostasis, brain activity, sleep-wake pattern, and cell regeneration) and behaviour (feeding, migration, breeding, etc.) via light-dark entrainment of the day-night cycles (Gwinner and Brandstaetter, 2001). At the molecular level, the rhythms are generated within the cells which contain specific molecular "clockworks" that are controlled within the cell (Brandstaetter, *et al.*, 2000a; Gwinner and Brandstaetter, 2001). These "clock" cells form functional units that transmit the cells' daily activity to influence the transcription and translation of the specific genes and proteins which affect the circadian functions in the organism (Figure 1.1.1.a.; Brandstaetter, *et al.*, 2000a; Gwinner and Brandstaetter, 2001).

The master clock, or oscillator, of the circadian system stores information (e.g. photic, etc.) on a daily basis to adapt to weather changes (cloudy, raining, etc.) which might alter the light lengths in the day. When organisms are held under constant conditions (i.e. 24 hours of darkness: laboratory or arctic conditions; Figure 1.1.1.b.) one complete cycle usual deviates slightly from the "normal" 24 hour, this deviation differs among species and within individuals, i.e. the mouse deviates to around 23.5 hours and the human deviates to about 24.1 hours (Figure 1.1.1.b.; Mistlberger, 2002).

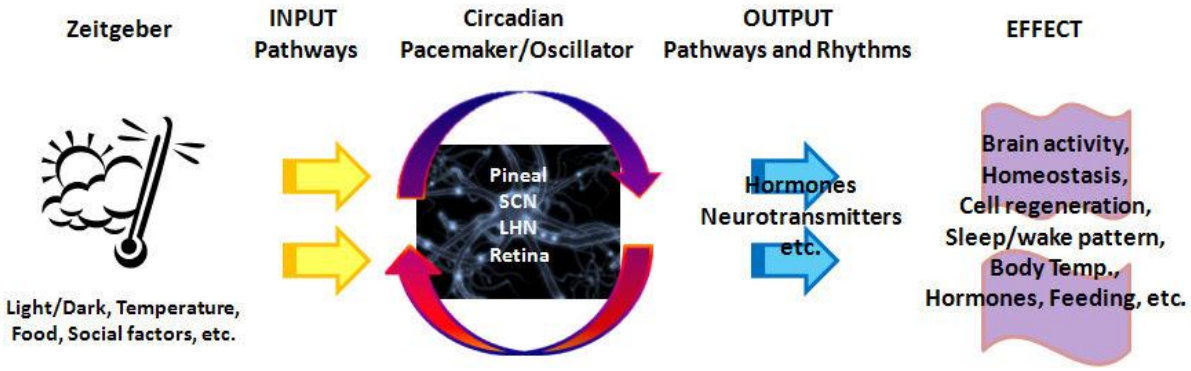

Figure 1.1.1.a. Overview of the core elements of the circadian system.

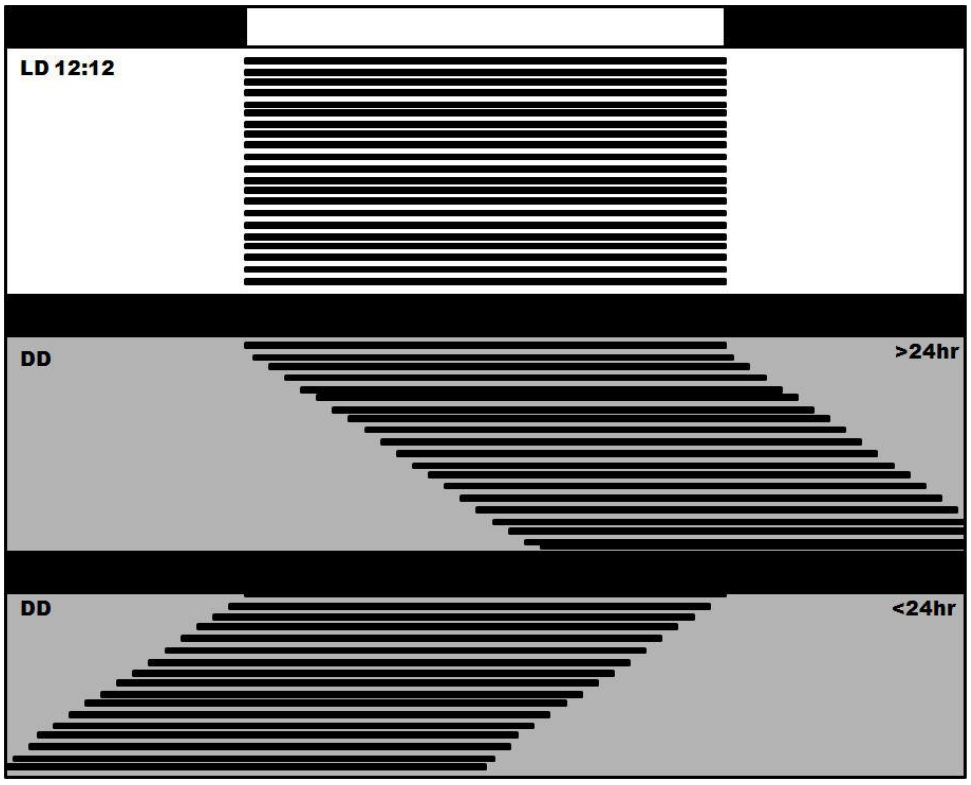

Figure 1.1.1.b. A schematic actogram chart showing the effect of light on synchronisation. Under laboratory (entrained) conditions circadian rhythms adjust their endogenous period to that of the zeitgeber. The actogram shows the change of the endogenous locomotor rhythms from entrained conditions (12:12 LD) to free running cycles under constant darkness (DD) with a endogenous rhythm longer than 24 hours (24>hr) and shorter than 24 hours (<24hr). LD conditions shown by the white and black bars at the top of the diagram. DD conditions shown by the black bar in the middle of the diagram and the grey boxed area beneath it.

1.1.2 The molecular clockwork

There are numerous genes (e.g. Per, Cry) and transcription factors (e.g. BMAL, CLOCK) that modulate the changes in the daily cycle by transcription/translation feedback loops to modulate themselves and other factors in the organism (Helfer, *et al*., 2006; Figure 1.1.2.a and

Table 1.1.2.a). The concentrations of these factors are an indication of the time of day and behaviour of the organism.

In most vertebrates studied so far, a circadian oscillators contains two 'clock' genes (period (*per*) and cryptochrome (*cry*)) which encode transcription factors *clock* (circadian locomotor output cycles kaput) and *Bmal* (brain and muscle ARNT-like). *Clock* and *Bmal* harbour a basic helix-loop-helix (bHLH) and Per-ARNT-Sim (PAS) domains which allow the mediation of DNA binding and heterodimerization (Gekakis, *et al.*, 1998; Hogenesch, *et al.*, 1998; Travnickova-Bendova, *et al.*, 2002; Yoo, *et al.*, 2005; Levi and Schibler, 2007). *Bmal* and *Clock* bind to the DNA element (E-boxes) in the promoter region of their target genes (*Per* and *Cry*) causing an increase in their transcription. PER and CRY proteins bind to form complexes in the cytoplasm before entering the nucleus (Griffin Jr., *et al.*, 1999; Kume, *et al.*, 1999; Levi and Schibler, 2007). Once CRY and PER expression has accumulated to high concentrations within the nucleus, the complex represses the expression of CLOCK and BMAL transcription, and thus has a negative effect on PER and CRY own expression, which is vital for the circadian timekeeping regulation (Field, *et al.*, 2000; Oishi, *et al.*, 1998; Shearman, *et al.*, 2000; Levi and Schibler, 2007). *Bmal* is the only gene whose inactivation immediately causes circadian behavioural arrhythmicity (Bunger, *et al*., 2000).

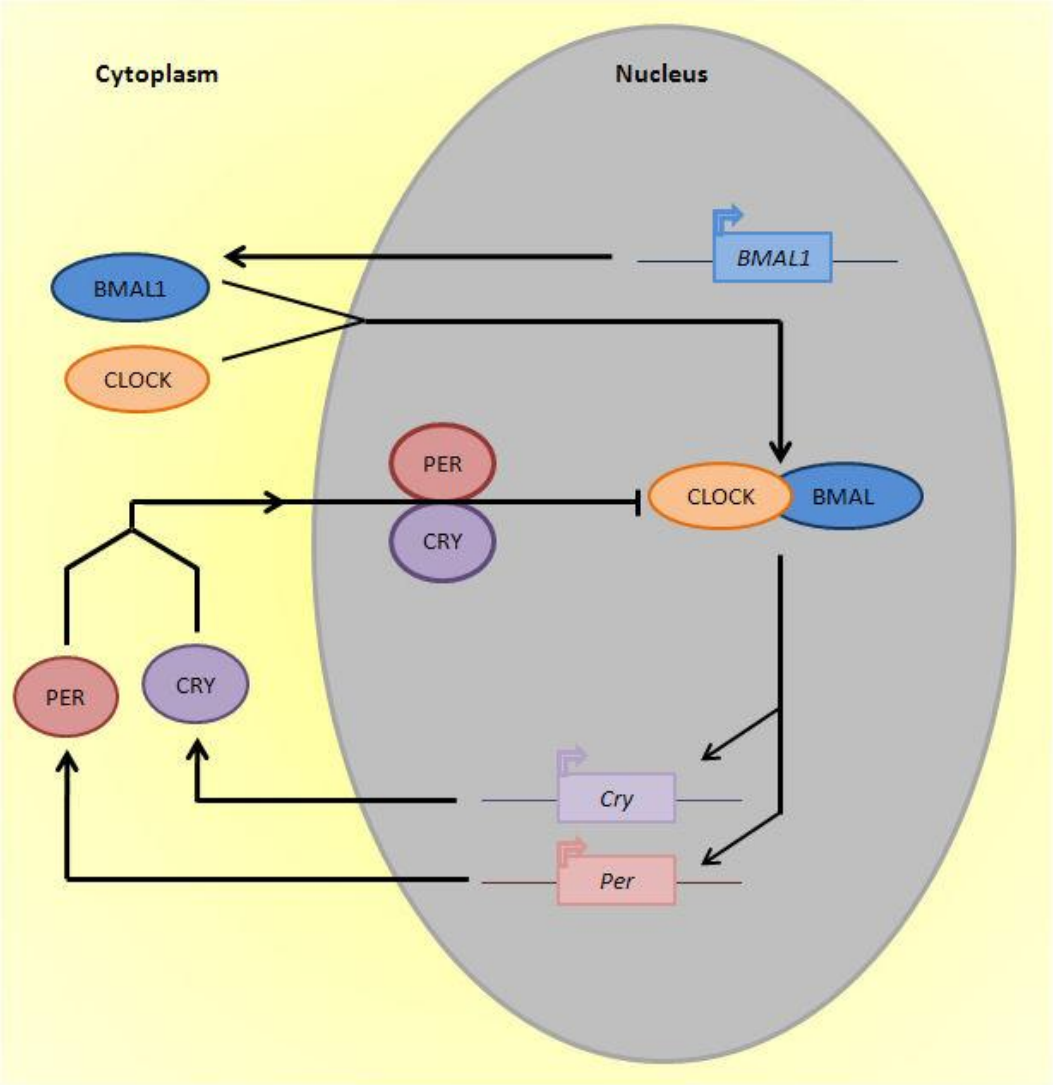

Figure 1.1.2.a. Schematic diagram of the regulatory feedback loops of clock genes in vertebrates. Positive elements CLOCK and BMAL dimerize and bind to E-boxes on promoter regions of clock-controlled genes and on negative element genes, period (Per) and cryptochrome (Cry), stimulating their transcription. These, in turn are translated, oligomerize and re-enter the nucleus, where they interfere with CLOCK/BMAL activity

.

Three *Per* genes have now been identified in the mammalian circadian system; *Per1*, *Per2* and *Per3*. Both *Per* and *Cry* are rhythmical produced in the mammalian central clock, suprachiasmatic nucleus (SCN) in the hypothalamus. *Per1-Cry1* are "morning" oscillators within the SCN cells, peaking in early morning and *Per2-Cry*2 are "evening" oscillators peaking in the late afternoon (Daan, *et al*., 2001). The stability and activity of the circadian gene (*Per* and *Cry*) and transcription factor (*Clock* and *Bmal*) regulation, in the feedback loop, are controlled by the protein kinases CK1ε/δ and CK2 (Levi and Schibler, 2007).

In birds, the *Per*1 gene has not yet been identified in any of the circadian oscillators. The avian *Per*2 gene has been shown have a similar rhythmic pattern to the mammalian *Per*1, (Yan and Okamura, 2002). In various species, avian *Per2* gene has been shown to be rhythmic in the pineal, retina and hypothalamus, under both light-dark (LD) and constant dark (DD) conditions, peaking in the early light phase (Yoshimura, *et al.*, 2000; Brandstaetter, *et al.*, 2001a; Doi, *et al.*, 2001; Okano, *et al.*, 2001; Takashi, *et al.*, 2001; Yamamoto, *et al.*, 2001; Abraham, *et al.*, 2002; Abraham, *et al.*, 2003; Yasuo, *et al.*, 2003). In the house sparrow, *Per*2 is cyclic in the photoperiod, being expressed in the most rostral part of the SCN before "lights on" at ZT24 and declining to a low concentration at "lights off" at ZT12; there is further decline to background levels by ZT18 (mid-dark phase), which is in reverse-phase of pineal melatonin levels, which is secreted during the night period (Abraham, *et al.*, 2003).

Avian *Per*2 has been identified in the pineal gland, retina and hypothalamus (preoptic nucleus (PON), SCN and lateral hypothalamic nuclei (LHN)), of the house sparrow brain (Brandstaetter, *et al.*, 2001a; Abraham, *et al.*, 2002). *Per*2 is rather dispersed in the preoptic nucleus, but strongly expressed along the ependymal wall of the third ventricle and the rostral

SCN (Abraham, *et al.,* 2002). There is a similar pattern of expression of the *Per*2 in both LD and DD conditions; the only slight difference was the reduced amplitude of the *Per*2 rhythm in DD, therefore showing that the *Per*2 expression is undoubtedly an endogenously circadian gene (Abraham, *et al.,* 2002). *Per*3 mRNA has been shown to be in 2h phase-advanced to *Per*2 expression, with its greatest peak around ZT22.5 (Helfer, *et al.,* 2006).

Cry1 expression in the house sparrow has a peak expression at ZT6.5 and *Cry2* expression peaked in the second half of the night at ZT 20.5 with the *Cry1* mRNA expression being four-fold higher than the *Cry2* mRNA expression (Helfer, *et al.,* 2006). *Cry2* expression is widespread throughout the various structures receiving visual input, in the chicken brain (Bailey, *et al.,* 2002).

The positive feedback factor *bmal1* is out of phase to the *Per* gene expression (Helfer, *et al.,* 2006). With similar results between avian species (e.g. chicken) and mammals, binding of BMAL to the CLOCK protein activates *Per*2 gene expression, which is an indicator that this basic mechanism of the circadian feedback loops is universal between mammal and avian species (Helfer, *et al.,* 2006).

Mammalian gene	Avian gene	Drosophila gene	Clock role	Mutant phenotype
Clock	*Clock*	*dClock*	Positive element	Lengthened period; loss of persistent rhythmicity in constant conditions
Per1	*Per2*	*period*	Negative element	Reduced amplitude, shortened period, or loss of rhythm
Per2	*Per3*			Shortened period, loss of rhythm
Per3				Modest shortening of period
CK1ε		*doubletime*	Facilitating element	Shortened period in hamster mutants
Cry1	*Cry1*	*dcry*	Negative element	Animals lacking the *Cry1* gene (i.e., *Cry1* knockouts) have shortened period
Cry2	*Cry2*			*Cry2* knockouts have lengthened period animals lacking both genes (i.e., double knockouts) have a loss of rhythm
	Cry4			
Bmal1	*Bmal1*	*cycle*	Positive element	Loss of rhythm
	Bmal2			
?*mTim*		*timeless*	Facilitating element	Role in mammals is not clear
?*DBP*				Modest lengthening of period

Table 1.1.2.a. Circadian clock genes. Comparing the known circadian clock genes in the mammal system and the avian systems and the drosophila (fruit fly) system. The effects of changes (i.e. mutations) in those genes on the behaviour (i.e. phenotype) of the mutated species (adapted from Vitaterna, *et al*., 2001).

1.1.3 Hypothalamus

The hypothalamus is a vital component of the brain (contained with the diencephalon): linking the nervous system to the endocrine system, via the infundibulum to the pituitary gland. It lies towards the posterior of the cerebrum, inferior to the thalamus, superior to the optic chiasma, around the third ventricle and posterior to the mammillary bodies (Daniel, 1976; Martini, *et al.,* 2001). The hypothalamus regulates the body's homeostasis, as well as generating behaviours involved in eating and digestion, sleep-wake pattern, drinking, emotions (limbic system), blood pressure, secretion of hormones, reproduction, and control of the circadian rhythms (Martini, *et al.,* 2001). There are numerous nuclei in the hypothalamus which have specific functions, in mammals: the supraoptic nucleus secretes anti-diuretic hormone (ADH); the preoptic area coordinates the activities of the other central nervous system (CNS) centres and regulates physiological systems, e.g. blood pressure (BP); the SCN synchronizes the circadian rhythms of daily day-night cycles (Kuhlman and McMahon, 2006).

The "master clock", or oscillator, in the mammalian circadian system is the SCN of the anterior hypothalamus; the SCN is a collection of nerve cell bodies either side of the third ventricle, above the optic chiasm and within the hypothalamic area. It receives photic information from specialised retinal ganglion cells via the retinohypothalamic tract (RHT) and projects to the pineal gland which is a small endocrine gland in the brain. The SCN synchronizes peripheral oscillators in the body which exhibit their own circadian rhythms, such as the liver, kidneys, gastro-intestinal (GI) tract and skin (Glossop and Hardin, 2002). SCN lesion studies on squirrel monkeys (*Simiri sciureus*) not only showed the total loss of their circadian rhythms but also a marked increase of 4 hours sleep, therefore suggesting that

the SCN output mechanisms may also enhance the wakefulness in diurnal mammals (Edgar, *et al.*, 1993).

The mammalian SCN is a densely packed pair of bilateral nuclei lateral to the third ventricle (Nolte, 2002), which can be subdivided into a smaller rostral part and a larger caudal part (van den Pol, 1980). The caudal part of the SCN is composed of two parts:

1) The ventrolateral area which is termed the "core" of the SCN (Figure 0.a.-A); this area receives photic information from the retina and rhythmically expresses the neuropeptide vasoactive intestinal polypeptide (VIP) and gastrin-releasing peptide (GRP) (Moore, *et al.*, 2002). The "core" receives visual afferents and input from the median raphe and projects upon shell, contralateral core and a select set of effector areas (Moore, *et al.*, 2002).

2) The dorsomedial part of the SCN is termed the "shell" (Figure 0.a.-A); which expresses vasopressin (AVP) and calretinin (CAR) neurons (Moore, *et al.*, 2002). The "shell" receives input from other areas of the hypothalamus, basal forebrain, limbic cortical areas, thalamus and brainstem and projects to a wider set of effector areas than core (Moore, *et al.*, 2002).

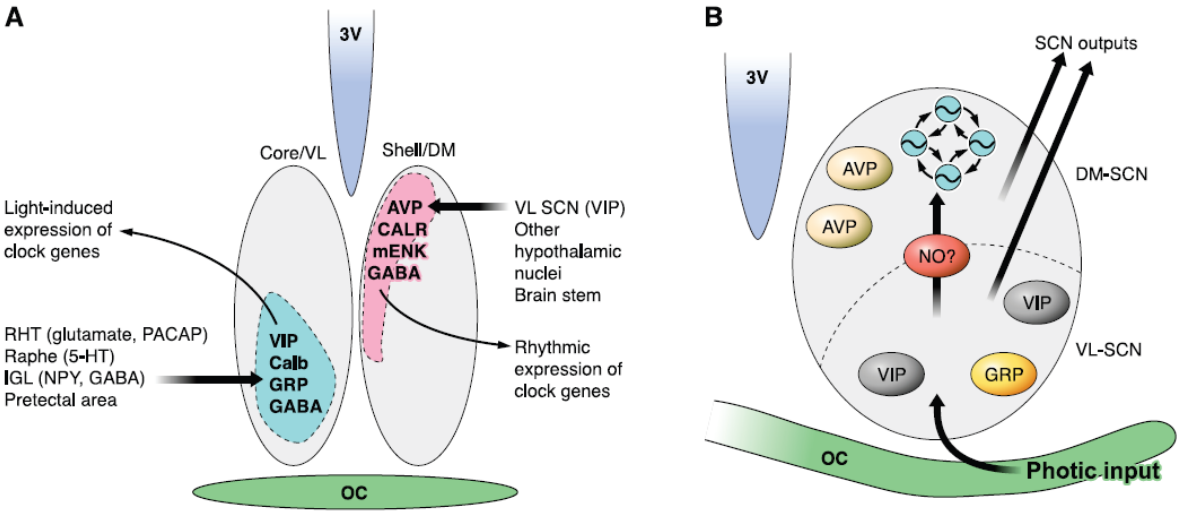

Figure 1.1.3.a. Diagram of the core-shell organization and connections of the SCN, with the neurotransmitter associated with each connection identified.

A: SCN functional and neurochemical subdivisions. The left SCN represents the neurochemical identity of the ventrolateral portion of the nuclei, in neurons that express clock genes in response to light and are directly innervated by the RHT, the raphe nuclei, and the IGL. The right SCN shows the neurotransmitters found in the dorsomedial portion of the nuclei, an area where clock genes are expressed rhythmically, and receives innervation from the ventrolateral SCN and other hypothalamic areas. RHT, retinohypothalamic tract; 3V, third ventricle; OC, optic chiasm; IGL, intergeniculate leaflet; VL, ventrolateral; DM, dorsomedial; VIP, vasoactive intestinal polypeptide; Calb, calbindin; GRP, gastrin-releasing peptide; AVP, arginine vasopressin; CALR, calretinin; mENK, Met-enkephalin.

B: coupling between ventrolateral and dorsomedial regions of the SCN. Ventrolateral neurons are light-responsive and convey the photic message to the dorsal portion of the nuclei. A candidate for this coupling message is nitric oxide (NO), a transcellular messenger. After scavenging extracellular NO, there is no light-induced phase shift nor c-Fos expression in the dorsal SCN (Golombek and Rosenstein, 2010).

1.1.4 Photic information

Photic information can be received by specialized ganglion cells of the retina (mammals and non-mammalian species), or the pineal gland (non-mammalian species) or directly through the skin or by deep encephalic photoreceptors of the brain (non-mammalian species; Lewis, *et al.*, 2000; Figure). This light energy is transmitted to the circadian oscillators in the brain (SCN, pineal gland, etc.: e.g. photoreceptors in the retina transmit via the optic nerve and into the RHT; Figure 1.1.4.a). This information on day length and seasonal changes is stored in the pineal gland and/or hypothalamic nuclei (SCN), and causes a cascade of gene transcription and hormone production (e.g. serotonin (5-HT) and melatonin), which then affects the endocrine function and behaviour (feeding, etc.) of the organism (Cassone and Menaker, 1984; Gwinner and Brandstaetter, 2001). Depending on the photic information received, hormones such as gonadotropin-releasing hormone (GnRH) can be released from the hypothalamus and stimulates the pituitary gland to secrete luteinizing hormone (LH) and follicle-stimulating hormone (FSH), which affect the sexual maturation and ovulatory cycle in animals and birds (Lewis, *et al.*, 2000).

The pineal gland plays an important role in the circadian rhythm, synthesising and secreting melatonin, at night, which regulates the sleep-wake pattern. It is derived from the caudal region of the embryonic dorsal diencephalic cell column (the epithalamus; Nolte, 2002). Many philosophers (such as Max Heindel's Rosicrucian) regarded the pineal gland as a third eye (or "the atrophied third eye"). The presence of photoreceptors, which have been identified in this gland in birds, play a significant role in influencing the circadian rhythm. In mammals the pineal gland has lost virtually all of its photoreceptive function (Flacón, 1999; Flacón, *et*

al., 2009) and has become a purely secretory organ from its parenchymal cells (Møller and Baeres, 2002). The vertebrate pinealocytes have evolved through a gradual loss of photoreceptor character and a gradual increase of neuroendocrine characters (Ekström and Meissl, 2003), suggesting that the mammal's non-sensory pinealocytes have evolved from a photoreceptor cell similar to those found in non-mammalian species that are still photoreceptive (Foster and Soni, 1998; Figure 1.1.4.b. and Table 1.1.4.a.).

In the retinal tissue a photopigment has been identified as being produced by specialized photosensitive ganglion cells in the retina that are involved in the regulation of circadian rhythms. This photopigment is called melanopsin. Melanopsin was originally discovered in 1998 in specialized light-sensitive cells of frog skin by Dr. I. Provencio and his colleagues (Provencio, *et al.*, 1998). The discovery of the function of melanopsin to light responses in specialized retinal ganglia where first recorded by Dr. Berson (Berson, *et al.*, 2002); showed that melanopsin ganglion cells are intrinsically photosensitive. In mammals, light activates the melanopsin ganglion cells which discharge nerve impulses to the SCN and other brain areas (olivary pretectal nucleus) (Berson, *et al.*, 2002).

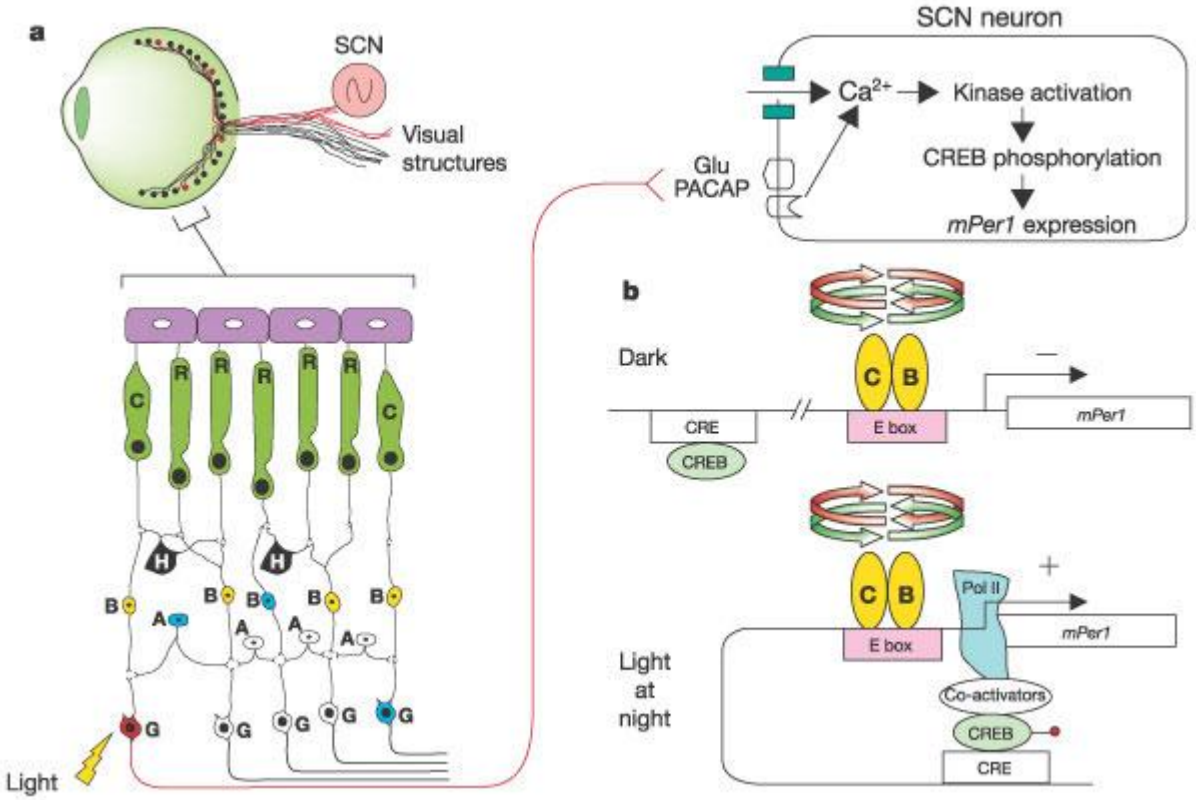

Figure 1.1.4.a. Visual pathway from retina to the SCN. a, A small population of widely dispersed, melanopsin-positive ganglion cells (red) form the retinohypothalamic tract that projects to the SCN. These ganglion cells (G) are directly light responsive. They also receive input from rods (R) and cones (C) through bipolar (B) and amacrine cells (A), some of which may contain crytochromes (blue). The precise anatomy of inputs to the melanopsin-positive neurons remains to be established. Glutamate (Glu) and PACAP mediate light effects on the mPer genes in SCN neurons. b, Light at night activates mPer1 expression through phosphorylated CREB, independent of CLOCK–BMAL1 E-box control. Red and green arrows indicate interacting negative and positive loops of the clockwork, respectively (Reppert and Weaver, 2002).

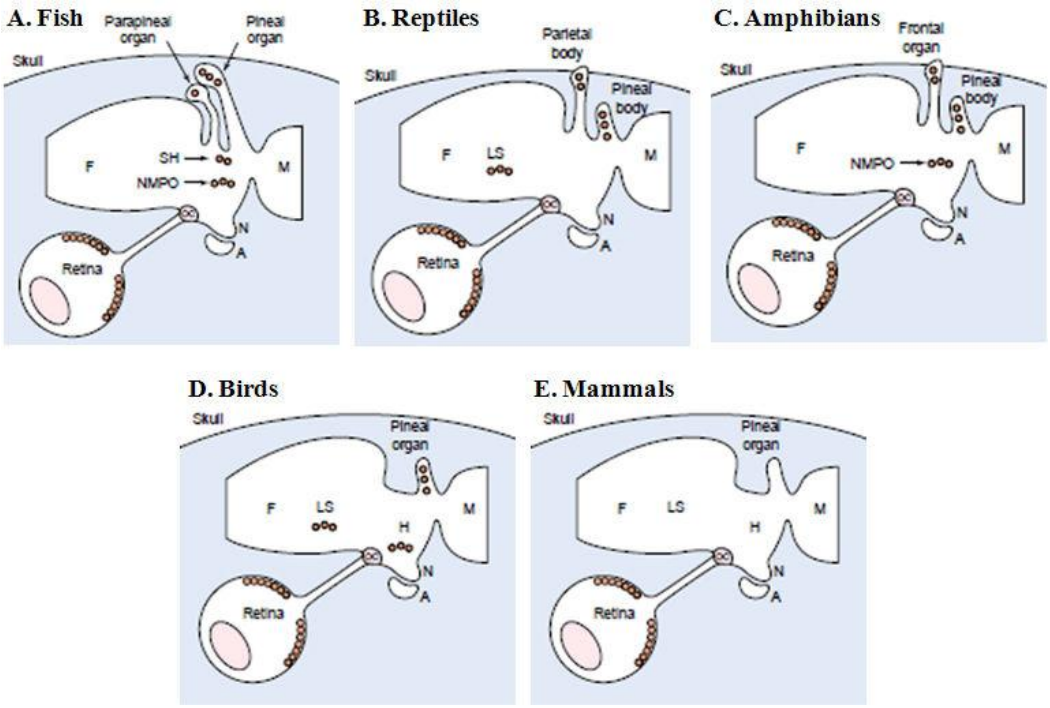

Figure 1.1.4.b. Diagrams illustrating the differences and some of the proposed sites of encephalic photoreception in vertebrates. (A) fish; (B) reptiles (note the extracranial parietal organ); (C) amphibian (note the extracranial frontal organ); (D) birds; (E) mammals. Those areas of the brain thought to contain photoreceptors (opsin immunopositive) are indicated by orange circles. Drawings are not to scale. A, adenohypophysis; F, forebrain; H, hypothalamus; LS, lateral septum; M, mid-brain; NMPO, nucleus magnocellularis preopticus; N, neurohypophysis; OC, optic chiasm; SH, subhabenular (edited from Foster and Soni, 1998).

	Pineal	Parietal Eye or Parapineal organ	Retina	Deep Brain Photoreceptors
Cyclostome	Yes	Yes	Yes	Yes
Fish	Yes	Ye	Yes	Yes
Amphibian	Yes	Yes	Yes	Yes
Reptile	Yes	Yes	Yes	Yes
Bird	Yes	No	Yes	Yes
Mammal	No	No	Yes	No

Table 1.1.4.a. Summary of the distribution of circadian photoreceptors within the vertebrate central nervous system. Extra-retinal photoreceptors are present in all the vertebrate classes, except mammals (edited from Menaker, *et al*., 1997).

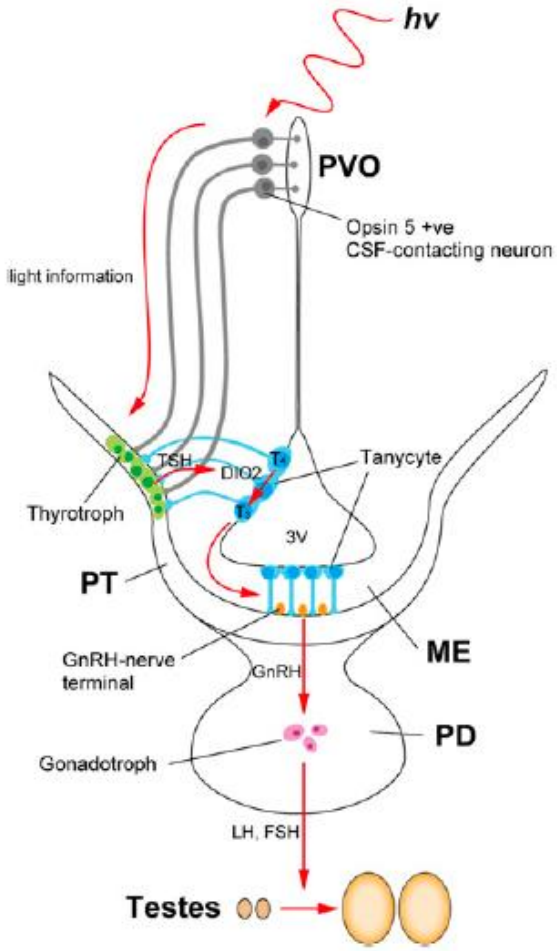

Figure 1.1.4.c. Model of photoperiodic signal transduction pathway in birds. Light detected by Opsin 5-positive PVO neurons that contact the CSF is transmitted to the pars tuberalis (PT) of the pituitary gland and induces thyroidstimulating hormone (TSH) expression in the PT. PT TSH induces expression of type 2 deiodinase (DIO2) in tanycytes lining the ventrolateral walls of the third ventricle (3V) (17). DIO2 converts prohormone T_4 to bioactive T_3 (6). Long-day–induced T_3 in the MBH causes morphologic changes in GnRH nerve terminals and glial processes and induces GnRH secretion. ME – median eminence; LH – luteinizing hormone; FSH – follicle stimulating hormone; PVO – paraventricular organ or nucleus (PVN); GnRH – gonadotropin-releasing hormone; MBH – mediobasal hypothalamus (Nakane, *et al.*, 2010).

1.2 Avian circadian system

The avian circadian system is more complex than the mammalian system: having the capacity to obtain environmental photic information from the retina, pineal gland and deep encephalic photoreceptors. The avian circadian system contains more than one master oscillator controlling the circadian rhythmicity of the organism, to date the pineal; hypothalamus and retina are recognised as separate master oscillators in birds, unlike in the mammalian system which contains one known master oscillator in the SCN of the hypothalamus. Different avian species have different hierarchical balances between the master oscillators but all of these oscillators have the ability to interact with one another to produce a stable circadian rhythmicity (Figure 1.2.a.; Lu and Cassone, 1993; Brandstaetter, 2002).

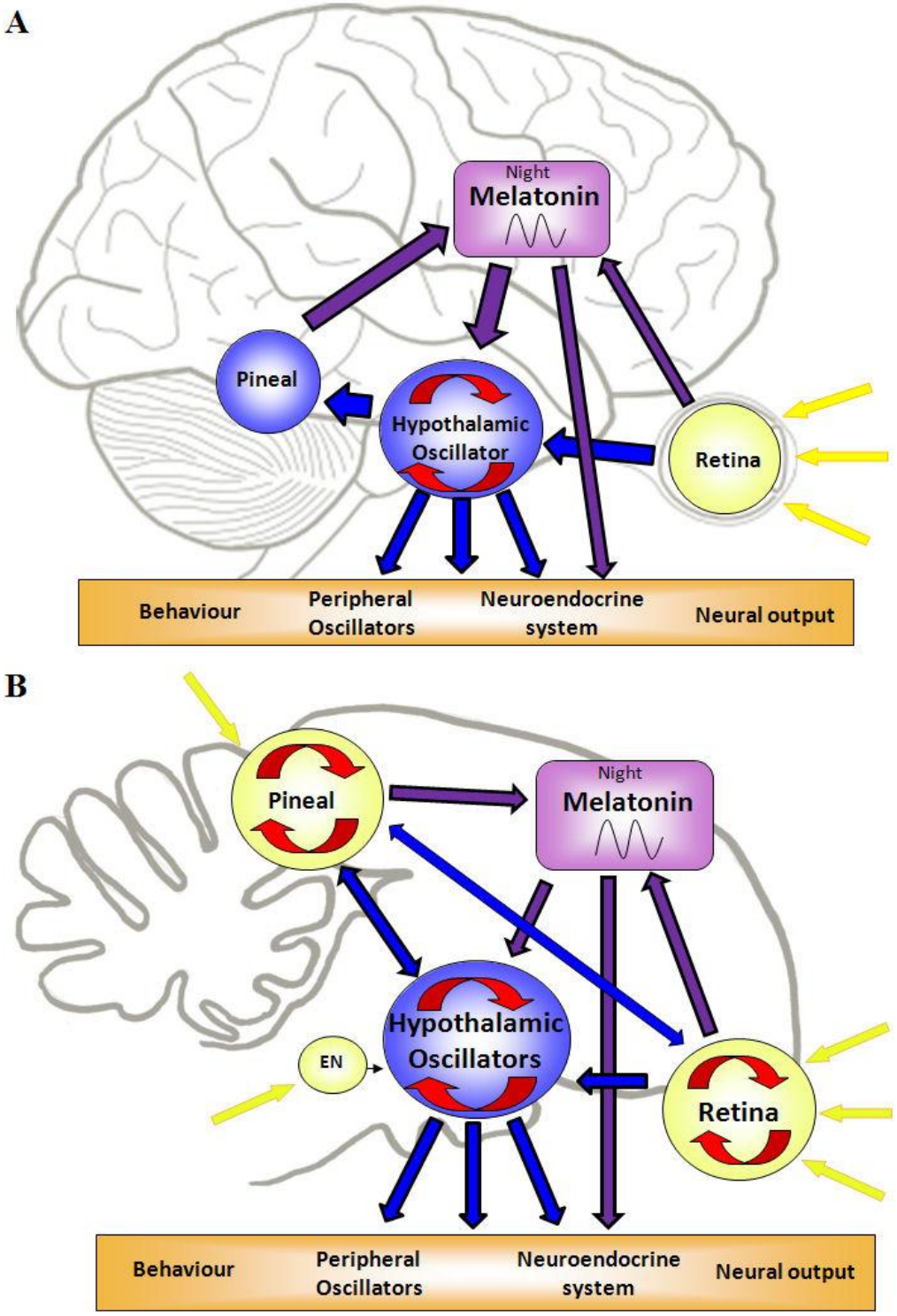

Figure 1.2.a. Comparative overview of the mammalian and avian circadian systems and oscillators. Circadian oscillators indicated by red circular arrows. Light input into the circadian system via photoreceptors is indicated by the yellow colouring; photoreception can occur in the retina, pineal gland and encephalic photoreceptors (EN) in the avian system (B) but only in the retina of the mammalian system (A). Melatonin signal pathways are indicated by purple arrows, neural pathways are indicated by blue arrows. Arrows with circular endings indicate an inhibitory effect.

1.2.1 Hypothalamus

In the avian brain, the circadian master clock has not yet been defined to one nucleus in the hypothalamus, as in the mammalian system. The classical anatomical location of the avian SCN is in the rostral diencephalon, but the RHT appears more caudally, medial to the nucleus geniculatus lateralis ventralis (GLv) and lateral to the supraoptic decussation (Cassone, 1988). Over the past 40 years numerous studies have been conducted to locate the avian homology to the mammalian SCN using anatomical, neurochemical, and neuro-projections (i.e. RHT) to find the answer. Over these 40 years as nuclei's are found to have different functions in different studies, these studies called named the same nuclei with different terminologies (see Figure 1.2.1.a and Table 1.2.1.a. for the terminologies used in this thesis).

In 1962 van Tienhoven identified a cell group above the optic chiasm and adjacent to the third ventricle, which had the similar anatomy to the mammalian SCN, so named this area the SCN (van Tienhoven and Juhasz, 1962). Since then this nucleus has also been termed the zone 1-3 (Meier, 1973), supraoptic nucleus (Ebihara and Kawamure, 1981), periventricular preoptic nucleus (PPN) and vSCN (Cassone and Moore, 1987), medial hypothalamic nucleus (Norgren and Silver, 1989), the medial hypothalamic retinorecipient nucleus (MHRN - Shimizu, *et al.*, 1994; Norgren and Silver, 1989) and mSCN (King and Follett, 1997).

King and Follett describe the avian SCN as having two areas; the medial (mSCN), which lies bilaterally around the lateral recess of the third ventricle, and the visual (vSCN) area, more caudo-lateral to the mSCN, which is now called the lateral hypothalamic nucleus (LHN)

(King and Follett, 1997). The avian vSCN has some important similarities to the mammalian SCN, lesions experiments in house sparrows and chickens abolished the circadian patterns and norepinephrine turnover in the pineal gland, which has the same effect in mammals such as mice and rats (King and Follett, 1997). It receives direct retinohypothalamic input, 2-de-oxy[lac]glucose (2-DG) uptake and 2[^{125}I]iodomelatonin (IMEL) rhythmic binding has been shown in this area (Lu and Cassone, 1993), thus suggesting that the vSCN could be the avian homolog to the mammalian SCN. In comparison, in the mSCN, as studies have shown, there are no melatonin binding sites (King and Follett, 1997); however the mSCN has VIP fibres, which are present in the cell bodies of the mammalian SCN (King and Follett, 1997).

The SCN, with other hypothalamic areas, has melatonin binding sites indicating that the pineal melatonin rhythm has an effect on the hypothalamic oscillator, and in turn the hypothalamic oscillator(s) influence(s) the rhythm of the pineal melatonin release (Gwinner and Brandstaetter, 2001). Lesions in the SCN area gave arrhythmic circadian patterns despite having an intact pineal gland (Gwinner and Brandstaetter, 2001). It has been shown that if one of the "oscillators" are removed, the remaining oscillators lacks the reinforcement and stability the other provided, resulting in loss of the normal circadian cycle, described by Cassone and Menaker as the "neuroendocrine loop" model (Cassone and Menaker, 1984). Another model is also proposed as the "internal resonance" model (Gwinner, 1989), which describes the pineal and hypothalamic oscillators stabilize and amplify each other by the secretion of neurotransmitters/hormones/genes from each tissue which can be perceived by the other tissue which in turn feeds back to the other tissue creating a feedback loop (resonance; Gwinner, 1989). Thus showing the importance of both of these oscillators (pineal and hypothalamus) in the generation of the circadian rhythmicity.

The importance of the retinal input in mammalian SCN has led some avian research groups to look at the RHT in different species to see whether this tract can highlight the master clock within the avian system. Cassone and Moore showed, in 1987, that the RHT projected to the anterior hypothalamus in the house sparrow: the tract had contralateral projections and the rostral extent of the tract projected to an area immediately lateral to the third ventricle and the periventricular preoptic nuclei (PPN), dorsally and ventrally surrounding the ventral supraoptic decussation (DSV): this area was the vSCN (Cassone and Moore, 1987). The vSCN also contained substances which have also been demonstrated in the mammalian SCN such as the glutamic acid decarboxylase and bombesin, but also a terminal field for substance P, 5-hydroxytryptamine, neuropeptide Y, avian pancreatic polypeptide and molluscan cardioexcitatory peptide fibres (Cassone and Moore, 1987).

In another area of the hypothalamus (lateral), a nucleus was also found to have retinal projections and lesions in this area also disrupted circadian behaviour; again over the years this area has been identified with numerous names such as zone 3 (Meier, 1973), supraoptic nucleus (Ebihara and Kwamura, 1981), vSCN (King and Follett, 1997) and the lateral hypothalamus (LHN) (Ehrlich and Mark, 1984). In this thesis it will be called the lateral hypothalamic nucleus, which can be split ventrally (LHNv) and dorsally (LHNd) as per Brandstaetter and Abraham, 2003. It could be that, in the avian brain, the distribution of the hypothalamic circadian pacemaker is divided between different nuclei with great interactions between the nuclei or that in birds the neurochemical circadian factors differs from the mammalian.

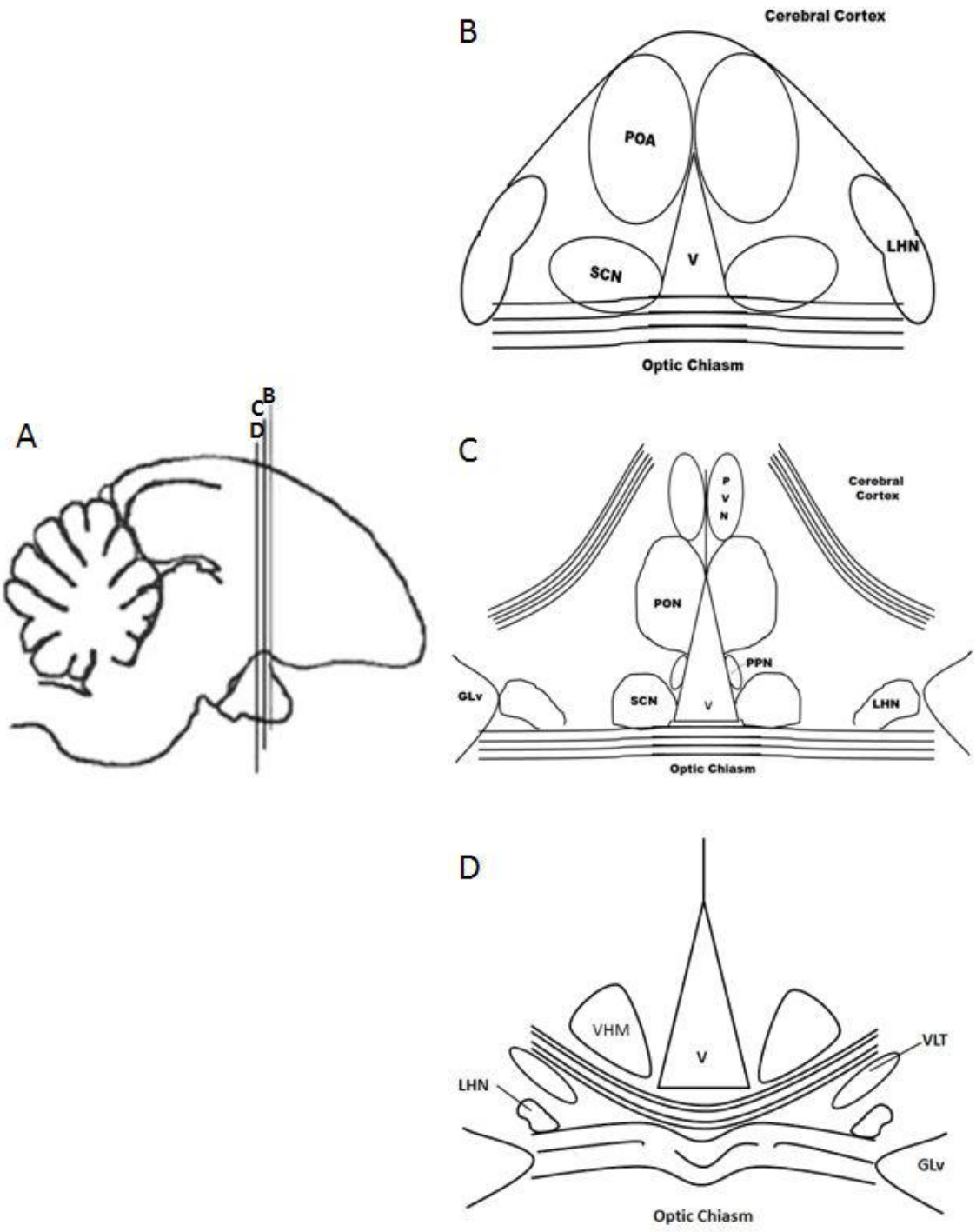

Figure 1.2.1.a. Sagittal section of a zebra finch brain (A) and coronal sections showing the hypothalamic nuclei at different regions through the brain (B-D). A) A sagittal section through the median plane, the vertical lines indicating the areas b-d; which illustrate the neuroanatomy in the rostral (B), medial (C) and caudal (D) hypothalamus. GLv – lateral geniculate nucleus pars ventralis, LHN – lateral hypothalamic nucleus, POA – anterior preoptic nucleus, PON – preoptic nucleus, PPN – periventricular preoptic nucleus, SCN – suprachiasmatic nucleus, V – third ventricle, VLT – ventrolateral thalamic nucleus, VMN – ventromedial hypothalamic nucleus. (Picture A edited from Abraham, *et al.*, 2002).

Name in thesis	Cell group terminology	Reference
SCN **Suprachiasmatic nucleus**	Suprachiasmatic nucleus (SCN)	van Tienhoven and Juhasz, 1962
	Zone 1-3	Meier, 1973
	Supraoptic nucleus	Ebihara, 1987
	Periventricular preoptic nucleus	Cassone and Moore, 1987
	Visual suprachiasmatic nucleus (vSCN)	Cassone and Moore, 1987
	Medial hypothalamic nucleus	Norgren and Silver, 1989
	Medial hypothalamic retinorecipient nucleus (MHRN)	Shimizu, *et al.*, 1994
	Medial suprachiasmatic nucleus (mSCN)	King and Follett, 1997
LHN **Lateral hypothalamic nucleus**	Supraoptic nucleus	Ebihara and Kawamura, 1981
	Suprachiasmatic nucleus (SCN)	Cooper, *et al.*, 1983
	Lateral hypothalamus	Ehrlich and Mark, 1984
	Visual suprachiasmatic nucleus (vSCN)	Cassone and Moore, 1987
	Lateral hypothalamic retinorecipient nucleus (LHRN)	Norgren and Silver, 1989
	Lateral hypothalamic nucleus (LHN)	Brandstaetter, *et al.*, 2001 Brandstaetter and Abraham, 2003

Table 1.2.1.a. Terminology of avian hypothalamic circadian oscillators in previous studies and terminology used in this thesis.

1.2.2. Pineal Gland

The pineal gland, in the avian brain, is found where the cerebellum and cerebral ridges meet on the dorsal surface of the brain, attached by the pineal stalk. The pineal gland, in non-mammalian vertebrates, has been shown to contain photosensitive receptors and contain self-sustaining oscillators (Brandstaetter, *et al*., 2001b). It receives the majority of its neural input via the supracervical ganglion from the RHT, as well as fibres from the preoptic hypothalamus (Brandstaetter, *et al*., 2001b). The major output from the pineal gland is via hormonal transport, i.e. melatonin, rather than neural output (Brandstaetter, 2002).

The pineal gland has the ability to store and retain biologically meaningful information about the time of season thus allowing a buffering system for weather-dependent short-term variations in the photoperiod (Gwinner and Brandstaetter, 2001). In the house sparrow and other passeriform birds the pineal gland secretion of melatonin is the only source of circulating melatonin which amplifies other pacemaker components (Brandstaetter, 2002). Melatonin secretions are rhythmically retained under constant conditions and free-runs in phase with circadian activity and environmental temperature (Brandstaetter, 2002).

Pinealectomy of birds kept under constant conditions have resulted in the complete abolition of their circadian rhythms in locomotor activity (house sparrow – Gaston and Menaker, 1968), core body temperature (house sparrow – Binkley, *et al.*, 1971) and feeding (house sparrow – Heigl and Gwinner, 1995), due to the lack of rhythmic melatonin. The circadian rhythm was restored by implantation of a donor pineal gland into the anterior region of the eye

(Zimmerman and Menaker, 1979) or by daily melatonin injections (Chabot and Menaker, 1992) or food supplements (Heigl and Gwinner, 1995). Although this finding was replicated in other passeriform birds (white-crowned sparrows – Gaston, 1971; white-throated sparrows – McMillan, 1972), other experiments (European starling) have shown only feeding and locomotor disturbances after pinealectomy (Gwinner, 1978); therefore suggesting that different avian species have different oscillatory dominance and control.

1.2.3. Retina

In birds the retina is also a component of the circadian pace making system. The retina transmits photic information about day length through the RHT to the lateral hypothalamic areas and to the SCN (Gwinner and Brandstaetter, 2001). There have been inconsistent results between species and between data from the same species about where the retinal photic information projects to in the hypothalamus, such as in the house sparrow, starling and quail (Abraham, *et al.,* 2003). The retina of some avian species also produces melatonin rhythmically (Cahill and Hasegawa, 1997; Brandstaetter, 2002). In some species retinal melatonin also enters the circulatory system, such as the galliform and columbiform species (Underwood, 1994), whereas in species such as songbirds the only source of circulating melatonin comes from the pineal gland (Gwinner, *et al.*, 1997).

1.3 Neurochemistry of circadian systems

There are various hormones, neurotransmitters and neuropeptides involved in the regulation of circadian rhythmicity and behaviour, projecting to and from numerous nuclei within the hypothalamus. In this next section I will discuss some of the hormones and neurotransmitters, identified so far, involved in the complex function controlling circadian behaviour.

1.3.1 Hormones

There are numerous hormones produced in the nuclei of the hypothalamus, which communicate and influence the production of hormones; these components play vital roles in the maintenance of the body's functions (Table) such as feeding activity, sleep/wake cycles, etc., which are in turn controlled by the rhythmicity of the circadian system. The synthesis and secretion of hormones is vital for maintaining the organism's internal homeostasis and metabolism; the production of hormones can change over a period of hours, months, years or even lifetimes (Hastings, *et al.,* 2007). The most persistent changes occur during the circadian (24 hour) cycle, as our bodies adapt to the changes in daylight which affect the metabolism between catabolic (awake/day-time) and anabolic (sleep/night-time) states (Hastings, *et al.*, 2007). This next section will discuss some of the main hormonal components and their interactions within the circadian system and within the hypothalamus.

Another function of the hypothalamus, which is vital for the circadian cycles and behaviours, is the endocrine system. Neural input to hypothalamic nuclei stimulates the synthesis and

secretion of numerous releasing factors which stimulate the production of other hormones in the pituitary gland (via the infundibular stalk) which then go on to act on peripheral endocrine glands and organs in the body (Table).

Hypothalamic Hormone	Area secreted	Effect
Thyrotropin releasing hormone (TRH)	Paraventricular Nucleus: Parvocellular neurosecretory neurons	Thyroid-stimulating hormone (TSH) is secreted from the anterior pituitary (primarily) and also stimulates prolactin (PRL) release from anterior pituitary.
Gonadotropin releasing hormone (GnRH)	Preoptic area: neuroendocrine cells	Anterior pituitary secretes FSH and LH
Growth hormone releasing hormone (GHRH)	Arcuate nucleus: neuroendocrine neurons	GH is released from anterior pituitary
Somatostatin (SS)	Periventricular nucleus: Neuroendocrince cells	Inhibits the release of TRH and GH from anterior pituitary
Corticotrophin releasing hormone (CRH)	Parvocellular neurosecretory neurons	Anterior pituitary gland secretes ACTH
Vasopressin (AVP) or anti-diuretic hormone (ADH)	Paraventricular Nucleus: Parvocellular neurosecretory neurons	Transported to the posterior pituitary gland and secreted. Release ACTH from anterior pituitary
Prolactin inhibiting hormone (PIH) or Dopamine (DA)	Arcuate nucleus: Dopamine neurons	Inhibit release of prolactin and TRH from anterior pituitary
Prolactin releasing hormone (PRH)	Neuroendocrine neurons in the hypothalamus	Release prolactin from anterior pituitary
Oxytocin	Supraoptic nucleus and paraventricular nucleus: magnocellular neurosecretory cells	Released into the blood from the posterior lobe of the pituitary gland

Table 1.3.1.a. Mammalian hypothalamic-controlled endocrine hormones.

1.3.1.1 Melatonin

A major contributor to the coordination of circadian behaviour is controlled the rhythmicity of the hormone melatonin. Melatonin (5-methoxy-N-acetyltrytamine) is a hormone found in all living creatures. Melatonin levels vary in a diurnal cycle (Brandstaetter, *et al*., 2001b). Rhythms of melatonin synthesis in the avian pineal gland are due primarily to changes in the activity of arylalkylamine-N-acetyltransferase (AA-NAT), converting serotonin into and then hydroxyl-Indole-O-methyl transferase (HIOMT) converts serotonin into melatonin (Bernard, 1997).

The production of melatonin by the pineal gland is entrained by the length of light and dark periods: the levels of melatonin increase under dark (night) conditions and during the day melatonin levels are low or completely absent (Figure 1.2.1.b.; Brandstaetter, *et al*., 2001b). Seasonal changes in day-night length are reflected in the duration and amplitude of the circulating melatonin, i.e. shorter duration but highest amplitude being in the summer, and a longer duration and lower amplitude in the winter period (Gwinner and Brandstaetter, 2001). The release of melatonin in house sparrows can be synchronized with advances/delays in light/dark cycles producing the corresponding shift in the rhythm (Brandstaetter, 2002).

The amplitude of the melatonin rhythmicity decreases, by 30%, in migratory birds in the migratory season, such as the garden warblers which are normally day active but migrate at night, and leading up to the migration, the birds become more nocturnally restless (Gwinner, 1977; Gwinner, *et al.*, 1997). The rhythm of melatonin secretion has been found in most avian

species irrespective of whether the species is a day active or night active bird; apart from the nocturnal barn owl which has low levels of melatonin in the night period, which is a prerequisite for night time activity of the bird (Wikelski, *et al.*, 2005).

The hypothalamus in birds has been shown to contain melatonin-binding sites, suggesting that the control of clock genes and neuropeptides are under the influence of the circulating melatonin levels (Lincoln, *et al*., 2002; Hazlerigg, *et al*., 2005; Johnston, *et al*, 2005). The melatonin rhythm has a dominant role in influencing the locomotor activity in some birds (Cassone, 1990; Bernard, 1997; Bernard, *et al*., 2002); these are mediated by melatonin receptors in the chicken brain (Bernard, *et al.*, 1997; Bernard, *et al*., 2002). The photic information (about the day and night length) received by the retinal ganglionic cells (expressing the photopigment melanopsin), is transmitted to the SCN and entrains the rhythmicity of pineal melatonin release. The concentration of melatonin is controlled by feedback loops from the pineal gland and the hypothalamus: during the night, melatonin is rhythmically released from the pineal gland and inhibits activity in the SCN; during the day the SCN inhibits the release of melatonin from the pineal gland. Melatonin binding site have also been identified in the testes and ovaries of chickens, ducks and quails; the density of binding sites in the quail brain and testes were shown to be dependent on the faction of the photoperiod of the season (Brandstaetter, *et al*., 2001b).

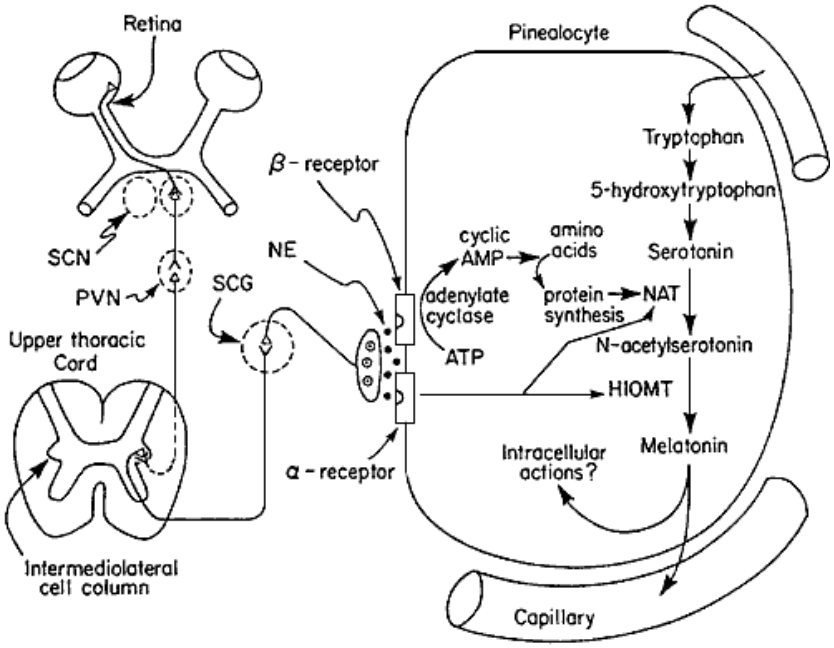

Figure 1.3.1.a. The biochemical mediation system for serotonin transformation to melatonin in the mammalian pinealocytes. Showing the signal transduction pathways from the retina to the cell and the cell receptor, through cyclic AMP and NAT to the transformation process. Although in birds the melatonin production does not need input from the retina, just photic light input directly to the pineal gland and to the pinealocytes, but the conversion pathway of melatonin is the same in both mammalian and non-mammalian systems. Cyclic AMP = cyclic adenosine monophosphate; ATP = adenosine 5'-triphosphate; HIOMT = hydroxylindole-O-methyltransferase; NAT = aralkylamine N-acetyltransferase; NE = norepinephrine (noradrenaline); PVN = paraventricular nucleus; SCN = suprachiasmatic nucleus; SCG = superior cervical ganglion (Reiter, 1994).

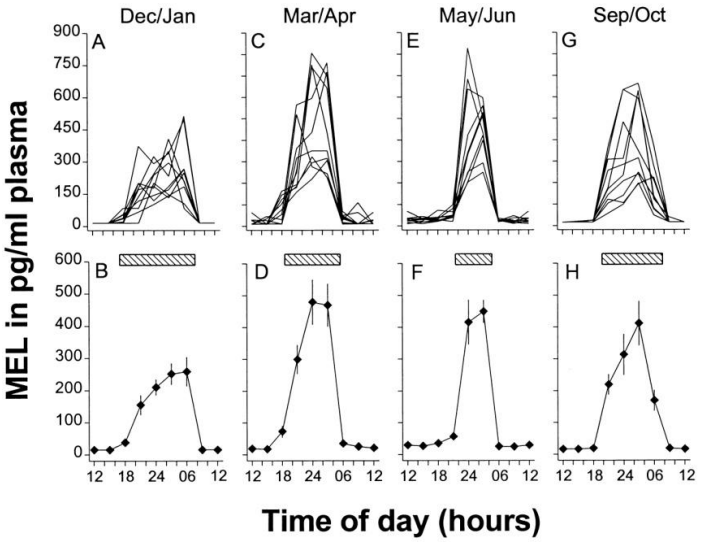

Figure 1.3.1.b. Twenty-four-hour profiles of circulating melatonin (MEL) in birds. In winter (A,B), spring (C,D), summer (E,F), and autumn (G,H). A, C, E, and G show profiles of individual birds; B, D, F, and H show mean values ± S.E.M. (n=10). Shaded areas indicate night length (Brandstaetter, *et al*., 2001b).

1.3.1.2 Arginine-Vasotocin (AVT)

Arginine-vasotocin (AVT) is the avian equivalent of the mammalian arginine-vasopressin (AVP or VP and also known as anti-diuretic hormone (ADH)) (Brandstaetter and Abraham, 2003). The hormone has been identified in the anterior nuclei, preoptic nuclei, periventricular preoptic nuclei, paraventricular nuclei and also in lateral parts of the hypothalamic area (Brandstaetter and Abraham, 2003). The vasotocinergic cells in the avian hypothalamus resemble the neurosecretory hypothalamohypophyseal systems in mammals (Brandstaetter and Abraham, 2003). AVT is synthesized by neurons in the anterior hypothalamus; to either salt loading or dehydration (Chaturvedi, *et al.*, 2000).

In mammals, vasopressin is regulated by the rhythmicity of the CLOCK/BMAL1 complex feedback loop (Jin, *et al*., 1999). AVT and AVP also have major roles in the endocrine stress response, where they have both been shown to directly stimulate the release of adrenocorticotropin (ACTH) and have a synergistic effect with corticotropin releasing factor (CRF) on ACTH release at the anterior pituitary in both mammals and birds (Nephew, *et al.*, 2005); this then stimulates the release of corticosterone (CORT), an important stress hormone in birds. AVT has been shown to decrease the frequency of maintenance behaviours (feeding, drinking, preening, beak wiping) as well as activity in resident starlings (Nephew, *et al.*, 2005).

Vasopressin was the first transmitter to be identified in the mammalian SCN; due to its pronounced rhythm during the day-night cycle within the cerebrospinal fluid (CSF)

(Kalsbeek, *et al.,* 2006). AVP can act as a hormone (possibly due to over spill of production within the SCN (Kalsbeek, *et al.,* 2006)) and neurotransmitter synthesized in the SCN and transmitted out; the daily fluctuations of AVP in the CSF are caused by the rhythm of firing rate of the AVP neurons within the SCN (Kalsbeek, *et al.,* 2006). Vasopressin concentrations cycle under both LD and DD conditions; with peak expression (both mRNA and protein) during the light phase (van Esseveldt, *et al.,* 2000). The $Clk^{-/-}$ mutant mice show an inability to control the AVP rhythm on generation; expressing a free-running period of locomotor activity which is shorter than the wild type and become arrhythmic after about 2-3 weeks in DD conditions (van Esseveldt, *et al.,* 2000).

1.3.1.3 Somatostatin

Somatostatin is a peptide hormone (14-28 amino acids) that is implicated in the endocrine system and in neurotransmission and cell proliferation. In mammalian systems somatostatin was first identified in hypothalamic extracts that strongly inhibited the release of growth hormone from the pituitary gland (Patel, 1999). It can inhibit the release of TSH secretion from the pituitary (Patel, 1999). The neuroendocrine neurons in the periventricular nucleus project to the median eminence of the hypothalamus; it is here that somatostatin is released from neurosecretory nerve endings into the hypothalamohypophyseal portal blood stream, which carries somatostatin to the anterior pituitary gland, so inhibiting the release of growth hormone (GH) from somatotrope cells (Patel, 1999). In the periventricular nucleus, somatostatin neurons also mediate a negative effect of growth hormone on its own release. Somatostatin is not only a powerful inhibitor of the secretion of growth hormone, insulin,

glucagon, and other hormones, but also inhibits functions in other systems including the gastrointestinal tract, such as secretion of stomach acid and pancreatic enzymes and intestinal absorption, therefore affecting other circadian behaviours such as feeding (Patel, 1999).

1.3.2 Other neurotransmitter and neuropeptides

Neurotransmitters and peptides play a vital role in the function of the brain, as well as the circadian system. They transmit information to and from nuclei all over the brain: about processes of the body (such as pain, hunger, fight or flight, alertness, etc.) and communication between different nuclei of the brain (such as pupil reflex, melatonin concentration), in order to maintain the body's homeostasis. Numerous studies have highlighted the presence of different neurotransmitters in the avian circadian system. In the mammalian hypothalamus numerous neurotransmitters have been identified and implicated in the function of the circadian system, such as acetylcholine, glutamate, neuropeptide Y (NPY), serotonin, vasoactive intestinal peptide (VIP) and peptide histidine isoleucine (PHI) (Reghunandanan and Reghunandanan, 2006). Neurotransmitters may have more than one function in a particular nucleus or in different nuclei. In this next section I will discuss the role and presence of the more vital/prominent neurotransmitters that have already been identified in the mammalian system and the avian circadian systems.

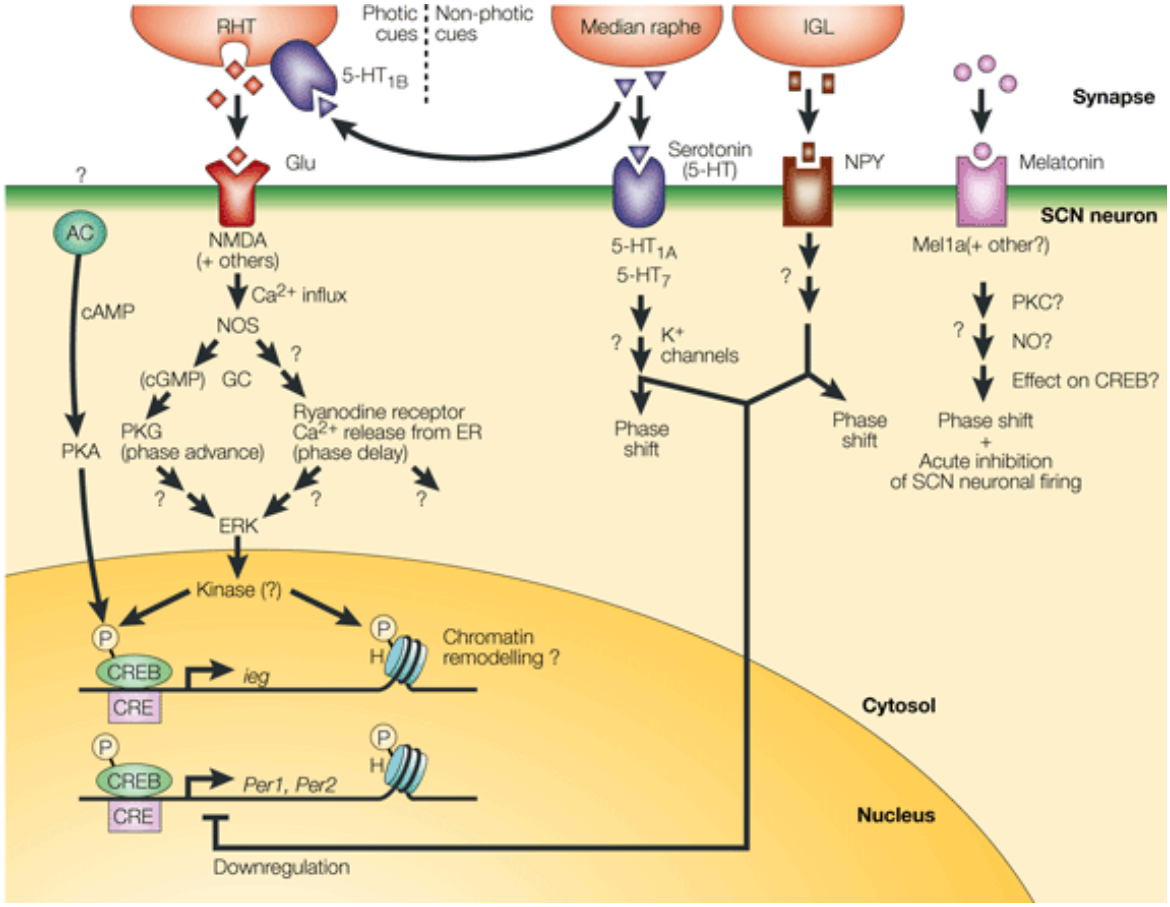

Figure 1.3.2.a. Signalling within a SCN synapse and neuron. The mammalian SCN circadian clock is affected by light (photic cues) through the retino-hypothalamic tract (RHT) leading to use of glutamate (Glu) as a neurotransmitter. Glutamate receptor triggering induces various intracellular responses, leading ultimately to gene expression and phase shifts. Non-photic cues involve a variety of other neurotransmitter and signalling pathways (three of which are shown here). The photic and non-photic pathways can cross-regulate each other pre- and postsynaptically, this scheme is therefore an oversimplification. AC, adenylate cyclase; CRE, cAMP response element; ER, endoplasmic reticulum; ERK, extracellular signal-regulated kinase; GC, guanylyl cyclase; H, histone; ieg, immediate early genes (for example, c-fos); IGL, nerve terminus from the intergeniculate leaflet (thalamus); NMDA, N-methyl-d-aspartate; NOS, nitric oxide synthase; NPY, neuropeptide Y; PKA, cAMP-dependent protein kinase; PKC, protein kinase C; PKG, cGMP-dependent protein kinase (Cermakian and Sassone-Corsi, 2000).

1.3.2.1 Serotonin (5-hydroxytryptamine, 5-HT)

As well as having a role in the production of melatonin, serotonin can also act as an important neurotransmitter throughout the central nervous system (CNS). Serotonin regulation plays a role in body temperature control, intestinal motility, pain modulation, sexual behaviour, appetite, mood and aggression, learning, sleep/wake cycle (via melatonin), anxiety and depression (Cozzi, *et al.*, 1991). Serotonin is formed via synthesis from tryptophan by the enzymes tryptophan-hydroylase and amino-acid decarboxylase. Serotoninergic cells have been found in the paraventricular nucleus (PVN) of the hypothalamus of the Japanese quail: the cells close to the third ventricle project knob-like fibres into the lumen (making a first layer of projections) which then connect to a second layer of fibres that are serotoninergic (immunoreactive) cells (Oishi, *et al.*, 2001). Serotonin has now been linked to photoperiodism, and/or circadian rhythms in the Japanese quail (Oishi, *et al.*, 2001).

1.3.2.2 Neuropeptide-Y

Neuropeptide-Y (NPY) is a 36 amino acid peptide, originally isolated from porcine brain extracts by Tatermoto in 1982 (Aste, *et al*., 1991). NPY has been associated with a number of physiologic processes in the brain, including the regulation of energy balance, memory and learning. The main effect of NPY secretion is (due to) an increase in food intake and decreased physical activity; these are examples of circadian behaviour (Aste, *et al*., 1991), as well as roles in the regulation of feeding behaviour, insulin secretion, sexual maturation and GnRH release in chicks (Esposito, *et al.*, 2001).

Studies have shown that NPY mimics the action of noradrenaline (norepinephrine) in controlling food and water intake (Aste, *et al*., 1991). Immunostaining studies have shown the presence of neuropeptide-Y in the arcuate nucleus, preoptic area and periventricular regions of the hypothalamus; the periventricular region had the greatest staining compared to the other areas (Aste, *et al*., 1991). In other studies, neuropeptide-Y immune-reactive (NPY-IR) cells have been observed along the walls of the third ventricle, inside the periventricular hypothalamic nucleus (PHN), PVN, LHN, nucleus infundibuli (IN) and the median eminence (ME) (Espositp, *et al.,* 2001).

NPY's role in regulating energy balance is well known, it forms part of the "lipostat" system in humans, along with leptin and corticotrophin-releasing hormone (CRH) (van Dijk, 2001). High levels of NPY in the cerebrospinal fluid (CSF) are associated with high food intake. In the arcuate nucleus high levels of fat is detected and leptin is produced by the adipocytes (van Dijk, 2001). The increased activity within the arcuate nucleus acts upon the paraventricular nucleus to inhibit the production of NPY at the site, thus reducing the animal's feeding behaviour and increasing energy expenditure. In 1994, Shimizu's studies on pigeons suggested that the MHRN could be the avian homolog to the mammalian SCN with neuropeptide-Y positive neurons strongly stained in this area, with similar results as the mammalian SCN (Shimizu, *et al.,* 1994).

1.3.2.3 Vasoactive intestinal polypeptide

Vasoactive intestinal peptide (VIP) is a 28 amino acid peptide hormone, originally isolated from porcine small intestine samples (Chaiseha and Halawani, 1999). VIP has been identified in many areas of the human body including the SCN of the hypothalamus (circadian pacemaker), the gut and pancreas. Within the SCN, VIP plays an important role in communication between hypothalamic nuclei. VIP is involved in the synchronisation of circadian timing within the light-dark cycle, in mammals. VIP has been shown as a major synchronizing agent among SCN neurons with light cues, in the mammalian hypothalamus (Vosko, *et al.*, 2007) modulating the molecular oscillations within the individual oscillators (Vosko, *et al.*, 2007).

Csernus's research group has shown that the pineal gland cells activity is controlled by numerous compounds such as VIP and NPY, in the chicken (Csernus, 2006). VIP has been shown to interact with serotonin and influence the neuroendocrine loop, with VIP-ir cells being found in the preoptic and hypothalamic areas in the collared dove (*Streptopelia decaocto).* This is a similar result to those found in other studies: Japanese quail (Yamada, *et al.*, 1982), chick (Kuenzel and Blähser, 1994) and ring dove (Norgren and Silver, 1990; den Boer-Visser and Dubbeldam, 2002). Injections of VIP (and PACAP) in chicks have been shown to significantly inhibit the intake of food, but their actions had a weaker effect than growth hormone releasing factor (GRF) and glucagon-like peptide-1 (GLP-1) (Furuse, 2007).

1.3.2.4 Gamma-aminobutyric acid (GABA)

GABA is the most abundant neurotransmitter found throughout the central nervous system (also the retina; Cutting, *et al*., 1991), converted from glutamate by enzyme L-glutamate decarboxylase (GAD) (van Esseveldt, *et al*., 2000). GABA is rhythmically secreted in the SCN on the mammalian hypothalamus (van Esseveldt, *et al*., 2000). Fluctuating under both LD and DD conditions; having an inhibitory action at night and excitatory action during the day (van Esseveldt, *et al*., 2000). It has also been identified in other organs around the body, including the kidney and the islet cells of the pancreas. In vertebrates, GABA works by binding to its specific receptors ($GABA_A$, $GABA_B$ and $GABA_C$) in the membrane of pre-synaptic and post-synaptic terminals of neurons. The GABA transmitter binding to the receptor causes the ion(s) channels on the membrane to open, allowing negative ions (e.g. chloride) into the cell and/or positive ions (e.g. potassium) out of the cell (van Esseveldt, *et al*., 2000)

GABAergic transmission manipulations at the paraventricular nucleus (PVN) has been shown to affect the release of melatonin from the pineal gland (Kalsbeek, *et al.*, 2006); GABAergic neurons in the SCN have a direct inhibitory effect on the excitatory effect of light on the melatonin release and are involved in the circadian rhythmicity of melatonin (Kalsbeek, *et al.*, 2006). The nocturnal peak of melatonin implies that the activity of the SCN GABA neurons are active during the day (inhibiting the melatonin) and inactive during the night (release of melatonin) (Kalsbeek, *et al.*, 2006).

1.4 Summary

Over the years there has been much debate over the avian hypothalamic homolog to the mammalian SCN "master clock" circadian oscillator: the avian SCN has been called the SCN (van Tienhoevn and Juhasz, 1962), zone 1-3 (Meier, 1973), SON (Ebihara and Kawamure, 1981), PPN and vSCN (Cassone and Moore, 1987), medial hypothalamic retinorecipient nucleus (Shimizu, *et al.,* 1994; Norgren and Silver, 1989); and mSCN (King and Follett, 1997). There has been another nucleus associated with the role as the avian hypothalamic homolog to the mammalian SCN, the LHN; this nuclei has also been referred to as the zone 3 (Meier, 1973), SON (Ebihara and Kwamura, 1981), lateral hypothalamus (Ehrlich and Mark, 1984) and the lateral hypothalamic retinorecipient nucleus (Norgren and Silver, 1989; Shimizu, *et al.,* 1994). The LHN was identified as a possible homolog due to the presence of retinal projections; lesions in this area also disrupted circadian behaviour (Brandstaetter and Abraham, 2003).

Since the avian circadian system has more than one master oscillator it could also be possible that the hypothalamic oscillatory role is not just confined to one cell group, like in the mammalian system, but acts between several nuclei in the hypothalamus (SCN and LHN both rhythmically produce clock genes), and that these nuclei may communicated with one another (though this is yet to be proven).

Along with the differences in circadian oscillatory functions and anatomy, avian species neurochemistry has similarities and differences with the mammalian system and differences

among avian species; i.e. the avian vasotocin hormone plays the role of both vasopressin and oxytocin hormones in the mammalian system. Looking at the mammalian system gives us clues and ideas about the avian system, but a lot more work is needed to characterise the avian circadian system.

1.5 Thesis aims and objectives

The aim of this project is to study and characterise circadian system input and output mechanisms of the zebra finch (*Taeniopygia guttata*). As previously discussed in this Chapter, in avian species so far there are two major hypothalamic nuclei are involved in the hypothalamic oscillation, the SCN and LHN. I will look at both of these areas using molecular and immunofluorescent protocols to study two input mechanisms and one output neuropeptide.

The first input mechanism I will be characterising and analysing the hormone melatonin's receptors. I will do this by cloning the three known melatonin receptors found in the zebra finch; Mel-1A, Mel-1B and Mel-1C, and comparing their location and rhythm over 24 hours in the circadian oscillators (hypothalamus, pineal and retina) and compare their levels to levels in other brain areas (optic tectum, cerebellum and telencephalon) and to several peripheral tissues (heart, liver, lung and kidney). From the data collected on the rhythm of these receptors I will then use immunofluorescent expression to see where the receptors are located in and around the two hypothalamic oscillatory nuclei.

The avian circadian system obtains environmental light information from the retina, pineal gland and deep encephalic photoreceptors. Light inhibits the synthesis and secretion of melatonin from the pineal gland during the day. Light input can be detected by looking at *c-fos* expression using immunofluorescent experiments. *c-fos* is involved in the light entrainment pathway and is a member of the *Fos* gene family (King & Follet, 1997). This

part of the thesis will examine the effect of a one hour light exposure in the early dark and late dark phase has on the hypothalamus by comparing the expression of c-fos in the hypothalamus.

The hypothalamic output neuropeptide I will be characterising is arginine-vasotocin (AVT or vasopressin in mammals), a neurotransmitter secreted by neurons in the supraoptic nucleus in the hypothalamus. I will use immunofluorescent experiments to characterise which hypothalamic nuclei express the hormone and compare the rhythms found in LD conditions and dimLL conditions to see if any rhythms present persist under darkness. I will also perform a species comparisons between the zebra finch, chicken and Japanese quail, at the time-point(s) with the greatest staining in the zebra finch.

1.6 Species of interest: Zebra Finch (Taeniopygia guttata)

(References in this section are from websites, noted with a W.; see end of reference section)

The avian species I will be studying throughout this thesis is the zebra finch, a Passeriform (songbird). The zebra finch is a resident bird of Australia which inhabits large open areas with scattered bushes and trees, but has adapted to human towns, cities and manmade structures (W.1.). The zebra finch is a small (~10g; 10-12cm) bird, native to Australia, though most zebra finches found outside Australia, were not born in Australia and therefore are considered domesticated to areas such as Indonesia, Timor, U.S.A, Puerto Rico and Portugal (W.1.). The zebra finch is a species of songbird, which can adapt or learn their song from whichever bird raised them: either the dominant male in the flock or, if raised with another species, they learn that species song instead; each male's song is different changing up until puberty and then, after puberty, the bird keeps the same song (W.1.).

Zebra finch cocks have chestnut/orange cheek feathers, with white and black markings along the neck, black breast bar, brown flanking along their sides, and black tear drop markings (Figure 1.6.a.-B; W.2.). While the female zebra finches do not have these chest barring, flankings, and cheeks, they do have the black tear drop markings and their beaks are orange (Figure 1.6.a.-C; W.2.). The infants are born with black beaks which turn red (male) or orange (female) during puberty (Figure 1.6.a-A; W.2.). Adult colours are usually complete by the time the young are 90 days old (W.3.; Figure 1.6.a.).

The Zebra finch is a species of great interest and an ideal model species due to a number of facts:

1. It is a highly adaptable species that can breed under the most adverse conditions. It can take extremes in temperature, is highly resistant to disease and parasites, can survive on minimal food and water of atrocious quality, requires minimal space and gets along well with others of its kind and other species and will attempt to breed in any of those conditions (W.3.).
2. Zebra finch can become opportunistic breeders under the right conditions, e.g. temperature, climate, light conditions, etc. which can be created in indoor breeding aviaries and in laboratory conditions. Domesticated Zebra finches are nearly always ready to breed (W.3.). The average clutch will consist of 4-7 laid at the rate of one per day. Incubation will usually begin in earnest after the third or fourth egg is laid. The eggs will begin to hatch after 12 or 13 days depending upon how tightly the pair sat during incubation (W.3.). This therefore allows a breeding stock for regular laboratory experiments for both behavioural and *in vivo/vitro* experiments.
3. Zebra finches have simple dietary requirements of standard finch mix. Grit and calcium in the form of crushed egg and oyster shells and cuttlebone should always be available to them, along with fresh fruit and vegetables.

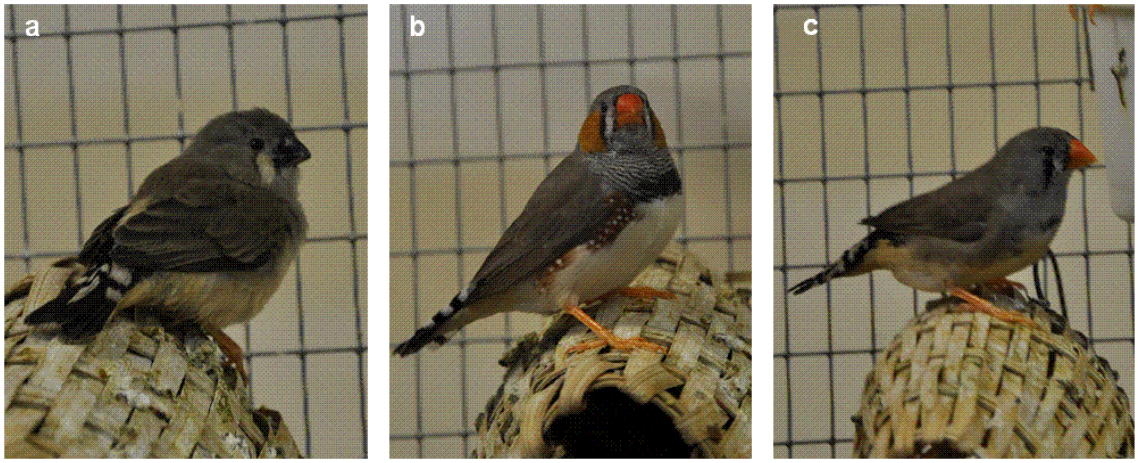

Figure 1.6.a. Zebra finches in the indoor breeding aviary. a) Infant zebra finch, with dark beak and no colouration to the cheeks. b) Male zebra finch with dark red beak, orange cheeks and black marking on the breast. c) Female zebra finch with orange beak, no colourations on the cheek or breast.

CHAPTER 2

Materials and Methods

CHAPTER TWO - MATERIALS AND METHODS

2.1 Animals and husbandry

2.1.1 Animals

2.1.1.1 Zebra finch

Male and female zebra finches where kept in indoor breeding aviaries until experimental work, when they were transferred into the synchronisation aviaries. The birds were supplied with water and food *ad libitum* (foreign finch diet seed, cuttlefish bone, baby spinach, lettuce, sliced apple and orange, and meal worms, with mineralise grit). Birds used for experimental procedures were all of adult plumage (see species of interest Chapter 1.6.).

2.1.1.2 Chicken and Japanese quail

The chicken and Japanese quail eggs were brought in from a reputable breeder. The chicken and Japanese quail eggs were placed in an incubator (37.5°C and 55% humidity) for 21 days (chickens) and 18 days (Japanese quail), and the eggs where turned regularly to prevent the embryo from sticking to the inside on the shell. Turning of the eggs was stopped in the final week to allow the chicks to settle in the correct hatching position. After the incubation time

was over the eggs were transferred to a hatcher. 24 hours after hatching the birds were transferred to the synchronisation aviaries; fitted with an infrared light (brooder) to provide heat, food and water *ad libitum*. Birds were kept in the synchronisation aviaries for two weeks before experimental procedures occurred, to ensure full synchronisation to the lighting conditions.

2.1.2 Synchronising aviaries

Each aviary was equipped with perches and branches. Infrared sensors connected to a data acquisition computer system to record the birds' activity, were situated in each aviary and used to monitor locomotor and feeding activity. Activity recordings were visualised on an actogram (Figure 2.1.3.a) and CLOCKLAB software (Actimetrics, Wilmette, USA) was used in order to assess full synchronisation with the light dark cycle. In each aviary the light source could be individually controlled.

2.1.3 Lighting conditions

All birds were kept in a light-dark (LD) cycle of 12 hours of bright light (1000 lux) from 09:00 hours to 21:00 hours and 12 hours of dark (0.01 lux) period from 21:00 hours to 09:00 hours (LD12:12) for at least two weeks to ensure the birds were fully synchronised before any

experimental procedures occurred. Zeitgeber times (ZT), ZT0/24 was defined as the onset of the light phase at 09:00; ZT6 was defined as 6 hours after the onset of light phase.

For dim constant low light (dimLL) conditions, birds where initially synchronized to LD 12:12 for two weeks conditions and then subjected to dimLL (1 lux ± 0.02 lux) and culled in the first circadian time (CT) cycle. A time-point at ZT23 was taken before the birds went into dimLL conditions; this was performed to check consistency of results between the LD and dimLL conditions, since they were performed in separate experiments.

After full synchronisation, all birds were killed (by dislocation and then decapitation) at set ZT (Chapter 2.3. and Table 2.3.1.a. and Table 2.3.1.b.).

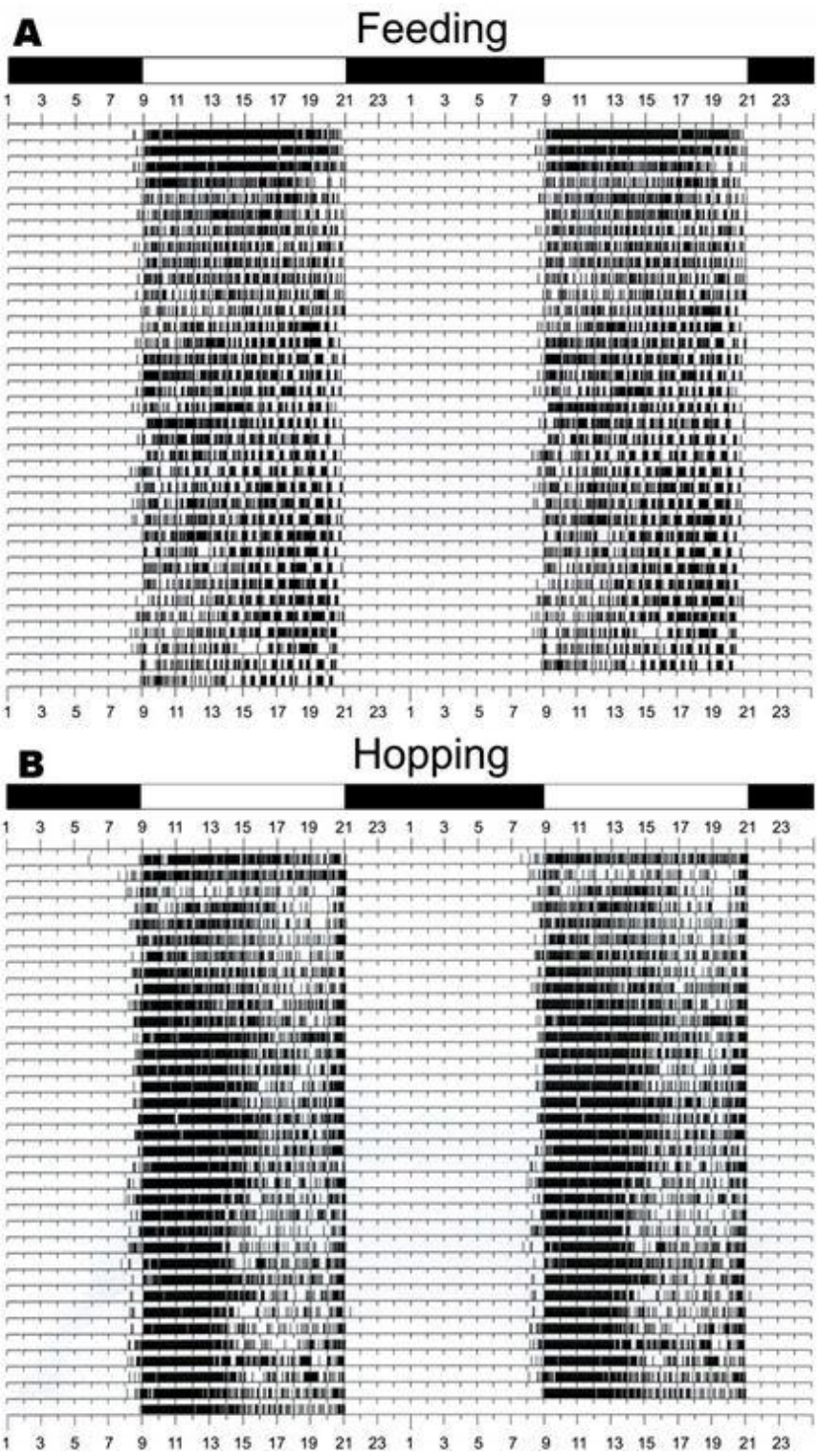

Figure 2.1.3.a. Representative double-plotted actograms showing the feeding (A) and hopping (B) activities of a zebra finch over a period of 34 days. The bird was kept in a LD cycle of 12:12 light:dark. Bars on the top of each graph indicate the light (white bars) and dark (black bars) phases. Each vertical black bar within the actogram marks at least one hopping or feeding event within a two minute interval.

2.2 Molecular procedures

For all solution and mediums used in this chapter see Appendix I – Section 1.1.1.

2.2.1 Tissue sampling

Zebra finches were killed at six different time points over 24 hours (ZT 2, 6, 10, 14, 18, and 22). The brains (n = 6/ZT) were quickly removed from the skull. After the pineal gland was removed, the brain was dissected into the cerebellum, diencephalon, telencephalon, tectum opticum and retina (Figure 2.2.1.a). For dissection of peripheral tissues (Figure 2.2.1.b), an incision was made along the chest bone and the rib cage was opened up and pinned back to remove the heart, liver, lungs and kidneys. All tissues were dissected as quickly as possible and frozen on dry ice and then transferred to a -80°C freezer until further use.

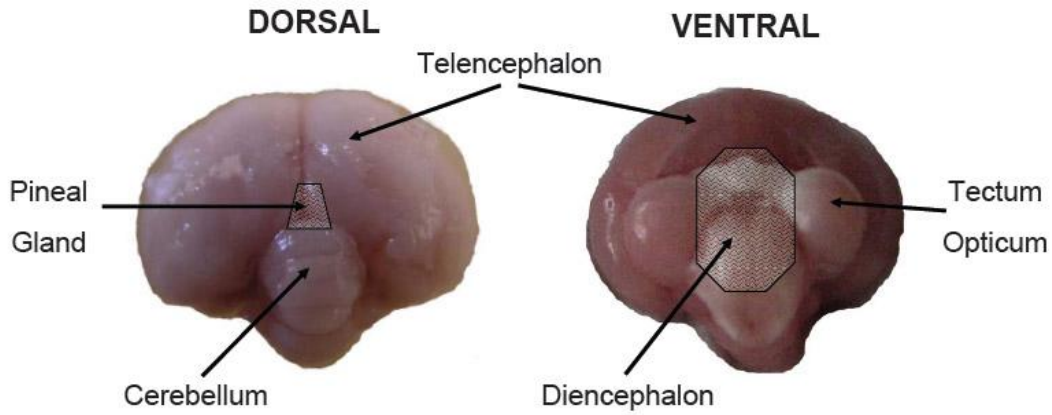

Figure 2.2.1.a. Dorsal and ventral view of a zebra finch brain showing the location of the brain tissues dissected and used in the molecular experiments. The pineal gland in the avian brain is found where the cerebellum and cerebral ridges meet on the dorsal surface of the brain, attached by the pineal stalk; found in the area of the grey triangle. The diencephalon is the area containing the hypothalamus which is found superior to the optic chiasm; indicated by the black outlined box.

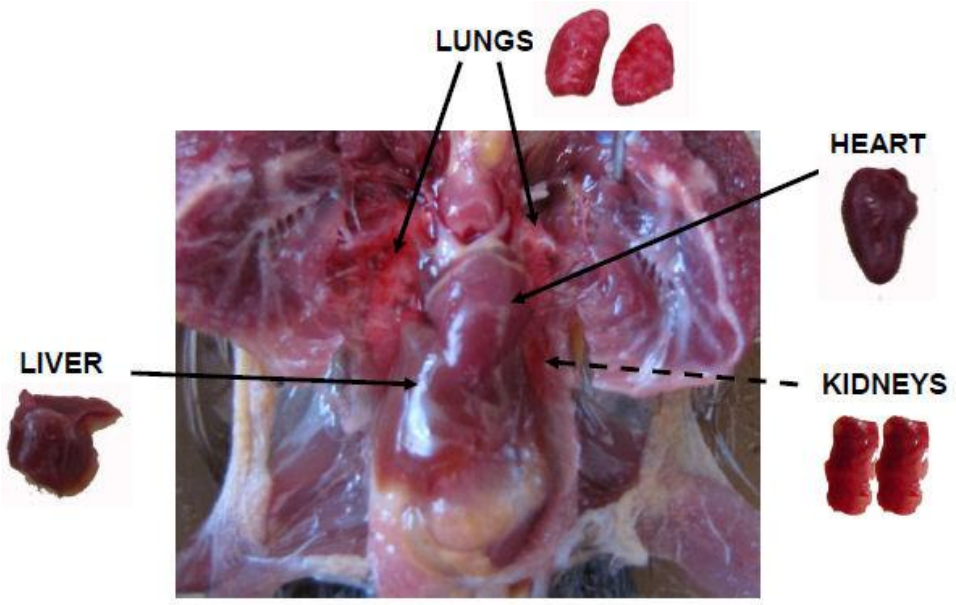

Figure 2.2.1.b. Dissection of zebra finch peripheral tissues for total RNA extraction showing the internal structure of the avian cavity. The tissues used in this study are highlighted by the black arrows and a isolated images: liver, lungs, heart and kidneys. In the image the heart and liver lie inferior to the opened rib cage and peritoneal; they are positioned most superiorly in the image. In the image the lungs and kidneys sit inferiorly to the heart and liver, along the back of the cavity.

2.2.2 RNA extraction

Total RNA was isolated from zebra finch tissues using Trizol™, following manufacturer's instructions (Invitrogen Life Technologies, Carlsbad, USA). Tissues were homogenized in 1ml of TRIZOL® (per 50-100 mg of tissue) and 0.2ml of chloroform were incubated for 5 minutes at room temperature before being vigorously shaken on a ball mill (Mixer Mill MM 300; Retsch, Haan, Germany) using 3mm tungsten carbide beads (Quiagen), for 15 seconds. The resulting solution was then incubated at 20°C for 3 minutes.

The solution was then centrifuged (Eppendorf Centrifuge 5810R) at 13,000 × g for 15 minutes at 4°C. Following centrifugation, the aqueous RNA phase in the upper phase of the solution was removed. The RNA solutions were then mixed with isopropyl alcohol to precipitate the RNA, by incubating for 10 minutes at 20°C. An RNA pellet was formed by centrifuging the samples. This pellet was then washed with 75% ethanol/DEPC and vortexed. This solution was then centrifuged and the RNA pellet dried. The resulting RNA pellet was mixed with RNase free water and incubated for 10 minutes at 55°C.

2.2.3 RNA analysis

The resulting total RNA samples were analysed by Nano-drop (Thermo scientific; all tissue samples), Agilent 2100 Bioanalyzer and the RNA 6000 LabChip® kit Nano assay (Caliper Labchip; all brain tissues). RNA gels stained with ethidium bromide (zebra finch peripheral

tissues), to check the quality and concentration of the isolated total RNA samples. RNA samples were then incubated with RNase-free DNase 1 (Roche Diagnostic, Mannheim, Germany) and RNase Inhibitor (RNA out Invitrogen) for 30 minutes at 37°C and then at 90°C for 10 minutes to deactivate the DNase I.

2.2.4 cDNA synthesis

1.0μg aliquot of the resulting RNA was reserve transcribed using oligo-p$(dT)_{15}$ primers (first strand cDNA synthesis kit; Roche Diagnostics) for the brain samples and oligo-p$(dT)_{18}$ primers (Bioline; cDNA synthesis kit) with RevertAidTM H minus M-MuLV reverse transcriptase (Fermentas) for the peripheral tissue samples. The solutions were incubated for 10 minutes at 25°C and transferred to 42°C for 60 minutes, before being inactivated at 70°C for 10 minutes. The resulting cDNA product was then subjected to reserve transcription polymerase chain reaction (RT-PCR) to amplify the cDNA content. Due to the small size of avian pineal gland less than 1μg of total RNA was used for the first strand cDNA synthesis.

2.2.5 Gene cloning of Mel-1A, Mel-1B and Mel-1C receptors

cDNA samples were taken from the diencephalon (DM) at time points ZT 6, 14 and 18 for the zebra finch. Relevant primer pairs (Table 2.2.5.a) where added to the cDNA samples and

amplified by RT-PCR (Applied Bioscience, Gene Amp PCR system 9700) using a Taq DNA Polymerase kit (Roche) see Chapter 0 for PCR cycle conditions. Each PCR reaction contained a negative control (no cDNA).

PCR products (n = 2/ZT 6, 14, 18) were separated on a low melting point 2% agarose (Sigma Aldrich) gel and stained with SYBR green I (Sigma Aldrich). The DNA bands were visualised on an UV light plate and dissected out. The DNA was extracted from the gel using a gel extraction kit (QIAGEN; QIAquick gel extraction kit).

2.2.5.1 Ligation

The DNA samples were ligated into pGEM-T easy vectors (Promega; Figure 2.2.5.a) using 2x rapid ligation buffer, for one hour at room temperature. The ligation reactions were set up as follows: pGEM-T Easy 0.5µl; Fragment (Quiagen Prep) 3.5µl; 2X Ligation Buffer 5.0µl; T4 DNA ligase 1.0µl. The reactions were mixed well and left at 4°C over night (this give the maximum number of transformations).

Gene	Primer pair nucleotide sequence (5' to 3')	Predicted product length
Mel-1A	Forward: TGCCACAG(C/T)CTCA(A/G)(A/G)TA(C/T)GAC Reverse: AT(T/C/G)GC(A/G)ATT(A/G)AGGCAGCTGTTGA	500bp
Mel-1B	Forward: GACAAAGTGTACAGCTGTTGG Reverse: CTGATTTGACTCGTCTTCGAAC	265bp
Mel-1C	Forward: TGCT(A/G)CATCTGCCACAGCCT Reserve: (GCT(C/T)A(G/A)(G/A)ACAAA(A/C)AGCCA(T/C)TCTG	463bp

Table 2.2.5.a. Primer sequences, and predicted product length, used to clone melatonin receptors Mel-1A, Mel-1B and Mel-1C from Zebra finch cDNA templates. The Mel-1B primers are based on the zebra finch Mel-1B receptor sequence (NCBO accession number NM_001048258). The Mel-1A and Mel-1C primers are based on sequenced published on house sparrow (Mel-1A - AY155489 and Mel-1C - AY743658) and personal communication with the authors.

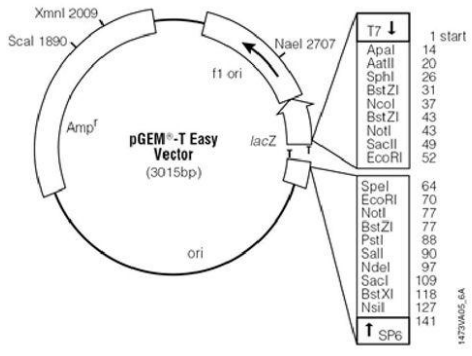

pGEM®-T Vector sequence reference points:

T7 RNA polymerase transcription initiation site	1
multiple cloning region	10–113
SP6 RNA polymerase promoter (–17 to +3)	124–143
SP6 RNA polymerase transcription initiation site	126
pUC/M13 Reverse Sequencing Primer binding site	161–177
*lac*Z start codon	165
lac operator	185–201
β-lactamase coding region	1322–2182
phage f1 region	2365–2820
lac operon sequences	2821–2981, 151–380
pUC/M13 Forward Sequencing Primer binding site	2941–2957
T7 RNA polymerase promoter (–17 to +3)	2984–3

Figure 2.2.5.a pGEM®-T easy vector circle map and sequence reference points (Promega datasheet).

2.2.5.2 Transformation of cells with vector ligated cells

Competent E.coli DH5α cells were transformed with the ligated vectors (50.0µl for each transformation). The ligation reaction was then denatured by heating at 65°C for 10 minutes. A negative control (cells without any DNA added) to check for any "background" of contaminating antibiotic resistant cells was included in every transformation. Reactions were incubated on ice for 30 minutes.

The cells were heat shocked at 37°C for 2 minutes and then placed on ice for 3 minutes: this allowed the cells to open and the vectors to enter the cell, placing on ice closed the cells again. SOC medium at pH 7 (Appendix I – Section 1.1) was added to each reaction and was incubated for 90 minutes at 37°C, gently shaken (110rpm).

The solution was centrifuged (Eppendorf; centrifuge 5810R) at 300rpm for 5 minutes; the supernatant discarded and the pellet plated out onto LB agar plates containing, ampicillin (10mg/ml or 20mg), Xgal (20mg/ml) and IPTG (0.1M) overnight at 37°C (Appendix I – Section 1.1). Liquid cultures were grown for ~16 hours at 37°C on a rotary shaker at ~200rpm. Agar plates were grown inverted for ~16 hours at 37°C. Inoculations of liquid culture and agar plates were carried out under aseptic conditions. White colonies (colonies with the DNA insert; Figure 2.2.5.b) where located, 2 colonies from each plate were removed and incubated in 5ml LB medium (with 50µl Amp) over night at 37°C on a shaker at 200 rpm.

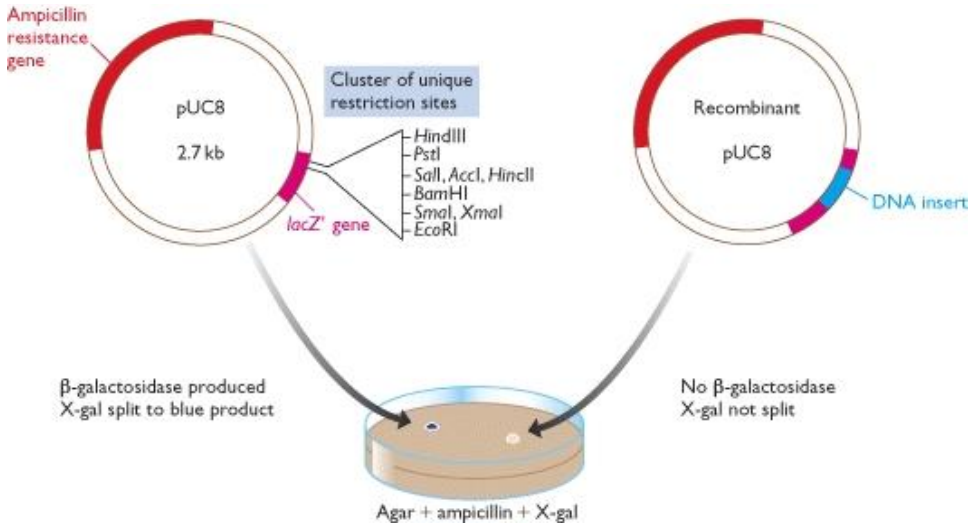

Figure 2.2.5.b Recombinant selection with pUC8. The blue/white colony identification occurs due the presence (blue) or absence (white) of the bacterial lacZ gene producing b-galactosidase (b-gal) in the plasmid's open reading frame. The alpha peptide expressed by hosting E.coli strain, functional b-galactosidase can be produced by transforming wild type lacZ containing plamid into e.coli cell and the b-galactosidase can turn the X-gal into blue colour products (Brown, 2002). When a foreign DNA is inserted into the multiple cloning sites within the lacZ gene, the open reading frame of lacZ is changed and will not produce b-galactosidase therefore the recombinant colony will be in white colour. Therefore if the insert DNA is present this interrupts b-gal from being produced and the colony turns white (Brown, 2002).

2.2.5.3 FastPlasmid Miniprep

A plasmid prep was carried out on each clone of the Mel-1A and Mel-1C plasmids, using fast plasmid mini kit (Eppendorf; 955150619) to collect the DNA using elution buffer (50µl), and stored at -20°C. Wizard® Plus SV minipreps (Promega) DNA purification system was used on the Mel-1B plasmids. The plasmid prep allowed the isolation of the plasmid from the cells. The plasmid vector carries two restriction sites for EcoR1, either side of the insert.

2.2.5.4 EcORI digestion

Samples were incubated at 37°C on a heating block for 55 minutes. The samples were visualised on a 1% agarose gel stained with SYBR green. The insert was then cut out of the gel and the plasmid discarded.

2.2.5.5Ethanol precipitation

Ethanol (EtOH) precipitation was performed using 100% Ethanol (x2 volume of solution) and sodium-acetate (1/10 vol. of solution) incubated at -80°C for 20 minutes and centrifuged for 30 minutes (14,000 rpm). The supernatant was removed and replaced with 70% ethanol and centrifuged for 15 minutes. The pellet was air dried and diluted with 10.0µl H_20/DEPC.

The EtOH precipitation was used to clean up the plasmid DNA; i.e. to remove buffers, etc. from the ligation. The EtOH precipitation was performed on the original plasmid prep. The presence of an insert was confirmed by Agarose gels.

2.2.6 DNA sequencing and identification of zebra finch Mel-1A, Mel-1B and Mel -1C receptors cDNA

The DNA sample was sequenced in house (Functional Genomics and Proteomics Services, School of Biosciences, University of Birmingham): 2µl Plasmid DNA (=200-500bp), 4µl M13 (-21) primer (=3.2 pmol) and 4µl H20/DEPC.

E.coli containing successfully sequenced clones were incubated overnight, on a shaker (200rpm) at 37°C in 2ml LB medium and 20µl of ampillicin (10mg/ml). 1ml of the clone culture was added to 1ml 30% glycerol/LB medium and stored at -80°C.

The sequencing results were analysed and aligned using:

- Chromas (Technelysium Pty Ltd),
- BioEdit (Ibis Biosciencs, Carlsbad, CA),
- NCBI Blast database (http://blast.ncbi.nim.nih.gov/Blast.cgi),
- Clustal W2 program from EMBL (http://www.ebi.ac.uk/Tools/clustalw2).

2.2.7 Reverse transcription polymerase chain reaction (RT-PCR)

All the PCR based reactions were performed on an Applied Biosystems GeneAmp® PCR system 9700. All PCR bases reactions used Roche Taq DNA polymerase and dNTPack kit.

Thermal Profile for cloning:

Initial heating:	94°C for 2 minutes,	1 cycle;
	94°C for 30 seconds,	
	55°C for 30 seconds,	
	72°C for 1 minute,	10 cycles;
Sequencing*:	94°C for 30 second,	
	60°C for 30 second,	
	72°C for 1 minute,	30 cycles;
Final stage:	72°C for 7 minutes,	1 cycle;
Hold:	4°C	

Thermal profile for Gene Analysis:

Initial heating:	94°C for 2 minutes,	1 cycle;
	94°C for 2 minutes	
	55°C for 3 minutes,	
	72°C for 5 minutes,	1cycle;
Sequencing*:	94°C for 30 seconds,	
	X°C for 30 seconds,	
	72°C for 1 minute,	Y cycles;
Final stage:	72°C for 7 minutes,	1 cycle;
Hold:	4°C	

*Alterations between the temperatures are done by ramping at 1°C/second.

Annealing temperatures (X°C), magnesium (Mg^{2+}) concentrations, and cycle numbers (Y cycles) were optimised for each set of primers for the melatonin receptor gene rhythmicity analysis, shown in Chapter 0.

2.2.7. 1 Primer design

For PCR amplification of melatonin receptor genes, primers were designed using Primer3 online program and supplied by MWG Biotec. All primers used were diluted to a working concentration of 10μM.

The specificity of a primers is controlled by the length and annealing temperature of the primer; oligonucleotides with a 18-24 bases tend to be more sequence-specific if the annealing temperature of the PCR is within a few degrees of the primer Tm (Dieffenbach and Dveksler, 2003). Primer length's of 18-24 base pairs is an optimum length for primers as it is long enough for adequate specificity, but short enough for primers to easily bind to the template cDNA at the annealing temperature. The melting temperature of a primer is calculated normally by one of two ways:

$$Tm = 4(G+C) + 2(A+T)$$ Suggs, *et al.*, (1981)

$$Tm = 64.9 + 0.41(\%C + \%G) - 600/n$$ Freier, *et al.*,(1986)

where G, C, A, T - respective nucleotides and n = the length in bases of the primer in question.

The melting temperature is the temperature at which the template DNA structure dissociates to become a single strand. The optimum melting temperature for most primers are between

55-65^{o}C, which will generally produce the best results; primers with melting temperatures above 65^{o}C tend to have a secondary annealing temperature.

The annealing temperature of the primers is the temperature at which the primers to anneal to the single stranded DNA template sequences, this is usually a few degrees below the Tm of the primers. The higher the annealing temperature the more specific binding there is, a too higher temperature produces insufficient primer-DNA hybridization lowering the PCR yield and too lower temperature leads to non-specific products being produced and more mismatches occur.

Minor alterations to a PCR protocol can significantly affect the yield of the reaction, the protocol carried out depended upon the reason the PCR was being carried out. The number of cycles used in a reaction was dependent upon the procedure being carried out and what stage of synthesis is needed for the experiment. Therefore for each primer pair designed the optimum conditions need to be worked out for the best PCR yield needed for the experiment in hand.

2.2.8 Optimising RT-PCR cycling conditions for Mel-1A, Mel-1B and Mel-1C primers

From the sequence and alignment data collected from the above experiments (Chapter 0) primers were designed for the Mel-1A, Mel-1B and Mel-1C receptors (Table 2.2.8.a). The cDNA for this part of the experiment was a mixture of all time-points and all five brain tissues.

Once the primers were designed using Primer3 online program, the primer conditions were optimised to obtain the specific receptor PCR products; be in the linear phase of synthesis. The primers used for semi-quantitative RT-PCR are summarised in Table 2.2.8.a and PCR setting in Chapter 0., unless otherwise stated. The PCR conditions were optimised in the following steps:

Step 1 – to obtain the specific amplified product annealing temperature, 2°C increments, and the Mg^{2+} ion concentration titrated over 0-2.5mM. The final annealing temperatures and Mg^{2+} for each receptor primer pair are stated in Table 2.2.8.a and will be used in steps 2 and 3.

Step 2 – the optimum cycle number to obtain a yield in the linear phase of synthesis. Thirteen identical reaction mixes were set up and removed from the PCR machine (Gene Amp PCR system 9700, Applied Bioscience, USA) at 10, 14, 16, 18, 20, 22, 24, 26, 28, 30, 34, 38 and 42 cycle numbers. The visualised products were analysed (Quantity one program; BioRad), quantified and plotted to produce a synthesis curve. The linear amplification phase range was selected and a cycle number was obtained for further use.

Step 3 - a cDNA dilution series (1:1) was used to confirm that the cycle number found in step 2 a in the linear phase.

At the end of each PCR step the products were visualised on an 8% polyacrylamide gel (Appendix I – Section 1.1.1.), stained with SYBR green I for 45 minutes.

Primer name	Primer nucleotide sequence (5' to 3')	Length (bp)	Tm (°C)	GC (%)
Mel-1A				
Mel1AQPfor1	CACAGTCTCAGATACGACAAGC	22	60.3	50.0
Mel1AQPrev1	GTAACTACGGCTATGGGAAGC	21	59.8	52.4
Mel1AQPfor2	**CCACAGTCTCAGATACGACAAGC**	**23**	**62.4**	**52.2**
Mel1AQPrev2	**ACCCTTCGCCTTACCTGGATAAC**	**23**	**62.4**	**52.2**
Mel-1B				
Mel1BQPfor1	CTTGTATCCATACCCACTGG	20	57.3	50.0
Mel1BQPrev1	GTGCATGAATAGATGCGTGG	20	57.3	50.0
Mel1BQPfor2	**GACAAAGTGTACAGCTGTTGG**	**21**	**57.9**	**48.0**
Mel1bQPrev2	**CTGATTTGACTCGTCTTCGAAC**	**22**	**58.4**	**45.0**
Mel-1C				
Mel1CQPfor1	ACATCTGCCACAGCCTTCGCT	21	61.8	57.1
Mel1CQPrev1	GCCCTGAGTTTCTGCTTGCAG	21	61.8	57.1
Mel1CQPfor2	CTTCTTTGTTGGCTCCTTGC	20	59.4	50.0
Mel1CQPrev2	GTCTTGTCTCACCCGGTGTT	20	57.3	55.0
Mel1CQPfor3	**TCTGCCTGACCTGGATACTCAC**	**22**	**55.3**	**54.5**
Mel1CQPrev3	**CTGCTTGCAGTCTTGTCTCACC**	**22**	**55.9**	**54.5**
Mel1CQPfor4	GAACACCTGCTGCTATCTCTGC	22	55.5	54.5
Mel1CQPrev4	TGCCCTGAGTTTCTGCTTGC	20	55.4	55.0
TBP				
TBPQPfor	**TACCACAGCCCCTTTACCTG**	**20**	**59.4**	**55.0**
TBPQPrev	**CTGTTCCTCGCTTTTTGCTC**	**20**	**57.3**	**50.0**

Table 2.2.8.a. Primers designed and used in optimising melatonin receptor expression experiments. One primer pair per receptor was optimised for future Melatonin receptor expression work. All Primers were supplied by MWG Biotec (Eurofins). TBP was designed and optimised by Dr. G. Helfer, (Bioscience, University of Birmingham) this gene is used to normalise the melatonin receptor expression. The bold highlighted primers where the primers fully optimised and used in the future experiments for the rhythmicity of all three receptors (Figure 2.2.8.a).

1) Mel-1A

5'>>>>>>>>>>>>>>>>>>>>>>>>>>

TTGCCACAGTCTCAGATACGACAAGCTGTACAGCGACAGGAATTCATTGTGCTAT
ATTGTTCTCATATGGCTCCTAACATTTGTTGCTATCGTGCCCAACCTGTTTGTGGG
ATCGCTCCAGTATGACCCCAGGATTTACTCCTGTACATTTGCACAGTCTGCGAGC
TCAGCATACACTATAGCAGTTGTGTTTTTCCACTTCCTGCTTCCCATAGCCGTAGT

<<<<<<<<<<<<<<<<<<<<<<<<<<<'5

TACTTTCTGTTACTTGCGAATATGGATCCTCGTTATCCAGGTAAGGCGAAGGGTTAA
ACCAGATAACAACCCTAGGCTGAAACCACATGACTTCAGAAACTTTGTAACCATGTT
TGTGGTATTTGTACTGTTTGCAGTCTGCTGGGCTCCTTTGAACTTTATAGGCATTGC
AGTGGCTGTCAATCCAAAAACTGTAATCCCTAGGATTCCAGAGTGGTTGTTTGTGC
TAGTTATTACATGGCATATTTCAACAGCTGCCTTAATCGCGATA

2) Mel-1B

5'>>>>>>>>>>>>>>>>>>>>>>>>

CTTTGCCTATGACAAAGTGTACAGCTGTTGGAATACAATGTTGTATGTCTCCTTAGT
CTGGATATTAACAGTAATTGCAACTGTGCCAAATTTTTTTGTTGGCTCTTTGAAGTAT
GATCCACGCATCTATTCATGCACATTTGTCCAAACTGCAAGCTCCTACTATACAATA
GCTGTTGTGGTCATTCACTTCATCGTCCCTATCACCATCGTCAGCTTCTGCTACCTT

<<<<<<<<<<<<<<<<<<<<<<<<'5

CGAATTTGGGTTTTAGTGCTTCAAGTTCGAAGACGAGTCAAATCAGAAACAAAGCC
AAGATTGAAGCCAAGTGACTTCAGAAACTTTCTTACCATGTTTGTTGTTTTTGTGATT
TTTGCCTTTTGCTGGGCACCTCTAAACTTCATTGGACTGGCTGTAGCCATTGATCCT
ACGGAAATGGCACCAAAAGTTCCTGAATGGCTATTCATTATAAGTTACTTAATGGCC
TATTTCAACAGCTGCCTTAATGCAAT

3) Mel-1C

5'>>>>>>>>>>>>>>>>>>>>>>>>

GCTGCTATCTCTGCCTGACCTGGATACTCACAGTGGTGGCAATTGTGCCAAACTTC
TTTGTTGGCTCCTTGCAGTACGACCCCCGGATTTACTCCTGCACCTTTGCCCAGAC
GGTGAGCACGTCGTACACCATCACGGTGGTGGTGGTTCACTTCATCGTCCCGCTC
TCCGTCGTGACGTTTTGCTACCTACGGATCTGGATTTTGGTGATTCAAGTCAAA

<<<<<<<<<<<<<<<<<<<<<<<<'5

CACCGGGTGAGACAAGACTGCAAGCAGAAACTCAGGGCAGCTGACACCCGAAACT
TCTTGACTATGTTTGTGGTTTTTGTCCTTTTTGCTGTGTGCTGGGGACCATTAAACT
TTATTGGCCTTGCTGTTTCAATTAATCCTTCAAAAGTGCAGCCACACATTCCAGAAT
GGCTTTTTGTCCTGAGCA

Figure 2.2.8.a. Partial sequences of the three cloned melatonin receptors, and their primer pair sequences (red) optimised for rhythmicity experiments.

2.29 Semi-quantitative analysis of RT-PCR for melatonin receptors Mel-1A, Mel-1B and Mel-1C

RT-PCR's were set up according to the optimised receptor primer pairs and conditions for each of the three receptor (Table 2.2.8.a and Figure 2.2.8.a), for each tissue and time-point. The PCR products were separated on an 8% polyacrylamide gel and stained with SYBR green I (Sigma Aldrich). To correct for gel staining variation, the optical densities of each sample were compared to a 50bp DNA ladder (Fermentas) with known marker concentrations (Figure 2.2.11.a). The raw data was plotted as absolute levels in graphs. The resulting data for each gene/time-point/tissue were then normalised to TATA-box binding protein (TBP) values for the same tissue and time-point and to the 24 hour mean value for each gene and plotted as relative gene expression, as described by (Helfer, *et al.*, 2006).

2.2.10 Gel electrophoresis

2.2.10 .1 Agarose gel electrophoresis

Agarose gels were used in the cloning experiments and RNA gels of this thesis. Visualisation of nucleic acid samples was accomplished by electrophoresis in 1x TAE buffer. An estimation of size was achieved by electrophoresis of an aliquot of 1kb ladder (Invitrogen). Agarose gels were constructed, depending on the size of nucleic acid of interest, between 1% (w/v) for a large molecular weight to 2% (w/v) for visualisation nucleic acids <300bp. Gels were poured

and electrophoresed using Biorad electrophoresis kits. PCR samples were mixed with 6x loading dye (Fermentas) and compared to either or both 1Kb DNA ladder (Fermentas) and GeneRuler^{TM} 100bp DNA ladder (Fermentas). For receptor cloning 1-2% agarose gels, and visualised by staining with SYBER green I (Sigma Aldrich) for 15mins.

2.2.10.1.1 RNA gels

RNA gels were performed on the peripheral tissue RNA samples to test the quality of the RNA extracted from the tissue sample. The RNA samples (5µg/5µl)) were denatured with 2x loading dye (5µl; Fermentas) at 75°C for 10 minutes, and the ladder was treated in the same manner. After denaturisation the samples were run on 1% agarose gel (made with 1xTAE). To allow visualisation of RNA extractions; samples were run on 1% agarose gels, post electrophoresis gels were stained for 30 minutes with ethidium bromide.

2.2.10.2 Polyacrylamide gel electrophoresis

Polyacrylamide gels were used in the optimising and melatonin receptor gene rhythmicity experiments. Polyacrylamide gels were used because they give much cleaner bands and can highlight DNA fragments differing by a single base-pair in length, therefore highlight the difference in rhythmicity of the genes over 24 hours in these studies with more accuracy. 8% Polyacrylamide gels were set up as per Appendix I – Section 1.1. mRNA samples were

mixed with 10x loading dye with Bromphenol Blue and 1x TE solution, prior to loading, and compared against GeneRuler™ 50bp DNA ladder (Fermentas SM0371; Figure 2.2.11.a). Gels were run in 1x TBE according to the manufacturer's instructions.

2.2.11 Visualisation and Analysis

Gels were stained with SYBER green I (Sigma Aldrich) and visualised with Gel Doc Imager (Gel Doc Imaging System; BioRad, Hercules, CA, USA). The amplified PCR products were quantified with Gel Doc Imaging System in combination with Quantity One imaging analysing software (BioRad), comparing the known fragment (bp) sizes and DNA quantity band of the DNA ladder to the PCR bands (Figure 2.2.11.a).

The rhythmicity of each melatonin receptor gene expression was analysed by one-way factorial analysis of variance (ANOVA) using Tukey's honest significant difference post hoc test (Tukey, 1959). Polynomial fourth order non-linear regression was fitted with GraphPad Prism software (GraphPad, San Diego, CA, USA) to compare expression.

	Fragment, bp	%	DNA quantity in band, (ng)
1	1031	14.6	146
2	900	12.8	128
3	800	11.4	114
4	700	10	100
5	600	8.5	85
6	**500**	**14.2**	**142**
7	400	5.7	57
8	300	4.3	43
9	250	3.6	36
10	**200**	**5.7**	**57**
11	150	2.1	21
12	**100**	**4.3**	**43**
13	50	2.8	28
	TOTAL	100	1000

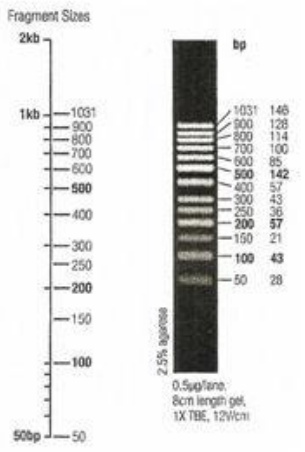

Figure 2.2.11.a. GeneRuler™ 50bp DNA Ladder and DNA quantity used to compare and analyse RT-PCR products for Melatonin receptor gene analysis.

2.3 Immunofluorescent procedures

For all solution and mediums used in this chapter see Appendix I – Section 1.1.1.

2.3.1 Tissue sampling, perfusion and processing of the brains

The birds were killed by dislocation of the neck and then decapitated at the ZT stated in Table 2.3.1.a and Table 2.3.1.b. The brains were dissected as quickly as possible (<5 minutes) after culling and transferred into a *in vitro* perfusion system filled with Hanks balanced salt solution (Sigma Aldrich).

The brains were perfused for 10 minutes with formalin solution 10% neutral buffered (Sigma Aldrich). Post *in vitro* perfusion, the brains were fixed in formalin solution 10%, neutral buffered (Sigma Aldrich) for 8 hours at room temperature. The brains were then transferred to 30% sucrose solution (Sigma Aldrich,) at room temperature for ~16 hours or until the brain has sunk to the bottom of the solution.

The eyes (for melatonin receptor immunofluorescent experiments) were removed from the eye sockets and then the retina was removed by puncturing the eye and removing the cornea and lens. The vitreous liquid was removed from the eye cup and the retina was placed in formalin solution 10% neutral buffered (Sigma Aldrich) and fixed as stated for the brain samples.

After fixation, the brains and retinas were mounted onto the cryostat specimen holders, with the caudal part facing the holder and the rostral end facing away from the holder; and the

retinas as per Figure 2.3.2.a, using cryomatrix (Thermo-Shandon) and frozen in the cryostat at -28°C, wrapped in aluminium foil and stored at -80°C until used.

Experiment		Time points of tissue collections (ZT –Zeitgeber)	Number per ZT
Melatonin Receptor	**Retina**	ZT06 ZT18	6
	Hypothalamus	ZT06 ZT18	4
Vasotocin	**LD 12:12**	ZT01 ZT06 ZT11 ZT13 ZT18 ZT23	5
	dimLL	ZT23 CT01 CT06 CT11 CT13 CT18 CT23	5

Table 2.3.1.a. Dissection time points (ZT) of zebra finch brains for melatonin receptor and vasotocin immunofluorescent experiments. Brain samples were immediately placed into the perfusion system (Chapter 0) and then into 10% Formalin solution, neutral buffered (Sigma Aldrich). Light cycle LD 12:12; ZT0 is 9am with the onset of light, light phase is from ZT0-ZT12 (9am-9pm) and dark phase is from ZT12-ZT0 (9am-9pm). dimLL; CT00 is subjective lights on, CT12 is subjective lights off; CT00-CT12 is subjective day and CT12-CT00 is subjective night.

Experiment	**Early Dark period**				**Late dark Period**			
Light pulse	No light pulse		ZT14-Z15		No light pulse		ZT21-22	
ZT (Collection time)	**ZT15** (12am)	**ZT15.5** (12.30am)	**ZT15** (12am)	**ZT15.5** (12.30am)	**ZT22** (7am)	**ZT22.5** (7.30am)	**ZT22** (7am)	**ZT22.5** (7.30am)
N value	3	3	3	4	3	3	3	4

Table 2.3.1.b. Dissection times for zebra finch brains for c-fos immunofluorescent experiments. Brain samples were immediately placed into the perfusion system (Chapter 0) and then into 10% Formalin solution, neutral buffered (Sigma Aldrich). n=3 per Zeitgeber time (ZT). RT= Room temperature. Light cycle LD 12:12; ZT0 is 9am with the onset of light, light phase is from ZT0-ZT12 (9am-9pm) and dark phase is from ZT12-ZT0 (9am-9pm).

2.3.1 Sectioning Tissues

The fixed and mounted brains were coronally sectioned with the cryostat (Bright, OTF500) at -15°C, taking sections 20μm thick that were thaw mounted onto superfrost plus slides (Roth) and dried at room temperature for two hours. Serial sections were taken from rostral to caudal through the hypothalamic region cut at 20μm thick (Figure 2.3.2.a-A). Eye cups were mounted (with the cornea, lens and iris removed) and serial transverse sections cut at 25μm thick (Figure 2.3.2.a-B) and dried at room temperature for two hours, before immunofluorescent procedures occurred.

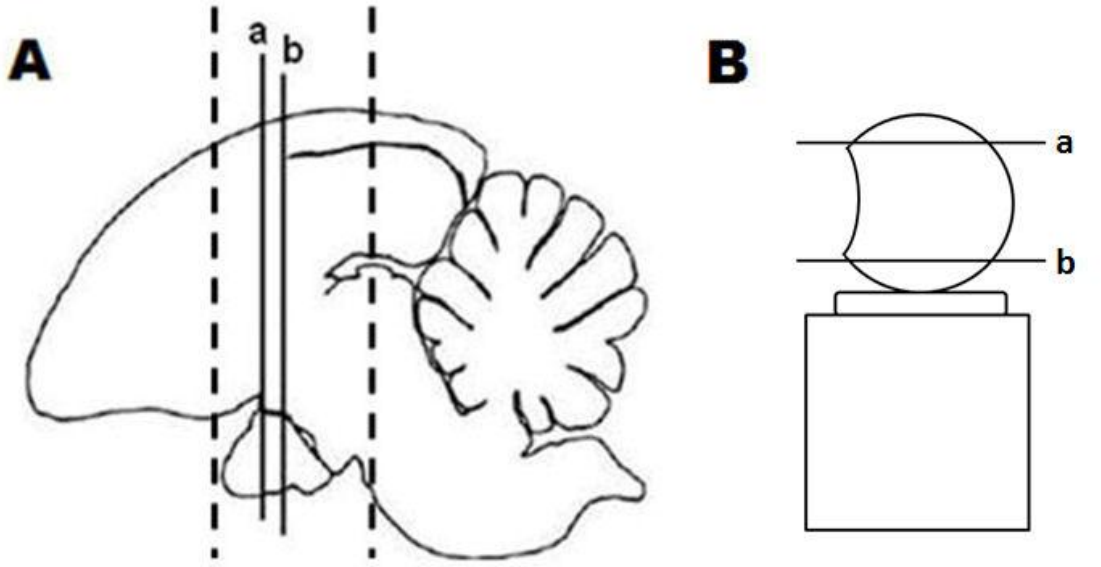

Figure 2.3.2.a. Slicing of the hypothalamus (A) and retinal (B) tissues for immunofluorescent experiments. A – Serial coronal sections of the hypothalamus were taken from zebra finch brain from rostral (a) to caudal (b), the brain is cut (along the dashed lines) to remove either end of the brain around the hypothalamus and mounted so the caudal area is closest to the top of the mount. B – Shows the eyecup as mounted onto the cryostat holder, with serial sections taken in the transverse plane from superior (a) to inferior (b).

2.3.3 Immunofluorescent protocol

Slides were mounted onto coverplate chambers (Shandon Coverplate, Figure 2.3.3.a) with 400µl of phosphate balanced saline (PBS; Sigma Aldrich), and placed into the coverplate/slide rack (Shandon Sequenza). 200µl of PBS was then applied to each coverplate chamber. The sections were incubated at room temperature for 20 minutes in CAS-block (Invitrogen, Zymed), which is a universal blocking agent for reducing nonspecific background staining in immunolabelling techniques. Primary antibody solution diluted as according to Table 2.3.3.a, 300µl, was applied to each slide chamber (apart from the antibody control sections), and placed in the dark overnight (18 hours) at room temperature. Control sections were incubated overnight in 300µl of antibody diluent (Zymed) and then treated the same as experimental sections.

Sections had three washes of 200µl PBS and incubated at room temperature for five minutes. 300µl of Secondary antibody solution (Table 2.3.3.b) was applied to each chamber, and incubated at room temperature in the dark for 3 hours. These steps were carried out in reduced lighting (in the dark) to avoid fading the fluorescent dye attached to the secondary antibody.

After the secondary antibody incubation, slides were washed with PBS for five minutes. Hoechst FluoroPure (Invitrogen) a nuclear staining protein, 200µl was applied to each chamber for five minutes (Table 2.3.3.c). The slides were then rinsed in PBS for five minutes. The slides mounted in fluorescent mounting medium (DAKO), cover slipped (Thermo shandon) and transferred to a 4°C fridge in the dark to allow the mounting medium to set before viewing under a fluorescent microscope (Chapter 0).

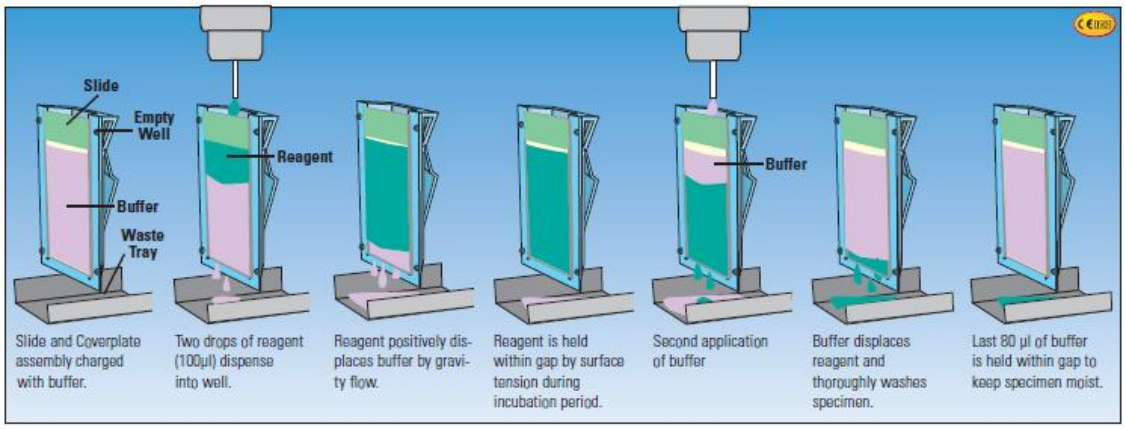

Figure 2.3.3.a. The immunofluorescent step by step coverplate system. The Coverplate is a plastic device that fits over a standard microscope slide allowing specimens to be immunostained with a minimum amount of reagent. The Coverplate system allows liquids to fill the gap between the coverplate and slide. The liquid stays in the gap by capillary attraction until the next reagent is dispensed into the well. Its pressure then causes the previous reagent to be displaced by gravity flow (Thermo Shandon datasheet).

Antibody	Host species	Monoclonal/ polyclonal	Supplier	Cat no.	Concentration	Dilution*	Incubation	Secondary Antibody
Anti-NeuN	Mouse	Monoclonal IgG	Chemicon Internation	MAB377	1.0 mg/ml	1:500	Over night at room temp.	Cy3 anti-mouse IgG
Anti-AVP	Rabbit	Polyclonal IgG	AbD serotec	9536-004	5.0 mg/ml	1:500	Over night at room temp	Cy3 anti-rabbit IgG
Anti-Mel1a	Goat	Polyclonal (Rada & Wiechmann, 2006)	Donated by Prof. Jody Summers Rada, University of Oklahoma Health Sciences Center, Oklahoma City.		3.5 mg/ml	1:200	Over night at room temp	Cy3 anti-Goat IgG
Anti-Mel1b	Rabbit				0.2 mg/ml	1:100	Over night at room temp	Cy3 anti-rabbit IgG
Anti-Mel1c	Chicken				0.2 mg/ml	1:100	Over night at room temp	Cy3 anti-Chicken IgY
Anti-c-fos	Rabbit Goat	Polyclonal	Santa Cruz	SC-253 SC-253-G	200µg/ml (0.2mg/ml)	1:200	Over night at room temp	Cy3 anti-rabbit IgG Cy3 anti-Goat IgG

Table 2.3.3.a. List of all primary antibodies, and specifications for each, used in immunofluorescent experiments. Host is what the primary antibody was raised in; the secondary antibody needs to be raised in anti this species. * All dilutions made with antibody diluent (Invitogen, Zymed), unless stated otherwise.

Antibody	Product	Supplier	Cat no.	Concentration	Dilution*	Incubation	Amax Emax	Microscope filter
Cy3-conjugated goat anti-mouse IgG (H+L)	AffiniPure F(ab') 2 Fragment	Jackson ImmunoResearch	115-166-003	1.5mg/ml	1:100	3h room temp in the dark	550nm 570nm	CY3 Excitation Filter, CWL = 565 nm, BW = 24 nm
Cy3-conjugated goat anti-rabbit IgG (H+L)	AffiniPure F(ab') 2 Fragment	Jackson ImmunoResearch	111-166-003	1.5mg/ml	1:100	3h room temp in the dark	550nm 570nm	
Cy3-conjugated rabbit anti-Goat IgG (H+L)	AffiniPure F(ab') 2 Fragment	Jackson ImmunoResearch	305-166-003	1.5mg/ml	1:100	3h room temp in the dark	550nm 570nm	
Cy3-conjugated rabbit anti-Chicken IgY (IG) (H+L)	AffiniPure F(ab') 2 Fragment	Jackson ImmunoResearch	303-166-003	1.5mg/ml	1:100	3h room temp in the dark	550nm 570nm	

Table 2.3.3.b. List of all secondary antibodies, and specifications for each, used in immunofluorescent experiments. * All dilutions made with antibody diluent (Invitogen, Zymed), unless stated otherwise. DDW= double distilled water.

Stain	Supplier	Cat no.	Concentration	Dilution	Incubation	Amax Emax	Filter
Hoechst (bisBenzimide H33258) nuclear staining protein	Sigma	B2883	10mg/ml	1:1000 (DDW)	5min room temp in the dark	356nm 465nm	UV

Table 2.3.3.c. List of additional stains, and specifications for each, used in immunofluorescent experiments. DDW= double distilled water.

2.3.4 Immunofluorescent stains

All antibodies underwent pre-absorption tests before immunofluorescent experiments occurred.

2.3.4.1 Melatonin receptors *MEL-1A, MEL-1B* and *MEL-1C*

Melatonin receptor antibodies were donated by Dr Jody Summer Rada and Professor Allan Wiechmann (The University of Oklahoma Health Sciences Centre, 1100 N. Lindsay, Oklahoma City, OK 73104). The antibodies were applied as stated above in Chapter 0, at ZT6 and ZT18; these ZT times correspond to the data found in Chapter 4, mRNA levels of the receptors showing the peak levels during the second half of the dark period and lowest levels during mid-light phase.

2.3.4.2 C-FOS

Zebra finch were synchronised to 12:12 LD conditions for two weeks. After two weeks synchronisation, a light exposure was emitted into the aviary in the early dark phase and in the late dark phase. One group of zebra finches were killed immediately after the 60 minute light

exposure, therefore 60 minutes after the onset of light, and one group was killed 90 minutes after the onset of light exposure, in order to get the full coverage of c-fos expression. Controls for this experiment were 1) antibody control – no primary antibody added during immunofluorescent protocol, 2) animal control – animals culled at the same time points as the experimental birds, but not subjected to the light pulse.

2.3.4.3 Arginine-vasotocin (AVT)

Arginine-vasotocin is a nine amino acid peptide secreted from the posterior pituitary in response to reductions in plasma volume and increases is plasma osmolarity. Its release triggers water reabsorption due to the insertion of aquaporins in the membranes of kidney tubules which transport solute-free water through tubular cells and back into the blood (AVP datasheet; AbD serotec).

2.3.4.3.1 Zebra finch

Immunohistochemistry was applied as stated above (Chapter 0) for AVT on zebra finches places under either LD (12:12 light/dark cycle) or dimLL (constant darkness) conditions.

LD rhythm: zebra finch were kept in the synchronisation aviaries for two weeks, before culling at ZT 1, 6 , 11, 13, 18 and 23 (n=5-6 per time point) for a 24 hour rhythmicity under 12:12 LD conditions.

dimLL rhythm: zebra finches were kept in the synchronisation aviaries for two weeks, before lights were switched off and put into dimLL conditions. Zebra finches were kept in dimLL conditions and culled in the first dimLL cycle; at the same time-points as the LD rhythm birds (ZT23, and CT 01, 06, 11, 13, 18 and 23).

2.3.4.3.2 Chicken and Japanese quail

The chicken and Japanese quails were used as a species comparison; to see if there is a species variation of AVP expression. Chicken and Japanese quails were kept in LD12:12 conditions from hatching and for two weeks to ensure synchronisation, before being culled at ZT1 (n=6 per species); perfused and processed by Dr. Linda Shaw, University of Birmingham. Immunofluorescent labels were applied as stated above for AVT on serial consecutive sections at ZT01.

2.3.4.4 Hoechst staining (Bisbenzimide H 33258)

Hoechst staining was applied for neuro-anatomical location through the hypothalamus, and for checking the perfusion and fixation of the brain. Hoechst (or NUNC) staining is a fluorescent staining that highlights the DNA present in any cells, it is therefore a good indicator for how well the tissue is perfused and fixed. The Hoechst stain is visible under purple/blue ultraviolet light at around 350nm, and emits at a maximum of 461nm. The positive cell staining appears blue against a black background. The staining was visualized and captured in the same manner as stated in Chapter 0 (Hoechst datasheet; Sigma Aldrich).

2.3.5 Microscopy and analysis

An Axioskop microscope (Zeiss, Germany) equipped with a mercury lamp (Zeiss, Germany). Metamorph Imaging software (Universal imaging, USA) with a black and white camera (Visitron, Germany) was used to record the images, and Corel Paint Shop Pro Photo X2 software was used for editing images. Cell counts were plotted and analysed using GraphPad Prism 5 software (GraphPad, San Diego, CA, USA) to compare expression. Fluorescent images were converted to the negative image by Corel Paint Shop Pro Photo X2 version 12.01, for clearer visualisation of staining.

RESULT CHAPTERS

HYPOTHALAMIC
INPUT MECHANISMS

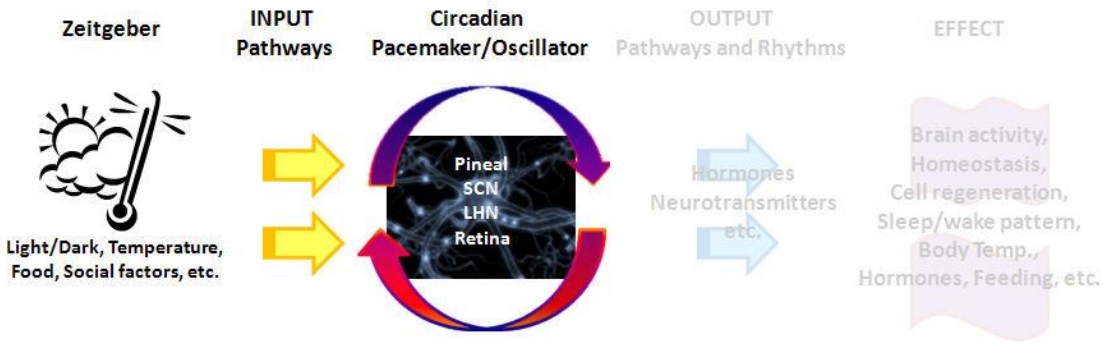

CHAPTER 3

Molecular methodology validation: RNA analysis; cloning, amplification and identification of melatonin receptors; optimisation of RT-PCR primer conditions

Data from this chapter was submitted to Chronobiology International April 2011, the manuscript was accepted in October 2011 and due for publication February 2012, see Appendix II for manuscript.

CHAPTER THREE - MOLECULAR METHODOLOGY VALIDATION: RNA ANALYSIS; CLONING, AMPLIFICATION AND IDENTIFICATION OF MELATONIN RECEPTORS; OPTIMISATION OF RT-PCR PRIMER CONDITIONS.

3.1 Introduction

Two major input mechanisms to the avian hypothalamic circadian oscillators are light and melatonin; conveying seasonal information needed for moulting, reproduction and migration, as well as daily information for sleep-wake cycle, feeding etc. The pineal and retinal melatonin inhibits the activity in the hypothalamus during the dark hours, and the hypothalamus inhibits the pineal melatonin production during the day in mammals (von Gall, *et al*., 2002) and birds (Karaganis, *et al*., 2009). Light information can be received by photoreceptors found in the retina (mammals and birds), pineal gland (non-mammalian systems) and deep brain (non-mammalian systems) receptors.

The biological effects of melatonin are produced through the activation of melatonin receptors (membrane (ML1) and nuclear (ML2)), while other effects are due to its role as a pervasive and extremely powerful antioxidant with a particular role in the protection of nuclear and mitochondrial DNA (Reiter, *et al*., 2003; Tan, *et al*., 2009). Nuclear receptors, such as retinoic-acid-receptor and retinoid-x-receptors, have been shown to be associated with melatonin signalling and act as transcription factors to directly regulate gene expression (Dubocovich, 1995). These receptors have a broad distribution in the nucleus and directly influence gene expression through activation by melatonin (Dubocovich, 1995; Rada and

Wiechmann, 2006). Melatonin has also been shown to have antioxidant roles, by scavenging free radicals, stimulating the activity of other antioxidant enzymes and enhancing mitochondrial oxidative phosphorylation (Rada and Wiechmann, 2006). In 1994, the first melatonin membrane receptor was cloned from *Xenopus laevis* immortalized melanophore, which was sensitive to guanine nucleotides and activation lead to an inhibition of adenylyl cyclase through a pertussis toxin-sensitive mechanism (Ebisawa, *et al.*, 1994).

There are now three known melatonin membrane receptors (Mel-1A, Mel-B and Mel-1C; Table 3.1.a) which comprise their own subtype within the guanine nucleotide binding proteins (G-protein-coupled) receptor superfamily (Figure 3.1.a; Ebisawa, *et al.*, 1994; Reppert, 1997). Zebra finch *Mel-1A*, *Mel-1B* and *Mel-1C* receptors are encoded by 353, 361 and 155 amino acids respectively. These receptors have a general structural motif of 7 hydrophobic transmembrane spanning α-helical domains, with the amino terminus located extracellularly and the carboxyl terminus found on the intracellular region (Figure 3.1.a; Ebisawa, *et al.*, 1994; Reppert, 1997). Transmembrane helices 3, 6 and 7 have been linked to the specific binding for melatonin (Witt-Enderby, *et al.*, 2003). The melatonin membrane receptors appear to form a unique group from the other groups of receptors, which comprise the prototypic G-protein-coupled receptor family, due to their distinct molecular structure and chromosomal localization (Reppert, *et al.*, 1994; Reppert, *et al.*, 1995a; Reppert, *et al.*, 1995b; Reppert, *et al.*, 1996).

IUPHAR name	Name in Thesis	Name Published	Species	Reference example
MT1	**Mel-1A**	MLR	Chick	Liu, *et al.*, 1995
		CKA	Chick	Reppert, *et al.*, 1995
		Mel-1a	Hamster	Gauer, *et al.*, 1998
		Mel1A Mel1a	Japanese Quail	Yasuo, *et al.*, 2002
			Chick	Natesan and Cassone, 2002
			Xenopus	Weichmann, 2003a-c
			Zebra finch	Jansen, *et al.*, 2005
			Human	Reppert, *et al.*, 1994
		MT1	Human	Niles, *et al.*, 1999
			Golden rabbit fish	Parkfield, 2007
			Rat	Audinot, *et al.*, 2008
			Mouse	Imbesi, *et al.*, 2009
		ML1a/ ML_{1A}	Mammal	Sugden, 1993
		Mel_{1a}	Chick	Rada and Wiechmann, 2006
MT2	**Mel-1B**	Mel1B Mel1b	Chick	Natesan and Cassone, 2002
			Zebra finch	Jansen, *et al.*, 2005
			Reef fish	Park, *et al.*, 2007
			Human	Reppert, *et al.*, 1995b
		MT2	Human	Niles, *et al.*, 1999
			Rat	Audinot, *et al.*, 2008
			Mouse	Imbesi, *et al.*, 2009
		MTNR1B	Rat	Lyssenku, *et al.*, 2009
		ML1B/ML_{1B}	Mammal	Sugden, 1993
		Mel_{1b}	Chick	Rada and Wiechmann, 2006
-	**Mel-1C**	CKB	Chick	Reppert, *et al.*, 1995b
		Mel1c	Japanese Quail	Yasuo, *et al.*, 2002
			Chick	Natesan and Cassone, 2002
			Chick	Weichmann, 2003a-c
			Zebra finch	Jansen, *et al.*, 2005
		Mel_{1c}	Chick	Rada and Wiechmann, 2006

Table 3.1.a. Nomaculture of the three membrane melatonin receptors, found to date, between different species and used in this thesis. Melatonin receptors named by the IUPHAR Committee on Receptor Nomenclature and Drug Classification are named and classified on the basis of operational and structural criteria. There is no Mel-1C classification as this receptor is not found in the mammalian system therefore melatonin receptors are referred to as Mel-1A, Mel-1B and Mel-1C in this thesis.

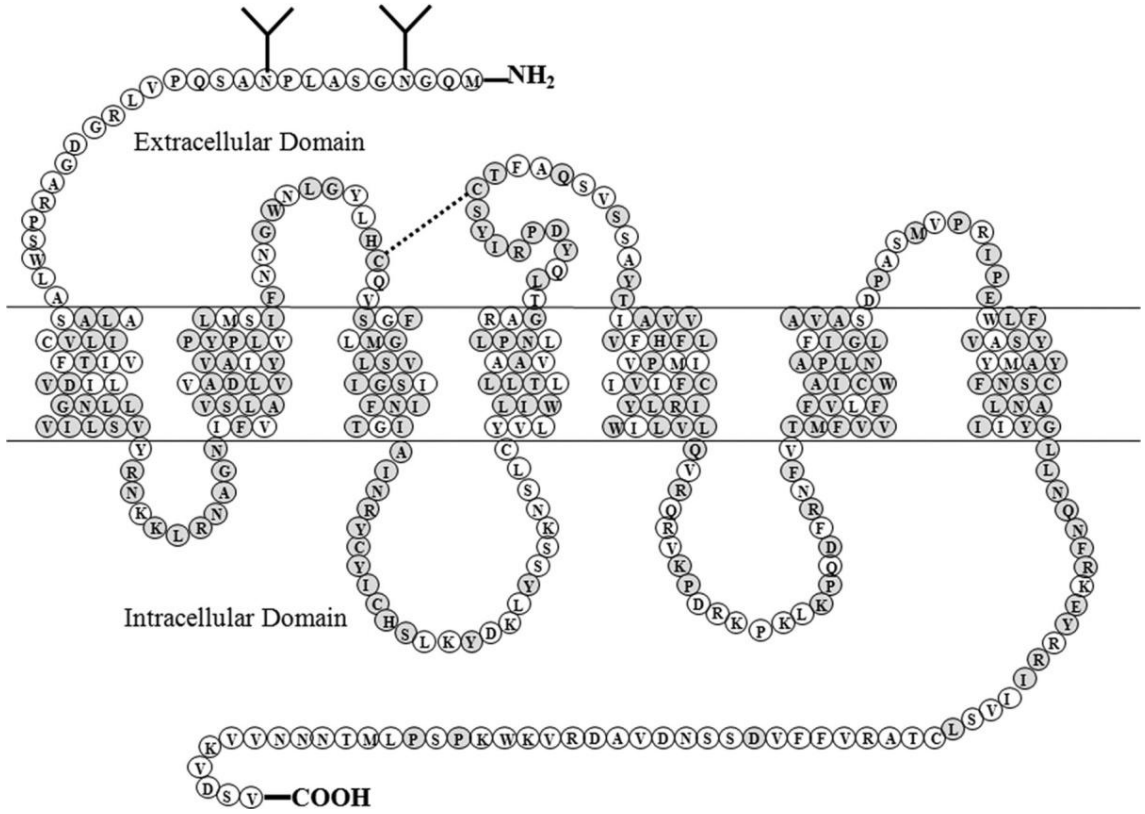

Figure 3.1.a. Membrane topology of the human melatonin receptor 1 (hMT_1) showing amino acids conserved in the hMT_2 receptor. Gray circles denote amino acids identical in the hMT_1 and hMT_2 melatonin receptors. The two glycosylation sites on the hMT_1 receptor are denoted (Y) in the N terminus (Dubocovich, *et al*., 2010).

The main differences between the membrane receptor types themselves are their kinetic and pharmacological properties for melatonin and its agonists: Mel-1A is a high affinity binding receptor and this affinity increases with temperature, whereas the Mel-1B receptor is a low affinity for binding and its affinity decreases with temperature (Dubocovich, 1995). G_i appears to be a common signalling pathway for all three membrane receptors (Reppert, *et al.*, 1995a-b). All three receptors have been linked to interact with G_{i2}, G_{i3} and $G_{q/ii}$. G_i causes the inhibition of intracellular cAMP levels; in the mammalian pituitary, SCN and cerebral arteries (Figure 3.1.b.; Capsoni, *et al*., 1994; Morgan, *et al*., 1994). This decrease in cAMP levels then caused a reduction in the protein kinase A (PKA) activity and decreases cAMP response element-binding (CREB) phosphorylation (Brydon, *et al*., 1999; Dubocovich, *et al*., 2010; Reppert, 1997; Jockers, 1997). Mel-1A receptor also couples to $G_{q/ii}$ protein which causes the mobilization of calcium from intracellular stores via phospholipase C (PLC) (Brydon, *et al.*, 1999). Mel-1A also activates the potassium inwardly-rectifying channel Kir3.1/3.1 which stimulates the PLC modulation of protein kinase C (PKC) and phospholipase A via $G_{\beta\gamma}$ during $G_{i/o}$ activation (Brydon, *et al.*, 1999). Activation of Mel-1A receptor has also been shown to inhibit the induction of c-fos and jun-B mRNA and c-Fos translation (Witt-Enderby, *et al*., 2003). Mel-1B also has shown to inhibit intracellular levels cGMP production stimulates JNK and phosphinositide turnover (Brydon, *et al*., 1999).

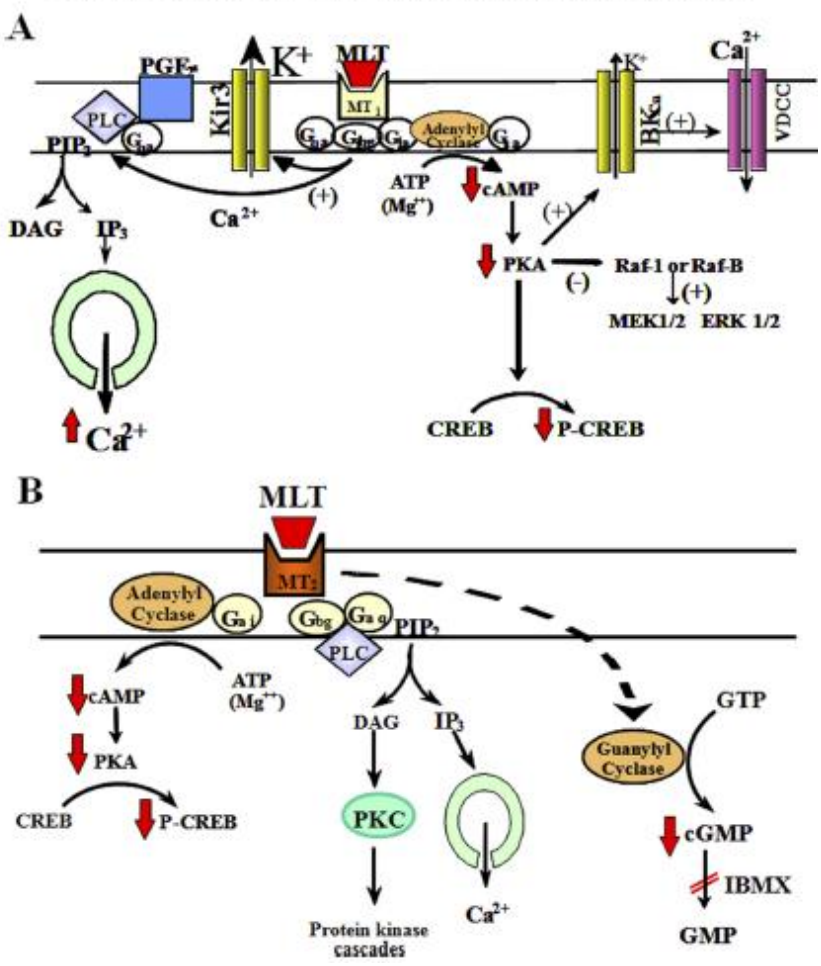

Figure 3.1.b. Mammalian Mel-1A and Mel-1B melatonin receptor signalling. A, melatonin (MLT) signals through activation of the Mel-1A (MT1) receptor via two parallel pathwaysmediated by the α-subunit (i.e., inhibition of cAMP formation) and the βγ-subunits [i.e., potentiation of phosphoinositide turnover stimulated by a Gq-coupled receptor (R)] of Gi. B, signaling pathways coupled to Mel-1B (MT2) melatonin receptor activation. Melatonin-mediated phase shifts of circadian rhythms through Mel-1B (MT2) receptors are mediated by PKC activation (the mechanism leading to PKC activation remains putative, however). DAG, diacylglycerol; PKA, protein kinase A; R, Gq-coupled receptor (i.e., prostaglandin F2 receptor FP and purinergic receptor P2Y) (Dubocovich, *et al*., 2010).

The chick Mel-1A (CKA) receptor is 80% identical to human Mel-1A and is the structural homolog of mammalian Mel-1A receptor (MT1; Reppert, *et al*., 1995b). Chick Mel-1C (CKB) receptor has an 80% homology to the Mel-1C found in *Xenopus*, and is 60% identical to the mammalian Mel-1A and Mel-1B receptors; though chick Mel-1C has a shorter (by 66 amino acids) carboxyl tail to that of the *Xenopus* Mel-1C (Reppert, *et al*., 1995b). Mel-1C of lower vertebrates has an Mel-1A-like (MT1-like) pharmacology and appears to be expressed in many brain areas (Sugden, *et al.*, 2004). Mel-1C shows a wide spread receptor distribution, suggesting that melatonin exerts temporal control over a broad range of physiological and behavioural events in birds (Reppert, *et al*., 1995b).

The Mel-1A receptor has been found in all avian species studied so far (chicken - (Reppert, *et al*., 1995b), zebra finch - (Jansen, *et al*., 2005)) and is found in mammals (e.g. humans – (Reppert, *et al*., 1994); rat - (Reppert, *et al.*, 1994) ; mice - (Slaugenhaupt, *et al*., 1995)), fish (e.g. Zebra fish - (Shang and Zhdanova, 2007); gold fish - (Ikegami, *et al*., 2009)) and frogs (e.g. *Xenopus laevis* - (Ebisawa, *et al*., 1994)). To date the Mel-1B receptor has not been found in the house sparrow but has been found and published in the chicken (Rada and Wiechmann, 2006; Sundaresan, *et al.*, 2009) and zebra finch (Jansen, *et al*., 2005). The Mel-1B receptor is also found in mammals (e.g. humans - (Reppert, *et al*., 1995b); rat – (Musshoff, *et al.*, 2002)), in fish (e.g. Zebra fish - (Shang and Zhdanova, 2007)); gold fish - (Ikegami, *et al*., 2009)) and amphibians (e.g. Xenopus laevis - (Ebisawa, *et al*., 1994)). The Mel-1C receptor has not been found in any mammalian species so far but has been described in fish (e.g. Zebra fish - (Shang and Zhdanova, 2007); gold fish - (Ikegami, *et al*., 2009)) and frogs (e.g. Xenopus laevis - (Ebisawa, *et al*., 1994)), as well as avian species (e.g. chicken – (Sundaresan, *et al.*, 2009); zebra finch - (Jansen, *et al*., 2005); house sparrow – unpublished

NCBI locus AY743658)). Over the years and in different species (both mammals and non-mammalian vertebrates) the receptors have been called numerous names (Table 3.1.a.).

So far, the Mel-1C receptor has only been identified in non-mammalian species such as frogs and birds (Reppert, 1997), whether mammals have evolved or adapted so the function of the Mel-1C receptor is no longer needed is still unknown. Whether the loss of photoreceptors and oscillatory function of the pineal gland in mammals has to do with the absence of this receptor in mammals is yet to be determined. Mammals have one dominant circadian oscillator which controls the pineal synthesis and secretion of nocturnal melatonin, and have photoreceptors only in the retina; though in the mammalian retina there has been an evolutionary loss of two cone classes (shortwave sensitive (SWS) and middle-wave sensitive (MWS); Bellingham, et al., 2003) and opsins which are found in the non-mammalian vertebrates (birds, fish, etc.; Bellingham, *et al*., 2003). In the early evolutionary history mammals went through what has been called elsewhere a "nocturnal bottleneck", which caused the nocturnal activity in small mammals due to predator's activity during the day; survival of the fittest (Menaker, *et al*., 1997). The loss of the two receptors might be because of this.

Recently a receptor was cloned from the human pituitary gland, this receptor was known as G protein-coupled orphan receptor 50 (GRP50) (Reppert, *et al*., 1996). GRP50 has been suggested to be the mammalian ortholog of the Mel-1C receptor found in non-mammalian species (Dufourny, *et al*., 2008). This GPR50 receptor has been shown to heterodimerize with the Mel-1A and Mel-1B receptors. However the GPR50 receptor cannot bind melatonin itself, but suppresses the Mel-1A receptors affinity to bind melatonin (Levoye, *et al*., 2006). Dufourny suggests a theory that the Mel-1C receptor rapidly evolved into the GPR50 receptor

in mammals by mutation of several critical amino acids and the addition of the C-terminus sequence; as both the GPR50 and Mel-1C genes are surrounded by the same genes, in syntenic genomic regions of the chicken, opossum and mammals (Dufourny, *et al*., 2008).

So far there is very little information on the rhythms and location of these receptors in any avian species. One major aspect of the thesis investigates this by looking at the expression of the three avian melatonin receptors in the zebra finch brain. In order to study and analyse the receptor rhythms I collected tissue samples from zebra finch, over a 24 hour period, and isolated the RNA from the samples. I cloned all three zebra finch receptors and compared their sequences to other published sequences. From the cloned sequences I designed primers for semi-quantitative reverse transcriptase polymerase chain reaction (RT-PCR) analysis of the receptor distribution. Each receptor primer pair was optimised to obtain PCR products in the linear phase of cycling in order to analyse the receptor mRNA content found in each tissue at each time-point. This chapter of the thesis shows the methodological stages leading up to the analysis of these melatonin receptors.

3.2 Results

3.2.1 RNA isolation and analysis

The RNA analysis of the extracted RNA samples from the dissected tissues is a vital step in the protocol; this was performed in order to assess whether the quality of the extracted RNA is good enough to use or if degradation or contamination had occurred.

In eukaryotic RNA samples, intact total RNA show sharp 28S and 18S rRNA bands. Partially degraded RNA has a smeared appearance and lacks the sharp rRNA bands. Completely degraded RNA appears as a very low molecular weight smear. Inclusion of RNA size markers on a gel allows for proper determination of the size of RNA or smears and also serves as a good control to ensure the gel was run properly.

3.2.2 Brain tissues

The brain tissue samples used in this thesis were analysed by the Bioanalysis (Agilent) and Nanodrop machines (Thermo scientific), allowing quantifying and calculating the RNA concentration for cDNA synthesis. Both give a concentration reading and a graph of the RNA (Figure 3.2.1.a). The Bioanalyzer also produces a gel image, from the ratio of the peak area of the ribosomal bands, for each sample, similar to an agarose/polyacrylamide image, an example of which is shown in Figure 3.2.1.a. for the tectum opticum samples.

3.2.1.2 Peripheral tissues

For the peripheral tissues used in this thesis, RNA gel and Nanodrop analysis was used to quantify and calculate the RNA concentration for cDNA synthesis. The Nanodrop was used to collect a concentration of the RNA sample and the RNA gel was used to visualise the RNA in order to assess the quality. An example of one of the RNA gels is shown in Figure 3.2.1.b, this gel shows lung and kidney samples.

The majority of the peripheral tissue RNA samples were uncontaminated and not degraded; any samples that were partly degraded or contaminated were discarded. A few of the samples showed a weak fluorescent band but when over-exposed, the samples showed two clear bands at 18s and 28s so the samples suggested low concentration of RNA. At each time point tissues samples of 6 birds were used. Before discarding any samples the gels were repeated to check for error.

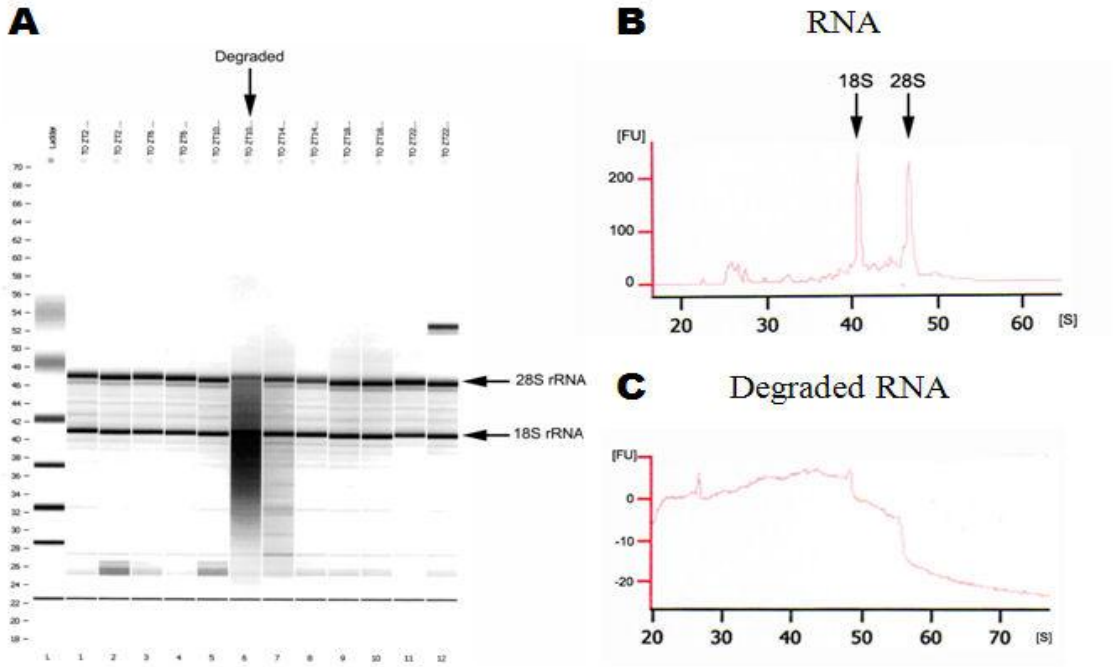

Figure 3.2.1.a. Output from the Bioanalysis program for tectum optium RNA isolation samples. The program puts the information from the samples into gel-like pictures. A, shows the gel images produced by the Bioanalyzer. B and C, show the graphs produced by the Bioanalyzer.

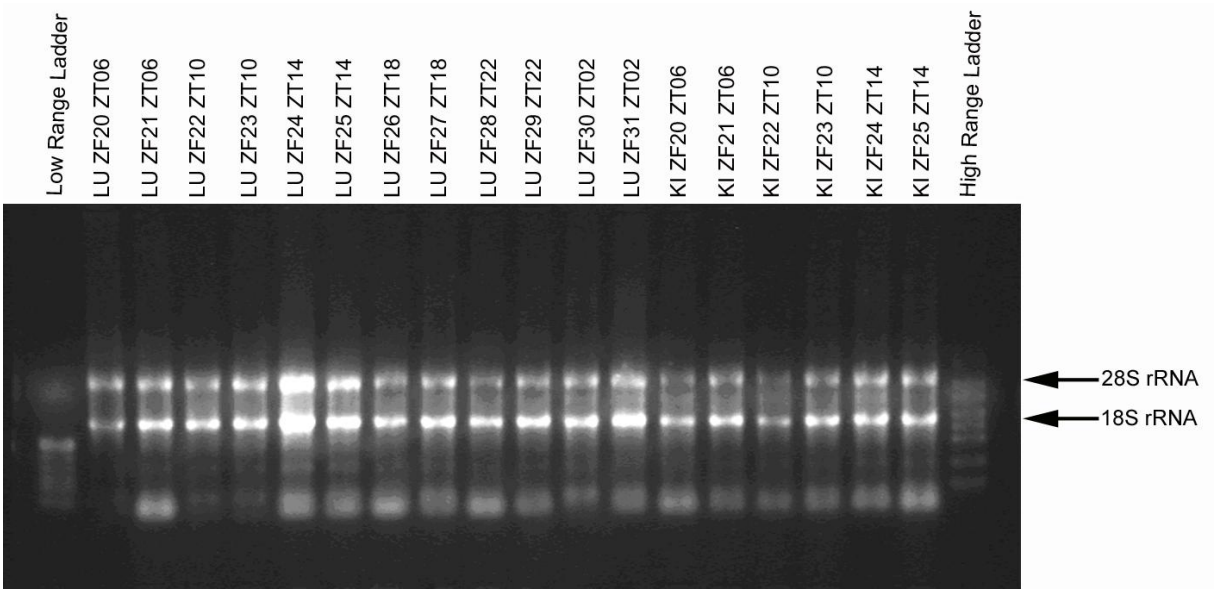

Figure 3.2.1.b. RNA gel for peripheral tissue samples from zebra finch. Abbreviations: LU lung, ZF animal number, KI kidney, ZT Zeitgeber time.

3.2.2 Cloning and DNA sequence analysis

I successfully cloned and sequenced partial cDNA for melatonin receptors 1A (494bp), 1B (265bp) and 1C (463bp) from the zebra finch brain tissues (Figure 3.2.2.a; Figure 3.2.2.b; Figure 3.2.2.c). The sequences were compared with other avian sequences using NCBI blast database and analysed accordingly showing 96% to 99% nucleotide sequence identities to previously published avian melatonin receptor sequences (Table 3.2.2.a).

The sequence analysis for melatonin receptor *Mel-1A* showed have 98% nucleotide sequence identity to the zebra finch Mel-1A (NM_001048257.1) receptor mRNA and 97% identity to the house sparrow *Mel-1A* receptor mRNA (AY155489.1) sequences already published on the database (Table 3.2.2.a). Thus only a few base-pair differences between this clone and the published data; grey blocks in Figure 3.2.2.a.

The *Mel-1B* receptor mRNA was highly identical to other *Mel-1B* receptors published in other avian species and virtually identical (99%) to the published sequence in the zebra finch (same species; DQ178665; Table 3.2.2.a). Unlike the other two receptors, there is no *Mel-1B* sequence available in the house sparrow; therefore in Figure 3.2.2.b the comparison is between the zebra finch and the chicken (EF197909.1).

The sequence for receptor *Mel-1C* showed to have 99% identity to the zebra finch *Mel-1C* receptor mRNA (AY803773.1) and 98% identity to the house sparrow *Mel-1C* receptor

mRNA sequences (AY743658.1) already published on the database; therefore only a few base pair difference between the clone and the published data (Figure 3.2.2.c). To date there has been no *Mel-1C* receptor identified or published in mammals, so I compared the identity to the human *GPR50* receptor, which had 67% identity, as these receptors have been shown to be orthologs (Dufourny, *et al*., 2008).

Cloned cDNA sequence	Melatonin Receptor (GenBank accession number)	Species	Percentage Identity
Mel-1A Receptor	Mel-1A receptor mRNA; complete cds (NM_001048257.1)	*Taeniopygia guttata* (zebra finch)	98%
	Mel-1A receptor mRNA; partial cds (AY155489.1)	*Passer domesticus* (house sparrow)	97%
	Mel-1A melatonin receptor mRNA, complete cds (GGU31820)	*Gallus gallus* (chicken)	89%
	Melatonin receptor 1A (MTNR1A) mRNA, complete cds (EU432127.1)	*Homo sapien* (human)	76%
Mel-1B Receptor	Mel-1B melatonin receptor mRNA, complete cds (DQ178665)	*Taeniopygia guttata* (zebra finch)	99%
	Mel-1B melatonin receptor mRNA, partial cds (DQ178663.1)	*Sylvia atricapilla* (blackcap)	96%
	Melatonin receptor 1B mRNA, partial cds (EF197909.1)	*Gallus gallus* (chicken)	90%
	Melatonin 1B receptor, complete cds (AB033598.2)	*Homo sapien* (human)	74%
Mel-1C Receptor	Mel-1C receptor mRNA; partial cds (AY803773.1)	*Taeniopygia guttata* (zebra finch)	99%
	Mel-1C receptor mRNA; partial cds (AY743658.1)	*Passer domesticus* (house sparrow)	98%
	Mel-1C melatonin receptor mRNA, complete cds (U31821.1)	*Gallus gallus* (chicken)	92%
	G protein-coupled receptor 50 (GPR50) mRNA (NM_004224)	*Homo sapien* (human)	67%

Table 3.2.2.a. Percentage nucleotide sequence identity of cloned melatonin receptors Mel-1A, Mel-1B and Mel-1C from zebra finch diencephalon tissue cDNA.

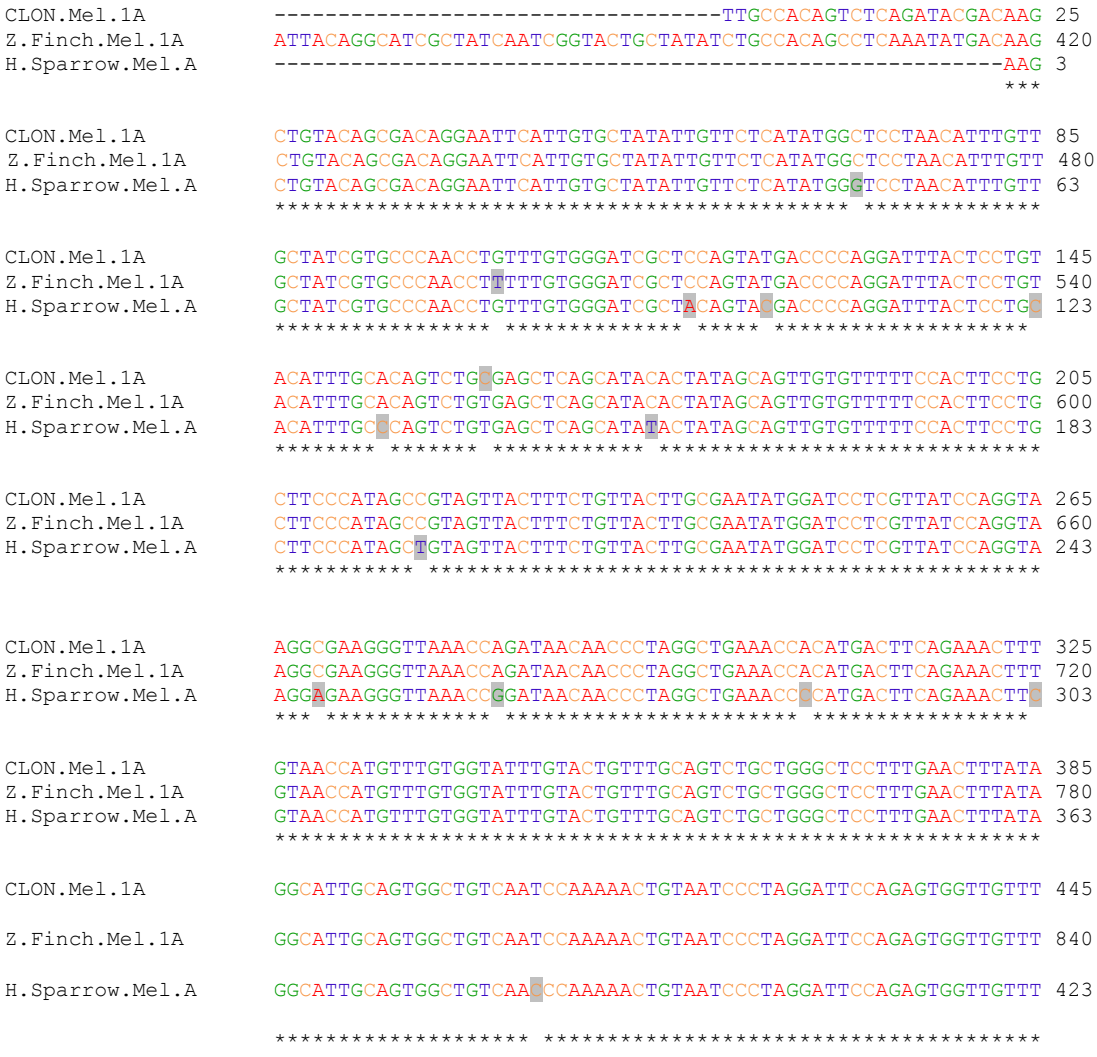

Figure 3.2.2.a. Alignment of nucleotide sequences for the *Mel-1A* receptor. The grey shaded residues highlight the nucleotide bases which differ from the consensus. CLON.Mel.1A indicates the sequence cloned in this thesis. ZebraFinch = zebra finch cDNA sequence NM_001048257, and H.Sparrow = house sparrow sequence AY155489 both from NCBI blast database.

Figure 3.2.2.b. Alignment of nucleotide sequences of the *Mel-1B* receptor. The grey shaded residues highlight the nucleotide bases which differ from the consensus. CLON.Mel.1B indicates the sequence cloned in this thesis. Z.Finch = zebra finch cDNA sequence DQ178665, and Chicken = chicken sequence EF197909.1 both from NCBI blast database.

Figure 3.2.2.c. Alignment of nucleotide sequences of the *Mel-1C* receptor. The grey shaded residues highlight the nucleotide bases which differ from the consensus. CLON.Mel.1C indicates the sequence cloned in this thesis. Z.Finch = zebra finch sequence AY803773, and H.Sparrow = house sparrow sequence AY743658 both from NCBI blast database.

3.2.2.1 Phylogenetic analysis

ClustalW2 phylogenetic analysis (Figure 3.2.2.d) revealed that all three receptors align with the relevant group of receptors, i.e. the melatonin receptor *Mel-1A* falls within the group of other avian *Mel-1A* receptors, the *Mel-1B* cloned sequence lies within the other *Mel-1B* sequences and the Mel-1C receptor cloned falls with the other avian *Mel-1C* receptors. The graph showed that the main branches of evolution for the *Mel-1B* and *Mel-1C* receptors are from the same division when *Mel-1A* and *GPR50* split from the other receptors. Only the fish *Mel-1B* and *Mel-1C* receptors seem to have split separately from the other receptors. For the full alignment of nucleotide sequences see Appendix I – Section 1.2.1.

Figure 3.2.2.d. (Page 105). Phylogenetic tree of melatonin receptors and melatonin-like receptor GPR50 in different species. Shows the relationships between families and species of the melatonin membrane receptors (see appendix for alignment of nucleotides). This graph was created using Clustal W2 program of EMBL website; based on the neighbour-joining method. Mel-1A, Mel-1B, and Mel-1C nucleotide sequences were cloned in this study. Other species nucleotides sequences were collected from the NCBI database: ZebraFinch.Mel1A = *Taeniopygia guttata* Mel-1A (DQ648558.1); HouseSparrow.Mel1A = *Passer domesticus* melatonin receptor-like protein MEL-1A mRNA (AY155489.1); Chicken.Mel1A = *Gallus gallus* Mel-1A (U31820.1); BlackCap.Mel1A = *Sylvia atricapilla* Mel-1A (DQ178662); Human.Mel1A = *Homo sapiens* melatonin receptor 1A (EU432127.1); Bovine.Mel1A = *Bos taurus* melatonin receptor 1A (BTU73327); BrownRat.Mel1A = *Rattus norvegicus* Mtnr1a (AB377274); Frog.Clone.X2.0 = *Xenopus laevis* clone X2.0 melatonin receptor mRNA (XLU31826); H.Mouse.Mel1A = *Mus musculus* melatonin receptor 1A (BC116900.1); Goldfish.Mel1A = *Carassius auratus* MT1 (AB481372); C.Salmon.Mel1A = *Oncorhynchus keta* melatonin-receptor 1A (AY356364); Sweetfish.Mel1A = *Plecoglossus altivelis* MT1 (AB481368); Z.Fish.Mel1A = *Danio rerio* melatonin receptor type 1B (NM_131395); Human.Mel1B = *Homo sapiens* melatonin receptor 1B (NM_005959); Frog.CloneX1.7 = *Xenopus laevis* clone X1.7 (U31827); H.Mouse.Mel1B = *Mus musculus* melatonin receptor 1B (NM_145712); Chicken.Mel1B = *Gallus gallus* Mel-1B (U30609.1); ZebraFinch.Mel1B = *Taeniopygia guttata* Mel-1B (AY803772.1); Z.Fish.Mel1B = *Danio rerio* melatonin receptor 1B (NM_131394); Goldfish.Mel1B = *Carassius auratus* MT2 (AB481374); C.Salmon.Mel1B = *Oncorhynchus keta* melatonin-receptor 1B (AY356365); Sweetfish.Mel1B = *Plecoglossus altivelis* MT2 (AB481369); ZebraFinch.Mel1C = *Taeniopygia guttata* Mel-1c (AY803773); HouseSparrow.Mel1C = *Passer domesticus* Mel-1c (AY743658); Chicken.Mel1C = *Gallus gallus* Mel-1C (U31821); BlackCap.Mel1C = *Sylvia atricapilla* Mel-1C (DQ178664.1); Sweetfish.Mel1C = *Plecoglossus altivelis* MEL1C (AB481370); Frog.Mel1C = *Xenopus laevis* Mel-1C (U09561); E.Starling.Mel1C = *Sturnus vulgaris* Mel-1C (DQ470810.1); Goldfish.Mel1C = *Carassius auratus* MEL1C (AB481375); RainbowTrout.Mel = *Oncorhynchus mykiss* melatonin receptor gene (AF178929).

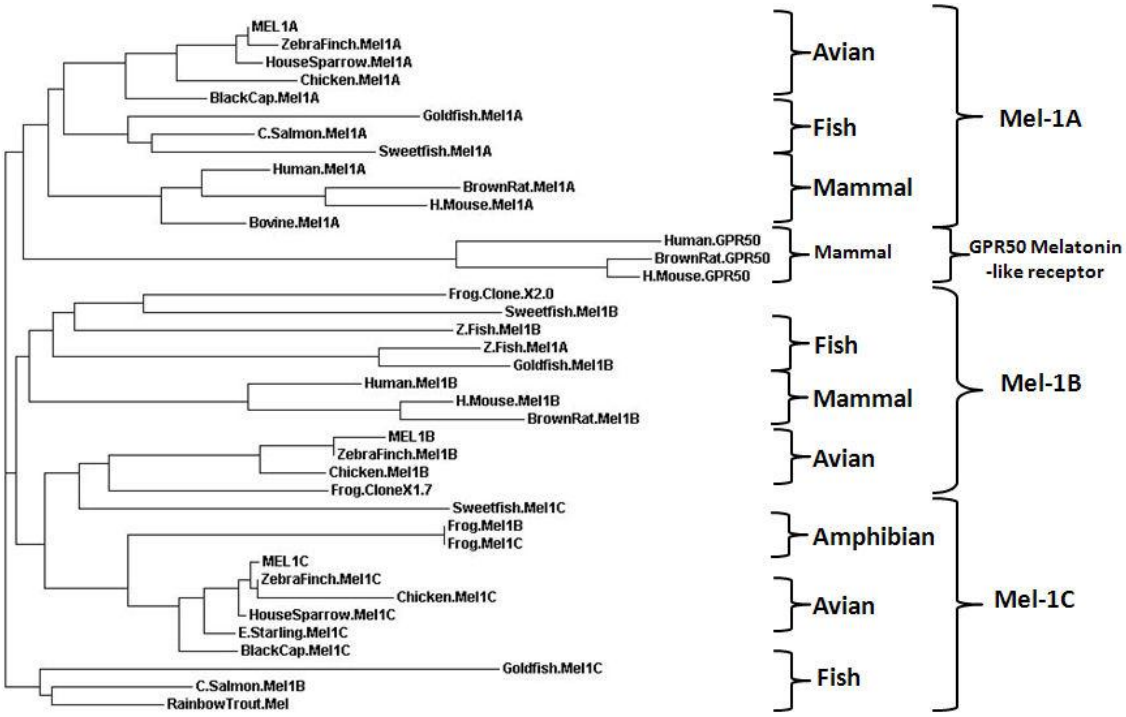

Figure 3.2.2.d. Phylogenetic tree of melatonin receptors and melatonin-like receptor GPR50 in different species. Shows the relationships between families and species of the melatonin membrane receptors (see appendix for alignment of nucleotides). This graph was created using Clustal W2 program of EMBL website.

3.2.3 Optimising RT-PCR conditions for melatonin receptor analysis

For RT-PCR reactions, reaction conditions were optimised to allow for semi-quantitative analysis of the melatonin receptors; these conditions are summarised in Table 3.2.3.a.

3.2.3.1 Optimising PCR Magnesium (Mg^{2+}) concentration and annealing temperatures

The optimal annealing temperatures (Tm) were calculated for each primer pair using the primer sequences, this temperature was then systematically tested in a series of annealing temperature variations (57°C to 62°C) along with varying magnesium concentrations (0mM to 2.5mM).

The RT-PCR results for Mel-1A receptor primer pair 1 resulted in no PCR products at any of the annealing temperatures, therefore discarded this primer pair and looked at the second set of primer pairs. The second primer pair set results showed the expected PCR product results at all annealing temperatures tested. The magnesium concentrations of 2mM showed the best results at 57°C and 62°C annealing temperatures; the rest of the PCR optimisation used this concentration. The Tm value for primer pair 2 (Mel1AQPfor2 and Mel1AQPrev2) was 62.4°C therefore I continued the rest of the PCR optimisation for Mel-1A receptor optimisation with 62°C temperature (Table 3.2.3.a).

The first primer pair set for Mel-1B receptor showed no/little results at lower Tm's; faint bands at Tm 57°C but nothing at Tm 60°C. So again I discarded this primer pair set and concentrated on the second primer pair. The second primer pair showed the best results with Tm of 60°C and a magnesium concentration at both 1.5mM and 2mM. Both of these concentrations were tested at the cycle number optimisation and the 2mM proved to be most suitable (Table 3.2.3.a).

The Mel-1C primer pair's 1 and 2 showed mixed results with the Tm and magnesium titration, but showed inconsistent results in the cycle number and cDNA titration experiments, therefore I discarded both of these primer pairs and designed two new primer pair sets. Primer pairs 3 and 4 showed consistent results to each other. The annealing temperature 62°C proved to be optimal, which coincides with the theoretical predicted annealing temperatures from the MWG datasheet. The Tm temperatures from the datasheet were most consistent with primer pair 3; therefore I continued the rest of the experiments and optimisation with this primer pair. At the annealing temperature of 62°C the 1.5mM magnesium concentration resulted in the best yield for this receptor primer pair (Table 3.2.3.a).

3.2.3.2 Optimising PCR cycle number

To determine the number of optimal cycles for each melatonin receptor gene amplification reaction, a RT-PCR was set up with the optimised conditions. A PCR tube was removed from the thermal cycler after 10 cycles and immediately stored on ice at 4°C. Tubes were

consecutively removed from the PCR thermal cycler after every second cycle, at the end of the cycle, up to cycle number 42.

Analysis from these experiments (Figure 3.2.3.a) showed a sigmoid curve, the initial plateau (cycle number 10-22), the linear phase of synthesis (cycle number 24-(30-34), and then plateau phase when the maximum yield is generated (cycle number 34-42). The optimal cycle number for each primer pair was picked to be in the linear range; cycle 26 for Mel-1A (Figure 3.2.3.a.-A), cycle 27 for Mel-B (Figure 3.2.3.a.-C) and Mel-1C (Figure 3.2.3.a.-E).

3.2.3.3 Testing cDNA concentrations

The cDNA dilution was performed in order to check whether the optimised conditions, from the previous experiments, were in linear correlation. This analysis is shown in Figure 3.2.3.a., the results showed a linear correlation for all three receptor cDNA dilution tests, indicating that conditions for each primer pair were in the linear correlation with each other.

Gene	RT-PCR Primer	Product length (bp)	Tm (X°C)	Cycle No. (Y)	Mg^{2+} Conc
Mel-1A	Forward: 5'-CCACAGTCTCAGATACGACAAGC-3' Reserve: 5'-ACCCTTCGCCTTACCTGGATAAC-3'	276	62°C	26	2mM
Mel-1B	Forward:5'-GACAAAGTGTACAGCTGTTGG-3' Reserve:5'-CTGATTTGACTCGTCTTCGAAC-3'	265	60°C	27	2mM
Mel-1C	Forward: 5'-TCTGCCTGACCTGGATACTCAC-3' Reserve: 5'- CTGCTTGCAGTCTTGTCTCACC-3'	239	62°C	27	1.5mM

Table 3.2.3.a. The final primer pair sequences and optimised PCR conditions for analysing the Mel-1A, Mel-1B and Mel-1C receptor mRNA levels in the zebra finch. bp – base pairs, Tm – annealing temperature, Mg^{2+} - magnesium concentration.

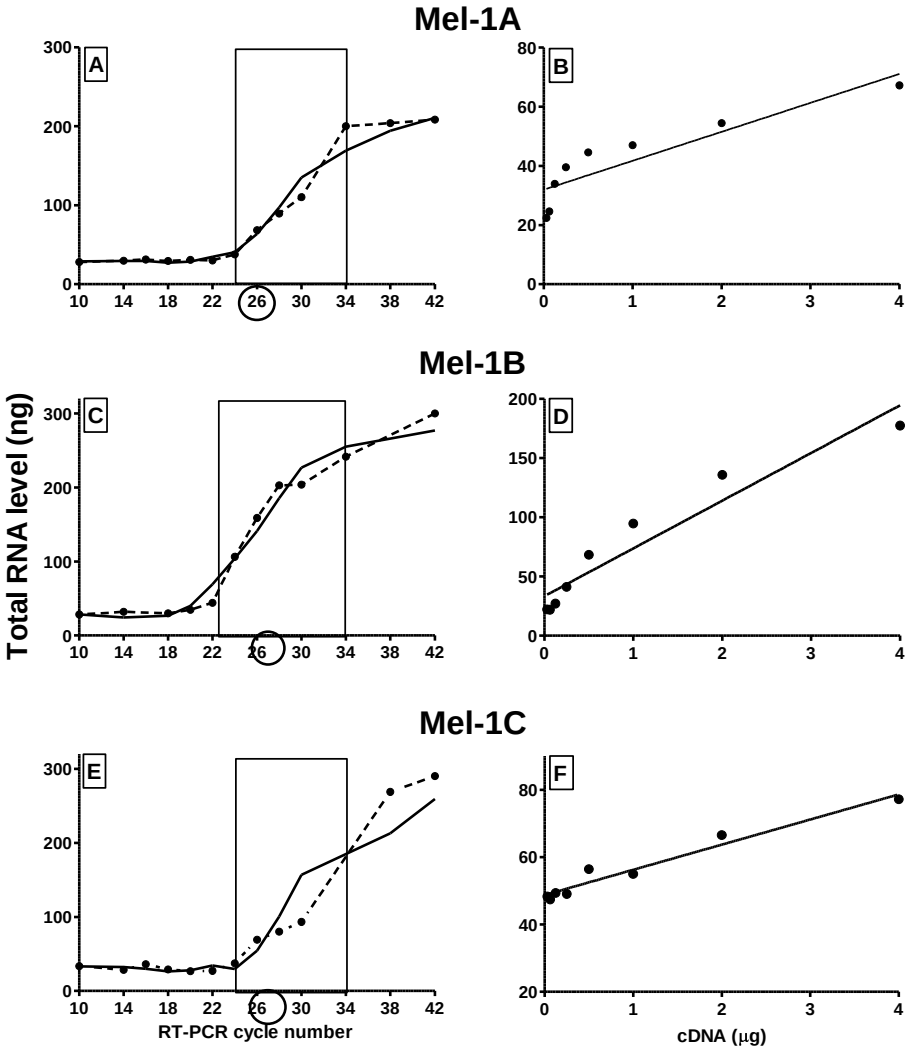

Figure 3.2.3.a. Receptor gene mRNA as a function of PCR cycles and cDNA dilution. Graphs A-B show results for the Mel-1A primer pair. Graphs C-D show results for Mel-1B primer pair. Graph E-F show results for the Mel-1C primer pair. Graphs A, C and E show the synthesis curve the PCR cycle number analysis; the cycle number for future mRNA expression analysis needs to be in the linear phase of the curve (boxed area) and the cycle number needed to be in the beginning-middle of this phase (circle). Graphs B, D and F show the cDNA dilution test for each receptor, the solid line in the graph represents the line of best fit through the values.

3.3 Discussion

So far, melatonin studies in birds have mostly concentrated on plasma melatonin levels and behavioural effects of exogenous melatonin on physiology and behaviour. Studies on avian melatonin receptors mainly focused on the retina (Rada and Wiechmann, 2006), gonads (Aste, *et al.*, 2001) and song-control nuclei in the brain (Cassone, *et al.*, 2008; Whitfield-Rucker and Cassone, 1996) while localisation of melatonin receptors in the brain and rhythmicity of expression received very little attention.

One of the main purposes of this study was to examine the melatonin receptor mRNA expression in different brain tissues of the zebra finch over 24 hour under LD 12:12 conditions. This was accomplished by ensuring that during tissue preparation all tissues were treated in the same manner, i.e. similar weight (± 0.010g) for whole tissue RNA extraction, and mRNA concentrations and therefore final cDNA concentrations. Due to the small size of the pineal gland and the kidney these measures could not be maintained for these tissues, they were treated in the same manner but due to their small size the weight was much lower than the other tissues collected and analysed. The RNA analysis showed very little tissues had degraded through the RNA isolation preparation, meaning all but a few could be used for the melatonin receptor cloning and analysis in the next chapter (Chapter 4).

Three melatonin membrane receptors were cloned in the zebra finch, Mel-1A, Mel-1B and *Mel-1C,* which show amino acid sequence homologies of 98-99% to previously published zebra finch melatonin receptors (Jansen, *et al*., 2005). Phylogenetic analysis showed that the

groupings of melatonin membrane receptors 1A, 1B and 1C have different lineage, though are structurally similar to each other. The cloned partial sequences of the melatonin membrane receptors showed that the zebra finch *Mel-1A* sequence grouped with other melatonin 1a receptors found in the other avian species. The appearance of the phylogenetic tree as a whole and the branching into the different melatonin receptor groups suggests an early evolutionary diversification of melatonin receptors in vertebrates. Interestingly, *Mel-1C* has not been detected in mammals and the question arises whether this receptor type has been lost during vertebrate diversification and mammalian development and, thus, was never present in mammals or whether mammals have reduced their number of melatonin receptors types during their own evolution. As compared to all other vertebrate classes, mammals have lost photosensitivity of the pineal gland as well as the circadian clock in the pineal gland, and have one dominant circadian brain oscillator which controls pineal synthesis and secretion of nocturnal melatonin. Mammals have photoreceptors only in the retina and there has been an evolutionary loss of two retinal cone classes (SWS and MWS; Bellingham, et al., 2003) and certain opsins which are found in lower vertebrates including birds and fishes (Bellingham, *et al*., 2003). These differences in circadian organisation are believed to be the consequence of a "nocturnal bottleneck" during early evolution of mammals (Foster, *et al*., 1993) and might have also lead to a loss of the third melatonin receptor.

The primers described in this Chapter, and, the PCR conditions were optimised for the specific needs of the gene analysis in Chapter Four. The optimal annealing temperature was theoretically predicted for each primer pair and then determined by preliminary experiments. A magnesium titration was performed for each primer pair to find the optimal magnesium concentration with annealing temperatures ranching from 55ºC to 62ºC. RT-PCR is very

magnesium sensitive as low magnesium concentration can result in failed reactions, whereas high magnesium concentration can result in high background staining. Therefore performing a magnesium titration is essential. The RT-PCR products must be in the linear phase of synthesis between the amplified products and the amounts of template DNA; for quantification of PCR products. The optimisation for all three primers pairs (receptors 1A, 1B and 1C) showed relevant base-pair bands for the PCR primer products, with all three receptors being optimised successfully. These finding are carried forward for the gene analysis work in different brain and peripheral tissues, the next Chapter.

CHAPTER 4

Melatonin receptor expression in the zebra finch brain and peripheral tissues

Data from this chapter was submitted to Chronobiology International April 2011, the manuscript was accepted in October 2011 and due for publication February 2012, see Appendix II for manuscript.

CHAPTER FOUR - MELATONIN RECEPTOR EXPRESSION IN THE ZEBRA FINCH BRAIN AND PERIPHERAL TISSUES

4.1 Introduction

Melatonin is a small lipophilic hormone (Carlberg, 2000) found in all living organisms from plants to humans, at levels that vary in a diurnal cycle (Brandstaetter, *et al*., 2001b). The chemical structure of melatonin was first identified by Aaron Lerner (Lerner, *et al*., 1958), who found that it caused aggregation of melanin granules within the melanocytes of frog skin (Ebisawa, *et al*., 1994; Lerner, *et al.*, 1958). Melatonin is produced by pinealocytes in the pineal gland but a small amount is also produced by the retina and the gastrointestinal tract (Brandstaetter, 2002). Due to the lipophilic nature of melatonin, it can diffuse through the pineal cell membrane and into the circulatory system, where it can bind to receptors of neuronal (and peripheral) tissues acting in a paracrine and autocrine manner (Wiechmann and Rada, 2003). Melatonin is rhythmically produced by the pineal gland, both into the circulation and into the CSF. Generally, melatonin levels are high during the dark phase and are completely absent during the light phase, levels drop just before the onset of light suggesting it is endogenously controlled (Brandstaetter, *et al*., 2001).

In the house sparrow the only source of circulating melatonin is the pineal gland (Brandstaetter, 2002), whereas in Japanese quail the retina supplies up to 50% of the circulating melatonin and the pineal gland contributes to the rest (Karaganis, *et al.*, 2009). So far studies have looked at the removal of the whole pineal gland (Gaston and Menaker, 1968),

circulating plasma melatonin levels (Gwinner, *et al*., 1997) and melatonin supplements (Heigl and Gwinner, 1995). The removal of the pineal gland abolishes circadian rhythmicity behaviour in songbirds highlighting the importance of circulating melatonin in these species.

Vakkuri, et al., (1984) provided the first radioligand analysis, using 2-[^{125}I]iodomelatonin as the tracer for melatonin uptake, since this study numerous other groups have reported the sites where melatonin is taken-up (Vakkuri, *et al*., 1984). Binding studies revealed 2-[^{125}I]iodomelatonin has a wide distribution of binding throughout the chicken brain, compared to that of the rodent brain where binding is restricted to a few discrete areas (i.e. SCN, PVN and ME) (Siuciak, *et al*., 1991). Binding in the chicken brain is most prominent in the regions associated with the visual system; such as the LHN (named vSCN in the paper), optic tectum, thalamofugal, median eminence, etc. (Siuciak, *et al*., 1991). The binding of 2-[^{125}I]iodomelatonin showed to have a high affinity, which was saturable and reversible, predominated in the major components of the chick's visual and auditory (Brooks and Cassone, 1992). In light/dark (LD) cycles, conditions the highest binding affinity was in the late afternoon (ZT10). When transferred to constant darkness (DD) conditions this rhythm persisted with a peak binding at CT10 with an increased amplitude between CT6 to CT10 (Brooks and Cassone, 1992).

Melatonin causes its stimulation by activating different receptors, such as membrane receptors and nuclear receptors. Although melatonin has other direct actions including powerful antioxidant and enhancing mitochondrial oxidative phosphorylation (Rada and Wiechmann, 2006). There are three known melatonin membrane receptors; Mel-1A, Mel-1B and Mel-1C.

Two melatonin receptors are found in the mammalian circadian system (Mel-1A and Mel-1B). All three are found in the avian circadian system.

In mammals the stimulation of melatonin has been shown to inhibit neuronal firing in the SCN in brain slices from wild-type and Mel-1B knock-out receptors, but not in Mel-1A knock-out mice which suggest the Mel-1A receptor mediates the inhibitory effects of melatonin in the SCN and thus disrupts the amplitude of the "daytime" circadian signal from the oscillator (Liu, *et al*., 1997b). Activation of this receptor (Mel-1A) was also shown to decrease neuronal firing in areas of the limbic system which are implicated in the regulation of sleep (Dubocovich, 2007). Activation of Mel-1A receptor causes the inhibition of pituitary adenylate cyclise activating polypeptide-stimulated phosphorylation (cAMP) of cAMP response element-binding (CREB) which is an early event in the signalling cascade leading to phase shifts of the endogenous clock (Jin, et al., 2003; Liu, et al., 1997b). Mel-1B activation also has been linked to phase shifting of neuronal firing rhythms in the SCN, at dusk (Dubocovich, 2007).

Chicken retinal *Mel-1A* mRNA has been found to be rhythmic under LD and DD cycles, peaking at midday and mid-subjective day (Natesan and Cassone, 2002). Chicken retinal *Mel-1C* mRNA is rhythmic in LD cycles (lower amplitude than Mel-1A): transcripts are high during the day and low during the night. In DD conditions, the rhythm becomes 180° out of phase with LD conditions (Natesan and Cassone, 2002). *Mel-1B* expression is highly variable and arrhythmic (Natesan and Cassone, 2002). Xenopus retinal *Mel-1B* and *Mel-1C* mRNA also peak during the day under 12:12 LD conditions, confirming the chick results (Natesan and Cassone, 2002), but being 180° out of phase with the circulating melatonin (Natesan and

Cassone, 2002); possibly suggesting a long delay between the presence of mRNA and the presence of a functional receptor (Natesan and Cassone, 2002), or that the receptor levels increase when there is low/no circulating melatonin in case melatonin is secreted, and therefore needed to receive the hormonal signal.

Although a lot of research has been conducted since the discovery of melatonin by Aaron Lerner (Lerner, *et al.*, 1958) and the first melatonin membrane receptor was cloned from *Xenopus laevis* in 1994 (Ebisawa, *et al.*, 1994). We still lack comprehensive information on the localisation and rhythmicity of melatonin receptors in the brain of birds. Therefore the aim for this study was to examine the expression levels of the three known melatonin membrane receptor mRNAs (*Mel-1A*, *Mel-1B* and *Mel-1C*) in the diencephalon, and compare these levels to those found in two other areas known to contain circadian oscillators (the pineal gland and retina). After comparing the oscillatory expression I examined the expression of these receptors in other regions of the brain, i.e. optic tectum, cerebellum and telencephalon, and then four peripheral tissues, i.e. the heart, liver, lung and kidney. The primers that were used for RT-PCR to amplify sections of the cloned melatonin receptors over a 24 hour period are described in Chapter 3. RT-PCR is a technique for *in-vitro* amplification of specific DNA sequences by simultaneous primer extension of complimentary strands of DNA. Semi-quantitative RT-PCR is a simple and rapid procedure for quantifying mRNA in the tissue samples of different species after RT-PCR. The intensity of the SYBR Green I Nucleic Acid Gel Stain luminescence of PCR products is measured directly from electrophoresis gels by a highly sensitive Gel Doc Imager camera combined with an image analysing computer system and compare the fluorescence to known concentrations.

4.2 Results

To investigate melatonin receptor gene expression in the brain of birds, expression levels of *Mel-1A, Mel-1B* and *Mel-1C* mRNA were analysed in the zebra finch, using RT-PCR techniques. The melatonin receptor mRNA expression was analysed by RT-PCR amplification, the PCR products were run on polyacrylamide gels. The polyacrylamide gels were analysed using a gel doc imaging system in combination with Quantity One imaging analysing software (BioRad; Functional genomics, proteomics and metabolomics facility at the University of Birmingham), comparing the known fragment (bp) sizes and DNA quantity of the DNA ladder band to the PCR product bands. The initial analysis of the gels produced an "absolute" reading from the raw data for the time point and that particular zebra finch. Six zebra finch readings were analysed for each time point in each tissue and the average absolute readings (i.e. raw data) were plotted into graphs (for example see Figure 4.2.1.a.-BD&F). In the absolute graph readings there will always be some natural fluorescence given off from any gel this is known as background level or "noise" which is around the 25ng readings on the plotted graphs. In the mRNA expression graphs there are normally peaks and dips found, the lowest levels found (or dips) are normally considered the base level expression for that gene in that particular tissue.

In the "absolute graphs" there is more deviations between the melatonin mRNA expressions due to natural variation. Therefore to remove or compensate variation in gel analysis, the absolute melatonin receptor mRNA data was compared to a known housekeeping gene, TATA-boxbinding protein (TBP) which encodes a transcription factor that plays a major role in the activation of eukaryotic genes transcribed by RNA Polymerase II, as an internal standard in accordance with previous circadian investigations (Doi, *et al*., 2001). The

housekeeping gene TBP was used for the comparative analysis as their expression levels remain relatively constant throughout the 24 hour period (Helfer, *et al*., 2006). The mRNA levels of the melatonin receptor gene mRNAs were then plotted as relative gene expression values compared to the TBP, these levels are plotted into graph as "normalised" or relative gene expression (for example see Figure 4.2.1.a.-A,B&C).

Due to the results obtained from the zebra finch brain tissues; I then went on to examine the expression in four peripheral tissues from the zebra finch. All tissues studied showed some level of receptor expression, but not all tissues showed a circadian rhythm, the statistical test performed on the receptor expression are summarised in Table 4.2.a.

		Statistical tests	
Receptor	**Tissue**	**ANOVA**	**Tukey's**
Mel-1A	Cerebellum	*	*
	Diencephalon	***	***
	Optic tectum	***	***
	Retina	**	**
	Telencephalon	**	*
	Pineal gland	-	-
	Heart	-	-
	Liver	**	**
	Lung	-	-
	Kidney	-	-
Mel-1B	Cerebellum	*	**
	Diencephalon	**	**
	Optic tectum	**	**
	Retina	**	**
	Telencephalon	-	-
	Pineal gland	*	*
	Heart	***	***
	Liver	***	***
	Lung	***	***
	Kidney	-	-
Mel-1C	Cerebellum	-	-
	Diencephalon	-	-
	Optic tectum	-	-
	Retina	-	-
	Telencephalon	*	-
	Pineal gland	*	-
	Heart	-	-
	Liver	-	-
	Lung	-	-
	Kidney	*	*

Table 4.2.a. Variation between time points of the three melatonin receptor mRNA levels in the different tissues studied in this Chapter over 24 hours. Summary of statistical test performed and significant findings, on zebra finch brain and peripheral tissues for variation in the expression of three melatonin receptors. *p<0.05, **p<0.01, ***p<0.001. For statistical analysis see Appendix I – Section 1.2.2 and Section 1.2.3.

4.2.1 Zebra finch expression of melatonin receptors in the brain tissues

All tissues associated with circadian oscillatory functions (diencephalon, pineal gland and retina) contained melatonin receptors and the levels varied throughout the 24 hour period.

In the diencephalon (Figure 4.2.1.a), both *Mel-1A* and *Mel-1B* had clear nocturnal rhythms of the mRNA. *Mel-1A* peaked at ZT22 and then immediately dropped at the onset of light (ZT00). Levels continued to drop throughout the light phase and minimal expression was seen between ZT6 and ZT10 (Figure 4.2.1.a.-A&B; Tukey's, ZT6vsZT22 q=7.595 and ZT10vsZT22 q=7.249). As the time progresses into the dark period (after ZT12) levels of the *Mel-1A* mRNA continued to increase into the mid-late dark period (ZT18). The *Mel-1A* expression in the absolute level graph (Figure 4.2.1.a.-B) showed the level of the *Mel-1A* mRNA receptor in the diencephalon as being fairly high; due to the baseline expression (~50ng) being much higher than that of the background level around 25ng. The *Mel-1B* mRNA levels (Figure 4.2.1.a.-C&D) showed a similar pattern to the *Mel-1A* rhythm, peaked during the dark period; though the rhythm in the *Mel-1B* gene peaked between ZT22 and ZT02, with the onset of light. The *Mel-1B* expression level remained high until after ZT2 (Figure 4.2.1.a.-C; Tukey's, ZT2vs10 q=5.998). The expression then dropped at ZT6 (lowest expression level) and remained low throughout the rest of the light period and into the dark phase. The expression levels rose slightly after the off-set of light at ZT12, it increased throughout the dark period to maximum expression at the turn of the light phase (ZT0). This rhythm was mirrored in the absolute levels (Figure 4.2.1.a.-D), but in the absolute level figure it showed a more gradual increase in receptor levels in the dark period. Between ZT6 and ZT14 *Mel-1B* mRNA levels are at its lowest (~30ng), across the light change. Indicating the

receptor in this tissue was either highly present or completely absent. There was no base line of expression. In the diencephalon, there appeared to be no rhythmicity in the *Mel-1C* gene in the relative data set (Figure 4.2.1.a.-E; one-way ANOVA, $F_{5,15}$=0.6741 p=0.6495). The absolute levels (Figure 4.2.1.a.-F) suggested that the receptor was present in the diencephalon region with a level higher than the base line (50ng).

In the pineal gland the only melatonin receptor mRNA which showed to be significantly rhythmic was the expression of *Mel-1B* receptor (Figure 4.2.1.b). The *Mel-1A* receptor mRNA showed very little rhythmicity in the pineal gland (Figure 4.2.1.b.-A&B; one-way ANOVA, $F_{5,15}$=0.9861 p=0.4582); being fairly constantly low, though the gene level dropped in mid-light phase at ZT6 and mid-dark phase at ZT18. This rhythm is mirrored by the fourth order polynomial curve (Figure 4.2.1.b.-A) which was confirmed by the absolute levels (Figure 4.2.1.b.-B), with all levels being below 50ng. *Mel-1B* mRNA was the only receptor that showed a rhythmic pattern in the pineal gland (Figure 4.2.1.b.-C&D). *Mel-1B* mRNA expression was constantly low throughout the 24 hours apart from a robust peak found at ZT22 (one-way ANOVA, $F_{5,14}$=4.233 p=0.0149, Tukey's, ZT18vs22 q=5.797) two hours before the on-set of light and then dropped immediately afterwards and remained low. The lowest levels were found at ZT6 (34ng; Tukey's, ZT6vs22 q=5.636) and ZT18 (35ng; Tukey's, ZT18vs22 q=5.797), again supported by the absolute levels (Figure 4.2.1.b.-D). After ZT18 the expression rose to the peak expression at ZT22 (85ng). The levels remained relatively low during the light phase and started to peak again at ZT10 before they dropped again at lights off and increased around the mid-to-late dark phase (after ZT18). The *Mel-1C* receptor mRNA showed a slight deviation around the mean value 1, in the normalised data (Figure 4.2.1.a.-E; one-way ANOVA, $F_{5,13}$=3.463 p=0.0330), with the fourth order

polynomial curve showing a peak around ZT12. The absolute levels showed no significant fluctuation from the baseline (25ng) although there was a slight increase in gene expression around ZT10-14 (Figure 4.2.1.b.-F).

In the retinal tissue (Figure 4.2.1.c), which receives photic information and where some melatonin can be synthesised, both *Mel-1A* and *Mel-1B* receptors showed strong rhythms. *Mel-1A* mRNA showed a nocturnal rhythm which peaked at ZT18 (Figure 4.2.1.c.-A&B) and low expression occurred during the day (lowest at ZT6). Levels then rose sharply around lights off and peaking at ZT18 (one-way ANOVA, $F_{5,20}$=5.836 p=0.0018, Tukey's, ZT6vs18 q=6.759). This rhythm was also mirrored in the absolute levels for this tissue; with the base line being 25ng (at ZT6) and peaking to around 85ng (at ZT18; Figure 4.2.1.c.-B). *Mel-1B* receptor mRNA showed a diurnal rhythm peaking at ZT10 just before the off-set of light at ZT12 (Figure 4.2.1.c.-C&D), eight hours before the peak in *Mel-1A*. The *Mel-1B* receptor peaked at ZT10 and the lowest expression was found at ZT22 (Figure 4.2.1.c.-C; one-way ANOVA, $F_{5,19}$=4.446 p=0.0075, Tukey's, ZT10vs22 q=6.422), two hours before the onset of light. After the peak of mRNA (ZT10) the expression gradually dropped after the on-set of the dark period, until it reached ZT22. Following ZT22, and with the onset of light (ZT0), the expression rapidly increased at ZT2, with a gradual increased thereafter until ZT10. This rhythm suggests that this receptor is anticipating the onset or release of circulating melatonin. Absolute levels (Figure 4.2.1.c.-D) showed an incredibly high level of mRNA at ZT10 (>350ng), although the SEM for this ZT is also very high. After both *Mel-1A* and *Mel-1B* receptors mRNA peak expression both receptor levels dropped immediately and the minimal expression was seen 12 hours after the peak expression, i.e. ZT6 for *Mel-1A* and ZT22 for *Mel-1B*. Again the levels of *Mel-1C* showed no rhythm and constant intermediate levels

(50ng) were seen in the absolute data (relative levels - Figure 4.2.1.c.-E and absolute levels - Figure 4.2.1.c.-F; one-way ANOVA, $F_{5,14}$=0.7569 p=0.5951).

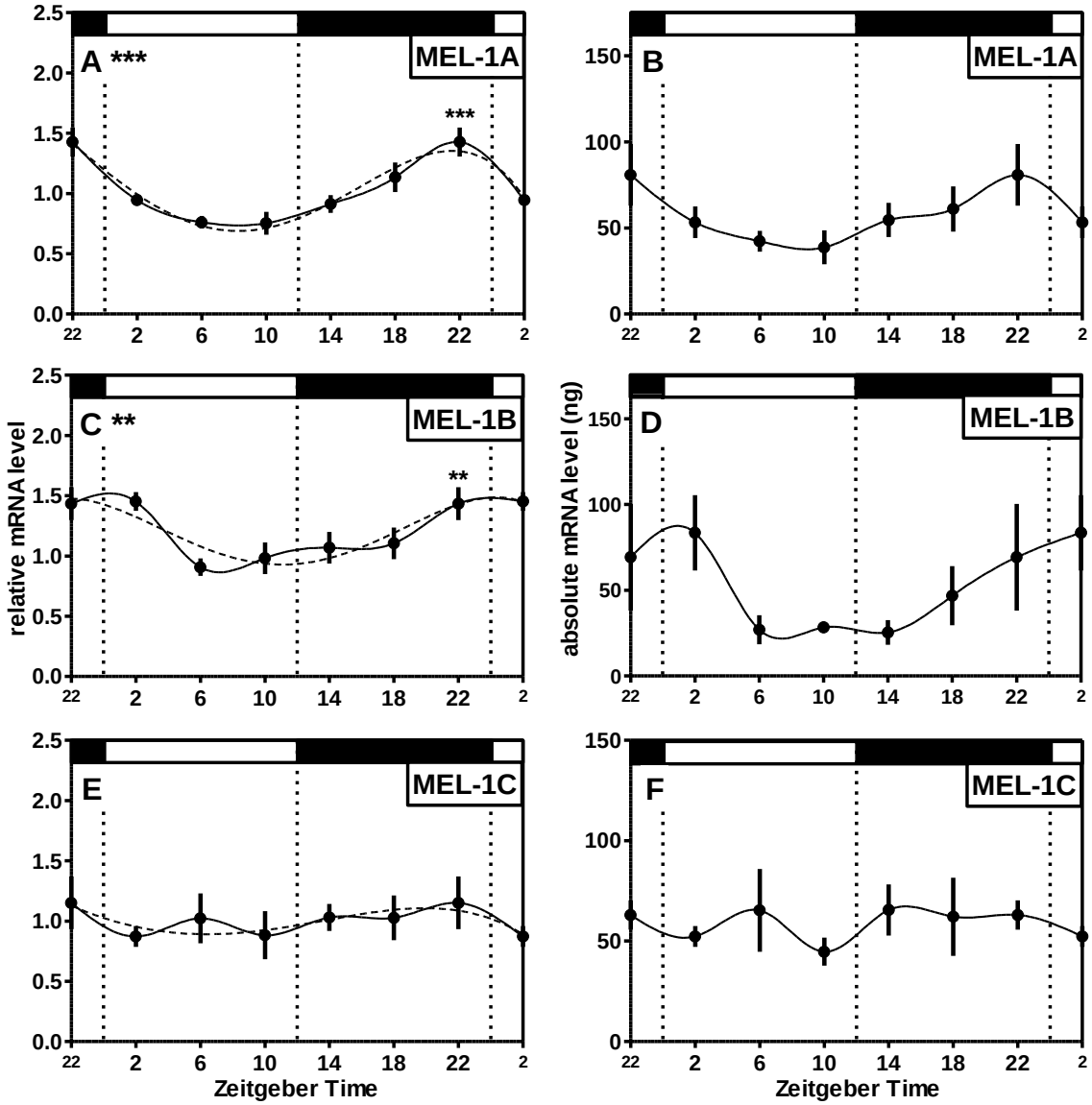

Figure 4.2.1.a. Expression profiles of melatonin receptors *Mel-1A*, *Mel-1B and Mel-1C* mRNA in the zebra finch diencephalon tissue. Temporal expression of normalised data (A,C,E), i.e. relative mRNA values normalised to *TBP* mRNA expression shown as variation from mean value, and (B,D,F) absolute mRNA values, i.e. raw data. The bars at the top of each graph indicate the LD 12:12 hrs light/dark schedule, i.e. light periods represented by white bars and dark period represented by black bars. The symbols represent mean values for each time point ± SEM (n=4-6). ZT2 and ZT22 are double plotted for better visualisation. Fourth order polynomial (dashed line) and lowess (black line) curves were fitted with GraphPad prism. Significant differences as revealed by ANOVA indicated by * on figure letter; significant differences between times points, i.e. to the lowest value of mRNA expression, as revealed by post hoc Tukey test indicated by * above the corresponding symbols: *p<0.05, **p<0.01, ***p<0.001. X-axis: Zeitgeber time. See Appendix I – Section 1.2.2 for statistical analysis.

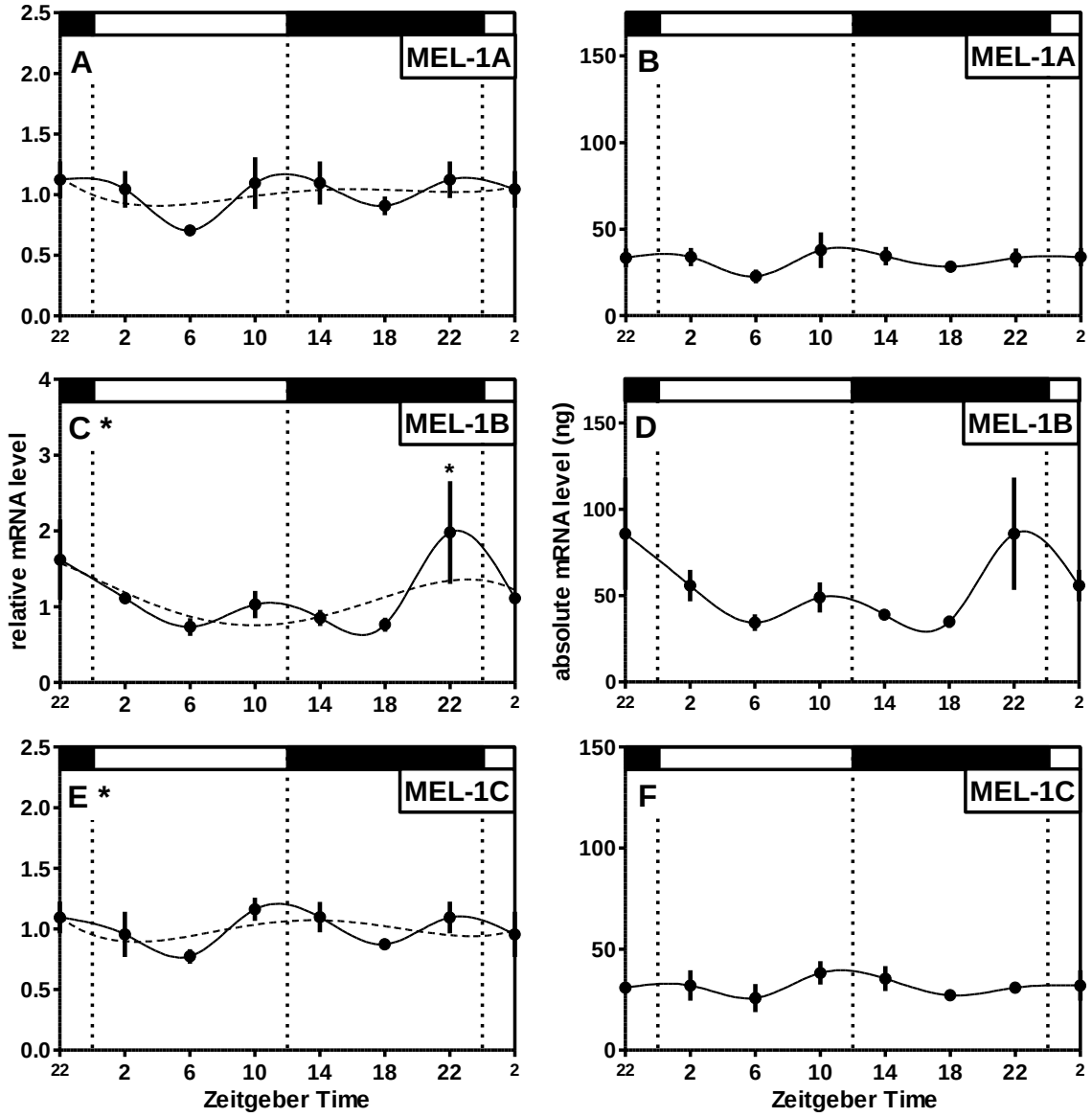

Figure 4.2.1.b. Expression profiles of melatonin receptors *Mel-1A, Mel-1B and Mel-1C* mRNA in the zebra finch pineal gland tissue. Temporal expression of normalised data (A,C,E), i.e. relative mRNA values normalised to *TBP* mRNA expression shown as variation from mean value, and (B,D,F) absolute mRNA values, i.e. raw data. The bars at the top of each graph indicate the LD 12:12 hrs light/dark schedule, i.e. light periods represented by white bars and dark period represented by black bars. The symbols represent mean values for each time point ± SEM (n=4-6). ZT2 and ZT22 are double plotted for better visualisation. Fourth order polynomial (dashed line) and lowess (black line) curves were fitted with GraphPad prism. Significant differences as revealed by ANOVA indicated by * on figure letter; significant differences between times points, i.e. to the lowest value of mRNA expression, as revealed by post hoc Tukey test indicated by * above the corresponding symbols: *p<0.05, **p<0.01, ***p<0.001. X-axis: Zeitgeber time. See Appendix I – Section 1.2.2 for statistical analysis.

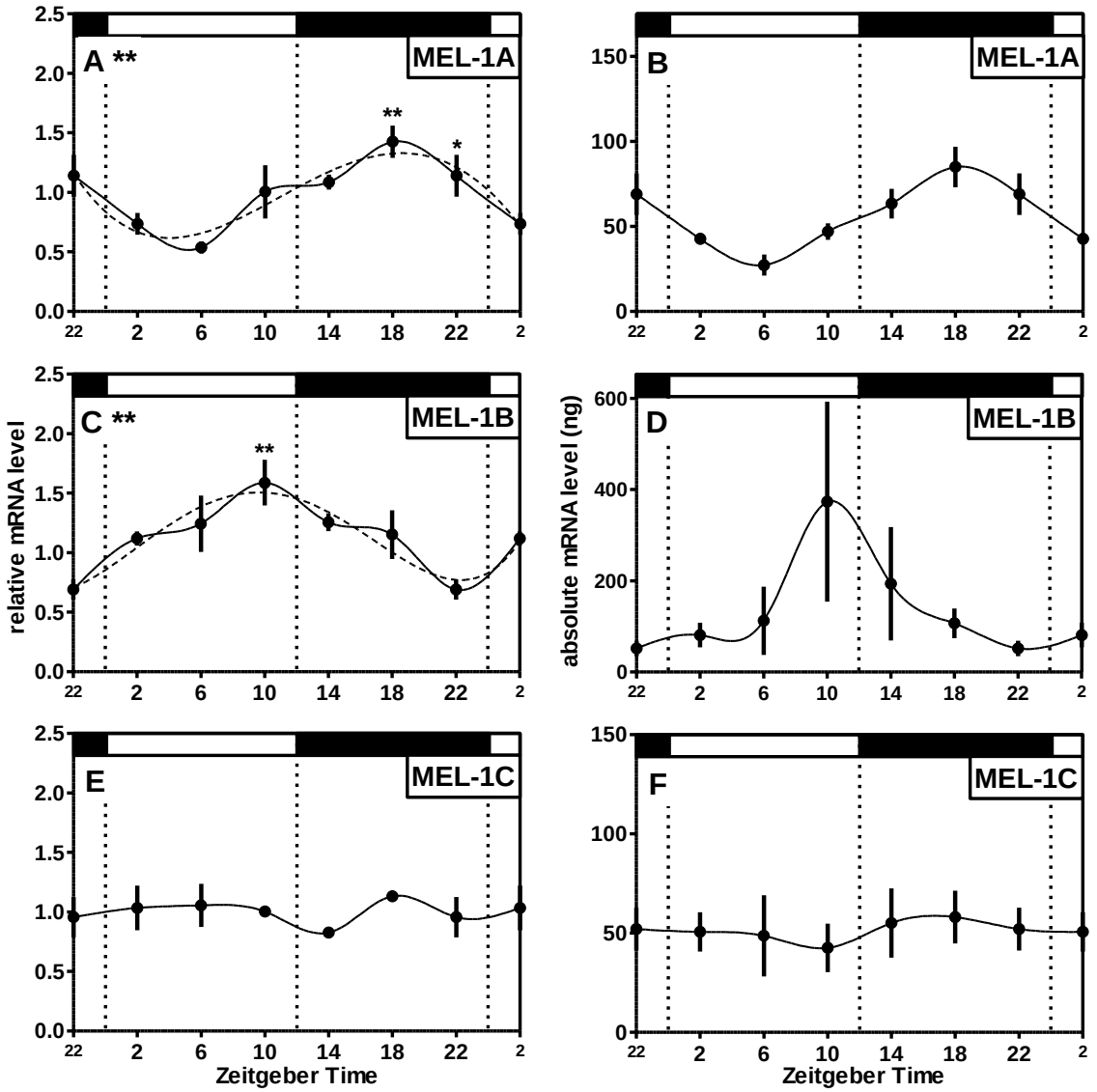

Figure 4.2.1.c. Expression profiles of melatonin receptors *Mel-1A, Mel-1B and Mel-1C* mRNA in the zebra finch retinal tissue. Temporal expression of normalised data (A,C,E), i.e. relative mRNA values normalised to *TBP* mRNA expression shown as variation from mean value, and (B,D,F) absolute mRNA values, i.e. raw data. The bars at the top of each graph indicate the LD 12:12 hrs light/dark schedule, i.e. light periods represented by white bars and dark period represented by black bars. The symbols represent mean values for each time point ± SEM (n=4-6). ZT2 and ZT22 are double plotted for better visualisation. Fourth order polynomial (dashed line) and lowess (black line) curves were fitted with GraphPad prism. Significant differences as revealed by ANOVA indicated by * on figure letter; significant differences between times points, i.e. to the lowest value of mRNA expression, as revealed by post hoc Tukey test indicated by * above the corresponding symbols: *p<0.05, **p<0.01, ***p<0.001. X-axis: Zeitgeber time. See Appendix I – Section 1.2.2 for statistical analysis.

In the non-oscillatory tissues (optic tectum, cerebellum and telencephalon) *Mel-1A* proved to be significantly rhythmic in all the tissues, *Mel-1B* was significantly rhythmic in the optic tectum and cerebellum but not in the telencephalon, and the *Mel-1C* receptor mRNA was not rhythmic in any of the tissues (Figure 4.2.1.d., Figure 4.2.1.e. and Figure 4.2.1.f.).

In the optic tectum, *Mel-1A* receptor mRNA was clearly rhythmically expressed (Figure 4.2.1.d.-A&B), with low levels (lowest at ZT10) during the day light and high levels in the dark phase, which peaked around ZT18-22 (Figure 4.2.1.d.-A; one-way ANOVA, $F_{5,26}$=8.944 p<0.0001, Tukey's, ZT10vs22 q=6.832). The absolute levels showed that mRNA levels were high in the optic tectum; the base line expression was 50ng at ZT10 and peaking at 100ng at ZT18-22 (Figure 4.2.1.d..-B). *Mel-1B* receptor mRNA expression appeared to be biphasic in the optic tectum (Figure 4.2.1.d.-C; one-way ANOVA, $F_{5,15}$=5.752 p=0.0037) with a peak expression two hours after the onset of the light period at ZT2 (Tukey's, ZT2vs22 q=6.187) and two hours after the onset of the dark period at ZT14 (Tukey's, ZT14vs22 q=4.679). After each peak the *Mel-1B* receptor expression decreased to the lowest levels two hours before the onset of darkness at ZT10 and the onset of the light at ZT22. The absolute levels for *Mel-1B* showed that there the peak levels were around the 50ng mark with the lowest levels being around the 25ng mark (Figure 4.2.1.d.-D). *Mel-1C* levels in the optic tectum appeared not to fluctuate over the 24 hour period (Figure 4.2.1.d.-E; one-way ANOVA, $F_{5,21}$=1.262 p=0.3169). The absolute levels for *Mel-1C* mRNA receptor showed a presence slightly higher than the base line in this tissue (50ng; Figure 4.2.1.d.-F).

Cerebellum tissue showed that *Mel-1A* was slightly rhythmic (Figure 4.2.1.e.-A; one-way ANOVA, $F_{5,27}$=3.170 p=0.0223; Tukey's, ZT10vs22 q=4.579). The expression was slightly higher in the dark phase than in the light phase, though this difference is only slightly difference. The absolute levels of *Mel-1A* for the cerebellum tissue (Figure 4.2.1.e.-B) showed that the mRNA levels varied between 25ng and 40ng. *Mel-1B* receptor mRNA appeared to be biphasic in the cerebellum tissue (Figure 4.2.1.e.-C) and also peaked at ZT2, similar to the optic tectum, but the peak was later in the dark phase at ZT18 (mid-dark phase). The greatest peak was found at ZT18 and the lowest level at ZT10 (one-way ANOVA, $F_{5,11}$=5.079 p=0.0117, Tukey's, ZT2vs10 q=4.839; ZT10vs18 q=6.351). This rhythm was clearly mirrored in the absolute data of the *Mel-1B* receptor in the cerebellum tissue (Figure 4.2.1.e.-D) with the low levels around 25ng and peak at ZT18 clearly at the 75ng level. *Mel-1C* expression in the cerebellum showed a slight variation around the mean value; with the lowest point of expression around ZT22 and gradually the expression rose to ZT18 (Figure 4.2.1.e.-E; one-way ANOVA, $F_{5,19}$=1.297 p=0.3066). The absolute levels for this tissue (Figure 4.2.1.e.-F) showed a clear rise in receptor expression; lowest at ZT 2 and rising throughout the day and peaking in the early dark phase (ZT14), but the standard errors for the rise in gene expression were too variable to significant.

In the telencephalon there appeared to be a significant rhythm in the *Mel-1A* receptor expression (Figure 4.2.1.f.-A). Receptor levels were high around the on-set of light (ZT0) and declined two hours after the on-set of light. Levels then dropped significantly between ZT6 and ZT10. Before levels increased steadily after the off-set of light and continuing to rise until ZT 22 (Figure 4.2.1.f.-A; one-way ANOVA, $F_{5,29}$=3.981 p=0.0072; Tukey's, ZT10vs22 q=4.759). The rhythm for the *Mel-1B* receptor in the telencephalon (Figure 4.2.1.f.-C; one-

way ANOVA $F_{5,23}$=1.834 p=0.1458) also appeared to be biphasic; with a peak in the middle of the light (ZT6) and dark (ZT18) periods. After each peak the expression rapidly decreased to be at the lowest levels (~40ng) two hours before the onset of light (ZT10) or the onset of the dark phase (ZT22). This rhythm was matched in both the normalised (Figure 4.2.1.f.-C) and absolute (Figure 4.2.1.f.-D) data sets; though the absolute data set showed a robust rhythm of the *Me-1B* receptor mRNA in the telencephalon tissue. Levels of the *Mel-1C* receptor gene are shown not to rhythmically expressed in the telencephalon (Figure 4.2.1.f.-E; one-way ANOVA, $F_{5,22}$=2.826 p=0. 0406) but there were very high levels seen in the tissue throughout the 24 hours (≤60ng; Figure 4.2.1.f.-F). No fourth-order polynomial curve could be fitted to the telencephalon data for the *Mel-1C* receptor gene.

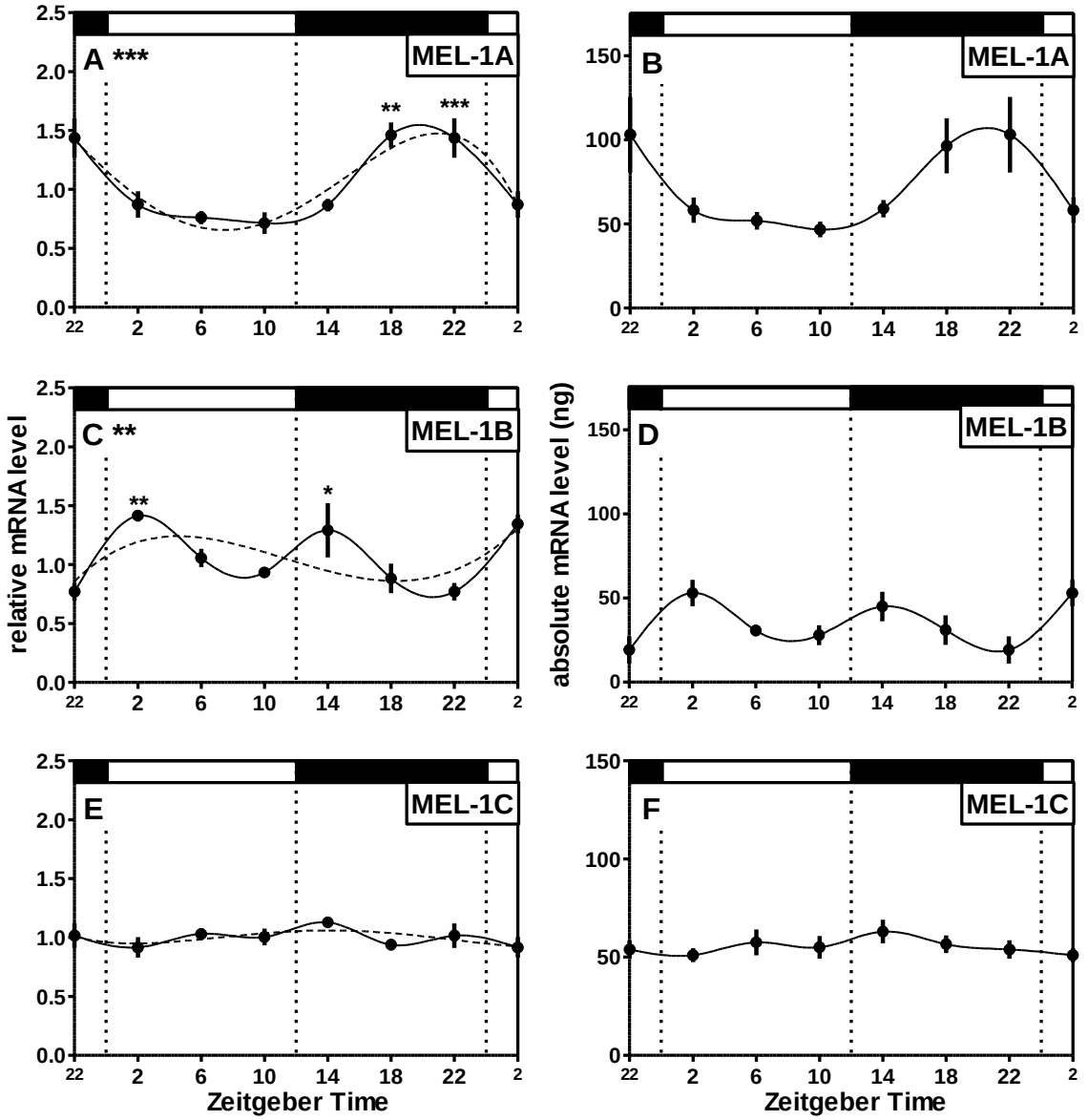

Figure 4.2.1.d. Expression profiles of melatonin receptors *Mel-1A, Mel-1B and Mel-1C* mRNA in the zebra finch optic tectum tissue. Temporal expression of normalised data (A,C,E), i.e. relative mRNA values normalised to *TBP* mRNA expression shown as variation from mean value, and (B,D,F) absolute mRNA values, i.e. raw data. The bars at the top of each graph indicate the LD 12:12 hrs light/dark schedule, i.e. light periods represented by white bars and dark period represented by black bars. The symbols represent mean values for each time point ± SEM (n=4-6). ZT2 and ZT22 are double plotted for better visualisation. Fourth order polynomial (dashed line) and lowess (black line) curves were fitted with GraphPad prism. Significant differences as revealed by ANOVA indicated by * on figure letter; significant differences between times points, i.e. to the lowest value of mRNA expression, as revealed by post hoc Tukey test indicated by * above the corresponding symbols: *p<0.05, **p<0.01, ***p<0.001. X-axis: Zeitgeber time. See Appendix I – Section 1.2.2 for statistical analysis.

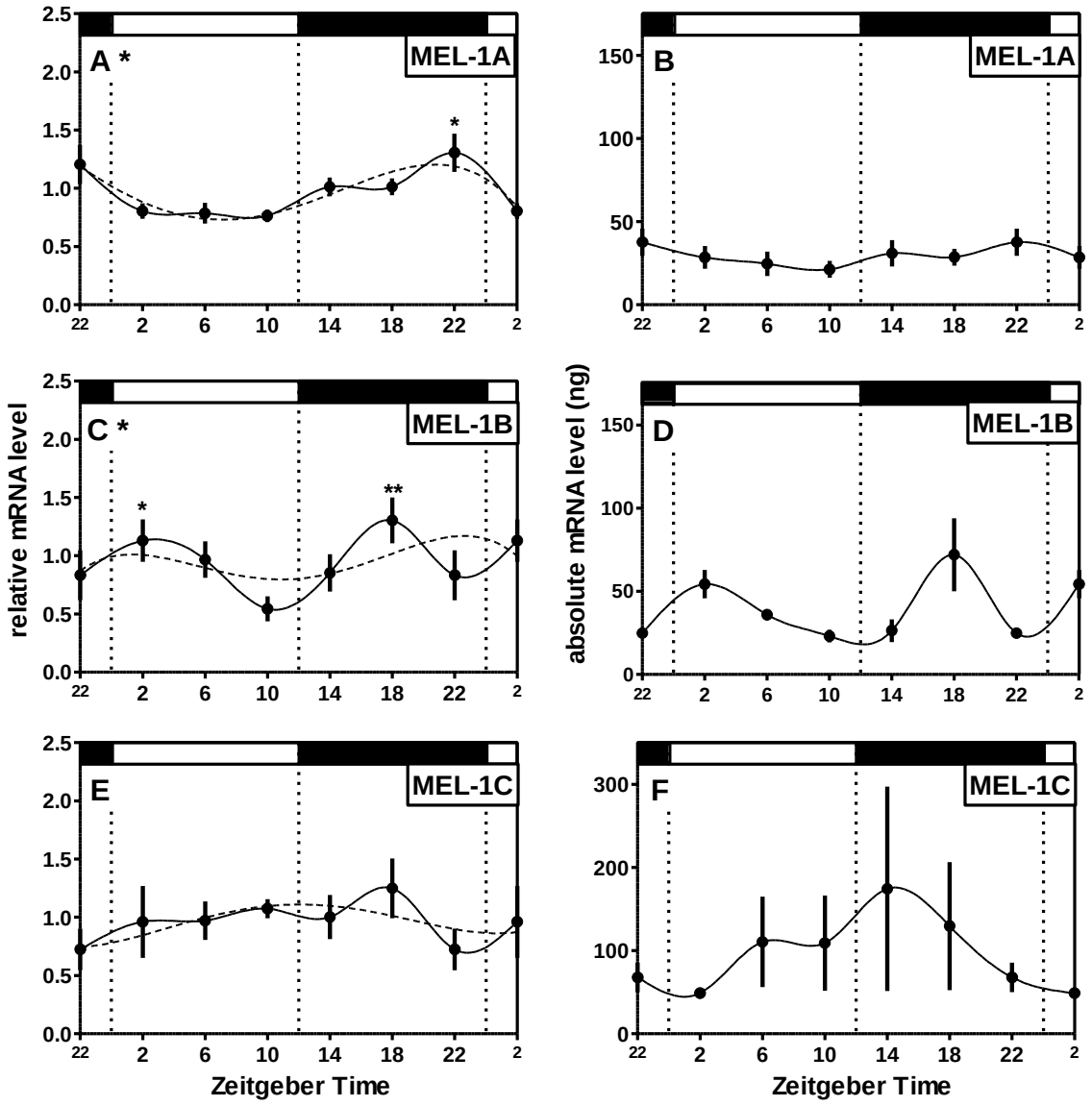

Figure 4.2.1.e. Expression profiles of melatonin receptors *Mel-1A, Mel-1B and Mel-1C* mRNA in the zebra finch cerebellum tissue. Temporal expression of normalised data (A,C,E), i.e. relative mRNA values normalised to *TBP* mRNA expression shown as variation from mean value, and (B,D,F) absolute mRNA values, i.e. raw data. The bars at the top of each graph indicate the LD 12:12 hrs light/dark schedule, i.e. light periods represented by white bars and dark period represented by black bars. The symbols represent mean values for each time point ± SEM (n=4-6). ZT2 and ZT22 are double plotted for better visualisation. Fourth order polynomial (dashed line) and lowess (black line) curves were fitted with GraphPad prism. Significant differences as revealed by ANOVA indicated by * on figure letter; significant differences between times points, i.e. to the lowest value of mRNA expression, as revealed by post hoc Tukey test indicated by * above the corresponding symbols: *p<0.05, **p<0.01, ***p<0.001. X-axis: Zeitgeber time. See Appendix I – Section 1.2.2 for statistical analysis.

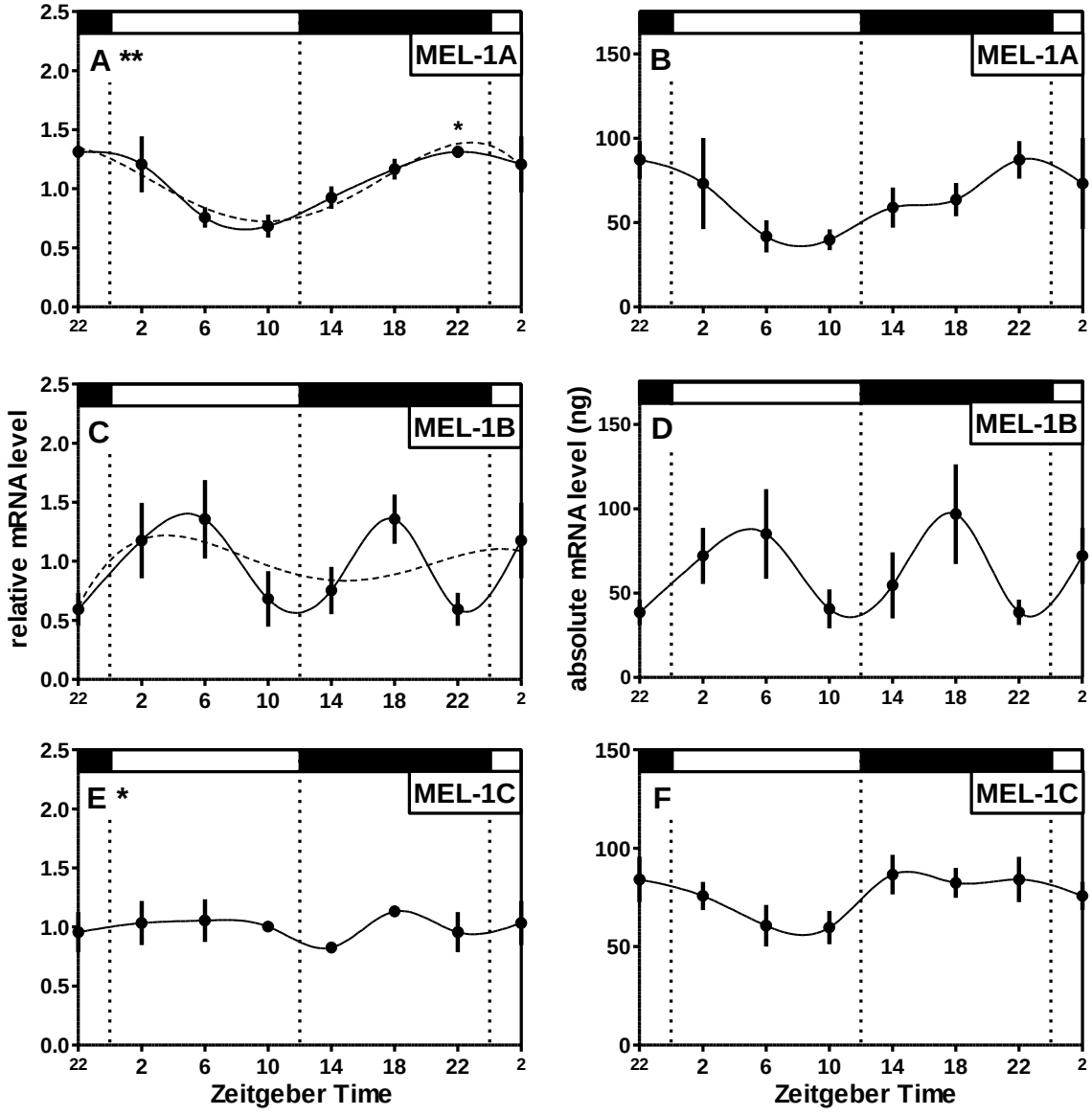

Figure 4.2.1.f. Expression profiles of melatonin receptors *Mel-1A, Mel-1B and Mel-1C* mRNA in the zebra finch telencephalon tissue. Temporal expression of normalised data (A,C,E), i.e. relative mRNA values normalised to *TBP* mRNA expression shown as variation from mean value, and (B,D,F) absolute mRNA values, i.e. raw data. The bars at the top of each graph indicate the LD 12:12 hrs light/dark schedule, i.e. light periods represented by white bars and dark period represented by black bars. The symbols represent mean values for each time point ± SEM (n=4-6). ZT2 and ZT22 are double plotted for better visualisation. Fourth order polynomial (dashed line) and lowess (black line) curves were fitted with GraphPad prism. Significant differences as revealed by ANOVA indicated by * on figure letter; significant differences between times points, i.e. to the lowest value of mRNA expression, as revealed by post hoc Tukey test indicated by * above the corresponding symbols: *p<0.05, **p<0.01, ***p<0.001. X-axis: Zeitgeber time. See Appendix I – Section 1.2.2 for statistical analysis.

4.2.1 Zebra finch expression of melatonin receptors in the peripheral tissues

To reveal whether the similar patterns of the different melatonin receptors (*Mel-1A*, *Mel-1B* and *Mel-1C*) mRNA expression found in the brain tissues were detectable in peripheral tissues, melatonin receptor expression was also analysed in the heart, liver, lung and kidney of the zebra finch (Figure 4.2.2.a; Figure 4.2.2.b; Figure 4.2.2.c).

Mel-1A mRNA receptor levels in heart, lung and kidney were low and arrhythmic (Figure 4.2.2.a.-A.C&D). There was a significant rhythm found in the liver (Figure 4.2.2.a.-B) with peak expression at ZT2 (one-way ANOVA, $F_{5,30}$=4.321 p=0.0044), two hours after the onset of light and then mRNA levels dropped throughout the rest of the time points. The lowest levels of the Mel-1A receptor were found in the dark period between ZT14 and ZT22. After ZT22, levels rose with the onset of light at ZT0. Absolute levels (Figure 4.2.2.a.-F) showed that a very low level of this receptor was found in the liver, it showed that there was a slight increase at ZT2. In the heart there was little variation of *Mel-1A* throughout the 24 hour period (Figure 4.2.2.a.-A; one-way ANOVA, $F_{5,30}$=2.258 p=0.0741). At ZT2 and ZT18, two hours after the onset of light and mid-dark period, there was a slight increase in the receptor mRNA. The lowest expression was between ZT14-18 (early-mid dark phase), after this *Mel-1A* mRNA expression rose at ZT18. In the lung, there was a slight rhythm of *Mel-1A* mRNA (Figure 4.2.2.a.-C; one-way ANOVA, $F_{5,29}$=0.8022 p=0.5573); with the lowest levels being around the onset of light (ZT0) and gradually increasing towards the off-set of light (ZT12). In the kidney, there was very little variation around the mean throughout the 24 hour period (Figure 4.2.2.a.-D; one-way ANOVA, $F_{5,14}$=1.116 p=0.3960). The absolute value for the *Mel-1A* receptor mRNA for each tissue showed that there were low amounts of mRNA found in

any of the tissues; the maximum was expression ≤30ng just above the "background noise" level (Figure 4.2.2.a.-E-H).

Interestingly, three out of the four studied peripheral tissues showed significant *Mel-1B* mRNA receptor rhythms with tissue-specific peak expression times (Figure 4.2.2.b.). *Mel-1B* receptor mRNA levels in the heart showed a rhythm (Figure 4.2.2.b.-A&E), with high levels throughout the light period, peaking at ZT2 (Figure 4.2.2.b.-A; Tukey's, ZT2vs22 q=5.544) and ZT10 (Figure 4.2.2.b.-A; Tukey's, ZT10vs22 q=7.079), with a slight decrease in between these two times points (one-way ANOVA, $F_{5,19}$=7.582 p=0.0005). After the beginning of the dark period (at ZT12) *Mel-1B* mRNA levels dropped in the heart to the lowest level ZT22. mRNA levels then rose sharply across the time points when the onset of light occurred lights, at ZT0. The absolute data (Figure 4.2.2.b.-E) showed a high level of the *Mel-1B* receptor throughout the 24 hours, i.e. even at the lowest level (ZT22) it was the level is higher than the 100ng level.

The *Mel-1B* rhythm in the liver (Figure 4.2.2.b.-B&F) again showed a high receptor level throughout the light period (ZT0-12; Figure 4.2.2.b.-B.; one-way ANOVA $F_{5,20}$=12.32 p=<0.0001; Tukey's, ZT2vs22 q=8.174, ZT6vs22 q=8.307, ZT10vs22 q=7.087). The *Mel-1B* receptor mRNA declined after ZT10, as the on-set of the dark period arrived. Levels dropped dramatically when the light period ended and two hours after the lights off at ZT14 levels remained low throughout the dark period. The receptor expression stayed low until two hours before lights on at ZT22 were *Mel-1B* mRNA increased rapidly, showing a clear endogenous rhythm rising before the activation of the light entrainment. The *Mel-1B* rhythm found in the liver had an opposite rhythm to the circulating melatonin rhythm. Similar to the heart, Mel-1B

in the liver was at a constantly high level (≥60ng absolute data; Figure 4.2.2.b.-F) even at the low plateau was above 50ng.

In the lung the *Mel-1B* receptor showed a different rhythm (Figure 4.2.2.b.-C&G) compared to the rhythms found in the heart and liver. The mRNA peaked at the on-set of the dark period between ZT10 and ZT14, with the onset occurring at ZT12 (Figure 4.2.2.b.-C; one-way ANOVA, $F_{5,22}$=8.591 p=0.0001; Tukey's, ZT10vs22 q=6.075 and ZT14vs22 q=7.126). Even though the rhythm had a different peak expression ZT, the lowest expression level was still found during the dark phase at ZT22, as with the other tissues. Absolute levels (Figure 4.2.2.b.-G), showed that the receptor was present at a high levels with the lowest level being 75ng at ZT22 and peak levels being around the 100ng at Z12.

In the kidney (Figure 4.2.2.-D&H) proved to be the only peripheral tissue with no significant rhythm of the *Mel-1B* receptor (Figure 4.2.2.b.-D; one-way ANOVA, $F_{5,12}$=0.6803 p=0.6470). Even though there is no statistical significance for this tissue, there are two peaks in the receptor level, one between ZT2-6 in the light phase and one at ZT18 in the dark phase, with the expression levels dropping, in between these peaks, to the lowest point at ZT10. Though, in this tissue the absolute data (Figure 4.2.2.b.-H) showed that the receptor was expressed around the 50ng mark (Figure 4.2.2.b.-D).

The *Mel-1C* receptor rhythms in the peripheral tissues are shown in Figure 4.2.2.c. Like the *Mel-1A* receptor, no significant rhythm was found in three of four peripheral tissue studied; heart (Figure 4.2.2.c.-A; one-way ANOVA, $F_{5,30}$=0.5104 p=0.7661), liver (Figure 4.2.2.c.-B; one-way ANOVA, $F_{5,30}$=0.4462 p=0.7982), or lung (Figure 4.2.2.c.-C; one-way ANOVA,

$F_{5,29}$=0.6603 p=0.6563), but there was a significant rhythm found in the kidney (Figure 4.2.2.c.-D; one-way ANOVA, $F_{5,10}$=5.449 p= 0.0112).

The absolute graphs for the heart liver and lung (Figure 4.2.2.c-E,F&G), showed there was constant very low levels of the Mel-1C receptor in all three tissues.

In the kidney *Mel-1C* receptor mRNA rhythm peaked in the early light phase at ZT2 (Figure 4.2.2.c.-D; Tukey's, ZT2vs18 q=6.281) two hours after the on-set of light. After the peak at ZT2, the expression dropped towards the mid-to-late light period (ZT6 and ZT10) and at ZT10 the expression seemed to plateau throughout the dark period (ZT14-18). Until around two hours (ZT22) before the on-set of light the expression started to rise again to ZT2. The rhythm found in the absolute data (Figure 4.2.2.c.-H) showed the peak expression at ZT6 not ZT2, this could be due to the variability of the raw data. The absolute data confirmed that a low level of Mel-1C mRNA expression was found in this tissue (Figure 4.2.2.c.-H).

Absolute mRNA levels indicated clear differences in melatonin receptor density between tissues with *Mel-1A* being generally low in all peripheral tissues, *Mel-1B* showing high mRNA levels in heart, lung, and liver, and *Mel-1C* being highest in liver and kidney.

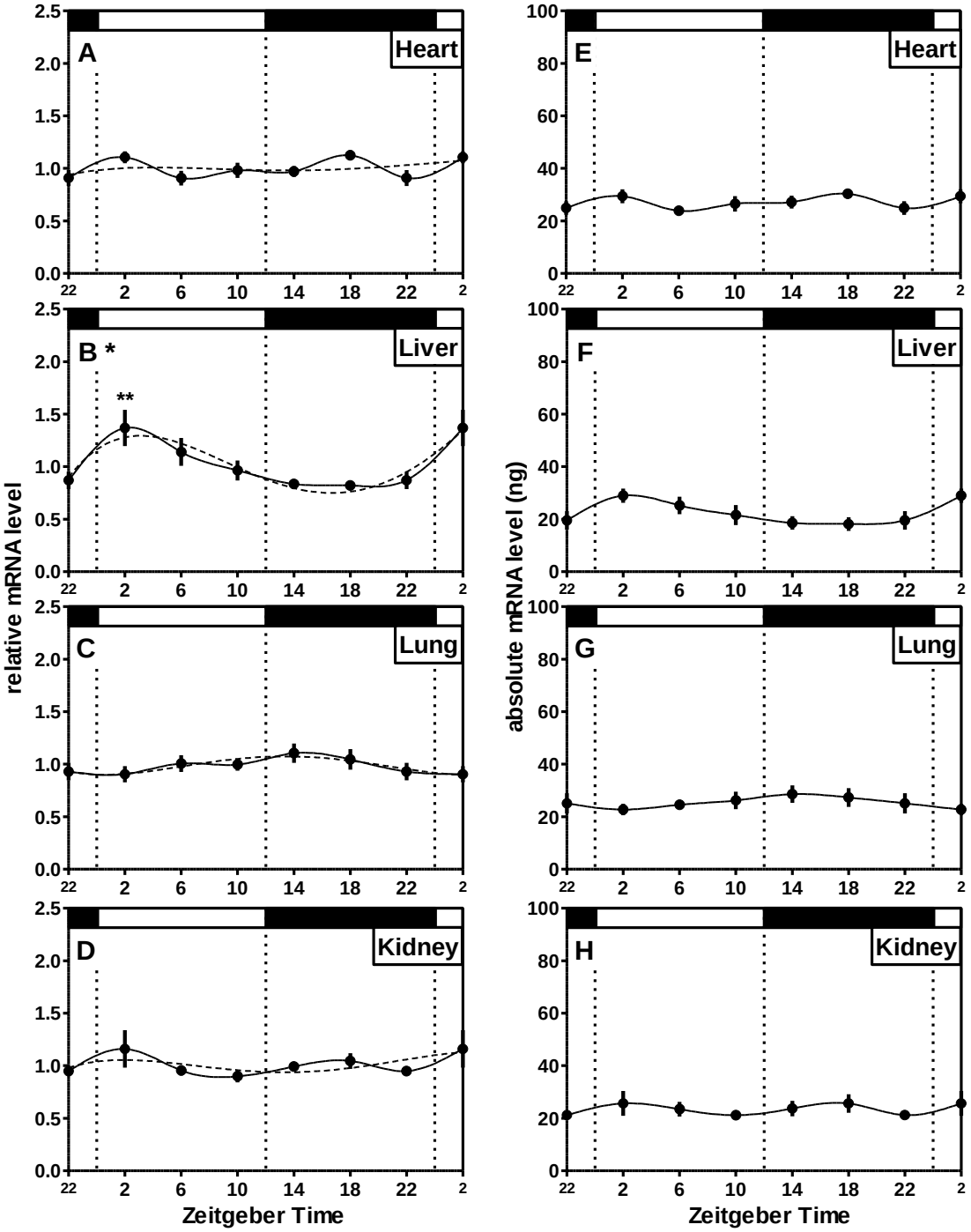

Figure 4.2.2.a. Expression profiles of melatonin receptor *Mel-1A* mRNA of zebra finch peripheral tissues. Temporal expression of normalised data (A-D), i.e. relative mRNA values normalised to *TBP* mRNA expression shown as variation from mean value, and (E-H) absolute mRNA values, i.e. raw data. The bars at the top of each graph indicate the LD 12:12 hrs light/dark schedule. The symbols represent mean values for each time point ± SEM (n=4-6). ZT2 and ZT22 are double plotted for better visualisation. Fourth order polynomial (dashed line) and lowess (black line) curves were fitted with GraphPad prism. Significant differences as revealed by ANOVA indicated by * on figure letter; significant differences between times points, i.e. to the lowest value of mRNA expression, as revealed by post hoc Tukey test indicated by * above the corresponding symbols: *p<0.05, **p<0.01, ***p<0.001. See Appendix I – Section 1.2.3 for statistical analysis.

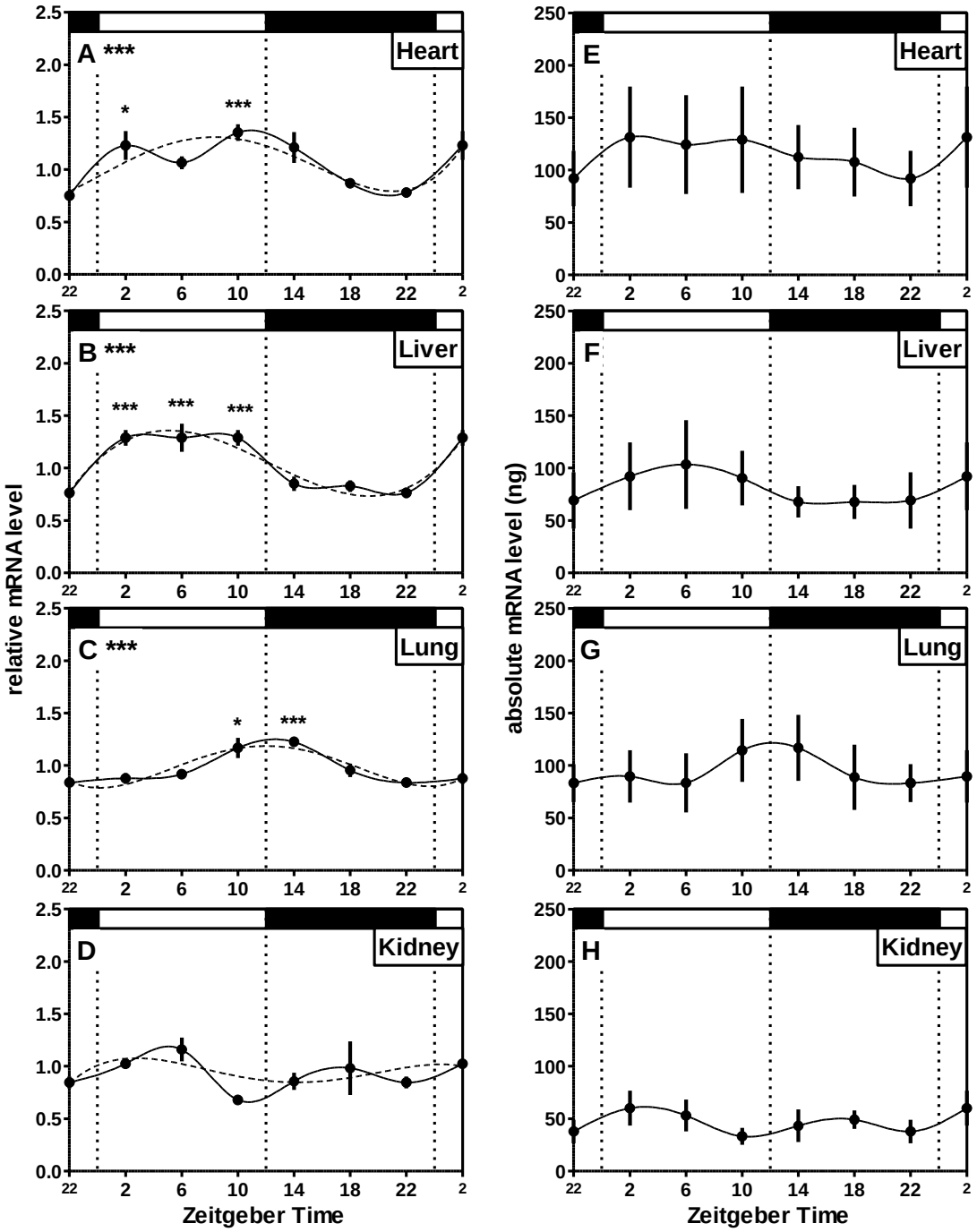

Figure 4.2.2.b. Expression profiles of melatonin receptor *Mel-1B* mRNA of zebra finch peripheral tissues. Temporal expression of normalised data (A-D), i.e. relative mRNA values normalised to *TBP* mRNA expression shown as variation from mean value, and (E-H) absolute mRNA values, i.e. raw data. The bars at the top of each graph indicate the LD 12:12 hrs light/dark schedule. The symbols represent mean values for each time point ± SEM (n=4-6). ZT2 and ZT22 are double plotted for better visualisation. Fourth order polynomial (dashed line) and lowess (black line) curves were fitted with GraphPad prism. Significant differences as revealed by ANOVA indicated by * on figure letter; significant differences between times points, i.e. to the lowest value of mRNA expression, as revealed by post hoc Tukey test indicated by * above the corresponding symbols: *p<0.05, **p<0.01, ***p<0.001. See Appendix I – Section 1.2.3 for statistical analysis.

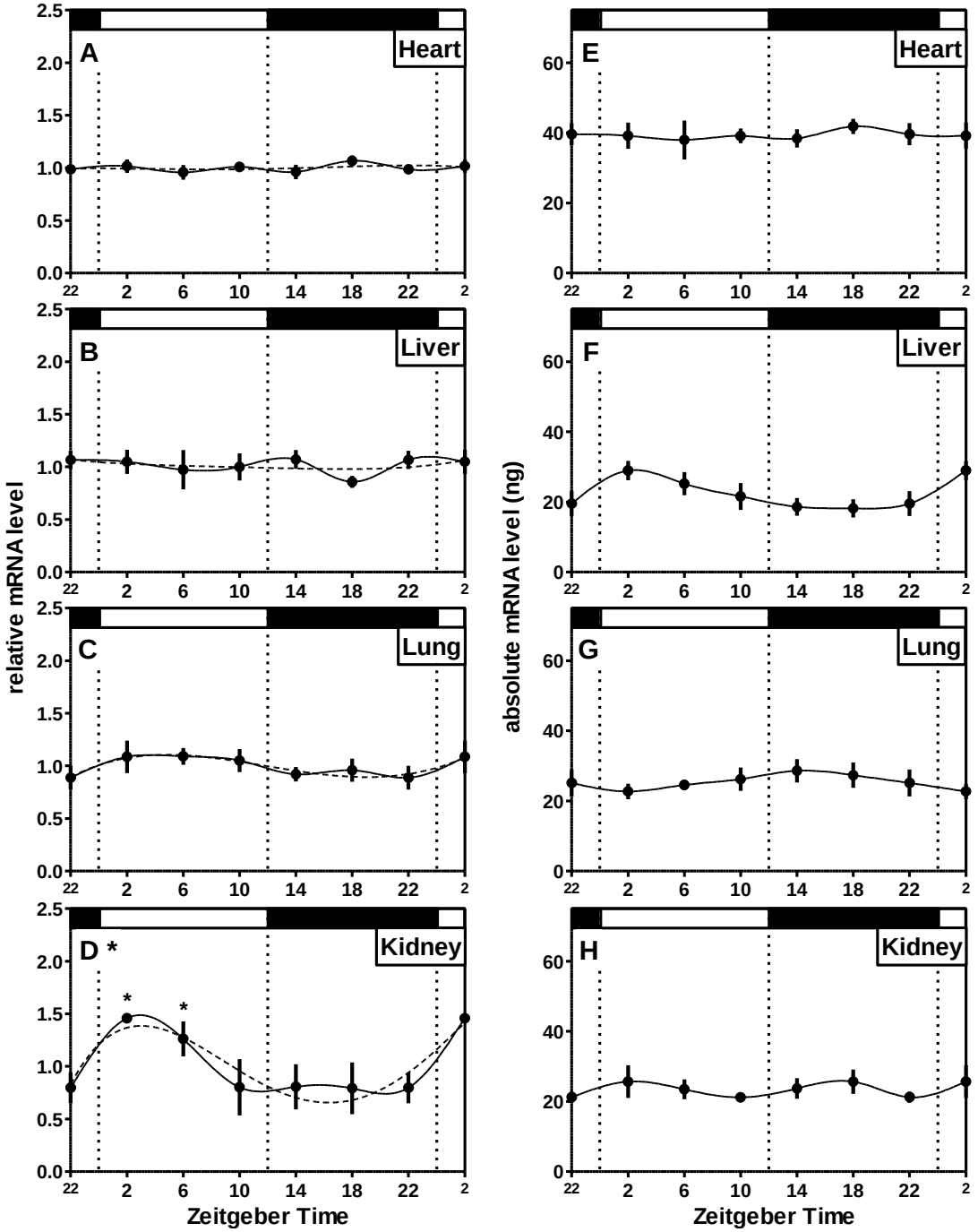

Figure 4.2.2.c. Expression profiles of melatonin receptor *Mel-1C* mRNA of zebra finch peripheral tissues. Temporal expression of normalised data (A-D), i.e. relative mRNA values normalised to *TBP* mRNA expression shown as variation from mean value, and (E-H) absolute mRNA values, i.e. raw data. The bars at the top of each graph indicate the LD 12:12 hrs light/dark schedule. The symbols represent mean values for each time point ± SEM (n=4-6). ZT2 and ZT22 are double plotted for better visualisation. Fourth order polynomial (dashed line) and lowess (black line) curves were fitted with GraphPad prism. Significant differences as revealed by ANOVA indicated by * on figure letter; significant differences between times points, i.e. to the lowest value of mRNA expression, as revealed by post hoc Tukey test indicated by * above the corresponding symbols: *p<0.05, **p<0.01, ***p<0.001. See Appendix I – Section 1.2.3 for statistical analysis.

4.3 Discussion

To date very few studies have looked at the mRNA rhythms of the known melatonin membrane receptors in mammalian and non-mammalian vertebrates. Non-vertebrates, including birds, possess complex circadian systems with multiple photic input mechanisms and multi-oscillator control of circadian rhythmicity (Gwinner and Brandstaetter, 2001). I found *Mel-1A*, *Mel-1B* and *Mel-1C* receptor mRNA expression in all parts of the zebra finch brain that are known to contain autonomous circadian clocks, i.e. retina, pineal gland and diencephalon. *Mel-1A* and *Mel-1B* were found to be rhythmic in the retina and diencephalon while *Mel-1C* receptor was found in these tissues its expression was not rhythmic. *Mel-1B* was found to be rhythmic in the pineal gland in contrast to *Mel-1A* and *Mel-1C* receptors. *Mel-1A* receptor was found to show nocturnal rhythms with peak expression levels during the second half of the night in all parts of the brain apart from the pineal gland. *Mel-1B* receptor expression was most variable with nocturnal rhythms in the pineal gland and the diencephalon reaching highest levels at the end of the night and in the transition from dark to light, a diurnal rhythm was found in the retina that peaked at ZT10, and biphasic expression patterns in tectum opticum, cerebellum, and telencephalon. *Mel-1C* receptor was not found to be significantly rhythmic in any of the brain regions studied although considerable mRNA levels were present.

In passerine birds, such as the zebra finch and house sparrow, the only source of circulating melatonin is the pineal gland (Brandstaetter, 2002). As melatonin production is controlled by an autonomous circadian clock in songbirds, one would predict that there would be no melatonin membrane receptors found in this gland unless they serve auto-regulatory feedback mechanisms. My data set confirms that all three melatonin receptors are present in the pineal

gland with *Mel-1B* being the only receptor that was rhythmically expressed. Interestingly, pineal *Mel-1B* receptor expression appears to peak at the end of the dark phase (ZT22) when melatonin production declines suggesting that *Mel-1B* receptors may indeed act as negative feedback and contribute to the termination of melatonin production at the end of the night. In birds melatonin levels declines before the onset of light, and has virtually disappeared when light is present, therefore the synthesis of melatonin is endogenously controlled since its decline occurs before the inhibitory factor of light becomes present (Brandstaetter, *et al*., 2001). The mechanism controlling this decline is still unknown, it could be controlled by the expression of clock genes and proteins or it could be coupled to a negative feedback loop controlled by clock up-regulating and melatonin receptors down-regulating or that melatonin controls the clock gene expression which initiated the morning oscillators *Per1-Cry1* (mammals) and *Per2-Cry1* (birds). It has been shown in the mammalian system that in the SCN rhythmic expression of clock genes (*Per1*, *Per2*, *Cry1* and *Rev-erbα*) and control clock controlled genes (e.g. arginine-vasopressin and D-element binding protein) are modulated by photoperiod, with a peak in expression earlier when subjected to long photo periods as to short photo periods (Hazlerigg, *et al*., 2005; Johnston, *et al*., 2005). In the long photo periods expression of the morning oscillators *Cry1* and *Per1* tracked the onset and offset of melatonin secretion, respectively, in the pituitary pars tuberalis; with *Cry1* also tracking the onset of melatonin under short photo periods (Johnston, *et al*., 2005). Thus with the data collected in this study that melatonin could drive the onset of the morning oscillatory genes in the avian system too, *Cry1-Per2*.

The mammalian MT2 receptor (homologue to the avian Mel-1B receptor) has been shown to be coupled to an inhibition of cyclic adenosine monophosphate (cAMP; MacKenziea, *et al*.,

2002) and cAMP has a positive effect on enzyme arylalkylamine-N-acetyl transferase (AANAT) which converts serotonin into N-acetylserotonin (Axelrod and Wurtman, 1968); a key enzyme in the synthesis of melatonin. Therefore if Mel-1B activation causes a decrease in cAMP in the pineal gland it is plausible that this causes a reduction of AANAT activity and therefore a reduction in melatonin production.

Interestingly, melatonin receptor expression mirrors the levels of nocturnal circulating melatonin in only some but not all tissues. While *Mel-1A* receptor expression reflects the presence of nocturnal melatonin in the diencephalon, retina, tectum opticum, cerebellum, and telencephalon with peak expression levels during the second half of the night, *Mel-1B* expression shows considerable variability between different brain regions. *Mel-1C* does not appear to be rhythmically expressed at all. The overall differences in absolute melatonin receptor mRNA levels are comparable with the findings of Reppert, *et al*., (1995b) in the chicken where no Mel-1A (CKA) was found within the cerebellum, liver, or pineal gland but within the diencephalon, telencephalon, retina and tectum opticum while high concentration of Mel-1C (CKB) were detected in the tectum opticum, hypothalamus, thalamus and pineal gland and low Mel-1C (CKB) concentration were found in the cerebellum and retina but not in the liver (Reppert, *et al*., 1995b)**.**

The non-rhythmic nature and the high expression of *Mel-1C* in some of the tissues is another remarkable outcome of this study. To exert the full physiological action, melatonin receptors may form functional dimers (Ayoub, *et al*., 2002) and it has been shown that the mammalian GPR50 modulates the function of mammalian Mel-1A (MT1) and Mel-1B (MT2) (Levoye, *et al*., 2006). Dufourny shows that the mammalian GPR50 is the mammalian ortholog of Mel-

1C (Dufourny, *et al*., 2008). The GPR50 receptor does not bind melatonin directly itself and can affect the affinity of the melatonin receptors (Dufourny, *et al*., 2008); heterodimerized with Mel-1A (MT1) receptor it has an inhibitory affect on the affinity of binding of melatonin; but not when it heterodimerized with the Mel-1B (MT2) receptor (Drew, *et al*., 1998). Data from this study could therefore suggest that this modulator role of Mel-1C/GPR50 is also important in birds, being the "constitutive" subunit of the hypothetical functional heterodimer (Mel-1A-Mel-1C or Mel-1B-Mel-1C). Rhythmic expression of the "regulatory" subunit (Mel-1A or Mel-1B) may decide the different role of melatonin on its target brain sites. The GPR50 receptor was shown to have limited distribution in the brain like the other melatonin receptors (MT1 and MT2) whereas in birds (chicken – (Natesan and Cassone, 2002) and zebra finch – this study) melatonin receptors (Mel-1A and Mel-1B) have a broad distribution throughout the brain as does the Mel-1C receptor. Therefore both Mel-1C and GPR50 mirror the distribution location of the other receptors to bind to and form their functional dimers. To examine this theory, future work of *in situ* hybridisation experiments for RNA levels or immunofluorescent localisation experiments for the receptor protein levels could determine whether the Mel-1C receptor does co-localise or dimerize with Mel-1A or Mel-1B receptor.

In the peripheral tissues of the zebra finch, melatonin receptor expression was highly variable. While liver showed rhythmic *Mel-1A* and *Mel-1B* expression, only *Mel-1B* receptor was found to be rhythmically expressed in lung and heart. Interestingly, kidney was the only tissue in this study that displayed a *Mel-1C* receptor rhythm. Peripheral tissues also differed in regard of the temporal organisation of melatonin receptor expression. While *Mel-1A* in the liver and *Mel-1C* in the kidney peak early in the day when circulating melatonin has declined

to baseline levels (Brandstaetter, *et al*., 2001b), *Mel-1B* is elevated throughout the day in heart and liver but peaks at the transition from light to dark in the lung but the kidney levels decline just before this transition. These data suggest distinct control mechanisms of melatonin in peripheral organs and diurnal rhythms of melatonin responsiveness that may relate to the rhythm of circulating melatonin mechanism (Gwinner and Brandstaetter, 2001; van't Hof and Gwinner, 1999).

The fascinating results seen in the kidney were the only receptor which was found to be rhythmic was Mel-1C mRNA, the fact that neither of the other two receptors were found to be rhythmic is very interesting. The mRNA level is very low in the kidney but it is found at the same level as other rhythmic receptors in the other tissues. Considering that the Mel-1C is thought to have a structural role and that Mel-1A and Mel-1B receptors are thought to be the rhythmical "regulatory" subunits. Along with the fact that the Mel-1C receptor was not found to be significantly rhythmic in any other tissue, it brings up the questions why this receptor is rhythmic in the kidney? Where AVT or AVP acts in a hormonal way on osmoregulation, could the Mel-1C receptor have an active role in this function?

In summary, the results represent a first comprehensive analysis of all three melatonin receptors at the mRNA level in a songbird species, the zebra finch. I show brain region-specific and peripheral tissue-specific rhythms in various brain and peripheral tissues of two of the melatonin receptors. With one receptor (*Mel-1B*) possibly highlighting a negative feedback mechanism, in the pineal gland, for the decline on circulating melatonin before the onset of light. The striking difference in melatonin receptor distribution between birds and mammals is another sign of the different evolutionary circadian paths of mammals as

compared to non-mammalian vertebrates. The ubiquitous presence of all melatonin receptor types throughout the brain and in all peripheral tissues of the zebra finch supports the hypothesis that melatonin acts as the major coordinator of circadian organisation at the whole-organism level in non-mammalian vertebrates such as birds. Non-mammalian vertebrates, including birds, possess complex circadian systems with multiple photic input mechanisms and multi-oscillator control of circadian rhythmicity with melatonin being believed to act as the major driver of coordinated circadian rhythmicity at the whole-organism level (Gwinner and Brandstaetter, 2001). This suggests or confirms how central melatonin is as an internal zeitgeber. Due to these result the next logical step was to examine the protein levels of melatonin receptors in and around the hypothalamus of the zebra finch (Chapter Five).

CHAPTER 5

Melatonin membrane receptor localisation in two avian circadian oscillatory regions

CHAPTER FIVE – MELATONIN MEMBRANE RECEPTOR LOCALISATION IN TWO AVIAN CIRCADIAN OSCILLATORY REGIONS

5.1 Introduction

The hormone melatonin is a vital competent in the circadian system, becoming active in the absence of light and inhibiting activity in the hypothalamus. In birds, noradrenaline (norepinephrine) is released during the day and binds to α2 adrenergic receptors in the pineal gland which inhibits AA-NAT activity and therefore melatonin production during the day (Zeman and Herichová, 2011), which creates the sleep stage of the sleep-wake cycle. Melatonin can act via membrane, nucleic and cytoplasmic receptors having numerous effects on different nuclei of the brain and different organs of the body. Since the identification of melatonin and its receptors, numerous studies have shown the presence of the membrane melatonin receptors to be wide spread in a number of brain regions, including the circadian oscillatory regions: the retina (Table 5.1.a), the hypothalamus (mammal – Dubocovich and Makowska, 2005; birds – Lu and Cassone, 1993; Reppert, *et al*., 1995b; Fish – Herrera-Pérez, *et al*., 2010) and the pineal gland.

The retina is a very important and specialised organ, composed of five different neuronal structures: the photoreceptors, horizontal cells, bipolar cells, amacrine cells and ganglion cells (Alarma-Estrany and Pintor, 2007). These different neurons conventionally form ten different cell layers in the retina which are the retinal pigmented epithelium, photoreceptor (rods and

cones), outer limiting membrane, the outer nuclear layer, outer plexiform layer, inner nuclear layer, inner plexiform, ganglion cell layer, nerve fibre layer and the inner limiting layer (Nolte, 2002; Figure 5.1.a.). The nuclear layers refer to the cell bodies, plexiform layers are where the nerve synapses are located and the inner and outer layers refer to the number of synapses by which the structure is separated from the brain, i.e. the photoreceptors are "outer" in respect to the bipolar cells in the inner nuclear layer (Nolte, 2002). Not only does the retina receive light and visual input, but also it can secrete melatonin (inner and outer retina - (Brandstaetter, 2002)). It has been reported that melatonin promotes dark-adaptive retinomotor movements, activates the photoreceptor disc shredding, it inhibits stimulation-evoked release of dopamine and acetylcholine, circadian changes to intraocular pressure, and also enhances the sensitivity of horizontal cells in the retina of the rat (Fujieda, *et al*., 1999; Rada and Wiechmann, 2006).

In some avian species, melatonin can be secreted into the circulating blood to affect the circadian oscillatory system, for example in chicken and quail, retinal melatonin secretion accounts for 50% of the circulating plasma melatonin (Karaganis, *et al*., 2009). However, not all avian species secret melatonin into the circulatory system; the house sparrow, a song bird, does not secret melatonin into the blood stream. Here the only source of circulating melatonin comes from the pineal gland (Heigl and Gwinner, 1995; Brandstaetter, *et al*., 2001b; Kumar and Gwinner 2005).

In the rat, the Mel-1A (MT1) receptor has been found in the inner and outer plexiform layers and in the horizontal cells of two week old rats, with staining in the plexiform layer in the ganglion and amacrine cells (Fujieda, *et al*., 1999). The MEL-1B (MT2) receptor was found

in the pigmented epithelial cells, in the photoreceptor inner segment, and the horizontal cells (Alarma-Estrany and Pintor, 2007). This is comparable to the melatonin binding sites that have been found in the chicken by *in situ* experiments, which show binding in the inner plexiform layer, ganglion cell layer, inner nuclear layer (Natesan and Cassone, 2002). *Mel-1A* and *Mel-1C* mRNA has been found in the chicken, primarily in the inner segment of the photoreceptor layer, the vitreal portion of the inner nuclear layer and the ganglion cell layer (Natesan and Cassone, 2002). Whereas the *Mel-1B* mRNA was seen to be much more widely spread with the receptor found throughout the entire photoreceptor layer, inner nuclear and ganglion layer (Natesan and Cassone, 2002). A summary of where the membrane melatonin receptors have been found within the retina and in which species can be seen in Table 5.1.a.

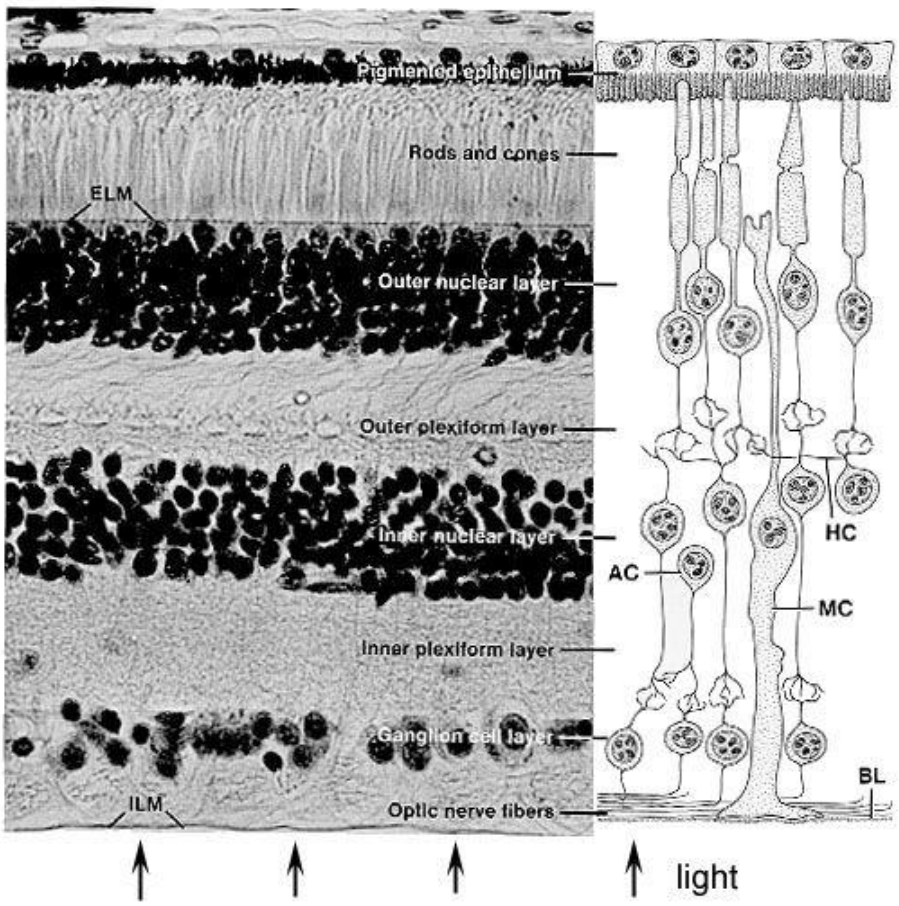

Figure 5.1.a. Schematic diagram of the retina showing the localization of the different cell types. Inner limiting membrane (ILM) is the boundary between the vitreous humor in the posterior chamber and the retina itself. Ganglion cell layer comprises the cell bodies and axons of ganglion cells. Inner plexiform layer (IPL) contains the synapses made between bipolar, amacrine and ganglion cells. The thickness of this layer varies considerably across species, where "simpler" organisms (such as frogs, pigeons and squirrels, for example) possess thicker IPL's than "higher" organisms like primates. The thicker IPL indicates that these retinas perform more peripheral and specialized image processing. Inner nuclear layer (INL) contains bipolar cell, horizontal and amacrine cell boides. Outer plexiform layer (OPL) contains bipolar cell, horizontal cell and receptor synapses. Outer nuclear layer (ONL) contains the nuclei of photoreceptors. Outer limiting membrane (OLM) is a membrane which coincides with the base of inner segments of photoreceptors. Photoreceptor layer contains the inner and outer segments of rod and cone photoreceptors. Pigment epithelium (PE) are darkly pigmented cells which absorb light not captured by photoreceptors, thus reducing scattering. HC – horizontal cell are laterally interconnecting neurons which help integrate and regulate the input from multiple photoreceptors; AC – amacrine cells are interneurons that interact at the second synaptic level of the vertically direct pathways; MC – Müller cells are the radial glial cells of the retina (from: http://www.psych.ndsu.nodak.edu/mccourt/Psy460 - Anatomy and Physiology of the Retina - retinal x-section.JPG).

Receptor subtype	Species & location	Reference
Mel-1A	Human - horizontal cells, amacrine cells, AII amacrine cells, inner segment of photoreceptor	Fujieda, *et al*., 1999 Meyer, *et al*., 2002 Savaskan, *et al*., 2002 Scher, *et al*., 2002 Scher, *et al*., 2003
	Rat - horizontal cells, inner/outer plexiform layers	Fujieda, *et al*., 1999 Fujieda, *et al*., 2000 Scher, *et al*., 2002
	Carp - horizontal cells, inner/outer plexiform layers	Huang, *et al*., 2005
	Guinea pig - Inner/outer plexiform layers	Fujieda, *et al*., 1999 Fujieda *et al*., 2000
	Chick - inner segment photoreceptors, inner nuclear layer, ganglion cell layer	Natesan and Cassone, 2002
	Monkey - AII amacrine cells	Scher, *et al*., 2003
	Xenopus - photoreceptors	Wiechmann and Smith, 2001
Mel-1B	Human	Reppert, *et al*., 1995b Scher, *et al*., 2002
	Xenopus - retinal pigmented epithelium, photoreceptors inner segments, horizontal cells	Wiechmann, *et al*., 2004
	Chick - retinal pigment epithelium, inner segment photoreceptor, nuclear layer, ganglion cell	Natesan and Cassone, 2002
Mel-1C	Chick - inner segment photoreceptor, inner nuclear layer, ganglion cell layer	Natesan and Cassone, 2002

Table 5.1.a. Melatonin receptor subtypes in the retinal tissue of different species (edited from Alarma-Estrany and Pintor, 2007).

As stated in pervious chapters, melatonin receptors have been found all over the avian brain using pharmacology and molecular techniques (Dubocovich, 1995) and 2-[^{125}I]iodomelatonin labelling (Reppert, *et al*., 1996). However, only a few studies compare the protein localisation of these receptors at different zeitgeber times (Rada and Wiechmann, 2006). In this chapter I examined the protein localisation of the three known melatonin membrane receptors studied in Chapter Three and Four of this thesis; MEL-1A, MEL-1B and MEL-1C. I performed immunofluorescent experiments on sections of retinal and hypothalamic tissues, two of the three oscillatory regions in birds, at ZT6 and ZT18. These times points were chosen due to the results obtained in Chapter Four which indicated that maximum mRNA expression of the receptors was found in the later dark period, between ZT18-22, for most tissues and ZT6-10 proved to have the lowest level of expression. The immunofluorescent experiments were performed to examine the exact anatomical distribution of these receptors.

5.2 Results

5.2.1 Antibodies and trials

Initially, Professor Jody Summer Rada and Professor Allan Wiechmann (The University of Oklahoma Health Sciences Centre, Oklahoma City, USA) provided information on dilution ratio's that they has successfully used in their immunofluorescent experiments with MEL-1A (1:200), but they were unsuccessful with the MEL-1B and MEL-1C antibodies. Due to this problem and since the antibodies were created for the chicken receptor sequences, I wanted to check that antibody sequences used by Professor Rada could be found in the zebra finch receptor sequences and therefore useable for these experiments. I compared the antibody sequences to the melatonin receptor sequences for zebra finch (Figure 5.2.1.a). I found that all three of the chicken antibody sequences were found in the zebra finch protein sequence, suggesting that the antibodies should react to the zebra finch melatonin receptors.

Initial dilution trials proved to be successful at 1:100 in the retinal tissues for both MEL-1B and MEL-1C antibodies using both ZT18 and ZT6 tissues, so future work was continued at this dilution. A 1:200 dilution for the MEL-1A antibody, described by Rada and Wiechmann (2006), was also successful using the protocols described in Chapter 2.3. Initial trials included controls to check for non-specific binding and that the receptors were present at these time points (Figure 5.2.1.b). The controls only showed slight fluorescence along the epithelia/choroid edge of the retinal tissue, whereas the tissues incubated with the melatonin antibodies show specific staining in the retinal tissue as well as along the epithelia/choroid edge.

Mel-1A

MRVNESELNSSVLPRDPPAEGAPRRQPWVTSTLAAILIFTIAVD
LLGNLLVILSVYRNKKLRNAGNVFVVSLAVADLIVAIYPYPLV
LTSVFHNGWKLGYLHCQISGFLMGLSVIGSIFNITGIAINRYCYI
CHSLKYDKLYSDRNSLCYIVLIWLLTFVAIVPNLFVGSLQYDP
RIYSCTFAQSVSSAYTIAVVFFHFLLPIAVVTFCYLRIWILVIQV
RRRVKPDNNPRLKPHDFRNFVTMFVVFVLFAVCWAPLNFIGI
AVAVNPKTVIPRIPEWLFVSSYYMAYFNSCLNAIVYGLLNQNF
RREYKRIIVNFCTAKVFFQDSSNDAGDRMRSKPSPLITNNNQV
KVDSV

Mel-1B

MLENGSLRNCCDPGGRGRLGLAEREAAAAGAPRPAWVVPVL
SSVLIFTTVVDILGNLLVILSVFKNRKLRNSGNAFVVSLALADL
VVALYPYPLVLLAIFHNGWTLGETHCKASGFVMGLSVIGSIFN
ITAIAINRYCYICHSFAYDKVYSCWNTMLYVSLVWILTVIATV
PNFFVGSLKYDPRIYSCTFVQTASSYYTIAVVVIHFIVPITIVSFC
YLRIWVLVLQVRRRVKSETKPRLKPSDFRNFLTMFVVFVIFAF
CWAPLNFIGLAVAIDPTEMAPKVPEWLFIISYLMAYFNSCLNAI
IYGLLNQNFRNEYKRISMSLWMPRLFFQDTSKGGTDGQKSKP
SPALNNNNQMKTETL

Mel-1C

MSHQRLPGTEQGEGGNIFVVSLSVADLVVAVYPYPLILSAIFH
NGWTMGNVHCQISGFLMGLSVIGSIFNITAIAINRYCYICHSLR
YDKLFNLKNTCCYLCLTWILTVVAIVPNFFVGSLQYDPRIYSC
TFAQTVSTSYTITVVVVHFIVPLSVVTFCYLRIWILVIQVKHRV
RQDCKQKLRAADIRNFLTMFVVFVLFAVCWGPLNFIGLAVSIN
PSKVQPHIPEWLFVLSYFMAYFNSCLNAVIYGLLNQNFRKEYK
RILLTLWTPRLLFIDVSKGGTEGMKSKHSPAITTNNNHAEIHL

Figure 5.2.1.a. Partial zebra finch melatonin receptor protein sequences and the antibody sequences (from NCBI: Mel-1A (NP_001041722), Mel-1B (NP_001041723) and Mel-1C (AAV66551)). The red highlighted sequences show the receptor antibody sequence for each receptor. The antibodies were donated by Prof. Jody Summers Rada, University of Oklahoma Health Sciences Centre, Oklahoma City and where created from the chicken receptor sequences.

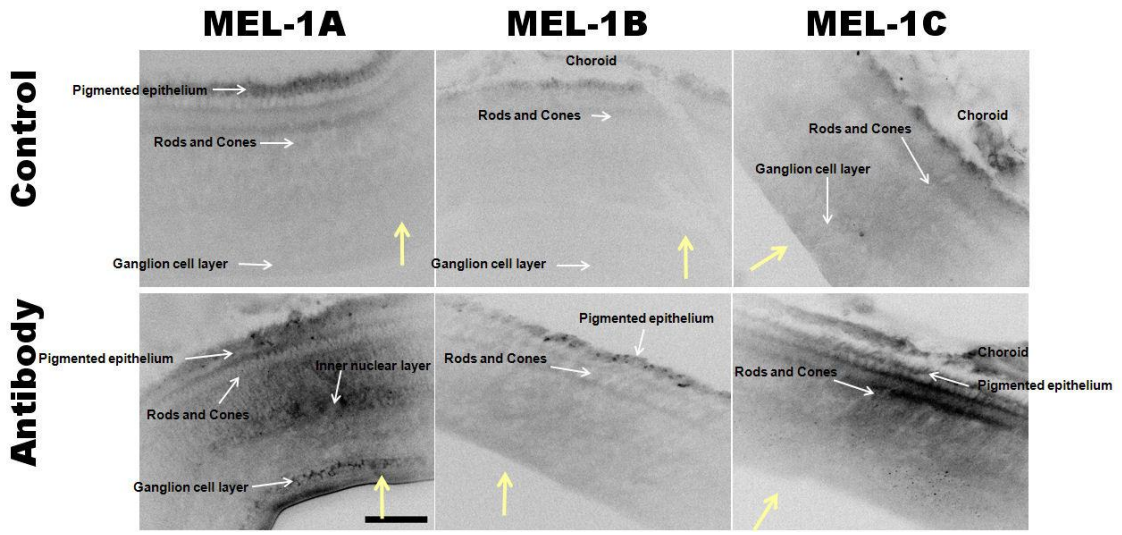

Figure 5.2.1.b. Melatonin receptor antibody tests at ZT18 in retinal tissues. Yellows arrows indicate the direction of light entering the retina. All images to the same scale bar of 50µm, as shown in MEL-1A antibody image.

5.2.2 Melatonin receptor expression in the hypothalamus at ZT6 and ZT18

A schematic diagram of the zebra finch brain is shown in Figure 5.2.2.a to help with the location of the cell groups mentioned in this section.

The melatonin receptor MEL-1A showed little expression localisation at ZT6 (Figure 5.2.2.b). The more dominant expression localisation was found in the rostral and medial areas of the hypothalamus. In the rostral region, the LHN staining appeared throughout this area (Figure 5.2.2.b.-B), whereas less expression was found in the cell groups around the third ventricle; PON, SCN and PPN (Figure 5.2.2.b.-A). More medially, the expression of MEL-1A receptor around the ventricle increased in the PON (Figure 5.2.2.b.-C), and expression in the LHN decreased (Figure 5.2.2.b.-D). Few cells containing MEL-1A receptors were found in the caudal areas of the hypothalamus at ZT6 (Figure 5.2.2.b.-E&F).

At ZT18, MEL-1A receptor expression appeared to increase. More positive cells were found throughout all the regions (rostral, medial and caudal) around the ventricle and lateral areas as compared to ZT6 (Figure 5.2.2.c). MEL-1A expression was found more rostrally around the ventricle particularly in the suprachiasmatic nucleus (SCN; Figure 5.2.2.c.-A), unlike at ZT6. Staining was also found in both areas (ventricle and LHN, Figure 5.2.2.c.-E&F respectively) in the caudal regions of the hypothalamus in contrast to ZT6. Additional staining was also found at ZT18 in the optic chiasm (Figure 5.2.2.c.-G) and optic tectum (Figure 5.2.2.c.-H).

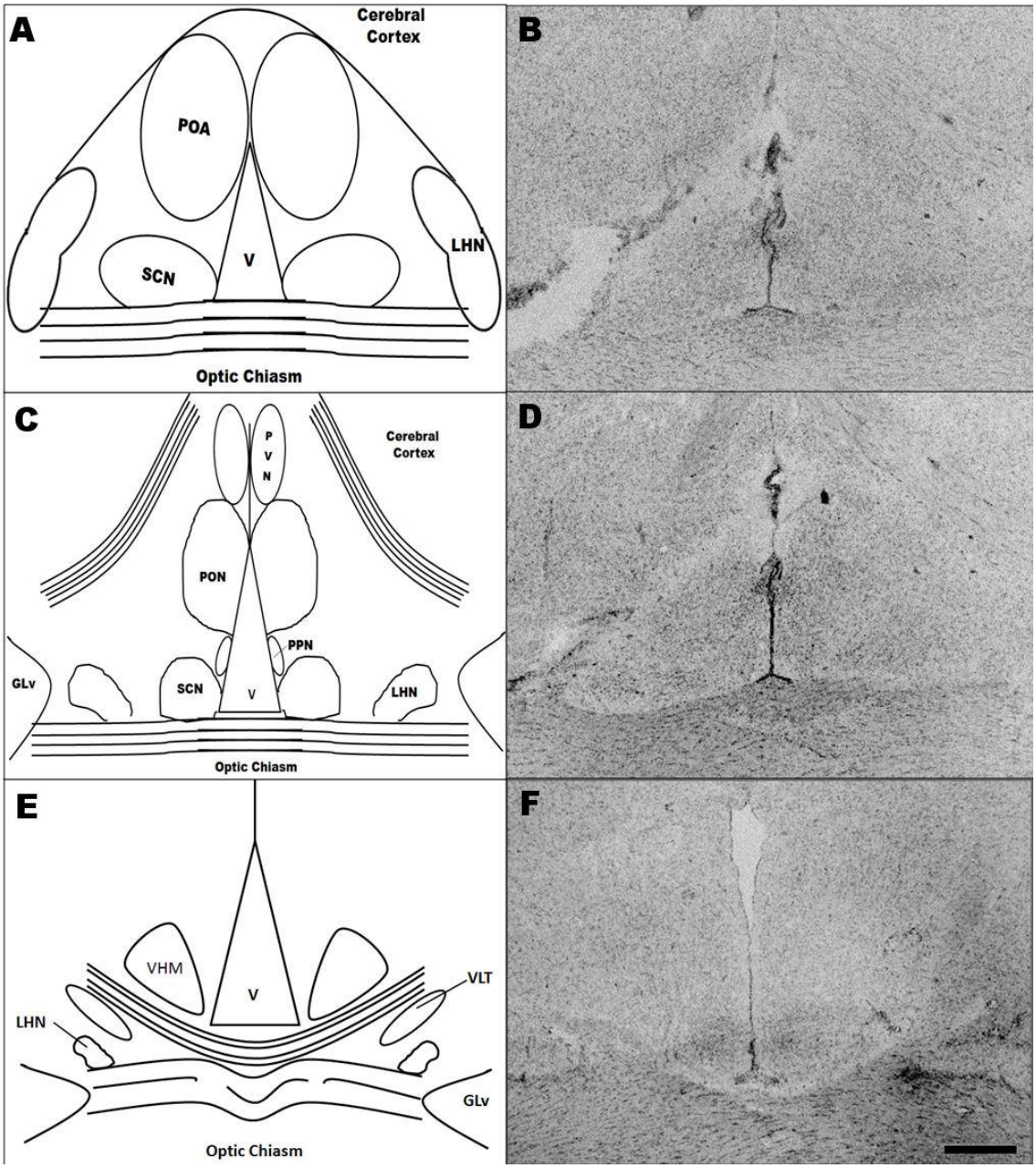

Figure 5.2.2.a. Schematic diagram (A,C,E) and Hoechst staining (B,D,F) in the hypothalamus, showing the three regions studied; rostral (A and B), medial (C and D) and caudal (E and F). These three regions are the areas examined in the following figures, to help showing the cell groups and their locations. GLv – lateral geniculate nucleus pars ventralis, LHN – lateral hypothalamic nucleus, POA – anterior preoptic nucleus, PON – preoptic nucleus, PPN – periventricular preoptic nucleus, SCN – suprachiasmatic nucleus, V – third ventricle, VLT – ventrolateral thalamic nucleus, VMN – ventromedial hypothalamic nucleus. All images to the same scale bar of 200µm, as shown in image F.

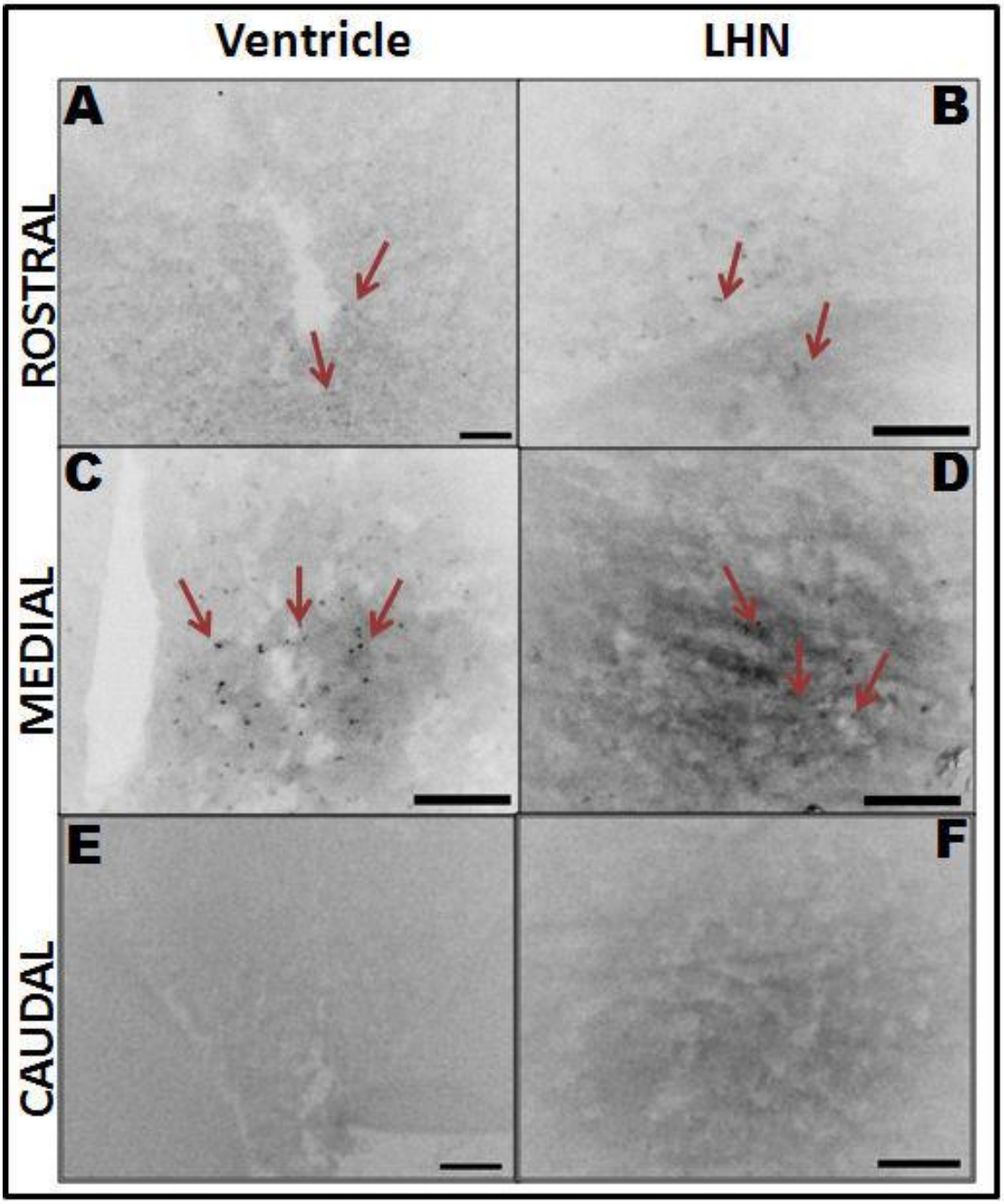

Figure 5.2.2.b. MEL-1A receptor localisation in the hypothalamus at ZT6. A&B show MEL-1A expression in the rostral region of the hypothalamus, around the ventricle area (A) and more laterally in the LHN (B). C&D show MEL-1A expression in the medial region of the hypothalamus, around the ventricle area (C) and more laterally in the LHN (D). E&F show MEL-1A expression in the caudal region of the hypothalamus, around the ventricle area (E) and more laterally in the LHN (F). Red arrows indicate the positive cells expressing MEL-1A receptor. The lighting schedule for the samples is highlighted by the colour of the background of the image; the samples here where taken at ZT6 in the light period and therefore has a white background. Scale bars: Image A, B, C, D & F= 50µm; E = 200µm

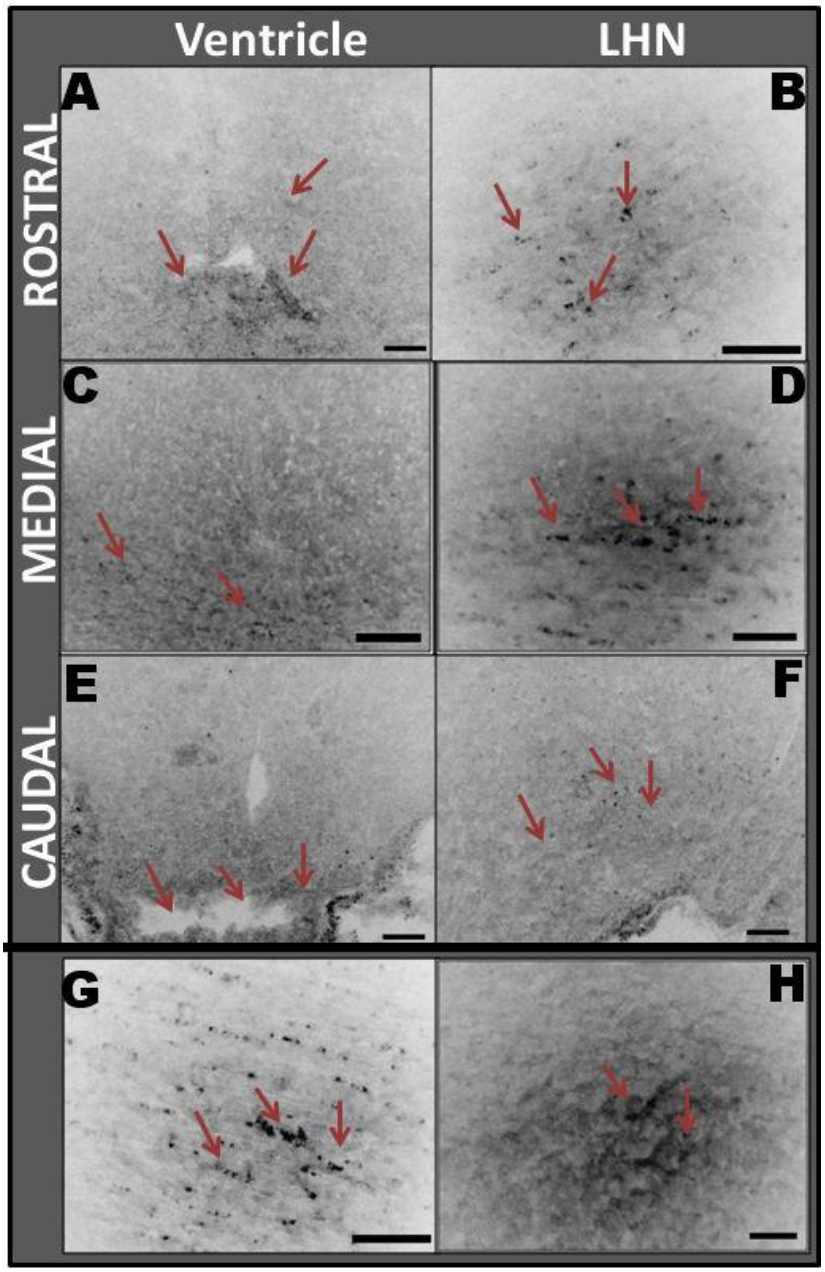

Figure 5.2.2.c. MEL-1A receptor localisation in the hypothalamus at ZT18. A&B show MEL-1A expression in the rostral region of the hypothalamus, around the ventricle area (A) and more laterally in the LHN (B). C&D show MEL-1A expression in the medial region of the hypothalamus, around the ventricle area (C) and more laterally in the LHN (D). E&F show MEL-1A expression in the caudal region of the hypothalamus, around the ventricle area (E) and more laterally in the LHN (F). G, shows positive cells found in the optic chiasm at ZT18. H, shows positive cells found in the optic tectum at ZT18. Red arrows indicate some of the positive cells expressing MEL-1A receptor. The lighting schedule for the samples is highlighted by the colour of the background of the image; the samples here where taken at ZT18 in the dark period and therefore has a dark background. Scale bars: Image A, B, D, E, F and G= 50µm; C and H = 100µm.

MEL-1B expression localisation at ZT6 (Figure 5.2.2.d) showed that there was little staining in cells around the third ventricle in any of the regions (rostral, medial or caudal; Figure 5.2.2.d.-A,C&E respectively). A few sporadic MEL-1B positive cells were found throughout the hypothalamus. In the LHN, there was a faint expression seen in the neuronal body of a few cells from rostral to caudal (Figure 5.2.2.d.-B,D&F). In contrast to the MEL-1B expression found at ZT6, expression seen at ZT18 was more intense throughout both the ventricle and lateral areas (Figure 5.2.2.e.). Expression in the rostral region of the PON (Figure 5.2.2.e.-A&B) show heavily stained cells with staining appearing to be around the membrane of the nerve cells. This expression pattern was seen throughout the other areas containing MEL-1B cells at ZT18. In the medial area around the third ventricle staining was found below the ventricle around the SCN region (Figure 5.2.2.e.-D&E), this shows again within the cell body but also along the axons away from the body of the cell. Cellular expression was also seen in the caudal region around the third ventricle in areas of the PON and PVN (Figure 5.2.2.e.-G&H). In the LHN of the hypothalamus there were cells positively expressing MEL-1B throughout the cell group, i.e. rostral (Figure 5.2.2.e.-C), medial (Figure 5.2.2.e.-F) and caudal (Figure 5.2.2.e.-I) areas, the staining in this nucleus appeared to be restricted to the soma of the neuronal cell.

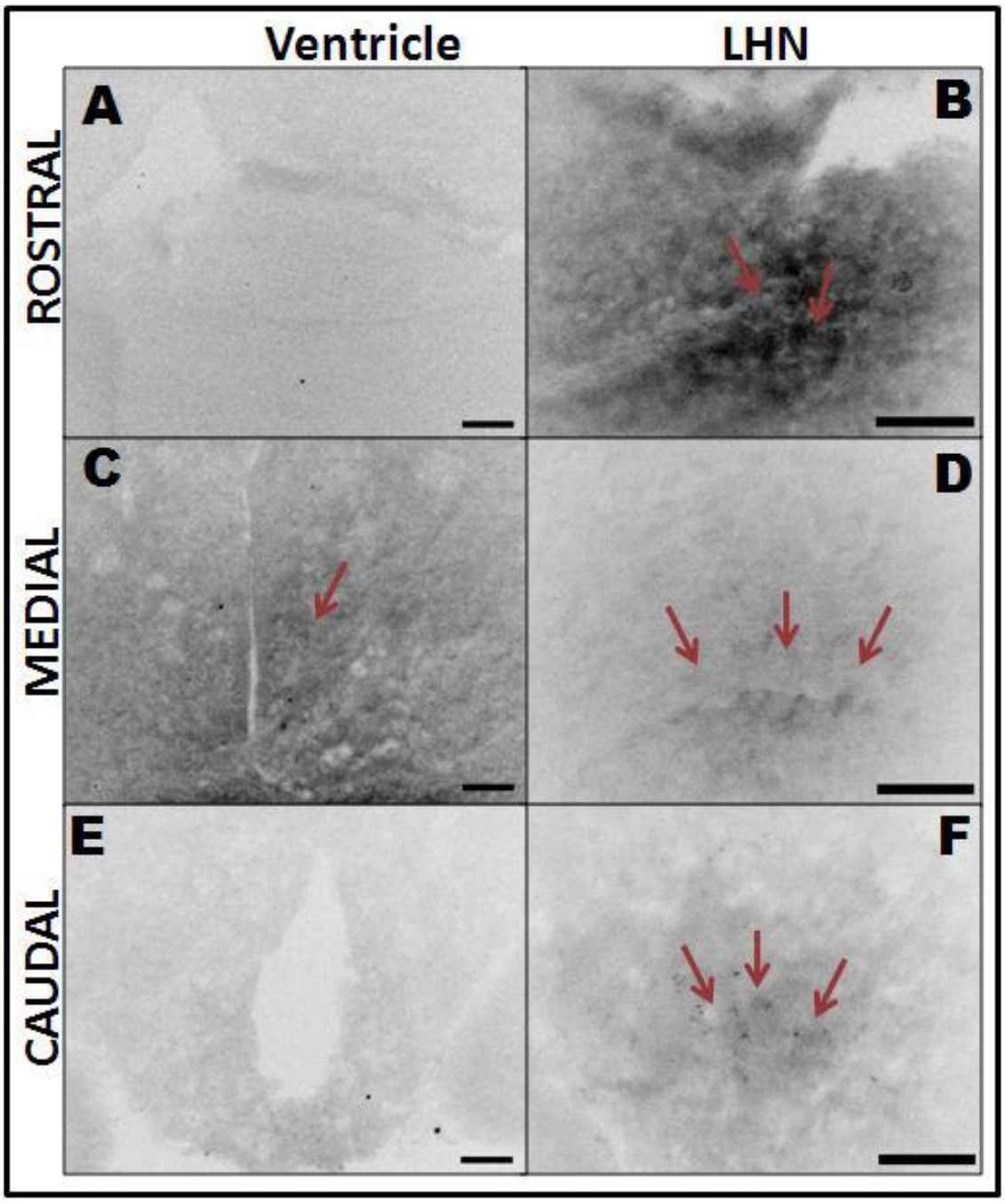

Figure 5.2.2.d. MEL-1B receptor localisation in the hypothalamus at ZT6. A&B show MEL-1B expression in the rostral region of the hypothalamus, around the ventricle area (A) and more laterally in the LHN (B). C&D show MEL-1B expression in the medial region of the hypothalamus, around the ventricle area (C) and more laterally in the LHN (D). E&F show MEL-1B expression in the caudal region of the hypothalamus, around the ventricle area (E) and more laterally in the LHN (F). Red arrows indicate some of the positive cells expressing MEL-1B receptor. The lighting schedule for the samples is highlighted by the colour of the background of the image; the samples here where taken at ZT6 in the light period and therefore has a white background. Scale bars: Image B, D, E, F = 50µm; A = 100µm.

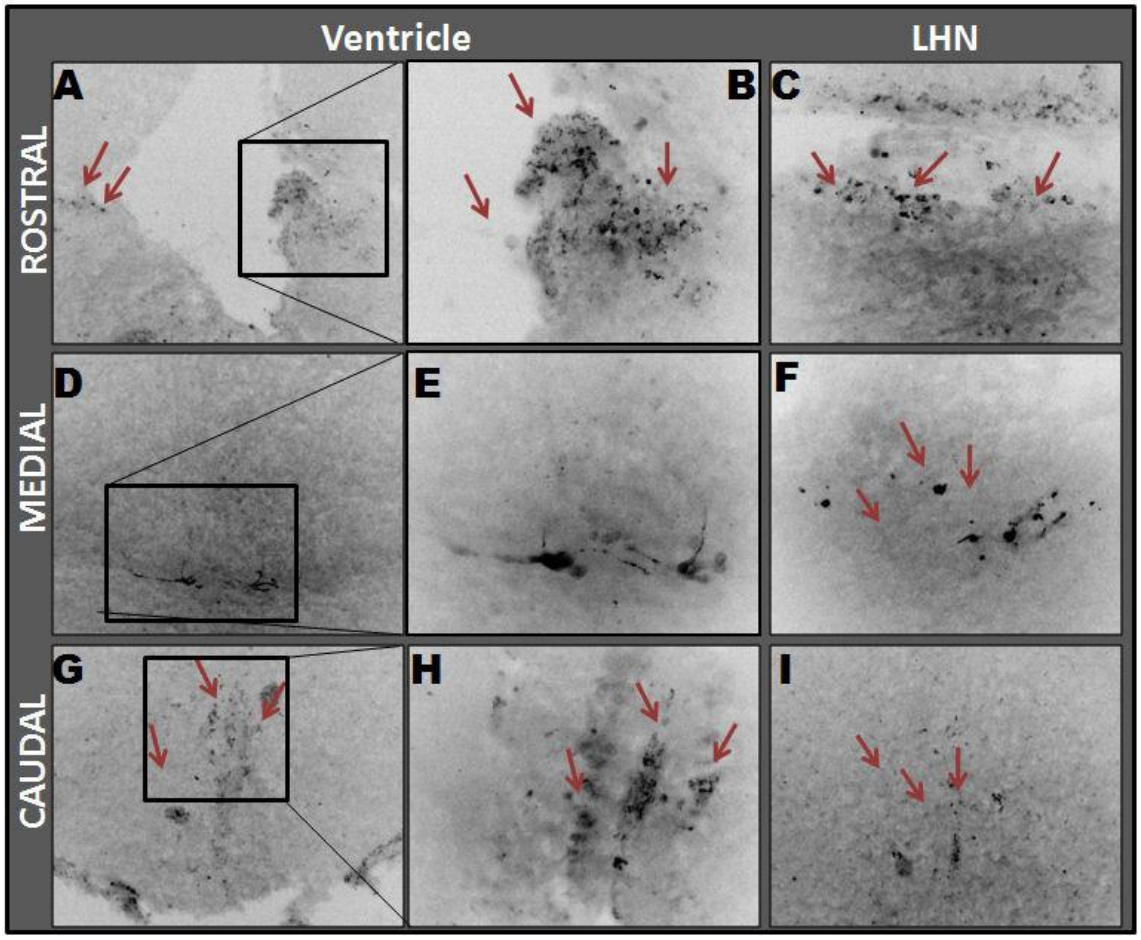

Figure 5.2.2.e. MEL-1B receptor localisation in the hypothalamus at ZT18. A,B&C show MEL-1B expression in the rostral region of the hypothalamus, around the ventricle area (A&B) and more laterally in the LHN (C). C,D&E show MEL-1B expression in the medial region of the hypothalamus, around the ventricle area (C&D) and more laterally in the LHN (E). F,G&H show MEL-1B expression in the caudal region of the hypothalamus, around the ventricle area (F&G) and more laterally in the LHN (H). Red arrows indicate some of the positive cells expressing MEL-1B receptor. The lighting schedule for the samples is highlighted by the colour of the background of the image; the samples here where taken at ZT18 in the dark period and therefore has a dark background. Scale bars: All Image = 50µm.

The MEL-1C receptor showed expression localisation throughout the hypothalamus at both ZT6 and ZT18 (Figure 5.2.2.f and Figure 5.2.2.g respectively). At ZT6, MEL-1C expression was seen in the rostral, medial and caudal regions around the ventricle (Figure 5.2.2.f.-A,C&E), in the PON and SCN, and the LHN (Figure 5.2.2.f.-B,D&F). In the high magnification images staining was shown to be along cells in the LHN and SCN (Figure 5.2.2.f.-G&I; respectively), in the SCN staining was also seen in the dendrites and axons leading away from the soma. MEL-1C positive cells were also found along the border between the optic tectum and optic chiasm (Figure 5.2.2.f.-H).

At ZT18, there was a dense collection of positive cells found in the inferior corner of the third ventricle leading towards the rostral SCN region (Figure 5.2.2.g.-A), these cells were staining along the neuronal cell and branching out away from the cell body. In the medial and caudal regions of the hypothalamus around the third ventricle staining was less dense with sporadic staining (medial - Figure 5.2.2.g.-C and caudal - Figure 5.2.2.g.-E). In the LHN, staining was seen in the cell bodies in the rostral and medial regions, but there was little staining present in the caudal areas of this nucleus (rostral - Figure 5.2.2.g.-B, medial - Figure 5.2.2.g.-D and caudal Figure 5.2.2.g.-E). High magnification images in the rostral regions of the PON (Figure 5.2.2.g.-G) LHN (Figure 5.2.2.g.-H) and within the PVN (Figure 5.2.2.g.-I) reveal the MEL-1C receptor towards the membrane and cytoplasm of the neuronal cells.

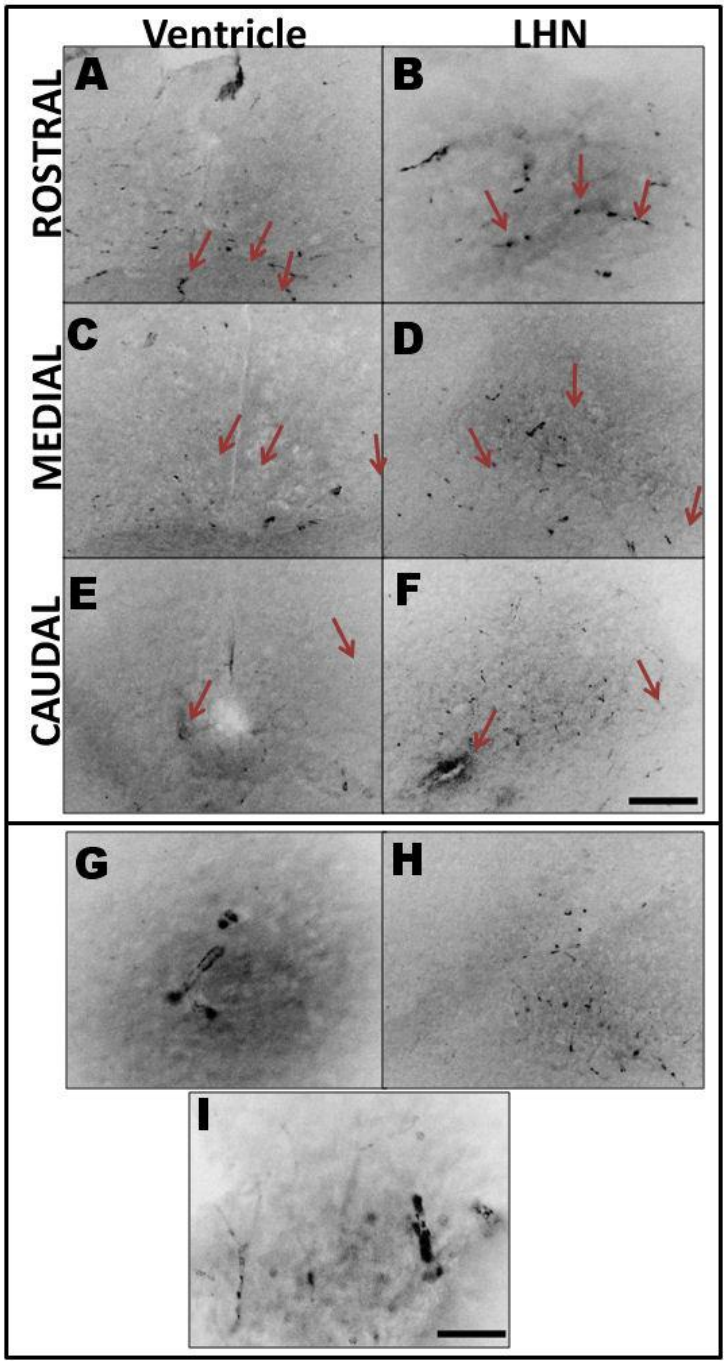

Figure 5.2.2.f. MEL-1C receptor localisation in the hypothalamus at ZT06. A&B shows MEL-1C expression in the rostral region of the hypothalamus, around the ventricle area (A) and more laterally in the LHN (B). C&D show MEL-1C expression in the medial region of the hypothalamus, around the ventricle area (C) and more laterally in the LHN (D). E&F show MEL-1C expression in the caudal region of the hypothalamus, around the ventricle area (E) and more laterally in the LHN (F). Additional staining was also found in the border between the optic chiasm and optic tectum (H). High magnification of cellular staining found in the LHN (G) and SCN (I). Red arrows indicate some of the positive cells expressing MEL-1C receptor. The lighting schedule for the samples is highlighted by the colour of the background of the image; the samples here where taken at ZT6 in the light period and therefore has a white background. All images are to scale bar of 50µm seen in image F & I.

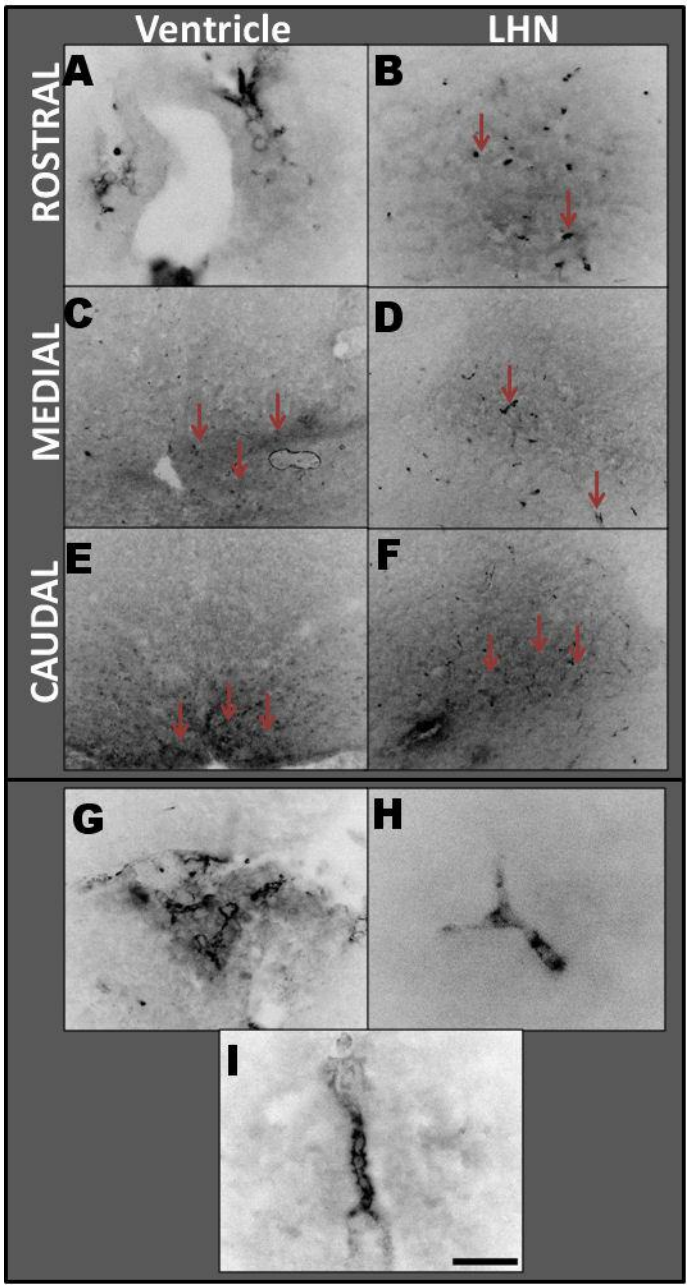

Figure 5.2.2.g. MEL-1C receptor localisation in the hypothalamus at ZT18. A&B shows MEL-1C expression in the rostral region of the hypothalamus, around the ventricle area (A) and more laterally in the LHN (B). C&D show MEL-1C expression in the medial region of the hypothalamus, around the ventricle area (C) and more laterally in the LHN (D). E&F show MEL-1C expression in the caudal region of the hypothalamus, around the ventricle area (E) and more laterally in the LHN (F). High magnification of cellular staining found in the PON (G), LHN (H) and within the paraventricular nucleus (I). H and I show blood vessel staining. Red arrows indicate some of the positive cells expressing the MEL-1C receptor. The lighting schedule for the samples is highlighted by the colour of the background of the image; the samples here where taken at ZT18 in the dark period and therefore has a dark background. All images are to scale bar of 50µm seen in image I.

From the results for the immunofluorescent experiments I summarised and compared the difference in receptor distribution. Figure 5.2.2.h shows a schematic diagram representing the results from the rostral and medial regions of the hypothalamus where to most abundant and variations of staining between the two time points were found (Figure 5.2.2.h).

There was a great difference in expression location and density between the receptors, in both the rostral and medial regions of the hypothalamus. MEL-1C appeared more widely expressed throughout the whole of the hypothalamic area, slightly increasing at ZT18 as compared to ZT6. Whereas the MEL-1A and MEL-1B receptors appeared in more isolated cell groups and dramatically increased in the dark phase (ZT18) compared to the light phase (ZT6) in both the rostral and medial regions. MEL-1A and MEL-1B receptors were limited to the LHN and PON in the rostral regions of the hypothalamus at ZT6 (Figure 5.2.2.h.-A), with expression increasing at ZT18 in these cell groups. MEL-1A and MEL-1B positive cells were also seen along ependymal layer of the third ventricle and in the SCN at ZT18 (Figure 5.2.2.h.-B). In the medial regions the MEL-1A receptor was seen only in the LHN and PON at both ZT6 and ZT18, though expression increased at ZT18 compared to the expression found at ZT18 (Figure 5.2.2.h.-C&D). The MEL-1B receptor had a greater distribution in the medial regions, being found in the LHN, PON, SCN and along the third ventricle border along the ependymal layer at ZT6 (Figure 5.2.2.h.-C) and at ZT18 this also increased in cell number but was also found in the PVN and close the PPN cell groups (Figure 5.2.2.h.-D).

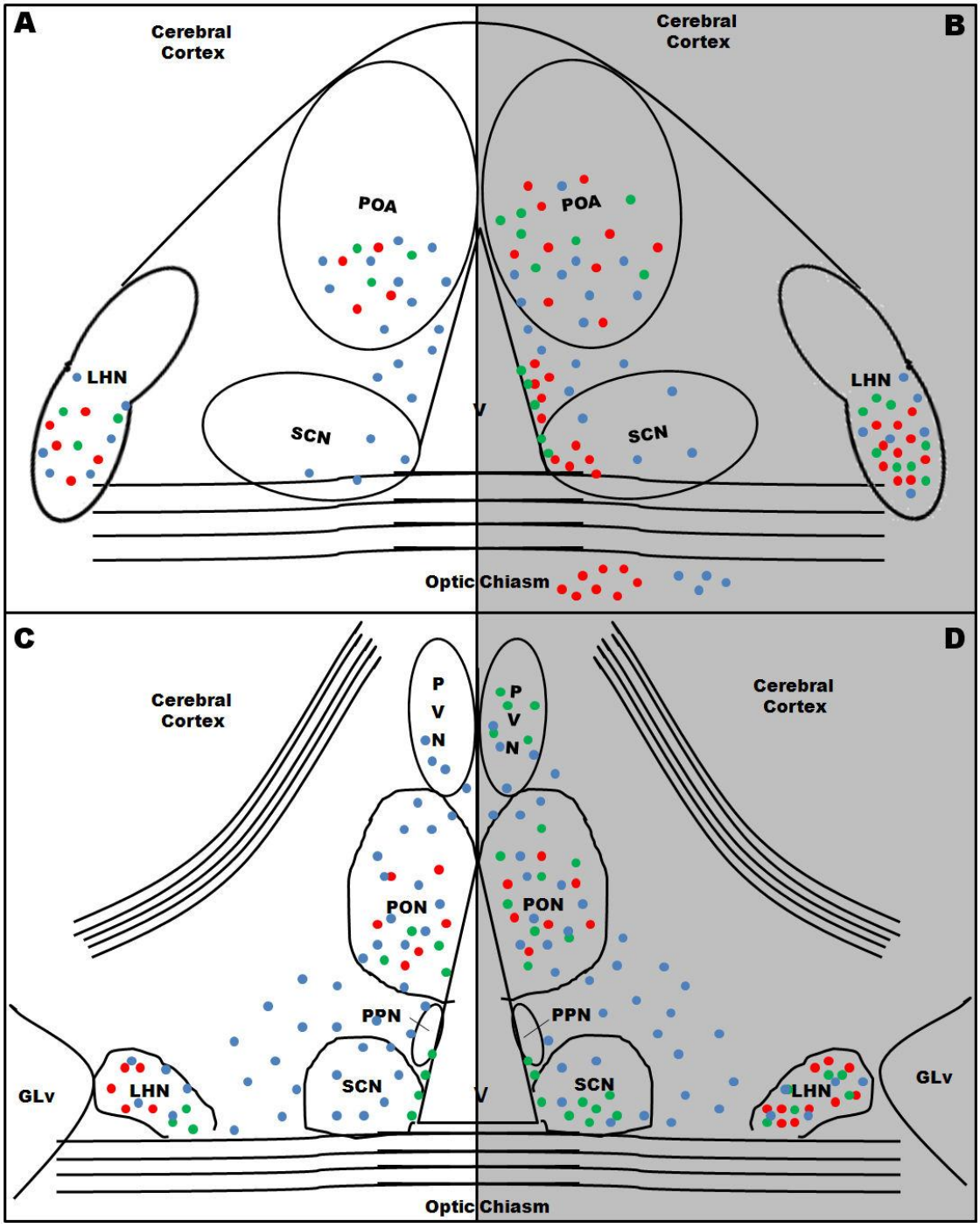

Figure 5.2.2.h. Schematic diagram comparing the location of the three melatonin membrane receptors, MEL-1A, MEL-1B and MEL-1C, in the hypothalamus at ZT6 and ZT18. Images A and B show the location of the different receptors in the rostral region of the hypothalamus at ZT6 (A) and ZT18 (B). Images C and D show the location of the different receptors in the medial region of the hypothalamus at ZT6 (C) and ZT18 (D). Red dots represent the location of MEL-1A receptor. Green dots highlight the areas where MEL-1B receptor was present. The blue dots show where the MEL-1C receptor was present. The background colour indicates the lighting schedule of the time points. GLv – lateral geniculate nucleus pars ventralis, LHN – lateral hypothalamic nucleus, POA/PON – anterior preoptic nucleus/preoptic nucleus, PPN – periventricular preoptic nucleus, SCN – suprachiasmatic nucleus, V – third ventricle.

5.2.3 Melatonin receptor expression in the retina at ZT6 and ZT18

A schematic diagram of the zebra finch retina is shown in Figure 5.2.3.a to help with the location of the cell layers mentioned in this section.

MEL-1A receptor expression was found throughout most of the layers in the retina (Figure 5.2.3.b and Figure 5.2.3.c). DNA (Hoechst) staining showed three clear bands of fluorescence along the epithelia and ganglion cell layers and a thick band covering the nuclear cell layers and the photoreceptor layer (ZT6 Figure 5.2.3.b.-A and ZT18 Figure 5.2.3.c.-A). Expression at ZT6 (Figure 5.2.3.b) was less intense than at ZT18 (Figure 5.2.3.c). At ZT6 expression was most prominent in the epithelia cell layer (Figure 5.2.3.b.-B.) and ganglion cell layer (Figure 5.2.3.b.C). Staining was also found within the photoreceptor layer and within the plexiform layers (Figure 5.2.3.b.-D,E&F).

Expression of the MEL-1A receptor at ZT18 showed more densely stained cells in the same regions as at ZT6; the ganglion cell layer, the epithelium, plexiform layers and nuclear cell layers (Figure 5.2.3.c.). Staining along the ganglion cell layer at ZT18 (Figure 5.2.3.c.-B,D,E&F) appeared more overtly than the staining found at ZT6 (Figure 5.2.3.b.-C). Staining was also seen along the axons of the nerve cells in the nuclear and plexiform layers (Figure 5.2.3.c.-D). Fluorescent expression of MEL-1A was seen in the pigmented epithelium layer and within the photoreceptor layer (Figure 5.2.3.c.-C) but at a lesser degree than at ZT6.

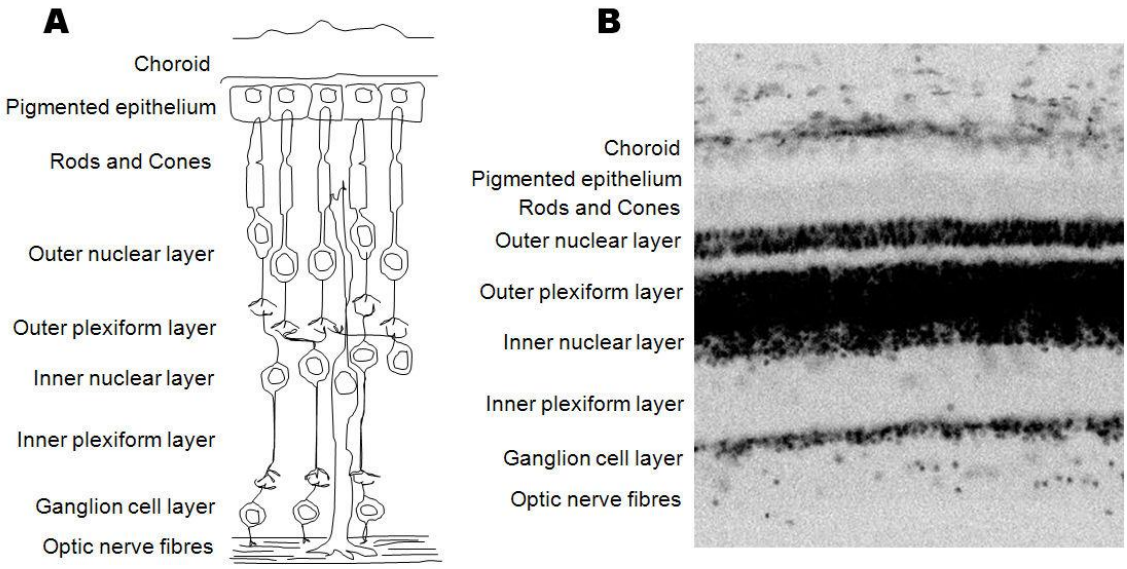

Figure 5.2.3.a. Schematic diagram (A) and Hoechst (DNA) staining (B) in the retina. Showing the layers of the retina examined in the following figures.

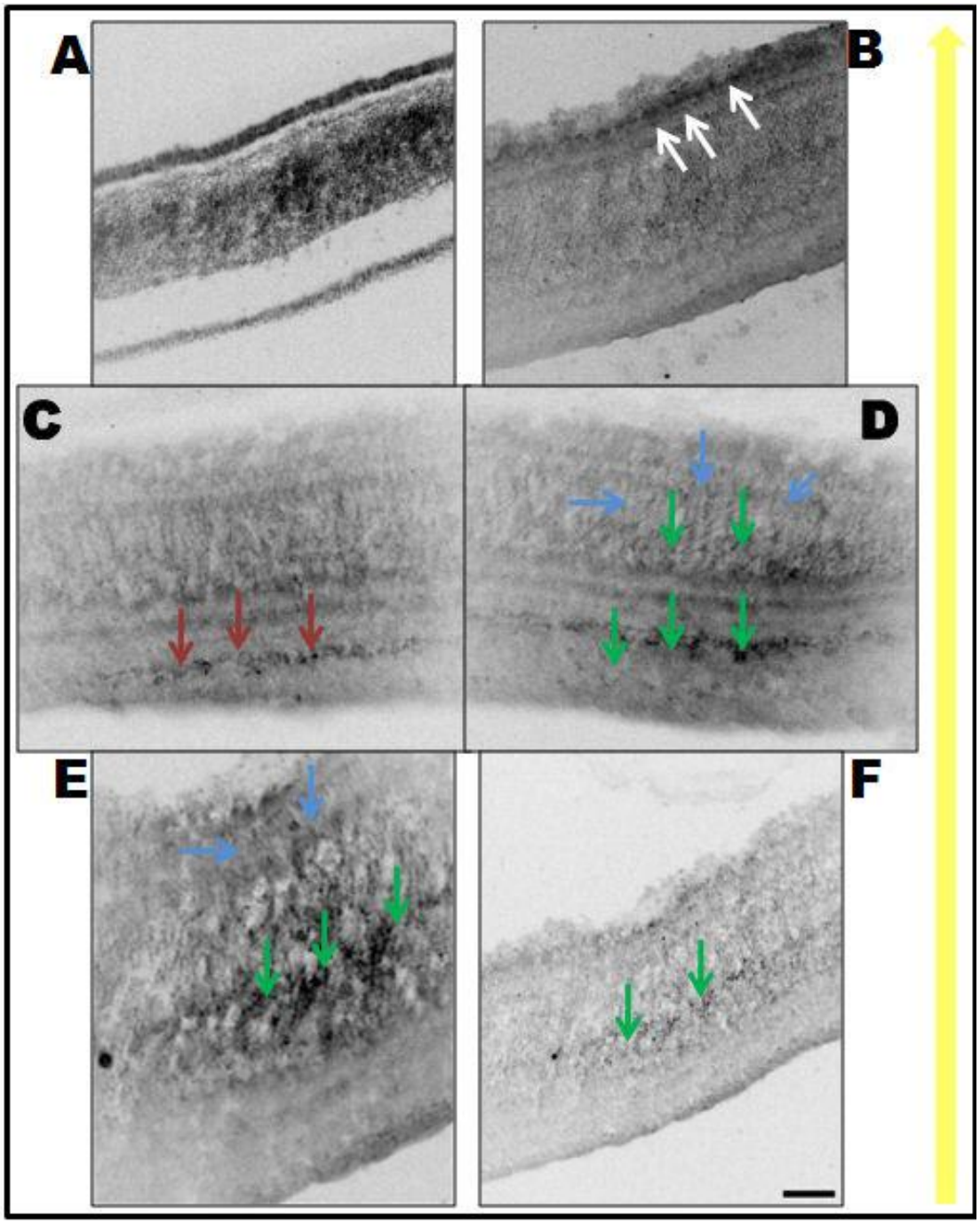

Figure 5.2.3.b. Melatonin receptor MEL-1A localisation in the retina at ZT6. A, shows the DNA content in the retinal tissue highlight by Hoechst staining. A&B are the same images with different staining, A with Hoechst and B with MEL-1A antibody staining. Staining was found in the pigmented epithelium layer (white arrows), photoreceptive layer (blue arrows), in the plexiform and nuclear cell layers (green arrows) and in the ganglion cell layer (red arrows). The yellow arrow on the right indicates the direction of light entering the retinal tissues. The lighting schedule for the samples is highlighted by the colour of the background of the image; the samples here where taken at ZT6 in the light period and therefore has a white background. All images are to scale bar of 50µm seen in image F.

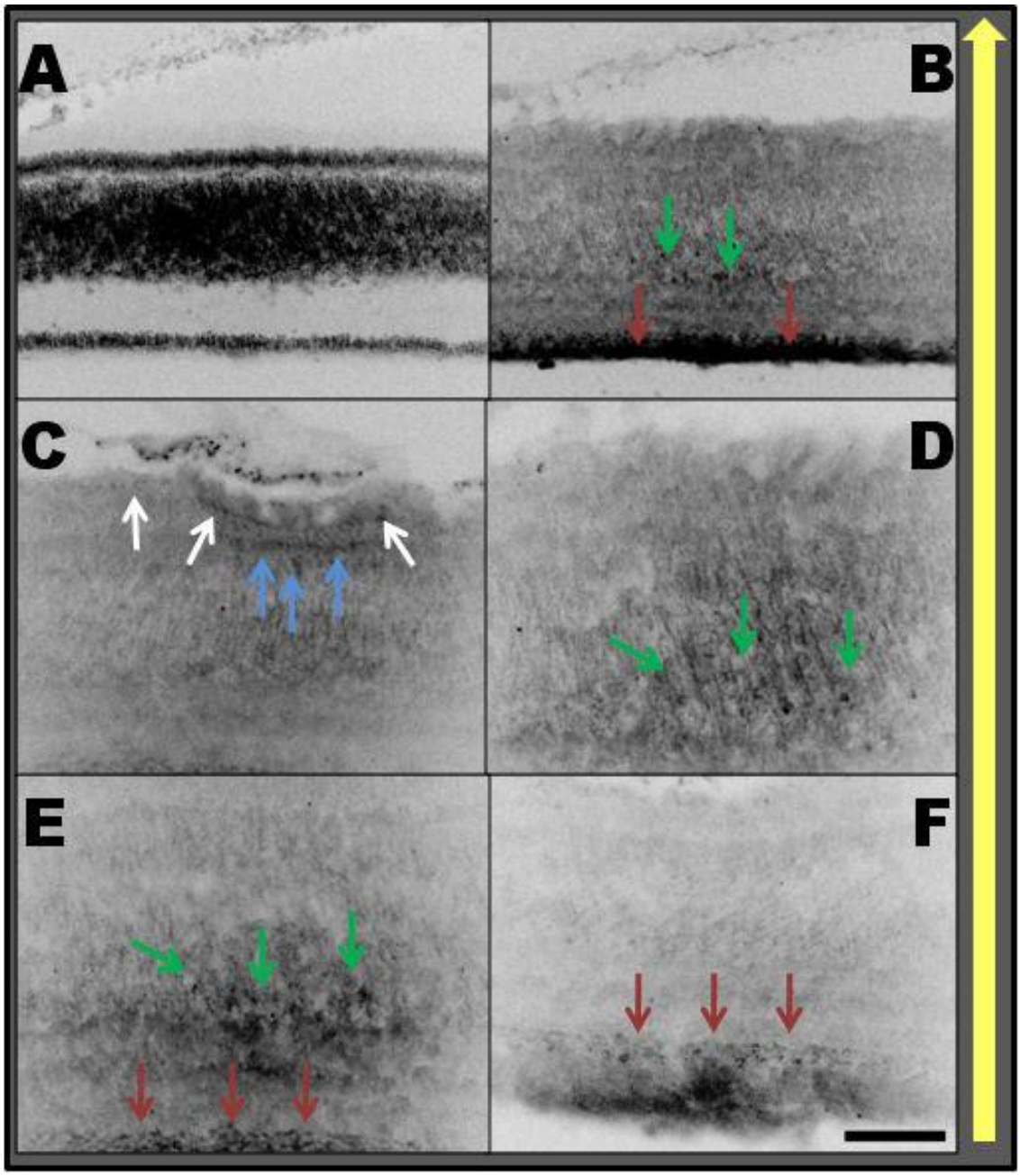

Figure 5.2.3.c. Melatonin receptor MEL-1A localisation in the retina at ZT18. A, shows the DNA content in the retinal tissue highlight by Hoechst staining. A&B are the same images with different staining, A with Hoechst and B with MEL-1A antibody. Staining is seen in the pigmented epithelium layer (white arrows), photoreceptive layer (blue arrows), in the plexiform and nuclear cell layers (green arrows) and in the ganglion cell layer (red arrows). The yellow arrow indicates the direction of light entering the retinal tissue. The lighting schedule for the samples is highlighted by the colour of the background of the image; the samples here where taken at ZT18 in the dark period and therefore has a dark background. All images are to scale bar of 50µm seen in image F.

Melatonin receptor MEL-1B expression in the retinal tissues was a lot weaker than the MEL-1A receptor, though staining was found throughout the retinal tissues (ZT6 Figure 5.2.3.d and ZT18 Figure 5.2.3.e). At ZT6, expression was seen in the pigmented epithelium layer (Figure 5.2.3.d.-B&C) and the photoreceptive layer (Figure 5.2.3.d.-B). There was also slight sporadic staining found in the plexiform layers (Figure 5.2.3.d.-D). At ZT18, the staining in these regions increased (Figure 5.2.3.e), with stronger expression in the epithelium layer and choroid connective tissue layer (Figure 5.2.3.e.-A,C&D). Sporadic staining can be seen along connective axons and fibres in the photoreceptor layer (Figure 5.2.3.e.-B).

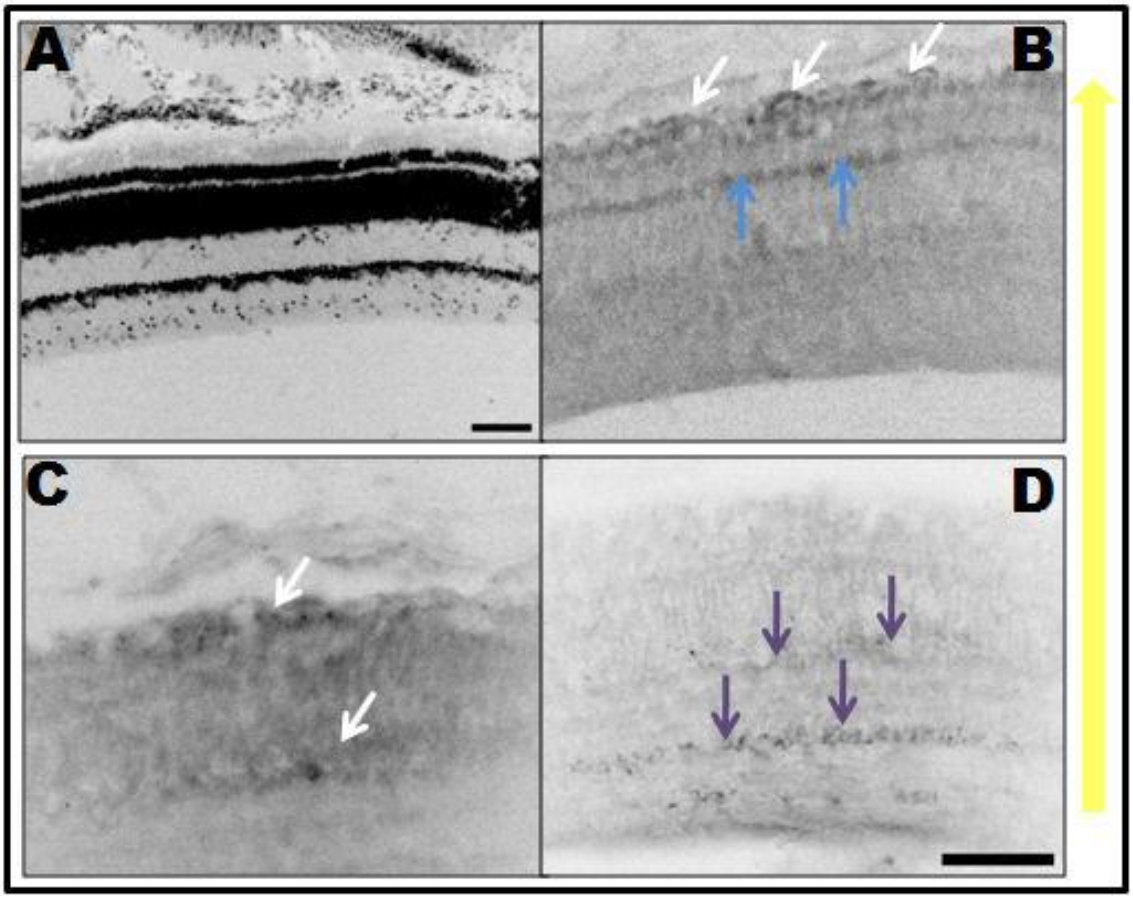

Figure 5.2.3.d. Melatonin receptor MEL-1B localisation in the retina at ZT6. A, shows the DNA content in the retinal tissue highlight by Hoechst staining. A&B are the same images with different staining, A with Hoechst and B with MEL-1B antibody. Staining is seen in the pigmented epithelium layer (white arrows) and the photoreceptive layer (blue arrows). The yellow arrow indicates the direction of light entering the retinal tissue. The lighting schedule for the samples is highlighted by the colour of the background of the image; the samples here where taken at ZT6 in the light period and therefore has a white background. All images are to scale bar of 50µm, image A's scale bar is for A & B and image D's scale bar is for C & D.

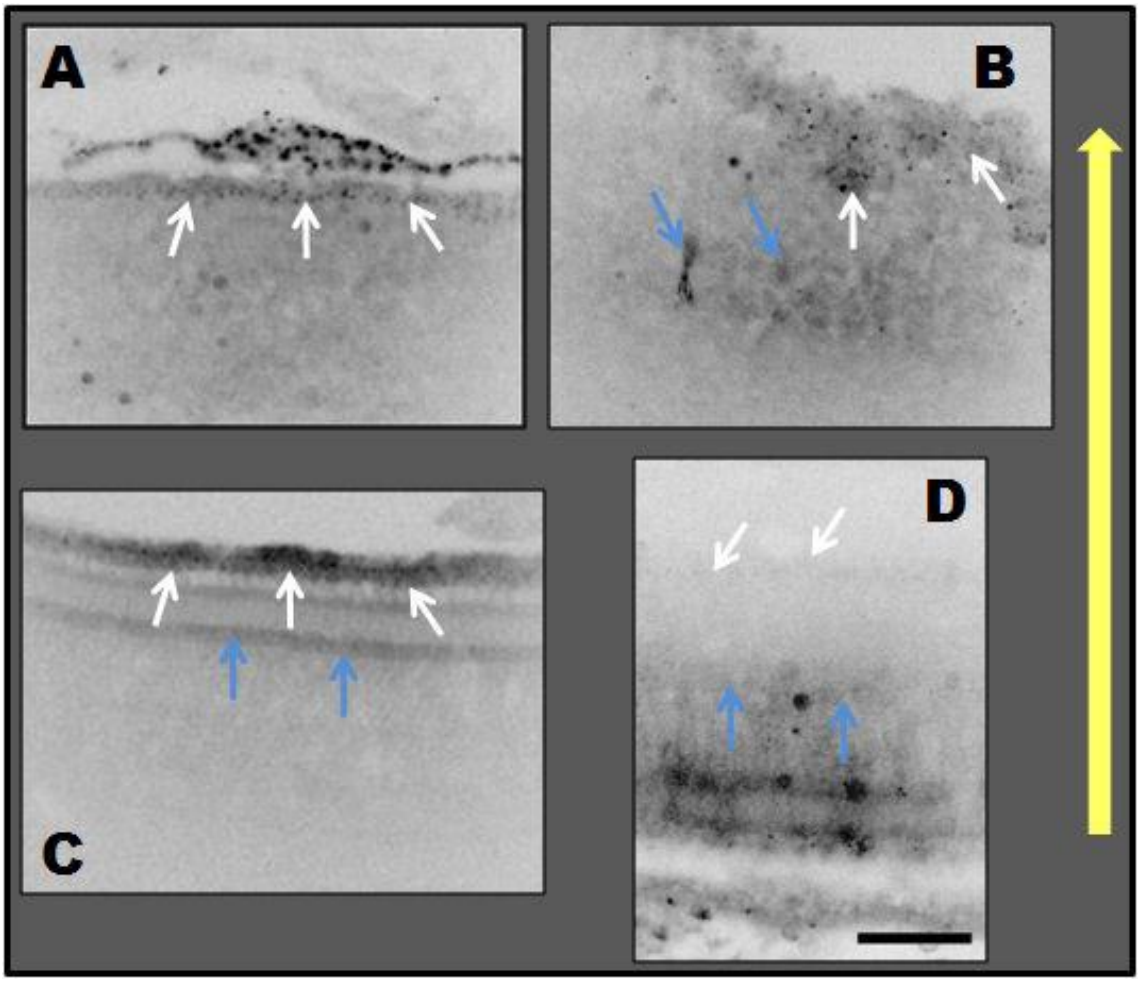

Figure 5.2.3.e. Melatonin receptor MEL-1B localisation in the retina at ZT18. Staining is seen in the pigmented epithelium layer (white arrows) and in the photoreceptive layer (blue arrows). The yellow arrow indicates the direction of light entering the retinal tissue. The lighting schedule for the samples is highlighted by the colour of the background of the image; the samples here where taken at ZT18 in the dark period and therefore has a dark background. All images are to scale bar of 50µm seen in image D.

MEL-1C receptor expression appeared to be more restricted than the other two receptors. It was only found in the pigmented epithelium layer and the photoreceptive layer of the retina at both ZT6 and ZT18 (Figure 5.2.3.f and Figure 5.2.3.g respectively). The expression of MEL-1C also appeared to be restricted to the cell body of the cells of the epithelium at both ZT6 and ZT18.Some staining was observed along the outer segments of the rods and cones and in the synaptic terminal of the photoreceptors at ZT6 (Figure 5.2.3.f.). At ZT18 the expression appeared to be stronger in both the cell layers, with intermittent cells stained amongst the photoreceptive layer (Figure 5.2.3.g). No MEL-1C expression was found in the plexiform or nuclear cell layers or along the ganglion cell layer as seen with MEL-1A and MEL-1B receptors.

From the results for the immunofluorescent experiments I summarised and compared the distinct receptor distributions. I created a schematic diagram representing the results from the retinal tissue to show where to most abundant and variations of staining between the two time points were found (Figure 5.2.3.h). There was a dramatic difference between receptor types, with MEL-1A being expressed throughout the retinal section and the MEL-1B and MEL-1C being more restricted to the areas along the epithelium.

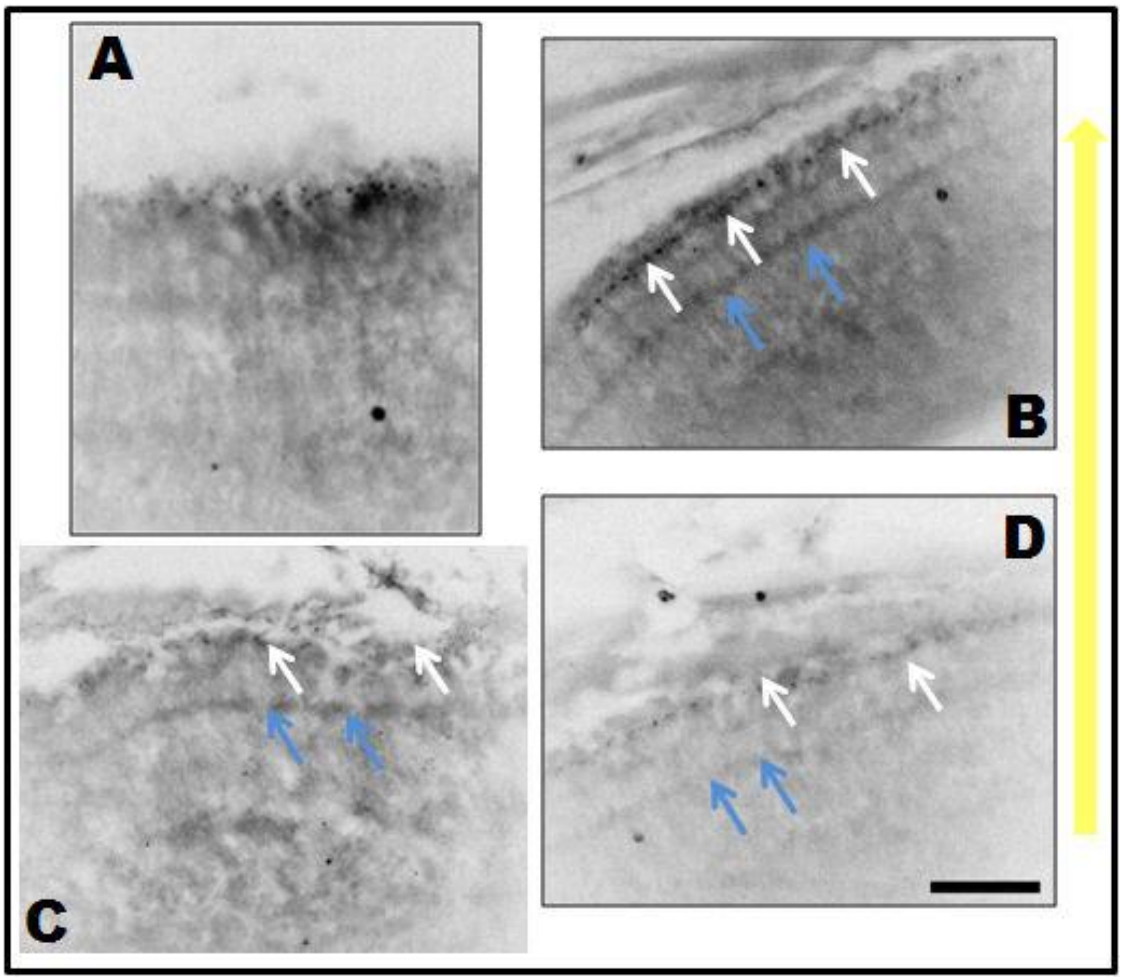

Figure 5.2.3.f. Melatonin receptor MEL-1C localisation in the retina at ZT6. Staining is seen in the pigmented epithelium layer (white arrows) and in the photoreceptive layer (blue arrows). The yellow arrow indicates the direction of light entering the retinal tissue. The lighting schedule for the samples is highlighted by the colour of the background of the image; the samples here where taken at ZT6 in the light period and therefore has a white background. All images are to scale bar of 50µm seen in image D.

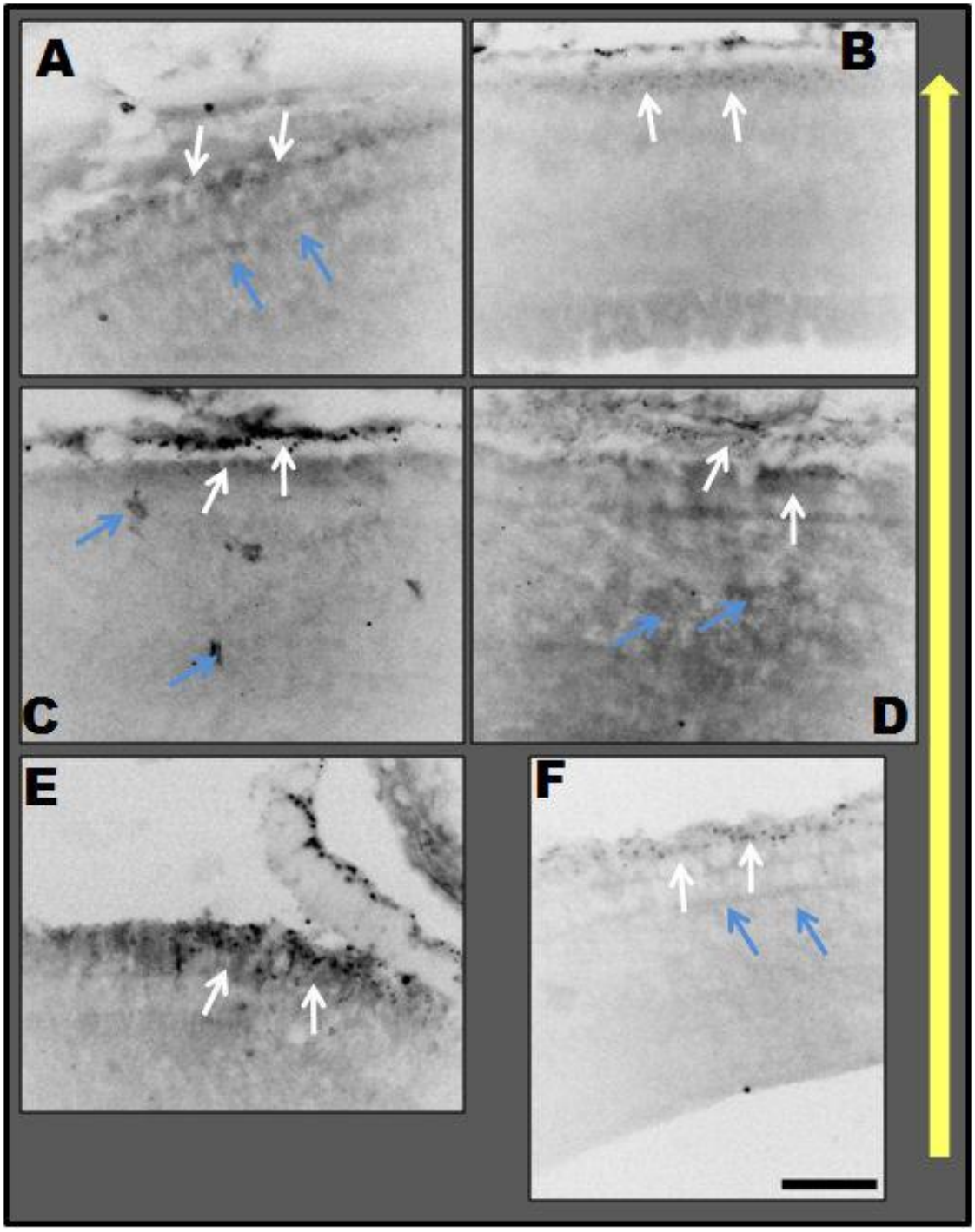

Figure 5.2.3.g. Melatonin receptor MEL-1C localisation in the retina at ZT18. Staining is seen in the pigmented epithelium layer (white arrows) and in the photoreceptive layer (blue arrows). The yellow arrow indicates the direction of light entering the retinal tissue. The lighting schedule for the samples is highlighted by the colour of the background of the image; the samples here where taken at ZT18 in the dark period and therefore has a dark background.

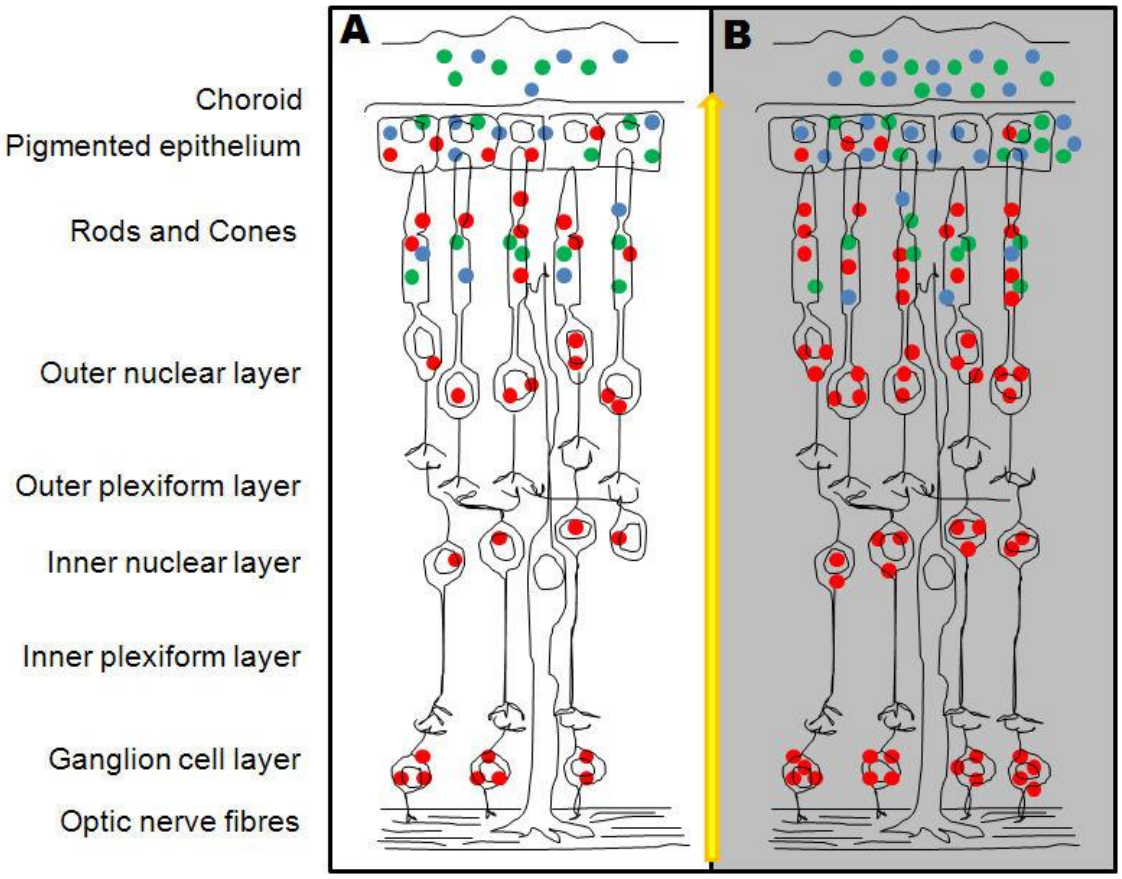

Figure 5.2.3.h. Comparative localisation of the three melatonin receptors MEL-1A (red), MEL-1B (green) and MEL-1C (blue) in the retinal sections at ZT6 (A) and ZT18 (B). The background colour indicates the lighting schedule of the time points. The yellow arrow in the middle indicates the direction of light.

5.3 Discussion

This chapter examined the expression of the three melatonin membrane receptors at two zeitgeber times (ZT), one in the mid-daylight (ZT6) and one in mid-darkness (ZT18), in two of the avian circadian oscillators, the retina and the hypothalamus. All three receptors were present in both the hypothalamus and retina at both time-points, but expression varied both in intensity and distribution. MEL-1A and MEL-1B appeared to fluctuate between ZT6 and ZT18. At ZT6 faint expression was found rostral and medially in the SCN, LHN and PON, but at ZT18 intense staining was found throughout these nuclei and in other areas such as the optic chiasm, tectum opticum and PVN. All three melatonin receptors were found in the two avian circadian hypothalamic areas, i.e. SCN and LHN, suggesting that melatonin acts in these nuclei during the night to inhibit the hypothalamic activity to stop the neural activity, possibly acting as an internal zeitgeber and having direct action on the circadian pacemakers (Stankov, *et al*., 1991). This could be testing with electrophysiological experiments with melatonin solutions added to the slices of hypothalamus to see if neuronal activity was indeed inhibited.

MEL-1C expression in the hypothalamus appeared not to be rhythmic and was found throughout the hypothalamus. MEL-1C receptor was also found in the optic chiasm and optic tectum. These results are consistent with the results found in Chapter Four for the receptor mRNA levels. It has been shown that Mel-1C and the mammalian GPR50 are orthologs (Dufourny, *et al*., 2008), and the GPR50 was found not to be rhythmic and it modulates the function of the mammal melatonin receptors (Levoye, *et al*., 2006). Melatonin receptor subtypes have been shown to form functional dimers with each other, i.e. Mel-1A-Mel-1B or

Mel-1B-Mel-1C etc. (Ayoub, *et al*., 2002). It has also been suggested that the GPR50 protein has a modulatory role, which is non-rhythmical and forms a constant subunit presence in the membrane that the regulatory subunits, such as Mel-1A and Mel-1B attach to (Dufourny, *et al*., 2008). It is these regulatory subunits which convey the melatonin signal into the target sites with different results, depending on the subunit formation. Since Mel-1C and the GPR50 receptor have been shown to be orthologs, it is feasible that the functional and modulatory role of the GPR50 receptor is the same as for the Mel-1C receptor subtype. The data from this chapter and Chapter Four would support this hypothesis.

The visual locations of the receptors within the neuronal cells shown in this study are highly important; here I have reported that the MEL-1C receptor is clearly shown both in the light (ZT6) and dark (ZT18) phases to be present throughout the different neuronal cells, i.e. within the cell body, down the axons and on the membrane of the cells. This suggests that MEL-1C is, like Dufourny suggests (Dufourny, *et al*., 2008), a functional subtype present and waiting for the rhythmical subtypes (Mel-1A and Mel-1B) to be translated and transported to the functional sites in the dendrites and synapses (Dufourny, *et al*., 2008). Both MEL-1A and MEL-1B appear in the cytoplasm of the cell body (expressed at ZT6 and ZT18) and along the membrane of the neuronal cells and synapses (ZT18). This result would suggest that these receptors are waiting for an internal signal to be transported to the cell membrane for activation by the melatonin hormone. MEL-1A and MEL-1B also are shown to be more highly present at ZT6 compared to the levels seen at ZT18.

In the retina, clear differences between the distributions of the three receptors were shown; MEL-1A was found throughout the retinal tissue sections with more dominant staining found at ZT18 than at ZT6. MEL-1B expression was found at a lower intensity than the MEL-1A receptor, but was found in the pigmented epithelium, photoreceptive and ganglionic layers, with sporadic staining in the plexiform layers, with expression increasing at ZT18 compared to the levels found at ZT18. Whereas MEL-1C expression appeared to be limited to the pigmented epithelium and a photoreceptive layer at both ZT6 and ZT18, there was a slight increase in expression at ZT18.

MEL-1A (MT1) receptor has been found in the inner segments of the photoreceptors, inner nuclear layer, inner plexiform layer and in the ganglion cells of the rat (Alcantara-Contreras, *et al*., 2011), xenopus and chick retina (Natesan and Cassone, 2002). The comparative expression between mammalian and non-mammalian models suggests that this is universal between species. Expression of MEL-1A receptors found in the nuclear and plexiform layers, the main cells found in these regions are the horizontal (inner nuclear layer) and amacrine (just below the inner nuclear layer bordering the inner plexiform layer) cells, which suggests that melatonin regulates the release of neurotransmitters, such as dopamine, acetylcholine, by acting on the amacrine cells (Alarma-Estrany and Pintor, 2007). It has been documented by other studies that melatonin inhibits the dopamine release at the postsynaptic sites in chick retina (Cassone and Natesan, 1997; Fujieda, et al., 1999), and enhances the sensitivity of the horizontal cells in the inner nuclear layer of the salamander (Alarma-Estrany and Pintor, 2007). The presence of melatonin receptors (MEL-1A and MEL-1B) in the photoreceptor layer suggests the role for the photoreceptor disc shedding (Fujieda, *et al*., 1999).

To summarise I have shown the location of the MEL-1A, MEL-1B and MEL-1C receptors in the hypothalamus and retina, highlighting areas that can be influenced by the hormone melatonin. Levels of MEL-1A and MEL-1B receptor were shown to vary between the light and dark phase, whereas MEL-1C expression remained constant throughout the lighting conditions, in both the retina and hypothalamus, two of the known avian circadian oscillatory regions.

CHAPTER 6

Light induced C-FOS expression in the zebra finch hypothalamus

CHAPTER SIX – LIGHT INDUCED C-FOS EXPRESSION IN THE ZEBRA FINCH HYPOTHALAMUS

6.1 Introduction

Organisms entrain their inherent circadian rhythms of biological processes to the external light cue. An organism's rhythm is maintained and adapted to the variability of the individual's internal and environment pressure, therefore the organism's rhythm is constantly being entrained to synchronize with the environmental cues. Light is the major external cue that entrains the internal clock; though there are other external cues that can enhance or inhibit the effectiveness of the entrainment; such as temperature (Barrett and Takahashi, 1995; Aschoff and Tokura, 1986; Herzog and Huckfeldt, 2003), locomotor stimuli (Stephan, 1972; Mrosovsky, 1996), stress (Harper, *et al*., 1996), melatonin (Heigl and Gwinner, 1995), and feeding schedules (Hau and Gwinner, 1996).

The light signal, or light period in 24 hours, synchronises the circadian oscillators which effects organisms' daily physiology (homeostasis, brain activity, sleep-wake pattern, hormone production and cell regeneration) and behaviour (feeding, migration, breeding, etc.) via light-dark entrainment of the day-night cycles (Gwinner and Brandstaetter, 2001). In the wild, the light phase reception also distinguishes seasonal changes from daily light variation due to clouds and rain etc., which would affect feeding, breeding, moulting and migration of some birds.

In laboratory conditions, exposure to light influences entrainment of the species, i.e. exposure to bright light in the early light period can phase advance the circadian rhythm and exposure before the dark phase delays the rhythm (Duffy, *et al.*, 1996; Warman, 2003). The length and intensity of the light exposure also effects the entrainment; with longer brighter exposures having greater influences (Duffy, *et al.*, 1996), consistent exposure is greater than random exposures (Baehr, *et al.*, 1999) and even dim light exposure can effect entrainment when the subject is placed into darkness (Gorman, *et al.*, 2005).

In most species the main source of photic information comes from the retina; though in non-mammalian species, photic light can be detected in the pineal gland, or parietal organ, and deep encephalic receptors. Photic information from the photoreceptors in the retina is carried along the retinohypothalamic tract (RHT) to the brain, glutamate being the primary neurotransmitter involved with this process. This signal initiates a complex signal transduction pathway that can advance or delay the circadian clock depending when the signal in transmitted (Porterfield and Mintz, 2009). In mammals the RHT terminates in the SCN which then relays this information to stimulate the ventrolateral or "core" cells which again is then relayed to the dorsomedial cells or "shell" portion of the SCN. The "shell" is not directly photosensitive but exhibits an endogenous rhythm in c-fos expression in DD conditions (Porterfield and Mintz, 2009). Nocturnal rodents exposed to light in the early night, delay their circadian rhythms, but exposure during the late night advances their rhythms. If exposed during normal daytime hours this has no effect (Porterfield and Mintz, 2009).

A neurological marker, c-fos, can be used to measure the initial neurological activation in the brain that light has, because *c-fos* is expressed when a neuron fires its action potential (van Elzakker, *et al*., 2008). The expression of *c-fos* reflects the intracellular state of the cell that varies primarily as a result of recent activation by intracellular signals such as hormones and neurotransmitters (van Elzakker, *et al*., 2008). Therefore if the only stimulus is a light exposure, *c-fos* can be used to examine the neurological localisation of the effect of light in brain regions, i.e. which nuclei are stimulated by light in the hypothalamus affecting circadian functions.

c-fos gene and C-FOS protein is the normal cellular counter-part of the viral oncogene v-fos (Sagar, *et al*., 1988). It is a member of the immediate early gene (IEGs) family which is rapidly and transiently expressed in many tissues in response to numerous stimuli (Sagar, *et al*. 1988; Basheer, *et al*., 1997); these genes are the first set of genes that are activated by external stimulus that do not require other proteins to be synthesised first (Herrera and Robertson, 1996). IEGs are believed to encode transcription factors which will modify the expression of other genes (known as target genes) which will then modify the phenotype of the cell (Herrera and Robertson, 1996).

c-Fos is rapidly induced in neuronal cells by neurotransmitters (Yoshida, *et al*., 1993; Figure 6.1.a). Light, or its downstream messenger glutamate, phosphorylates CREB and the activation of several immediate early genes and the core clock gene *Per1* (Porterfield and Mintz, 2009). The c-fos protein levels are dramatically elevated after light impulses administered in either the dark phase in LD conditions or the “subjective night” in DD

conditions, in hamsters, mice and rats (Schwartz, 1995). Under 8:16 LD conditions, an one hour light exposure at either CT8 or CT20 can induce c-fos expression in the LHN in quails and starlings (vSCN) but not in the SCN (mSCN) of either species (King and Follett, 1997). This study also reports that a more significant phase shift was seen after the one hour light exposure at CT20 than at CT8 (King and Follett, 1997).

In this chapter I qualitatively analysed the effect that light exposure in the early dark period and late dark period had on the protein level of C-FOS in different cell groups of the hypothalamus. I compared the c-fos localisation in cell groups in experimental controls samples without light exposure at the same time points, and c-fos levels in light conditions. The immunofluorescent protocol allowed me to visually identify the anatomical distribution of C-FOS in the brain after light exposure in the dark period of an LD cycle, and what effect the light exposure had in the brain. The immunofluorescent protocol offered cellular resolution since the c-fos staining is localised in the cell's nucleus (Sagar, *et al*., 1988). I examined the C-FOS localisation in the zebra finch hypothalamus 60 minutes and 90 minutes after the onset of light exposure (OLE); because the immunoreactive protein's peak expression is 1-2 hour after the light onset (Schwartz, 1995).

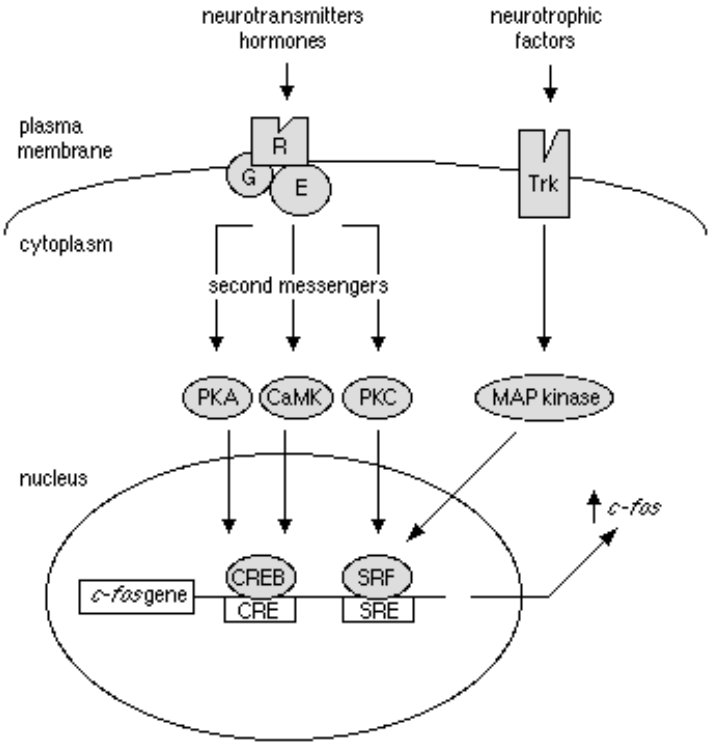

Figure 6.1.a. Receptor-coupled signal transduction pathways and regulation of *c-fos* expression. The expression of *c-fos* mRNA is regulated by several different neurotransmitters, hormones, and neurotrophic factors via receptor-coupled signal transduction pathways. Neurotransmitters and hormones stimulate G protein–coupled receptors (R) that activate second messenger effectors (E). Second messengers such as cAMP, Ca^{2+}, diacylglycerol, and inositol trisphosphate activate second messenger–dependent protein kinases such as cAMP-dependent protein kinase (PKA), Ca^{2+}/calmodulin-dependent protein kinase (CaMK), and protein kinase C (PKC). Activation of these protein kinases leads to induction of *c-fos* gene expression via two different promoter elements: the cAMP response element (CRE) and the serum response element (SRE). PKA and CaMK (as well as PKC) phosphorylate and activate the cAMP response element binding protein (CREB), and PKC phosphorylates and activates the serum response factor (SRF). Activation of neurotrophic factor receptors leads to stimulation of MAP kinase via several intermediary steps (not shown). MAP kinase increases the expression of *c-fos* via phosphorylation of the SRF or, depending on the cell system, can activate CREB via phosphorylation of CREB kinase, also referred to as Rsk (not shown). This model demonstrates the complexity of the receptor-coupled signal transduction cascades that regulate *c-fos* expression (Duman, 2001).

6.2 Results

This chapter examined the effect light has on cell groups within the hypothalamus in the early and late dark period of a normal 12:12LD cycle. C-FOS-immunoreactive (C-FOS-IR) cells were found at all time points, including the experimental controls, as c-fos is an immediate early gene which is stimulated by the numerous factors (such as temperature, motion, etc.). The experimental controls gave a "background" level of C-FOS-IR cells which are present during normal LD dark period and no light exposure conditions. Immunofluorescent antibody controls were carried out on each immunofluorescent procedure to ensure the accuracy of the results, all immunofluorescent controls proved negative for C-FOS-IR cells. In all experimental sections C-FOS-IR cells were also seen in the telencephalon at all time points showing consistency between experiments. Experimental samples were taken at either 60 minutes, at ZT15 or ZT21, after the onset of light exposure (OLE) or 90 minutes after OLE, at ZT15.5 or ZT21.5. The time points taken after 90 minutes were exposed to light for 60 minutes and then subjected back into dark conditions for 30 minutes (Figure 6.2.a).

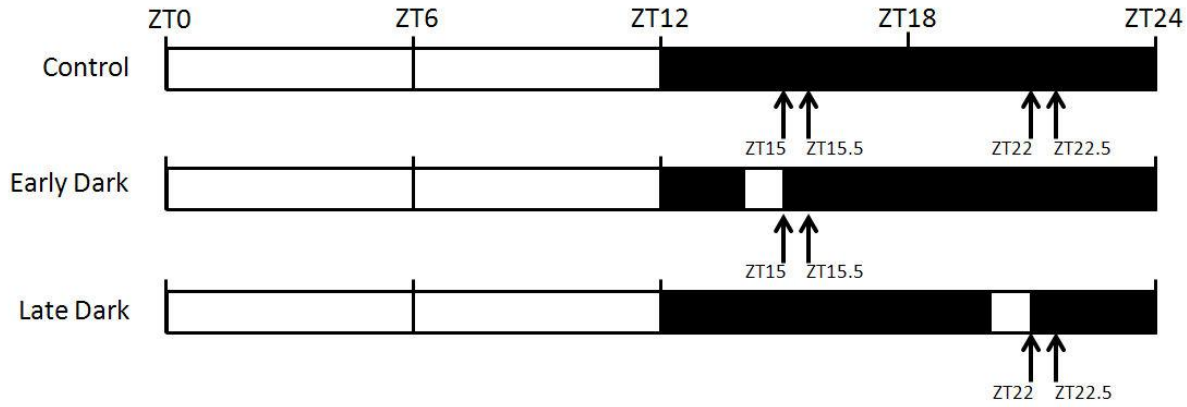

Figure 6.2.a. Schematic diagram showing the lighting conditions and dissection time points of the zebra finch. The control samples are taken void of the OLE under "normal 12:12 LD conditions. The light exposure in the early dark is highlighted by the white box in the dark period, with dissections occurring immediately after the 60 minute OLE (ZT15) and 90 minutes after the OLE (ZT15.5). The late dark exposure is again highlight by the white box, but occurred between ZT21 and ZT22, with dissections again occurring immediately after the 60 minute OLE (ZT22) and 90 minutes after the OLE (ZT22.5). Arrows indicate the dissection time points.

6.2.1 C-FOS expression in the zebra finch hypothalamus after one hour light exposure in the early dark period

Experimental control samples, i.e. taken at the same ZT's as the experimental tissues but not subjected to the one hour light exposure, showed similar results at both the time-points (ZT15 and ZT15.5) in the early dark phase (Figure 6.2.1.a and Figure 6.2.1.b respectively). In the rostral regions of the hypothalamus (Figure 6.2.1.a.-C and Figure 6.2.1.b.-C), there were sporadic C-FOS-IR cells found in the preoptic area (POA) and there were a few C-FOS-IR cells found through the rest of the hypothalamus. More medially (Figure 6.2.1.a.-D-G and Figure 6.2.1.b.-D-F) C-FOS-IR cells were also seen in the POA leading into the PON, in the medial hypothalamus, and around the GLv. The C-FOS expression was seen in all the controls had a scattered pattern not defined to one cell group.

60 minutes after the OLE (Figure 6.2.1.c), in the rostral region of the hypothalamus the most abundant C-FOS-IR cells were seen in the POA and LHN (Figure 6.2.1.c.-B), similar to the staining found at the experimental control time point (Figure 6.2.1.c.-C) but more intensely populated numbers of C-FOS-IR cells were found. C-FOS-IR cells were also seen towards the top of the third ventricle around were the PVN is found in more medial sections.

90 minutes after OLE (Figure 6.2.1.d.), there were still an abundant collection of C-FOS-IR cells present in the PON, LHN and GLv cell groups of the hypothalamus, the staining appeared to be more prominent than that found after 60 minutes OLE. Rostrally, the number of C-FOS-IR cells and intensity of staining increased throughout all the cell groups, as well as in the cortex (Figure 6.2.1.d.-B). Again more medially (Figure 6.2.1.d.-D) the staining of C-

FOS-IR cells was more densely, lateral the GLv cell group was dominantly full of C-FOS-IR cells. More medially to the GLv, C-FOS-IR cells were seen in the LHN cell group, and around the third ventricle more C-FOS-IR cells were found in the PON than immediately after the 60 minutes of light exposure (Figure 6.2.1.b.-D-F).

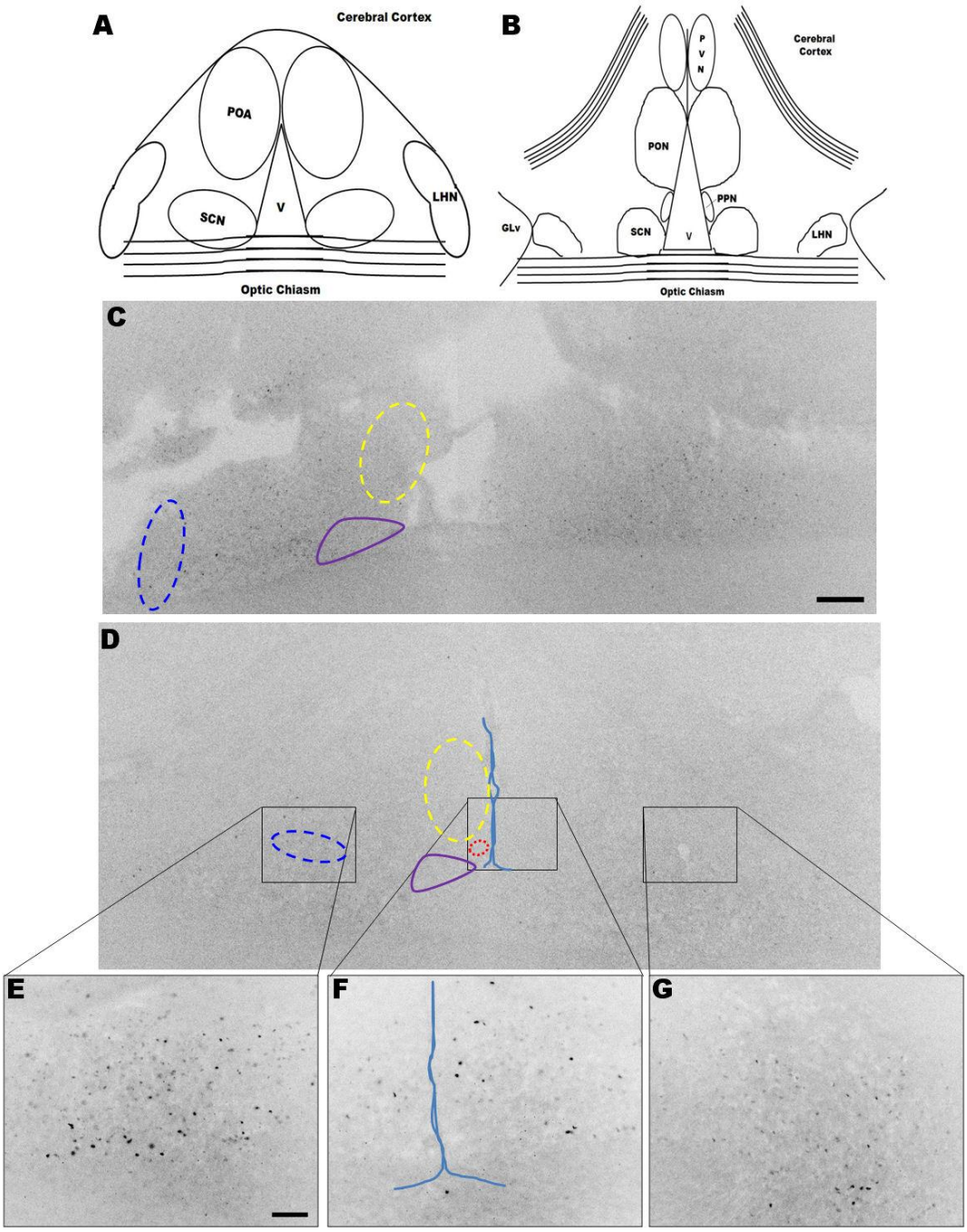

Figure 6.2.1.a. C-FOS-IR cells in the hypothalamus at ZT15 without a 60 minute light exposure (control). Schematic diagrams showing the cell groups found in the rostral (A) and medial (B) areas of the hypothalamus. C-FOS-IR cells were found in cell groups in the rostral (C) and medial (D-G) regions of the hypothalamus. High magnification images of the lateral medial cell groups (E and G) and central medial cell groups around the third ventricle of the hypothalamus (F). GLv – lateral geniculate nucleus pars ventralis, LHN – lateral hypothalamic nucleus, POA – anterior preoptic nucleus, PON – Preoptic nucleus, PPN – periventricular preoptic nucleus, SCN – suprachiasmatic nucleus, V – third ventricle. Scale bar for images C & D is 200µm, shown in image A. Scale bar for images E-G is 50µm, shown in image E. The blue lines indicate the third ventricle walls. Purple dashed circle indicates the SCN; blue dashed circle indicates the LHN; yellow dashed circle indicates the PON; red dashed circle indicates the PPN.

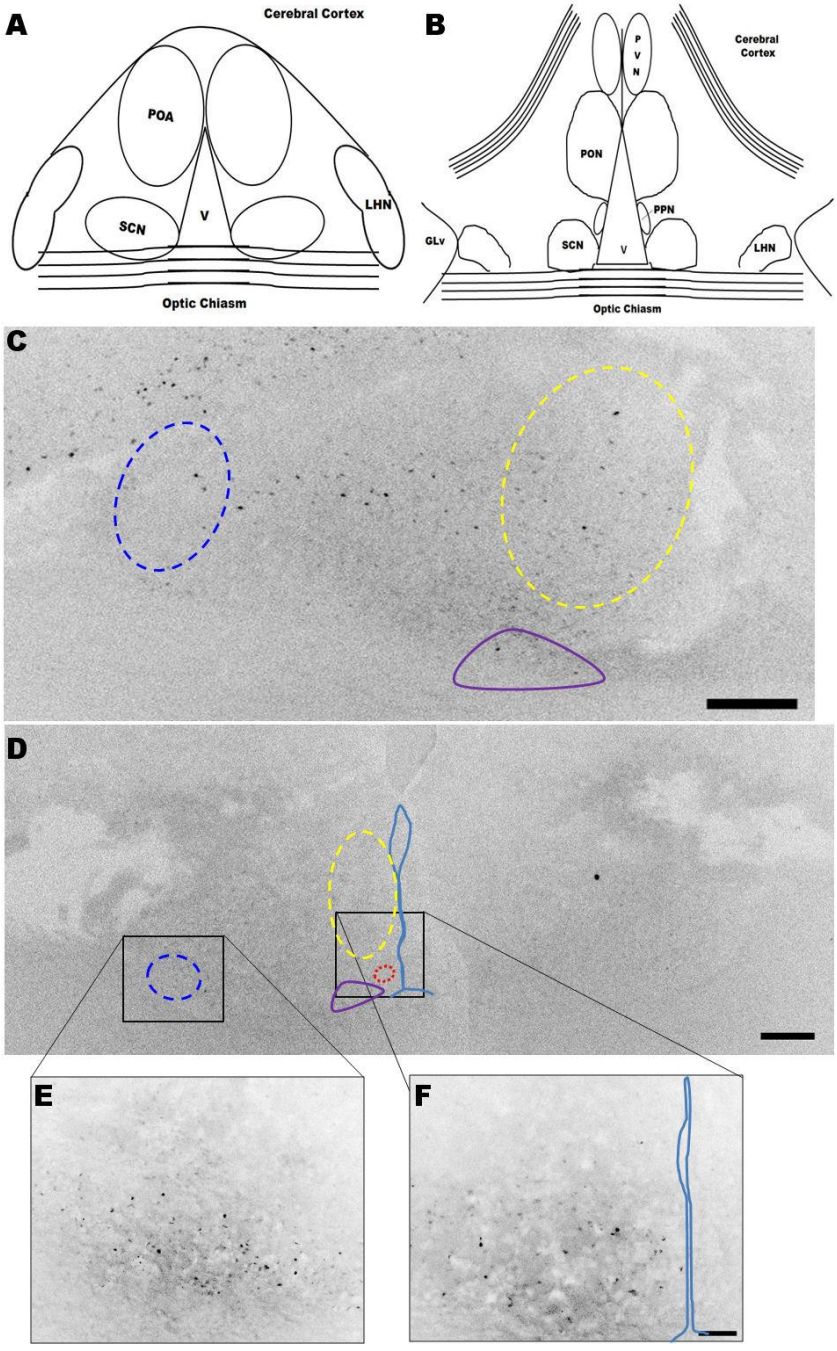

Figure 6.2.1.b. C-FOS-IR cells in the hypothalamus at ZT15.5 without a 60 minute light exposure (control). Schematic diagrams showing the cell groups found in the rostral (A) and medial (B) areas of the hypothalamus. C-FOS-IR cells were found in cell groups in the rostral (C) and medial (D-F) regions of the hypothalamus. High magnification images of the lateral medial cell groups (E) and central medial cell groups around the third ventricle of the hypothalamus (F). GLv – lateral geniculate nucleus pars ventralis, LHN – lateral hypothalamic nucleus, POA – anterior preoptic nucleus, PON – Preoptic nucleus, PPN – periventricular preoptic nucleus, SCN – suprachiasmatic nucleus, V – third ventricle. Scale bar for images C is 200µm; image D is 100µm and images E-F is 50µm, shown in image E. The blue lines indicate the third ventricle walls. Purple dashed circle indicates the SCN; blue dashed circle indicates the LHN; yellow dashed circle indicates the PON; red dashed circle indicates the PPN.

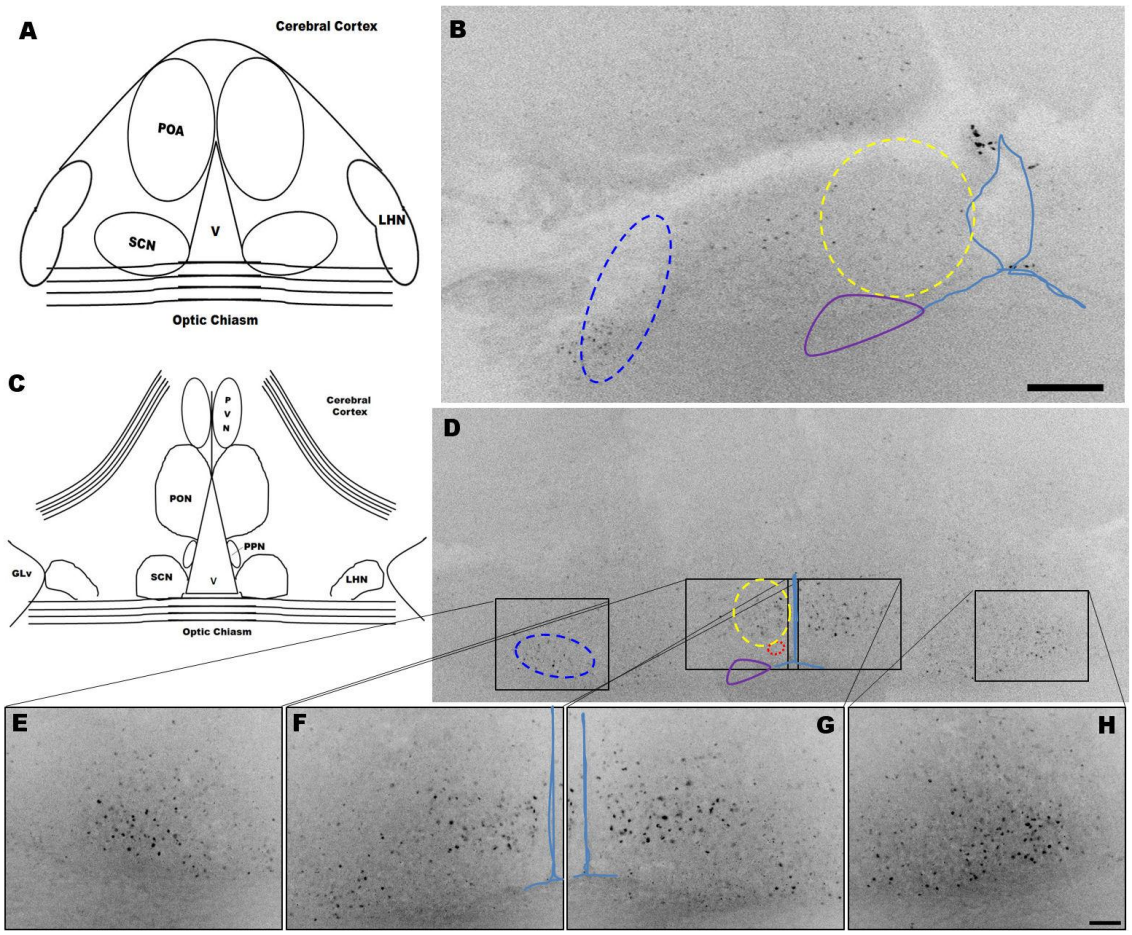

Figure 6.2.1.c. C-FOS-IR cells in the hypothalamus 60 minutes (ZT15) after the OLE. Zebra finches where subjected to a 60 minute light exposure and then immediately culled. Schematic diagrams showing the cell groups found in the rostral (A) and medial (C) areas of the hypothalamus. C-FOS-IR cells were found in cell groups in the rostral (B) and medial (D-H) regions of the hypothalamus. High magnification images of the lateral medial cell groups (E and H) and central medial cell groups around the third ventricle of the hypothalamus (F and G). The blue lines indicate the third ventricle walls. GLv – lateral geniculate nucleus pars ventralis, LHN – lateral hypothalamic nucleus, POA – anterior preoptic nucleus, PON – Preoptic nucleus, PPN – periventricular preoptic nucleus, SCN – suprachiasmatic nucleus, V – third ventricle. Scale bars: image A and B = 100µm and images E-H = 50µm. The blue lines indicate the third ventricle walls. Purple dashed circle indicates the SCN; blue dashed circle indicates the LHN; yellow dashed circle indicates the PON; red dashed circle indicates the PPN.

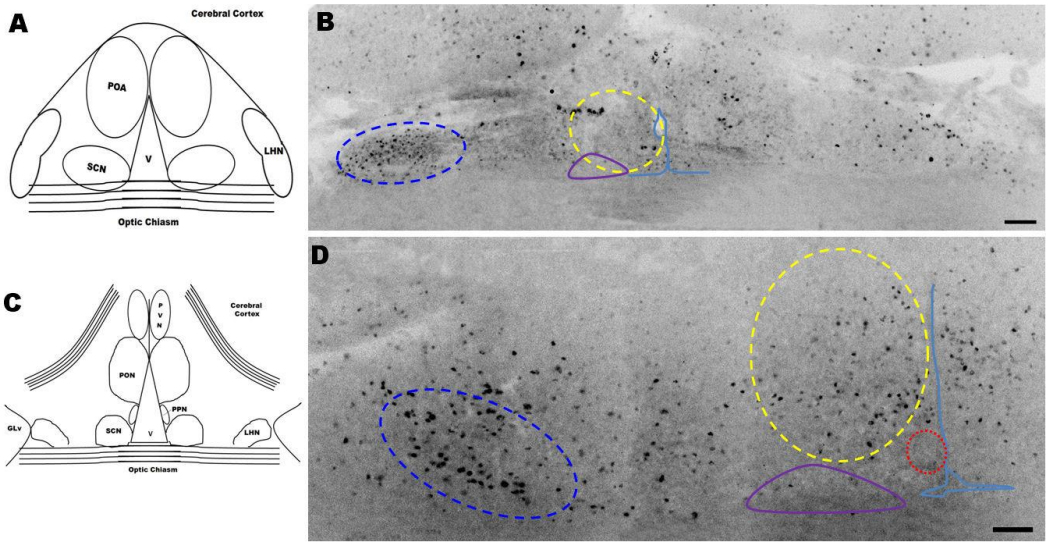

Figure 6.2.1.d. C-FOS-IR cells in the hypothalamus 90 minutes (ZT15.5) after OLE. Zebra finches where subjected to a 60 minute light exposure and then placed back into darkness for 30 minutes and culled. Schematic diagrams showing the cell groups found in the rostral (A) and medial (C) areas of the hypothalamus. C-FOS-IR cells were found in cell groups in the rostral (B) and medial (D) regions of the hypothalamus. The blue lines indicate the third ventricle walls. GLv – lateral geniculate nucleus pars ventralis, LHN – lateral hypothalamic nucleus, POA – anterior preoptic nucleus, PON – Preoptic nucleus, PPN – periventricular preoptic nucleus, SCN – suprachiasmatic nucleus, V – third ventricle. Scale bars: image B = 200µm and images D = 100µm. The blue lines indicate the third ventricle walls. Purple dashed circle indicates the SCN; blue dashed circle indicates the LHN; yellow dashed circle indicates the PON; red dashed circle indicates the PPN.

6.2.2 C-FOS expression in the zebra finch hypothalamus after one hour light exposure in the late dark period

In both the experimental control samples in the late dark period (Figure 6.2.2.a and Figure 6.2.2.b), there was a sporadic number of C-FOS-IR cells seen in the POA (rostrally), PON (medially) and more laterally in the GLv cell groups. At ZT21 (Figure 6.2.2.a.) which corresponded to the immediate end of the 60 minute light exposure, experimentally, there was very few C-FOS-IR cells seen in both the rostral (Figure 6.2.2.a.-B) and medial (Figure 6.2.2.a.-D) regions of the hypothalamus. Whereas at ZT21.5 (Figure 6.2.2.b) which corresponded with the 90 minute time point after the OLE, experimentally, there appeared to be more C-FOS-IR cells present in both the rostral (Figure 6.2.2.b.-C-E) and medial (Figure 6.2.2.b.-F) cell groups; POA, PON and GLv.

Immediately after the end of the 60 minute OLE (Figure 6.2.2.c), rostrally, C-FOS-IR cells were found again in the POA and LHN cell groups, as in the previous figures, but a large number of densely stained C-FOS-IR cells were also seen in the suprachiasmatic nucleus (SCN), just at the inferior corner of the third ventricle (Figure 6.2.2.c.-C&D). This population of C-FOS-IR cells were found throughout the SCN, as the sections go more medially into the hypothalamus (Figure 6.2.2.c.-E&H). In the medial hypothalamus (Figure 6.2.2.c.-E-H) C-FOS-IR cells were present in more laterally in the GLV (Figure 6.2.2.c.-F) and LHN (Figure 6.2.2.c.-G) cell groups. At this time point there were a lesser number of C-FOS-IR cells found in the POA (rostrally; Figure 6.2.2.c.-C&D) and in the PON (medially; Figure 6.2.2.c.-E&H) cell groups, as seen in all the previous figures.

Ninety minutes after the OLE (Figure 6.2.2.d), C-FOS-IR cells were again found in the POA of the rostral region of the hypothalamus (Figure 6.2.2.d.-C&D). There was faint staining of C-FOS-IR cells in the SCN, rostrally (Figure 6.2.2.d.-C&D). C-FOS-IR cells were also found along the border of the superior part of the third ventricle. In the medial region of the hypothalamus (Figure 6.2.2.d.-E), C-FOS-IR cells were located in the GLv, LHN and also appeared around the third ventricle in the PPN, again there was a low number of C-FOS-IR cells in the PON at this time point.

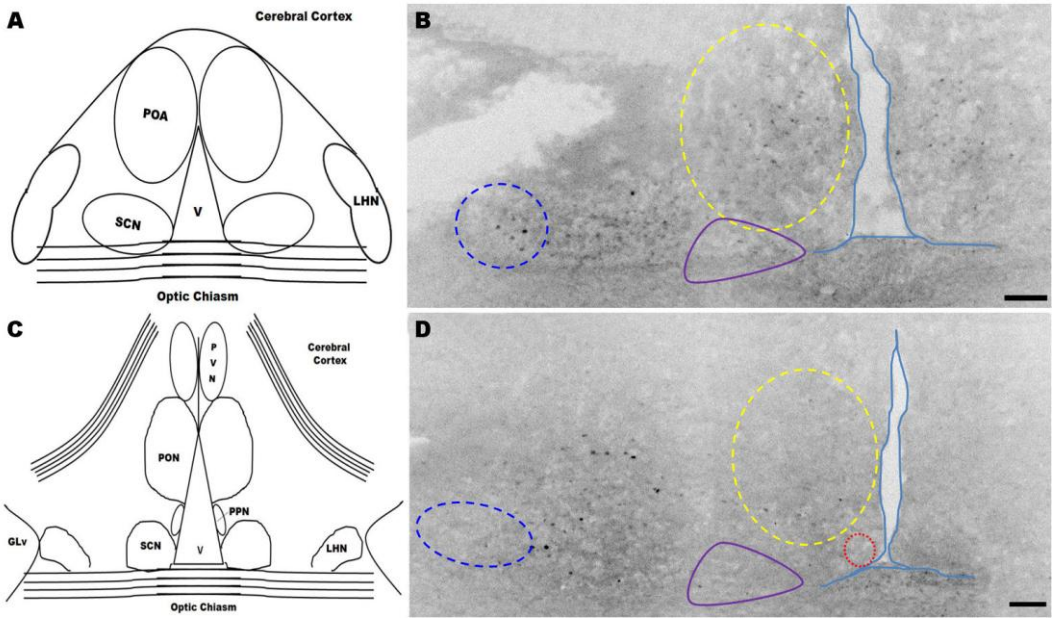

Figure 6.2.2.a. C-FOS-IR cells in the hypothalamus at ZT21 without a 60 minute light exposure (control). Schematic diagrams showing the cell groups found in the rostral (A) and medial (C) areas of the hypothalamus. C-FOS-IR cells were found in cell groups in the rostral (B) and medial (D) regions of the hypothalamus. The blue lines indicate the third ventricle walls. GLv – lateral geniculate nucleus pars ventralis, LHN – lateral hypothalamic nucleus, POA – anterior preoptic nucleus, PON – Preoptic nucleus, PPN – periventricular preoptic nucleus, SCN – suprachiasmatic nucleus, V – third ventricle. Scale bars = 100µm. The blue lines indicate the third ventricle walls. Purple dashed circle indicates the SCN; blue dashed circle indicates the LHN; yellow dashed circle indicates the PON; red dashed circle indicates the PPN.

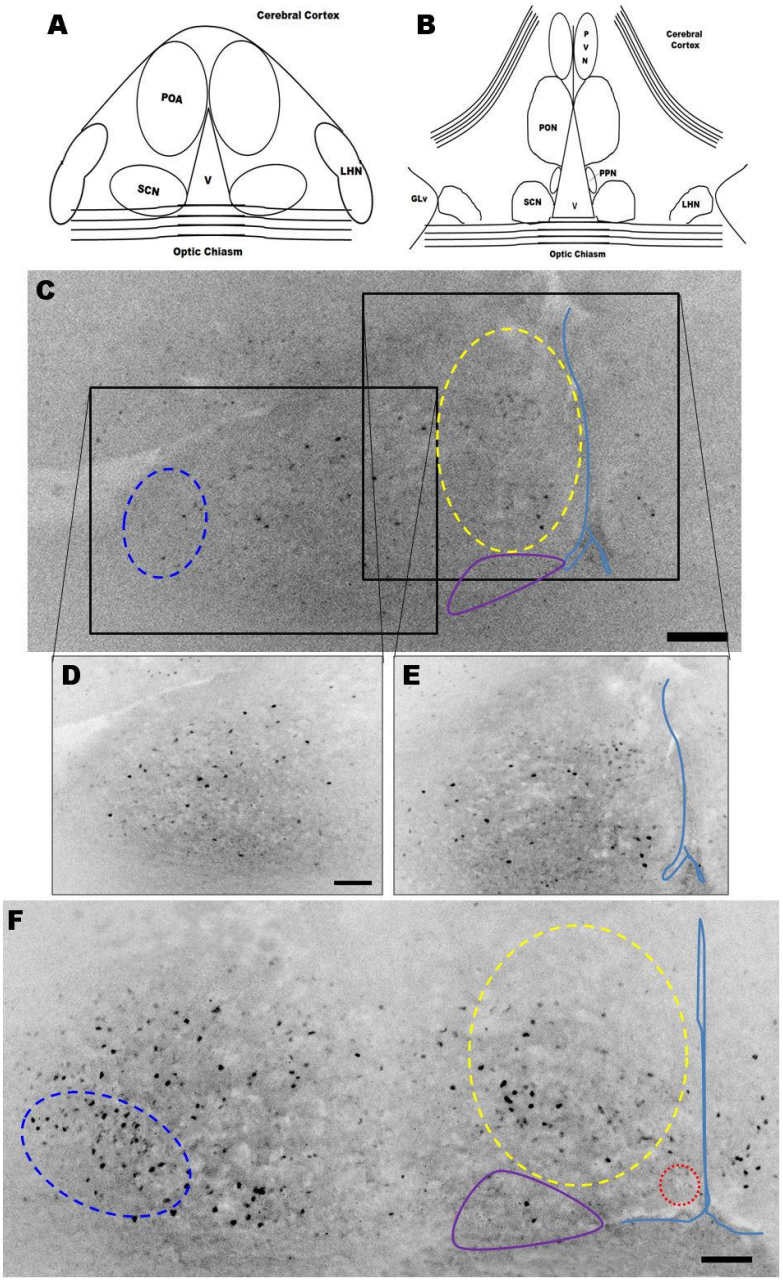

Figure 6.2.2.b. C-FOS-IR cells in the hypothalamus at ZT21.5 without a 60 minute light exposure (control). Schematic diagrams showing the cell groups found in the rostral (A) and medial (B) areas of the hypothalamus. C-FOS-IR cells were found in cell groups in the rostral (C-E) and medial (F) regions of the hypothalamus. High magnification images of the lateral rostral cell groups (D) and central rostral cell groups around the third ventricle of the hypothalamus (E). The blue lines indicate the third ventricle walls. GLv – lateral geniculate nucleus pars ventralis, LHN – lateral hypothalamic nucleus, POA – anterior preoptic nucleus, PON – Preoptic nucleus, PPN – periventricular preoptic nucleus, SCN – suprachiasmatic nucleus, V – third ventricle. Scale bars: image C = 100µm; image D and E (bar shown in D) = 50µm; image F = 50µm. The blue lines indicate the third ventricle walls. Purple dashed circle indicates the SCN; blue dashed circle indicates the LHN; yellow dashed circle indicates the PON; red dashed circle indicates the PPN.

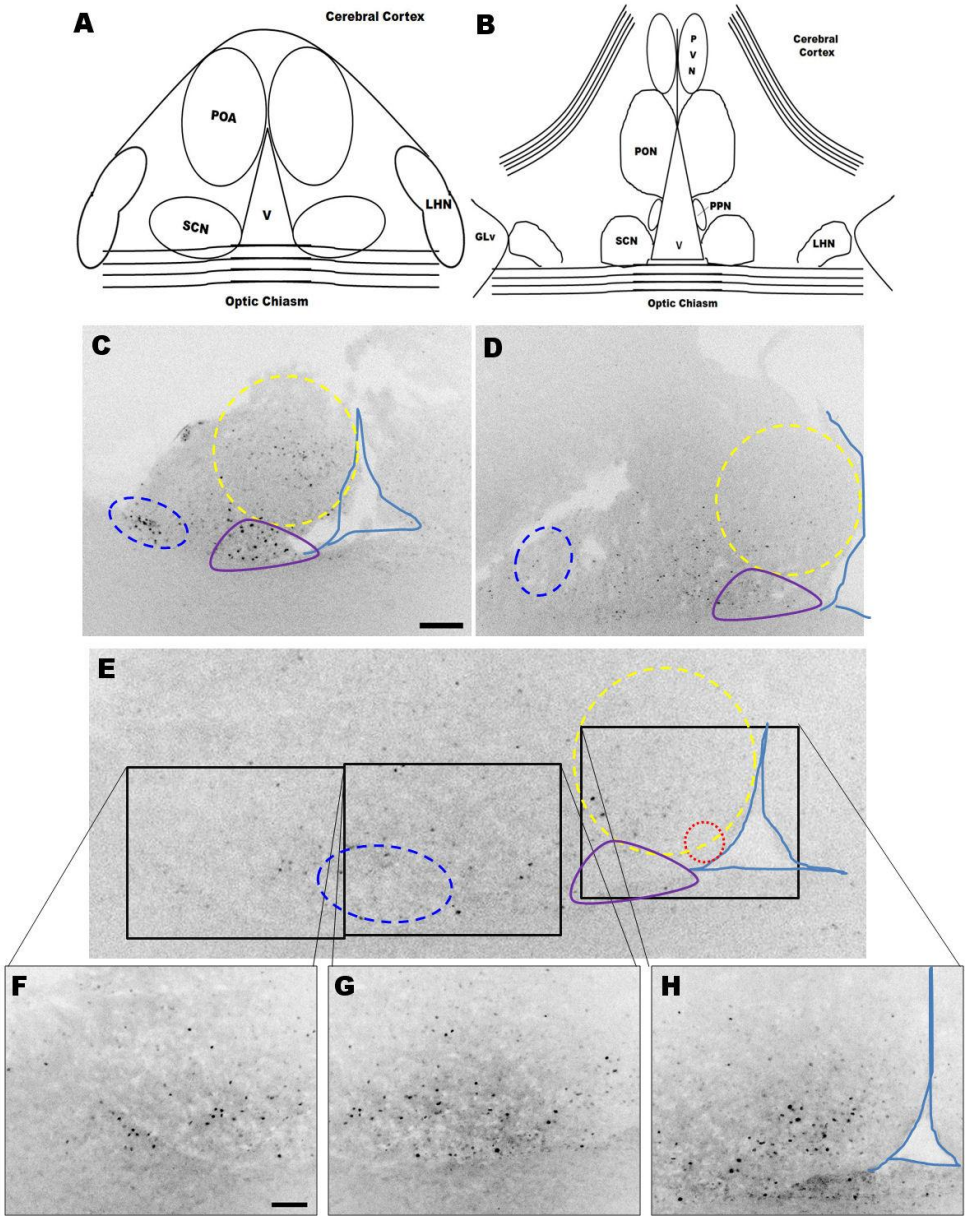

Figure 6.2.2.c. C-FOS-IR cells in the hypothalamus 60 minutes (ZT21) after the OLE. Schematic diagrams showing the cell groups found in the rostral (A) and medial (B) areas of the hypothalamus. C-FOS-IR cells were found in cell groups in the rostral (C and D) and medial (E-H) regions of the hypothalamus. High magnification images of the lateral rostral cell groups (F), lateral-medial medial cell groups (G) and central rostral cell groups around the third ventricle of the hypothalamus (H). The blue lines indicate the third ventricle walls. GLv – lateral geniculate nucleus pars ventralis, LHN – lateral hypothalamic nucleus, POA – anterior preoptic nucleus, PON – Preoptic nucleus, PPN – periventricular preoptic nucleus, SCN – suprachiasmatic nucleus, V – third ventricle. Scale bars: image C, D and E = 100µm (bar shown in C); images F-H = 50µm (bar shown in F). The blue lines indicate the third ventricle walls. Purple dashed circle indicates the SCN; blue dashed circle indicates the LHN; yellow dashed circle indicates the PON; red dashed circle indicates the PPN.

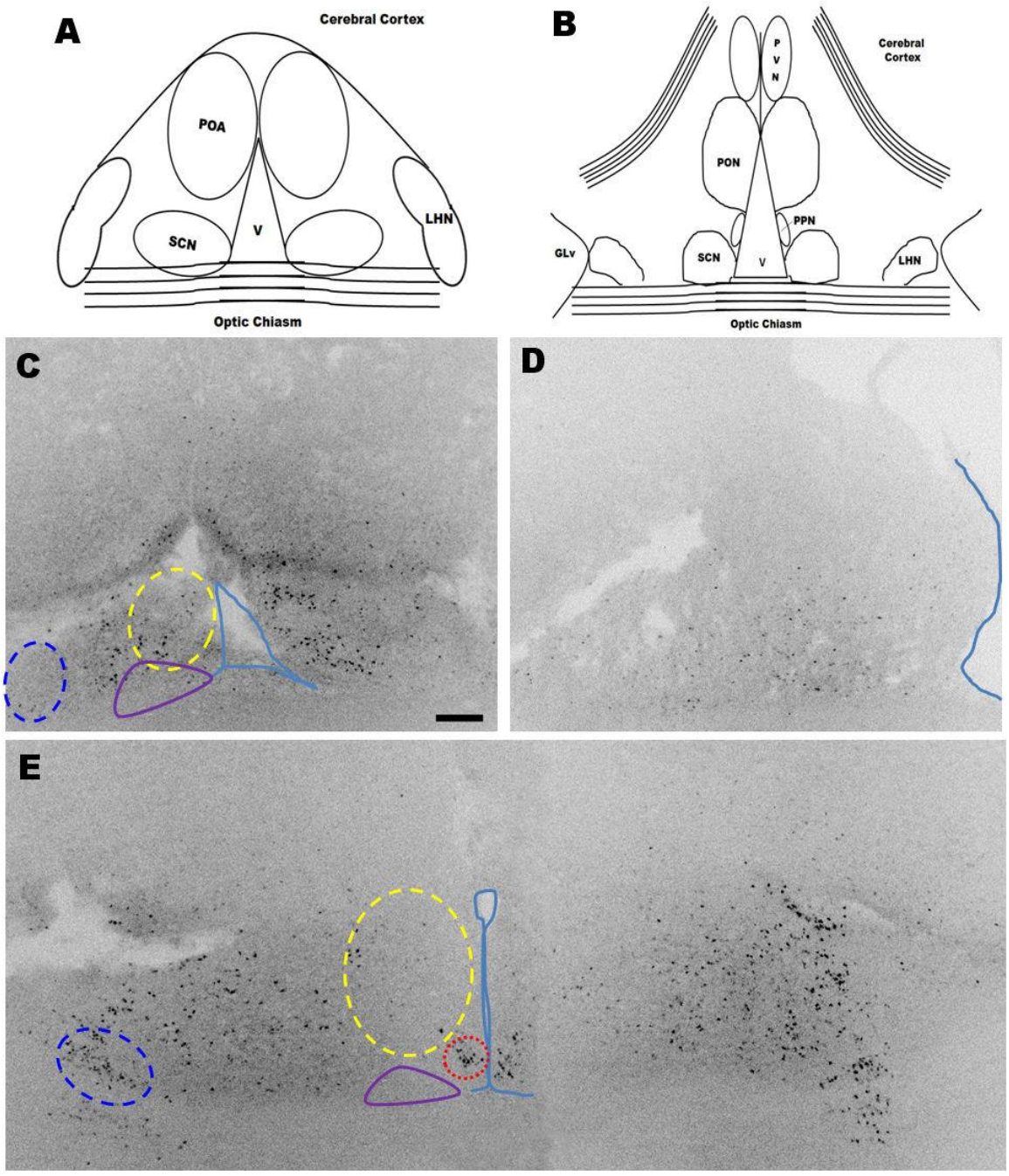

Figure 6.2.2.d. C-FOS-IR expression in the hypothalamus 90 minutes (ZT21.5) after OLE. Schematic diagrams showing the cell groups found in the rostral (A) and medial (B) areas of the hypothalamus. C-FOS-IR cells were found in cell groups in the rostral (C and D) and medial (E) regions of the hypothalamus. The blue lines indicate the third ventricle walls. GLv – lateral geniculate nucleus pars ventralis, LHN – lateral hypothalamic nucleus, POA – anterior preoptic nucleus, PON – Preoptic nucleus, PPN – periventricular preoptic nucleus, SCN – suprachiasmatic nucleus, V – third ventricle. All image scale 100µm (bar shown in C).The blue lines indicate the third ventricle walls. Purple dashed circle indicates the SCN; blue dashed circle indicates the LHN; yellow dashed circle indicates the PON; red dashed circle indicates the PPN.

6.2.3 Comparing the effect of a one hour light exposure in the early dark period to one hour light exposure in the late dark period in the zebra finch hypothalamus

Due to the interesting results from the past two sections, comparing results of the C-FOS-IR cells within the early and late dark period, I decided to compare the differences between the two time periods. C-FOS-IR differences in experimental controls (Figure 6.2.3a), rostral area of the hypothalamus (Figure 6.2.3.b) and the medial area of the hypothalamus (Figure 6.2.3.c). The experimental control time points, i.e. without the light exposure, showed similar results through the hypothalamus (Figure 6.2.3a); with sporadic C-FOS-IR cells found in the POA, PON, LHN and GLv.

The most interesting results between time points (i.e. between early and late dark periods) were seen in the rostral region of the hypothalamus (Figure 6.2.3.b). Hypothalamic sections seen 60 minutes after the OLE in the late dark period showed C-FOS-IR cells to be present in the SCN in the late dark period (Figure 6.2.3.b.-D). This reaction was not seen at all in the early dark period. After 90 minutes after the OLE in the late dark period there were some C-FOS-IR cells found in the SCN cell group (Figure 6.2.3.b.-E), but not as prominent as seen after the 60 minute time point (Figure 6.2.3.b.-D). In the early dark period this reaction was not seen, apart from a few sporadic C-FOS-IR cells, the main cell groups containing C-FOS-IR cells were the POA, LHN and GLv (Figure 6.2.3.b.-B&C). These cell groups were also seen to contain C-FOS-IR cells in the rostral region in the late dark period (Figure 6.2.3.b.-D&E). Thus suggesting that the C-FOS-IR cells found in the SCN in the late dark period is a novel finding in one of the hypothalamic circadian cell groups.

In the medial region of the hypothalamus (Figure 6.2.3.c), again an interesting result occurred in the late dark period compared to the early dark period; after 90 minutes from the OLE a small densely populated number C-FOS-IR cells were seen in the PPN (Figure 6.2.3.c.-E). This finding was also not seen in any of the experimental controls or any of the experimental time points, apart from the 60 minute time point in the late dark period (Figure 6.2.3.c.-D) when a few sporadic C-FOS-IR cells were found. C-FOS-IR cells in the early dark period were generally confined to the PON, LHN and GLv (Figure 6.2.3.c.-B&C). This could also be a novel reaction to light in the later part of the dark period.

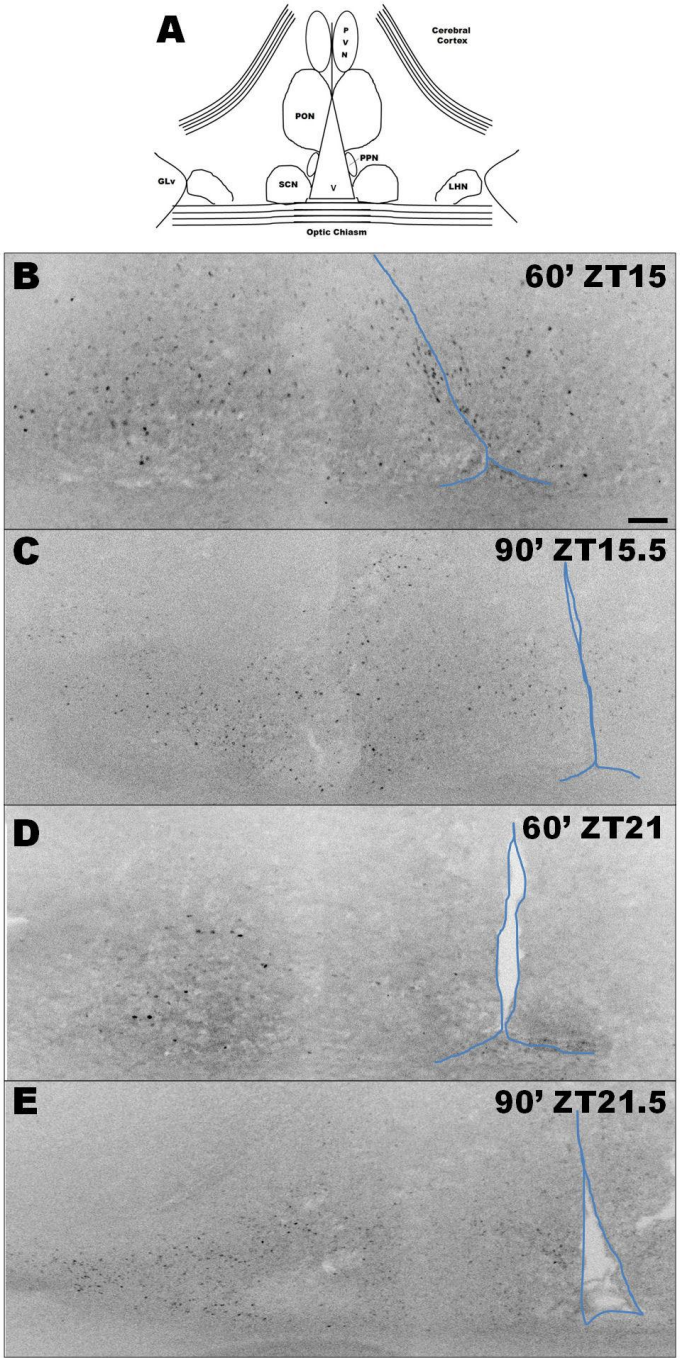

Figure 6.2.3a. Comparison of C-FOS-IR cells in the experimental control time points, in the medial region of the hypothalamus in the early dark period (B and C) and in the late dark period (D and E), immediately after a 60 minute OLE (B and D) and 90 minutes after the OLE (C and E). A shows a schematic diagram of the rostral region of the hypothalamus showing the cell groups found in this region; GLv – lateral geniculate nucleus pars ventralis, LHN – lateral hypothalamic nucleus, PON – Preoptic nucleus, PPN – periventricular preoptic nucleus, SCN – suprachiasmatic nucleus, V – third ventricle. All image scale 100µm (bar shown in B).The blue lines indicate the third ventricle walls.

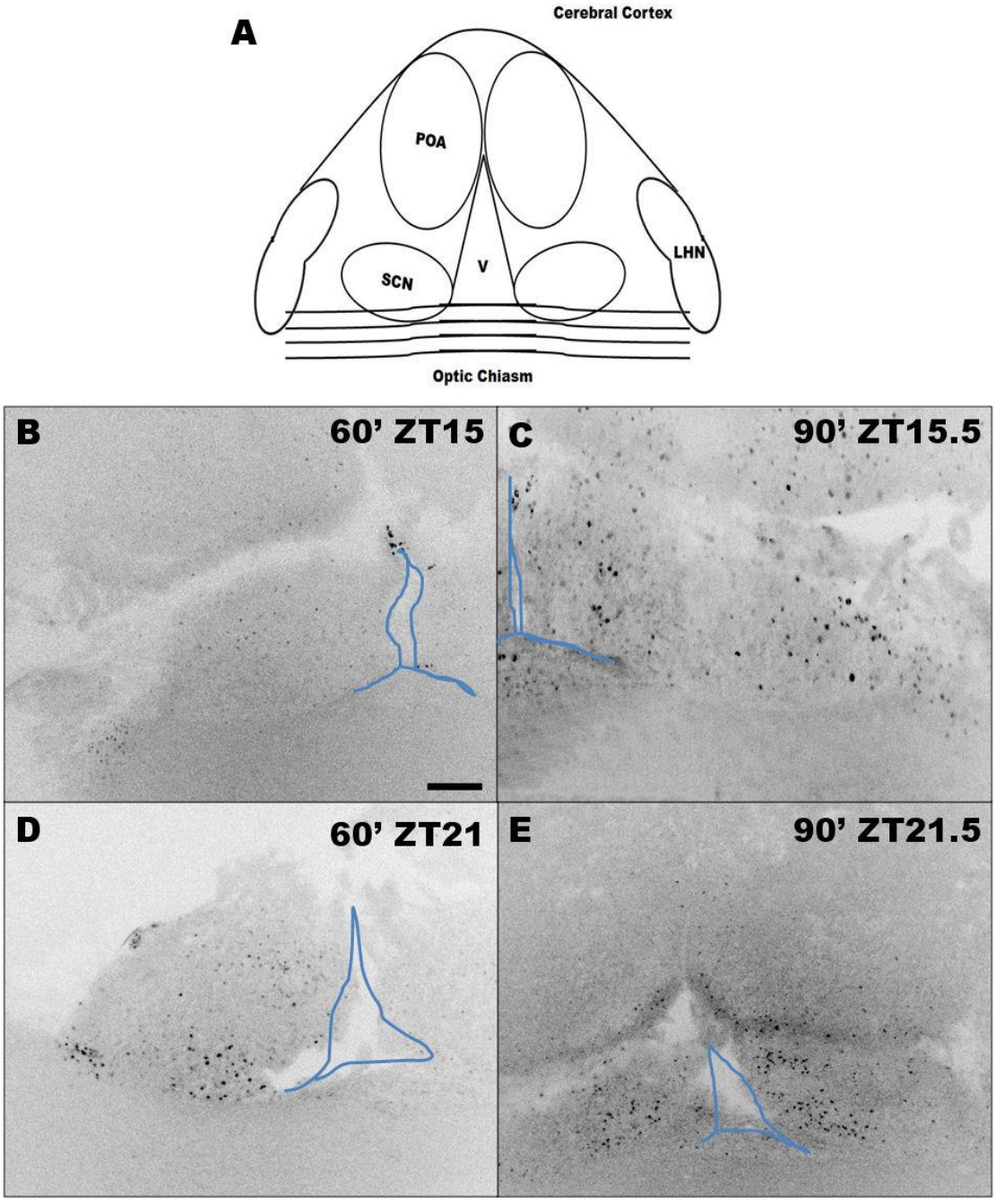

Figure 6.2.3.b. Comparison of C-FOS-IR cells in the rostral region of the hypothalamus in the early dark period (B and C) and in the late dark period (D and E). Immediately after a 60 minute OLE (B and D) and 90 minutes after the onset OLE (C and E). A shows a schematic diagram of the rostral region of the hypothalamus showing the cell groups found in this region; LHN – lateral hypothalamic nucleus, POA – anterior preoptic nucleus, SCN – suprachiasmatic nucleus, V – third ventricle. All image scale 100µm (bar shown in B).The blue lines indicate the third ventricle walls.

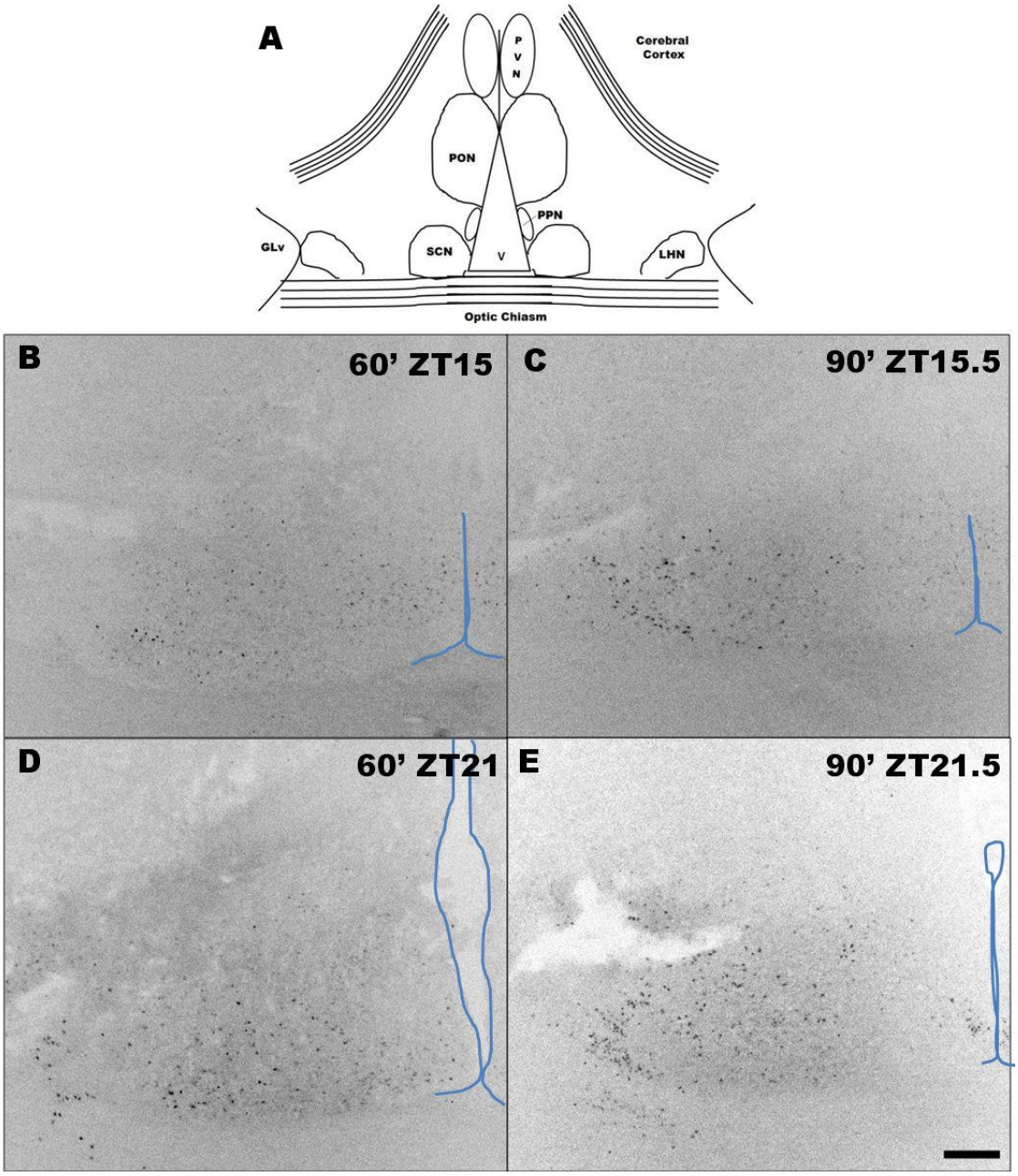

Figure 6.2.3.c. Comparison of C-FOS-IR cells in the medial region of the hypothalamus in the early dark period (B and C) and in the late dark period (D and E). Immediately after a 60 minute OLE (B and D) and 90 minutes after the OLE (C and E). A shows a schematic diagram of the rostral region of the hypothalamus showing the cell groups found in this region; GLv – lateral geniculate nucleus pars ventralis, LHN – lateral hypothalamic nucleus, PON – Preoptic nucleus, PPN – periventricular preoptic nucleus, SCN – suprachiasmatic nucleus, V – third ventricle. All image scale 100µm (bar shown in E).The blue lines indicate the third ventricle walls.

6.3 Discussion

c-fos is an immediate early gene that responds to different stimuli to the cell. In this study it highlights the effect of light in the hypothalamus, which cell groups respond to the light stimulation and which do not. *c-fos* is rapidly phosophorylated in response to UV light exposure (Tanos, *et al*., 2005), and plays a key role in the subsequent regulation of genes involved in the DNA repair, cell proliferation, cell cycle, and tissues and extracellular matrix remodelling proteases (Tanos, *et al*., 2005). *c-fos* has been shown to be expressed in reaction to spontaneous wakefulness in rats. Proteins levels were seen to be high during wakefulness and low during sleepfulness in the cortex (Basheer, *et al*., 1997). Other studies have shown C-FOS immunoreactivity in the PVN, immediately dorsal to the SCN of the hamster after light exposure (Kornhauser, *et al*., 1990). In this study, C-FOS-IR cells highlighted a dramatic effect of light in the POA and PON, the GLv and LHN in the hypothalamus, all of which are areas associated with light transduction. These cells groups all contained C-FOS-IR cells at all time points, but the intensity and density dramatically varied with more C-FOS-IR cells numbers at a greater intensity after stimulation of light in both the early and late dark periods found.

I identified two cell groups that contained C-FOS-IR cells in the late dark period which appeared at no other time point in this study, the SCN and the PPN. C-FOS-IR cells appeared in the SCN immediately after the 60 minute light exposure, in the late dark period, the prominent staining in this cell group had faded slightly 30 minutes later at the 90 minute time point, in which the birds had been transferred back into darkness. This suggests that in the late dark period the SCN has an immediate respond to light and this response gradually disappears

as the intensity and density of C-FOS-IR cells increases in the other cell groups, i.e. PON, LHN and GLv, which contain C-FOS-IR cells in the early dark period and after 90 minutes in the late dark period. C-FOS-IR cells in the PPN only appear in the sections of the medial hypothalamus 90 minutes after the OLE, in the late dark period. The C-FOS-IR cells in the PPN occurs after the SCN staining starts to decline, this suggests that the immediate reaction in the SCN could then relay the photic information to the PPN, the name of the nuclei preoptic suggests its relevance to the light information. Interestingly, studies in the starling and quail showed that the SCN did not respond to light stimulation at CT8 or CT20 under constant darkness (King and Follett, 1997), which could be due to species difference in light transduction or that this experiment was performed under constant darkness and not LD conditions. Under 8L:16D conditions the quail and starling study showed that a one hour light exposure at CT20 caused a greater phase shift in locomotor rhythms (King and Follett, 1997). This result together with my data suggests that the SCN stimulation could be linked with the phase advancing/delaying mechanisms in the zebra finch.

In avian species, studies have shown that the hypothalamus contains more than one circadian oscillator, these cell groups are called the SCN and the LHN (Abraham, *et al*., 2002). The results in this study show that both of these cell groups are responsive to light, but at different times. The LHN appears to contain C-FOS-IR cells under most conditions but increases in intensity after stimulation of light, whereas the SCN is only responsive in the late dark period. This finding suggests that the SCN is involved in the detection of the onset of the photoperiod, i.e. OLE in the morning, as once the birds were placed back in to darkness for 30 minutes, the number of C-FOS-IR cells starts to diminish. Similar findings have been shown in the hamster; C-FOS immuno-reactivity has been shown in the SCN following light

exposure (Kornhauser, *et al*., 1990). In mammals the circadian hypothalamic oscillator resides in the SCN. Light or its downstream messenger, glutamate, activates the phosphorylation of CREB and several immediate early genes, like *c-fos*, and the core clock gene *Per1* (mammals; Porterfield and Mintz, 2009). Therefore this activation in the late dark period in the SCN of the zebra finch could highlight the activation of the avian *Per2* gene, which is the morning oscillator in birds (Abraham, *et al*., 2002; Brandstaetter, *et al*., 2001a). This exposure to light and activation of core clock genes causes a phase advance of circadian rhythms, as shown is other studies on the rodent SCN where a light exposure anytime between ZT18-22 caused a large phase advance of >60 minutes (Guido, *et al*., 1999). In future studies, it will be interesting to examine whether light exposure indeed activates the avian *Per2* gene.

This study shows the effect of light in the hypothalamus of the zebra finch, in numerous cell groups associated with the transduction of photic information: the lateral geniculate nucleus pars ventralis, preoptic regions (POA and PON), and lateral hypothalamic nucleus. It also shows a novel immediate respond of the suprachiasmatic nucleus, and in the periventricular preoptic nucleus, in the late dark period under exposure to light, a key cell group in circadian system.

HYPOTHALAMIC

OUTPUT MECHANISM

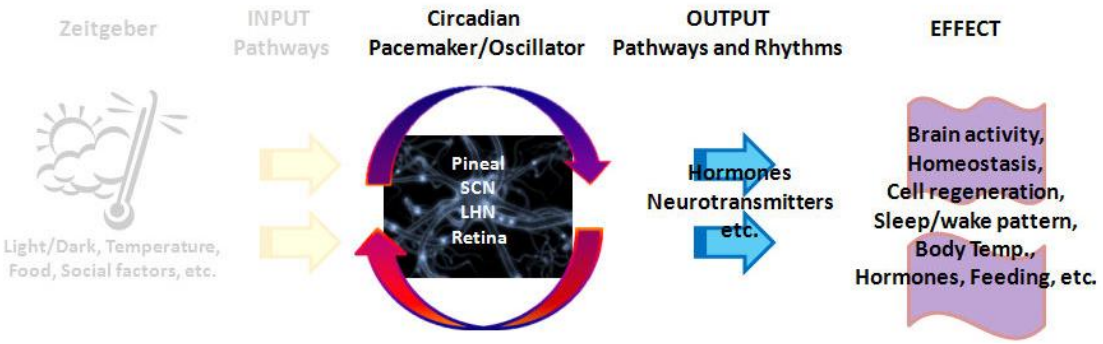

CHAPTER 7

Arginine-vasotocin (AVT) expression in the zebra finch hypothalamus

CHAPTER SEVEN - ARGININE-VASOTOCIN (AVT) EXPRESSION IN THE ZEBRA FINCH HYPOTHALAMUS

7.1 Introduction

A complex system of transcriptional and translational feedback loops is known to control the circadian oscillations in organisms; in mammals the SCN in the hypothalamus controls this and in birds there is a balance between retinal, pineal and hypothalamic oscillators to control the regulation of these feedback loops. These feedback loops control output genes, clock-controlled genes (CCGs), which signal a variety of neurotransmitters, peptides and hormones; these are rhythmically regulated by the same transcriptional mechanisms that control the feedback loops (Li, *et al*., 2009). Three known CCGs peptides, prokineticin 2 (PK2), cardiotrophin-like cytokine and AVP, are implicated as critical SCN output molecules that link the SCN and its efferent targets, in mammals (Li, *et al*., 2009). The neurohypophysial hormone AVP has been shown to be present in the cerebral spinal fluid (CSF), rhythmically, as in the circadian cycle: morning levels are shown to be five times higher than those found in the dark hours (Li, *et al*., 2009).

Arginine-vasotocin (AVT) is the avian homologue to mammalian arginine-vasopressin; there is only an amino acid difference between the two peptides. In the body it is known to regulate the body's retention of water in the kidneys (osmotic balance), it acts in the cardiovascular system to increase blood pressure and produces smooth muscle contraction in the avian oviduct associated with oviposition (Jurkevich, *et al.*, 2008). In the central nervous system it

plays a role in memory formation, rapid eye movement sleep (REM), aggression, social and stress reactions (Jurkevich, *et al.*, 2008). It also stimulates the release of ACTH from the pituitary gland, prolactin-releasing activity in turkeys, prolactin and thyroid-stimulating hormone activity in rats and LH from gonadotropes in hamsters and rats (Jurkevich and Grossmann, 2003). AVT in avian species plays the role which both oxytocin for oviposition and AVP for osmoregulation play in mammalian species (Grossmann, *et al.*, 2002).

The AVT hormone appears to be the archetypal neurohypophyseal hormone in vertebrates, having originated approximately 500 million years ago in cyclostomes (Cornett, *et al*., 2003). The evolution of the other neurohypophyseal hormones may have occurred following the duplication of the AVT gene leading to the "oxytotic-like" (i.e. oxytocin, mesotocin, etc.) and the "vasopressin-like" (i.e. AVP and lysine-vasopressin) lineages (Cornett, *et al*., 2003). Signal sequence followed by conopressin and a remarkably conserved neurophysin domain having a divergent copeptin-homologous c-terminal sequence; this unequivocally demonstrates that the typical architecture of the precursors of the vasopressin and oxytocin hormone superfamily must have been present in the archaemetazoa, a stem group from which both the vertebrate and invertebrates diverged about 600 million years ago (van Kesteren, *et al*., 1992). Vasotocin is therefore the evolutionary precursor of vasopressin (de Kloet, 2010; Table 7.1.a.).

Hormone	Species	Sequence
Vertebrate vasopressin family		
Vasopressin	Mammals[a]	Cys-Tyr-Phe-Gln-Asn-Cys-Pro-Arg-Gly-NH2
Lysipressin	Pigs, warthogs, hippopotamuses, Some marsupials	Cys-Tyr-Phe-Gln-Asn-Cys-Pro-Lys-Gly-NH2
Phenypressin	Some marsupials	Cys-Phe-Phe-Gln-Asn-Cys-Pro-Arg-Gly-NH2
Vasotocin[b]	Non-mammals	Cys-Tyr-Ile-Gln-Asn-Cys-Pro-Arg-Gly-NH2
Vertebrate oxytocin family		
Oxytocin	Mammals[c], ratfish	Cys-Tyr-Ile-Gln-Asn-Cys-Pro-Leu-Gly-NH2
Mesotocin	Marsupials, birds, reptiles, lungfishes, amphibians	Cys-Tyr-Ile-Gln-Asn-Cys-Pro-Ile-Gly-NH2
Isotocin	Bony fishes	Cys-Tyr-Ile-Ser-Asn-Cys-Pro-Ile-Gly-NH2
Various tocins	Sharks	Cys-Tyr-Ile-N/Q-Asn-Cys-Pro-L/V-Gly-NH2
Invertebrate vasopressin/oxytocin superfamily		
Diuretic hormone	Locust	Cys-Leu-Ile-Thr-Asn-Cys-Pro-Arg-Gly-NH2
Annetocin	Earthworm	Cys-Phe-Val-Arg-Asn-Cys-Pro-Thr-Gly-NH2
Lys-Connopressin	Geography and imperial cones, pond snail, seahare, leech	Cys-Phe-Ile-Arg-Asn-Cys-Pro-Lys-Gly-NH2
Arg-Connopressin	Striped cone	Cys-Ile-Ile-Arg-Asn-Cys-Pro-Arg-Gly-NH2
Cephalotocin	Octopus	Cys-Tyr-Phe-Arg-Asn-Cys-Pro-Ile-Gly-NH2
Octopressin	Octopus	Cys-Phe-Trp-Thr-Ser-Cys-Pro-Ile-Gly-NH2

Table 7.1.a. Peptide sequences of vasopressin/oxytocin superfamily. [a] Vasopressin is not found in some marsupials, pigs, and some other mammals. [b] Vasotocin is the progenitor of the vertebrate neurohypophysial hormones; only vasotocin is found in hagfish and lampreys. [c] Oxytocin is also found in some marsupials (Agnatha appeared 500 million years ago; Acher and Chauvet, 1995).

AVT is synthesised in the magnocellular diencephalic vasotocinergic cells from the hypothalamo-neurohypophysial-neurosecretory system (Jurkevich and Grossmann, 2003; Seth, *et al*., 2004). AVT is transported from these cells along the axon terminals to the neurohypophysis (posterior pituitary gland) where the peptide is released into the blood stream (Jurkevich and Grossmann, 2003). Parvocellular vasotocin neurons may also release the peptide, but they release the peptide directly into the brain's interstitial fluid where it modulates the neural circuits controlling brain functions, such as behaviour (Jurkevich and Grossmann, 2003). Experiments in mice have shown that AVP may specifically enhance the output signals of the hypothalamic circadian oscillator, the SCN, by increasing the firing activity of the neurons (Li, *et al*., 2009) which can act as a feedback loop regulator since vasopressin receptor (V1a) has been identified in 40% of SCN neurons (Li, *et al*., 2009). AVP is also released locally into the SCN, or even from the SCN itself, as one third of SCN neurons synthesise AVP, and from the collateral output projections may regulate the expression of certain clock-related genes (Li, *et al*., 2009).

In mammals, AVP is synthesised in the hypothalamus and vesicles stored in the posterior pituitary (Caldwell and Young, 2006). AVP is also released into the brain from the neurons in the supraoptic nucleus (at the base of the brain by the optic chiasm), from centrally projecting hypothalamic neurons, controlling aggression, blood pressure and temperature, and from the paraventricular nucleus (PVN) (Caldwell and Young, 2006; Lim and Young, 2004). The parvocellar neurons of the SCN, bed nucleus of the stria terminalis, and medial amygdale all express AVP (Caldwell and Young, 2006). Axon's from the supraoptic nucleus and paraventricular nucleus project through the infundibulum, into the posterior pituitary gland (Caldwell and Young, 2006; Lim and Young, 2004).

In birds, AVT has been shown be synthesized in the magnocellular diencephalic neurons, such as the supraoptic nucleus (SON) and PVN, in the Japanese quail and chicken and released in to the blood circulation (Jurkevich and Grossmann, 2003; Saito, *et al*., 2010; Seth, *et al*., 2004): this, is the same as in the mammalian system suggesting that the synthesis and secretion mechanisms are conserved between mammals and birds. Cassone and Moore found large AVTergic cells in the SCN, but these cells were smaller than the cell found in the magnocellular paraventricular cells of the house sparrow (Cassone and Moore, 1987). In other song birds (canary and zebra finch) AVTergic cells were found in extra-hypothalamic locations such as the bed nucleus of the stria terminalis (BnST) and these influence reproductive and sexual behaviours in birds (Grossmann, *et al*., 2002). Japanese quails have also shown AVTergic cells in the septo-preoptic-hypothalamic area, later septum, and periventricular hypothalamus and in the preoptic region (Aste, *et al*., 1998). The wide distribution of AVT shows the varied role that AVT has in the organism, from reproduction to aggressive behaviour and osmoregulation.

This study looked at the vasotocin protein rhythm in the hypothalamus of the zebra finch. Immunofluorescent procedures were used to examine the 24 hour expression profile of this hormone under 12:12 LD conditions and under constant dimLL conditions (Figure 7.1.a). The immunofluorescent protocol allowed me to see the neuro-anatomical location and distribution of the peptide AVT in the zebra finch hypothalamus over a 24 hour period and to see whether the expression of AVT is circadian in nature under 12:12 LD conditions and under constant dimLL conditions. Performing cell counts of the AVTergic cells allowed me to quantify and analyse the findings.

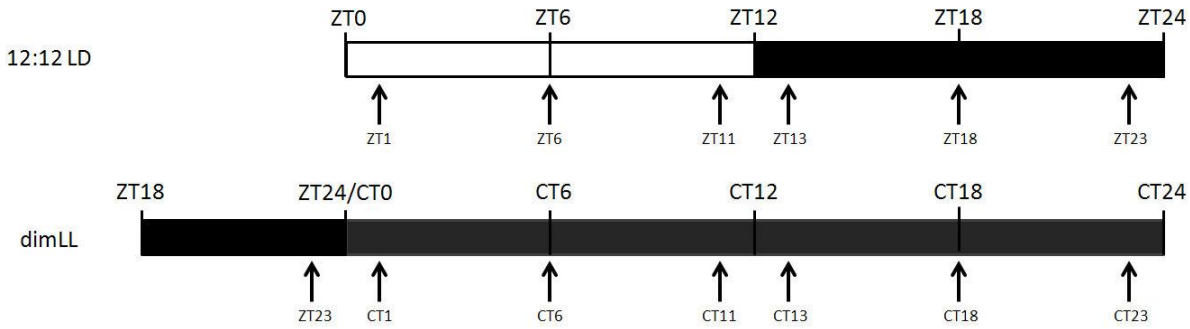

Figure 7.1.a. Schematic diagram showing the lighting conditions and dissection time points of the zebra finch under 12:12LD conditions and dimLL conditions. Dissection time points are highlight by the arrows.

7.2Results

7.2.1 AVTergic cell expression in the hypothalamus under LD conditions

7.2.1.1 Immunofluorescent image analysis

Zebra finches were maintained under 12:12 LD conditions for two weeks, immunofluorescent analysis was performed at ZT1, 06, 11, 13, 18 and 23. Immunofluorescent cellularization of AVT occurred in the perikarya of the neurons stained (Figure 7.2.1.a-A), and not in the nucleus of the neuron, as seen by the dark staining in the cytoplasm with a white/clear oval (nucleus) in the cell. In the POA in the hypothalamus the AVTergic cells are heavily stained with some staining down the axons of the neuron (Figure 7.2.1.a-B). Fibre staining of the axons and dendrites, along with the cell body staining, was also visible in some sections in the caudal areas of the hypothalamus above the LHN region (Figure 7.2.1.a-D) and below the third ventricle in the optic chiasm (Figure 7.2.1.a-C).

The main regions of the hypothalamus containing AVTergic cells were found around the third ventricle including PON and PPN, as well as a small nucleus more lateral to the ventricle, known as the LHN. In avian species this cell group can be split into the ventral and dorsal regions: LHNv and LHNd respectively. Though there was staining found in other regions, such as the paraventricular nucleus, this cell group had sporadic AVTergic cells found throughout the time points (Figure 7.2.1.a.-E&F).

Out of the four cell groups (PON, PPN, LHNv and LHNd), the most profoundly stained areas were the PON and the LHNv: the expression in all the areas appeared to differ over the 24 hour period (Figure 7.2.1.b; Figure 7.2.1.c; Figure 7.2.1.d) with most prominent staining around the onset of light and then diminishing throughout the light period and into the dark period. Toward the mid-late dark period the expression of AVT levels started to increase.

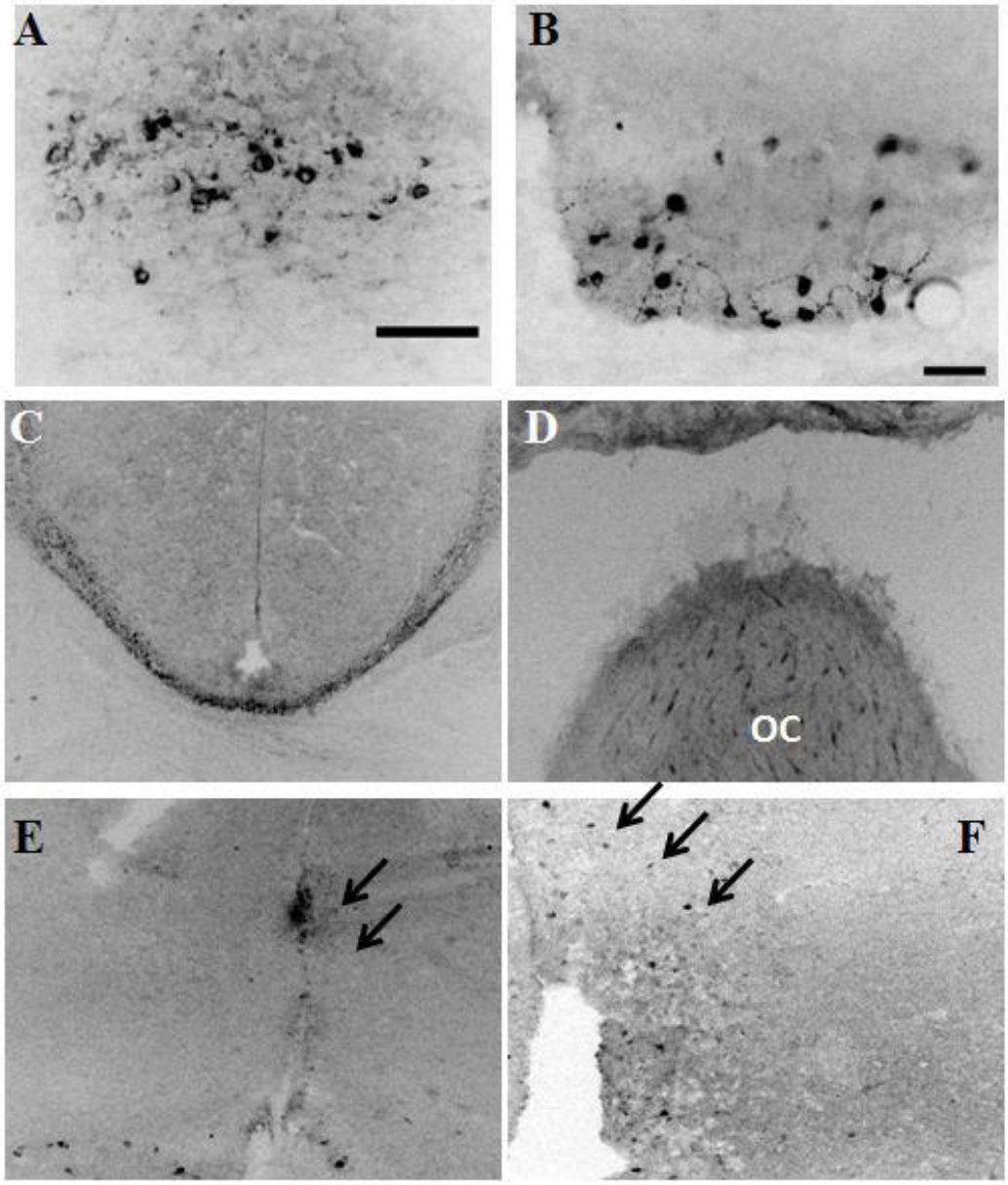

Figure 7.2.1.a. AVTergic cells in the zebra finch hypothalamus. A, shows AVTergic cells with expression confined to the cytoplasm and not the nucleus of the neuron. B, shows AVTergic cells in the PON, showing expression along the axons as well as the body of the nerve cells. C, shows fibrous and cellular staining along the border below the ventricle. D, shows staining in the optic chiasm (OC) in very rostral section, in the formation of the third ventricle, staining here appeared to be in the nerve cell and along the axon. E&F, show cellular staining in the paraventricular nucleus above the third ventricle. Scale bars: image A = 50 µm; B, C, D, E and F = 100µm (bar shown in B).

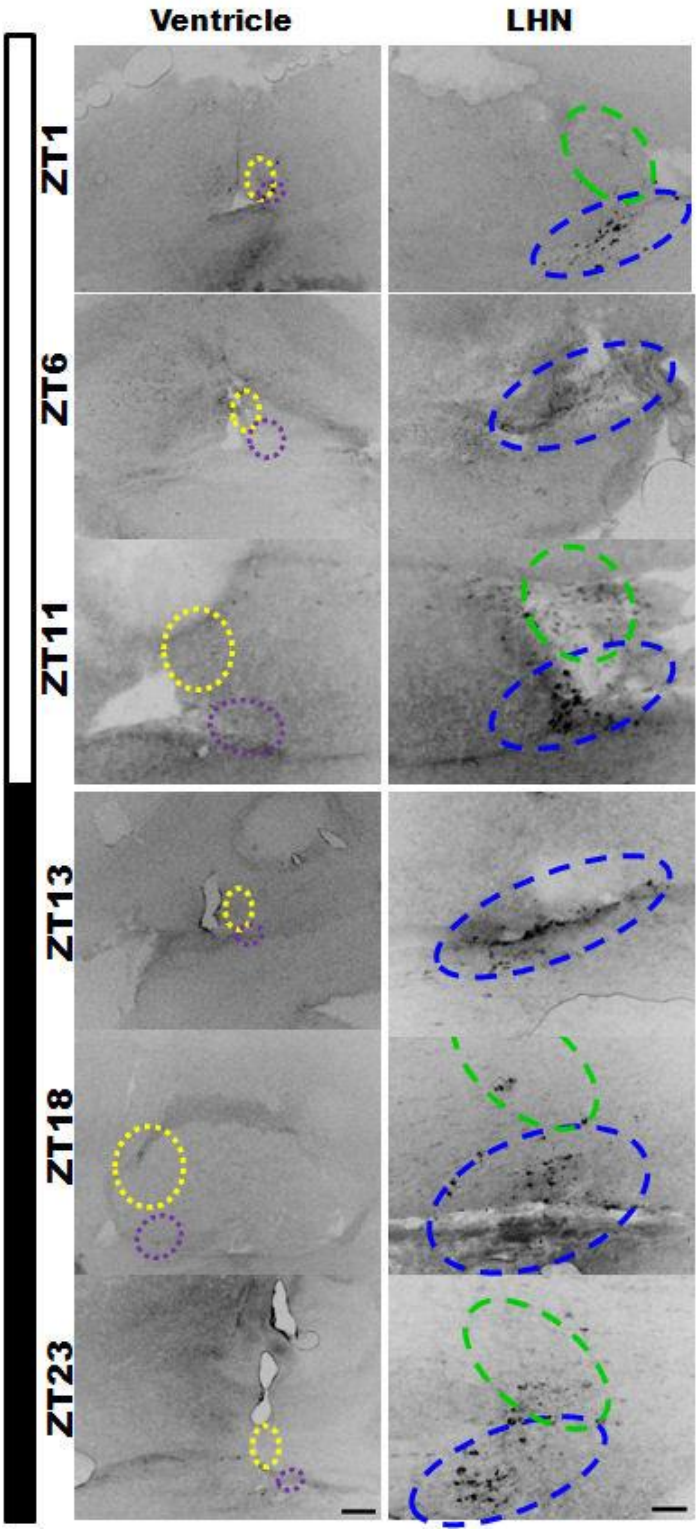

Figure 7.2.1.b. AVTergic cells in the rostral region of the hypothalamus under LD conditions. At ZT1, ZT6 and ZT11, in the light phase of 24 hours, and ZT13, ZT18 and ZT23, in the dark phase of 24 hours, under 12:12 LD conditions, as shown by the white (light period) and black (dark period) bars along the edge of the figure. Purple dashed circle indicates the SCN; blue dashed circle indicates the LHNv; green dashed circle indicates the LHNd; yellow dashed circle indicates the PON. Scale bars: ventricle = 100 µm; LHN = 100µm.

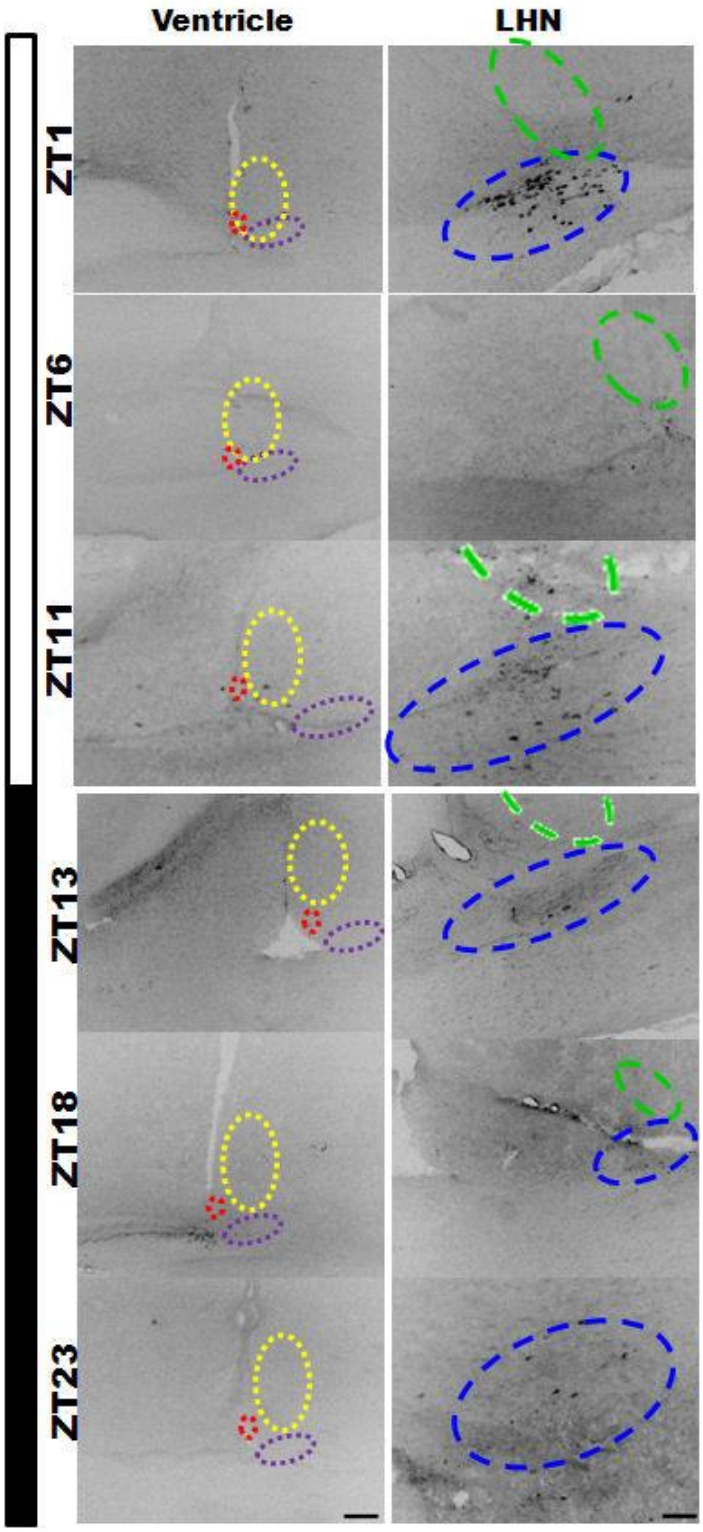

Figure 7.2.1.c. AVTergic cells in the medial region of the hypothalamus under LD conditions. At ZT1, ZT6 and ZT11, in the light phase of 24 hours, and ZT13, ZT18 and ZT23, in the dark phase of 24 hours, under 12:12 LD conditions, as shown by the white (light period) and black (dark period) bars along the edge of the figure. Purple dashed circle indicates the SCN; blue dashed circle indicates the LHNv; green dashed circle indicates the LHNd; yellow dashed circle indicates the PON; red dashed circle indicates the PPN. Scale bars: ventricle = 200µm; LHN = 50µm.

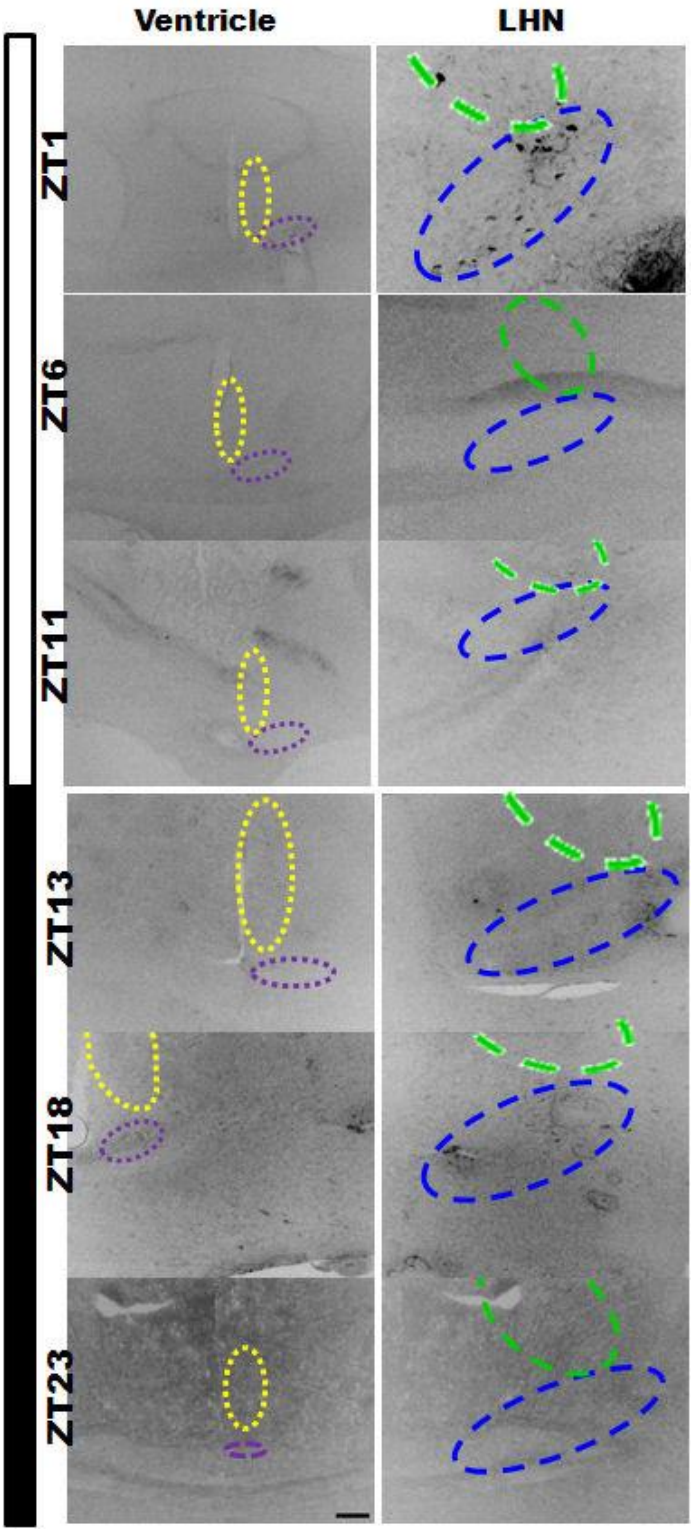

Figure 7.2.1.d. AVTergic cells through the caudal region of the hypothalamus under LD conditions. At ZT1, ZT6 and ZT11, in the light phase of 24 hours, and ZT13, ZT18 and ZT23, in the dark phase of 24 hours, under 12:12 LD conditions, as shown by the white (light period) and black (dark period) bars along the edge of the figure. Purple dashed circle indicates the SCN; blue dashed circle indicates the LHNv; green dashed circle indicates the LHNd; yellow dashed circle indicates the PON. Scale bars: ventricle and LHN = 100µm.

7.2.1.2 Immunofluorescent cell counts analysis

In the zebra finch, AVTergic cells were found in numerous cell groups within the hypothalamus (i.e. PPN, LHN, PON; Figure 7.2.1.e); cell groups with the greatest number of AVTergic cells are the PON and LHN-v of the hypothalamus.

In the PON area (Figure 7.2.1.e.-A-F; yellow bars), the most profuse staining was found at ZT1 (Figure 7.2.1.e.-A): staining was found throughout the whole of the region. After ZT1 the number of AVTergic cells rapidly drops, so that AVTergic cells were only found in the most rostral areas of the PON by ZT6 (sections 1-10; Figure 7.2.1.e.-B). This low level of expression continued throughout the light period and into the dark period, apart from a few more rostral-medial (sections number 15-20) cells being found at ZT11 (Figure 7.2.1.e.-C) and ZT13 (Figure 7.2.1.e.-D). In the dark period (ZT12-ZT24) AVTergic cell numbers were still low right up until ZT23, one hour before the onset of light (Figure 7.2.1.e.F).

The AVTergic cells found in the PPN cell group (Figure 7.2.1.e.-A-F and Figure 7.2.1.e.-M-R – red bars) appeared more sporadically localised and only appeared towards the middle of the dark period, at ZT18 (Figure 7.2.1.e.-E&Q). The first few AVTergic cells were found at ZT18 and then the number increased at ZT23 (Figure 7.2.1.e.-F&R). The number of AVTergic cells dropped at ZT1 (Figure 7.2.1.e.-A&M), one hour into the light period. After ZT1 AVTergic cells disappeared (Figure 7.2.1.e.-B-D and Figure 7.2.1.e.-N-P).

AVTergic cells were found through the LHNv region of the hypothalamus (Figure 7.2.1.e.-G-L – blue bars) and varied throughout the 24 hour period. The most rostral sections of the

LHNv always contained AVTergic cells, but, as the time changes, the AVTergic cell number fluctuates in more medial and caudal sections of the hypothalamus. At ZT1 (Figure 7.2.1.e.-G), AVTergic cells were found throughout the LHNv cell group, but after ZT1 the caudal sections AVTergic cell number dropped, peaking again just before lights off at ZT11 (Figure 7.2.1.e.-I). The number of AVTergic cells in the caudal area starts to significantly reduce until only the rostral area that contained AVTergic cells at ZT13, with a few sporadic AVTergic cells found more medially (Figure 7.2.1.e.-J). At ZT18, there was a large number of AVTergic cells found in the medial area of the LHNv (Figure 7.2.1.e.K); then one hour before lights on, ZT23, the number of AVTergic cells increased more caudally, with high levels in the rostral area (Figure 7.2.1.e.-L).

In the dorsal area of the LHN (LHNd; Figure 7.2.1.e.-G-L – green bars), AVTergic cells appears to be sporadic throughout the cell group, similar to the PPN cell group. The LHNd only appears to contain AVTergic cells around the onset of light (ZT00); positive cells are found sporadically throughout the region at ZT1 (Figure 7.2.1.e.-G) and more rostrally at ZT23 (Figure 7.2.1.e.-L). These patterns were confirmed in the graphs showing total cell counts for each cell groups at each ZT (Figure 7.2.1.e.-M-R).

Figure 7.2.1.e. (Page 225) AVTergic cell profiles in the zebra finch hypothalamus under 12:12 LD conditions. AVTergic cell expression profiles through the zebra finch hypothalamus at different zeitgeber times (A-L). Each point represents an average cell count for that section through the hypothalamus from rostral to caudal. (M-R)Total cell counts of AVTergic cells in the different cell groups of the hypothalamus over 24 hours. Each point represents an averaged total cell count ± SEM for that cell group. ZT0 is when lights are turned on at 9am and ZT12 is when lights are turned off at 9pm. The bar along the edge of the graphs indicates the lighting condition for that time point, i.e. white bars indicate the light period and black bars indicate the dark priod. Red bars indicate the periventricular preoptic nucleus (PPN); blue bars indicate lateral hypothalamic nucleus ventral portion (LHNv); green bars indicate the lateral hypothalamic nucleus dorsal portion (LHNd); yellow bars indicate the preoptic nucleus (PON). ANOVA indicated by * on figure letter; significant differences between times points as revealed by post hoc Tukey test indicated by * above the corresponding symbols: *p<0.05, **p<0.01, ***p<0.001. See Appendix I – Section 1.2.4 for statistical analysis.

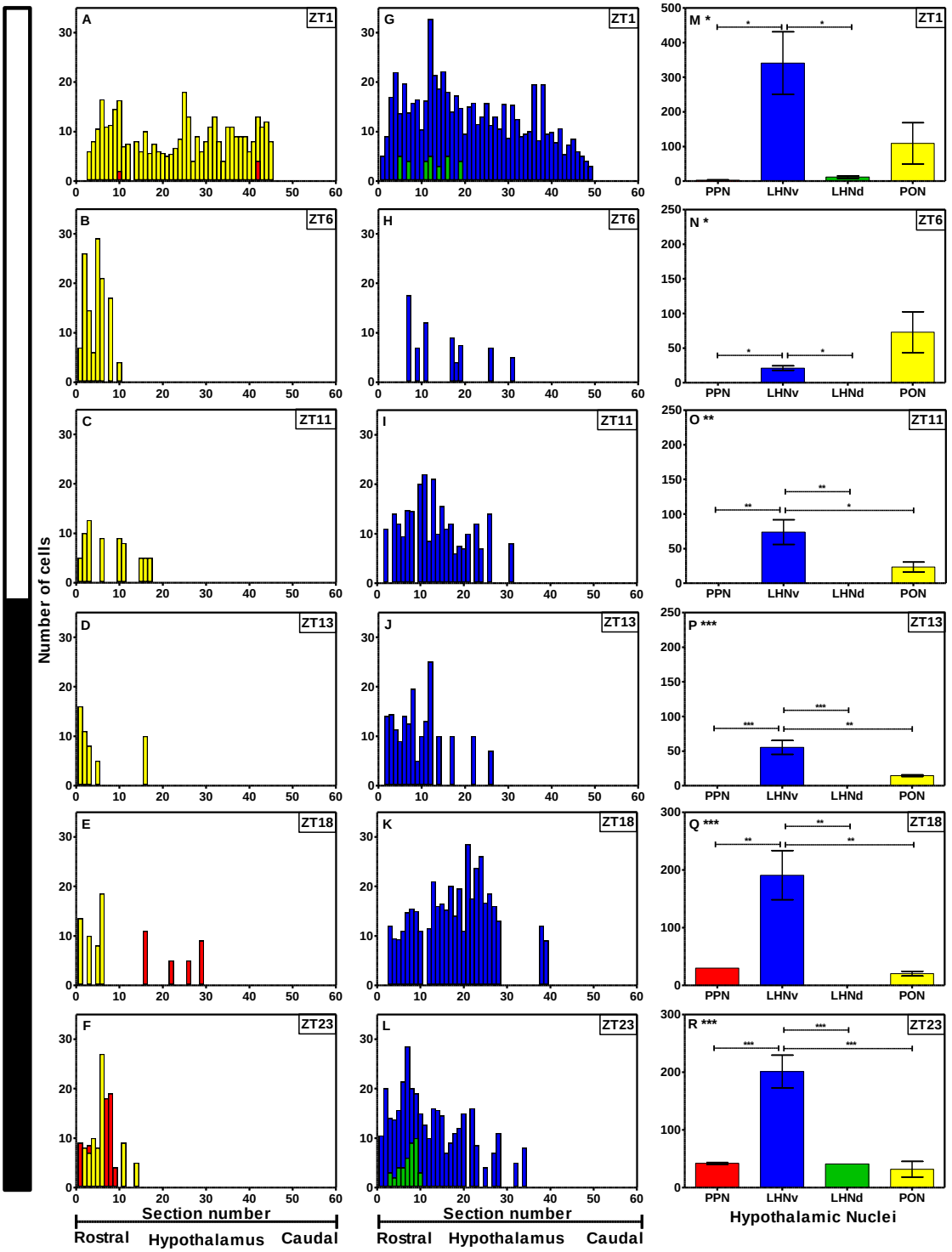
A
ZT1
B
ZT6
C
ZT11
D
ZT13
E
ZT18
F
ZT23
G
ZT1
H
ZT6
I
ZT11
J
ZT13
K
ZT18
L
ZT23
M *
ZT1
N *
ZT6
O **
ZT11
P ***
ZT13
Q ***
ZT18
R ***
ZT23
PPN
LHNv
LHNd
PON
Hypothalamic Nuclei
Number of cells
Section number
Rostral
Hypothalamus
Caudal

7.2.2 AVTergic cell expression in the hypothalamus under constant dimLL conditions

7.2.2.1 Immunofluorescent images analysis

Under dimLL conditions AVTergic cells were found in all the four cell groups examined in this chapter; the PPN, LHNv, LHNd and the PON (Figure 7.2.2.a; Figure 7.2.2.b; Figure 7.2.2.c). The more prominent AVTergic cells were seen in the rostral (Figure 7.2.2.a) and medial (Figure 7.2.2.b) regions of the cell groups, with no AVTergic cells found in the caudal extension of the cell groups (Figure 7.2.2.c). The most prominently stained AVTergic cells were found in the LHNv and PON cell groups, the same cell groups prominently stained under the LD conditions, but neither cell group had the number of AVTergic cells as seen under LD conditions. The LHNv had staining in the medial region of this nucleus, but only at CT1, CT18 and CT23. The AVTergic cells found in the PON were restricted to the rostral regions of this cell group.

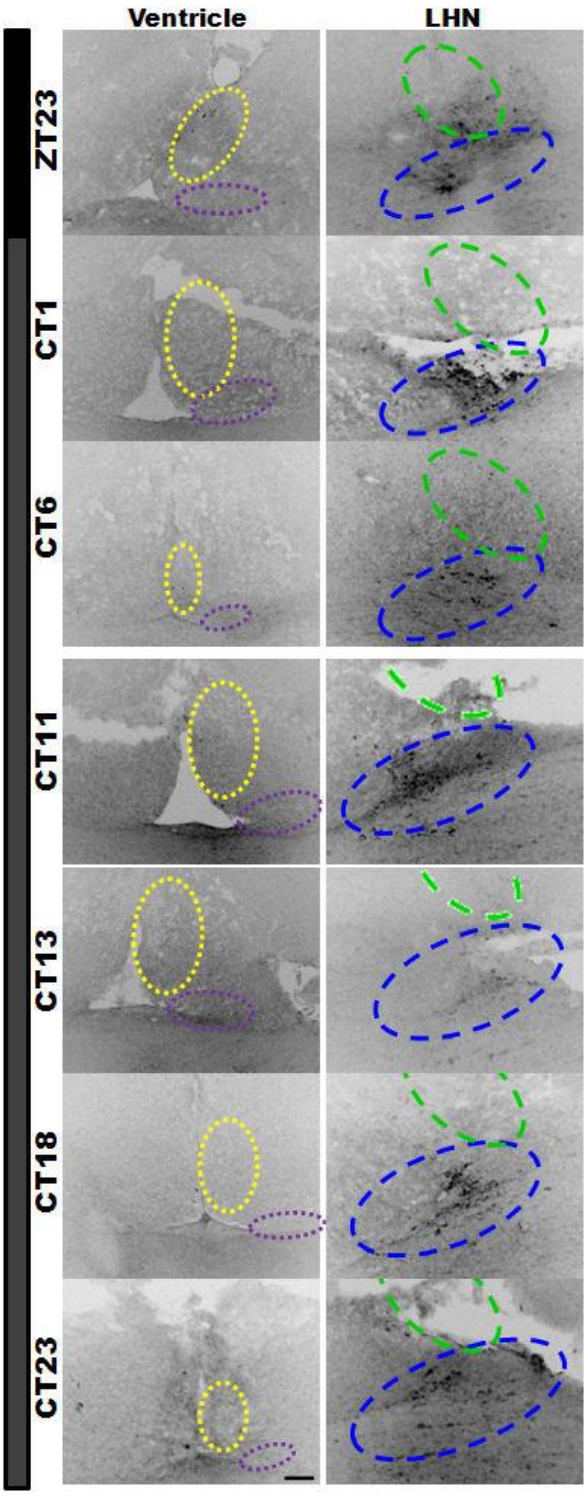

Figure 7.2.2.a. AVTergic cells in the rostral region of the hypothalamus. At ZT23 (LD), CT1, CT6, CT11, CT13, CT18 and CT23 time points under dimLL conditions. CT1-CT11 would normally be under light conditions and CT1, CT6 and CT11 would normally be in the dark phase of the 24 hour cycle, as shown by the black and dark grey bars along the edge of the figure. Purple dashed circle indicates the SCN; blue dashed circle indicates the LHNv; green dashed circle indicates the LHNd; yellow dashed circle indicates the PON. Scale bars: ventricle and LHN = 50µm.

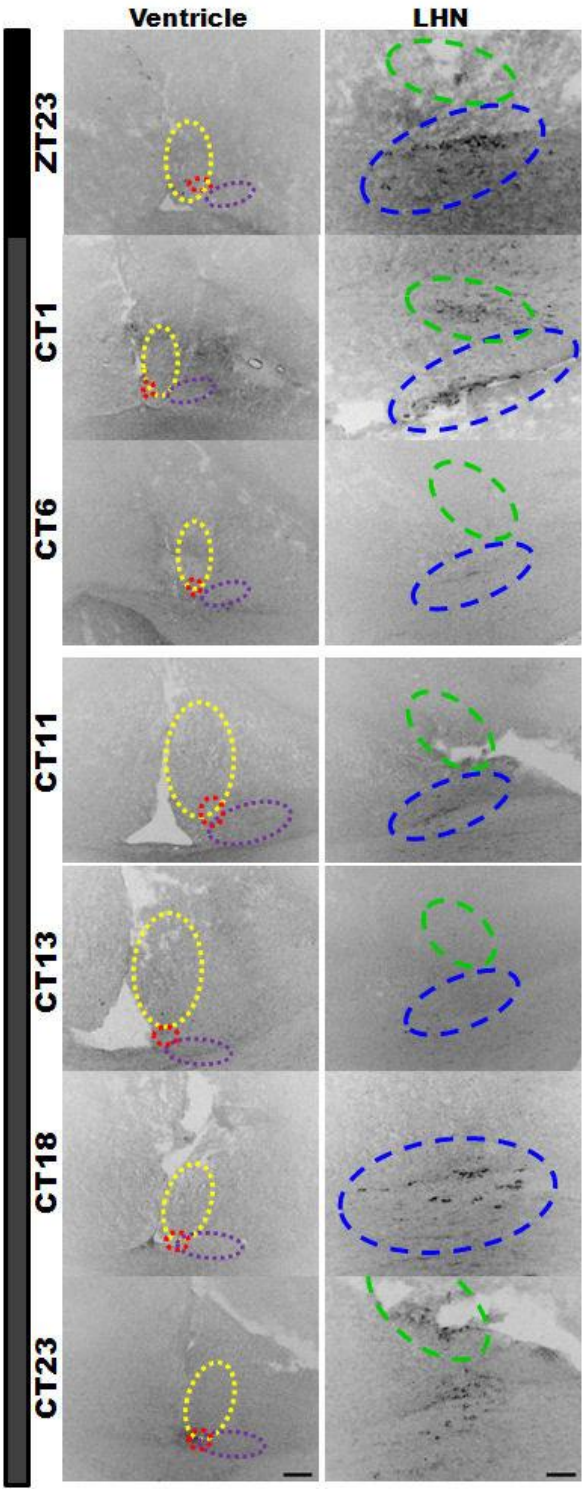

Figure 7.2.2.b. AVTergic cells in the medial region of the hypothalamus. At ZT23 (LD), CT1, CT6, CT11, CT13, CT18 and CT23 time points under dimLL conditions. CT1-CT11 would normally be under light conditions and CT1, CT6 and CT11 would normally be in the dark phase of the 24 hour cycle, as shown by the black and dark grey bars along the edge of the figure. Purple dashed circle indicates the SCN; blue dashed circle indicates the LHNv; green dashed circle indicates the LHNd; yellow dashed circle indicates the PON; red dashed circle indicates the PPN. Scale bars: ventricle = 100µm and LHN = 50µm.

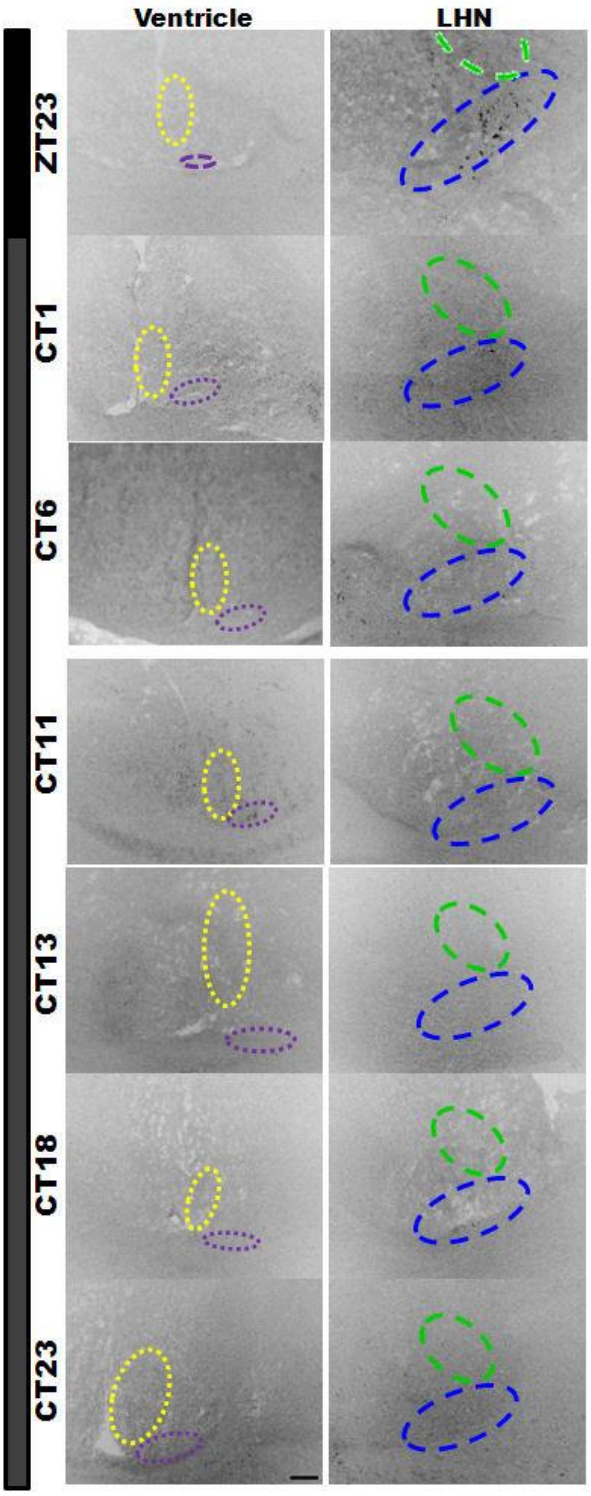

Figure 7.2.2.c. AVTergic cells in the caudal region of the hypothalamus. At ZT23 (LD), CT1, CT6, CT11, CT13, CT18 and CT23 time points under dimLL conditions. CT1-CT11 would normally be under light conditions and CT1, CT6 and CT11 would normally be in the dark phase of 24 hour, as shown by the black and dark grey bars along the edge of the figure. Purple dashed circle indicates the SCN; blue dashed circle indicates the LHNv; green dashed circle indicates the LHNd; yellow dashed circle indicates the PON. Scale bars: ventricle and LHN = 50µm.

7.2.2.2Immunofluorescent cell count analysis

The AVTergic cell staining under dimLL conditions showed a similar pattern to the staining found under LD conditions; AVTergic cells were found in the PON, PPN around the ventricle and in areas of the LHN (Figure 7.2.2.d). ZT23 was repeated in this experiment because the birds were placed under experimental conditions at a separate time to the LD conditions; therefore I wanted to check for continuity between the experiments.

Under the dimLL conditions, AVTergic cell numbers in the PON were minimal, only rostral areas of this cell group contained AVTergic cells at all CT times (Figure 7.2.2.d.-A-G). There was slight variation in AVTergic cell numbers in the most rostral areas, the lowest numbers of cells were found at CT6, in the middle of the subjective day (Figure 7.2.2.d.-C&Q). Time points around the subjective lights on CT1 and CT23, and mid-subjective night at CT18 had the highest number of AVTergic cells (Figure 7.2.2.d.-A,F&G and Figure 7.2.2.d.-P,T&U respectively).

A sporadic number of AVTergic cells were found in the PPN throughout the time-points (Figure 7.2.2.d.A-G). AVTergic cells found in this cell group were also contained in the most rostral regions; with CT1 having the highest number of AVTergic cells found and CT13 had the least amount of AVTergic cells (Figure 7.2.2.d.-B&P and Figure 7.2.2.d.-E&S respectively).

The most abundant number of AVTergic cells were found in the LHNv at CT1 (Figure 7.2.2.d.-I); levels in this cell group then rapidly decrease at ZT6 (Figure 7.2.2.d.-J) and continued to be seen only in the more rostral regions of the LHNv throughout the subjective light and subjective dark phases. AVTergic cell numbers then increased in more medial areas of the LHNv towards the mid-subjective dark period at CT18 (Figure 7.2.2.d.-M) when numbers remain high until CT1.

There were low numbers of AVTergic cells found in the LHNd (Figure 7.2.2.d-H-N – green bars). Again AVTergic cells were found at around the subjective onset of light CT1 and CT23, and mid-subjective night at CT18. This is a similar pattern to AVTergic cells found in LD conditions with expression around the presumed onset of light. These patterns are supported by the total cell counts for each cell group (Figure 7.2.2.d.-O-U).

Figure 7.2.2.d. (Page 232) AVTergic cell profiles in the zebra finch hypothalamus under constant dimLL conditions. (A-N) AVTergic cell expression profiles through the zebra finch hypothalamus at different zeitgeber times. Each point represents an average cell count for that section through the hypothalamus from rostral to caudal. (O-U)Total cell counts of AVTergic cells in the different cell groups of the hypothalamus over 24 hours. Each point represents an averaged total cell count ± SEM for that cell group. The bar along the edge of the graphs indicates the lighting condition for that time point, i.e. black bar represents the dark period under the LD conditions and the dark grey bar indicates the constant dim light (dimLL) conditions. Red bars indicate the periventricular preoptic nucleus (PPN); blue bars indicate lateral hypothalamic nucleus ventral portion (LHNv); green bars indicate the lateral hypothalamic nucleus dorsal portion (LHNd); yellow bars indicate the preoptic nucleus (PON). ANOVA indicated by * on figure letter; significant differences between times points as revealed by post hoc Tukey test indicated by * above the corresponding symbols: *p<0.05, **p<0.01, ***p<0.001. See Appendix I – Section 1.2.4 for statistical analysis.

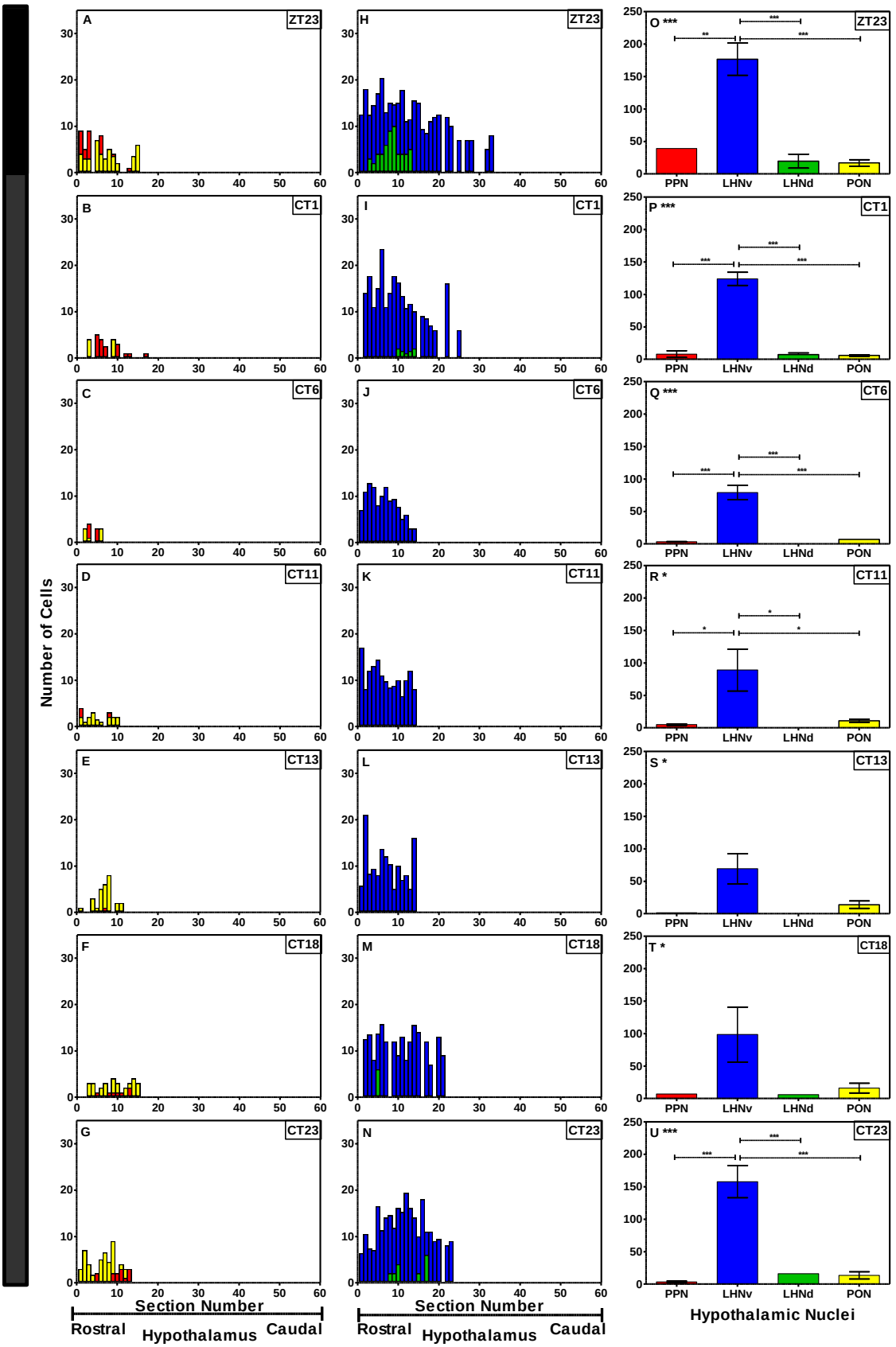
A
ZT23
H
ZT23
O ***
ZT23
B
CT1
I
CT1
P ***
CT1
C
CT6
J
CT6
Q ***
CT6
D
CT11
K
CT11
R *
CT11
E
CT13
L
CT13
S *
CT13
F
CT18
M
CT18
T *
CT18
G
CT23
N
CT23
U ***
CT23
Number of Cells
PPN
LHNv
LHNd
PON
Section Number
Rostral
Hypothalamus
Caudal
Hypothalamic Nuclei

7.2.3 Comparing AVTergic cell expression under LD conditions and dimLL conditions in the hypothalamus

To compare the AVTergic cells between the different cell groups under different lighting conditions, I calculated the total cell count for each ZT/CT in the four different nuclei: the results are shown in Figure 7.2.3.a. The AVTergic expression in the PPN appeared in the dark and constant dark periods (Figure 7.2.3.a.-A; one-way ANOVA, $F_{12,34}$=58.01 p= <0.0001). There is a low number of AVTergic cells found at ZT1; after this time point the number of AVTergic cells disappeared until mid-dark period at ZT18, with the peak number of AVTergic cells at ZT23, with the anticipation of light. The number of AVTergic cells then decreased at CT1 and remained consistently low throughout the subjective light and dark periods, the number did not increase again at CT18 (ZT18-CT18 q=10.86 p<0.001) and CT23 (ZT23-CT23 q=19.35 p<0.001) as in the LD conditions at ZT18 and ZT23.

In the LHNv, the total number AVTergic cells at different time points was shown to be significantly variable (Figure 7.2.3.a.-B – one-way ANOVA, $F_{12,57}$=4.774 p<0.0001). ZT1 has the most abundant number of AVTergic cells over any other time point; ZT1 has a mean number of 334 AVTergic cells, whereas the closest comparative expression at ZT18-23 has a mean of 205-14 (see Appendix I – Section 1.2.6 page 236 for statistical break down). There was a significant reduction of AVTergic cells after ZT1 (Tukeys, ZT1-ZT6 q=8.155 p<0.001); there was more than a 10 fold difference in total cells expressing AVT between ZT1 and ZT6 (mean values ZT1=334.33, ZT6=21.2). Again, the number of cells remains low throughout the rest of the light period (ZT6-ZT12) and into the dark period of the LD cycle. After the mid-dark period (ZT18) cell numbers increase, and continue to increase towards the end of the dark period (ZT23). Once the birds are subjected to the constant dim light period

(dimLL), AVTergic cell numbers drop. CT1 AVTergic cell numbers are significantly lower compared to the cell counts ZT1 (q=5.139). These low numbers continued for the rest of the subjective light period (CT00-CT12), as did those found under LD conditions (Figure 7.2.3.a.-B). In the subjective dark period (CT12-CT24) the level remains low at CT13. AVTergic cell numbers then increase towards the mid-subjective dark period (CT18) and continue to increase towards the end of the subjective dark period at CT23, again as in the numbers found in LD. Cell counts at CT23 were greater than those found at CT1 (CT1=124 and CT23=157). Although the level remains low during the constant dimLL period, the cell numbers found at CT6 are higher than those found at ZT6, showing an increase in AVTergic cell numbers from the light period. The rhythm was more smoothly pronounced during the constant dimLL period, suggesting that AVT expression could be due to sleep or with the anticipation of light.

AVTergic cells in the LHNd (Figure 7.2.3.a.-C; one-way ANOVA, $F_{12,57}$=4.774 p<0.05) clearly occurred around the onset of light at ZT00. Under LD conditions, expression is only found in this nucleus at ZT1 and ZT23, but under dimLL conditions expression is also found at CT18, as well as CT1 and CT23. There are no AVTergic cells found throughout the rest of the time-points, in both the LD and dimLL conditions.

Total cell counts for the PON cell group (Figure 7.2.3.a.-D; one-way ANOVA, $F_{12,48}$=2.346 p<0.0001) show that the peak expression was found in the light period, at ZT1 and ZT6. The number of AVTergic cells under LD conditions was higher than that found under the dimLL conditions. Though the cell numbers in the subjective dark period (CT12-CT00) were higher than those found in the subjective light period (CT00-CT12), under LD conditions levels

peaked at ZT1 and ZT6, then dropped and cell numbers increased towards the end of the dark period at ZT23.

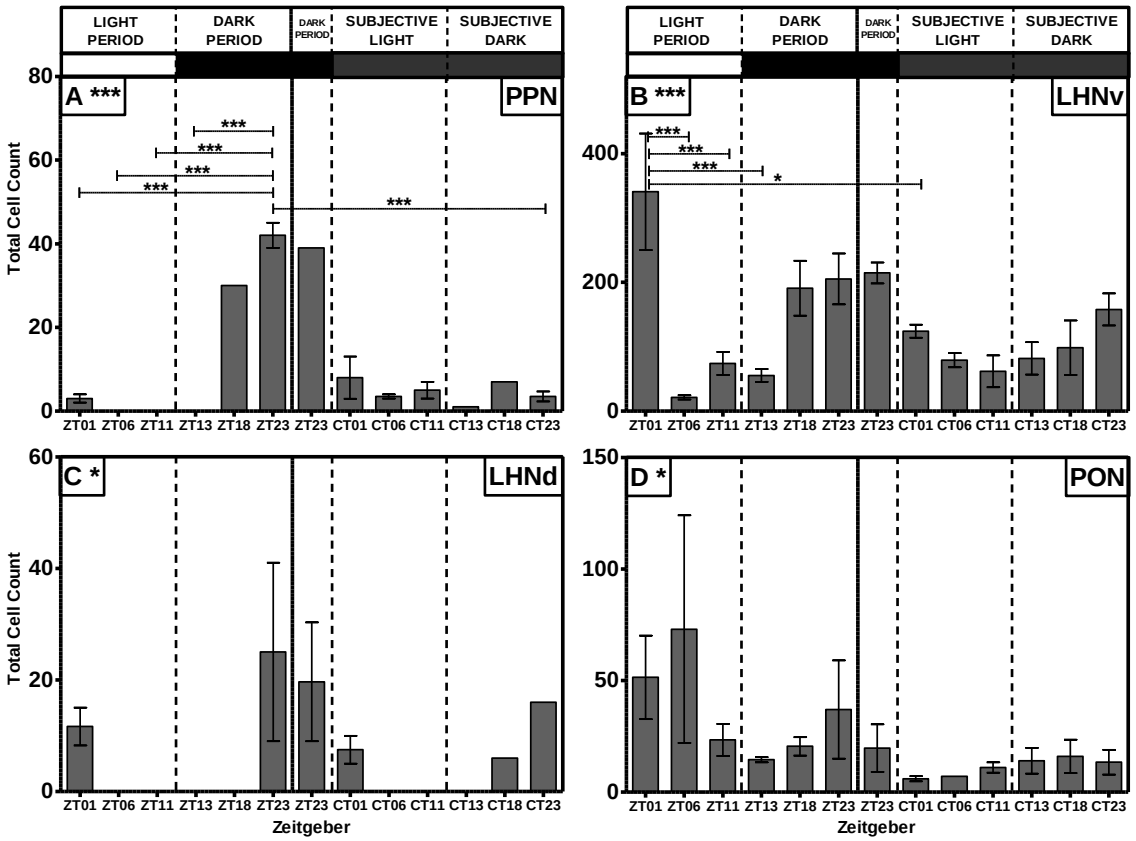

Figure 7.2.3.a. Comparative total AVTergic cell counts in different hypothalamic cell groups under different light conditions in different hypothalamic cell groups. Each point represents an averaged total cell count ± SEM for that ZT through the hypothalamus. ZT23 is repeated as the samples of the LD and dimLL were collected at different times, therefore a repeat of ZT23 was needed to check for continuity. Under 12:12 LD conditions, ZT 0 is when lights are turned on at 9am and ZT12 is when lights are turned off at 9pm. Under dimLL conditions, CT00-CT12 is the subjective light period and CT12-CT00 is the subjective dark period. Bars at the top of each graph represent the lighting conditions at that set ZT. Significant differences as revealed by ANOVA indicated by * on figure letter; significant differences between times points, i.e. to the lowest value of mRNA expression, as revealed by post hoc Tukey test indicated by * above the corresponding symbols: *p<0.05, **p<0.01, ***p<0.001. X-axis: Zeitgeber time. PPN - periventricular preoptic nucleus; LHNv – lateral hypothalamic nucleus ventral portion; LHNd - lateral hypothalamic nucleus dorsal portion; PON – preoptic nucleus. See Appendix I – Section 1.2.6 for statistical analysis.

The previous figures showing AVTergic cell expression under LD (Figure 7.2.1.e) and dimLL conditions (Figure 7.2.2.d); highlighted that AVTergic cells through the hypothalamus from rostral to caudal vary over the 24 hour period. AVTergic cells are consistently found in the rostral regions of the hypothalamus, e.g. LHN-v, PON, LHN-d and the PPN, but not in the medial and caudal regions. Therefore I wanted to see whether the area of the cell group containing AVTergic cells does change over the time-points. Since each section is a set thickness (20μm), I converted the area containing AVTergic cells to a distance (μm) and compared this distance over the time-points collected under LD and dimLL conditions (Figure 7.2.3.b).

In the PPN (Figure 7.2.3.b.A; one-way ANOVA, $F_{12,43}$= 63.14 p=<0.0001) AVTergic cells mainly appear in the dark phase(s) of the study, i.e. ZT18-ZT23 under LD conditions and throughout the dimLL conditions. The maximum length, from rostral to caudal, of the PPN cell group containing AVTergic cells, is ~200μm of the cell group, throughout most of the time-points which contain AVTergic cells. ZT18 is shown to have an expression range of ~600μm, but looking at the profiles for this time-point, it appears that there were only a few AVTergic cells in the medial area of this cell group and no AVTergic cells in the rostral area. The dimLL conditions show that there were AVTergic cells at CT6 (80μm), CT11 (140μm) and CT13 (140μm), whereas these time-points under LD conditions (ZT6, ZT11 and ZT13) contain no AVTergic cells.

The most abundant number of AVTergic cells through the LHNv was at ZT1, at just under 800μm length of this cell group containing AVTergic cells (Figure 7.2.3.b.-B; one-way

ANOVA, $F_{12,53}$=10.20 p=<0.0001; see Appendix I – Section 1.2.6 for a full statistical break down). During the rest of the LD conditions the expression dropped to below the 400μm mark at ZT6 (352μm), ZT11 (393μm) and ZT13 (395μm; Figure 7.2.3.b.-B). Then as the dark period continued towards the mid-dark period AVTergic cell number started to increase through the LHNv from rostral into more medial extensions of this cell group at ZT18 (500μm) and ZT23 (468μm; Figure 7.2.3.b.-B). The rhythm found under the LD conditions was maintained and more pronounced under the dimLL subjective light and dark periods. At CT1 (400μm) a lot less of the LHNv contains AVTergic cells as compared to the distance found at ZT1 (856μm; Figure 7.2.3.b.-B; Tukey's ZT1-CT1 q=8.520 p<0.001). As seen in the LD conditions, the distance or amount of the LHNv containing AVTergic cells decreased dramatically at CT6 (by 145μm) and continued to drop to its lowest amount of the LHNv at CT13 (216μm) in the early subjective dark period. At CT18, mid-subjective dark period, AVTergic cells are seen slightly more medially into the LHNv, covering 285μm of this cell group, and this distance increases further at CT23 to 384μm (Figure 7.2.3.b.-B).

In the LHNd the AVTergic cells appeared to be expressed in the very rostral parts of this cell group, within the first 200μm (Figure 7.2.3.b.-C; one-way ANOVA, $F_{12,47}$=<0.0001 p<0.0001), if found at all, in time points found around the onset or subjective onset of light, ZT1, ZT23, CT1 and CT23.

At ZT1 AVTergic cells in the PON (Figure 7.2.3.b.-D; one-way ANOVA, $F_{12,43}$=3.934 p<0.0010) are contained through most (~500μm) of this cell group, into the more caudal extension. The distance found at ZT1 is significantly greater than that found at CT1 under

dimLL conditions (~200μm; Tukey's, ZT1-CT1 q=5.559 p<0.05) or the level found at most of the other time points (see Appendix I – Section 1.2.6 for full details). At all the other time points, AVTergic cells are found within the first 300μm of the PON cell group, with most being far below this distance (≤200μm) in the very rostral regions of the PON (Figure 7.2.3.b.-D).

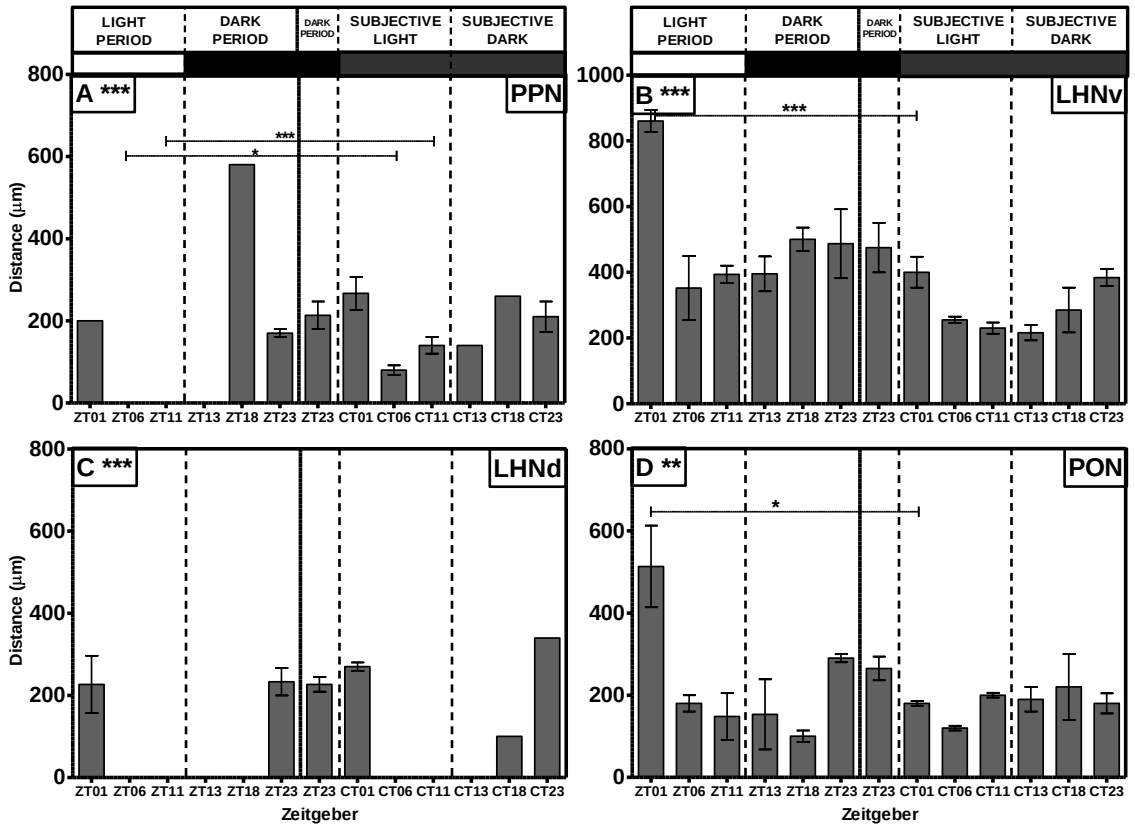

Figure 7.2.3.b. AVTergic cells along the longitudinal axis of the hypothalamus in different cell groups. Each point represents an averaged total cell count ± SEM for that ZT through the hypothalamus. ZT23 is repeated as the samples of the LD and dimLL were collected at different times, therefore a repeat of ZT23 was needed to check for continuity. Under 12:12 LD conditions, ZT0 is when lights are turned on at 9am and ZT12 is when lights are turned off at 9pm. Under dimLL conditions, CT00-CT12 is the subjective light period and CT12-CT00 is the subjective dark period. Bars at the top of each graph represent the lighting conditions at that set ZT. Significant differences as revealed by ANOVA indicated by * on figure letter; significant differences between times points, i.e. to the lowest value of mRNA expression, as revealed by post hoc Tukey test indicated by * above the corresponding symbols: *p<0.05, **p<0.01, ***p<0.001. PPN - periventricular preoptic nucleus; LHNv – lateral hypothalamic nucleus ventral portion; LHNd - lateral hypothalamic nucleus dorsal portion; PON – preoptic nucleus. See Appendix I – Section 1.2.6 for statistical analysis.

In the previous figures I have shown that, in the zebra finch, the most abundant cell group containing AVTergic cells occurs in the LHNv, with variation of AVTergic cell numbers from rostral to caudal, within this cell group. I felt that closer examination of this nuclei expression was needed. Therefore I separated the nuclei into three regions, the rostral, medial and caudal, and averaged the total cell count readings for each of the regions and compared them over the set time-points taken (Figure 7.2.3.c).

Closer examination of this cell group revealed that the most medial and rostral areas of the LHNv contained the greatest numbers of AVTergic cells throughout the 24 hours period, in both the LD conditions and dimLL conditions (Figure 7.2.3.c.-A&B respectively; A - one-way ANOVA, $F_{12,53}$=4.365 p=0.0002 and B - one-way ANOVA, $F_{12,48}$=3.077 p<0.01). Only a few time points mainly around the onset or subjective onset of light (ZT1, ZT23, CT1, CT23), contained AVTergic cells in the caudal extension of this cell group (Figure 7.2.3.c.-C; one-way ANOVA, $F_{12,45}$= 2.113 p<0.05).

In the rostral region of the LHNv (Figure 7.2.3.c.-A), the time points with the greatest number of AVTergic cells was found to be around the onset (LD) or subjective onset of light under dimLL conditions, e.g. ZT1, ZT23, CT1 and CT23. After a peak at ZT1, the number of AVTergic cells in the rostral area dramatically dropped at ZT6 (by 152 cells; Figure 7.2.3.c.-A; Tukey's ZT1-ZT6 q=6.182 p<0.01). After ZT6 the AVTergic cell count began to increase through the rest of the light period and through the dark period, with another dramatic increase in cell numbers between ZT18 and ZT23 (increasing by 82 cells) and peaking in the late dark period at ZT23 (Figure 7.2.3.c.-A). The two ZT23 time point values are consistent

with each other. Under dimLL conditions AVTergic cell counts drop at the first time point (CT1) compared to the level seen at the end of the dark period (ZT23; decreasing by 50 cells; Figure 7.2.3.c.-A). The level at CT1 then continued to decrease throughout the rest of the dimLL conditions until CT23 where there was a dramatic increase in AVTergic cell numbers, compared to CT18 (increasing by 60 cells; Figure 7.2.3.c.-A). Under dimLL conditions the lowest AVTergic cell count occurred at CT11, whereas under LD conditions the lowest count was found at ZT6. At CT1 and CT23 the number of AVTergic cells was not as high as ZT1 and ZT23, but not significantly different (Tukey's, q=1.541 p<0.01), suggesting that this level or peak is endogenous to the zebra finch and is therefore linked to the end of sleep or the beginning of arousal or the activation of endogenous core clock genes.

Medially the highest number of AVTergic cells occurred in the LD conditions and around what would have been the "on set of light" in the *dim*LL conditions, i.e. CT1 and CT23 (Figure 7.2.3.c.-B). Following a similar pattern to the rostral sections (Figure 7.2.3.c.-A), greatest AVTergic cell numbers were found at ZT1 before decreasing at ZT6, ZT11 and ZT13, and into the dark period. In the mid-dark period AVTergic cell numbers increased at ZT18 and ZT23 (Figure 7.2.3.c.-B). Under the dimLL conditions, this pattern continued with peak cell counts found at CT1, CT18 and CT23; although these levels are a lot lower than the "peaks" in the LD conditions. No AVTergic cells were found between CT6 and CT13 (Figure 7.2.3.c.-B). AVTergic cell numbers found at CT1 are more similar to the levels found at ZT6 (LD), both around the ~15 cell mark. This therefore suggests that the level of cell numbers found in the medial regions are endogenous in nature, peaking when light should be appearing, the levels, however, and then increased with light exposure.

In the caudal region of the LHNv (Figure 7.2.3.c.-C) AVTergic cells only occurred around the "on-set of light" at ZT1, ZT18, ZT23, CT1, CT18 and CT23 (Figure 7.2.3.c.-C). The finding that this expression is continued in the dimLL conditions suggests that this rhythm is deeply entrained or takes more than 24 hours to become "free-running" or that the rhythm found at these time points is endogenous to the zebra finch hypothalamus.

The patterns are clearly shown when comparing the variation of AVTergic cell counts in the different regions at each time-point (Figure 7.2.3.d). The expression and significance changes through the 24 hours under both LD and dimLL conditions; under LD conditions the most significant variations are found in the mid-light period until the early dark period (ZT6, ZT11 and ZT13; Figure 7.2.3.d.-B,C&D; ANOVA, ZT6 – $F_{2,10}$=15.24 p<0.01; ZT11 – $F_{2,15}$=5.018 p<0.05; ZT13 – $F_{2,12}$=12.31 p<0.01). At these time points no AVTergic cells are found in the caudal regions of the LHNv. Whereas, at time-points when AVTergic cells are found in the caudal regions, around the onset of light (ZT1 - Figure 7.2.3.d.-A; ZT18 - Figure 7.2.3.d.-E; ZT23 - Figure 7.2.3.d.-F) there is no significant difference between the regions of the LHNv. Under dimLL conditions it was the time points around the subjective onset of light which appear to be more significantly variable; CT1 (Figure 7.2.3.d.-H; ANOVA, $F_{2,9}$=42.14 p=0.0001), CT6 (Figure 7.2.3.d.-I; ANOVA, $F_{2,9}$=35.52 p=0.0002) and CT23 (Figure 7.2.3.d.-M; ANOVA, $F_{2,11}$=24.03 p=0.0002). The time-point around the subjective lights-off CT11 and CT13 only have expression in the most rostral areas and less of a significant variation (Figure 7.2.3.d.-J&K respectively; ANOVA, CT11 - $F_{2,9}$=5.275 p<0.05; CT13 - $F_{2,10}$=4.879 p<0.05).

As the time-points are lined up with their relevant time-point under the different conditions, i.e. ZT1 with CT1 are next to each other, it is easy to see the variation of expression in the caudal region of the LHNv. Under the dimLL conditions (Figure 7.2.3.d.-H-M) the cell counts are greater in the rostral regions and the medial cell counts decrease, compared to their counter-part. CT1 and CT18 both have a much lower AVTergic cell count in the rostral and medial regions and no cells were found in the caudal regions, under the dimLL conditions as compared to the counts found at ZT1 and ZT18 under LD conditions (Figure 7.2.3.d.-A and Figure 7.2.3.d.-E respectively). At ZT6 (Figure 7.2.3.d.-B), expression was found in both the rostral and medial areas but at CT6 (Figure 7.2.3.d.-I) there was only expression found in the rostral expression and this pattern continued at time-points ZT11/CT11 (Figure 7.2.3.d.-C&J), ZT13/CT13 (Figure 7.2.3.d.-D&K) and ZT23/CT23 (Figure 7.2.3.d.-F&M).

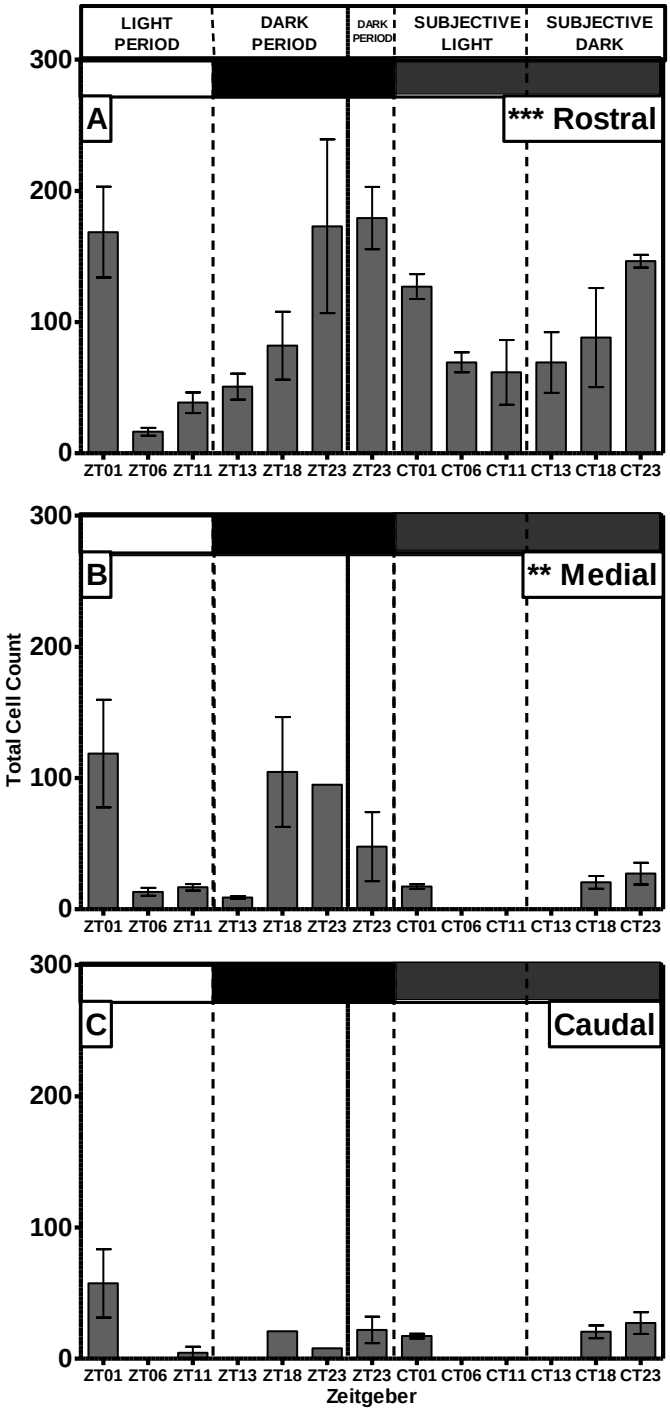

Figure 7.2.3.c. Total AVTergic cell counts in rostral (A), medial (B) and caudal (C) regions of the LHNv. ZT23 is double plotted as the LD and dimLL samples were taken at different periods, so ZT23 was repeated to check for continuity. The bars at the top of each graph indicates the light schedule the birds where under, LD 12:12 light period (white bars) and dark period (black bars), and constant dimLL (dark grey bars). The bars represent the mean values for each time point ± SEM (n=4-6). Graphs were fitted with GraphPad prism. Significant differences as revealed by ANOVA indicated by * on figure letter; significant differences between times points, i.e. to the lowest value of mRNA expression, as revealed by post hoc Tukey test indicated by * above the corresponding symbols: *p<0.05, **p<0.01, ***p<0.001. See Appendix I – Section 1.2.6 for statistical analysis.

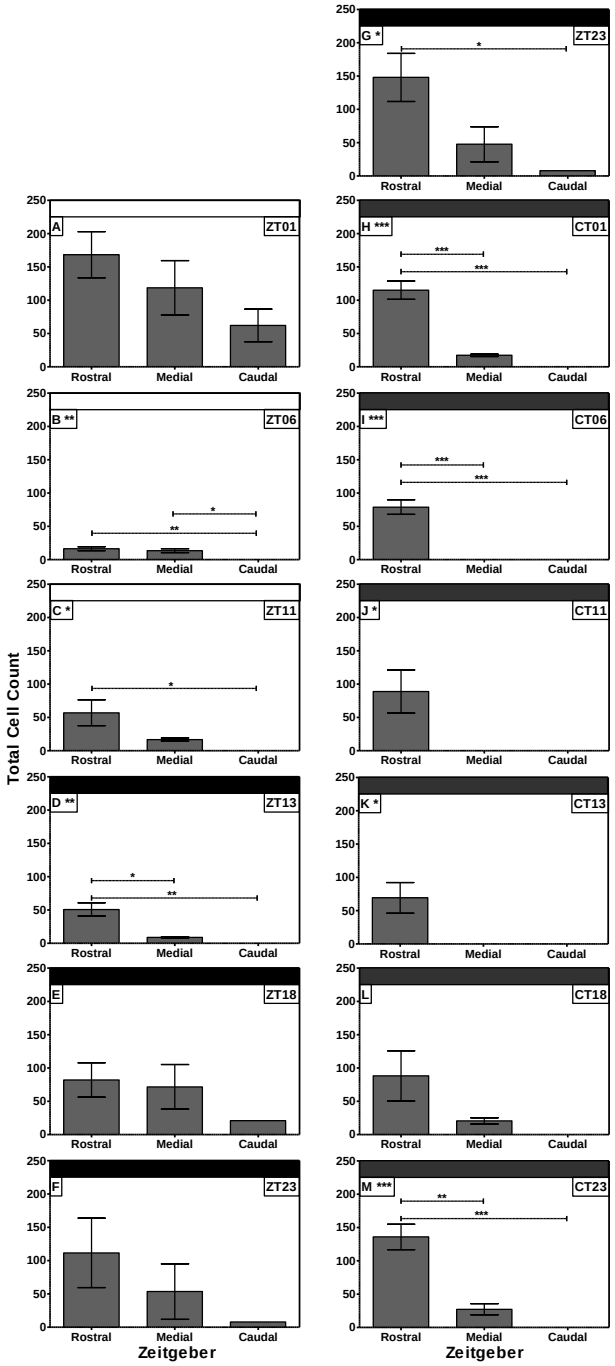

Figure 7.2.3.d. Total AVTergic cell counts in different regions of the LHNv at set zeitgeber times. There are two ZT23 as the LD and dimLL samples were taken at different periods, so ZT23 was repeated to check for continuity. The bars at the top of each graph indicates the light schedule the birds were under, LD 12:12 light period (white bars) and dark period (black bars), and constant dimLL (dark grey bars). The bars represent the mean values for each time point ± SEM (n=4-6). Graphs were fitted with GraphPad prism. Significant differences as revealed by ANOVA indicated by * on figure letter; significant differences between times points, i.e. to the lowest value of mRNA expression, as revealed by post hoc Tukey's test indicated by * above the corresponding symbols: *p<0.05, **p<0.01, ***p<0.001. See Appendix I – Section 1.2.6 for statistical analysis.

7.3 Discussion

This study explored the rhythmicity of the vasotocin (vasopressin) hormone in the zebra finch hypothalamus; I have shown that there is dominant expression in the LHNv as well as the preoptic nucleus PON which varies throughout the 24 hour period and this rhythm is sustained under constant dimLL conditions. Previous studies looking at vasotocin in the avian brain, have shown expression in the preoptic area, including the supraoptic region, and in the paraventricular hypothalamic nucleus of the chicken (Jurkevich and Grossmann, 2003). AVT has been found in cells and fibres bordering the ventral aspect of the vSCN and extending into the optic chiasm and into the *retinohypothalamic* tract in the house sparrow (Cassone and Moore, 1987).

The AVTergic cells in the LHNv and PON of this study were predominantly found in the rostral sections throughout the 24 hours under both light dark cycle (LD) and dimLL conditions. The variation in the AVTergic cell number was in the caudal regions of each nucleus; with staining only found in this region around the onset of light and mid-dark period at ZT1, ZT18, ZT23, CT1, CT18 and CT23; this was confirmed with profile through the hypothalamus and calculated amount in distance of the nuclei containing AVT cells. In the PON, cell numbers were constant throughout the rostral region, with a sharp increase in AVTergic cell numbers throughout this cell group at ZT1, suggesting that light triggers AVTergic stimulation in this cell group.

The rhythm found in the LHNv under LD conditions persisted under dimLL conditions, suggesting that vasopressin in this nucleus is endogenously produced, but the expression is enhanced under the presence of light, as shown by the abundant staining at ZT1. The AVTergic cell number starts to increase towards the end of the dark period and peaks an hour after lights on at ZT1; suggesting a role of this hormone in end of sleep phase or the start of consciousness. In mammals vasopressin (AVP) has been shown to be rhythmically regulated by the positive and negative elements of the core molecular genes of the circadian system (Li, *et al*., 2009). The CLOCK/BMAL1 complex positively activates the expression of the AVP gene and the AVP gene is suppressed by the Per and Cry elements of the clock genes (Li, *et al*., 2009). The rhythm of the AVT hormone shown in this study is comparable with the morning oscillators *Per2* and *Per3* genes in the house sparrow (Helfer, *et al*., 2006), which peak at the onset of light and decline during the light period and then escalate during the mid-to-late dark phase. The avian*Per2* gene has been shown to be widespread in the hypothalamus (PON, SCN and LHN; Abraham, *et al*., 2002; Brandstaetter, *et al*., 2001a), and not restricted to one nucleus as in mammalian*Per1* (Brandstaetter, *et al*., 2001a; Abraham, *et al*., 2002). Therefore the avian*Per2* could activate the transcription of the AVT hormone (a clock-controlled gene - Li, *et al*., 2009) in the LHN and PON as shown in this study.

In mammals rhythmic *Per* expression under constant conditions is most prominent in the vasopressinergic cells of the dorsal SCN (Bittman, 2009). These cells have been regarded as down-stream from the critical core of the pacemaker and, rather than serving exclusively as an output signal, vasopressin may play a role over the long term in coordinating oscillations (Bittman, 2009). I found no visible staining in the SCN of the zebra finch and, due to the fact that there are multiple hypothalamic circadian oscillators in birds, the findings in this study of

the LHNv suggest it may be that this vasotocinergic role is provided by the LHNv in the zebra finch instead of the SCN as in mammals.

This study has shown that the arginine-vasotocin hormone in the zebra finch hypothalamus is endogenously found and that the rhythm persisted under LD and dimLL conditions, in one of the known areas of the hypothalamus containing circadian oscillatory functions, the LHN. The fascinating results in this study help to increase the knowledge of the AVT rhythmicity in the avian hypothalamus. In the next Chapter of this thesis I will perform a species comparison of AVTergic cell expression at ZT1 to see whether this high level of AVT is consistent amongst avian species.

CHAPTER 8

Species comparison of AVTergic cells in the hypothalamus at ZT1

CHAPTER 8 - SPECIES COMPARISON OF AVTergic CELLS IN THE HYPOTHALAMUS AT ZT1

8.1 Introduction

The neuroendocrine system in the brain is a vital feature in maintaining the body's homeostatic balance; the hypo-thalamic–pituitary-adrenal (HPA) axis senses homeostatic disturbances which causes the release of hypothalamic hormones which stimulate the release of other hormones from the anterior pituitary gland, such as ACTH (Cornett, *et al*., 2003). The mammalian hormone AVP or the non-mammalian homolog AVT is one of the principal releasing factors for ACTH from the pituitary (Cornett, *et al*., 2003). Vasopressin has been shown to be more than just an output signal: it has also been linked to a role in the long term coordinating of oscillators by stimulating VIP cells in the mammalian hypothalamic oscillator, the SCN (Bittman, 2009). Since the HPA in avian systems have been shown to be similar the mammalian HPA (Cornett, *et al*., 2003), this suggests that vasotocin may have an active role in the avian hypothalamic oscillatory regions, i.e. LHN and the SCN.

Vasotocin, or vasopressin, has been associated with multiple roles in the body such osmoregulation, vasomotor and thermoregulatory effect, oviposition (birds), stress behaviours, sexual and aggressive behaviours, and links to REM sleep and memory formation (Jurkevich, *et al*., 2005; Jurkevich and Grossmann, 2003; Li, *et al*., 2009; Maurizi, 2000). Therefore the expression of AVP/AVT has been found in numerous brain regions across the

animal kingdom (Table 8.1.a.). Avian AVT is abundantly synthesized in the supraoptic and paraventricular nucleus and released into the blood stream in response to hyper-osmotic stimuli (Saito, *et al*., 2010). In zebra finches and white-crowned sparrows, central infusions of AVT were shown to facilitate aggressive behaviours whereas, in the violet-eared waxbill and field sparrows, it inhibits them (Leung, *et al*., 2009), showing great variations between avian species in the response to the same hormone.

Cassone and Moore, found house sparrows to express AVT in neuron cells and fibres bordering the ventral aspects of the vSCN and extending 50-100μm into the optic chiasm (Cassone and Moore, 1987). The AVT-like cells were smaller than the AVT-like cells in the hypothalamic magnocellular Paraventricular nuclei. The AVT-like cells in the vSCN and retinohypothalamic tract were more fusiform in shape and extended their dendritic arbors well into the optic chiasm (Cassone and Moore, 1987). In contrast, Grossman and colleagues found staining in the preoptic area including the supraoptic nucleus as well as the paraventricular nucleus and bed nucleus of the stria terminalis, during *in situ* hybridization experiments in the chick (Grossmann, *et al.*, 2002). Song birds (i.e. canary and the zebra finch) showed AVT cells in extra-hypothalamic locations; clusters of AVT perikarya were located in the bed nucleus of the stria terminalis on the border between lateral septum and dorsal diencephalon; males had more intense staining than females (Grossmann, *et al.*, 2002). In chicken, the concentration of circulating AVT has been implicated with oviposition; AVT increases around the time of oviposition with a sharp increase in plasma AVT causing oviduct contractions: the concentration subsides within 30 minutes of egg laying (Jurkevich and Grossmann, 2003). There are also differences between sexes: male Japanese quail showed

discrete clusters of AVT-IR (immune-reactive) structures whereas females quails showed AVT-IR fibres around negative cell bodies (Aste, *et al*., 1998).

Due to the interesting results obtained in Chapter Seven, this chapter will expand on the examination of the expression of AVT by looking at the expression in other avian species to see whether the results found in Chapter Seven, i.e. staining patterns found at ZT1, were the same across species or whether there was a difference in nuclei expression. ZT1 was chosen for the comparison because in the last Chapter (Seven) showed that ZT1 had the most AVTergic cells in different nuclei. I compared the AVT expression in the chicken (*Gallus gallus domesticus*) and the Japanese quail (*Coturnix japonica*); both species are in the Galliform order of birds, whereas the zebra finch (*Taeniopygia guttata*) is in the passeriform order. The passeriform order covers half of all bird species; birds in this order are also known as perching birds or as songbirds. Galliforms are birds also known as game-birds or game-fowls, so include species of turkey, grouse, pheasants as well as quail and chicken; they are heavy-bodied ground-feeders. Therefore this part of the thesis is a comparative study across different species/orders on the expression of vasotocin in the hypothalamus

Brain Region	Fish	Amphibians	Reptiles	Birds	Mammals
Diencephalon		V6, Bed nucleus of the decussation of the fassiculus lateralis telencephali			Anterior commissural nucleus
		V7, Anterior preoptic area	Anterior hypothalamic-preoptic area	Anterior preoptic area	Anterior hypothalamic-preoptic area lateral to the anterior commissural nucleus in males
		V8, Pars ventralis thalami	Dorsomedial thalamic Ventromedial thalamic nucleus	Thalamus	
	Magnocellular preoptic area	V9, Magnocellular preoptic area	Supraoptic area	Supraoptic nucleus	Supraoptic nucleus

Table 8.1.a. Distribution of potential vasotocinergic and vasopressinergic cell bodies in the diencephalon region of different vertebrate species. See Appendix I – Setion 1.2.7 for the full comparative table showing the distribution of potential vasotocinergic and vasopressinergic cell bodies in brain regions of different vertebrate species (Moore and Lowry, 1998).

8. 2 Results

Zebra finch, Japanese quail and chickens were maintained under LD 12:12 conditions and killed at ZT1, one hour after lights on, and AVT antibody was used in immunofluorescent protocol (Chapter 2.3.) to see the expression of vasotocin in the hypothalamus.

8.2.1 Immunofluorescent image analysis

AVTergic cells were found in the PON and PPN around the third ventricle (Figure 8.2.1.a): expression in the PON was more abundant in all three of the species studied, with sporadic staining in the PPN. In the zebra finch the AVTergic cell numbers were greatest in the LHN, and the zebra finch had more abundant staining than that found in the chicken and quail (Figure 8.2.1.b), though AVTergic cells were found in both the chicken and quail in the more rostral-medial regions. There was sporadic staining in the PVN in all three species (Figure 8.2.1.a).

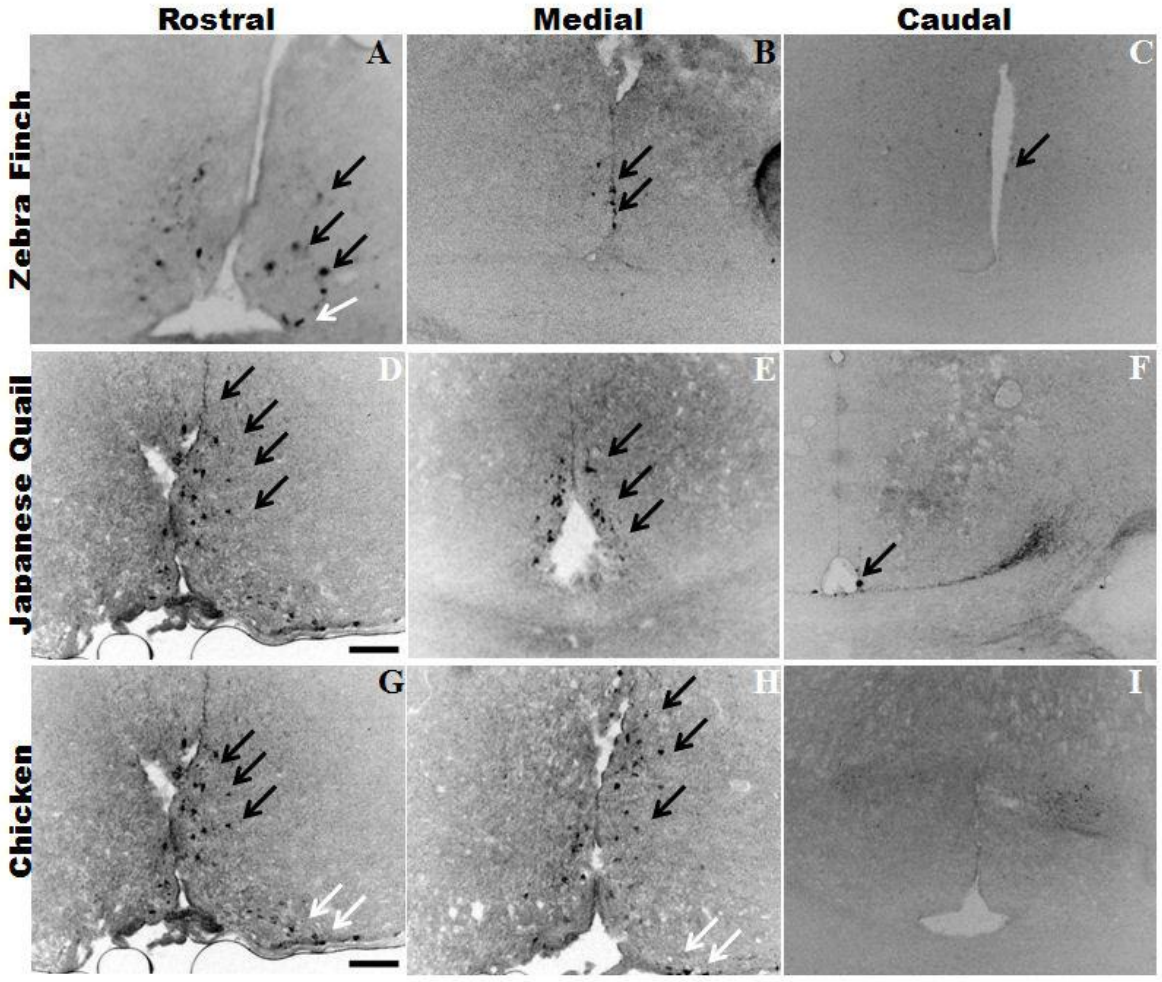

Figure 8.2.1.a. AVTergic cells found through the hypothalamus around the third ventricle. Comparison between three species: zebra finch, chicken and Japanese quail. Black arrows indicate the AVTergic cells in the preoptic area (POA) and the white arrows indicate the AVTergic cells in the periventricular preoptic nucleus (PPN). Scale bars: Image A, D, E and H = 50µm (Bar in D); Image B, C, F, G and I = 100µm (bar in G).

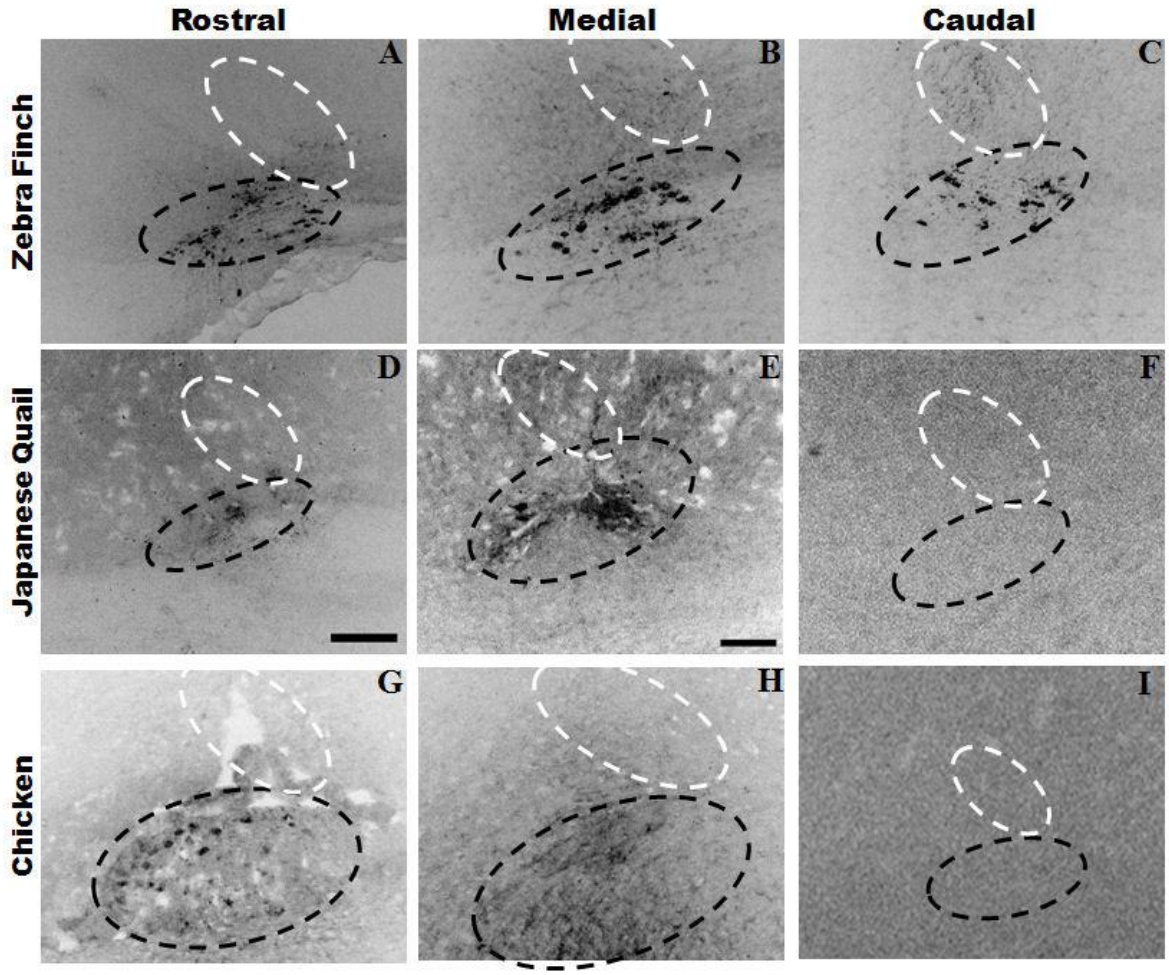

Figure 8.2.1.b. AVTergic cells found in the lateral hypothalamic nucleus (LHN). Comparison between three avian species: zebra finch, chicken and Japanese quail. Black dashed oval indicates ventral portion (LHNv) and white dashed oval indicates dorsal portion (LHNd). Scale bars: Image B, C, E and H = 50µm (Bar in E); Image A, D, F, and I = 100µm (bar in D).

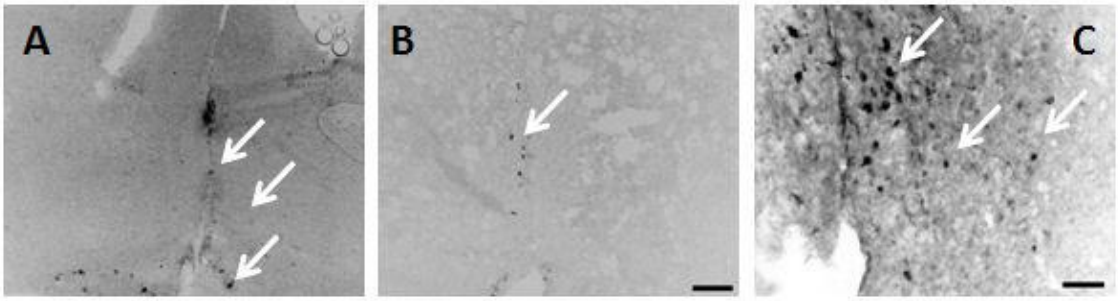

Figure 8.2.1.c. AVTergic cells found in the paraventricular nucleus (PVN). In the zebra finch (A), Japanese quail (B) and chicken (C). White arrows indicate some of the AVPergic cells. Scale bars: Image A and B = 100µm (Bar in B); Image C = 50µm.

8.2.2 Comparative AVTergic cell profiles in different species at ZT1

Fluorescent image analysis of AVTergic cells allowed for cell counts to be taken which showed the nuclei expression profiles at ZT1 in the zebra finch and comparing the expression to the Japanese quail and chicken. I then performed statistical analysis; one-way ANOVA (ANOVA) and pos hoc Tukey's test (Tukey's), to see if the expression of AVT varied between species in different nuclei.

The profile figures of AVTergic cells counts in different cell groups in the three different species at ZT1 showed a very clear distinction between each species and cell groups (Figure 8.2.2.a). AVTergic cell counts in the PON were found to be very similar between species (Figure 8.2.2.a.-A-C); AVTergic cells were found throughout the whole of this cell group in all three species. AVTergic cell counts of around 100 cells in each species (Figure 8.2.2.a.-G-I), suggest that the findings of this study are reliable and consistent. The interesting difference between species in the AVTergic cell counts occurred in the LHN region (Figure 8.2.2.a.-D-F). In LHN, the zebra finch has high cell numbers throughout the ventral portion of this cell group (Figure 8.2.2.a.-D), whereas, in the Japanese quail and chicken there were less AVTergic cells found in the LHNv cell groups (Figure 8.2.2.a.-E and Figure 8.2.2.a.-F respectively). In the LHNd there were very few AVTergic cells found in any of the species examined in this study.

In the zebra finch, LHNv had the most abundant number of AVTergic cells compared to the other cell groups that express AVT (Figure 8.2.2.a.-G; ANOVA, $F_{3,16}$=3.607 p<0.05). AVTergic cells are seen along the whole of the rostral to caudal extension of the

hypothalamus (Figure 8.2.2.a.-A&D). The LHNv has a peak number of AVTergic cell count in the rostral area of the hypothalamus, and maintains this cell count in at least 10 cells for the length of the LHNv (Figure 8.2.2.a.-D). LHNd had a sporadic pattern of AVTergic cells in the rostral and rostral-medial regions (Figure 8.2.2.a.-D). In the PON, a consistent number of AVTergic cells were seen throughout the length of this cell group, of around 5-10 AVTergic cells. Few positive cells were found in the PPN (Figure 8.2.2.a.-A).

The Japanese quail hypothalamus has AVTergic cells throughout length of the hypothalamus (Figure 8.2.2.a.-B; Figure 8.2.2.a.-E; Figure 8.2.2.a.-H). Three of the four cell groups (SCN, LHN-v and PON) all contain AVTergic cells (Figure 8.2.2.a.-H; one-way ANOVA $F_{3,14}$=18.30 p=0.0003; Tukey's - PPN vs PON q=8.482 p<0.001, LHNv vs PON q=5.999 p<0.001, and LHNd vs PON q=7.733 p<0.001). The PON has the most abudant quantity of AVTergic cells in this species (Figure 8.2.2.a.-B). The PPN and LHNv do contain some AVTergic cells (Figure 8.2.2.a.-B and Figure 8.2.2.a.-E). The LHNd had no AVTergic cells present (Figure 8.2.2.a.-E).

The chicken hypothalamus shows similar results to the Japanese quail; there are AVTergic cells found in three of the four cell groups (Figure 8.2.2.a.-C; Figure 8.2.2.a.F; Figure 8.2.2.a.-I). In the LHNv, there are AVTergic cells found along the rostral and rostro-medial area (Figure 8.2.2.a.-F). There were no AVTergic cells found in the LHNd cell group (Figure 8.2.2.a.-F). A few sporadic AVTergic cells were seen in the PPN (Figure 8.2.2.a.-C). The most abundant number AVTergic cells occured in the PON, with cells found along the whole of the cell group (Figure 8.2.3.a.-C&I; one way ANOVA p= 0.088).

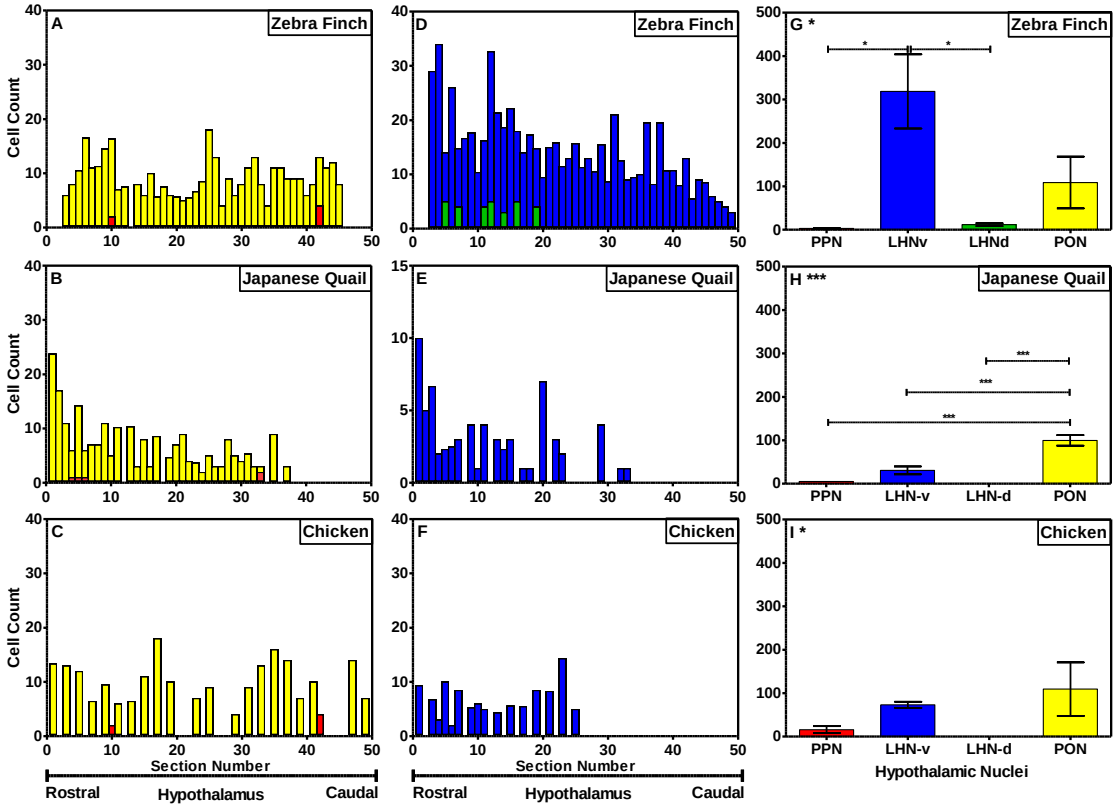

Figure 8.2.2.a. Profiles of AVTergic cells count through different cell groups of the hypothalamus in different species at ZT1. Zebra finch (A, D, G), Japanese quail (B, E, H) and chicken (C, F, I). Graphs A-F show AVTergic cells found along the rostral-caudal axis through the hypothalamus, from rostral to caudal, of zebra finch (A&D), Japanese quail (B&E) and chicken (C&F) at ZT1. Graphs A-C show the expression in the preoptic nucleus (PON; yellow bars) and periventricular preoptic nucleus (PPN; red bars); Graphs D-F show the AVPergic cells through the lateral hypothalamic nucleus ventral portion (LHN-v; blue bars) and the lateral hypothalamic nucleus dorsal portion (LHN-d; green bars). Graphs G-I show the total cell counts for each hypothalamic nuclei expressing AVT at ZT1, in the zebra finch (D), Japanese quail (E) and chicken (F). Graphs A-F, bars represents the mean total cell count value for that section (n=6). G-I, bars represent the average total cell count for that cell group (n=6) ± SEM. Birds were synchronised and maintained under 12:12 LD lighting conditions and killed at ZT1; ZT0 being when lights are turned on at 9am and ZT12 being when lights are turned off at 9pm. ANOVA indicated by * on figure letter; significant differences between times points as revealed by post hoc Tukey test indicated by * above the corresponding symbols: *p<0.05, **p<0.01, ***p<0.001. See Appendix I – Section 1.2.4 for statistical analysis.

8.2.3 Comparative AVTergic cell count analysis at ZT1

Since the results from the previous profile figures showed an interesting variation in AVTergic cell expression between species (Figure 8.2.2.a); I wanted to compare and contrast these results across species to see if there were any significant differences. I therefore compared the total cell counts for each nucleus and compared their results between each species (Figure 8.2.3.a).

In the PPN (Figure 8.2.3.a.-A) all three species have AVTergic cells present, with the most abundant number of cells found in the Japanese quail (one-way ANOVA, $F_{2,7}$=17.34 p<0.001; Tukey's - ZF-JQ q=4.899 *p*<0.05 and JQ-CH q=8.216 *p*<0.001).

The LHNv, showed a high number of AVTergic cells in the zebra finch (300), with lower number of AVTergic cells found in the Japanese quail (70) and chicken (70) of this cell group (Figure 8.2.3.a.B; one-way ANOVA, $F_{2,15}$=6.670 p<0.05; Tukey's, ZF vs JQ q=4.093 *p*<0.05, ZF vs CH q=4.046 *p*<0.05).

In the LHNd, no staining was found in the chicken or Japanese quail, but a few AVTergic cells were found in the zebra finch (Figure 8.2.3.a.-C; one-way ANOVA, $F_{2,8}$=11.89 p=0.0082).

In the PON all three avian species showed a similar level of AVTergic cell number (100) contained within this cell group (Figure 8.2.3.a.-D; one-way ANOVA, $F_{2,14}$=0.0136 p=0.9865).

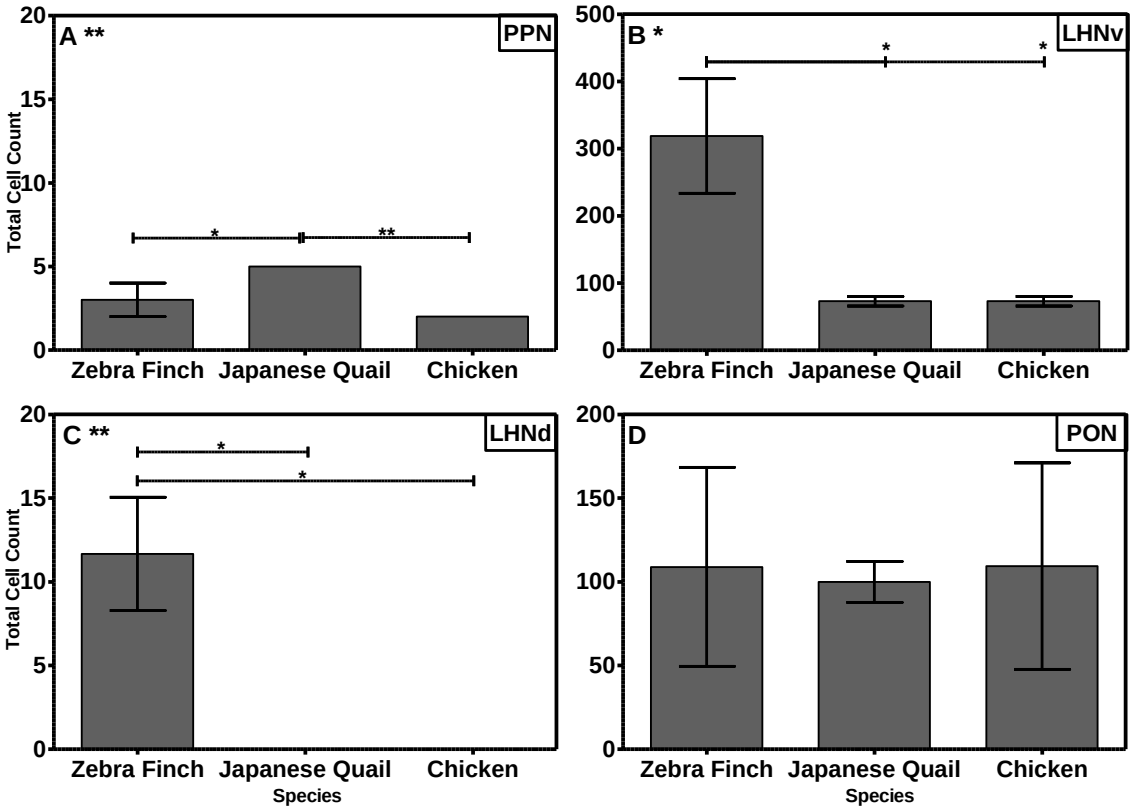

Figure 8.2.3.a. Comparative total AVTergic cell counts in different cell groups of the hypothalamus between different avian species at ZT1. Each bar represents an averaged total cell count ± SEM. Under 12:12 LD conditions, ZT 0 being when lights are turned on at 9am and ZT12 being when lights are turned off at 9pm. Significant differences as revealed by ANOVA indicated by *on figure letter; significant differences between species as revealed by post hoc Tukey test indicated by * above the corresponding symbols: *p<0.05, **p<0.01, ***p<0.001. PPN - periventricular preoptic nucleus; LHN-v – lateral hypothalamic nucleus ventral portion; LHN-d - lateral hypothalamic nucleus dorsal portion; PON – preoptic nucleus. See Appendix I – Section 1.2.8 for statistical analysis.

From the initial figures of profiles of AVTergic cells in the different cell groups of each species (Figure 8.2.2.a.-A-C); I noticed a variation in the spread of expression throughout each cell group from rostral to caudal regions. Therefore I wanted to compare the length of each cell group which contained AVTergic cells, for each cell group and species. Since the section thickness was a set value (20μm) I converted section numbers containing the AVTergic cells into a length and compared these values against each species for each cell group (Figure 8.2.3.b.-A-D).

AVTergic cells appeared to be within similar range along the length of the PPN (Figure 8.2.3.b.-A) in all three species, though due to the high variability of these data no significant differences were found between species (one-way ANOVA, $F_{2,9}$=0.08857 p= 0.9163). In the Japanese quail expression in this nucleus was only found in one sample, with this staining being sporadic through the length of this cell group.

In the lateral hypothalamic area, the AVTergic cells in the LHNv (Figure 8.2.3.b.-B) showed that the zebra finch had the most profuse staining, with virtually this entire cell group containing AVTergic cells. The AVTergic cells were mainly found in the rostral to medial regions of the LHNv in the Japanese quail and chicken (one-way ANOVA, $F_{2,14}$=7.184 p<0.001; Tukey's, ZF vs JQ q=4.089 p<0.05, ZF vs CH q=7.101 *p*<0.05).

There were no AVTergic cells found in the LHNd in the chicken and Japanese quail species. AVTergic cells were found in the rostral regions in the zebra finch (≤200μm; Figure 8.2.3.b.C; one-way ANOVA, $F_{2,8}$=8.816 p=0.0164).

AVTergic cells found were found in all three species in the PON (Figure 8.2.3.b.-D). The AVTergic cells were found to be more rostro-medial (≤650μm). The AVTergic cells found through the PON cell group was consistent between species, which suggests that this is conserved between species. This comparable staining also shows the reliability of the staining in the other nuclei.

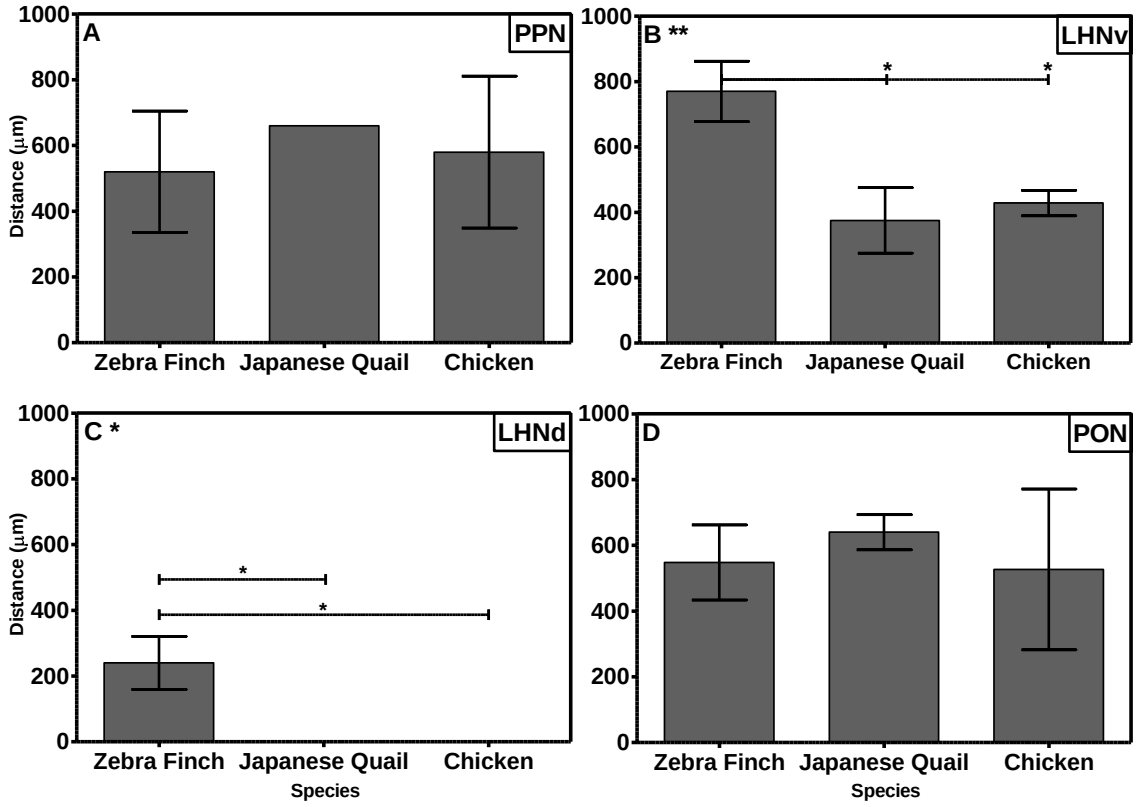

Figure 8.2.3.b. Species comparison of the AVTergic cells along the longitudinal axis different hypothalamic cell groups. A, Periventricular preoptic nucleus (PPN). B, Lateral hypothalamic nuclei, ventral portion (LHNv). C, Lateral hypothalamic nuclei, dorsal portion (LHNd). D, Preoptic nucleus (PON). The birds were synchronised under LD 12:12 lighting conditions. The bars represent the mean values for each time point ± SEM (n=3-6). Significant differences as revealed by ANOVA indicated by *on figure letter; significant differences between species as revealed by post hoc Tukey test indicated by * above the corresponding symbols: *p<0.05, **p<0.01, ***p<0.001. See Appendix I – Section 1.2.8 for statistical analysis.

Following the results from the previous figures, which showed that the LHNv and the PON have the most prolific AVTergic cell counts, varying along the rostral to caudal regions of the cell groups, I wanted to investigate these findings further by splitting these two cell groups into three regions; rostral, medial and caudal. This would allow comparison of these AVTergic cells in the three regions in each species to see if the expression pattern varies significantly (Figure 8.2.3.c and Figure 8.2.3.d).

The zebra finch pattern through the LHNv shows a clear difference in AVTergic cells from rostral to caudal (Figure 8.2.3.c.-A) with dominant staining in the rostral areas and AVTergic cell number declining through to the caudal region. This pattern is similar in the quail and chicken (Figure 8.2.3.c.-B and Figure 8.2.3.c.-C), though the AVTergic cells are restricted to the rostral and medial regions of the LHNv. In the Japanese quail there appears to be greater decline in cell numbers between the rostral and medial regions, compared to the other two species. Both the rostral and medial contained a higher number of cells in the chicken compared to the Japanese quail. The AVTergic cell count numbers were a lot higher in the zebra finch compared to the Japanese quail and chicken. These patterns were confirmed by the species comparison analysis (Figure 8.2.3.c.-D-F); the most abundant number of AVTergic cells in the LHNv was found in the zebra finch. In the rostral regions (Figure 8.2.3.c.-D), the zebra finch total cells counts were significantly higher than the levels found in the Japanese quail and chicken (one-way ANOVA, $F_{2,14}=10.32$ $p<0.01$; Tukey's, ZF vs JQ $q=4.579$ $p<0.01$, ZF vs CH $q=5.291$ $p<0.01$). This pattern was also shown in the medial region, with the zebra finch having the most profuse number of cells (Figure 8.2.3.c.-E). The zebra finch is the only species to have staining in the caudal region of the LHNv cell group (Figure 8.2.3.c.-F).

In the PON, the cell counts in the zebra finch and chicken are pretty comparable; both have most abundant AVTergic cell counts in the rostral and caudal regions of the PON but the cell count drops in the medial region in both species (zebra finch - Figure 8.2.3.d.-A and chicken - Figure 8.2.3.d.-C). In the Japanese quail, however, (Figure 8.2.3.d.-B) there is a significant number of AVTergic cells in the rostral region compared to the medial and caudal regions (one-way ANOVA, $F_{2,14}$=14.90 p=0.0006; Tukey's, rostral vs medial q=6.061 p<0.01, rostral vs caudal q=6.840 p<0.01). In the rostral regions of the PON, all three species showed a similar high number of AVTergic cells (Figure 8.2.3.d.-D). Then in the medial region, AVTergic cells in the zebra finch and quail drop dramatically, whereas in the chicken the cell count remains significantly high compared to the other two species (one-way ANOVA, F2,11=6.165 p<0.05; Tukey's, ZF vs CH q=4.532 p<0.05, JQ-CH q=4.640 p<0.05). As the expression progresses into the caudal region (Figure 8.2.3.d.-F) the AVTergic cells numbers in the chicken remain high, the zebra finch cell count increases again, and the Japanese quail levels drop again.

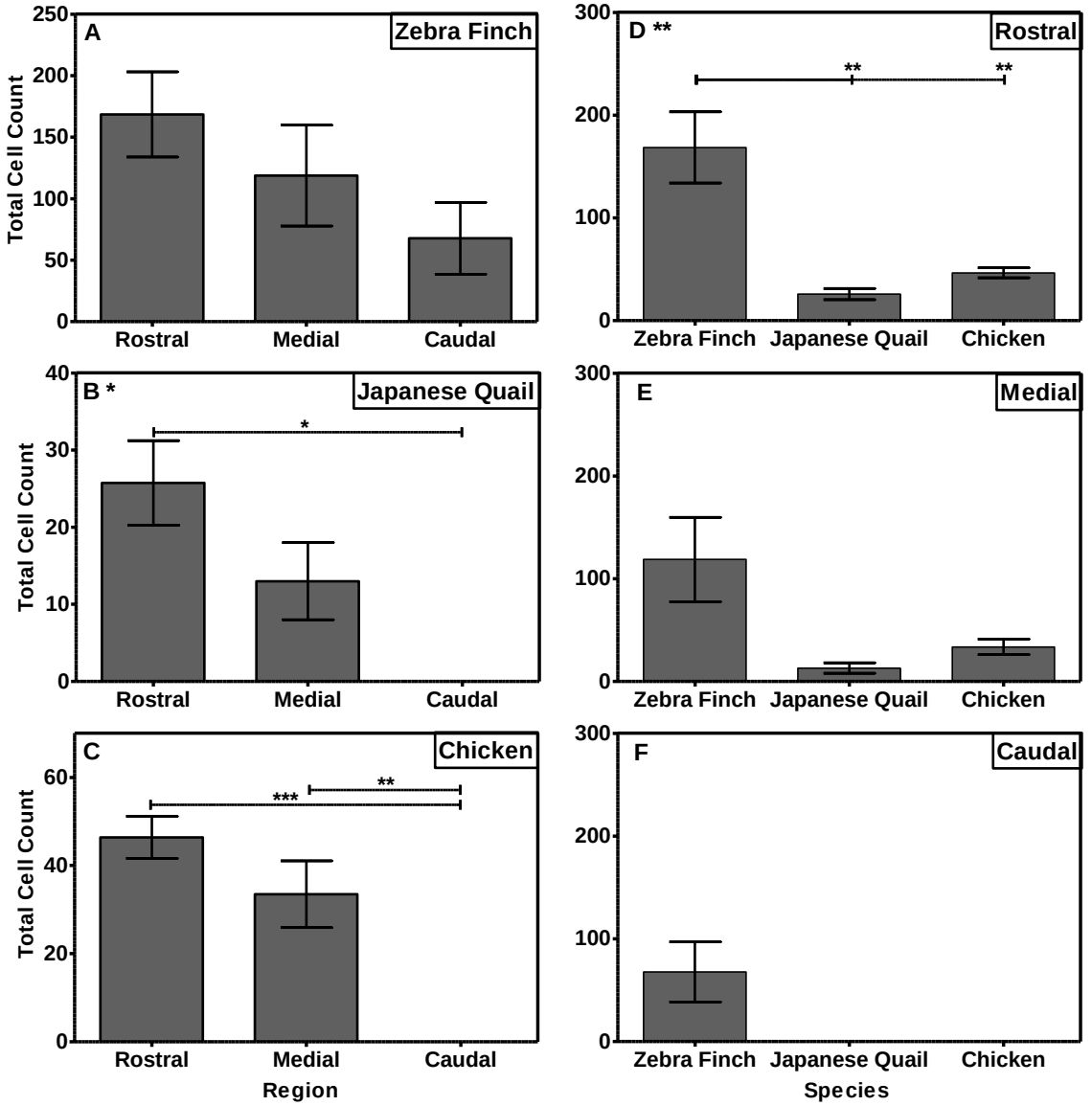

Figure 8.2.3.c. Total AVTergic cell counts in different regions of the LHNv cell group. A-C, shows the total cell counts through the LHNv of the zebra finch (A), Japanese quail (B) and the chicken (C). D-F, show species comparison of total cell counts in the different regions of the LHNv; rostral (D), medial (E) and caudal (F). The bars represent the mean values for the total cell counts in the region/species ± SEM (n=5-6). Significant differences as revealed by ANOVA indicated by *on figure letter; significant differences between species as revealed by post hoc Tukey test indicated by * above the corresponding symbols: *p<0.05, **p<0.01, ***p<0.001. See Appendix I – Section 1.2.8 for statistical analysis.

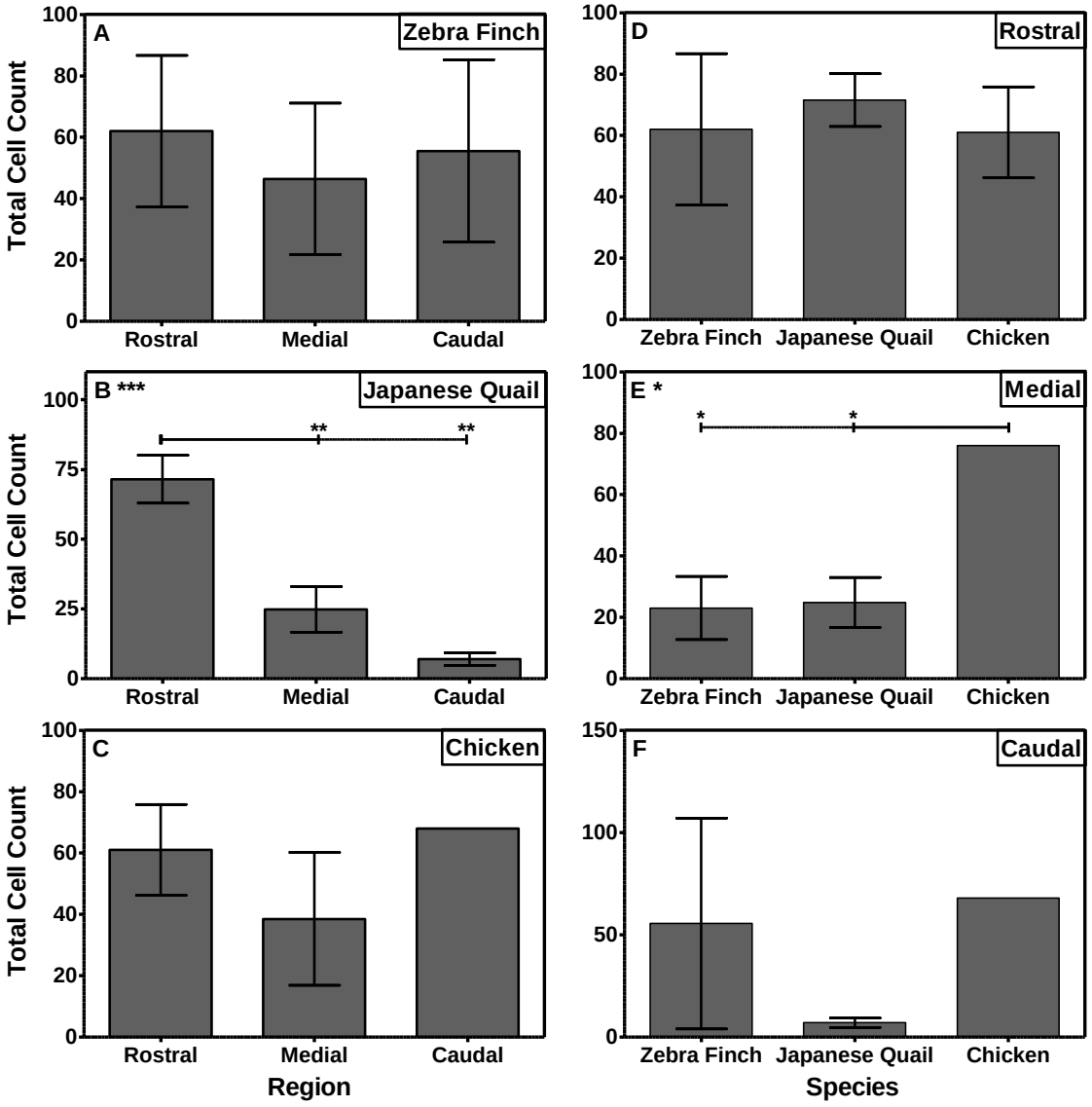

Figure 8.2.3.d. Total AVTergic cell counts in different regions of the PON. A-C, shows the total cell counts through the PON of the zebra finch (A), Japanese quail (B) and the chicken (C). D-F, shows the species comparison of total cell counts in the different regions of the PON; rostral (D), medial (E) and caudal (F). The bars represent the mean values for the total cell counts in the region/species ± SEM (n=5-6). Significant differences as revealed by ANOVA indicated by *on figure letter; significant differences between species as revealed by post hoc Tukey test indicated by * above the corresponding symbols: *p<0.05, **p<0.01, ***p<0.001. See Appendix I – Section 1.2.8 for statistical analysis.

8.3 Discussion

This study showed a detailed analysis of the expression of vasotocin cells in three species of birds at ZT1. It showed a large variation between AVTergic cells in different cell groups in the hypothalamus; all three species contain AVTergic cells in different hypothalamic cell groups studied, apart from the chicken, which did not contain any AVTergic cells in the LHNd. All three species had the most abundant staining in the LHNv and PON cell groups, with AVTergic cell number varying along the rostral-to-caudal axis of the LHNv cell group. The AVTergic neurons have been shown to build a dense network between the lateral hypothalamic area, the preoptic region and the paraventricular nucleus: this system is known as the hypothalamic-hypophysial neurosecretory system (Yoshimura, *et al*., 2003).

This study shows species specific difference in the number of AVTergic cells. All three species show consistent results in AVTergic cell numbers in the PON and sporadic number of cells in the PPN of the hypothalamus. The main differences between species are in the lateral hypothalamic area, with both the Japanese quail and chicken having less AVTergic cells than the zebra finch. All three species had a very low number of AVTergic cells in the LHNd, with the chicken and Japanese quail having no AVTergic in this area. The differences highlighted in this study are not taxonomical as all three species lack AVTergic cells in the LHNd. The three species studied here all now are non-seasonal breeders: the zebra finch is natively a non-seasonal breeder (opportunistic breeder), and the chicken and Japanese quail have been forced to become non-seasonal breeders due to farming for poultry meat. In house sparrows, however, and other seasonal breeding birds (such as the blackbird, European starling,

stonechat and garden warbler) which all have intact photorefractoriness, i.e. the process responsible for the termination of gonadal activity (Hazlerigg and Wagner, 2006), show a pronounced AVTergic cells in the LHNd. This study shows that birds without an intact photorefractoriness which do not breed seasonally (i.e. zebra finch, Japanese quail and chicken) do not have this LHNd AVTergic cell group. This suggests an evolutionary novelty in the brain of seasonal breeding birds, which is the presence of a higher control centre in the lateral region of the hypothalamus.

With such contrasting results between the species in this study and the seasonal breeders (personal communication with Dr Roland Brandstaetter, 2011 (see Appendix I – Section 1.2.9.)) could suggest that the LHNd has a role in seasonal breeding in avian species and that species such as the domesticated chicken has evolved or lost the AVT function in the LHNd, with the PON AVT becoming more dominant in these species. With the variations between avian species in the balance of circadian oscillatory mechanisms, i.e. the hypothalamus, retina and pineal gland, it could be that the mechanisms involved in the galliform species influence the expression of AVT in different nuclei. There are clear differences between the mammalian and avian system: in mammals AVP is predominantly found in the SCN; three-quarters of SCN neurons synthesise AVP and a high proportion of these neurons (>40%) can be excited by AVP through the V1 receptors, which may specifically enhance the output signals from the SCN in the mouse (Li, *et al*., 2009). The data I collected in this chapter, showed no staining in the SCN of any avian species, and data collected in the previous chapter (Chapter 7) shows that in the zebra finch (a songbird) expression was predominantly found in the LHNv and PON. All this data put together suggests different nuclei dominance of AVT expression between species in birds.

In addition to the detailed analysis of the four nuclei shown in this study (PON, PPN, LHNv and LHNd), AVTergic cells were also found in the paraventricular nucleus of all three species. These findings coincide with previous studies of chicken AVT which show AVTergic cells to be concentrated in the preoptic and supraoptic regions and within the paraventricular nucleus; the magnocellular vasotocinergic neurons form the hypothalamo-neurohypophysial-neurosecretory system (Jurkevich & Grossmann, 2003). AVT is synthesized in the magnocellular cells and transported along the axons terminals to the neurohypophysis (pituitary gland) where the peptide is released into the blood stream (Jurkevich & Grossmann, 2003). As in mammals, the parvocellular vasotocin neurons release AVT directly into the brain interstitial fluid where it modulates the neural circuits controlling behaviour (Jurkevich & Grossmann, 2003).

This Chapter has shown the AVTergic cell expression at ZT1 in the zebra finch, Japanese quail and chicken, with great differences found in the hypothalamic location of this hormone between species. A consistent finding was the low level of the vasotocin hormone in the LHNd. Comparing this finding with previous studies into vasotocin expression in other avian species. I believe I have found a link between seasonal breeding or intact photorefractoriness and the expression of this hormone in the dorsal portion of one of the hypothalamic cell groups associated with circadian oscillatory functions, the LHNd.

CHAPTER 9

General Discussion

CHAPTER 9 - GENERAL DISCUSSION

9.1 General Discussion

The avian circadian system is a complex network of multiple oscillators functioning together to create a stable system: areas such as the retina, the pineal and the hypothalamus have so far been identified as containing oscillatory functions. At the whole-organism level, our knowledge of circadian biology in birds is better than other non-mammalian vertebrates, but it still lags behind that of mammals. Over the years with the chicken (Wallis, *et al*., 2004), and now zebra finch (Warren, *et al*., 2010), genome sequencing projects, our knowledge is increasing in avian species. Currently research being performed on non-galliform species is helping to increase our knowledge on avian systems and highlight the differences between species. Since species such as the chicken and Japanese quail have been subjected to domestication, and as a result their circadian properties, examining species that have not been so heavily domesticated will provide greater insight into avian systems.

Non-mammalian vertebrate studies provide a useful alternative to develop an understanding of circadian systems and mechanisms, since non-mammalian species such as birds have photoreceptors in extra-retinal locations and, therefore, respond to the input of light in different pathways. Comparative studies between mammals and birds are of great significance in addressing how the circadian clock has evolved and developed over the years. This thesis has looked at the input and output mechanisms involved in the retina, the pineal and the hypothalamus, the three core oscillators, of the zebra finch, an example of a song bird. This

has been done by studying the effect light has on the hypothalamus, by investigating the location and rhythmicity of three melatonin membrane receptors in the brain and peripheral tissues, and examining the expression of AVT in the hypothalamus. This will help to further our knowledge of the zebra finch circadian system, an important avian "model" species.

In Chapter Three, I reported the cloning of three melatonin receptor gene homologues. Sequence analysis revealed high sequence similarities at the nucleotide level with other published avian and mammalian genes. Phylogenetic analysis showed that the groupings of melatonin membrane receptors from the zebra finch brain tissue Mel-1A, Mel-1B and Mel-1C have different lineages, though are structurally very similar to each other. The cloned partial sequences of the melatonin membrane receptors showed one of the genes had highest similarities to Mel-1A group, and were therefore termed Mel-1A. The genes cloned from the Mel-1B and Mel-1C receptor sequences showed to be highly similar to the other gene sequences for their respective groups. The appearance of the phylogenetic tree as a whole and the branching into the different melatonin receptor groups suggests an early evolutionary diversification of melatonin receptors in vertebrates.

Interestingly Mel-1C has not been detected in mammals, and the question arises whether this receptor type has been lost during vertebrate diversification and mammalian development, or was never present in mammals. Recently the Mel-1C receptor has been shown to have similar roles and properties to the mammalian GPR50 receptor, which cannot bind melatonin directly but heterodimerizers with either the Mel-1A or Mel-1B receptors to bind melatonin and changes their affinity to melatonin (Jin, *et al*., 2003; Levoye, *et al*., 2006; Dufourny, *et al*., 2008).

Compared to all other vertebrate classes, mammals have lost photosensitivity, as well as the circadian clock, in the pineal gland, and have one dominant circadian brain oscillator which controls pineal synthesis and secretion of nocturnal melatonin. Mammals only have photoreceptors in the retina, and there has been an evolutionary loss of two retinal cone classes (SWS and MWS; Barrett, *et al*., 2003) and certain opsins, which are found in lower vertebrates including birds and fishes (Bellingham, *et al*., 2003). These differences in circadian organisation are believed to be the consequence of a 'nocturnal bottleneck' during early evolution of mammals (Foster, *et al*., 1993).

The main object of the melatonin receptor study in Chapter Four was to objectively compare the gene expression in different brain tissues of the zebra finch. This was achieved by ensuring that tissue preparation of all tissues were treated in the same manner, i.e. similar weight for whole tissue RNA extraction, and mRNA and cDNA concentrations. Non-mammalian vertebrates, including birds, possess complex circadian systems with multiple photic input mechanisms and multi-oscillator control of circadian rhythmicity (Gwinner and Brandstaetter, 2001). I found Mel-1A, Mel-1B and Mel-1C receptor expression in all parts of the avian brain that have been shown to contain autonomous circadian clocks, i.e. retina, pineal and diencephalon.

In this thesis, the diencephalon showed robust rhythms of Mel-1A and Mel-1B receptor mRNA peaking in the late dark period (ZT22), with the Mel-1C being present in this tissue but not rhythmic, coinciding with the decline in pineal melatonin levels (Brandstaetter, *et al*., 2001b) and onset of light at ZT0 (Chapter 4). This rhythm was confirmed with the protein immunofluorescent experiments which showed a different in fluorescent intensity and density

between ZT6 (light period) and ZT18 (dark period) of Mel-1A and Mel-1B receptors and that Mel-1C receptor protein levels appeared constant between the two time points (Chapter Five).

In passerine birds, such as the zebra finch and house sparrow, the only source of circulating melatonin is the pineal gland (Brandstaetter, 2002). As melatonin production is controlled by an autonomous circadian clock in songbirds, one would predict that there would be no melatonin membrane receptors found in this gland unless they serve auto-regulatory feedback. The data from Chapter 4 shows that all three melatonin receptors are present in the pineal gland with Mel-1B being the only receptor that was rhythmically expressed. The pineal Mel-1B receptor expression peaks at the end of the dark phase (ZT 22) when melatonin production declines suggesting that Mel-1B receptors may indeed act as negative feedback and contribute to the termination of melatonin production at the end of the night. To the best of my knowledge, previous studies using 2-[^{125}I]iodomelatonin radiograph have shown melatonin receptors site to be wide spread the avian brain but these experiments do not show which receptor subtype is found in each location or that any sites were found in the pineal gland (e.g. Vakkuri, et al., 1984; Siuciak, et al., 1991; Brooks and Cassone, 1992; Reppert, *et al*., 1996). This suggests that the finding of the melatonin receptors is this thesis is a novel result and considering one of the receptors (Mel-1B) was rhythmically expressed, further work is needed to examine these findings.

Mel-1A and Mel-1B were found to be rhythmic in the retina with peak time differences, Mel-1A peaked towards the end of the dark phase (like the diencephalon) while Mel-1B peaked towards the onset of the dark period. This suggests possible different roles in the two different oscillatory regions; the level of Mel-1A receptor declines with the drop in melatonin levels,

but Mel-1B appears to peak just before the start of the melatonin secretions in the dark phase. The Mel-1A receptor protein level appears to vary between light and dark, with high intensity and distribution at ZT18 compared to ZT6, whereas there appeared to be low levels of the Mel-1B seen in the retinal tissues at ZT6 and ZT18 (Chapter Five).This suggests different roles for each of the receptor sub-types. In the mammalian system, the Mel-1A (MT1) receptor has been implicated in inhibiting neuronal firing within the SCN (Dubocovich, 2007) possibly due to the inhibitory responses on the cAMP signal transduction cascade by decreasing PKA activity and CREB phosphorylation (Witt-Enderby, *et al*., 2003). Mel-1A (MT1) has also been shown to inhibit the induction of c-fos and junB mRNA and c-fos translation (Witt-Enderby, *et al*., 2003). Circadian phase shifting of the neuronal firing rhythms, however, has been linked to the activation of Mel-1B (MT2) receptor (Dubocovich, 2007) and recent findings indicate that melatonin mainly acts by altering neuronal excitability in SCN neurons by modulating inhibitory GABAergic transmission within the SCN (Scott, *et al*., 2010). In contrast to mammals, very little is known about the physiological cellular effects of melatonin in birds but there is clear evidence that the pineal melatonin rhythm acts on at least one other oscillator within the circadian pacemaking system, presumably the hypothalamic clock, which in turn feeds back onto the pineal gland (Gwinner and Brandstaetter, 2001).

The Mel-1C receptor appeared not to be rhythmic in the tissues studied but had high levels in the diencephalon, retina, optic tectum, cerebellum and telencephalon, and weaker levels in the pineal, heart, liver, lung and kidney. This suggests that the Mel-1C receptor has a structural role, but can heterodimerize with the other two receptors (Mel-1A and Mel-1B) in order to bind melatonin to initiate the effect of the hormone. Mammal and non-mammal species have

Mel-1A and Mel-1B orthologues (~80% MT1, 67% MT2). However, the mammalian GPR50 protein has been shown to perform a similar role to Mel-1C, although the two genes share only ~50% homology (Dufourny, *et al*., 2008).

Melatonin receptor expression was highly variable in peripheral tissues of the zebra finch, and while liver showed rhythmic Mel-1A and Mel-1B expression, only the Mel-1B receptor was rhythmically expressed in lung and heart. Interestingly, kidney was the only tissue in this study that showed a rhythm in Mel-1C receptor expression. Peripheral tissues also differed in regard of the temporal organisation of melatonin receptor expression. While Mel-1A in the liver and Mel-1C in the heart peak early in the day when circulating melatonin has declined to baseline levels (Brandstaetter, *et al*., 2001b), Mel-1B is elevated throughout the day in heart and liver but peaks at the transition from light to dark in the lung. These data suggest distinct control mechanisms of melatonin in peripheral organs and diurnal rhythms of melatonin responsiveness that may relate to the rhythm of circulating melatonin mechanism (Gwinner and Brandstaetter, 2001; van't Hof and Gwinner, 1999).

In Chapter Six it was shown that light exposure affected numerous cell groups within the hypothalamus (PON, GLv, LHN, SCN, PPN), notably the suprachiasmatic nucleus (SCN) and the lateral hypothalamic nucleus (LHN), two of the nuclei associated with circadian oscillatory functions. The LHN appears to be stimulated by light at all the experimental time points, showing its importance in the light signal transduction pathway. The effect of light showed a novel result in the late dark period, compared to the finding in the early dark period. Expression of c-fos in the SCN is seen in the late dark phase and more dominantly after 60 minutes, when compared to 90 minutes. This suggests that the SCN becomes stimulated by

the light in the second half of the dark phase and detects the onset of the light period, or detects differences in lighting conditions and buffers abnormal conditions. After 90 minutes from the onset of light, the dominant c-fos expression in the SCN became weaker, but expression in the periventricular preoptic nucleus (PPN) cell group became more dominant. The PPN is part for the preoptic and periventricular areas that are involved in secreting hormones/releasing factors to the pituitary gland. Therefore, the fact that light has stimulated this area in the late dark could suggest its role in releasing factors to stimulate the arousal of the individual with the onset of the morning light.

In Chapter Seven, arginine-vasotocin (AVT) expression was examined in the hypothalamus using immunofluorescent localisation experiments. AVTergic cells were also seen to peak in the LHN towards to the late dark period and into the light period, but AVTergic cells were not found in the SCN of the zebra finch. Vasopressin/Vasotocin is one of the most documented circadian output neuropeptide in circadian work in both mammals and birds, showing autonomic and behavioural features; from osmoregulation to aggressive and sexual behaviours. It has been shown to be one of the so-called 'clock controlled genes' which are rhythmically regulated using the same transcriptional mechanisms that control the clock feedback loops in mice (Li, *et al*., 2009).

Vasotocin data from Chapter Seven in this thesis showed a robust diurnal rhythm that is sustained under darkness, showing the endogenous nature of this neuropeptide in the zebra finch circadian system. The highest number and most rhythmical of AVTergic cells was seen in the LHNv of the zebra finch, where avianPer2 has been shown to be expressed in the early morning (Brandstaetter, *et al*., 2001b). AVTergic cells were also found in the LHNv of the

chicken and Japanese quail at ZT1 but with lower numbers, as seen in Chapter Eight. Together with previous data from Dr Roland Brandstaetter (personal communication 2011 – appendix I -) we have shown a novel hypothalamic cell group in the dorsal part of the LHN which is associated with seasonal breeding of the house sparrow, blackbird, European starling, stonechat and garden warbler, which all have intact photorefractoriness. Avian species such as the chicken, Japanese quail and zebra finch, lack the AVTergic cells in the LHNd and are now non-seasonal breeders without an intact photorefractoriness. These results significantly increase the knowledge of the working model of avian photoperiodism by linking the circadian and hypothalamo-hypophysial systems, with the LHNd appearing to be an evolutionary novelty of seasonally breeding birds.

In the mammalian hypothalamus it is well documented that the 'master' oscillator lies within the suprachiasmatic nucleus (SCN). In birds, there are at least two cell groups in the hypothalamus that have been shown to be comparable with the mammalian SCN circadian functions. These are the SCN and a more lateral cell group known as the lateral hypothalamic nucleus (LHN). Both of these cell groups are vital in maintaining circadian rhythmicity (Takahashi and Menaker, 1982) by expressing vital circadian core genes (Abraham, 2002; Abraham, *et al*., 2002; Albrecht, *et al*., 1997) and have light input mechanisms (King and Follett, 1997).

This thesis has shown that the SCN and LHN areas are responsive to light (c-fos expression), contain AVTergic cells (LHN), and cells within these groups contain melatonin membrane receptors. Two out of the three receptors (Mel-1A and Mel-1B) are rhythmically expressed in the diencephalon (hypothalamus), whereas the Mel-1C receptor is constantly expressed in the

diencephalon. This has increased knowledge of how important the LHN is in the circadian system of the zebra finch. This work represents another step forward in disentangling the numerous signalling events that take place in the circadian system in birds. Future work should help to confirm the roles of other neuropeptides have in circadian organisation in the lateral hypothalamic nuclei and hopefully shed light on other signalling networks that take place in order to successfully maintain the circadian rhythms in the zebra finch.

9.2 Future work

This thesis has shown rhythmic cycles of two of the three melatonin receptors (*Mel-1A* and *Mel-1B*) and one receptor that is constantly expressed in tissues (*Mel-1C*). The mRNA rhythmicity of the melatonin receptors studied were under 12:12 LD conditions it would be interesting to further this work by changing the lighting schedule to constant light and constant darkness as seen in previous circadian work in order to determine endogenous rhythms like (de Mairan, 1729). This would determine if the rhythms of these receptors are endogenous like the cycle of secreting melatonin hormone levels (Brandstaetter, *et al*., 2001b), or whether the rhythms found are entrained to light presences. Since this part of the thesis looked at whole tissue levels of the receptors, *in situ* hybridisation studies would show the location of the receptors in the hypothalamic nuclei, and how these nuclei are relevant to circadian biology. Previous studies using 2-[^{125}I]odomelatonin radiograph techniques have shown melatonin receptors sites throughout the avian brain but these experiments do not show which receptor subtype is found in each location or that any sites were found in the pineal

gland (e.g. Vakkuri, *et al*., 1984; Siuciak, *et al*., 1991; Brooks and Cassone, 1992; Reppert, *et al*., 1996), therefore it would be interesting to see the spread of the three different receptor mRNA in cell groups of the hypothalamus.

The findings of the *Mel-1C* mRNA shown in this thesis, it would be interesting to see if the *in situ* experiments showed any differences in the expression the receptor, i.e. whether the *Mel-1C* receptor levels are rhythmic in set nuclei or whether the receptor is constantly expressed in the nuclei the receptor is found in. To the best of my knowledge this occurrence has not been shown, that whole tissue sample can dampen single cell group rhythmicity, so therefore this would be an interesting methodology examination to see if this does or can occur. Since the protein expression experiments (Chapter Five) showed that the Mel-1C receptor levels were constantly expressed in the mid-light phase and in the mid-dark phase, it would be interesting to compare the cell group localization of the protein levels to the mRNA levels, a more precise technique for this would be to use real time polymerase chain reaction which gives specific quantitative readings on mRNA level rather than the comparative readings in this thesis. Since the protein work for the melatonin receptors showed the cell group localisation it would be fascinating to quantify this data with western blot experiments, or cell counts of the immunofluorescent images, over a 24 hour series at the same ZT's studied in the mRNA experiments in Chapter 4. Another approach to the protein expression would be to look at the new proteomic techniques such as fourier-transform ion cyclotron resonance mass spectrometry (FT-ICR-MS) to examine the proteins in a sample of brain tissue at set time points over the 24 hour period, so see whether the protein levels differ. Such techniques have been used in a variety of different research studies ranging from the diagnostics of diabetes

and other disease (Griffin and Nicholls, 2006; Theodorescu and Mischak, 2007) to plant physiology (Weckwerth, 2008).

The putative effect of the melatonin receptors are documented in the mammalian system (Dubocovich, 2007), it would be interesting to perform experiments to see how they differed from the mammalian, such as firing rates of SCN or LHN neurons. GPR50 melatonin like receptor has been shown to reduce the Mel-1A receptor affinity to binding melatonin (Levoye, *et al*., 2006; Dufourny, *et al*., 2008; Pandi-Perumal, *et al*., 2008), if the GPR50 and Mel-1C are orthologues of one another, could Mel-1C receptor do the same in avian species. It has also been suggested that the melatonin receptor subtypes heterodimerize with one another (Levoye, *et al*., 2006; Dufourny, *et al*., 2008). Yeast two-hybrid (Y2H) technique could be used to examine whether Mel-1a, Mel-1b and Mel1c receptors can heterodimerize with each other in different combinations (i.e. Mel-1A-Mel-1B, Mel-1A-Mel-1C and Mel-1B-Mel-1C) like suggested in the mammalian system.

Considering the interesting result from the AVT study in this thesis which showed different results in the LHN cell group of birds with different photorefractoriness, a comparative studying of melatonin receptor levels (either protein or mRNA) looking at seasonal breeders (e.g. house sparrow, blackbird, European starling, stonechat, garden warbler) and non-seasonal breeders/or birds that have lost their photorefractoriness (e.g. Japanese quail, chicken) would be interesting, to see if the melatonin receptors are linked seasonal breeders. We know that melatonin levels vary over seasonal changes in light lengths (Brandstaetter, *et al*., 2000; Brandstaetter, *et al*., 2001b) and in migratory birds melatonin levels are reduced at night close to the start of the migration (Brandstaetter, 2003; Fusani and Gwinner, 2004;

Kumar, *et al*., 2010). A comparative study looking at the how the melatonin receptor levels vary in accordance to the melatonin level changes throughout these periods, i.e. look at the melatonin receptor levels in migratory birds (e.g. house sparrow, European starling, etc.) and non-migratory birds (e.g. zebra finch, chicken, Japanese quail). As well as looking comparing difference between the two types of species, it would also be interesting to see the different expression patterns just in the migratory birds, i.e. when they are resident to when they are about to migrate as some migratory birds become night active close to migration.

In light of the exciting results of the light exposure experiments in this thesis, it would be interesting to compare the c-fos levels during the normal 12:12 LD light phase to compare the levels 60 minutes (ZT1) and 90 minutes (ZT1.5) after the "normal" onset of light at ZT0. This would allow us to see if the same responses occur due to the initial response to light or whether the responses seen in this study occur just during the dark phase. To further this study, reaction to light exposure at the same time-point used in these experiments could be performed after the birds are placed in constant darkness for 24 hour, to see if there are any differences to the response to light.

The AVT work here confirmed an endogenous rhythm of AVT in the zebra finch hypothalamus, i.e. experiments in DD conditions showed the same results (but slightly dampened) to that seen in 12:12 LD over 24 hours. It would be interesting to see what changing the lighting conditions in LD cycles has on the number of AVTergic cells in the LHN, i.e. would changing the lighting conditions to 8:16 LD or 16:8 LD still have a strong response at ZT1 or would this change. Since changing the light length has shown to vary the during and amplification of other neuropeptides and hormones such as melatonin

(Brandstaetter, 2003; Brandstaetter, *et al*., 2001b), could this also occur in the AVT rhythm. Light enhances the rhythm of AVTergic cells; it would be interesting to compare the result under constant bright light or after 48 hours under constant dimLL. With the comparative results from the Japanese quail and chicken (Chapter Eight) immunofluorescent experiments over 24 hours could be performed under LD and dimLL conditions, like in the zebra finch experiments, which would show whether a rhythm is found in these two species and whether their rhythm is endogenous as well.

Although this thesis has provided a new understanding of input and output mechanisms in the circadian system of the zebra finch, there are still major gaps in knowledge of both general circadian biology and avian circadian biology. As stated in birds so far, three regions of the brain have been identified to contain circadian oscillatory functions, but as more work goes on more regions maybe uncovered. The avian system is more complex than mammalian model, and as multiple regions can influenced in the avian system there must be different signal pathways involved with the photo-transduction (Gwinner, 1978; Gwinner, *et al*., 1997; Brandstaetter, et al., 2001b). Avian species comparisons are needed to reveal the differences in the species with different oscillatory balances and functions.

Currently the most widely studied avian species or "model" species are the chicken and quail, but both of these birds have become domesticated and lost their natural photoperiodism, i.e. seasonal breeding. Although these species are good for comparative studies because of this loss, generalisations may not be able to be drawn between domesticated and non-domesticated species. Due to the diverse range of habitual characteristics of avian species, such as seasonal breeders, opportunistic breeders, migratory birds and resident birds other species need to be

studied to look at the life-style related circadian biology, i.e. same species found in different conditions (or latitudes). Comparative studies are greatly needed to understand the evolution of the circadian system, with different species having slightly different systems with different number of oscillators, different homologues of genes, photoreceptors distributions, with different habitats and "life styles" i.e. migration, resident, etc. Even though birds have a remarkable uniformity amongst their species bird inhabit all regions of the world and therefore a wide variety of ecological roles (Konishi, *et al*., 1989). The avian species also explore and communicate with other members of their species by the same sense as we do (i.e. sight, smell, touch and hearing) they therefore have similar sense organs as we do, but these sense are more highly developed in birds compared to us, which make birds ideal subjects for neural research (Konishi, et al., 1989). Time and time again the avian species prove their importance as a species to test and develop new ideas in numerous research fields. Therefore comparisons between vertebrates and invertebrates (e.g. drosophila and mammalian species - Sun, *et al*., 1997; Panda, *et al*., 2002; Glossop and Hardin, 2002; Stanewsky, 2003; Yu and Hardin, 2006), between vertebrate species (e.g. Foster and Menaker, 1993 and Menaker, *et al*., 1997) and between species (e.g. between avian species – Japanese quail and chicken compared to zebra finch in this thesis) are all of high importance due to the differences even between different vertebrate species highlight vital evolutionary changes. This will help reveal more vital circadian mechanisms and evolution across species.

References

REFERENCES

Abraham, U. (2002). *Molecular and neurochemical characterization of the hypothalamic circadian oscillator in the house sparrow (Passer domesticus)*. Ludwig-Maximilian-Universität.

Abraham, U., Albrecht, U., Gwinner, E., and Brandstaetter, R. (2002). Spatial and temporal variation of passer Per2 gene expression in two distinct cell groups of the suprachiasmatic hypothalamus in the house sparrow (Passer domesticus). *European Journal of Neuroscience*, *16*(3), pp.429–436.

Abraham, U., Albrecht, U., and Brandstaetter, R. (2003). Hypothalamic circadian organization in birds. II. Clock gene expression. *Chronobiology international*, *20*(4), pp.657–669.

Acher, R., and Chauvet, J. (1995). The neurohypophysial endocrine regulatory cascade: precursors, mediators, receptors, and effectors. *Frontiers in neuroendocrinology*, *16*(3), pp.237–289.

Alarma-Estrany, P., and Pintor, J. (2007). Melatonin receptors in the eye: location, second messengers and role in ocular physiology. *Pharmacology and therapeutics*, *113*(3), pp.507-22.

Albrecht, U., Sun, Z.S., Eichele, G., and Lee, C.C. (1997). A differential response of two putative mammalian circadian regulators, mper1 and mper2, to light. *Cell*, *91*(7), pp.1055-64.

Alcantara-Contreras, S., Baba, K., and Tosini, G. (2011). Removal of melatonin receptor type 1 increases intraocular pressure and retinal ganglion cells death in the mouse. *Neuroscience letters*, *494*(1), pp.61-64.

Aschoff, J., and Tokura, H. (1986). Circadian Activity Rhythms in Squirrel Monkeys: Entrainment by Temperature Cycles 1. *Journal of Biological Rhythms*, *1*(2), pp.91-99.

Aste, N., Balthazart, J., Absil, P., Grossmann, R., Mülhbauer, E., Viglietti-Panzica, C., and Panzica, G.C. (1998). Anatomical and neurochemical definition of the nucleus of the stria terminalis in Japanese quail (Coturnix japonica). *The Journal of comparative neurology*, *396*(2), pp.141-57.

Aste, N., Cozzi, B., Stankov, B., and Panzica, G. C. (2001). Sexual differences and effect of photoperiod on melatonin receptor in avian brain. *Microscopy research and technique*, *55*(1), pp.37-47.

Audinot, V., Bonnaud, A., Grandcolas, L., Rodriguez, M., Nagel, N., Galizzi, J.-P., Balik, A., Messager, S., Hazlerigg, D.G., Barrett, P., Delagrange, P., and Boutin, J.A. (2008). Molecular cloning and pharmacological characterization of rat melatonin MT1 and MT2 receptors. *Biochemical pharmacology*, *75*(10), pp.2007-2019.

Axelrod, J., and Wurtman, R.J. (1968). Photic and neural control of indoleamine metabolism in the rat pineal gland. *Advances in pharmacology*, *6*(Pt A), pp/157-166.

Ayoub, M. a, Couturier, C., Lucas-Meunier, E., Angers, S., Fossier, P., Bouvier, M., and Jockers, R. (2002). Monitoring of ligand-independent dimerization and ligand-induced conformational changes of melatonin receptors in living cells by bioluminescence resonance energy transfer. *The Journal of biological chemistry*, *277*(24), pp.21522-8.

Bae, K., Jin, X., Maywood, E.S., Hastings, M.H., Reppert, S.M., and Weaver, D.R. (2001). Differential Functions of mPer1, mPer2, and mPer3 in the SCN Circadian Clock. *Neuron*, *30*(2), pp.525-536.

Baehr, E.K., Fogg, L.F., and Eastman, C.I. (1999). Intermittent bright light and exercise to entrain human circadian rhythms to night work. *American Journal of Physiology: Regulatory, Integrative Comparative Physiology*, *277*(6), R1598-1604.

Bailey, M., Chong, N.W., Xiong, J., and Cassone, V.M. (2002). Chickens' Cry2: molecular analysis of an avian cryptochrome in retinal and pineal photoreceptors. *FEBS Letters*, *513*(2-3), pp.169-174.

Bargiello, T.A., and Young, M.A. (1984). Molecular Genetics of a Biological Clock in Drosophila. *Proceedings of the National Academy of Sciences*, *81*(7), 2142-2146.

Barrett, P., Conway, S., and Morgan, P.J. (2003). Digging deep - structure-function relationships in the melatonin receptor family. *Journal of Pineal Research*, *35*(4), pp.221-230.

Barrett, R., and Takahashi, J. (1995). Temperature compensation and temperature entrainment of the chick pineal cell circadian clock. *J. Neurosci.*, *15*(8), pp.5681-5692.

Basheer, R., Sherin, J. E., Saper, C.B., Morgan, J.I., McCarley, R.W., and Shiromani, P. J. (1997). Effects of Sleep on Wake-Induced c-fos Expression. *J. Neurosci.*, *17*(24), pp.9746-9750.

Bellingham, J., Wells, D., and Foster, R.G. (2003). In silico characterisation and chromosomal localisation of human RRH (peropsin) – implications for opsin evolution. *BMC Genomics*, *4*(1), p.3.

Bernard, M. (1997). Chick pineal clock regulates serotonin N-acetyltransferase mRNA rhythm in culture. *Proceedings of the National Academy of Sciences*, *94*(1), pp.304-309.

Bernard, M., Iuvone, P.M., Cassone, V.M., Roseboom, P.H., Coon, S. L., and Klein, D.C. (2002). Avian Melatonin Synthesis: Photic and Circadian Regulation of Serotonin N-Acetyltransferase mRNA in the Chicken Pineal Gland and Retina. *Journal of Neurochemistry*, *68*(1), pp.213-224.

Berson, D.M., Dunn, F.A., and Takao, M. (2002). Phototransduction by retinal ganglion cells that set the circadian clock. *Science (New York, N.Y.)*, *295*(5557), pp.1070-3.

Berson, D.M. (2007). Phototransduction in ganglion-cell photoreceptors. *European Journal of Physiology*, *54*, pp.849-855.

Binkley, S., Kluth, E., and Menaker, M. (1971). Pineal Function in Sparrows: Circadian Rhythms and Body Temperature. *Science*, *174*(4006), pp.311-314.

Bittman, E.L. (2009). Vasopressin: more than just an output of the circadian pacemaker? Focus on "Vasopressin receptor V1a regulates circadian rhythms of locomotor activity and expression of clock-controlled genes in the suprachiasmatic nuclei". *American journal of physiology. Regulatory, integrative and comparative physiology*, *296*(3), pp.R821-3.

den Boer-Visser, A., and Dubbeldam, J.L. (2002). The distribution of dopamine, substance P, vasoactive intestinal polypeptide and neuropeptide Y immunoreactivity in the brain of the collared dove, *Streptopelia decaocto*. *Journal of Chemical Neuroanatomy*, *23*(1), pp.1-27.

Brandstaetter, R., Kumar, V., Abraham, U., and Gwinner, E. (2000). Photoperiodic information acquired and stored in vivo is retained in vitro by a circadian oscillator, the avian pineal gland. *Proceedings of the National Academy of Sciences of the United States of America*, *97*(22), pp.12324-8.

Brandstaetter, R., Abraham, U., and Albrecht, U. (2001a). Initial demonstration of rhythmic Per gene expression in the hypothalamus of a non-mammalian vertebrate, the house sparrow. *Neuroreport*, *12*(6), pp.1167-1170.

Brandstaetter, R., Kumar, V., van't Hof, T.J., and Gwinner, E. (2001b). Seasonal variations of *in vivo* and *in vitro* melatonin production in a passeriform bird, the house sparrow (Passer domesticus). *Journal of Pineal Research*, *31*(2), pp.120-126.

Brandstaetter, R. (2002). The circadian pacemaking system of birds. *Biological Rhythms* (Kumar 5th., pp. 144-163). Narosa Publishing House, New Delhi.

Brandstaetter, R. (2003). Encoding time of day and time of year by the avian circadian system. *Journal of neuroendocrinology*, *15*(4), pp.398-404.

Brandstaetter, R., and Abraham, U. (2003). Hypothalamic Circadian Organization in Birds. I. Anatomy, Functional Morphology, and Terminology of the Suprachiasmatic Region. *Chronobiology International*, *20*(4), pp.637-655.

Bringmann, A., Pannicke, T., Grosche, J., Francke, M., Wiedemann, P., Skatchkov, S. N., Osborne, N. N., and Reichenbach, A. (2006). Müller cells in the healthy and diseased retina. *Progress in Retinal and Eye Research*, *25*(4), pp.397-424.

Brooks, D.S., and Cassone, V.M. (1992). Daily and circadian regulation of 2-[125I]iodomelatonin binding in the chick brain. *Endocrinology*, *131*(3), pp.1297-1304.

Brydon, L., Roka, F., Petit, L., Coppet, P. D., Tissot, M., Barrett, P., Morgan, P. J., Nanoff, C., Strosberg, A.D., and Jockers, R. (1999). Dual Signaling of Human Mel1a Melatonin Receptors via Gi2, Gi3, and Gq/11 Proteins. *Molecular Endocrinology*, *13*(12), pp.2025-2038.

Bunger, M., Wilsbacher, L.D., Moran, S., and Clendenin, C. (2000). Mop3 is an essential component of the master circadian pacemaker in mammals. *Cell*, *103*, 1009−1017.

Cahill, G.M., and Hasegawa, M. (1997). Circadian Oscillators in Vertebrate Retinal Photoreceptor Cells. *Neurosignals*, *6*(4-6), pp.191-200.

Caldwell, H., and Young, W. (2006). *Handbook of Neurochemistry and Molecular Neurobiology*. (A. Lajtha and R. Lim, Eds.)*Handbook of Neurochemistry and Molecular Neurobiology* (pp. 573-607). Boston, MA: Springer US.

Cantwell, E.L., and Cassone, V.M. (2006). Chicken suprachiasmatic nuclei: I. Efferent and afferent connections. *The Journal of Comparative Neurology*, *496*(1), pp.97–120.

Capsoni, S., Viswanathan, M., Oliveira, A.M.D., and Saavedra, J.M. (1994). Characterization of melatonin receptors and signal transduction system in rat arteries forming the circle of Willis. *Endocrinology*, *135*(1), pp.373-378.

Carlberg, C. (2000). Gene Regulation by Melatonin. *Annals of the New York Academy of Sciences*, *917*(1), pp.387-396.

Cassone, V.M., and Menaker, M. (1984). Is the avian circadian system a neuroendocrine loop? *The Journal of experimental zoology*, *232*(3), pp.539-49.

Cassone, V.M., and Moore, R.Y. (1987). Retinohypothalamic projection and suprachiasmatic nucleus of the house sparrow, Passer domesticus. *The Journal of Comparative*, *182*, pp.171-182.

Cassone, V.M. (1988). Circadian variation of [14C]2-deoxyglucose uptake within the suprachiasmatic nucleus of the house sparrow,Passer domesticus. *Brain Research, 459*(1), pp.178-182.

Cassone, V. M. (1990). Effects of melatonin on vertebrate circadian systems. *Trends in Neurosciences*, *13*(11), pp.457-464.

Cassone, V.M., and Brooks, D.S. (1991). Sites of melatonin action in the brain of the house sparrow,Passer domesticus. *Journal of Experimental Zoology, 260*(3), pp.302-309.

Cassone, V.M., Bartell, P.A., Earnest, B.J., and Kumar, V. (2008). Duration of melatonin regulates seasonal changes in song control nuclei of the house sparrow, Passer domesticus: independence from gonads and circadian entrainment. *Journal of biological rhythms*, *23*(1), pp.49-58.

Cermakian, N., and Sassone-Corsi, P. (2000). Multilevel regulation of the circadian clock. *Nature reviews. Molecular cell biology, 1*(1), pp.59-67.

Chabot, C., and Menaker, M. (1992). Effects of physiological cycles of infused melatonin on circadian rhythmicity in pigeons. *Journal of Comparative Physiology A, 170*(5), pp.615-622.

Chaiseha, Y., and El Halawani, M.E. (1999). Expression of vasoactive intestinal peptide/peptide histidine isoleucine in several hypothalamic areas during the turkey reproductive cycle: relationship to prolactin secretion. *Neuroendocrinology*, *70*(6), pp.402-412.

Chaiseha, Y., Youngren, O.M., and El Halawani, M.E. (1998). Vasoactive Intestinal Peptide Secretion by Turkey Hypothalamic Explants. *Biology of Reproduction, 59*(3), pp.670-675.

Chaturvedi, C. M., Chowdhary, A., Wall, P.T., Koike, T.I., and Cornett, L.E. (2000). A sexual dimorphism in hypothalamic arginine vasotocin (AVT) gene expression and AVT plasma levels in the Japanese quail (Coturnix coturnix japonica) in response to water deprivation. *General and comparative endocrinology, 117*(1), pp.129-137.

Chen, J., Kuei, C., Sutton, S., Wilson, S., Yu, J., Kamme, F., Mazur, C., Lovenberg, T. and Liu, C. (2005). Identification and pharmacological characterization of prokineticin 2 beta as a selective ligand for prokineticin receptor 1. *Molecular pharmacology*, *67*(6), pp.2070-2076.

Cheng, M.Y., Bittman, E.L., Hattar, S., and Zhou, Q.-Y. (2005). Regulation of prokineticin 2 expression by light and the circadian clock. *BMC neuroscience*, *6*(1), pp.17.

Cheng, M.Y., Bullock, C.M., Li, C., Lee, A.G., Bermak, J.C., Belluzzi, J., Weaver, D.R., Leslie, F.M. and, Zhou, Q.-Y. (2002). Prokineticin 2 transmits the behavioural circadian rhythm of the suprachiasmatic nucleus. *Nature*, *417*(6887), pp.405-10.

Cooper, M.L., Pickard, G.E., and Silver, R. (1983). Retinohypothalamic Pathway in the Dove Demu ~ st ~ ated by Antero ~ ad ~ HRP. *Brain Research Bulletin*, *10*, pp.715-718.

Cornett, L.E., Kirby, J.D., Vizcarra, J.A., Ellison, J.C., Thrash, J., Mayeux, P.R., Crew, M.D., Jones, S.M., Ali, N., and Baeyens, D.A. (2003). Molecular cloning and functional characterization of a vasotocin receptor subtype expressed in the pituitary gland of the domestic chicken (Gallus domesticus): avian homolog of the mammalian V1b-vasopressin receptor. *Regulatory peptides*, *110*(3), pp.231–239.

Cottet, M., Albizu, L., Perkovska, S., Jean-Alphonse, F., Rahmeh, R., Orcel, H., Méjean, C., Granier, S., Mendre, C., Mouillac, B., and Durroux, T (2010). Past, present and future of vasopressin and oxytocin receptor oligomers, prototypical GPCR models to study dimerization processes. *Current opinion in pharmacology*, *10*(1), pp.59-66.

Cottrell, G. T., Zhou, Q.-Y., and Ferguson, A. V. (2004). Prokineticin 2 modulates the excitability of subfornical organ neurons. *The Journal of neuroscience : the official journal of the Society for Neuroscience*, *24*(10), pp.2375-2379.

Cozzi, B., Viglietti-Panzica, C., Aste, N., and Panzica, G.C. (1991). The serotoninergic system in the brain of the Japanese quail. *Cell and Tissue Research*, *263*(2), pp.271-284.

Csernus, V. J. (2006). The avian pineal gland. *Chronobiology international*, *23*(1-2), pp.329-339.

Cutting, G. R., Lu, L., O'Hara, B.F., Kasch, L.M., Montrose-Rafizadeh, C., Donovan, D.M., Shimada, S., Antonarakis, S.E., Guggino, W.B., and Uhl, G.R. (1991). Cloning of the -Aminobutyric Acid (GABA) 1 cDNA: A GABA Receptor Subunit Highly Expressed in the Retina. *Proceedings of the National Academy of Sciences*, *88*(7), pp.2673-2677.

Daan, S., and Pittendrigh, C.S. (1976). A Functional analysis of circadian pacemakers in nocturnal rodents. *Journal of Comparative Physiology A*, *106*(3), pp.253-266.

Daan, S., Albrecht, U., van der Horst, G., Illnerova, H., Roenneberg, T., Wehr, T., and Schwartz, W. (2001). Assembling a clock for all seasons: are there M and E oscillators in the genes? *Journal of Biology Rhythms*, *16*(2), pp.105-116.

Daniel, P.M. (1976). Anatomy of the hypothalamus and pituitary gland. *Journal of Clinical Pathology*, *s1-7*(1), pp.1-7.

Dardente, H., and Cermakian, N. (2007). Molecular circadian rhythms in central and peripheral clocks in mammals. *Chronobiology international*, *24*(2), pp.195-213.

Day, H.E.W., Kryskow, E.M., Nyhuis, T.J., Herlihy, L., and Campeau, S. (2008). Conditioned fear inhibits c-fos mRNA expression in the central extended amygdala. *Brain research*, *1229*, pp.137-46.

de Mairan, J. (1729). Observation botanique. *oir de l'Academie Royale des Science*, pp.35-36.

Dieffenbach, C.W., and Dveksler, G.S. (2003). *PCR primer: a laboratory manual* (p. 520). CSHL Press.

van Dijk, G. (2001). The Role of Leptin in the Regulation of Energy Balance and Adiposity. *Journal of Neuroendocrinology*, *13*(10), pp.913-921.

Doi, M., Nakajima, Y., Okano, T, and Fukada, Y. (2001). Light-induced phase-delay of the chicken pineal circadian clock is associated with the induction of cE4bp4, a potential transcriptional repressor of cPer2 gene. *PNAS*, *98*(14), pp.8089-8094.

Drew, J.E., Barrett, P., Williams, L.M., Conway, S., and Morgan, P.J. (1998). The Ovine Melatonin-Related Receptor: Cloning and Preliminary Distribution and Binding Studies. *Journal of Neuroendocrinology, 10*(9), pp.651-661.

Dubocovich, M.L. (1988). Pharmacology and function of melatonin receptors. *FASEB J, 2*(12), pp.2765-2773.

Dubocovich, M.L. (1988). Luzindole (N-0774): a novel melatonin receptor antagonist. *Journal of Pharmacology and Experimental Therapeutics, 246*(3), pp.902-910.

Dubocovich, M. L. (1995). Melatonin receptors: Are there multiple subtypes? *Trends in Pharmacological Sciences, 16*(2), pp.50-56.

Dubocovich, M. L. (2007). Melatonin receptors: role on sleep and circadian rhythm regulation. *Sleep medicine, 8 Suppl 3*, pp.34-42.

Dubocovich, M.L., Rivera-Bermudez, M.A., Gerdin, M.J., and Masana, M.I. (2003). Molecular pharmacology, regulation and function of mammalian melatonin receptors. *Frontiers in Bioscience, 8*, d1093-1108.

Dubocovich, M.L., and Markowska, M. (2005). Functional MT1 and MT2 melatonin receptors in mammals. *Endocrine, 27*(2), pp.101-110.

Dubocovich, M.L., Delagrange, P., and Krause, D.N. (2010). International union of basic and clinical pharmacology. LXXV. Nomenclature, classification, and pharmacology of G protein-coupled melatonin receptors. *Pharmacological, 62*(3), pp.343.

Duffy, J.F., Kronauer, R.E., and Czeisler, C.A. (1996). Phase-shifting human circadian rhythms: influence of sleep timing, social contact and light exposure. *Journal of Physiology, 495*(1), pp.289-297.

Dufourny, L., Levasseur, A., Migaud, M., Callebaut, I., Pontarotti, P., Malpaux, B., and Monget, P. (2008). GPR50 is the mammalian ortholog of Mel1c: evidence of rapid evolution in mammals. *BMC evolutionary biology, 8*, pp.105.

Duman, R.S. (2001). *Analysis of Early Gene Responses*. (S. J. Enna, M. Williams, J. F. Barret, J. W. Ferkany, T. Kenakin, and R. D. Porsolt, Eds.) (pp. 2.5.1–2.5.20.). Hoboken, NJ, USA: John Wiley and Sons, Inc.

Ebihara, S., and Kawamura, H. (1981). The role of the pineal organ and the suprachiasmatic nucleus in the control of circadian locomotor rhythms in the Java sparrow,Padda oryzivora. *Journal of Comparative Physiology A*, *141*(2), pp.207-214.

Ebihara, S., Oshima, I., Yamada, H., Maki, G., and Koji, S. (1987). Circadian organization in the pigeon. *In: Hiroshige, T., Honma, K., eds. Comparative Aspects of Circadian Clocks* (pp. 84–94). Sapporo: Hokkaido University Press.

Ebisawa, T., Karne, S., Lerner, M.R., and Reppert, S.M. (1994). Expression cloning of a high-affinity melatonin receptor from Xenopus dermal melanophores. *Proceedings of the National Academy of Sciences of the United States of America*, *91*(13), pp.6133-6137.

Edgar, D., Dement, W., and Fuller, C. (1993). Effect of SCN lesions on sleep in squirrel monkeys: evidence for opponent processes in sleep-wake regulation. *Journal of Neuroscience*, *13*(3), pp.1065-1079.

Ehrlich, D., and Mark, R. (1984). An atlas of the primary visual projections in the brain of the chick Gallus gallus. *The Journal of comparative neurology*, *223*(4), pp.592-610.

Ekström, P., and Meissl, H. (2003). Evolution of photosensory pineal organs in new light: the fate of neuroendocrine photoreceptors. *Phil. Trans. R. Soc. Lond. B*, *358*(August), pp.1679-1700.

van Elzakker, M., Fevurly, R.D., Breindel, T., and Spencer, R.L. (2008). Environmental novelty is associated with a selective increase in Fos expression in the output elements of the hippocampal formation and the perirhinal cortex. *Learning and memory (Cold Spring Harbor, N.Y.)*, *15*(12), pp.899-908.

Emery, P., So, W.V., Kaneko, M., Hall, J.C., and Rosbash, M. (1998). CRY, a Drosophila Clock and Light-Regulated Cryptochrome, Is a Major Contributor to Circadian Rhythm Resetting and Photosensitivity. *Cell*, *95*(5), pp.669-679.

Esposito, V., Pelagalli, G.V., De Girolamo, P., and Gargiulo, G. (2001). Anatomical distribution of NPY-like immunoreactivity in the domestic chick brain (Gallus domesticus). *The Anatomical record*, *263*(2), pp.186-201.

van Esseveldt, L., Lehmanb, M.N., and Boer, G.J. (2000). The suprachiasmatic nucleus and the circadian time-keeping system revisited. *Brain Research Reviews*, *33*(1), pp.34-77.

Falcón, J. (1999). Cellular circadian clocks in the pineal. *Progress in Neurobiology*, *58*(2), pp.121-162.

Falcón, J., Besseau, L., Fuentès, M., Sauzet, S., Magnanou, E., and Boeuf, G. (2009). Structural and functional evolution of the pineal melatonin system in vertebrates. *Annals of the New York Academy of Sciences*, *1163*(ii), pp.101-11.

Field, M.D., Maywood, E.S., O'Brien, J.A., Weaver, D.R, Reppert, St.M., and Hastings, M.H. (2000). Analysis of Clock Proteins in Mouse SCN Demonstrates Phylogenetic Divergence of the Circadian Clockwork and Resetting Mechanisms. *Neuron*, *25*(2), pp.437-447.

Folk, G., Thrift, D., Zimmerman, M., and Reimann, P. (2006). Mammalian activity – rest rhythms in Arctic continuous daylight. *Biological Rhythm Research*, *37*(6), pp.455-469.

Foster, R.G., and Menaker, M. (1993). Circadian photoreception in mammals and other vertebrates. *Light and Biological Rhythms in Man* (pp. 73–91). Wetterberg, Pergamon Press, Oxford.

Foster, R.G., Garcia-Fernandez, J.M., Provencio, I., and de Grip, W.J. (1993). Opsin localization and chromophore retinoids identified within the basal brain of the lizard Anolis carolinensis. *Journal of Comparative Physiology A, 172*(1), pp.33-45.

Foster, R.G., and Soni, B.G. (1998). Extraretinal photoreceptors and their regulation of temporal physiology. *Reviews of reproduction*, *3*(3), pp.145-50.

Freier, S.M. (1986). Improved Free-Energy Parameters for Predictions of RNA Duplex Stability. *Proceedings of the National Academy of Sciences*, *83*(24), pp.9373-9377.

Fujieda, H., Hamadanizadeh, S.A., Wankiewics, E., Pang, S.F., and Brown, G.M. (1999). Expression of mt1 melatonin receptor in rat retina: evidence for multiple cell targets for melatonin. *Neuroscience*, *93*(2), pp.793-799.

Fujieda, H., Scher, J., Hamadanizadeh, S.A, Wankiewicz, E, Pang, S.F., and Brown, G.M. (2000). Dopaminergic and GABAergic amacrine cells are direct targets of melatonin: immunocytochemical study of mt1 melatonin receptor in guinea pig retina. *Visual neuroscience*, *17*(1), pp.63-70.

Furuse, M. (2007). Behavioral regulators in the brain of neonatal chicks. *Animal Science Journal*, *78*(3), pp.218-232.

Fusani, L., and Gwinner, E. (2004). Simulation of migratory flight and stopover affects night levels of melatonin in a nocturnal migrant. *Processing of the Royal Society B*, *271*, pp.205-211.

Gahr, M., and Kosar, E. (1996). Identification, distribution, and developmental changes of a melatonin binding site in the song control system of the zebra finch. *The Journal of comparative neurology*, *367*(2), pp.308-18.

von Gall, C., Garabette, M.L., Kell, C.A., Frenzel, S., Dehghani, F., Schumm-Draeger, P.-M., Weaver, David R, Korf, H.-W., Hastings, M.H., and Stehle, J.H. (2002). Rhythmic gene expression in pituitary depends on heterologous sensitization by the neurohormone melatonin. *Nature neuroscience*, *5*(3), pp.234-238.

von Gall, C., Weaver, DR, Kock, M., Korf, H.-W., and Stehle, J.H. (2000). Melatonin limits transcriptional impact of phosphoCREB in the mouse SCN via the Mel1a receptor. *Neuroreport*, *11*(9), pp.1803-1807.

Gallego, M., and Virshup, D.M. (2007). Post-translational modifications regulate the ticking of the circadian clock. *Nature reviews. Molecular cell biology*, *8*(2), pp.139-148

Ganguly, S., Coon, S.L., and Klein, D.C. (2002). Control of melatonin synthesis in the mammalian pineal gland: the critical role of serotonin acetylation. *Cell and tissue research*, *309*(1), pp.127-137.

Gaston, S., and Menaker, M. (1968). Pineal Function: The Biological Clock in the Sparrow? *Science, 160*(3832), pp.1125-1127.

Gaston, S. (1971).The influence of the pineal organ on the circadian activity rhythm in birds. In: Menaker, M. (Ed.), Biochronometry. Natl. Acad. Sciences, Washington DC, pp. 541–549.

Gekakis, N., Staknis, D., Nguyen, H.B., Davis, F.C., Wilsbacher, L.D., King, D.P., Takahashi, Joseph S., and Weitz, C.J.. (1998). Role of the CLOCK Protein in the Mammalian Circadian Mechanism. *Science, 280*(5369), pp.1564-1569.

van Gelder, R.N. (2008). How the clock sees the light. *Nature neuroscience, 11*(6), pp.628-630.

Glossop, N.R., and Hardin, P.E. (2002). Central and peripheral circadian oscillator mechanisms in flies and mammals. *Journal of Cell Science, 115*(17), pp.3369-3377.

Golombek, D.A., and Rosenstein, R.E. (2010). Physiology of circadian entrainment. *Physiological reviews, 90*(3), pp.1063-102.

Gorman, M.R., Kendall, M., and Elliott, J.A. (2005). Scotopic illumination enhances entrainment of circadian rhythms to lengthening light:dark cycles. *Journal of biological rhythms, 20*(1), pp.38-48.

Griffin Jr., E.A., Staknis, D., and Weitz, C.J. (1999). Light-Independent Role of CRY1 and CRY2 in the Mammalian Circadian Clock. *Science, 286*(5440), pp.768-771.

Griffin, J.L., and Nicholls, A.W. (2006). Metabolomics as a functional genomic tool for understanding lipid dysfunction in diabetes, obesity and related disorders. *Pharmacogenomics, 7*(7), pp.1095-1107.

Grossmann, R., Jurkevich, A., and Köhler, A. (2002). Sex dimorphism in the avian arginine vasotocin system with special emphasis to the bed nucleus of the stria terminalis. *Comparative Biochemistry and Physiology - Part A: Molecular and Integrative Physiology, 131*(4), pp.833-837.

Gauer, F., Schuster, C., Poirel, V.-J., Pévet, P., and Masson-Pévet, M. (1998). Cloning experiments and developmental expression of both melatonin receptor Mel1A mRNA and melatonin binding sites in the Syrian hamster suprachiasmatic nuclei. *Molecular Brain Research, 60*(2), pp.193-202.

Guido, M.E., Goguen, D., De Guido, L., Robertson, H.A., and Rusak, B. (1999). Circadian and photic regulation of immediate-early gene expression in the hamster suprachiasmatic nucleus. *Neuroscience, 90*(2), pp.555-571.

Guilding, C., and Piggins, H.D. (2007). Challenging the omnipotence of the suprachiasmatic timekeeper: are circadian oscillators present throughout the mammalian brain? *European Journal of Neuroscience, 25*(11), pp.3195–3216. J

Gwinner, E. (1977). Circannual Rhythms in Bird Migration. *Annual Review of Ecology and Systematics, 8*(1), pp.381-405.

Gwinner, E. (1978). Effects of pinealectomy on circadian locomotor activity rhythms in european starlings,Sturnus vulgaris. *Journal of Comparative Physiology A, 126*(2), pp.123-129.

Gwinner, E. (1989). Melatonin in the circadian system of birds: model of internal resonance. *Hiroshige T, Honma K, eds. Circadian Clocks and Ecology* (pp. 27–53). Sapporo: Hokkaido University Press.

Gwinner, E., Hau, M., and Heigl, S. (1997). Melatonin: Generation and Modulation of Avian Circadian Rhythms. *Brain Research Bulletin, 44*(4), pp.439-444.

Gwinner, E., and Brandstaetter, R. (2001). Complex bird clocks. *Philosophical transactions of the Royal Society of London. Series B, Biological sciences, 356*(1415), pp.1801-1810.

Halberg, F. (1946). Merizin. *Jahrbuch der international Hochschi* (pp. 336-351).

Harper, D.G., Tornatzky, W., and Miczek, K.A. (1996). Stress induced disorganization of circadian and ultradian rhythms: Comparisons of effects of surgery and social stress. *Physiology and Behaviour*, *59*(3), pp.409-419.

Hartwig, H.G. (1974). Electron microscopic evidence for a retinohypothalamic projection to the suprachiasmatic nucleus of Passer domesticus. *Cell and Tissue Research*, *153*(1), pp.89-99.

Hastings, M., O'Neill, J.S., and Maywood, E.S. (2007). Circadian clocks: regulators of endocrine and metabolic rhythms. *The Journal of endocrinology*, *195*(2), pp.187-198.

Hau, M., and Gwinner, E. (1996). Food as a circadian Zeitgeber for house sparrows: the effect of different food access durations. *Journal of biological rhythms*, *11*(3), pp.196-207.

Hazlerigg, D.G., Ebling, F.J.P., and Johnston, J.D. (2005). Photoperiod differentially regulates gene expression rhythms in the rostral and caudal SCN. *Current Biology*, *15*(12), R449-450.

Heigl, S., and Gwinner, E. (1995). Synchronization of Circadian Rhythms of House Sparrows by Oral Melatonin: Effects of Changing Period. *Journal of Biological Rhythms*, *10*(3), pp.225-233.

Helfer, G., Fidler, A.E., Vallone, D., Foulkes, N., and Brandstaetter, R. (2006). Molecular analysis of clock gene expression in the avian brain. *Chronobiology international*, *23*(1-2), pp.113-27.

Herrera-Pérez, P., Del Carmen Rendón, M., Besseau, L., Sauzet, S., Falcón, J., and Muñoz-Cueto, J.A. (2010). Melatonin receptors in the brain of the European sea bass: An in situ hybridization and autoradiographic study. *The Journal of comparative neurology*, *518*(17), pp.3495-511.

Herzog, E. D., and Huckfeldt, R. M. (2003). Circadian entrainment to temperature, but not light, in the isolated suprachiasmatic nucleus. *Journal of neurophysiology*, *90*(2), pp.763-770.

van't Hof, T.J., and Gwinner, E. (1999). Influence of pinealectomy and pineal stalk deflection on circadian gastrointestinal tract melatonin rhythms in zebra finches (*Taeniopygia guttata*). *Journal of biological rhythms*, *14*(3), pp.185-189.

Hogenesch, J.B., Gu, Y.-Z., Jain, S., and Bradfield, C.A. (1998). The basic-helix-loop-helix-PAS orphan MOP3 forms transcriptionally active complexes with circadian and hypoxia factors. *Proceedings of the National Academy of Sciences*, *95*(10), pp.5474-5479.

Huang, H., Lee, S.-C., and Yang, X.-L. (2005). Modulation by melatonin of glutamatergic synaptic transmission in the carp retina. *The Journal of physiology*, *569*(Pt 3), pp.857-71.

Husband, S., and Shimizu, T. (2001). Evolution of the Avian Visual System. *Cook, Robert G.*

Hätönen, T. (2000). *The impact of light on the secretion of melatonin in humans*. University of Helsinki: Helsinki, Finland.

Ikegami, T., Azuma, K., Nakamura, M., Suzuki, N., Hattori, A., and Ando, H. (2009). Diurnal expressions of four subtypes of melatonin receptor genes in the optic tectum and retina of goldfish. *Comparative biochemistry and physiology. Part A, Molecular and integrative physiology*, *152*(2), pp.219-24.

Imbesi, M., Arslan, A.D., Yildiz, S., Sharma, R., Gavin, D., Tun, N., Manev, H., and Uz, T. (2009). The melatonin receptor MT1 is required for the differential regulatory actions of melatonin on neuronal "clock" gene expression in striatal neurons in vitro. *Journal of pineal research*, *46*(1), pp.87-94.

Jansen, R., Metzdorf, R., van der Roest, M., Fusani, L., ter Maat, A., and Gahr, M. (2005). Melatonin affects the temporal organization of the song of the zebra finch. *The FASEB journal: official publication of the Federation of American Societies for Experimental Biology*, *19*(7), pp.848-50.

Jin, X., von Gall, C., Pieschl, R. L., Gribkoff, V. K., Stehle, J. H., Reppert, Steven M., and Weaver, D. R. (2003). Targeted Disruption of the Mouse Mel1b Melatonin Receptor. *Molecular and Cellular Biology*, *23*(3), pp.1054-1060.

Jin, Xiaowei, von Gall, C., Pieschl, R.L., Gribkoff, V.K., Stehle, J. H., Reppert, S.M., and Weaver, D.R. (2003). Targeted disruption of the mouse Mel1b melatonin receptor. *Molecular and cellular biology*, *23*(3), pp.1054–1060.

Jockers, R. (1997). Novel Isoforms of Mel1c Melatonin Receptors Modulating Intracellular Cyclic Guanosine 3',5'-Monophosphate Levels. *Molecular Endocrinology*, *11*(8), pp.1070-1081.

Johnston, J.D., Ebling, F.J.P., and Hazlerigg, D.G. (2005). Photoperiod regulates multiple gene expression in the suprachiasmatic nuclei and pars tuberalis of the Siberian hamster (Phodopus sungorus). *European Journal of Neuroscience*, *21*, pp.2967-2974.

Jurkevich, A., and Grossmann, R. (2003). Vasotocin and reproductive functions of the domestic chicken. *Domestic Animal Endocrinology*, *25*(1), pp.93-99.

Jurkevich, A., Berghman, L.R., Cornett, L.E., and Kuenzel, W.J. (2005). Characterization and immunohistochemical visualization of the vasotocin VT2 receptor in the pituitary gland of the chicken, Gallus gallus. *General and comparative endocrinology*, *143*(1), pp.82-91.

Jurkevich, A., Berghman, L.R., Cornett, L.E., and Kuenzel, W.J. (2008). Immunohistochemical characterization of chicken pituitary cells containing the vasotocin VT2 receptor. *Cell and Tissue Research*, *333*, pp.253-262.

Kalsbeek, A., Perreau-Lenz, S., and Buijs, R.M. (2006). A network of (autonomic) clock outputs. *Chronobiology International*, *23*(3), pp.23521-535.

Karaganis, S.P., Bartell, P.A., Shende, V.R., Moore, A.F., and Cassone, V.M. (2009). Modulation of metabolic and clock gene mRNA rhythms by pineal and retinal circadian oscillators. *General and comparative endocrinology*, *161*(2), pp.179-192.

van Kesteren, R.E., Smit, A.B., Dirks, R.W., With, N.D.D., Geraerts, W.P., and Joosse, J. (1992). Evolution of the Vasopressin/Oxytocin Superfamily: Characterization of a cDNA Encoding a Vasopressin-Related Precursor, Preproconopressin, from the Mollusc Lymnaea stagnalis. *Proceedings of the National Academy of Sciences*, *89*(10), pp.4593-4597.

King, V.M., and Follett, B.K. (1997). c-fos expression in the putative avian suprachiasmatic nucleus. *Journal of Comparative Physiology A: Sensory, Neural, and Behavioral Physiology*, *180*(5), pp.541-551.

de Kloet, E.R. (2010). From vasotocin to stress and cognition. *European Journal of Pharmacology*, *626*(1), pp.18–26.

Konishi, M., Emlen, S.T., Ricklefs, R.E., and Wingfield, J.C. (1989). Contributions of Bird Studies to Biology. *Advancement Of Science*, *246*(4929), pp.465-472.

Konopka, R.J. (1971). Clock Mutants of Drosophila melanogaster. *Proceedings of the National Academy of Sciences*, *68*(9), pp.2112-2116.

Kornhauser, J.M., Nelson, D.E., Mayo, K.E., and Takahashi, J.S. (1990). Photic and circadian regulation of c-fos gene expression in the hamster suprachiasmatic nucleus. *Neuron*, *5*(2), pp.127-134.

Kräuchi, K., and Wirz-Justice., A. (2001). Circadian Clues to Sleep Onset Mechanisms. *Neuropsychopharmacology*, *25*(5), pp.S92-S96.

Kuenzel, W.J., and Blähser, S. (1994). Vasoactive intestinal polypeptide (VIP)-containing neurons: distribution throughout the brain of the chick (Gallus domesticus) with focus upon the lateral septal organ. *Cell and Tissue Research*, *275*(1), pp.91-107.

Kuhlman, S.J., and McMahon, D.G. (2006). Encoding the ins and outs of circadian pacemaking. *Journal of biological rhythms*, *21*(6), pp.470-81.

Kumar, V., Singh, B.P., and Rani, S. (2004). The Bird Clock: A Complex, Multi-Oscillatory and Highly Diversified System. *Biological Rhythm Research*, *35*(1), pp.121-144.

Kumar, V., and Gwinner, E. (2005). Pinealectomy shortens resynchronisation times of house sparrow (Passer domesticus) circadian rhythms. *Naturwissenschaften*, *92*, pp.419-422.

Kumar, V., Wingfield, J.C., Dawson, A., Ramenofsky, M., Rani, S., and Bartell, P.A. (2010). Biological Clocks and Regulation of Seasonal Reproduction and Migration in Birds. *Physiological and biochemical zoology: PBZ*, *83*(5), pp.827-835.

Kume, K., Zylka, M. J., Sriram, S., Shearman, L.P, Weaver, D.R, Jin, Xiaowei, Maywood, E.S., Hastings, M.H., and Reppert, S.M. (1999). mCRY1 and mCRY2 Are Essential Components of the Negative Limb of the Circadian Clock Feedback Loop. *Cell*, *98*(2), pp.193-205.

Lall, G., and Biello, S. (2003). Neuropeptide y, gaba and circadian phase shifts to photic stimuli. *Neuroscience*, *120*(4), pp.915-921.

Lerner, A.B., Case, J.D., Takahashi, Y., Lee, T.H., and Mori, W. (1958). Isolation of melatonin, the pineal gland factor that lightens melanocytes. *Journal of the American Chemical Society*, *80*(10), pp.2587.

Leung, C., Goode, C., and Young, L. (2009). Neural distribution of nonapeptide binding sites in two species of songbird. *The Journal of Comparative Neurology*, *513*(August 2008), pp.197-208.

Levi, F., and Schibler, U. (2007). Circadian Rhythms: Mechanisms and Therapeutic Implications. *Annual Review of Pharmacology and Toxicology*, *47*, pp.593-628.

Levoye, A., Dam, J., Ayoub, M.A., Guillaume, J.-L., Couturier, C., Delagrange, P., and Jockers, R. (2006). The orphan GPR50 receptor specifically inhibits MT1 melatonin receptor function through heterodimerization. *The EMBO journal*, *25*(13), pp.3012-23.

Lewis, P. D., and Morris, T. R. (2000). Poultry and coloured light. *World's Poultry Science Journal*, *56*(03), pp.189-207.

Li, J.-D., Hu, W.-P., Boehmer, L., Cheng, M. Y., Lee, A. G., Jilek, A., Siegel, J. M., and Zhou, Q.-Y. (2006). Attenuated circadian rhythms in mice lacking the prokineticin 2 gene. *The Journal of neuroscience*, *26*(45), pp.11615-11623.

Li, J.-D., Burton, K.J., Zhang, C., Hu, S.-B., and Zhou, Q.-Y. (2009). Vasopressin receptor V1a regulates circadian rhythms of locomotor activity and expression of clock-controlled genes in the suprachiasmatic nuclei. *American journal of physiology. Regulatory, integrative and comparative physiology*, *296*(3), R824-830.

Lim, M.M., and Young, L.J. (2004). Vasopressin-dependent neural circuits underlying pair bond formation in the monogamous prairie vole. *Neuroscience*, *125*(1), pp.35-45.

Lin, D. C.-H., Bullock, C.M., Ehlert, F.J., Chen, J.-L., Tian, H., and Zhou, Q.-Y. (2002). Identification and molecular characterization of two closely related G protein-coupled receptors activated by prokineticins/endocrine gland vascular endothelial growth factor. *The Journal of biological chemistry*, *277*(22), pp.19276-19280.

Lincoln, G., Messager, S., Andersson, H., and Hazlerigg, D.G. (2002). Temporal expression of seven clock genes in the suprachiasmatic nucleus and the pars tuberalis of the sheep: evidence for an internal coincidence timer. *Proceedings of the National Academy of Sciences of the United States of America*, *99*(21), pp.13890-13895.

Liu, F., Yuan, H., Sugamori, K.S., Hamadanizadeh, A., Lee, F.J.S., Pang, S.F., Brown, G. M., Pristupa, Z.B., and Niznik, H.B. (1995). Molecular and functional characterization of a partial cDNA encoding a novel chicken brain melatonin receptor. *FEBS Letters*, *374*(2), pp.273-278.

Liu, C, Weaver, D.R., Strogatz, S.H., and Reppert, S.M. (1997a). Cellular construction of a circadian clock: period determination in the suprachiasmatic nuclei. *Cell*, *91*(6), pp.855–860.

Liu, C., Weaver, D.R., Jin, X., Shearman, L.P., Pieschl, R.L., Gribkoff, V.K., and Reppert, S.M. (1997b). Molecular dissection of two distinct actions of melatonin on the suprachiasmatic circadian clock. *Neuron*, *19*(1), pp.91-102.

Lu, J., and Cassone, V.M. (1993). Pineal regulation of circadian rhythms of 2-deoxy[^{14}C]glucose uptake and 2[^{125}I]iodomelatonin binding in the visual system of the house sparrow, *Passer domesticus. Journal of Comparative Physiology A, 173*, pp.765-774.

Lyssenko, V., Nagorny, C. L. F., Erdos, M. R., Wierup, N., Jonsson, A., Spégel, P., Bugliani, M., Saxena, R., Fex, M., Pulizzi, N., Isomaa, B., Tuomi, T., Nilsson, P., Kuusisto, J., Tuomilehto, J., Boehnke, M., Altshuler, D., Sundler, F., Eriksson, J.G., Jackson, A.U., Laakso, M., Marchetti, P., Watanabe, R.M., Mulder, H., and Groop, L. (2009). Common variant in MTNR1B associated with increased risk of type 2 diabetes and impaired early insulin secretion. *Nature genetics*, *41*(1), pp.82-8.

MacKenziea, R.S., Melanb, M.A., Passeya, D.K., and Witt-Enderby, P.A. (2002). Dual coupling of MT1 and MT2 melatonin receptors to cyclic AMP and phosphoinositide signal transduction cascades and their regulation following melatonin exposure. *Biochemical Pharmacology*, *63*(4), pp.587-595.

Martini, F., Ober, W.C., Garrison, C.W., Welch, K., and Hutchings, R.T. (2001). *Fundamentals of Anatomy and Physiology* (5th ed.). Prentice Hall College Div.

Maurizi, C. (2000). A preliminary understanding of mania: roles for melatonin, vasotocin and rapid-eye-movement sleep. *Medical hypotheses*, *54*(1), pp.26–29.

McMillan, J.P. (1972) Pinealectomy abolishes the circadian rhythm of migratory restlessness. *Journal of Comparative Physiology*, *79*, pp.105-112.

Meier, R. (1973). Autoradiographic evidence for a direct retino-hypothalamic projection in the avian brain. *Brain Research*, *53*(2), pp.417-421.

Meijer, J.H., Michel, S., and Vansteensel, M.J. (2007). Processing of daily and seasonal light information in the mammalian circadian clock. *General and comparative endocrinology*, *152*(2-3), pp.159-164.

Menaker, M., Moreira, L.F., and Tosini, G. (1997). Evolution of circadian organization in vertebrates. *Braziliant Journal of Medical and Biological Research*, *30*(3), pp.305-313.

Merrow, M., Spoelstra, K., and Roenneberg, T. (2005). The circadian cycle: daily rhythms from behaviour to genes. *EMBO reports*, *6*(10), pp.930-935.

Meyer, P., Pache, M., Loeffler, K. U., Brydon, L., Jockers, R., Flammer, J., Wirz-Justice, A., and Savaskan, E. (2002). Melatonin MT-1-receptor immunoreactivity in the human eye. *The British journal of ophthalmology*, *86*(9), pp.1053-1057.

Mistlberger, R.E. (2002). Circadian Rhythms. *Encyclopedia of cognitive science*. MacMillian Reference Ltd: London.

Mollay, C., Wechselbergera, C., Mignognab, G., Negric, L., Melchiorric, P., Barrab, D., and Kreila, G. (1999). Bv8, a small protein from frog skin and its homologue from snake venom induce hyperalgesia in rats. *European Journal of Pharmacology*, *374*(2), pp.189-196.

Møller, M., and Baeres, F.M.M. (2002). The anatomy and innervation of the mammalian pineal gland. *Cell and tissue research*, *309*(1), pp.139-50.

Moore, R.Y., and Eichler, V. (1972). Loss of a circadian adrenal corticosterone rhythm following suprachiasmatic lesions in the rat. *Brain Research*, *42*(1), pp.201-206.

Moore, F.L., and Lowry, C.A. (1998). Comparative neuroanatomy of vasotocin and vasopressin in amphibians and other vertebrates. *Comparative Biochemistry and Physiology Part C: Pharmacology, Toxicology and Endocrinology*, *119*(3), pp.251-60.

Moore, R.Y., Speh, J.C., and Leak, R.K. (2002). Suprachiasmatic nucleus organization. *Cell and tissue research*, *309*(1), pp.89–98.

Morgan, P.J., Barrett, P., Howell, H.E., and Helliwell, R. (1994). Melatonin receptors: Localization, molecular pharmacology and physiological significance. *Neurochemistry International*, *24*(2), pp.101-146.

Mrosovsky, N. (1996). Locomotor activity and non-photic influences on the circadian clocks. *Biological Reviews*, *71*(3), pp.343-372.

Musshoff, U., Riewenherm, D., Berger, E., Fauteck, J.-D., and Speckmann, E.-J. (2002). Melatonin receptors in rat hippocampus: molecular and functional investigations. *Hippocampus*, *12*(2), pp.165-73.

Naji, L., Carrillo-Vico, A., Guerrero, J.M., and Calvo, J.R. (2004). Expression of membrane and nuclear melatonin receptors in mouse peripheral organs. *Life sciences*, *74*(18), pp.2227-2236.

Nakane, Y., Ikegami, K., Ono, H., Yamamoto, N., Yoshida, S., Hirunagi, K., Ebihara, Shizufumi, Kubo, Y., and Yoshimura, T. (2010). A mammalian neural tissue opsin (Opsin 5) is a deep brain photoreceptor in birds. *Proceedings of the National Academy of Sciences of the United States of America*, *107*(34), pp.15264-15268.

Natesan, A.K., and Cassone, V.M. (2002). Melatonin receptor mRNA localization and rhythmicity in the retina of the domestic chick, Gallus domesticus. *Visual Neuroscience*, *19*(03), pp.265-274.

Nephew, B.C., Aaron, R.S., and Romero, L.M. (2005). Effects of arginine vasotocin (AVT) on the behavioral, cardiovascular, and corticosterone responses of starlings (Sturnus vulgaris) to crowding. *Hormones and behavior*, *47*(3), pp.280-289.

Newman, E., and Reichenbach, A. (1996). The Müller cell: a functional element of the retina. *Trends in neurosciences*, *19*(8), pp.307-12.

Niles, L.P., Wang, J., Shen, L., Lobb, D.K., and Younglai, E.V. (1999). Melatonin receptor mRNA expression in human granulosa cells. *Molecular and cellular endocrinology*, *156*(1-2), pp.107-10.

Nolte, J. (2002). *The Human Brain: An Introduction to its functional anatomy* (5th ed.). Mosby.

Norgren, J., and Silver, R. (1989). Retinohypothalamic Projections and the Suprachiasmatic Nucleus in Birds. *Brain, Behavior and Evolution*, *34*(2), pp.73-83.

Oishi, K., Sakamoto, K., Okada, T., Nagase, T., and Ishida, N. (1998). Antiphase circadian expression between BMAL1 and period homologue mRNA in the suprachiasmatic nucleus and peripheral tissues of rats. *Biochemical and Biophysical Research Communications*, *253*, pp.199-203.

Oishi, T., Yamao, M., Kondo, C., Haida, Y., Masuda, A., and Tamotsu, S. (2001). Multiphotoreceptor and multioscillator system in avian circadian organization. *Microscopy research and technique*, *53*(1), pp.43-47.

Okano, Toshiyuki, Yamamoto, K., Okano, K., Hirota, T., Kasahara, T., Sasaki, M., Takanaka, Y., and Fukada, Y. (2001). Chicken pineal clock genes: implication of BMAL2 as a bidirectional regulator in circadian clock oscillation. *Genes to Cells*, *6*(9), pp.825-836.

van Oort, B.E.H., Tyler, N.J.C., Gerkema, M.P., Folkow, L., Blix, A.S., and Stokkan, K.-A. (2005). Circadian organization in reindeer. *Nature*, *438*(7071), pp.1095-1096.

Panda, S., Hogenesch, J.B., and Kay, S.A. (2002). Circadian rhythms from flies to human. *Nature*, *417*(6886), pp.329-35.

Pandi-Perumal, S.R., Trakht, I., Srinivasan, V., Spence, D.W., Maestroni, G.J.M., Zisapel, N., and Cardinali, D.P. (2008). Physiological effects of melatonin: role of melatonin receptors and signal transduction pathways. *Progress in neurobiology*, *85*(3), pp.335-53.

Park, Y.-ju, Park, J.-gweon, Jeong, H.-bok, Takeuchi, Y., Kim, S.-jae, Lee, Y.-don, and Takemura, A. (2007). Expression of the melatonin receptor Mel 1c in neural tissues of the reef fish Siganus guttatus. *Comparative Biochemistry and Physiology, Part A*, *147*, pp.103 - 111.

Patel, Y.C. (1999). Somatostatin and its receptor family. *Frontiers in neuroendocrinology*, *20*(3), pp.157-98.

Peirson, S.N., Halford, S., and Foster, R.G. (2009). The evolution of irradiance detection: melanopsin and the non-visual opsins. *Philosophical transactions of the Royal Society of London. Series B, Biological sciences*, *364*(1531), pp.2849-65.

van den Pol, A.N. (1980). The hypothalamic suprachiasmatic nucleus of rat: intrinsic anatomy. *The Journal of Comparative Neurology. 191*, pp.661–702.

Porterfield, V.M., and Mintz, E.M. (2009). Temporal patterns of light-induced immediate-early gene expression in the suprachiasmatic nucleus. *Neuroscience letters*, *463*(1), pp.70–73.

Prosser, H.M., Bradley, A., Chesham, J.E., Ebling, F.J.P., Hastings, M.H., and Maywood, E.S. (2007). Prokineticin receptor 2 (Prokr2) is essential for the regulation of circadian behavior by the suprachiasmatic nuclei. *Proceedings of the National Academy of Sciences of the United States of America*, *104*(2), pp.648-53.

Provencio, I., Jiang, G., de Grip, W.J., Hayes, W.P., and Rollag, M.D. (1998). Melanopsin: An opsin in melanophores, brain, and eye. *Proceedings of the National Academy of Sciences*, *95*(1), pp.340-345.

Rada, J.A.S., and Wiechmann, A.F. (2006). Melatonin receptors in chick ocular tissues: implications for a role of melatonin in ocular growth regulation. *Investigative ophthalmology and visual science*, *47*(1), pp.25-33.

Rattenborg, N.C., Mandt, B.H., Obermeyer, W.H., Winsauer, P.J., Huber, R., Wikelski, M., and Benca, R.M. (2004). Migratory Sleeplessness in the White-Crowned Sparrow. *PLoS Biology*, *2*(7), pp.924-936.

Reddy, P., Zehring, W.A., Wheeler, D.A., Pirrotta, V., Hadfield, C., Hall, Jeffrey C., and Rosbash, M. (1984). Molecular analysis of the period locus in Drosophila melanogaster and identification of a transcript involved in biological rhythms. *Cell*, *38*(3), pp.701-710.

Reghunandanan, V., and Reghunandanan, R. (2006). Neurotransmitters of the suprachiasmatic nuclei. *Journal of circadian rhythms*, *4*, 2.

Reiter, R.J. (1994). Melatonin suppression by static and extremely low frequency electromagnetic fields: relationship to the reported increased incidence of cancer. *Reviews on Environmental Health*, *10*, pp.171-186.

Reiter, R.J., Tan, D.-X., Mayo, J.C., Sainz, R.M., Leon, J., and Czarnocki, Z. (2003). Melatonin as an antioxidant: biochemical mechanisms and pathophysiological implications in humans. *Acta biochimica Polonica*, *50*(4), pp.1129-46.

Reppert, S.M., Weaver, D.R., and Ebisawa, T. (1994). Cloning and characterization of a mammalian melatonin receptor that mediates reproductive and circadian responses. *Neuron*, *13*(5), pp.1177-1185.

Reppert, S.M., and Weaver, D.R. (1995). Melatonin Madness. *Cell*, *83*(7), pp.1059.

Reppert, S.M., Godson, C, Mahle, C.D., Weaver, D.R., Slaugenhaupt, S.A., and Gusella, J.F. (1995a). Molecular characterization of a second melatonin receptor expressed in human retina and brain: the Mel1b melatonin receptor. *Proceedings of the National Academy of Sciences of the United States of America*, *92*(19), pp.8734-8.

Reppert, S.M., Weaver, D.R., Cassone, V.M., Godson, C., and Kolakowski Jr.,L.F. (1995b). Melatonin receptors are for the birds: Molecular analysis of two receptor subtypes differentially expressed in chick brain. *Neuron*, *15*(5), pp.1003-1015.

Reppert, S.M., Weaver, D.R., Ebisawa, T., Mahle, C.D., and Kolakowski, L.F. (1996). Cloning of a melatonin-related receptor from human pituitary. *FEBS Letters*, *386*, pp.219-224.

Reppert, S.M. (1997). Melatonin Receptors: Molecular Biology of a New Family of G Protein-Coupled Receptors. *Journal of Biological Rhythms*, *12*(6), pp.528-531.

Reppert, S.M., and Weaver, D.R. (2002). Coordination of circadian timing in mammals. *Nature*, *418*(6901), pp.935-41.

Robertson, L., and Takahashi, J. (1988). Circadian clock in cell culture: II. In vitro photic entrainment of melatonin oscillation from dissociated chick pineal cells. *Journal of Neuroscience*, *8*(1), pp.22-30.

Sagar, S. M., Sharp, F., and Curran, T. (1988). Expression of c-fos protein in brain: metabolic mapping at the cellular level. *Science*, *240*(4857), pp.1328-1331.

Saito, N., Fujii, M., Sugiura, K., Aste, N., and Shimada, K. (2010). TonEBP regulates hyperosmolality-induced arginine vasotocin gene expression in the chick (Gallus domesticus). *Neuroscience letters*, *468*(3), pp.334-8.

Savaskan, E., Wirz-Justice, A., Olivieri, G., Pache, M., Krauchi, K., Brydon, L., Jockers, R., Muller-Spahn, F., and Meyer, P. (2002). Distribution of Melatonin MT1 Receptor Immunoreactivity in Human Retina. *Journal of Histochemistry and Cytochemistry*, *50*(4), pp.519-525.

Scher, J., Wankiewicz, Ellen, Brown, Gregory M, and Fujieda, H. (2002). MT(1) melatonin receptor in the human retina: expression and localization. *Investigative ophthalmology and visual science*, *43*(3), pp.889-897.

Scher, J., Wankiewicza, E., Browna, G.M., and Fujieda, H. (2003). AII amacrine cells express the MT1 melatonin receptor in human and macaque retina. *Experimental Eye Research*, *77*(3), pp.375-382.

Schwartz, W.J. (1995). Towards a molecular biology of the suprachiasmatic nucleus: photic and temporal regulation of c-fosgene expression. *Seminars in Neuroscience*, *7*(1), pp.53-60.

Scott, F.F., Belle, M.D.C., Delagrange, P., and Piggins, H.D. (2010). Electrophysiological effects of melatonin on mouse Per1 and non-Per1 suprachiasmatic nuclei neurones in vitro. *Journal of neuroendocrinology*, *22*(11), pp.1148-56.

Seth, R., Köhler, A, Grossmann, R., and Chaturvedi, C.M. (2004). Expression of hypothalamic arginine vasotocin gene in response to water deprivation and sex steroid administration in female Japanese quail. *The Journal of experimental biology*, *207*(Pt 17), 3025-33.

Shang, E.H., and Zhdanova, I.V. (2007). The circadian system is a target and modulator of prenatal cocaine effects. (S. Akbarian, Ed.)*PloS one*, *2*(7), e587.

Shearman, L. P., Sriram, S., Weaver, David R., Maywood, E. S., Chaves, I., Zheng, B., Kume, K., Lee, C.C., Horst, van der Gijsbertus, T.J., Hastings, M.H., and Reppert, S.M. (2000). Interacting molecular loops in the mammalian circadian clock. *Science*, *288*(5468), pp.1013-1019.

Shearman, L.P, Jin, X., Lee, C., Reppert, S.M., and Weaver, D.R. (2000). Targeted Disruption of the mPer3 Gene: Subtle Effects on Circadian Clock Function. *Molecular and Cellular Biology*, *20*(17), pp.6269-6275.

Shimizu, T., Cox, K., Karten, H.J., and Britto, L.R.G. (1994). Cholera toxin mapping of retinal projections in pigeons (*Columba livia*), with emphasis on retinohypothalamic connections. *Visual Neuroscience*, *11*(03), pp.441-446.

Siuciak, J.A., Krause, D.N., and Dubocovich, M.L. (1991). Quantitative Pharmacological Analysis of 2- 1251-lodomelatonin Binding Sites in Discrete Areas of the Chicken Brain. *The Journal of Neuroscience*, *11*(9), pp.2855-2864.

Slaugenhaupt, S.A., Roca, A.L., Liebert, C.B., Altherr, M.R., Gusella, J.F., and Reppert, S.M. (1995). Mapping of the gene for the Mel1a-melatonin receptor to human chromosome 4 (MTNR1A) and mouse chromosome 8 (Mtnr1a). *Genomics*, *27*(2), pp.355-357.

Stanewsky, R. (2003). Genetic analysis of the circadian system in Drosophila melanogaster and mammals. *Journal of neurobiology*, *54*(1), 111-47.

Stanewsky, R., Kaneko, M., Emery, P., Beretta, B., Wager-Smith, K., Kay, S.A., Rosbash, M., and Hall, J.C. (1998). The cryb Mutation Identifies Cryptochrome as a Circadian Photoreceptor in Drosophila. *Cell*, *95*(5), pp.681-692.

Stankov, B., Fraschini, F., and Reiter, R.J. (1991). Melatonin binding sites in the central nervous system. *Brain Research Reviews*, *16*(3), pp.245-256.

Stankov, B., and Fraschini, F. (1993). High affinity melatonin binding sites in the vertebrate brain. *Neuroendocrinology Letters*, *15*, pp.149-164.

Stephan, F. K. (1972). Circadian Rhythms in Drinking Behavior and Locomotor Activity of Rats are Eliminated by Hypothalamic Lesions. *Proceedings of the National Academy of Sciences*, *69*(6), pp.1583-1586.

Sugden, D. (1993). Melatonin receptors. *Receptor*, (800).

Sugden, D., Davidson, K., Hough, K. A., and Teh, M.-T. (2004). Melatonin , Melatonin Receptors and Melanophores: A Moving Story. *Pigment Cell Research*, *17*, pp.454-460.

Suggs, V.C., Hirose, T., Myake, E.H., Kawashima, M.J., Johnson, K.I., and Walace, R.B. (1981). Using Purified Genes. *ICN-UCLA symposium on Molecular Biology*, *25*, pp.683-693.

Sun, Zhong Sheng, Albrecht, U., Zhuchenko, O., Bailey, J., Eichele, Gregor, and Lee, Cheng Chi. (1997). RIGUI, a Putative Mammalian Ortholog of the Drosophila period Gene. *Cell*, *90*(6), pp.1003-1011.

Sundaresan, N.R., Marcus Leo, M.D., Subramani, J., Anish, D., Sudhagar, M., Ahmed, K. A., Saxena, M., Tyagi, J.S., Sastry, K.V.H., and Saxena, V.K. (2009). Expression analysis of melatonin receptor subtypes in the ovary of domestic chicken. *Veterinary research communications*, *33*(1), pp.49-56.

Takahashi, J., and Menaker, M. (1982). Role of the suprachiasmatic nuclei in the circadian system of the house sparrow, Passer domesticus. *J. Neurosci.*, *2*(6), pp.815-828.

Takahashi, J., Kishi, E., Ishimaru, H., Ikarashi, Y., and Maruyama, Y. (2001). Role of preoptic and anterior hypothalamic cholinergic input on water intake and body temperature. *Brain Research*, *889*(1-2), pp.191-199.

Tan, D.-X., Hardeland, R., Manchester, L. C., Paredes, S. D., Korkmaz, A., Sainz, R. M., Mayo, J. C., Fuentes-Broto, L., and Reiter, R.J. (2009). The changing biological roles of melatonin during evolution: from an antioxidant to signals of darkness, sexual selection and fitness. *Biological reviews of the Cambridge Philosophical Society*, *85*(3), pp.607-623.

Tan, F.-l, Lolait, S. J., Brownstein, M. J., Saito, N., MacLeod, V., Baeyens, Dennis A., Mayeux, Philip R., Jones, S.M., and Cornett, L.E. (2000). Molecular Cloning and Functional Characterization of a Vasotocin Receptor Subtype That Is Expressed in the Shell Gland and Brain of the Domestic Chicken. *Biology of Reproduction*, *62*(1), pp.8-15.

Tanos, T., Marinissen, M.J., Leskow, F.C., Hochbaum, D., Martinetto, H., Gutkind, J.S., and Coso, O.A. (2005). Phosphorylation of c-Fos by members of the p38 MAPK family.

Role in the AP-1 response to UV light. *The Journal of biological chemistry*, *280*(19), pp.18842-18852.

Theodorescu, D., and Mischak, H. (2007). Mass spectrometry based proteomics in urine biomarker discovery. *World journal of urology*, *25*(5), pp.435-443.

van Tienhoven, A., and Juhasz, L. (1962). The chicken telencephalon, diencephalon and mesencephalon in stereotaxic coordinates. *The Journal of Comparative Neurology*, *118*(2), pp.185–197.

Travnickova-Bendova, Z., Cermakian, N., Reppert, S.M., and Sassone-Corsi, P. (2002). Bimodal regulation of mPeriod promoters by CREB-dependent signaling and CLOCK/BMAL1 activity. *Proceedings of the National Academy of Sciences of the United States of America*, *99*(11), pp.7728-7733.

Tukey, J. W. (1959). A Quick, Compact, Two-Sample Test to Duckworth's Specifications. *Technometrics*, *1*(1), pp.31-48.

Underwood, H. (1994). The circadian rhythm of thermoregulation in Japanese quail. I. Role of the eyes and pineal. *Journal of comparative physiology. A, Sensory, neural, and behavioral physiology*, *175*(5), pp.639-53.

Underwood, H.A., Steele, C.T., and Zivkovic, B. (2001). Circadian organization and the role of the pineal in birds. *Microscopy research and technique*, *53*(1), pp.48-62.

Vakkuri, O., Lämsä, E., Rahkamaa, E., Ruotsalainen, H., and Leppäluoto, J. (1984). Iodinated melatonin: preparation and characterization of the molecular structure by mass and 1H NMR spectroscopy. *Analytical biochemistry*, *142*(2), 284-9.

Vitaterna, M.H., Takahashi, J.S., and Turek, F.W. (2001). Overview of circadian rhythms. *Alcohol research and health : the journal of the National Institute on Alcohol Abuse and Alcoholism*, *25*(2), pp.85-93.

Vosko, A.M., Schroeder, A., Loh, D.H., and Colwell, C.S. (2007). Vasoactive intestinal peptide and the mammalian circadian system. *General and comparative endocrinology*, *152*(2-3), pp.165-175.

Wallis, J.W., Aerts, J., and Groenen, M.A.M. (2004). A physical map of the chicken genome. *Nature*, *432*(December), pp.761-764.

Warman, V. (2003). Phase advancing human circadian rhythms with short wavelength light. *Neuroscience Letters*, *342*(1-2), pp.37-40.

Warren, W.C., Clayton, D.F., Ellegren, H., Arnold, A.P., Hillier, L.W., Künstner, A., Searle, S., et al. (2010). The genome of a songbird. *Nature*, *464*(7289), pp.757-62.

Weckwerth, W. (2008). Integration of metabolomics and proteomics in molecular plant physiology--coping with the complexity by data-dimensionality reduction. *Physiologia plantarum*, *132*(2), pp.176-89.

Whitfield-Rucker, M.G., and Cassone, V.M. (1996). Melatonin binding in the house sparrow song control system: sexual dimorphism and the effect of photoperiod. *Hormones and behavior*, *30*(4), pp.528-37.

Wiechmann, A.F., and Smith, A.R. (2001). Melatonin receptor RNA is expressed in photoreceptors and displays a diurnal rhythm in Xenopus retina. *Molecular Brain Research*, *91*(1-2), pp.104-111.

Wiechmann, A.F. (2003a). Direct Modulation of Rod Photoreceptor Responsiveness through a Mel1c Melatonin Receptor in Transgenic Xenopus laevis Retina. *Investigative Ophthalmology and Visual Science*, *44*(10), pp.4522-4531.

Wiechmann, A.F. (2003b). Differential distribution of Mel1a and Mel1c melatonin receptors in Xenopus laevis retina. *Experimental Eye Research*, *76*(1), pp.99-106.

Wiechmann, A.F., and Rada, J.A.S. (2003). Melatonin receptor expression in the cornea and sclera. *Experimental Eye Research*, *77*(2), pp.219-225.

Wiechmann, A.F., Udin, S.B., and Rada, J. S.A. (2004). Localization of Mel1b melatonin receptor-like immunoreactivity in ocular tissues of Xenopus laevis. *Experimental eye research*, *79*(4), pp.585-594.

Wikelski, M., Tarlow, E.M., Eising, C.M., Groothuis, T.G.G., and Gwinner, E. (2005). Do night-active birds lack daily melatonin rhythms? A case study comparing a diurnal and a nocturnal-foraging gull species. *Journal of Ornithology*, *147*(1), pp.107-111.

Witt-Enderby, P.A., Bennett, J., Jarzynkaa, M.J., Firestinea, S., and Melan, M.A. (2003). Melatonin receptors and their regulation: biochemical and structural mechanisms. *Life Sciences*, *72*(20), pp.2183-2198.

Yamada, S., Mikami, S.-ichi, and Yanaihara, N. (1982). Immunohistochemical localization of vasoactive intestinal polypeptide(VIP)-containing neurons in the hypothalamus of the Japanese quail, Coturnix coturnix. *Cell and Tissue Research*, *226*(1), pp.13-26.

Yamamoto, S., Shigeyoshi, Y., Ishida, Y., Fukuyama, T., Yamaguchi, S., Yagita, K., Moriya, T., Shibata, S., Takashima, N., and Okamura, H. (2001). Expression of the Per1 gene in the hamster: brain atlas and circadian characteristics in the suprachiasmatic nucleus. *The Journal of comparative neurology*, *430*(4), pp.518-32.

Yan, L., and Okamura, H. (2002). Gradients in the circadian expression of Per1 and Per2 genes in the rat suprachiasmatic nucleus. *European Journal of Neuroscience*, *15*(7), pp.1153-1162.

Yasuo, S., Yoshimura, T., Bartell, P.A., Iigo, M., Makino, E., Okabayashi, N., and Ebihara, S. (2002). Effect of melatonin administration on qPer2, qPer3, and qClock gene expression in the suprachiasmatic nucleus of Japanese quail. *European Journal of Neuroscience*, *16*, pp.1541-1546.

Yasuo, S, Watanabe, M., Okabayashi, N., Ebihara, S., and Yoshimura, T. (2003). Circadian Clock Genes and Photoperiodism: Comprehensive Analysis of Clock Gene Expression in the Mediobasal Hypothalamus, the Suprachiasmatic Nucleus, and the Pineal Gland of Japanese Quail under Various Light Schedules. *Endocrinology*, *144*(9), pp.3742-3748.

Yoo, S.-H., Ko, C.H., Lowrey, P.L., Buhr, E.D., Song, E.-joo, Chang, S., Yoo, O. J., Yamazaki, S., Lee, C., and Takahashi, J.S. (2005). A noncanonical E-box enhancer drives mouse Period2 circadian oscillations in vivo. *Proceedings of the National Academy of Sciences of the United States of America*, *102*(7), pp.2608-2613.

Yoshida, K., Kawamura, K., and Imaki, J. (1993). Differential expression of c-fos mRNA in rat retinal cells: Regulation by light/dark cycle. *Neuron*, *10*(6), pp.1049-1054.

Yoshimura, T., Suzuki, Y, Makino, E, Suzuki, T., Kuroiwa, A., Matsuda, Y., Namikawa, T., and Ebihara, S. (2000). Molecular analysis of avian circadian clock genes. *Brain research. Molecular brain research*, *78*(1-2), pp.207-215.

Yoshimura, T., Yasuo, S., Suzuki, Y., Makino, E., Yokota, Y., and Ebihara, S. (2001). Identification of the suprachiasmatic nucleus in birds. *American Journal of Physiology-Regulatory, Integrative and Comparative Physiology*, *280*(4), R1185

Yoshimura, T., Yasuo, S., Watanabe, M., Iigo, M., Yamamura, T., Hirunagi, K., and Ebihara, S. (2003). Light-induced hormone conversion of T4 to T3 regulates photoperiodic response of gonads in birds. *Nature*, *426*(6963), pp.178-181.

Yu, W., and Hardin, P.E. (2006). Circadian oscillators of Drosophila and mammals. *Journal of cell science*, *119*(Pt 23), pp.4793-4795.

Yuill, E.A., Hoyda, T.D., Ferri, C.C., Zhou, Q.-Y., and Ferguson, A.V. (2007). Prokineticin 2 depolarizes paraventricular nucleus magnocellular and parvocellular neurons. *The European journal of neuroscience*, *25*(2), pp.425-434.

Zeman, M., and Herichová, I. (2011). Circadian melatonin production develops faster in birds than in mammals. *General and comparative endocrinology*. 172(1), pp.23-30.

Zhou, Q.-Y., and Cheng, M.Y. (2005). Prokineticin 2 and circadian clock output. *The FEBS journal*, *272*(22), pp.5703-5709.

Zimmerman, N.H. (1979). The Pineal Gland: A Pacemaker within the Circadian System of the House Sparrow. *Proceedings of the National Academy of Sciences*, *76*(2), pp.999-1003.

Websites Referenced in the species of interest Chapter 1.5:

W.1. www.zebrafinch.co.uk

W.2. The Zebra Finch Society (United Kingdom): www.zebrafinchsociety.co.uk

W.3. http://www.efinch.com/species/zebra.htm

Appendices

Appendix I

Supplementary material

APPENDIX I

Supplementary material

1.1 Supplementary material for Materials and Methods, Chapter Two

1.1.1 Solutions and mediums

1% Agarose Gel

- 0.5g Agarose Crystals (Sigma; A9539-250G)
- 50ml TAE
- Boil until solution is clear

10% APS

- 0.5g APS (Sigm; A3678-100G)
- 5ml Double Distilled Water (autoclaved)

AIX Plates

- Autoclaved LB Agar medium
- 1.8ml Ampicillin (10mg/ml or 20mg)
- 0.25ml 0.1M IPTG
- 0.3ml 20mg/ml Xgal
- Plate out in fume cupboard and store in fridge once set

EcORI digestion

- 2µl 10x H buffer,
- 0.5µl EcORI,
- 13.5µl H20/DEPC,
- 4µl plasmid DNA

0.5M EDTA pH8.0 (500ml)

- 93.05g EDTA (fw 372.24 p/mol) (Fisher Scientific; D/O700/53)
- Make up to 480ml with Double Distilled Water
- Adjust pH to 8.0 with NaOH (solution will turn clear)
- Make up to 500ml with Double Distilled Water

- Autoclave

LB Agar for plates (makes up to 10 plates)

- 8g LB Agar (Invitrogen; 22700-025)
- 250ml Water
- Autoclave

LB Medium

- 6.25g Luria Broth base (Invitrogen; 12795-027)
- 250ml Double Distilled Water
- Autoclave

PBS

- 1 Phosphate Buffered Saline table (Sigma; P4417-100TAB)
- 200ml Double Distilled Water

8% Poly-Acrylamide Gel

- 2.7ml 30% Acrylamide (Sigma; A3574-100ml)
- 5.3ml Water (autoclaved)
- 2ml 5xTBE
- 140µl 10% APS
- 3.5µl TEMED (Sigma; T9281-50ml)

APS and TEMED are added immediately prior to pouring.

SOC Medium

- 2g Tryptone (Sigma; T-2559-250G)
- 0.5g Yeast extract (Sigma; Y1626-250G)
- 0.5g NaCl (BDH; 10241AP)
- 1ml 25mM KCl
- Make up to 100ml with Double Distilled Water
- Adjust to pH 7.0
- Autoclave

30% Sucrose

- 30g Sucrose (Sigma; S0389-500G)
- 100ml Double Distilled Water

x1 TAE

- 20ml x50 TAE
- 980ml Double Distilled Water

x50 TAE

- 242g Tris Base (mw 121.1) (Fisher Scientific; T/P630/53)
- 57.1ml Glacial Acetic Acid
- 100ml 0.5M EDTA pH8
- Dilute with H_2O/DEPC

5x TBE (1L)

- 54g Tris Base (mw 121.1) (Fisher Scientific; T/P630/53)
- 27.5g Boric Acid (Sigma; B6768-1KG)
- 20ml 0.5M EDTA pH8.0

1x TE pH 7.0 (100ml)

- 1ml 1M TrisHCl pH7.0 (10mM)
- 200µl 0.5M EDTA pH8.0 (1mM)
- Up to 100ml Water
- Adjust pH to 7.0 with 1:100 HCl/H2O

1M Tris HCl (50ml)

- 6.05g Tris Base (mw 121.1) (Fisher Scientific; T/P630/53)
- 50ml Double Distilled Water
- Adjust pH to 7 with HCl solution

1.2 Supplementary material for results Chapters Three-Eight

1.2.1 Sequence alignments for the phylogenetic tree analysis (Chapter 3.2.2.1; Figure 3.2.2.d).

Created using Clustal W2 program of EMBL website. MEL1A, MEL1B and MEL1C (boxed in red) nucleotides cloned in this study. Other species nucleotides sequences were collected from the NCBI database**:** ZebraFinch.Mel1A = *Taeniopygia guttata* Mel-1A (DQ648558.1); HouseSparrow.Mel1A = *Passer domesticus* melatonin receptor-like protein MEL-1A mRNA (AY155489.1); Chicken.Mel1A = *Gallus gallus* Mel-1A (U31820.1); BlackCap.Mel1A = *Sylvia atricapilla* Mel-1A (DQ178662); Human.Mel1A = *Homo sapiens* melatonin receptor 1A (EU432127.1); Bovine.Mel1A = *Bos taurus* melatonin receptor 1A (BTU73327); BrownRat.Mel1A = *Rattus norvegicus* Mtnr1a (AB377274); Frog.Clone.X2.0 = *Xenopus laevis* clone X2.0 melatonin receptor mRNA (XLU31826); H.Mouse.Mel1A = *Mus musculus* melatonin receptor 1A (BC116900.1); Goldfish.Mel1A = *Carassius auratus* MT1 (AB481372); C.Salmon.Mel1A = *Oncorhynchus keta* melatonin-receptor 1A (AY356364); Sweetfish.Mel1A = *Plecoglossus altivelis* MT1 (AB481368); Z.Fish.Mel1A = *Danio rerio* melatonin receptor type 1B (NM_131395); Human.Mel1B = *Homo sapiens* melatonin receptor 1B (NM_005959); Frog.CloneX1.7 = *Xenopus laevis* clone X1.7 (U31827); H.Mouse.Mel1B = *Mus musculus* melatonin receptor 1B (NM_145712); Chicken.Mel1B = *Gallus gallus* Mel-1B (U30609.1); ZebraFinch.Mel1B = *Taeniopygia guttata* Mel-1B (AY803772.1); Z.Fish.Mel1B = *Danio rerio* melatonin receptor 1B (NM_131394); Goldfish.Mel1B = *Carassius auratus* MT2 (AB481374); C.Salmon.Mel1B = *Oncorhynchus keta* melatonin-receptor 1B (AY356365); Sweetfish.Mel1B = *Plecoglossus altivelis* MT2 (AB481369); ZebraFinch.Mel1C = *Taeniopygia guttata* Mel-1c (AY803773); HouseSparrow.Mel1C = *Passer domesticus* Mel-1c (AY743658); Chicken.Mel1C = *Gallus gallus* Mel-1C (U31821); BlackCap.Mel1C = *Sylvia atricapilla* Mel-1C (DQ178664.1); Sweetfish.Mel1C = *Plecoglossus altivelis* MEL1C (AB481370); Frog.Mel1C = *Xenopus laevis* Mel-1C (U09561); E.Starling.Mel1C = *Sturnus vulgaris* Mel-1C (DQ470810.1); Goldfish.Mel1C = *Carassius auratus* MEL1C (AB481375); RainbowTrout.Mel = *Oncorhynchus mykiss* melatonin receptor gene (AF178929).

```
MEL1A                   --------------------TTGCCACAGTCTCAGATACGACAAGCTGTACAGCGACAGG 40
ZebraFinch.Mel1A        ATCAATCGGTACTGCTATATCTGCCACAGCCTCAAATATGACAAGCTGTACAGCGACAGG 435
HouseSparrow.Mel1A      ------------------------------------------AAGCTGTACAGCGACAGG 18
Chicken.Mel1A           ATCAATCGATACTGCTATATCTGCCACAGTCTCAAATATGACAAGCTGTACAGTGACAAG 438
BlackCap.Mel1A          -----------CTGCTACATCTGCCACAGCCTCAAATACGACAAGCTGTACAGCGACAAG 49
C.Salmon.Mel1A          ------------------ATATGTCACAGCCTTAAGTACGACAAGCTGTACAGCGACAAG 42
Sweetfish.Mel1A         ATCAACCGCTACTGTTACATCTGCCACAGCCTCAAGTACGACAAGCTGTACAGCGACAAG 613
Goldfish.Mel1A          ATCAACCGCTACTGTTATATCTGCCACAGCCTCAAATATGACAAACTCTACAGTGACAAA 618
BrownRat.Mel1A          ATGAACCGCTACTGCTACATTTGCCACAGTCTCAAGTATGATAGGATATACAGTAACAAG 641
H.Mouse.Mel1A           ATGAACCGTTACTGCTACATTTGCCACAGCCTCAAGTACGACAAAATATACAGTAACAAG 508
Human.Mel1A             ATCAACCGCTACTGCTACATCTGCCACAGTCTCAAGTACGACAAACTGTACAGCAGCAAG 426
Bovine.Mel1A            ATCAACCGCTATTGCTGCATCTGCCACAGCCTCAGATACGACAAGCTGTATAGCAGCACG 69
C.Salmon.Mel1B          ------------------ATATGTCACAGCCTTAAGTACGACAAGCTCTTCTCCAACCAG 42
RainbowTrout.Mel        ------------TGCTACATATGTCACAACCTGAAGTACGACAAGCTCTTCTCCAACCAG 48
Goldfish.Mel1C          ATCAACCGCTACTGCTACATCTGCCACAGTCTCCGCTACGACCGGCTGTATTCTCGTCAG 762
Frog.Clone.X2.0         ------------------------CACAGCAGCTGGTACAATCGCCTATTCTCTAATTCC 36
Sweetfish.Mel1B         GTGAACCGCTACTGCTACATCTGCCACTCCTTCTCCTACCACCGCCTGTACAGCTTCCGC 1121
Z.Fish.Mel1B            ATTAACCGCTACTGCTACATCTGCCACAGCTTTGCCTACGGACGTCTGTACAGCTTCCGA 810
Z.Fish.Mel1A            ATCAACCGCTACTGCTTCATCTGTCAAGCCAACACTTACGAGAAGATCTACGGCCGAGCT 592
Goldfish.Mel1B          ATCAACCGCTACTGTTTCATCTGCCAGGCCAACACCTACGAGAAGATCTACGGCCGCGCA 745
H.Mouse.Mel1B           ATCAACCGCTACTGCTGCATCTGTCATAGTACCACCTACCACCGGGTCTGCAGTCACTGG 561
BrownRat.Mel1B          ATCAACCGCTACTGGTGCATCTGTCACAGTGCGACCTACCACCGAGCCTGCAGTCAGTGG 580
Human.Mel1B             ATTAACCGCTACTGCTACATCTGCCACAGCATGGCCTACCACCGAATCTACCGGCGCTGG 465
MEL1B                   ------------------------------------GACAAAGTGTACAGCTGTTGG 21
ZebraFinch.Mel1B        ATAAACAGATATTGCTACATATGTCATAGCTTTGCCTATGACAAAGTGTACAGCTGTTGG 193
Chicken.Mel1B           ATAAACCGATATTGCTATATATGTCATAGCTTTGCCTATGACAAAGTGTATAGCTGTTGG 243
Frog.CloneX1.7          ------------------------CATAGCTTTGTCTATGAAAAGCTGTTCAGCCTGTGG 36
Sweetfish.Mel1C         ATCAACCGCTACTGCTACATCTGCCACAGTCTTCACTACGATCGACTGTACAGCCTCAGG 819
Frog.Mel1B              ATCAACAGGTATTGCTACATCTGCCACAGCCTGAGATATGACAAGCTTTATAATCAAAGA 472
Frog.Mel1C              ATCAACAGGTATTGCTACATCTGCCACAGCCTGAGATATGACAAGCTTTATAATCAAAGA 472
ZebraFinch.Mel1C        -----------CTGCTACATCTGCCACAGCCTTCGCTATGATAAGCTCTTCAACCTGAAG 49
Chicken.Mel1C           ATCAATCGCTACTGCTACATCTGCCACAGCCTTCGGTATGATAAGCTCTTCAACCTGAAG 438
MEL1C                   ------------TGCTACATCTGCCACAGCCTTCGCTATGATAAGCTCTTCAACCTAAAG 48
HouseSparrow.Mel1C      ------------TGCTACATCTGCCACAGCCTTCGGTACGATAAGCTCTTCAACCTGAAG 48
E.Starling.Mel1C        ------------------------------------------------------------
BlackCap.Mel1C          -----------CTGCTGCATCTGCCACAGCCTGCGGTACGACAAGCTCTTCAACCTGAAG 49
BrownRat.GPR50          ATCAACCGGTACTGCTACATCTGCCACAGCCTCCAGTACAAGCGGATCTTCAGCCTGCGC 478
H.Mouse.GPR50           ATCAACCGTTACTGCTACATCTGCCACAGCCTCCAATACAAGCGGATCTTCAGCCTGCGC 478
Human.GPR50             ATCAACCGTTACTGCTACATCTGCCACAGCCTCCAGTACGAACGGATCTTCAGTGTGCGC 567

MEL1A                   AATTCATTGTGCTATATTGTTCTCATATGGCTCCTAACATTTGTTGCTATCGTGCCCAAC 100
ZebraFinch.Mel1A        AATTCATTGTGCTATATTGTTCTCATATGGCTCCTAACATTTGTTGCTATCGTGCCCAAC 495
HouseSparrow.Mel1A      AATTCATTGTGCTATATTGTTCTCATATGGGTCCTAACATTTGTTGCTATCGTGCCCAAC 78
Chicken.Mel1A           AATTCTTTGTGTTATGTTGGTCTTATCTGGGTCCTAACAGTTGTTGCTATTGTGCCCAAC 498
BlackCap.Mel1A          AATTCTCTGTGCTATATTGTCCTTATTTGGGCCCTGACATTCGTGGCCATAGTGCCCAAC 109
C.Salmon.Mel1A          AACTCAGTGTTATGTCCTACTCATCTGGGCGTTGACCATTGTGGCCATCGTGCCGAAT 102
Sweetfish.Mel1A         AACTCTGTGTGCTACGTTCTGCTCATATGGGTGCTGACGGTAGTGGCCATTGTGCCCAAC 673
Goldfish.Mel1A          AACTCAGTTTGCTATGTACTGTTAATTTGGGCTTTGACGGTGCTTGCTATTGTACCCAAC 678
BrownRat.Mel1A          AATTCCCTGTGCTACGTGTTCCTGATATGGACACTGACACTCATAGCCATCATGCCCAAC 701
H.Mouse.Mel1A           AACTCGCTCTGCTACGTGTTCCTGATATGGATGCTGACACTCATCGCCATCATGCCCAAC 568
Human.Mel1A             AACTCCCTCTGCTACGTGCTCCTCATATGGCTCCTGACGCTGGCGGCCGTCCTGCCCAAC 486
Bovine.Mel1A            AATTCCCTCTGCTACGTGTTCCTGATATGGATGCTGACGCTCGTGGCGATCGTGCCCAAC 129
C.Salmon.Mel1B          AACACCGTGTGTTACGTCATCCTGGTGTGGGCGCTGACTGTGTTGGCCATCGTGCCCAAC 102
RainbowTrout.Mel        AACACCGTGTGTTACGTCATCCTGGTGTGGTCGCTGACTGTGTTGGCCATCGTGCCCAAC 108
Goldfish.Mel1C          AACACCTGTCTGTACCTGCTGCTCACCTGGACGCTAACCGCTTTGGCCACTGTGCCCAAC 822
Frog.Clone.X2.0         GGCACAATTTGCTATGTGGGTCTTGTATGGGTGTTGGCCCTGGGGGCCATTTTGCCAAAC 96
Sweetfish.Mel1B         AACACCCTGCTCTTCGTCGCCCTCATCTGGCTGCTCACCGTCCTGGCCATCCTTCCCAAC 1181
Z.Fish.Mel1B            AACACACTGCTGCTCGTGGCTCTGATCTGGGCGCTTACCGTACTTGCAATTCTGCCCAAT 870
Z.Fish.Mel1A            GGGACGCTAGTGCTCCTGACGCTAGTATGGGTTCTCACCGCTATCGCTATTCTTCCAAAC 652
Goldfish.Mel1B          GGAACCCTGGCGCTACTGATGTTAGTCTGGGTGCTCACCGCCATCGCCATTCTTCCAAAC 805
H.Mouse.Mel1B           TATACTCCCATCTACATCAGCCTCGTCTGGCTCCTCACTCTGGTGGCTTTGGTGCCCAAT 621
BrownRat.Mel1B          CATGCTCCCCTCTACATCAGCCTCATCTGGCTTCTCACTCTGGTGGCCTTGGTGCCCAAT 640
Human.Mel1B             CACACCCCTCTGCACATCTGCCTCATCTGGCTCCTCACCGTGGTGGCCTTGCTGCCCAAC 525
MEL1B                   AATACAATGTTGTATGTCTCCTTAGTCTGGATATTAACAGTAATTGCAACTGTGCCAAAT 81
ZebraFinch.Mel1B        AATACAATGTTGTATGTCTCCTTAGTCTGGATATTAACAGTAATTGCAACTGTGCCAAAT 253
Chicken.Mel1B           AACACAATGCTCTATGTGTCCTTAATCTGGGTATTAACAGTAATTGCAACTGTGCCAAAT 303
Frog.CloneX1.7          AATACAATACTTTATGTCTGTTTAATTTGGACCCTCACCGTAGTTGCAACTGTCCCAAAC 96
Sweetfish.Mel1C         AACACCTGCTGCTACCTTGGTCTCACCTGGCTGCTCACCGCCCTCGCCACCGTGCCCAAC 879
Frog.Mel1B              AGCACCTGGTGCTACCTTGGCCTGACATGGATACTAACTATAATTGCAATCGTGCCAAAC 532
Frog.Mel1C              AGCACCTGGTGCTACCTTGGCCTGACATGGATACTAACTATAATTGCAATCGTGCCAAAC 532
ZebraFinch.Mel1C        AACACCTGCTGCTATCTCTGCCTGACCTGGATACTCACAGTGGTGGCAATTGTGCCAAAC 109
Chicken.Mel1C           AACACCTGCTGCTATATCTGTCTGACGTGGACGCTCACGGTGGTGGCCATTGTGCCAAAC 498
MEL1C                   AACACCTGCTGCTATCTCTGCCTGACCTGGATACTCACAGTGGTGGCAATTGTGCCAAAC 108
```

```
HouseSparrow.Mel1C      AACACCTGCTGCTATCTCTGCCTGACCTGGATACTCACGGTGGTGGCAATTGTGCCAAAC 108
E.Starling.Mel1C        --------------------------TGGATACTCACAGTGGTGGCAATCGTGCCTAAC 33
BlackCap.Mel1C          AACACCTGCTGCTATCTCTGCCTGACCTGGGTGCTCACCGTGGTGGCAATCGTGCCCAAC 109
BrownRat.GPR50          AACACTTGCATCTATCTGGTTGTTACCTGGGTCATGACTGTTCTGGCTGTCCTGCCTAAT 538
H.Mouse.GPR50           AACACTTGCATCTATCTGGTCGTTACCTGGGTCATGACTGTCCTGGCTGTCCTGCCTAAC 538
Human.GPR50             AATACCTGCATCTACCTGGTCATCACCTGGATCATGACCGTCCTGGCTGTCCTGCCCAAC 627
                                                ***    *  *       **     * ** **

MEL1A                   CTGTTTGTGGGATCGCTCCAGTATGACCCCAGGATTTACTCCTGTACATTTGCACAGTCT 160
ZebraFinch.Mel1A        CTTTTTGTGGGATCGCTCCAGTATGACCCCAGGATTTACTCCTGTACATTTGCACAGTCT 555
HouseSparrow.Mel1A      CTGTTTGTGGGATCGCTACAGTACGACCCCAGGATTTACTCCTGCACATTTGCCCAGTCT 138
Chicken.Mel1A           CTGTTTGTGGGATCTCTACAGTATGACCCCAGGATTTATTCGTGCACATTTGCACAGTCT 558
BlackCap.Mel1A          CTGTTCGTGGGGTCGCTGCAGTACGACCCCAGGATTTACTCCTGTACTTTTGCCCAGTCT 169
C.Salmon.Mel1A          CTCTTCGTGGGTTCGTTGCAGTATGACCCCAGGGTGTATTCGTGTACGTTCGAGCAGTCG 162
Sweetfish.Mel1A         CTGTTCGTGGGCTCGCTCCAATACGACCCTCGCATTTACTCCTGCACTTTTGAACAGTCA 733
Goldfish.Mel1A          TTGTTCGTAGGTTCCCTGCAGTATGATCCACGGGTTTATTCCTGTACATTCGAGCAGTCG 738
BrownRat.Mel1A          CTGCAAACCGGAACTCTCCAGTACGACCCCCGGATCTACTCCTGTACCTTCACCCAGTCC 761
H.Mouse.Mel1A           CTGCAAACCGGAACACTCCAGTACGATCCCCGGATCTACTCCTGTACCTTCACCCAGTCT 628
Human.Mel1A             CTCCGTGCAGGGACTCTCCAGTACGACCCGAGGATCTACTCGTGCACCTTCGCCCAGTCC 546
Bovine.Mel1A            CTGTGTGTGGGGACCCTGCAGTACGACCCGAGGATCTATTCCTGTACCTTCACGCAGTCC 189
C.Salmon.Mel1B          TGGTTTATGGAGTCTCTGCAGTACGACCCGAGGGTCTACTCGTGTACCTTCGCCCAGTCG 162
RainbowTrout.Mel        TGGTTTATGGAGTCTCTGCAGTACGACCCGAGGGTCTACTCGTGTACCTTCGCCCAGTCG 168
Goldfish.Mel1C          TTCCTGGTGGGTTCCCTAAAATATGACCCACGCGTCTTCTCCTGCACGTTCACCCAGACA 882
Frog.Clone.X2.0         CTCTTTGTGGGATCCCTACGATGCGACCCTCGTATATTCTCCTGCACATTCGCTCAATAT 156
Sweetfish.Mel1B         CTGTTCGTGGGCTCCCTGCGCTATGACCCTAGAGTCTACTCCTGCACCTTTGCCCAGAAC 1241
Z.Fish.Mel1B            TTCTTTGTGGGTTCGCTGAGTTACGACCCTCGAGTTTACTCCTGCACGTTCACACAGACT 930
Z.Fish.Mel1A            CTGTCGCTTGGGTCGCTGACGTATGACCCGCGCGTTTATTCCTGCACCTTCAGTCAGACG 712
Goldfish.Mel1B          CTGGCACTGGGGTCATTGACGTACGACCCTCGCGTTTACTCCTGCACCTTTAGTCAGACA 865
H.Mouse.Mel1B           TTCTTTGTGGGGTCTTTAGAGTATGATCCACGCATCTATTCCTGCACCTTCATCCAGACA 681
BrownRat.Mel1B          TTCTTTGTGGGGTCTCTAGAATATGACCCGCGAATCTATTCCTGCACCTTCATCCAGACA 700
Human.Mel1B             TTCTTTGTGGGGTCCCTGGAGTACGACCCACGCATCTATTCCTGCACCTTCATCCAGACC 585
MEL1B                   TTTTTTGTTGGCTCTTTGAAGTATGATCCACGCATCTATTCATGCACATTTGTCCAAACT 141
ZebraFinch.Mel1B        TTTTTTGTTGGCTCTTTGAAGTATGATCCACGCATCTATTCATGCACATTTGTCCAAACT 313
Chicken.Mel1B           TTTTTTGTCGGCTCTCTGAAGTATGATCCACGCATCTATTCATGCACATTTGTTCAGACT 363
Frog.CloneX1.7          TTTTTTGTCGGCTCATTAGAGTACGATCCCCGGATCTACTCATGTACTTTTGTTCAAACT 156
Sweetfish.Mel1C         TTCTTTGTGGGCTCGCTGCAGTACGACCCGCGCATCTACTCCTGCACCTTTGCCCAGACG 939
Frog.Mel1B              TTTTTTGTTGGATCACTACAGTATGACCCCAGGATTTTTTCTTGCACATTTGCGCAGACA 592
Frog.Mel1C              TTTTTTGTTGGATCACTACAGTATGACCCCAGGATTTTTTCTTGCACATTTGCGCAGACA 592
ZebraFinch.Mel1C        TTCTTTGTTGGCTCCTTGCAGTACGACCCCCGGATTTACTCCTGCACCTTTGCCCAGACG 169
Chicken.Mel1C           TTCTTTGTTGGCTCCTTGCAGTATGACCCCCGGATTTACTCTTGCACCTTTGCCCAGACT 558
MEL1C                   TTCTTTGTTGGCTCCTTGCAGTACGACCCCCGGATTTACTCCTGCACCTTTGCCCAGACG 168
HouseSparrow.Mel1C      TTCTTTGTTGGCTCCTTGCAGTATGACCCCCGGATTTACTCCTGCACCTTTGCCCAGACC 168
E.Starling.Mel1C        TTCTTTGTTGGCTCCTTGCAGTATGACCCCCGGATTTACTCCTGCACCTTTGCCCAGACA 93
BlackCap.Mel1C          TTCTTTGTTGGCTCCTTGCAGTACGACCCCCGGATTTACTCGTGCACCTTTGCGCAGACG 169
BrownRat.GPR50          GTGTACATTGGCACCATTGAGTATGACCCTCGCACCTACACCTGCATCTTCAACTATGTG 598
H.Mouse.GPR50           ATGTACATTGGCACCATTGAGTATGACCCTCGCACCTACACCTGCATCTTCAACTATGTG 598
Human.GPR50             ATGTACATTGGCACCATCGAGTACGATCCTCGCACCTACACCTGCATCTTCAACTATCTG 687
                              *   *  *    *  ** **  *    *   * ** *  **     *

MEL1A                   GCGAGCTCAGCATACACTATAGCAGTTGTGTTTTTCCACTTCCTGCTTCCCATAGCCGTA 220
ZebraFinch.Mel1A        GTGAGCTCAGCATACACTATAGCAGTTGTGTTTTTCCACTTCCTGCTTCCCATAGCCGTA 615
HouseSparrow.Mel1A      GTGAGCTCAGCATATACTATAGCAGTTGTGTTTTTCCACTTCCTGCTTCCCATAGCTGTA 198
Chicken.Mel1A           GTGAGTTCCGCATATACAATAGCAGTGGTGTTTTTCCACTTCATACTTCCCATAGCCATA 618
BlackCap.Mel1A          GTGAGCTCAGCCTACACTATAGCAGTGGTGTTTTTCCACTTCCTGCTCCCCATAGCCGTC 229
C.Salmon.Mel1A          GCGAGTTCGGCGTACACCATCGCCGTGGTCTTCTTCCACTTCATCCTACCGATCATGATC 222
Sweetfish.Mel1A         GCGAGCTCAGCCTACACCATTGCGGTGGTCTTCTTCCACTTCATCCTACCTATCATGATC 793
Goldfish.Mel1A          GCGAGCTCGGCATACACGATCGCTGTCGTGTTCTTCCATTTTATTCTTCCCATCATGATT 798
BrownRat.Mel1A          GTCAGCTCGGCGTACACGATTGCCCTGGTGGTTTTCCATTTCGTAGTTCCAATGATTATT 821
H.Mouse.Mel1A           GTCAGCTCAGCGTACACGATAGCAGTGGTGGTTTTCCATTTCATCGTGCCTATGATTATT 688
Human.Mel1A             GTCAGCTCCGCCTACACCATCGCCGTGGTGGTTTTCCACTTCCTCGTCCCCATGATCATA 606
Bovine.Mel1A            GTCAGCTCAGCCTACACGATCGCCGTGGTGGTGTTCCATTTCATCGTTCCGATGCTCGTA 249
C.Salmon.Mel1B          GTGAGTTCCTTGTACACCATCACCGTGGTCGTGGTTCACTTCATCCTCCCCATCAGTATC 222
RainbowTrout.Mel        GTTAGTTCCTCGTACACCATCACTGTGGTGGTGATTCATTTCTTCGTGCCCATCGCCGTG 228
Goldfish.Mel1C          GCAAGTTCTTCCTATACCGTTTGCGTTGTTCTGATCCACTTTCTGGTTCCTCTGGGTGTG 942
Frog.Clone.X2.0         GTCAGCTCCTATTACACCATTGCTGTTGTGATCTTCCATTTTTTTTTGCCTATCGGGGTG 216
Sweetfish.Mel1B         GTTAGCAGCTCCTACACTGTGGCCGTGGTGGTGATTCACTTCCTGGTCCCCATCGCTGTG 1301
Z.Fish.Mel1B            GCCAGCAGCTCCTACACTGTGGTGGTGGTAGTGGTTCACTTTCTAGTGCCCATCGCTGTG 990
Z.Fish.Mel1A            ACAAGTGCGGGATACACCATCGCAGTGGTGACTGTGCATTTTCTGCTTCCTATCGCTGTG 772
Goldfish.Mel1B          ACAAGTGCAGGCTACACCATCGCCGTGGTGACTGTGCACTTCCTGCTTCCTATAGCGGTA 925
H.Mouse.Mel1B           GCCAGCACACAGTACACGGCAGCTGTGGTGGCCATCCACTTCCTCCTTCCCATGGCTGTG 741
BrownRat.Mel1B          GCCAGCACCCAATACACTATGGCTGTGGTGGCCATCCACTTCCTCCTTCCAATTGCTGTG 760
Human.Mel1B             GCCAGCACCCAGTACACGGCGGCAGTGGTGGTCATCCACTTCCTCCTCCCTATCGCTGTC 645
MEL1B                   GCAAGCTCCTACTATACAATAGCTGTTGTGGTCATTCACTTCATCGTCCCTATCACCATC 201
ZebraFinch.Mel1B        GCAAGCTCCTACTATACAATAGCTGTTGTGGTCATTCACTTCATCGTCCCTATCACCATC 373
```

```
Chicken.Mel1B          GCAAGCTCCTACTATACAATTGCAGTTGTGGTAATTCATTTCATCGTCCCTATTACTGTT 423
Frog.CloneX1.7         GTAAGCTCGTCCTACACGATTACTGTAGTCGTCATTCATTTCATTTTACCAATCACTGTG 216
Sweetfish.Mel1C        GTCAGTTCCTACTATACCATCTCTGTGGTGGTCATCCACTTCCTCATCCCCCTGCTGGTC 999
Frog.Mel1B             GTGAGTTCCTCATACACCATAACAGTAGTGGTGGTGCATTTTATAGTCCCTCTTAGTGTT 652
Frog.Mel1C             GTGAGTTCCTCATACACCATAACAGTAGTGGTGGTGCATTTTATAGTCCCTCTTAGTGTT 652
ZebraFinch.Mel1C       GTGAGCACATCGTACACCATCACGGTGGTGGTGGTTCACTTCATCGTCCCGCTCTCCGTC 229
Chicken.Mel1C          GTGAGTACATCGTACACGATCACAGTGGTGGTTGTCCACTTCATTGTCCCACTGTCCATC 618
MEL1C                  GTGAGCACGTCGTACACCATCACGGTGGTGGTGGTTCACTTCATCGTCCCGCTCTCCGTC 228
HouseSparrow.Mel1C     GTGAGCACGTCGTACACCATCACGGTGGTGGTGGTTCACTTCATCGTCCCGCTCTCCGTC 228
E.Starling.Mel1C       GTGAGCACATCATACACCATCACGGTGGTAGTGGTTCACTTCATTGTTCCACTCTCTGTT 153
BlackCap.Mel1C         GTGAGCACGTCGTACACCATCACGGTGGTGGTGGTTCACTTCATCGTCCCCCTCTCCGTC 229
BrownRat.GPR50         AACAACCCTGCCTTTACTGTGACCATTGTCTGCATCCACTTCGTCCTCCCTCTCATCATA 658
H.Mouse.GPR50          AACAATCCTGCCTTTACCGTGACCATTGTCTGCATCCACTTCGTCCTCCCTCTCATCATA 658
Human.GPR50            AACAACCCTGTCTTCACTGTTACCATCGTCTGCATCCACTTCGTCCTCCCTCTCCTCATC 747
                          *        *  **        * **     * ** **  *  * **  *     *

MEL1A                  GTTACTTTCTGTTACTTGCGAATATGGATCCTCGTTATCCAGGTAAGGCGAAGGGTTAAA 280
ZebraFinch.Mel1A       GTTACTTTCTGTTACTTGCGAATATGGATCCTCGTTATCCAGGTAAGGCGAAGGGTTAAA 675
HouseSparrow.Mel1A     GTTACTTTCTGTTACTTGCGAATATGGATCCTCGTTATCCAGGTAAGGAGAAGGGTTAAA 258
Chicken.Mel1A          GTTACTTATTGTTACTTGAGAATATGGATCCTTGTTATTCAGGTAAGACGAAGAGTTAAA 678
BlackCap.Mel1A         GTCACTTTCTGCTACTTGAGAATATGGATCCTCGTCATTCAGGTAAGGAGAAGGGTGAAA 289
C.Salmon.Mel1A         GTCACTTACTGCTACCTGAGGATCTGGATCCTGGTCATTCAGGTTAGGCGACGTGTCGAA 282
Sweetfish.Mel1A        GTTACCTATTGCTACCTGAGAATCTGGATCCTCGTCATCCAGGTGAGACGAAGGGTGAAG 853
Goldfish.Mel1A         GTCACCTACTGTTACTTGCGAATCTGGGTTCTGGTCATACAGGTGCGAAGACGAGTGAAG 858
BrownRat.Mel1A         GTCACTTTCTGCTACTTAAGGATATGGATCCTGGTTCTTCAGGTCAGACGGAGGGTGAAA 881
H.Mouse.Mel1A          GTCATCTTCTGCTACTTAAGGATATGGGTCCTGGTCCTTCAGGTCAGACGGAGGGTGAAA 748
Human.Mel1A            GTCATCTTCTGTTACCTGAGAATATGGATCCTGGTTCTCCAGGTCAGACAGAGGGTGAAA 666
Bovine.Mel1A           GTCATCTTCTGTTACCTGAGAATCTGGGCCCTAGTTCTTCAGGTCAGATGGAGGGTGAAA 309
C.Salmon.Mel1B         GTCACGTACTGCTACCTGAGGATCTGGATCCTGGTCTTACAGGTGAGGAGACGGGTGAAA 282
RainbowTrout.Mel       GTTACCTTCTGCTACCTGAGGATCTGGATCCTGGTCATCCAGGTGAGGAGGAAGGTGAAG 288
Goldfish.Mel1C         GTTTCTTTCTGCTACCTGCGCATATGGACGTTGGTGATAAGAGTCAAAGGTCGCGTGCGG 1002
Frog.Clone.X2.0        GTGAGCTACTGCTATCTACGCATCTGGGTGCTTGTTCTCAATATTAGGCACAGGGTCAAA 276
Sweetfish.Mel1B        GTGACCTTCTGCTACCTGCGAATATGGGTGCTGGTCATCCAGGTGCGGAAAAAAGTGAAG 1361
Z.Fish.Mel1B           GTGACCTTCTGCTACCTGCGGATTTGGGTTCTGGTGATCCAGGTGAGGAGGAAGGTGAAA 1050
Z.Fish.Mel1A           GTTACCTTCTGCTATCTGAGGATTTGGGTGCTGGTTCTTCGCGTGAGGAGGCGGGTCACA 832
Goldfish.Mel1B         GTTACATTCTGCTATCTGAGGATTTGGGTGCTGGTGCTCCGCGTAAGGAGGCGGGTCAAA 985
H.Mouse.Mel1B          GTGTCCTTCTGCTACCTGCGAATCTGGGTACTGGTGCTCCAGGCCCGAAGGAAGGCCAAG 801
BrownRat.Mel1B         GTGTCCTTTTGCTACCTGCGAATATGGATACTGGTGCTCCAGGCCCGAAGGAAGGCAAAG 820
Human.Mel1B            GTGTCCTTCTGCTACCTGCGCATCTGGGTGCTGGTGCTTCAGGCCCGCAGGAAAGCCAAG 705
MEL1B                  GTCAGCTTCTGCTACCTTCAAATTTGGGTTTTAGTGCTTCAAGTTCGAAGACGAGTCAAA 261
ZebraFinch.Mel1B       GTCAGCTTCTGCTACCTTCGAATTTGGGTTTTAGTGCTTCAAGTTCGAAGACGAGTCAAA 433
Chicken.Mel1B          GTGAGCTTCTGCTATCTTCGAATTTGGGTCTTAGTGCTTCAAGTTAGAAGACGAGTCAAG 483
Frog.CloneX1.7         GTGACTTTTTGTTACCTCCGGATATGGATTTTGGTGATTCAGGTGAGGAGGAAAGTCAAG 276
Sweetfish.Mel1C        GTGTCTTTCTGCTACATGAGGATCTGGGTTCTGGTCATCCAGGTCAAGCACAGGGTGAAA 1059
Frog.Mel1B             GTGACATTCTGTTACTTAAGAATATGGGTTTTAGTGATCCAAGTCAAACACAGAGTTAGA 712
Frog.Mel1C             GTGACATTCTGTTACTTAAGAATATGGGTTTTAGTGATCCAAGTCAAACACAGAGTTAGA 712
ZebraFinch.Mel1C       GTGACGTTTTGCTACCTACGGATCTGGATTTTGGTGATTCAAGTCAAACACCGGGTGAGA 289
Chicken.Mel1C          GTGACTTTTTGCTACCTTCGGATCTGGATTTTGGTGATTCAAGTCAAACACCGGGTGAGA 678
MEL1C                  GTGACGTTTTGCTACCTACGGATCTGGATTTTGGTGATTCAAGTCAAACACCGGGTGAGA 288
HouseSparrow.Mel1C     GTGACGTTTTGCTACCTACGGATCTGGATTCTGGTCATTCAAGTCAAACACCGGGTGAGA 288
E.Starling.Mel1C       GTGACATTTTGCTACCTACGGATCTGGATTTTGGTGATTCAAGTCAAACACCGGGTGAGA 213
BlackCap.Mel1C         GTGACGTTTTGCTACCTGAGGATCTGGATTTTGGTGATCCAGGTCAAGCACAGGGTGAGG 289
BrownRat.GPR50         GTCGGTTATTGCTACACAAAAATCTGGATCAAAGTGCTGGCAGCCCGGGACCCAGCTGGA 718
H.Mouse.GPR50          GTTGGTTATTGCTACACGAAAATCTGGATCAAAGTGCTGGCAGCCCGTGACCCAGCTGGA 718
Human.GPR50            GTGGGTTTCTGCTACGTGAGGATCTGGACCAAAGTGCTGGCGGCCCGTGACCCTGCAGGG 807
                       **    *  ** **        ** ***      **  *                 *

MEL1A                  CCAGATAACAACCCTAGGCTGAAA------CCACATGACTTCAGAAACTTTGTAACCATG 334
ZebraFinch.Mel1A       CCAGATAACAACCCTAGGCTGAAA------CCACATGACTTCAGAAACTTTGTAACCATG 729
HouseSparrow.Mel1A     CCGGATAACAACCCTAGGCTGAAA------CCCCATGACTTCAGAAACTTCGTAACCATG 312
Chicken.Mel1A          CCAGACAACAACCCCCGATTGAAA------CCACATGACTTCAGAAACTTTGTAACCATG 732
BlackCap.Mel1A         CCAGATAACAACCCCAGGCTGAAG------CCACACGACTTCAGGAACTTTGTCACCATG 343
C.Salmon.Mel1A         CCGGACAATAGACCGAAACTGACG------CCACACGACGTGAGGAACTTCGTGACTATG 336
Sweetfish.Mel1A        CCGGACAACCGGCCCAAGCTGACC------CCGCACGACGTCAGGAACTTTGTCACCATG 907
Goldfish.Mel1A         CCCGACAATCGTCCCAAGCTCACG------CCACACGATGTGCGAAACTTCGTAACAATG 912
BrownRat.Mel1A         CCGGACAGCAAACCCAAACTGAAG------CCGCAGGACTTCAGGAACTTTGTCACCATG 935
H.Mouse.Mel1A          CCCGACAACAAGCCCAAACTGAAG------CCCCAGGACTTCAGGAACTTTGTCACCATG 802
Human.Mel1A            CCTGACCGCAAACCCAAACTGAAA------CCACAGGACTTCAGGAATTTTGTCACCATG 720
Bovine.Mel1A           CCTGACGACAAACCGAAACTGAAG------CCCCAGGACTTCAGGAATTTTGTCACCATG 363
C.Salmon.Mel1B         CCGGACACGAGGCCCAAGATCAAA------CCACACGACTTCCGTATCTTCCTGACTATG 336
RainbowTrout.Mel       TCAGAGGTGAAGTCTCGACTCAAA------CCCAGCGACATGCGCAACTTCATCACCATG 342
Goldfish.Mel1C         CCCAATCCGAAG------GTCAGG------GCGGCCGACCTGCGGAATTTCTTGACGATG 1050
Frog.Clone.X2.0        CCAGATAGGCACCTCCATCACCAGACATGGCCTTACAATATCCATGGGTTTATCACCATG 336
Sweetfish.Mel1B        ACCAACGAGGGCCCCCGCCTTAAA------CCGAGTGACATGCGGAACTTCGTCACAATG 1415
```

```
Z.Fish.Mel1B            AGCGAGGAACGTTCGAGGGTCAGG------CCCAGCGACCTGCGCAACTTTGTCACCATG 1104
Z.Fish.Mel1A            ACTGATGTCAGGCCACGCCTCCGT------CCTAGTGAGTTGCGCCATTTCTTGACCATG 886
Goldfish.Mel1B          ACCGATGTCAGGCCACGCCTCCGT------CCAAGTGAACTGCGTCACTTCTTGACCATG 1039
H.Mouse.Mel1B           GCTGAGAGGAAGCTGCGTCTGAGA------CCGAGTGATTTGCGCAGTTTCCTAACCATG 855
BrownRat.Mel1B          GCTGAGAGAAAGCTACGCCTGAGA------CCCAGTGACCTGCGCAGTTTCCTAACCATG 874
Human.Mel1B             CCAGAGAGCAGGCTGTGCCTGAAG------CCCAGCGACTTGCGGAGCTTTCTAACCATG 759
MEL1B                   TCAG---------------------------------------------------------- 265
ZebraFinch.Mel1B        TCAGAAACAAAGCCAAGATTGAAG------CCAAGTGACTTCAGAAACTTTCTTACCATG 487
Chicken.Mel1B           TCAGAAACAAAGCCAAGACTGAAA------CCAAGTGACTTCAGAAACTTTCTTACCATG 537
Frog.CloneX1.7          TCTGAATTCAAGCCAAGGATGAAA------CAAAGCGATTTCCGTAATTTTCTTACCATG 330
Sweetfish.Mel1C         CCAGAATACAGGACCAAAGTGAAG------CCGAGTGATGTCAGGAACTTCCTGACTATG 1113
Frog.Mel1B              CAAGACTTCAAGCAAAAGTTGACA------CAAACAGACTTGAGAAATTTCTTGACCATG 766
Frog.Mel1C              CAAGACTTCAAGCAAAAGTTGACA------CAAACAGACTTGAGAAATTTCTTGACCATG 766
ZebraFinch.Mel1C        CAAGACTGCAAGCAGAAACTCAGG------GCAGCTGACATCCGAAACTTCTTGACTATG 343
Chicken.Mel1C           CAAGACTGCAAGCAGAAGATCAGA------GCTGCTGACATACGGAATTTCTTGACTATG 732
MEL1C                   CAAGACTGCAAGCAGAAACTCAGG------GCAGCTGACACCCGAAACTTCTTGACTATG 342
HouseSparrow.Mel1C      CAAGACTGCAAGCAGAAACTCAGG------GCAGCTGACATCCGAAACTTCTTGACTATG 342
E.Starling.Mel1C        CAAGACTGCAAGCAGAAACTCAGG------GCAACTGACATCCGAAACTTCTTGACTATG 267
BlackCap.Mel1C          CAAGACTGCAAGCAGAAACTCAGG------GCAGCTGACATCCGAAACTTCTTGACTATG 343
BrownRat.GPR50          CAGAATCCTGACAACCAGTTTGCT------------GAGGTTCGAAATTTTCTAACCATG 766
H.Mouse.GPR50           CAGAATCCTGACAACCAGTTTGCT------------GAGGTTCGAAATTTTCTAACCATG 766
Human.GPR50             CAGAATCCTGACAACCAACTTGCT------------GAGGTTCGCAATTTTCTAACCATG 855

MEL1A                   TTTGTGGTATTTGTACTGTTTGCAGTCTGCTGGGCTCCTTTGAACTTTATAGGCATTGCA 394
ZebraFinch.Mel1A        TTTGTGGTATTTGTACTGTTTGCAGTCTGCTGGGCTCCTTTGAACTTTATAGGCATTGCA 789
HouseSparrow.Mel1A      TTTGTGGTATTTGTACTGTTTGCAGTCTGCTGGGCTCCTTTGAACTTTATAGGCATTGCA 372
Chicken.Mel1A           TTTGTGGTATTTGTACTGTTTGCAGTCTGTTGGGCTCCATTGAACTTCATTGGCCTTGCT 792
BlackCap.Mel1A          TTTGTGGTGTTTGTACTCTTTGCAGTCTGCTGGGCTCCTTTGAACTTCATAGGCCTTGCG 403
C.Salmon.Mel1A          TTCGTGGTGTTTGTGCTTTTCGCCGTGTGCTGGGCGCCGCTCAACTTCATTGGGCTGGC- 395
Sweetfish.Mel1A         TTCGTGGTGTTTGTGCTGTTCGCTGTATGCTGGGCACCGCTCAACTTTATTGGTCTTGCG 967
Goldfish.Mel1A          TTTGTTGTTTTCGTGCTCTTTGCCGTGTGCTGGGCACCATTAAATTTCATCGGGTTGGCA 972
BrownRat.Mel1A          TTTGTAGTTTTTGTACTTTTTGCCCTGTGCTGGGCCCCACTCAACTTCATAGGTCTTATT 995
H.Mouse.Mel1A           TTCGTAGTTTTTGTACTTTTTGCCATTTGTTGGGCCCCACTCAACCTCATAGGTCTTATT 862
Human.Mel1A             TTTGTGGTTTTTGTCCTTTTTGCCATTTGCTGGGCTCCTCTGAACTTCATTGGCCTGGCC 780
Bovine.Mel1A            TTTGTGGTTTTTGTCCTCTTTGCCATTTGCTGGGCTCCTCTGAACTTCATTGGTCTTGTT 423
C.Salmon.Mel1B          TTTGTGGTGTTTGTGTTGTTCGCTGTCTGCTGGGCTCCTCTGAACTTCATTGGGCTGGC- 395
RainbowTrout.Mel        TTTGTGGTGTTCGTGCTCTTCGCCATCTGCTGGGCGCCGCTCAACTTCATTGGGCTGGCC 402
Goldfish.Mel1C          TTTGTGGTGTTCGTGCTGTTTGCCGTGTGCTGGGCGCCCTTGAACTTCATCGGGCTCGCC 1110
Frog.Clone.X2.0         TTTGTGGTGTTTGTCCTCTTTGCAGTATGCTGGGGCCCGTTGAATATCATTGGACTGACA 396
Sweetfish.Mel1B         TTTGTGGTCTTCGTTCTATTCGCCATCTGCTGGGCTCCTCTCAACCTGATTGGGTTGGCT 1475
Z.Fish.Mel1B            TTCGTGGTGTTTGTTTTGTTTGCCATCTGCTGGGCCCCGCTCAATCTCATCGGTTTGGTG 1164
Z.Fish.Mel1A            TTTGTGGTTTTTGTGTTATTCGCTGTGTGTTGGGCGCCGCTCAATCTGATTGGCCTGGCT 946
Goldfish.Mel1B          TTCGTCGTCTTTGTGCTGTTCGCCGTCTGCTGGGCGCCGCTGAATCTGATTGGCTTGGCT 1099
H.Mouse.Mel1B           TTTGCAGTGTTTGTGGTTTTTGCCATATGCTGGGCCCCCCTCAACTGTATCGGCCTTGCA 915
BrownRat.Mel1B          TTCGCAGTGTTTGTGGTTTTCGCCATATGCTGGGCCCCCCTCAACTGTATTGGCCTTGCA 934
Human.Mel1B             TTTGTGGTGTTTGTGATCTTTGCCATCTGCTGGGCTCCACTTAACTGCATCGGCCTCGCT 819
MEL1B                   ------------------------------------------------------------
ZebraFinch.Mel1B        TTTGTTGTTTTTGTGATTTTTGCCTTTTGCTGGGCACCTCTAAACTTCATTGGACTGGCT 547
Chicken.Mel1B           TTTGTGGTTTTTGTGATTTTTGCCTTTTGCTGGGCACCTCTAAACTTCATAGGACTGGCT 597
Frog.CloneX1.7          TTCGTAGTATTTGTTATTTTTGCCTTTTGTTGGGCTCCTCTAAACTTCATCGGCTTAGCA 390
Sweetfish.Mel1C         TTTATGGTGTTTGTGCTGTTTGCCGTGTGCTGGGCGCCGCTGAACCTGATTGGCCTGGCT 1173
Frog.Mel1B              TTTGTGGTCTTTGTACTTTTTGCAGTTTGCTGGGCCCCCTTAAACTTTATCGGCCTTGCT 826
Frog.Mel1C              TTTGTGGTCTTTGTACTTTTTGCAGTTTGCTGGGCCCCCTTAAACTTTATCGGCCTTGCT 826
ZebraFinch.Mel1C        TTTGTGGTTTTTGTCCTTTTTGCTGTGTGCTGGGGACCATTAAACTTTATTGGCCTTGCT 403
Chicken.Mel1C           TTTGTGGTTTTTGTCCTTTTTGCTGTGTGCTGGGGACCATTAAACTTTATCGGCCTTGCT 792
MEL1C                   TTTGTGGTTTTTGTCCTTTTTGCTGTGTGCTGGGGACCATTAAACTTTATTGGCCTTGCT 402
HouseSparrow.Mel1C      TTTGTGGTTTTTGTCCTTTTTGCTGTGTGCTGGGGACCATTAAACTTTATTGGCCTTGCT 402
E.Starling.Mel1C        TTTGTGGTTTTTGTCCTTTTTGCTGTGTGCTGGGGACCACTAAACTTTATTGGCCTTGCT 327
BlackCap.Mel1C          TTTGTGGTTTTTGTCCTTTTCGCCGTGTGCTGGGGACCATTAAACTTTATTGGCCTCGCT 403
BrownRat.GPR50          TTTGTGATCTTCCTCCTTTTTTGCAGTGTGCTGGTGCCCTGTCAATGTGCTCACTGTGCTG 826
H.Mouse.GPR50           TTTGTGATCTTCCTCCTTTTTGCAGTGTGCTGGTGCCCTGTCAATGTGCTCACTGTGTTG 826
Human.GPR50             TTTGTGATCTTCCTCCTCTTTGCAGTGTGCTGGTGCCCTATCAACGTGCTCACTGTCTTG 915

MEL1A                   GTGGCTGTCAATCCAAAAACTGTAATCCCTAGGATTCCAGAGTGGTTGTTTGTGTCTAGT 454
ZebraFinch.Mel1A        GTGGCTGTCAATCCAAAAACTGTAATCCCTAGGATTCCAGAGTGGTTGTTTGTGTCTAGT 849
HouseSparrow.Mel1A      GTGGCTGTCAACCCAAAAACTGTAATCCCTAGGATTCCAGAGTGGTTGTTTGTGTCTAGT 432
Chicken.Mel1A           GTGGCTGTTGACCCAGAAACTATAATCCCTAGAATTCCAGAGTGGTTGTTCGTGTCTAGC 852
BlackCap.Mel1A          GTGGCTGTCAACCCCAAAACTGTAATCCCTAGGATTCCAGAGTGGTTGTTTGTGTCCAGT 463
C.Salmon.Mel1A          ------------------------------------------------------------
Sweetfish.Mel1A         GTGGCTATTAACCCTGAAGCGGTGGTGCCAATTATCCCTGAATGGCTTTTTGTGGCCAGC 1027
Goldfish.Mel1A          GTAGCGATTTCTCCTGAGCACGTGGTTCCTTTAATACCCGAATGGCTCTTTGTGGCAAGT 1032
BrownRat.Mel1A          GTGGCCTCAGATCCGGCCGCCATGGCCCCCAGGATCCCGGAGTGGCTCTTCGTGGCTAGT 1055
```

```
H.Mouse.Mel1A           GTGGCCTCAGACCCTGCCACCATGGTCCCCAGGATCCCAGAGTGGCTGTTCGTGGCTAGT 922
Human.Mel1A             GTGGCCTCTGACCCCGCCAGCATGGTGCCTAGGATCCCAGAGTGGCTGTTTGTGGCCAGT 840
Bovine.Mel1A            GTGGCCTCGGACCCGGCCAGCATGGCACCCAGGATCCCCGAGTGGCTGTTTGTGGCCAGT 483
C.Salmon.Mel1B          ------------------------------------------------------------
RainbowTrout.Mel        GTGGCCATCGACCCGGAGACGGTGGCGCCACGGATCCCAGAGTGGCTGTTCGTGGTCAGC 462
Goldfish.Mel1C          GTGGCGATAAACCCCGCAAGAGTGGCGCCGAATGTACCAGAGTGGCTGTTTGTTACCAGC 1170
Frog.Clone.X2.0         GTGGCCATCTATCCACCCCTTGGAGATTCT---ATACCTCAATGGCTCTTTGTAGCTAGT 453
Sweetfish.Mel1B         GTAGCCATAGACCCGCCCCGTCTGGCCCCTCGCATCCCTGAGTGGCTTTTTGTGGTCAGC 1535
Z.Fish.Mel1B            GTGGCCATCAATCCAGAGGTCATGGCTCCACGTGTTCCAGAATGGTTGTTTGTCGTAAGC 1224
Z.Fish.Mel1A            GTAGCAGTGGACCCACCTCGGGTCGGGCCATTGGTCCCTGATTGGCTGTTCGTGATGAGT 1006
Goldfish.Mel1B          GTAGCGGTGGACCCGCCCCGCGTAGGGCCCTTGGTCCCTGATTGGCTATTTGTGGTGAGT 1159
H.Mouse.Mel1B           GTGGCCATCAACCCAGAGGCAATGGCTCTCCAGGTCCCAGAAGGGCTCTTTGTCACCAGT 975
BrownRat.Mel1B          GTGGCCATCAATCCAGAGGCAATGGCTCTTCAGATCCCAGAAGGGCTTTTTGTCACCAGT 994
Human.Mel1B             GTGGCCATCAACCCCCAAGAAATGGCTCCCCAGATCCCTGAGGGGCTATTTGTCACTAGC 879
MEL1B                   ------------------------------------------------------------
ZebraFinch.Mel1B        GTAGCCATTGATCCTACGGAAATGGCACCAAAAGTTCCTGAATGGCTATTCATTATAAGT 607
Chicken.Mel1B           GTAGCCATCAATCCTTCAGAAATGGCACCAAAAGTTCCTGAATGGTTATTCATTATAAGC 657
Frog.CloneX1.7          GTGTCCATCAACCCTACAGAAGTAGCACCCAAAATTCCAGAATGGCTCTTCGTTGTTAGC 450
Sweetfish.Mel1C         GTGGCCATTAACCCCATGAGGGTGGCGCCCAACATCCCAGAATGGCTCTTTGTCACAAGC 1233
Frog.Mel1B              GTGGCCATTAATCCGTTTCATGTGGCACCAAAGATTCCAGAATGGCTGTTTGTTTTAAGC 886
Frog.Mel1C              GTGGCCATTAATCCGTTTCATGTGGCACCAAAGATTCCAGAATGGCTGTTTGTTTTAAGC 886
ZebraFinch.Mel1C        GTTTCAATTAATCCTTCAAAAGTGCAGCCACACATTCCAGAATGGCTTTTTGTCCTGAGC 463
Chicken.Mel1C           GTTTCAATTAATCCTTCCAAAGTGCAGCCACACATTCCAGAGTGGCTTTTTGTCCTAAGC 852
MEL1C                   GTTTCAATTAATCCTTCAAAAGTGCAGCCACACATTCCAGAATGGCTTTTTGTCCTGAGC 462
HouseSparrow.Mel1C      GTTTCAATTAATCCTTCAAAAGTGCAGCCACACATTCCAGAATGGCTTTTTGTCCTGAGC 462
E.Starling.Mel1C        GTTTCAATTAATCC-------------------------------------------- 341
BlackCap.Mel1C          GTTTCAATTAATCCTTCAAAAGTGCAGCCACACATTCCAGAATGGCTTTTTGTCCTGAGC 463
BrownRat.GPR50          GTGGCTGTCATTCCAAAGGAAATGGCAGGCAAGATCCCCAACTGGCTTTATCTTGCAGCC 886
H.Mouse.GPR50           GTGGCTGTCATTCCAAAGGAAATGGCAGGCAAGATCCCCAACTGGCTTTATCTTGCAGCC 886
Human.GPR50             GTGGCTGTCAGTCCGAAGGAGATGGCAGGCAAGATCCCCAACTGGCTTTATCTTGCAGCC 975

MEL1A                   TATTACATGGCATATTTCAACAGCTGCCTTAATCGCGATA---------------------- 494
ZebraFinch.Mel1A        TATTACATGGCATATTTCAACAGCTGCCTTAAT-GCTATAGTATATGGACTCCTGAACCA 908
HouseSparrow.Mel1A      TATTACATGGCATATT------------------------------------------- 448
Chicken.Mel1A           TATTACATGGCATATTTCAACAGCTGCCTTAAT-GCCATTATATATGGACTCCTGAATCA 911
BlackCap.Mel1A          TATTAC---------------------------------------------------- 469
C.Salmon.Mel1A          ------------------------------------------------------------
Sweetfish.Mel1A         TACTTCATGGCATACTTCAACAGCTGCCTTAAC-GCCATCGTGTATGGGGTGCTGAACCA 1086
Goldfish.Mel1A          TATTTCATGGCATACTTTAACAGTTGTCTCAAT-GCAATCGTCTATGGAGTTTTGAACCA 1091
BrownRat.Mel1A          TACTACCTGGCGTATTTCAACAGCTGCCTCAAC-GCAATCATATACGGACTACTGAACCA 1114
H.Mouse.Mel1A           TACTACCTGGCGTACTTCAACAGCTGCCTCAAC-GCAATTATATACGGACTACTGAATCA 981
Human.Mel1A             TACTACATGGCGTATTTCAACAGCTGCCTCAAT-GCCATTATATACGGGCTACTGAACCA 899
Bovine.Mel1A            TACTATATGGCATATTTCAACAGCTGCCTCAAT-GCGATCATATATGGACTACTGAACCA 542
C.Salmon.Mel1B          ------------------------------------------------------------
RainbowTrout.Mel        TACTTCATGGCGTACTTCAACAGT---------------------------------- 486
Goldfish.Mel1C          TACTTCATGGCGTATTTCAACAGCTGTCTGAAT-GCTGTCATCTATGGGTTGCTCAACCA 1229
Frog.Clone.X2.0         TACTTC---------------------------------------------------- 459
Sweetfish.Mel1B         TACTTCATGGCTTATTTTAACAGCTGCCTGAAT-GCCATCATCTATGGCCTCCTCAACAG 1594
Z.Fish.Mel1B            TACTTTATGGCTTATTTTAACAGCTGCCTCAAT-GCTATCATTTATGGCCTCCTGAACAG 1283
Z.Fish.Mel1A            TATTTCATGGCATACTTTAACTCCTGCCTGAAC-GCTGTAGTGTATGGACTGCTCAATCA 1065
Goldfish.Mel1B          TATTTCATGGCATATTTTAACTCCTGCCTGAAC-GCCGTAGTGTACGGACTGCTCAATCA 1218
H.Mouse.Mel1B           TACTTCTTAGCTTACTTTAACAGCTGCCTTAAT-GCCATTGTTTATGGGCTCCTGAACCA 1034
BrownRat.Mel1B          TACTTCCTAGCTTACTTCAACAGCTGCCTTAAT-GCTATTGTTTATGGGCTTCTGAACCA 1053
Human.Mel1B             TACTTACTGGCTTATTTCAACAGCTGCCTGAAT-GCCATTGTCTATGGGCTCTTGAACCA 938
MEL1B                   ------------------------------------------------------------
ZebraFinch.Mel1B        TACTTA---------------------------------------------------- 613
Chicken.Mel1B           TACTTCATGGCCTATTTCAACAGCTGCCTTAAT-GCAATAATATATGGACTTCTTAACCA 716
Frog.CloneX1.7          TATTTC---------------------------------------------------- 456
Sweetfish.Mel1C         TACTTTATGGCGTACTTCAACAGCTGCTTGAAT-GCCATCATATACGGACTGCTCAACCA 1292
Frog.Mel1B              TATTTCATGGCCTATTTTAACAGTTGTCTCAAT-GCTGTTATATATGGTGTGCTAAATCA 945
Frog.Mel1C              TATTTCATGGCCTATTTTAACAGTTGTCTCAAT-GCTGTTATATATGGTGTGCTAAATCA 945
ZebraFinch.Mel1C        TATTTT---------------------------------------------------- 469
Chicken.Mel1C           TATTTTATGGCCTATTTTAACAGCTGCCTCAAT-GCTGTGATCTATGGGCTGCTTAACCA 911
MEL1C                   A--------------------------------------------------------- 463
HouseSparrow.Mel1C      ------------------------------------------------------------
E.Starling.Mel1C        ------------------------------------------------------------
BlackCap.Mel1C          TATTTT---------------------------------------------------- 469
BrownRat.GPR50          TACTGCATAGCCTACTTCAACAGCTGCCTCAAC-GCCATCATCTACGGTATCCTCAATGA 945
H.Mouse.GPR50           TACTGCATAGCCTACTTCAACAGCTGCCTCAAC-GCCATCATCTACGGTATCCTCAATGA 945
Human.GPR50             TACTTCATAGCCTACTTCAACAGCTGCCTCAAC-GCTGTGATCTACGGGCTCCTCAATGA 1034
```

1.2.2 Statistical analysis for the melatonin receptor mRNA expression in the zebra finch the brain tissues, in Chapter Four. NS = not significant; *p<0.05, **p<0.01, ***p<0.001.

		Statistical tests						
Tissue	**Receptor**	**One-way ANOVA**			**Post hoc Tukey's Multiple Comparison test**			
		F Value	**p Value**	**Summary**	**Comparison**	**q value**	**Significant? P<0.05**	**Summary**
Diencephalon Figure 4.2.1.a.	Mel-1A	8.210	0.0002	***	ZT02vsZT22	5.500	Yes	**
					ZT06vsZT22	7.595	Yes	***
					ZT10vsZT22	7.249	Yes	***
					ZT14vsZT22	5.532	Yes	**
	Mel-1B	7.010	0.0015	**	ZT02vsZT06	6.694	Yes	**
					ZT02vsZT10	5.477	Yes	*
					ZT06vsZT22	6.019	Yes	**
					ZT10vsZT22	4.957	Yes	*
	Mel-1C	0.6741	0.6495	NS	-	-	-	-
Pineal Gland Figure 4.2.1.b.	Mel-1A	0.9861	0.4582	NS	-	-	-	-
	Mel-1B	4.233	0.0149	*	ZT06vsZT22	5.636	Yes	*
					ZT14vsZT22	5.374	Yes	*
					ZT18vsZT22	5.797	Yes	*
	Mel-1C	3.463	0.0330	*	-	-	-	-
Retina Figure 4.2.1.c.	Mel-1A	5.836	0.0018	**	ZT02vsZT18	5.568	Yes	**
					ZT06vsZT18	6.759	Yes	**
					ZT06vsZT22	4.593	Yes	*
	Mel-1B	4.446	0.0075	**	ZT10vsZT22	6.422	Yes	**
	Mel-1C	0.7569	0.5951	NS	-	-	-	-
Optic tectum Figure 4.2.1.d.	Mel-1A	8.944	<0.0001	***	ZT02vsZT18	4.985	Yes	*
					ZT02vsZT22	5.338	Yes	**
					ZT06vsZT18	5.932	Yes	**
					ZT06vsZT22	6.396	Yes	**
					ZT10vsZT18	6.321	Yes	**
					ZT10vsZT22	6.832	Yes	***
					ZT14vsZT18	4.595	Yes	*
					ZT14vsZT22	4.823	Yes	*
	Mel-1B	5.752	0.0037	**	ZT02vsZT10	4.982	Yes	*
					ZT02vsZT18	5.094	Yes	*
					ZT02vsZT22	6.187	Yes	**
					ZT14vsZT22	4.679	Yes	*
	Mel-1C	1.262	0.3169	NS	-	-	-	-
Cerebellum Figure 4.2.1.e.	Mel-1A	3.170	0.0223	*	ZT06vsZT22	4.359	Yes	*
					ZT10vsZT22	4.579	Yes	*
	Mel-1B	5.079	0.0117	*	ZT02vsZT10	4.839	Yes	*
					ZT10vsZT18	6.351	Yes	**
	Mel-1C	1.297	0.3066	NS	-	-	-	-
Telencephalon Figure 4.2.1.f.	Mel-1A	3.981	0.0072	**	ZT10vsZT22	4.759	Yes	*
	Mel-1B	1.834	0.1458	NS	-	-	-	-
	Mel-1C	2.826	0.0406	*	-	-	-	-

1.2.3 Statistical analysis for the melatonin receptor mRNA expression in the zebra finch the peripheral tissues, in Chapter Four. NS = not significant; *p<0.05, **p<0.01, ***p<0.001.

		Statistical tests						
Receptor	Tissue	One-way ANOVA			Post hoc Tukey's Multiple Comparison test			
		F Value	p Value	Summary	Comparison	q value	Significant? P<0.05	Summary
Mel-1A Figure 4.2.2.a.	Heart	2.258	0.0741	NS	-	-	-	-
	Liver	4.321	0.0044	**	ZT02vsZT14	5.141	Yes	*
					ZT02vsZT18	5.276	Yes	**
					ZT02vsZT22	4.797	Yes	*
	Lung	0.8022	0.5573	NS	-	-	-	-
	Kidney	1.116	0.3960	NS	-	-	-	-
Mel-1B Figure 4.2.2.b.	Heart	7.582	0.0005	***	ZT02vsZT18	4.469	Yes	*
					ZT02vsZT22	5.544	Yes	*
					ZT10vsZT18	6.004	Yes	**
					ZT10vsZT22	7.079	Yes	***
					ZT14vsZT22	4.891	Yes	*
	Liver	12.32	<0.0001	***	ZT02vsZT18	5.880	Yes	**
					ZT02vsZT22	8.174	Yes	***
					ZT06vsZT14	4.616	Yes	*
					ZT06vsZT18	6.321	Yes	**
					ZT06vsZT22	8.307	Yes	***
					ZT10vsZT18	5.101	Yes	*
					ZT10vsZT22	7.087	Yes	***
	Lung	8.591	0.0001	***	ZT02vsZT10	5.323	Yes	*
					ZT02vsZT14	6.373	Yes	**
					ZT06vsZT14	5.325	Yes	*
					ZT10vsZT22	6.075	Yes	**
					ZT14vsZT18	4.684	Yes	*
					ZT14vsZT22	7.126	Yes	***
	Kidney	0.6803	0.6470	NS	-	-	-	-
Mel-1C Figure 4.2.2.c.	Heart	0.5104	0.7661	NS	-	-	-	-
	Liver	0.4662	0.7982	NS	-	-	-	-
	Lung	0.6603	0.6563	NS	-	-	-	-
	Kidney	5.449	0.0112	*	ZT02vsZT18	6.281	Yes	*
					ZT02vsZT22	5.099	Yes	*
					ZT06vsZT18	5.193	Yes	*

1.2.4 Statistical analysis for the AVTergic cell expression profiles under LD conditions in the zebra finch, in Chapter Seven. NS = not significant; *p<0.05, **p<0.01, ***p<0.001.

		Statistical tests						
Figure	Graph	One-way ANOVA			Post hoc Tukey's Multiple Comparison test			
		p Value	Signif. P<0.05	Summary	Comparison	q value	Signif P<0.05	Summary
Nuclei Cell Counts Figure 7.2.1.e	ZT01	0.0430	Yes	*	-	-	-	-
	ZT06	0.0600	No	NS	-	-	-	-
	ZT11	0.0012	Yes	**	LHNvvsPPN	6.085	Yes	**
					LHNvvsLHNd	6.085	Yes	**
					LHNvvsPON	4.431	Yes	*
	ZT13	<0.0001	Yes	***	LHNvvsPPN	8.328	Yes	***
					LHNvvsLHNd	8.328	Yes	***
					LHNvvsPON	6.146	Yes	**
	ZT18	0.0007	Yes	***	LHNvvsPPN	5.643	Yes	**
					LHNvvsLHNd	7.289	Yes	**
					LHNvvsPON	6.506	Yes	**
	ZT23	<0.0001	Yes	***	LHNvvsPPN	9.667	Yes	***
					LHNvvsLHNd	9.006	Yes	***
					LHNvvsPON	9.512	Yes	***

1.2.5 Statistical analysis for the AVTergic cell expression profiles under dimLL conditions in the zebra finch, in Chapter Seven. NS = not significant; *p<0.05, **p<0.01, ***p<0.001.

		Statistical tests						
Figure	Graph	One-way ANOVA			Post hoc Tukey's Multiple Comparison test			
		p Value	Signif P<0.05	Summary	Comparison	q value	Signif. P<0.05	Summary
Nuclei cell counts Figure 7.2.2.d.	ZT23	0.0002	Yes	***	LHNvvsPPN	7.309	Yes	**
					LHNvvsLHNd	8.336	Yes	***
					LHNvvsPON	8.477	Yes	***
	CT01	0.0001	Yes	***	LHNvvsPPN	18.11	Yes	***
					LHNvvsLHNd	19.36	Yes	***
					LHNvvsPON	19.90	Yes	***
	CT06	0.0001	Yes	***	LHNvvsPPN	12.42	Yes	***
					LHNvvsLHNd	12.04	Yes	***
					LHNvvsPON	10.97	Yes	***
	CT11	0.0117	Yes	*	LHNvvsPPN	4.945	Yes	*
					LHNvvsLHNd	4.851	Yes	*
					LHNvvsPON	4.592	Yes	*
	CT13	0.0262	Yes	*	-	-	-	-
	CT18	0.0630	No	NS	-	-	-	-
	CT23	<0.0001	Yes	***	LHNvvsPPN	10.29	Yes	***
					LHNvvsLHNd	8.689	Yes	***
					LHNvvsPON	10.22	Yes	***

1.2.6 Statistical analysis of the AVTergic cell counts under LD conditions and dimLL conditions in the zebra finch hypothalamus, in Chapter Seven. NS = not significant; *p<0.05, **p<0.01, ***p<0.001.

		Statistical tests							
Figure	Graph	One-way ANOVA				Post hoc Tukey's Multiple Comparison test			
		F Value	p Value	Sign.P <0.05	Summary	Comparison	q value	Sign. P <0.05	Summary
Total Cell Counts Figure 7.2.3.a.	PPN	58.01	<0.0001	Yes	***	ZT01vsZT18	32.59	Yes	***
						ZT01vsZT23	50.85	Yes	***
						ZT06vsZT23	54.76	Yes	***
						ZT11vsZT23	54.76	Yes	***
						ZT13vsZT23	54.76	Yes	***
						ZT18vsZT23	14.49	Yes	***
						ZT01vsCT01	1.378	No	-
						ZT06vsCT06	1.042	No	-
						ZT11vsCT11	1.488	No	-
						ZT13vsCT13	0.243	No	-
						ZT18vsCT18	10.86	Yes	***
						ZT23vsCT23	19.35	Yes	***
	LHNv	4.774	<0.0001	Yes	***	ZT01vsZT06	8.155	Yes	***
						ZT01vsZT11	7.115	Yes	***
						ZT01vsZT13	7.621	Yes	***
						ZT01vsCT01	5.319	Yes	*
						ZT06vsCT06	1.432	No	-
						ZT11vsCT11	0.391	No	-
						ZT13vsCT13	0.381	No	-
						ZT18vsCT18	3.121	No	-
						ZT23vsCT23	1.814	No	-
	LHNd	2.302	0.0434	Yes	*	ZT01vsCT01	2.414	No	-
						ZT06vsCT06	0	No	-
						ZT11vsCT11	0	No	-
						ZT13vsCT13	0	No	-
						ZT18vsCT18	0.8604	No	-
						ZT23vsCT23	1.178	No	-
	PON	2.346	<0.0240	Yes	*	ZT01vsCT01	4.422	No	-
						ZT06vsCT06	4.724	No	-
						ZT11vsCT11	1.208	No	-
						ZT13vsCT13	0.0462	No	-
						ZT18vsCT18	0.4158	No	-
						ZT23vsCT23	0.5607	No	-
Distance Figure 7.2.3.b.	PPN	63.14	<0.0001	Yes	***	ZT01vsZT06	10.23	Yes	***
						ZT01vsZT11	10.23	Yes	***
						ZT01vsZT13	10.23	Yes	***
						ZT06vsZT23	12.60	Yes	***
						ZT11vsZT23	12.60	Yes	***

						ZT13vsZT23	8.697	Yes	***
						ZT18vsZT23	17.13	Yes	***
						ZT01vsCT01	3.051	No	-
						ZT06vsCT06	5.177	Yes	*
						ZT11vsCT11	7.162	Yes	***
						ZT13vsCT13	8.787	Yes	***
						ZT18vsCT18	17.39	Yes	***
						ZT23vsCT23	0.926	No	-
	LHNv	10.20	<0.0001	Yes	***	ZT01vsZT06	9.988	Yes	***
						ZT01vsZT11	7.941	Yes	***
						ZT01vsZT13	8.613	Yes	***
						ZT01vsZT18	6.652	Yes	**
						ZT01vsZT23	7.119	Yes	***
						ZT01vsCT01	8.520	Yes	***
						ZT06vsCT06	1.812	No	-
						ZT11vsCT11	2.680	No	-
						ZT13vsCT13	3.344	No	-
						ZT18vsCT18	3.811	No	-
						ZT23vsCT23	1.762	No	-
	LHNd	6.921	<0.0001	Yes	***	ZT01vsZT06	7.999	Yes	***
						ZT01vsZT11	7.999	Yes	***
						ZT01vsZT13	7.999	Yes	***
						ZT01vsZT18	7.999	Yes	***
						ZT01vsCT01	2.149	No	-
						ZT06vsCT06	0	No	-
						ZT11vsCT11	0	No	-
						ZT13vsCT13	0	No	-
						ZT18vsCT18	1.676	No	-
						ZT23vsCT23	1.699	No	-
	PON	3.934	0.0010	Yes	**	ZT01vsZT11	7.115	Yes	**
						ZT01vsZT13	6.004	Yes	**
						ZT01vsZT18	7.552	Yes	***
						ZT01vsCT01	5.559	Yes	*
						ZT06vsCT06	0.7752	No	-
						ZT11vsCT11	0.8397	No	-
						ZT13vsCT13	0.4737	No	-
						ZT18vsCT18	1.634	No	-
						ZT23vsCT23	1.551	No	-
Cell counts through the LHNv regions Figure 7.2.3.c.	**Rostral**	4.365	0.0002	Yes	***	ZT01vsZT06	6.182	Yes	**
						ZT01vsZT11	5.632	Yes	*
						ZT01vsZT13	5.351	Yes	*
						ZT06vsZT23	6.043	Yes	**
						ZT11vsZT23	5.505	Yes	*
						ZT13vsZT23	5.223	Yes	*
						ZT01vsCT01	1.541	No	-
						ZT06vsCT06	1.816	No	-
						ZT11vsCT11	0.842	No	-
						ZT13vsCT13	0.7964	No	-
						ZT18vsCT18	0.2446	No	-

						ZT23vsCT23	0.8575	No	-
	Medial	3.077	0.0045	Yes	**	ZT01vsCT01	4.568	No	-
						ZT06vsCT06	0.521	No	-
						ZT11vsCT11	0.759	No	-
						ZT13vsCT13	0.351	No	-
						ZT18vsCT18	3.081	No	-
						ZT23vsCT23	1.454	No	-
	Caudal	2.113	0.0443	Yes	*	ZT01vsCT01	3.620	No	-
						ZT06vsCT06	0	No	-
						ZT11vsCT11	0	No	-
						ZT13vsCT13	0	No	-
						ZT18vsCT18	0.034	No	-
						ZT23vsCT23	0.047	No	-
Cell counts through the LHNv ZT Figure 7.2.3.d.	**ZT01**	1.897	0.1897	No	NS	-	-	-	-
	ZT06	15.24	0.19	Yes	**	RvsC	7.433	Yes	**
						MvsC	5.561	Yes	*
	ZT11	5.018	0.0243	Yes	*	RvsC	4.187	Yes	*
	ZT13	12.31	0.0020	Yes	**	RvsM	4.869	Yes	*
						RvsC	6.481	Yes	**
	ZT18	1.242	0.3339	No	NS	-	-	-	-
	ZT23	1.251	0.3432	No	NS	-	-	-	-
	ZT23	5.489	0.0316	Yes	*	RvsC	4.397	Yes	*
	CT01	42.15	0.0001	Yes	***	RvsM	9.997	Yes	***
						RvsC	11.77	Yes	***
	CT06	35.52	0.0002	Yes	***	RvsM	10.07	Yes	***
						RvsC	10.07	Yes	***
	CT11	5.275	0.0401	Yes	*	-	-	-	-
	CT13	4.879	0.0412	Yes	*	-	-	-	-
	CT18	3.598	0.0768	No	NS	-	-	-	-
	CT23	24.03	0.0002	Yes	***	RvsM	7.614	Yes	**
						RvsC	8.746	Yes	***

1.2.7 Table showing the distribution of potential vasotocinergic and vasopressinergic cell bodies in brain regions of different vertebrate species (Moore & Lowry, 1998). For Chapter Eight - Species comparison of AVT expression in the hypothalamus at ZT01.

Brain Region	Fish	Amphibians	Reptiles	Birds	Mammals
Pallial telencephalon		V1, Dorsal pallium-nucleus olfactorius anterior pars dorsalis continuum V2, Medial pallium (Hippocammpal)			
Subpallial telencephalon		V3, Caudal septum medial basal forebrain continuum (amygdale pars medialis)	Medial septum-medial basal forebrain continuum	Basal septal area	Lateral septum
					Medial septum
					Vertical limb of the diagonal band of Broca (ventral part)
					Angular portion of the diagonal band of Broca
					Horizontal limb of the diagonal band of Broca
					Basal nucleus of Meynert
					Substantia innominata sublenticularis (extending into the ventral globus pallidus)
		V4, Bed nucleus of the stria terminalis (caudal striatum)	Bed nucleus of the stria terminalis	Bed nucleus of the stria terminalis	Bed nucleus of stria terminalis
					Internal capsule
		V5, Nucleus amygdalae dorsolateralis (Amygdala pars lateralis)			Medial amygdaloid nucleus
Diencephalon		V6, Bed nucleus			Anterior

		of the decussation of the fassiculus lateralis telencephali			commissural nucleus
		V7, Anterior preoptic area	Anterior hypothalamic-preoptic area	Anterior preoptic area	Anterior hypothalamic-preoptic area lateral to the anterior commissural nucleus in males
		V8, Pars ventralis thalami	Dorsomedial thalamic Ventromedial thalamic nucleus	Thalamus	
	Magnocellular preoptic area	V9, Magnocellular preoptic area	Supraoptic area	Supraoptic nucleus	Supraoptic nucleus
Hypothalamic accessory nuclei			Accessory cells between the rostral hypothalamic area and the supraoptic and paraventricular nuclei	Accessory cells between supraoptic and paraventricular nuclei Accessory cells in the lateral hypothalamus	Perifornical region Nucleus circularis Lateral hypothalamic area Zona incerta
			Accessory cells around the lateral forebrain bundle		
	Parvocellular preoptic area	V10, Posterior preoptic area	Paraventricular nucleus	Paraventricular nucleus	Paraventricular nucleus
		V11, Ventral preoptic area Suprachiasmatic nucleus		Suprachiasmatic nucleus	Suprachiasmatic nucleus Intrachiasmatic nucleus possibly equivalent to the rostromedian division of the SCN, or dorsal chiasmatic nucleus
	Nucleus periventricularis hypothalami	V12, Pars dorsalis hypothalami			Dorsomedial hypothalamic nucleus Posterior dorsal hypothalamic area
		V13, Posterior lobe of the pars ventralis hypothalami	Ventral hypothalamus		Dorsal capsule of the ventromedial hypothalamic nucleus

		V14, Primordial mammillary region		Tuberomammillary area (near or within the ectomammillary tract)	Tuber cinereum, caudal, lateral, arcuate nucleus
Brainstem		V15, Rostral ventromedial mesencephalon	Interpeduncular nucleus		Rare cells in deep mesencephalic nucleus
		V16, Nucleus visceralis Superior nucleus isthmi region			
		V17, Nucleus cerebella			Cerebellum (Purkinjie cells)
		V18, Inferior colliculus			Inferior colliculus
		V19, Lateral auricle-area, acusticolateralis continuum			
		Area lateral to presumed locus coeruleus			Locus coeruleus Locus coeruleus region Subcoeruleus Medioventral zone of the periolivary region
		Area adjacent to the solitary tract	Caudal rhombencephalon		Ventral subnucleus of the nucleus of the solitary tract
		Thoracic spinal cord			Dorsal horn of the cervical spinal cord

1.2.8 Statistical analysis for the comparative AVTergic cell expression under LD conditions in the zebra finch (ZF), Japanese quail (JQ) and chicken (CH), in Chapter Eight. NS = not significant; *p<0.05, **p<0.01, ***p<0.001.

		Statistical tests							
Figure	Graph	One-way ANOVA				Post hoc Tukey's Multiple Comparison test			
		F Value	p Value	Sign. P<0.05	Summary	Comparison	q value	Sign. P<0.05	Summary
Nuclei cells counts Figure 8.2.2.a.	Zebra Finch (G)	3.607	0.043	Yes	*	-	-	-	-
	Japanese Quail (H)	15.92	0.00003	Yes	***	PPNvsPON	7.994	Yes	***
						LHNvvsPON	5.999	Yes	**
						LHNdvPON	7.489	Yes	**
	Chicken (I)	3.448	0.0888	-	-	-	-	-	-
Nuclei total cell counts Figure 8.2.3.a	PPN (A)	17.34	0.0056	Yes	**	ZFvsJQ	4.899	Yes	*
						JQvsCH	8.216	Yes	*
	LHNv (B)	5.960	0.0250	Yes	*	ZFvsCH	4.078	Yes	*
	LHNd (C)	11.89	0.0082	Yes	*	ZFvsJQ	5.973	Yes	*
						ZFvsCH	5.973	Yes	*
	PON (D)	0.0136	0.9865	No	NS	-	-	-	-
Distance Figure 8.2.3.b	PPN (A)	0.0886	0.9163	No	NS	-	-	-	-
	LHNv (B)	6.240	0.0020	Yes	**	ZFvsJQ	4.089	Yes	*
						ZFvsCH	7.101	Yes	**
	LHNd (C)	8.816	0.0164	Yes	*	ZFvsJQ	5.143	Yes	*
						ZFvsCH	5.143	Yes	*
	PON	0.2736	0.7657	No	NS	-	-	-	-
Total cell counts in LHNv Figure 8.2.3.c	Zebra Finch (A)	1.876	0.1897	No	NS	-	-	-	-
	Japanese Quail (B)	3.680	0.0906	No	NS	-	-	-	-
	Chicken (C)	15.98	-	-	-	-	-	-	-
	Rostral (D)	8.911	0.0066	Yes	**	ZFvsJQ	4.579	Yes	*
						ZFvsCH	5.291	Yes	*
	Medial (E)	2.701	0.0861	No	NS	-	-	-	-
	Caudal (F)	2.928	0.1111	No	NS	-	-	-	-

Total cell counts in PON Figure 8.2.3.d	**Zebra Finch (A)**	0.0963	0.9090	No	NS	-	-	-	-
	Japanese Quail (B)	14.90	0.0006	Yes	***	RvsM	6.061	Yes	**
						RvsC	6.840	Yes	**
	Chicken (C)	0.8554	0.4652	No	NS	-	-	-	-
	Rostral (D)	0.1174	0.8903	No	NS	-	-	-	-
	Medial (E)	6.165	0.0206	Yes	*	ZFvsCH	4.532	Yes	*
						ZFvsCH	4.640	Yes	*
	Caudal (F)	1.984	0.2520	No	NS	-	-	-	-

1.2.9 Personal communication from Dr Roland Brandstaetter for the AVT comparison between species in Chapter Eight - The lateral hypothalamic nucleus in the avian brain – an evolutionary novelty for the control of seasonal reproduction

Birds, like most organisms, have the ability to read the annual progression of certain environmental factors and to utilize this information to regulate their annual biological rhythms[1]. The most important environmental signal for annual rhythms of physiology and behaviour, including gonadal activity, moult, and migration, is the annual cycle of photoperiod, i.e. daylength, and it is the circadian system that is responsible for photoperiodic time measurement[2,3]. As with all animal species, birds concentrate their reproductive efforts to times when environmental conditions are optimal for the survival of their offspring[4]. This timing mechanism requires detection of changing daylength, comparison of these changes with an internal reference system, a response system that transduces environmental information into neural and endocrine signals to change the reproductive status of the animal, and a mechanism to terminate gonadal activity.

While photoperiodism and the control of seasonal reproduction are well understood in mammals[5], our knowledge in lower vertebrates including birds is still very limited. Recently, a working model has been developed based on molecular and endocrine investigations in one bird species, the Japanese quail[6,7]. This working model, however, has its focus on photoinduction of gonadal activity only and neural mechanisms related to the distinct reproductive strategies of birds, understanding of the link

between the circadian system and the pituitary gland, and the mechanism of termination of reproductive activity remain elusive.

Here we show a cell group in the lateral hypothalamus of birds that i) contains rhythmic clock gene expression and circadian neuropeptidergic output, i.e. vasotocin (VT), ii) responds to light, and iii) is only present in seasonally reproducing species.

This lateral hypothalamic nucleus (LHN) of birds consists of two interconnected parts; while the ventral part appears anatomically comparable to the supraoptic nucleus of mammals, the dorsal part that extends into the lateral hypothalamus is unique to birds. It is characterised by a dense population of vasotocinergic cells that anatomically co-localize with rhythmic period clock gene expression. Detailed analysis of VTergic cells in the hypothalamus of the house sparrow, a well established model species in circadian research, reveals VT rhythmicity in both parts of the LHN in light/dark conditions as well as in constant darkness indicating circadian control while none of the neighbouring VT-containing preoptic cell groups show VT rhythmicity. VT maxima temporally coincide with the decline of circulating melatonin, increased *Per3* mRNA expression, and with the onset of locomotor activity of the animal at the transition from dark to light. Furthermore, immediate early response gene expression can be found in both parts of the LHN following light exposure at night and a comparison of 6 passeriform and 2 galliform species shows a striking correlation of the presence of the VTergic dorsal LHN with the patterns of reproduction and photoperiodism. All photoperiodic and seasonally reproducing species (house sparrow, blackbird, European starling, stonechat, garden warbler) with intact photorefractoriness, i.e. the process responsible for the termination of gonadal activity, show a pronounced VTergic dorsal LHN while this cell group is absent in less photoperiodic species with impaired photorefractoriness that do not reproduce seasonally (zebra finch, chicken, Japanese quail). VTergic LHN neurons build a dense network with the preoptic nuclei and the paraventricular nucleus, known as the hypothalamo-hypophysial neurosecretory system; axons of these cells form a prominent vasotocinergic fibre tract towards the mediobasal hypothalamus and median eminence where photoinduction of reproduction is believed to be initiated[6].

Our results demonstrate an evolutionary novelty in the brain of photoperiodic seasonally reproducing birds. While the existing working model[6,7] suggests photoperiodic responsiveness to be controlled by the mediobasal hypothalamus as revealed in Japanese quail, our results suggest the presence of a higher control center in the lateral hypothalamus of birds. Our results significantly expand the existing working model on avian photoperiodism by revealing the link between the circadian and hypothalamo-hypophysial systems. This cell group, termed lateral hypothalamic nucleus according to

its anatomical localisation in the avian brain, appears to be an evolutionary novelty of seasonally breeding birds.

1 Brandstaetter R (2002) The circadian pacemaking system of birds. Biological Rhythms (V Kumar, ed), Narosa Publishing House, pp 144-163.

2 Pittendrigh CS & S Daan (1976) A functional analysis of circadian pacemakers in nocturnal rodents. V. Pacemaker structure: a clock for all seasons. J Comp Physiol **106**, 333–355.

3 Brandstaetter R (2003) Encoding time of day and time of year by the avian circadian system. J Neuroendocrinol **15**, 398-404.

4 Okamura H (2008) Physiology: Brain comes to light. Nature **452**, 294-295.

5 Hazlerigg DG & GC Wagner (2006) Seasonal photoperiodism in vertebrates: from coincidence to amplitude. Trends Endocrinol Metabol **17**: 83-91.

6 Yoshimura T et al (2003) Light-induced hormone conversion of T-4 to T-3 regulates photoperiodic response of gonads in birds. Nature **426**, 178-181.

7 Provencio I (2010) Shedding light on photoperiodism. Proc Natl Acad Sci U S A **107**, 15662-15663

Appendix II

Publications

APPENDIX II

Publications

1) **Melatonin receptor expression in the zebra finch brain and peripheral tissues**
Submitted to Chronobiology International in April 2011, Accepted in November 2011, due to be February 2012 edition.

Melatonin receptor expression in the zebra finch brain and peripheral tissues

Catherine Jones, Gisela Helfer, Roland Brandstaetter

Biological Rhythms Research Group, School of Biosciences, LES College, University of Birmingham, Edgbaston, Birmingham, B15 2TT, UK. E-Mail: r.brandstaetter@bham.ac.uk

Abstract

The circadian endocrine hormone melatonin plays a significant role in many physiological processes such as modulating sleep/wake cycle and oxidative stress. Melatonin is synthesised and secreted during the night by the pineal gland and released into the circulatory system. It binds to numerous membrane, cytosolic and nuclear receptors in the brain and peripheral organs. Three G-protein linked membrane receptors (Mel-1A, Mel-1B and Mel-1C) have been identified in numerous species. Considering the importance of this hormone and its receptors, this study looks at the location and rhythmicity of three avian melatonin receptors *Mel-1A*, *Mel-1B* and *Mel-1C* using reserve transcription-polymerase chain reaction (RT-PCR) mRNA analysis techniques. This study shows successful partial cloning of the three receptors and gene expression analysis revealed significant rhythms of the *Mel-1A* receptor in the cerebellum, diencephalon, tectum opticum, telencephalon, and retina. Significant rhythms where found in the diencephalon, pineal gland, retina, tectum opticum and cerebellum of the *Mel-1B* receptor whereas *Mel-1C* appeared not to be rhythmically expressed in brain tissues studied. *Mel-1A*, *Mel-1B* and *Mel-1C* receptor mRNA where also present in peripheral tissues showing tissue-specific expression patterns.

Keywords: brain; melatonin receptors; pineal gland; rhythm;

Address correspondence to Dr Roland Brandstaetter, Biological Rhythms Research Group, School of Biosciences, LES College, University of Birmingham, B15 2TT Birmingham, UK.
E-Mail: r.brandstaetter@bham.ac.uk

INTRODUCTION

Organisms time behavioural and physiological processes by synchronizing them with periodically changing environmental factors such as the light/dark cycle (Pittendrigh, 1993). In vertebrates, three central nervous structures have been identified to contain autonomous oscillators that are involved in the regulation of circadian rhythms: the retina, the pineal gland and the hypothalamus (Menaker et al., 1997). The relative contribution of these oscillators to the overall functioning of the circadian system at the whole-organism level varies among vertebrate species. In mammals, it is the hypothalamic oscillator that plays a major role in circadian organisation; it is located in a paired cell group in the hypothalamus, the suprachiasmatic nucleus (SCN) (van Esseveldt et al., 2000).

In birds, melatonin released from the pineal gland (e.g. songbirds) or from the retina and the pineal gland (e.g. galliform birds) appears to act as the major circadian coordinator and neural and physiological interactions of the retina, pineal gland, and hypothalamic oscillators determine circadian organisation at the whole-organism level (Gwinner and Brandstaetter, 2001; Brandstaetter, 2002; Brandstaetter, 2003). The two major input mechanisms to the hypothalamic circadian oscillators are light and melatonin; light can be perceived by photoreceptors found in the retina (mammals and birds), pineal gland (birds and lower invertebrates) and brain (birds and lower vertebrates) (Peirson et al., 2009). Pineal and retinal melatonin appear to inhibit activity in the hypothalamus during the dark phase, and the hypothalamus inhibits pineal melatonin production during the day (Karaganis et al., 2009).

Melatonin (5-methoxy-N-acetyltryptamine) is a small lipophilic hormone found in all living organisms from plants to humans (Carlberg, 2000) and has been found to be synthesized in both the retina (inner and outer retina) and the pineal gland (pinealocytes) of vertebrates. Early receptor studies revealed a wide distribution of 2-[^{125}I]iodomelatonin binding

throughout the chicken brain as compared to the rodent brain where binding was restricted to a few discrete areas (i.e. suprachiasmatic nucleus (SCN), periventricular nucleus (PVN) and median eminence (ME)) (Siuciak, et al., 1991). Melatonin binding in the chicken brain was most prominent in regions associated with the visual system, such as the visual SCN (vSCN), tectum opticum, and thalamofugal areas (Siuciak et al., 1991). In LD conditions, highest binding was found in the late afternoon (Zeitgeber time 10) and rhythmicity was shown to persist in constant conditions (Brooks and Cassone, 1992).

The biological effects of melatonin are produced through the activation of three melatonin receptor types, while other effects are due to its role as a pervasive and powerful antioxidant with a particular role in the protection of nuclear and mitochondrial DNA (Reiter et al. 2003; Rada and Wiechmann 2006; Dufourny et al., 2008). In 1994, the first membrane receptor was cloned from *Xenopus laevis* immortalized melanophores, which was sensitive to guanine nucleotides and its activation lead to an inhibition of adenylyl cyclase through a pertussis toxin-sensitive mechanism (Ebisawa et al., 1994). Since then, three melatonin receptor genes have been identified, melatonin receptor 1A (in mammals and non-mammalian vertebrates), 1B (in mammals and some non-mammalian vertebrates) and 1C (in non-mammalian vertebrates). All three receptors contain 7 hydrophobic transmembrane domains, and are linked to the guanine nucleotide binding proteins (G-protein-coupled) receptor superfamily (Ebisawa et al., 1994; Reppert, 1997). The main differences between the membrane receptor types are their kinetic and pharmacological properties for melatonin and its agonists: Mel-1A is a high affinity binding receptor, whereas the Mel-1B receptor has a low affinity for binding (Dubocovich 1995). Chicken Mel1A is 80% identical to human Mel1A (Reppert et al. 1995) and is the structural homolog of the mammalian MT1 receptor. Chicken Mel-1C receptor has an 80% homology to the Mel-1C found in Xenopus, and is 60% identical to the mammalian Mel-1A and -1B receptors (Reppert, 1997; Reppert et al. 1995). Mel-1C of lower vertebrates has an MT1-like pharmacology and receptor distribution suggests that melatonin may exert temporal control over a broad range of physiological and behavioural events in birds (Reppert et al., 1995; Sugden et al. 2004). Mel-1C has rapidly evolved from fishes and birds to mammals to the so-called GPR50 receptor that is believed to act as a modulator of melatonin responsiveness (Dufourny et al., 2008). There is a third transmembrane receptor (MT3) identified in mammals that is neither structurally nor physiologically comparable to the

receptors found in lower invertebrates; it has a 95% homology to human quinine reductase 2, a detoxification enzyme (Witt-Enderby et al., 2003).

Generally, removal of the pineal gland abolishes circadian rhythmicity of behaviour in songbirds highlighting the importance of circulating melatonin. Studies so far have looked at the removal of the whole gland (Gaston and Menaker, 1968), circulating plasma melatonin levels (Gwinner et al., 1997) and melatonin supplements (Heigl and Gwinner, 1995), but we still lack comprehensive information on the localisation and regulation of melatonin receptors in the brain of birds. The present study provides a first comprehensive investigation of melatonin receptor 1A (also referred to as Mel-1A, CKA MT1, MNRT1), 1B (also referred to as Mel1B, MT2, MTNR1B, ML1B) and 1C (also referred to as Mel1C, CKB) expression in the brain of a songbird, the zebra finch; we used the most frequently used non-mammalian nomenclature, i.e. Mel-1A, Mel-1B, and Mel-1C, in this paper as the present classification and nomenclature of melatonin receptors were applied only to mammalian receptors and there is no consensus on classifying nonmammalian receptors at present (Dubocovich et al., 2010).

MATERIALS AND METHODS

Animals and synchronisation

Adult male and female zebra finches were kept in light-tight and sound proof indoor aviaries with water and food *ad libitum* (Foreign finch diet seed, cuttlefish bone, mineralise grit and fresh fruit and vegetables). The aviaries were equipped with passive infrared sensors connected to a data acquisition computer system to record locomotor and feeding activities with CLOCKLAB software. The birds were kept in a light-dark cycle of 12hrs of bright light from 09:00h (ZT 0) to 21:00h (ZT12) and 12hrs of dim light (0.1lux) from 21:00h (ZT12) to 09:00h (ZT0) (LD12:12) for at least three weeks to ensure the birds where fully synchronised before tissue sampling. All experimental procedures were performed according to the UK home office regulations and international ethical standards (Portaluppi et al., 2010).

Tissue Sampling

Zebra finches were killed by dislocation of the neck and decapitation at six different time points over 24hrs (ZT 2, 6, 10, 14, 18, and 22). The brains (n = 6/ZT) were quickly removed from the skull; after the pineal gland was removed, the brain was dissected into the cerebellum, diencephalon, telencephalon, tectum opticum and the retina was sampled thereafter. For peripheral tissues, an incision was made along the chest bone and the rib cage was opened up and tissue samples of heart, liver, lungs and kidneys obtained. All tissues were immediately frozen on dry ice and then stored at -80°C until further use.

RNA extraction and cDNA synthesis

Total RNA was isolated by homogenising tissue samples with a ball mill (Mixer Mill MM 300, Retsch, Haan, Germany) following the protocol of Helfer et al. (2006). 3mm tungsten carbide beads were used to ensure full homogenisation of all tissue samples. The total RNA fractions from the samples were isolated using Trizol™ (Invitrogen Life Technologies, Carlsbad, USA). The resulting RNA samples were analysed by Nano-drop (Thermo Scientific, Wilmington, USA), Bioanalyzer RNA 6000 Nano assay (Agilent Technologies, Santa Clara, USA) and RNA gels. RNA samples were incubated with RNase-free DNase l (Roche Diagnostic, Mannheim, Germany) before 1.0µg aliquot of the resulting RNA was reverse transcribed using oligo(dT) primers. The product was then subjected to Reserve Transcription Polymerase Chain Reaction (RT-PCR) to amplify the cDNA content. Due to the small size of the avian pineal gland less than 1µg of total RNA was available for the first strand cDNA synthesis.

Amplification and Identification of zebra finch Mel-1A, Mel-1B and Mel -1C receptors cDNA

cDNA samples were taken from the diencephalon (DI) at time points ZT 6, 14 and 18. Primer pairs (Table. 1) were added to the relevant cDNA samples and amplified with RT-PCR using the Taq DNA Polymerase kit (Roche Diagnostics; thermocycler, Applied Bioscience, Gene Amp PCR system 9700) under the following conditions: 94^{o}C/2 min, 1 cycle; 94^{o}C/30seconds, 55^{o}C/30seconds, 72^{o}C/1min, 10 cycles; 94^{o}C/30seconds, 60^{o}C/30seconds,

72°C/1min (+ 5 sec to each subsequent run), 30 cycles; 72°C/7 min, 1 cycle; 4°C/hold. In every PCR reaction negative controls, i.e. no cDNA, were included to control for contamination. PCR products (n = 2/ZT 6, 14, 18) were separated on a 2% agarose gel and visualised on a UV light plate and dissected out. The DNA was extracted from the gel using gel extraction kit (QIAGEN, QIAquick gel extraction kit). The DNA sample from each band were ligated into a T-tail cloning vector, using pGEM-T easy vectors (Promega, Madison, USA). The plasmid vectors with the DNA insert were purified from transformed competent DH5α cell colonies by alkaline lysis (High pure plasmid isolation, Roche Diagnostics) and digested with EcORI (37°C for 55min). The relevant PCR products were sequenced, analysed and aligned using Chromas (Technelysium Pty Ltd), BioEdit (Ibis Biosciencs, Carlsbad, CA), NCBI Blast database (http://blast.ncbi.nlm.nih.gov/Blast.cgi), and Clustal W2 program (http://www.ebi.ac.uk/Tools/clustalw2).

Optimising RT-PCR conditions for Mel-1A, Mel-1B and Mel-1C receptors

PCR conditions were optimised to obtain amplified specific receptor PCR products in the linear phase of synthesis in three steps; Step 1: magnesium concentrations (0-2.5mM) and annealing temperatures (55°C, 57°C, 60°C, 62°C), Step 2: cycle numbers (10-42 cycles, every 2 cycle numbers were tested), and Step 3: cDNA dilution series . Optimised values for each gene primer pair are shown in Table 2.

Semi-quantitative Reserve Transcription-PCR (RT-PCR) for Melatonin receptors 1A, 1B and 1C

The PCR conditions were 94°C/2 min, 1 cycle; 94°C/30seconds, 55°C/30seconds, 72°C/1min, 1 cycles; 94°C/30seconds, X°C/1min, 72°C/1min (5 sec increments in each subsequent run), Y cycles; 72°C/7 min, 1 cycle; 4°C/hold (optimised X and Y values see Table 2). PCR products were run on an 8% polyacrylamide gel electrophoresis and stained with SYBR green I (Roche Diagnostics). The amplified products were quantified with a Gel Doc Imaging System in combination with Quantity One imaging analysing software (BioRad, Hercules,

USA). To correct for gel staining variation, the optical densities of each sample were compared to a 50bp DNA ladder (Fermentas) with known marker concentration.

The resulting data for each gene/time-point/tissue were normalised to TATA-box binding protein (TBP) values for the same tissue as previously described (Helfer et. al, 2006). Melatonin receptor gene expression was analysed by one-way factorial analysis of variance (ANOVA) using Tukey's honest significant difference (HSD) post hoc test. Polynomial fourth order non-linear regression and Lowess curves were fitted with GraphPad Prism software (GraphPad, San Diego, CA, USA) to compare expression patterns as previously described (Brandstaetter et al., 2000).

Declaration of Interest

The authors report no conflicts of interest.

RESULTS

Amplification and Identification of zebra finch Mel-1A, Mel-1B and Mel-1C receptors cDNA

Using RT-PCR, we successfully cloned and sequenced partial cDNA for melatonin receptors 1A (494bp), 1B (265bp) and 1C (463bp) in zebra finch brain tissues. The sequences were compared with other avian DNA sequences using NCBI blast database and analysed accordingly showing 96% to 99% nucleotide sequence identities to previously published avian melatonin receptor sequences (Table 3).

Semi-quantitative RT-PCR for Melatonin receptors 1A, 1B and 1C in the zebra finch brain

Mel1A mRNA showed robust significant rhythmicity in two of the circadian oscillator regions, i.e. diencephalon and retina, with peak expression levels between ZT18 and ZT22 (ANOVA, $F_{5,27}$=8.210, p=0.0002 for diencephalon, $F_{5,25}$=5.836, p=0.0018 for retina). No

clear rhythmicity could be detected in the pineal gland with *Mel-1A* mRNA levels being low near the detection limit throughout light and dark phases (Fig. 1). *Mel-1B* mRNA was rhythmically expressed in all three of the oscillator regions with peak expression times of ZT22 to ZT2 in the diencephalon (ANOVA, $F_{5,20}$=7.010, p=0.0015), ZT22 in the pineal gland (ANOVA, $F_{5,19}$=4.233, p=0.0149), and ZT10 in the retina (ANOVA, $F_{5,24}$=4.446, p=0.0075) (Fig. 2). *Mel-1C* mRNA was present in all three oscillatory regions but did not show any rhythmicity (Fig. 3).

In the tectum opticum, *Mel-1A* mRNA was rhythmically expressed with low levels during the day and high levels during the dark phase with significant peak expression from ZT 18 to ZT 22 (ANOVA, $F_{5,31}$=8.944, p<0.0001) comparable to the cerebellum (ANOVA, $F_{5,32}$=3.170, p=0.0223) and the telencephalon (ANOVA, $F_{5,34}$=3.981, p=0.0072) (Fig. 1).

In the tectum opticum (ANOVA, $F_{5,20}$=5.752, p=0.004), cerebellum (ANOVA, $F_{5,16}$=5.079, p=0.001), and telencephalon, *Mel-1B* mRNA showed biphasic patterns of rhythmic expression with peak expression levels during the light phase as well as during the dark phase. While peak expression levels for *Mel-1B* mRNA were at ZT2 and ZT14 in the tectum opticum, i.e. two hours after the onset of light and two hours after the onset of darkness, peak expression levels in the cerebellum were reached at ZT2 and ZT 18 (Fig. 2). A similar pattern was observed in the telencephalon where expression values were found not to be significantly rhythmic.

Intermediate to high absolute *Mel-1C* mRNA levels could be found throughout the brain but without any clear signs of rhythmicity in any of the parts of the brain that were studied (Fig. 3). Absolute mRNA levels were comparable in all parts of the brain for *Mel-1A* while peak levels of *Mel-1B* where about four times higher in the retina as compared to all other parts of the brain.

Semi-quantitative RT-PCR for Melatonin receptors 1A, 1B and 1C in zebra finch peripheral tissues

To reveal whether similar patterns of melatonin receptor expression were detectable in peripheral tissues, melatonin receptor expression was also analysed in the heart, liver, lung

and kidney of the zebra finch. *Mel-1A* receptor mRNA levels in heart, lung and kidney were low and arrhythmic while there was a significant rhythm in the liver with peak expression at ZT2 (ANOVA, $F_{5,35}$=4.321, p=0.0044), two hours after the onset of light (Fig. 4).

Interestingly, three out of the four studied peripheral tissues showed significant *Mel-1B* receptor rhythms with tissue-specific peak expression times. In the heart, expression levels were high throughout the light period with peak expression at ZT2 and ZT10 (ANOVA, $F_{5,24}$=7.582, p=0.0005). Similarly, liver *Mel-1B* mRNA was significantly elevated throughout the light phase as compared to darkness (ANOVA, $F_{5,25}$=12.32, p<0.0001). In variance to heart and liver, lung *Mel1B* mRNA showed peak expression times at ZT10 and ZT12, i.e. at the transition from light to dark (ANOVA, $F_{5,27}$=8.591, p=0.0001). Although *Mel-1B* levels in the kidney were variable during the 24-hr cycle studied, no significant rhythm could be detected (Fig. 5).

Mel-1C receptor expression showed no apparent rhythmicity in either heart, liver or lung while there was a significant diurnal rhythm found in the kidney with peak expression levels at ZT2 (ANOVA, $F_{5,15}$= 5.449, p=0.01) (Fig. 6).

Absolute mRNA levels indicate clear differences in melatonin receptor density between tissues with *Mel-1A* being generally low in all peripheral tissues, *Mel-1B* showing high mRNA levels in heart, lung, and liver, and *Mel-1C* being highest in liver and kidney.

DISCUSSION

So far, melatonin studies in birds have mostly concentrated on plasma melatonin levels and behavioural effects of exogenous melatonin on physiology and behaviour. Studies on avian melatonin receptors mainly focused on the retina (Rada and Wiechmann, 2006), gonads (Aste et al., 2001) and song-control nuclei in the brain (Cassone et al., 2008; Whitfield-Rucker and Cassone, 1996) while localisation of melatonin receptors in the brain and rhythmicity of expression received very little attention. We cloned three melatonin membrane receptors in the zebra finch, *Mel-1A, Mel-1B* and *Mel-1C*, that show amino acid sequence homologies of 98-99% to previously published zebra finch melatonin receptors (Jansen et al., 2005); we found all of these melatonin receptor types to be expressed in all major divisions of the brain

as well as in all peripheral tissues studied. This is in remarkable contrast to the very restricted distribution of melatonin receptors in the mammalian brain. As compared to all other vertebrate classes, mammals have lost photosensitivity of the pineal gland as well as the circadian clock in the pineal gland, and have one dominant circadian brain oscillator, i.e. the suprachiasmatic nucleus, that controls pineal synthesis and secretion of nocturnal melatonin; photoreception takes place in the retina only and there has been an evolutionary loss of two retinal cone classes (Barrett et al., 2003) and of certain opsins which are found in non-mammalian vertebrates including birds and fishes (Bellingham et al., 2003). These differences in circadian organisation are believed to be the consequence of a "nocturnal bottleneck" during early evolution of mammals (Foster et al., 1993). The striking difference in melatonin receptor distribution between birds and mammals is another sign of the different evolutionary circadian paths of mammals as compared to non-mammalian vertebrates. The ubiquituous presence of all melatonin receptor types throughout the brain and in all peripheral tissues of the zebra finch supports the hypothesis that melatonin acts as the major coordinator of circadian organisation at the whole-organism level in non-mammalian vertebrates such as birds. Non-mammalian vertebrates, including birds, possess complex circadian systems with multiple photic input mechanisms and multi-oscillator control of circadian rhythmicity with melatonin being believed to act as the major driver of coordinated circadian rhythmicity at the whole-organism level (Gwinner & Brandstaetter, 2001). We found *Mel-1A*, *Mel-1B* and *Mel-1C* receptor mRNA expression in all parts of the avian brain that have been shown to contain autonomous circadian clocks, i.e. retina, pineal gland and diencephalon. *Mel-1A* and *Mel-1B* were found to be rhythmic in the retina and diencephalon while although *Mel-1C* was found in these tissues its expression was not rhythmic. *Mel-1B* was found to be rhythmic in the pineal gland in contrast to *Mel-1A* and *Mel-1C* mRNA. *Mel-1A* mRNA was found to show nocturnal rhythms with peak expression levels during the second half of the night in all parts of the brain apart from the pineal gland. *Mel-1B* receptor expression was most variable with nocturnal rhythms in the pineal gland and the diencephalon reaching highest levels at the end of the night and the transition from dark to light, a diurnal rhythm in the retina, and biphasic expression patterns in the tectum opticum, cerebellum, and telencephalon. *Me-l1C* receptor was not found to be rhythmic in any of the brain regions studied although considerable mRNA levels were present. These results show the widespread distribution of all melatonin

receptors in the avian brain and suggest tissue-specific regulation of melatonin receptor expression.

The non-rhythmic but considerable expression of *Mel-1C* in all tissues studied is another remarkable outcome of this study. To exert full physiological action, melatonin receptors may form functional dimers (Ayoub et al., 2002) and it has been shown that the mammalian GPR50 receptor modulates the function of mammalian MT1 and MT2 receptors (Levoye et al. 2006). Our results showing the ubiquitous presence of all three receptors throughout the brain and in all peripheral tissues studied suggests that the modulatory role of Mel-1C/GPR50 found in mammals may also be important in birds with Mel1C possibly being the partner of the Mel1A/Mel1B receptor heterodimers. Rhythmic expression of either *Mel-1A* or *Mel-1B* or both was indeed what we found in our study in all parts of the brain and in all peripheral organs. Strikingly, the only tissue where neither *Mel-1A* nor *Mel-1B* mRNA was rhythmically expressed was the kidney where rhythmic *Mel-1C* receptor expression was found instead.

In passerine birds, such as the zebra finch and house sparrow, the only source of circulating melatonin is the pineal gland (Brandstaetter, 2002). As melatonin production is controlled by an autonomous circadian clock in songbirds, one would predict that there would be no melatonin membrane receptors found in this gland unless they serve auto-regulatory feedback. Our data set confirms that all three melatonin receptors are present in the pineal gland with *Mel-1B* being the only receptor that was rhythmically expressed. Interestingly, pineal *Mel-1B* receptor expression appears to peak at the end of the dark phase (ZT 22) when melatonin production declines suggesting that *Mel-1B* receptors may indeed act as negative feedback and contribute to the termination of melatonin production at the end of the night.

Interestingly, melatonin receptor expression mirrors nocturnal circulating melatonin in some but not all tissues; while *Mel-1A* receptor expression reflects the presence of nocturnal melatonin in the diencephalon, retina, tectum opticum, cerebellum, and telencephalon with peak expression levels during the second half of the night, *Mel-1B* expression shows considerable variability between brain regions, and *Mel-1C* does not appear to be rhythmically expressed at all. The overall differences in absolute melatonin receptor mRNA levels are comparable with the findings of Reppert et al. (1995) in the chicken where no Mel1A was found within the cerebellum, liver, or pineal gland but within the diencephalon, telencephalon, retina and tectum opticum while high concentration of *Mel-1B* were detected

in the tectum opticum, hypothalamus, thalamus and pineal gland and low *Mel-1B* concentration were found in the cerebellum and retina but not in the liver (Reppert et al., 1995).

Rada and Wiechmann (2006) identified all three melatonin receptor types in the chicken retina-RPE-choroid and found Mel-1A and Mel-1B to have similar expression patterns with low levels occurring in the early morning and highest levels in the evening (Mel-1A peaked at ZT12 (lights off) and Mel-1B peaked at ZT20 (mid-late dark period) while Mel-1C showed out-of-phase oscillation to Mel-1A and Mel-1B with high levels in the early morning and low levels during the early-mid dark phase (ZT16). Chicken retinal *Mel-1A* mRNA has been found to be rhythmic under light/dark (LD) cycles and in constant darkness (DD), peaking at midday and mid-subjective day (Natesan and Cassone 2002). Chicken retinal *Mel-1C* mRNA was also found to be rhythmic in LD with high expression levels during the day but opposite phasing in DD while *Mel-1B* was highly variable and arrhythmic (Natesan and Cassone, 2002). A comparison of our mRNA data with melatonin receptor protein levels in the chicken retina revealed certain differences in peak expression times; while the *Mel-1A* receptor was found to peak at ZT12 at the transition from light to dark, *Mel-1B* peaked at ZT20, and *Mel-1C* at ZT0 in the chicken retina (Rada & Wiechmann, 2006) we found mRNA in the retina to peak at ZT18 (*Mel-1A*), ZT10 (*Mel1B*), and *Mel1C* mRNA to be arrhythmic. These differences could be caused by differential expression of melatonin receptors in the different layers of the retina as both studies used whole tissue samples or by species-specific differences between the role the retina plays in galliform and passeriform circadian organisation (Brandstaetter, 2002).

Generally, the actions of melatonin at the cellular level are very complex due to the presence of several receptor types with different affinities for melatonin, due to complex interaction mechanisms between the receptors, and due to possible melatonin action via membrane receptors but also nuclear and cytosolic binding (Reiter et al. 2003; Levoye et al., 2006; Rada and Wiechmann 2006). In mammals, the MT1 receptor has been implicated in inhibiting neuronal firing within the SCN (Dubocovich, 2007) possibly due to the inhibitory responses on the cAMP signal transduction cascade by decreasing PKA activity and CREB phosphorylation (Witt-Enderby et al., 2003). MT1 has also been shown to inhibit the induction of c-fos and junB mRNA and c-fos translation (Witt-Enderby et al., 2003).

Circadian phase shifting of the neuronal firing rhythms, however, has been linked to the activation of MT2 receptor (Dubocovich, 2007) and recent findings indicate that melatonin mainly acts by altering neuronal excitability in SCN neurons by modulating inhibitory GABAergic transmission within the SCN (Scott et al., 2010). In contrast to mammals, very little is known about the physiological cellular effects of melatonin in birds but there is clear evidence that the pineal melatonin rhythm acts on at least one other oscillator within the circadian pacemaking system, presumably the hypothalamic clock, which in turn feeds back onto the pineal gland (Gwinner and Brandstaetter, 2001).

In variance to melatonin receptor expression in the brain of the zebra finch, peripheral tissues showed considerable variability; while liver showed rhythmic *Mel1A* and *Mel1B* expression, only *Mel1B* receptor mRNA was found to be rhythmically expressed in lung and heart. Interestingly, kidney, as the only tissue in this study, showed a *Mel1C* receptor rhythm which is of particular interest regarding its possible role as a modulator of melatonin receptor function (Levoye et al., 2006). Peripheral tissues also differed in regard of the temporal organisation of melatonin receptor expression. While *Mel1A* in the liver and *Mel1C* in the heart peak early in the day when circulating melatonin has already declined to baseline levels (Brandstaetter et al., 2001), *Mel1B* is elevated throughout the day in heart and liver but peaks at the transition from light to dark in the lung. These data suggest complex control mechanisms of melatonin receptor expression in peripheral organs and diurnal rhythms of melatonin responsiveness that may relate to the rhythm of circulating melatonin (Gwinner & Brandstaetter, 2001; Van't Hof & Gwinner, 1999).

In summary, our results represent a first comprehensive analysis of all three melatonin receptors at the mRNA level in a songbird species, the zebra finch. Although we cannot conclude on the physiological effects of melatonin nor on the dynamics of melatonin receptors at the protein level at present, we show brain region-specific and peripheral tissue-specific rhythms of two of the melatonin receptors *Mel-1A* and *Mel-1B* while *Mel-1C* receptor was present throughout the brain and in all peripheral tissues studied but no rhythmic expression pattern was found apart from one peripheral tissue, the kidney. Our results show very clearly that melatonin, in strong contrast to mammals, has the general ability to exert its actions throughout the brain and body in birds via all three receptor types. The differences in temporal regulation and overall receptor levels as indicated by our mRNA data set suggest

tissue-specific melatonin action in the different parts of the brain and in peripheral organs. The presence of each of the three receptor types in every tissue studied suggests widespread melatonin responsiveness throughout the brain and body of birds and has to be considered in future physiological and behavioural experiments to elucidate the multiple roles melatonin may play in co-ordinating circadian organisation at the whole-organism level in birds.

ACKNOWLEDGEMENTS

Financial support was provided by the Max Planck Society and the Biotechnology and Biological Sciences Research Council. We gratefully acknowledge information on melatonin receptor sequence data provided by M. Gahr (Max-Planck-Institute of Ornithology).

REFERENCES

Aste N, Cozzi B, Stankov B, Panzica G. (2001). Sexual differences and effect of photoperiod on melatonin receptor in avian brain. *Microsc. Res. Tech.* 55: 37-47.

Ayoub MA, Couturier C, Lucas-Meunier E, Angers S, Fossier P, Bouvier M, Jockers R (2002). Monitoring of ligand-independent dimerization and ligand-induced conformational changes of melatonin receptors in living cells by bioluminescence resonance energy transfer. *J. Biol. Chem.* 277: 21522-21528.

Barrett P, Conway S, Morgan PJ. (2003). Digging deep – structure–function relationships in the melatonin receptor family. *J. Pineal Res.* 35: 221-230.

Bellingham J, Wells DJ, Foster RG. (2003). In silico characterisation and chromosomal localisation of human RRH (peropsin) – implications for opsin evolution. *BMC Genomics* 4: 3.

Brandstaetter R. (2003). Encoding time of day and time of year by the avian circadian system. *J.Neuroendocrinol.* 15: 398-404.

Brandstaetter R. 2002. The Circadian Pacemaking System of Birds. In: *Biological Rhythms* (Ed) V Kumar: 144-163.

Brandstaetter R, Kumar V, Abraham U, Gwinner E (2000). Photoperiodic information acquired and stored in vivo is retained in vitro by a circadian oscillator, the avian pineal gland. *Proc. Natl. Acad. Sci. U S A.* 97:12324-12328.

Brandstaetter R, Kumar V, Van'T Hof TJ, Gwinner E. (2001). Seasonal variations of in vivo and in vitro melatonin production in a passeriform bird, the house sparrow (*Passer domesticus*). *J. Pineal Res.* 31: 120-126.

Brooks DS, Cassone VM. (1992). Daily and circadian regulation of 2-[125]iodomelatonin binding in the chick brain. *Endocrinol*. 131: 1297-1304.

Carlberg C. (2000). Gene Regulation by Melatonin. *Ann. New York Acad.Sci.* 917: 387-396.

Cassone VM, Bartell PA, Earnest BJ, Kumar V. (2008). Duration of Melatonin Regulates Seasonal Changes in Song Control Nuclei of the House Sparrow, *Passer domesticus*: Independence from Gonads and Circadian Entrainment. *J. Biol. Rhythms* 23: 49-58.

Dubocovich ML. (1995). Melatonin receptors: Are there multiple subtypes? *Trends Pharmacol. Sci.* 16: 50-56.

Dubocovich ML, Delagrange P, Krause DN, Sugden D, Cardinali DP, Olcese J. International Union of Basic and Clinical Pharmacology. (2010). LXXV. Nomenclature, classification, and pharmacology of G protein-coupled melatonin receptors. *Pharmacol Rev.* 62: 343-380.

Dubocovich ML. (2007) Melatonin receptors: role on sleep and circadian rhythm regulation. *Sleep Med.* 8, Suppl 3: 34-42.

Dufourny L, Levasseur A, Migaud M, Callebaut I, Pontarotti P, Malpaux B,

Monget P. (2008) GPR50 is the mammalian ortholog of Mel1c: evidence of rapid evolution in mammals. *BMC Evol. Biol.* 8: 105.

Ebisawa T, Karne S, Lerner MR, Reppert SM. (1994). Expression cloning of a high-affinity melatonin receptor from Xenopus dermal melanophores. *Proc. Natl. Acad. Sci. USA* 91: 6133-6137.

Foster RG, Garcia-Fernandez JM, Provencio I, DeGrip WJ. (1993). Opsin localization and chromophore retinoids identified within the basal brain of the lizard Anolis carolinensis. *J. Comp. Physiol. A.* 172: 33-45.

Gaston S, Menaker M. (1968). Pineal Function: The Biological Clock in the Sparrow? *Science* 160: 1125-1127.

Gwinner E, Brandstaetter R. (2001). Complex bird clocks. *Philos. Trans. R. Soc. Lond. B Biol. Sci.* 356: 1801-1810.

Gwinner E, Hau M, Heigl S. (1997). Melatonin: Generation and Modulation of Avian Circadian Rhythms. *Brain Res. Bull.* 44: 439-444.

Heigl S, Gwinner E. (1995). Synchronization of Circadian Rhythms of House Sparrows by Oral Melatonin: Effects of Changing Period. *J. Biol. Rhythms* 10: 225-233.

Helfer G, Fidler AE, Vallone D, Foulkes ND, Brandstaetter R. (2006). Molecular Analysis of Clock Gene Expression in the Avian Brain. *Chronobiol. Int.* 23: 113 - 127.

Jansen R, Metzdorf R, van der Roest M, Fusani L, ter Maat A, Gahr M. (2005). Melatonin affects the temporal organization of the song of the zebra finch. *FASEB J.* 19: 848-850.

Karaganis SP, Bartell PA, Shende VR, Moore AF, Cassone VM. (2009). Modulation of metabolic and clock gene mRNA rhythms by pineal and retinal circadian oscillators. *Gen. Comp. Endocrinol.* 161: 179-192.

Levoye A, Dam J, Ayoub MA, Guillaume JL, Couturier C, Delagrange P, Jockers R. (2006) The orphan GPR50 receptor specifically inhibits MT1 melatonin receptor function through heterodimerization. *EMBO J.* 25: 3012-3023.

Menaker M, Moreira LF, Tosini G.(1997). Evolution of circadian organization in vertebrates. *Braz J Med Biol Res.* 30: 305-313.

Natesan A, Cassone VM. (2002). Melatonin receptor mRNA localization and rhythmicity in the retina of the domestic chick, *Gallus domesticus*. *Visual Neurosci.* 19: 265-274.

Peirson SN, Halford S, Foster RG. (2009) The evolution of irradiance detection: melanopsin and the non-visual opsins. *Philos. Trans. R. Soc. Lond. B Biol. Sci.* 364: 2849-2865.

Pittendrigh CS. (1993). Temporal organization: reflections of a Darwinian clock-watcher. *Annu. Rev. Physiol.* 55: 16-54.

Portaluppi F, Smolensky MH, Touitou Y. (2010) Ethics and methods for biological rhythm research on animals and human beings. *Chronobiol. Int.* 27:1911-1929.

Rada JAS, Wiechmann AF. (2006). Melatonin Receptors in Chick Ocular Tissues: Implications for a Role of Melatonin in Ocular Growth Regulation. *Invest. Ophthalmol. Visual Sci.* 47: 25-33.

Reiter RJ, Tan DX, Mayo JC, Sainz RM, Leon J, Czarnocki Z. (2003). Melatonin as an antioxidant: biochemical mechanisms and pathophysiological implications in humans. *Acta Biochim. Polon.* 50: 1129-1146.

Reppert SM. (1997). Melatonin Receptors: Molecular Biology of a New Family of G Protein-Coupled Receptors. *J. Biol. Rhythms.* 12: 528-531.

Reppert SM, Weaver DR, Cassone VM, Godson C, Kolakowski LF. (1995). Melatonin Receptors Are for the Birds: Molecular Analysis of Two Receptor Subtypes Differentially Expressed in Chick Brain. *Neuron* 15: 1003-1015.

Scott FF, Belle MD, Delagrange P, Piggins HD. (2010) Electrophysiological effects of melatonin on mouse Per1 and non-Per1 suprachiasmatic nuclei neurones in vitro. *J Neuroendocrinol.* 22: 1148-1156.

Sugden D, Davidson K, Hough KA, Teh MT. (2004). Melatonin, Melatonin Receptors and Melanophores: A Moving Story. *Pigment Cell Res.* 17: 454-460.

Siuciak J, Krause D, Dubocovich M. (1991). Quantitative pharmacological analysis of 2-[125I]-iodomelatonin binding sites in discrete areas of the chicken brain. *J. Neurosci.* 11: 2855-2864.

Van Esseveldt KE, Lehman MN, Boer GJ. (2000). The suprachiasmatic nucleus and the circadian time-keeping system revisited. *Brain Res. Rev.* 33: 34-77.

Van't Hof TJ, Gwinner E. (1999). Influence of pinealectomy and pineal stalk deflection on circadian gastrointestinal tract melatonin rhythms in zebra finches (*Taeniopygia guttata*). J. Biol. Rhythms. 14: 185-189.

Whitfield-Rucker MG, Cassone VM. (1996). Melatonin Binding in the House Sparrow Song Control System: Sexual Dimorphism and the Effect of Photoperiod. *Horm. Behav.* 30: 528-537.

Witt-Enderby PA, Bennett J, Jarzynka MJ, Firestine S, Melan MA. (2003). Melatonin receptors and their regulation: biochemical and structural mechanisms. *Life Sci.* 72: 2183-2198.

Table 1. Primer sequences and predicted product length used to clone melatonin receptors Mel-1A, Mel-1B and Mel-1C from zebra finch cDNA templates. The Mel-1B primers are based on the published zebra finch Mel-1b receptor sequence (NM_001048258). The Mel-1A

and Mel-1C primers are based on sequences published on house sparrow (Mel-1A - AY155489 and Mel-1C - AY743658).

Table 2. Primer sequences and optimised PCR conditions for the Mel-1A, Mel-1B and Mel-1C partial cDNA gene homologues.

Table 3. Percentage nucleotide sequence identity of cloned Melatonin receptors Mel-1A, Mel-1B and Mel-1C from Zebra Finch diencephalon tissue cDNA at time points ZT=14 (CLON 2.1), ZT=6 (CLON 4.2) and ZT=14 (CLON 5.2).

Figure 1. Expression profiles of *Melatonin receptor 1A* mRNA of zebra finch brain tissues. Temporal expression of normalised data (A-F), i.e. relative mRNA values normalised to *TBP* mRNA expression shown as variation from mean value, and (G-L) absolute mRNA values, i.e. raw data. The bars at the top of each graph indicate the LD 12:12 hrs light/dark schedule the birds were exposed to. The symbols represent mean values for each time point ± SEM (n=4-6). ZT2 and ZT22 are double plotted for better visualisation. Fourth order polynomial (dashed line) and lowess (black line) curves were fitted with GraphPad prism. Significant differences as revealed by ANOVA indicated by * on figure letter; significant differences between times points, i.e. to the lowest value of mRNA expression, as revealed by post hoc Tukey test indicated by * above the corresponding symbols: *$p<0.05$, **$p<0.01$, ***$p<0.001$. X-axis: Zeitgeber time in hrs.

Figure 2. Expression profiles of Melatonin receptor 1B mRNA of zebra finch brain tissues. Temporal expression of normalised data (A-F), i.e. relative mRNA values normalised to *TBP* mRNA expression shown as variation from mean value, and (G-L) absolute mRNA values, i.e. raw data. The bars at the top of each graph indicate the LD 12:12 hrs light/dark schedule the birds were exposed to. The symbols represent mean values for each time point ± SEM (n=4-6). ZT2 and ZT22 are double plotted for better visualisation. Fourth order polynomial (dashed line) and lowess (black line) curves were fitted with GraphPad prism. Significant differences as revealed by ANOVA indicated by * on figure letter; significant differences between times points, i.e. to the lowest value of mRNA expression, as revealed by post hoc Tukey test indicated by * above the corresponding symbols: *$p<0.05$, **$p<0.01$, ***$p<0.001$. X-axis: Zeitgeber time in hrs.

Figure 3. Expression profiles of Melatonin receptor 1C mRNA of zebra finch brain tissues. Temporal expression of normalised data (A-F), i.e. relative mRNA values normalised to *TBP* mRNA expression shown as variation from mean value, and (G-L) absolute mRNA values, i.e. raw data. The bars at the top of each graph indicate the LD 12:12 hrs light/dark schedule the birds were exposed to. The symbols represent mean values for each time point ± SEM

(n=4-6). ZT2 and ZT22 are double plotted for better visualisation. Fourth order polynomial (dashed line) and lowess (black line) curves were fitted with GraphPad prism. Significant differences as revealed by ANOVA indicated by * on figure letter; significant differences between times points, i.e. to the lowest value of mRNA expression, as revealed by post hoc Tukey test indicated by * above the corresponding symbols: *p<0.05, **p<0.01, ***p<0.001. X-axis: Zeitgeber time in hrs.

Figure 4. Expression profiles of Melatonin receptor 1A mRNA of zebra finch peripheral tissues. Temporal expression of normalised data (A-D), i.e. relative mRNA values normalised to *TBP* mRNA expression shown as variation from mean value, and (E-H) absolute mRNA values, i.e. raw data. The bars at the top of each graph indicate the LD 12:12 hrs light/dark schedule the birds were exposed to. The symbols represent mean values for each time point ± SEM (n=4-6). ZT2 and ZT22 are double plotted for better visualisation. Fourth order polynomial (dashed line) and lowess (black line) curves were fitted with GraphPad prism. Significant differences as revealed by ANOVA indicated by * on figure letter; significant differences between times points, i.e. to the lowest value of mRNA expression, as revealed by post hoc Tukey test indicated by * above the corresponding symbols: *p<0.05, **p<0.01, ***p<0.001. X-axis: Zeitgeber time in hrs.

Figure 5. Expression profiles of Melatonin receptor 1B mRNA of zebra finch peripheral tissues. Temporal expression of normalised data (A-D), i.e. relative mRNA values normalised to *TBP* mRNA expression shown as variation from mean value, and (E-H) absolute mRNA values, i.e. raw data. The bars at the top of each graph indicate the LD 12:12 hrs light/dark schedule the birds were exposed to. The symbols represent mean values for each time point ± SEM (n=4-6). ZT2 and ZT22 are double plotted for better visualisation. Fourth order polynomial (dashed line) and lowess (black line) curves were fitted with GraphPad prism. Significant differences as revealed by ANOVA indicated by * on figure letter; significant differences between times points, i.e. to the lowest value of mRNA expression, as revealed by post hoc Tukey test indicated by * above the corresponding symbols: *p<0.05, **p<0.01, ***p<0.001. X-axis: Zeitgeber time in hrs.

Figure 6. Expression profiles of Melatonin receptor 1C mRNA of zebra finch peripheral tissues. Temporal expression of normalised data (A-D), i.e. relative mRNA values normalised to *TBP* mRNA expression shown as variation from mean value, and (E-H) absolute mRNA values, i.e. raw data. The bars at the top of each graph indicate the LD 12:12 hrs light/dark schedule the birds were exposed to. The symbols represent mean values for each time point ± SEM (n=4-6). ZT2 and ZT22 are double plotted for better visualisation.

Fourth order polynomial (dashed line) and lowess (black line) curves were fitted with GraphPad prism. Significant differences as revealed by ANOVA indicated by * on figure letter; significant differences between times points, i.e. to the lowest value of mRNA expression, as revealed by post hoc Tukey test indicated by * above the corresponding symbols: *p<0.05, **p<0.01, ***p<0.001. X-axis: Zeitgeber time in hrs.

Table 1

Gene	**Primer Pair**	**Predicted Product length**
Mel-1A	Forward: 5'- TGCCACAG(C/T)CTCA(A/G)(A/G)TA(C/T)GAC-3' Reverse: 5'- AT(T/C/G)GC(A/G)ATT(A/G)AGGCAGCTGTTGA-3'	500bp
Mel-1B	Forward: 5'-GACAAAGTGTACAGCTGTTGG-3' Reverse: 5'-CTGATTTGACTCGTCTTCGAAC-3'	265bp
Mel-1C	Forward: 5'- TGCT(A/G)CATCTGCCACAGCCT-3' Reserve: 5'-(GCT(C/T)A(G/A)(G/A)ACAAA(A/C)AGCCA(T/C)TCTG-3'	463bp

Table 2

Gene	RT-PCR Primer	Product length	Tm (X°C)	Cycle No. (Y)	Mg^{2+} Conc
Mel-1A	Forward: 5'-CCACAGTCTCAGATACGACAAGC-3' Reserve: 5'-ACCCTTCGCCTTACCTGGATAAC-3'	276	62°C	26	2mM
Mel-1B	Forward: 5'-GACAAAGTGTACAGCTGTTGG-3' Reserve: 5'-CTGATTTGACTCGTCTTCGAAC-3'	265	60°C	27	2mM
Mel-1C	Forward: 5'-TCTGCCTGACCTGGATACTCAC-3' Reserve: 5'- CTGCTTGCAGTCTTGTCTCACC-3'	239	62°C	27	1.5mM

Table 3

Cloned DNA sequence	Melatonin Receptor (GenBank accession number)	Species	Percentage Identity
Mel-1A Receptor	Mel-1A receptor mRNA; complete cds (NM_001048257.1)	Taeniopygia guttata (Zebra Finch)	98%
	Mel-1A receptor mRNA; partial cds (AY155489.1)	Passer domesticus (House Sparrow)	97%
	Mel-1A melatonin receptor mRNA, complete cds (GGU31820)	Gallus gallus (Chicken)	89%
	Melatonin receptor 1A (MTNR1A) mRNA, complete cds (EU432127.1)	Homo sapien (human)	76%
Mel-1B Receptor	Mel-1b melatonin receptor mRNA, complete cds (DQ178665)	Taeniopygia guttata (Zebra Finch)	99%

	Mel-1b melatonin receptor mRNA, partial cds (DQ178663.1)	Sylvia atricapilla (Blackcap)	96%
	Melatonin receptor 1b mRNA, partial cds (EF197909.1)	Gallus gallus (Chicken)	90%
	Melatonin 1b receptor, complete cds (AB033598.2)	Homo sapien (Human)	74%
Mel-1C Receptor	Mel-1C receptor mRNA; partial cds (AY803773.1)	Taeniopygia guttata (Zebra Finch)	99%
	Mel-1C receptor mRNA; partial cds (AY743658.1)	Passer domesticus (House Sparrow)	98%
	Mel-1C melatonin receptor mRNA, complete cds (U31821.1)	Gallus gallus (Chicken)	92%
	G protein-coupled receptor 50 (GPR50), mRNA (NM_004224)	Homo sapien (Human)	67%

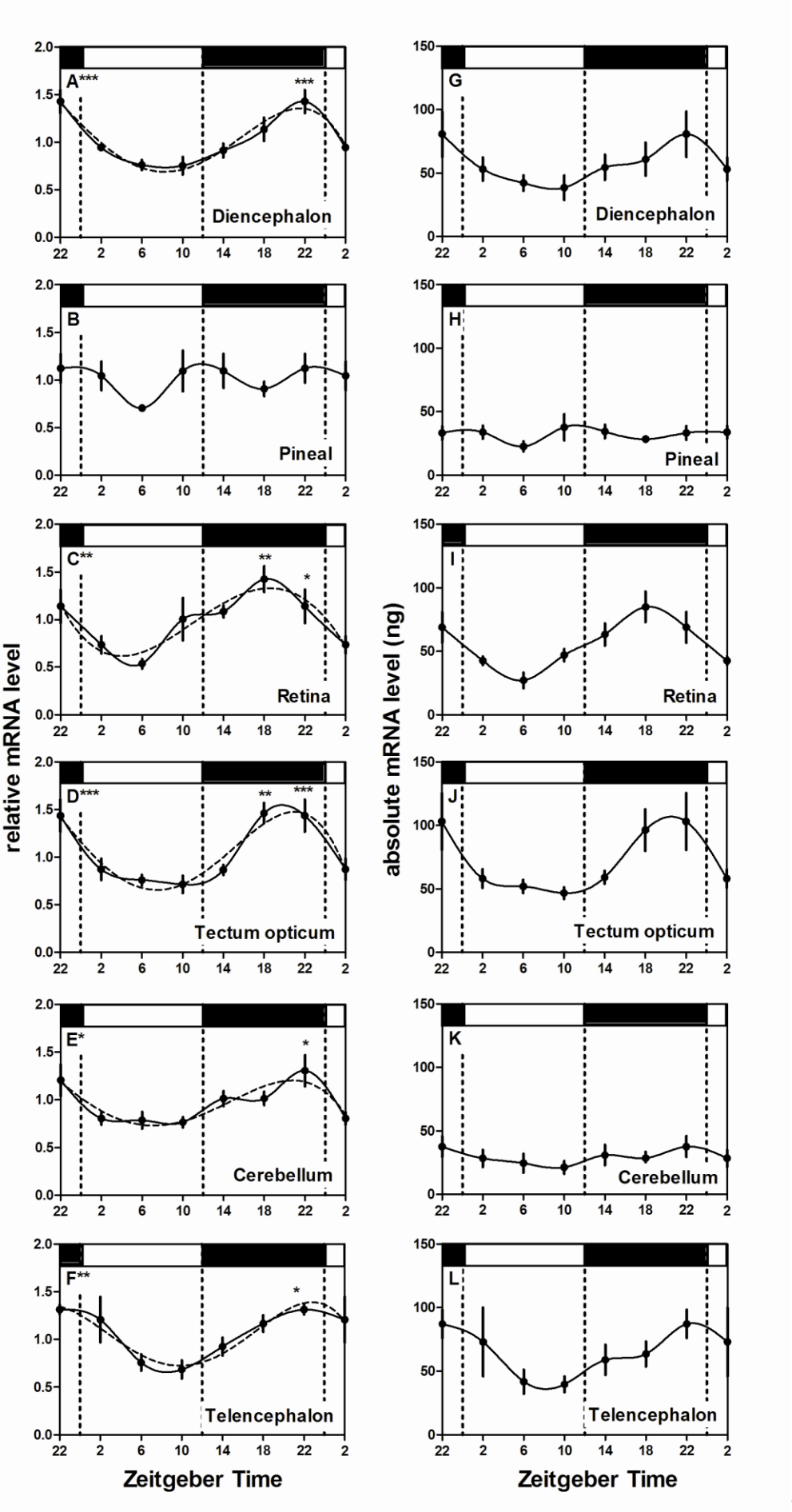
A***
***
Diencephalon
G
Diencephalon
B
Pineal
H
Pineal
C**
**
*
Retina
I
Retina
D***
**
***
Tectum opticum
J
Tectum opticum
E*
*
Cerebellum
K
Cerebellum
F**
*
Telencephalon
L
Telencephalon
relative mRNA level
absolute mRNA level (ng)
Zeitgeber Time
Zeitgeber Time

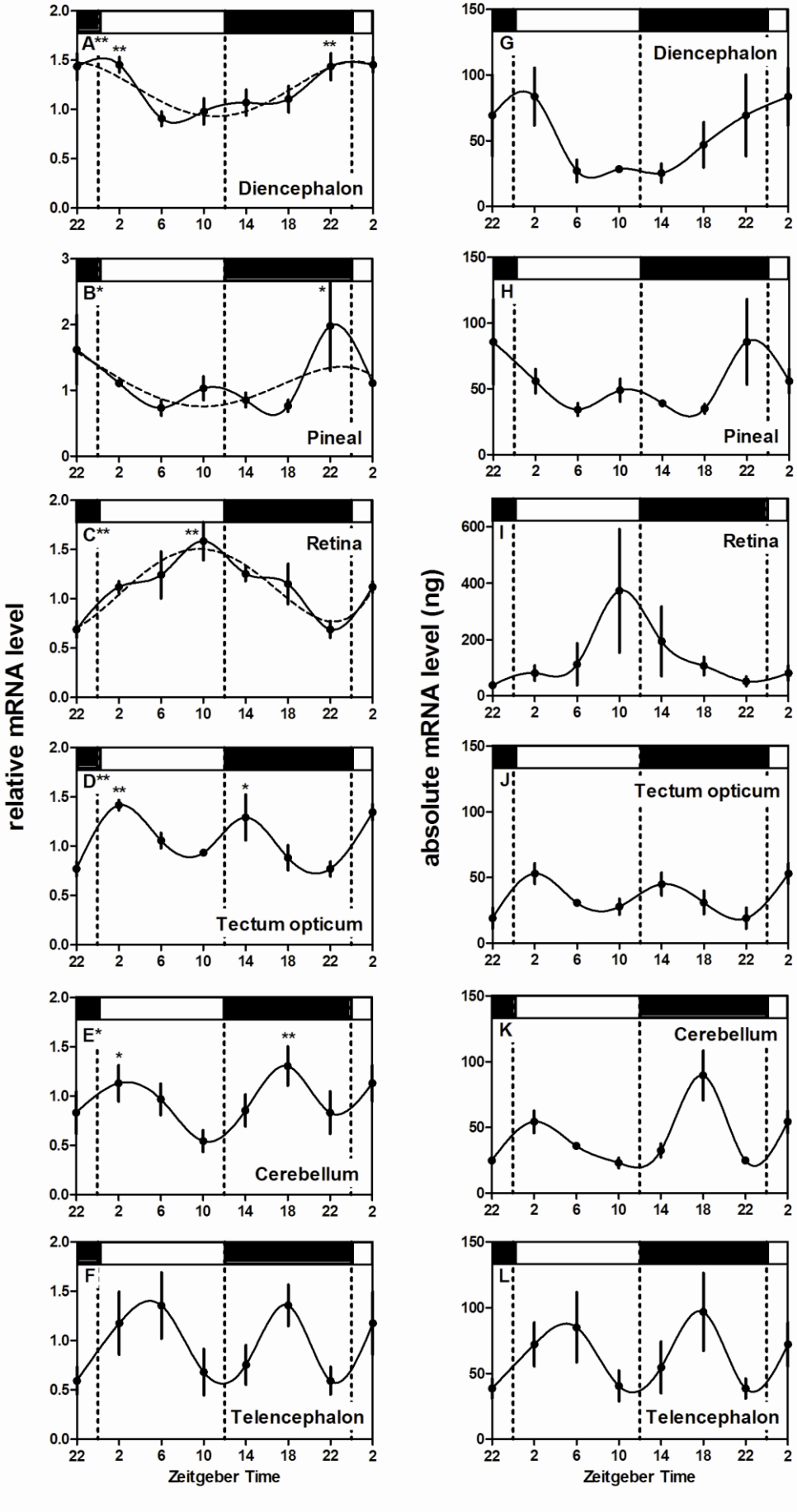
relative mRNA level
absolute mRNA level (ng)
A**
B*
C**
D**
E*
F
G
H
I
J
K
L
Diencephalon
Pineal
Retina
Tectum opticum
Cerebellum
Telencephalon
Zeitgeber Time
22 2 6 10 14 18 22 2

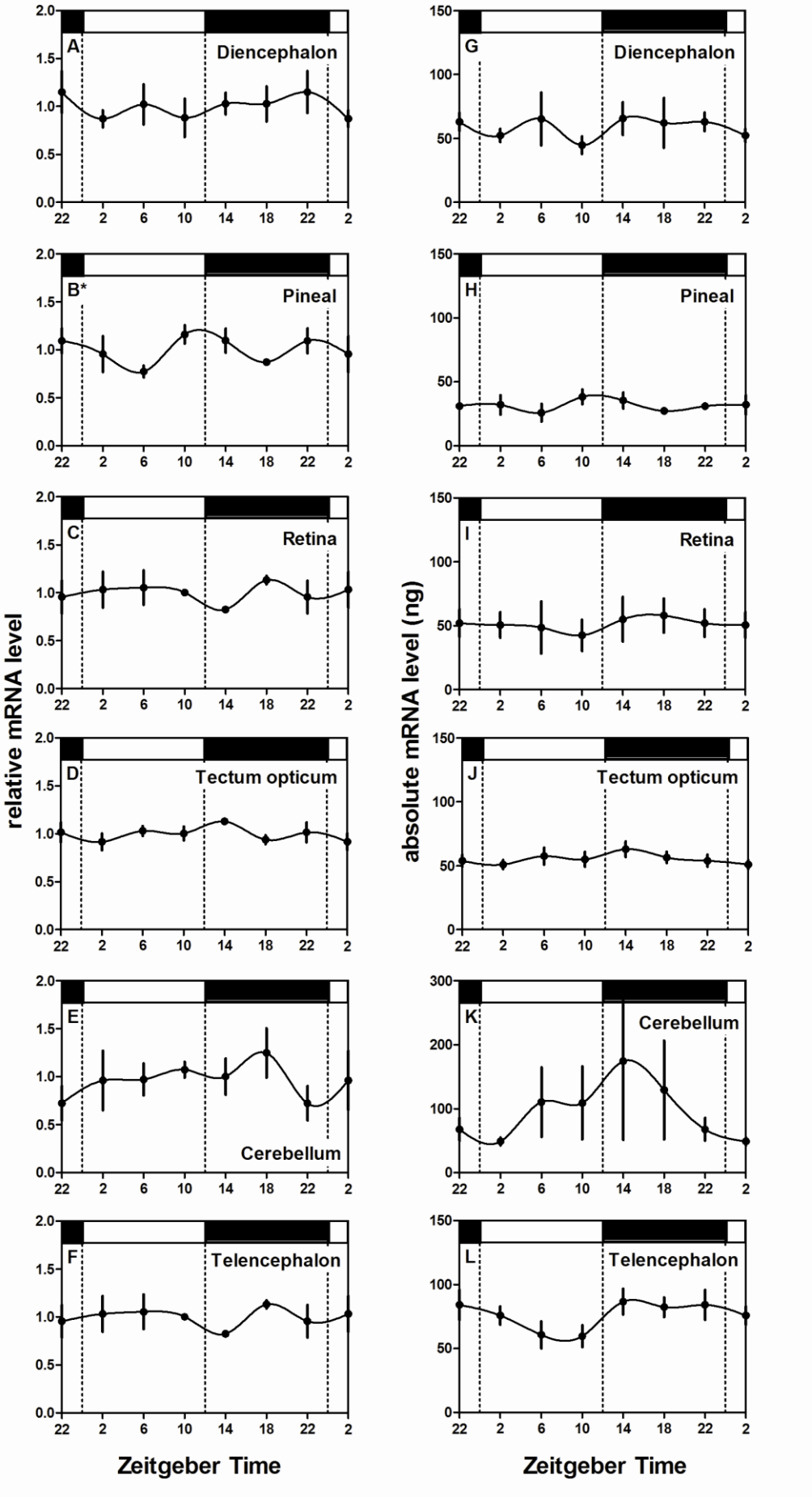
A
Diencephalon
G
Diencephalon
B*
Pineal
H
Pineal
C
Retina
I
Retina
D
Tectum opticum
J
Tectum opticum
E
Cerebellum
K
Cerebellum
F
Telencephalon
L
Telencephalon
relative mRNA level
absolute mRNA level (ng)
Zeitgeber Time
Zeitgeber Time

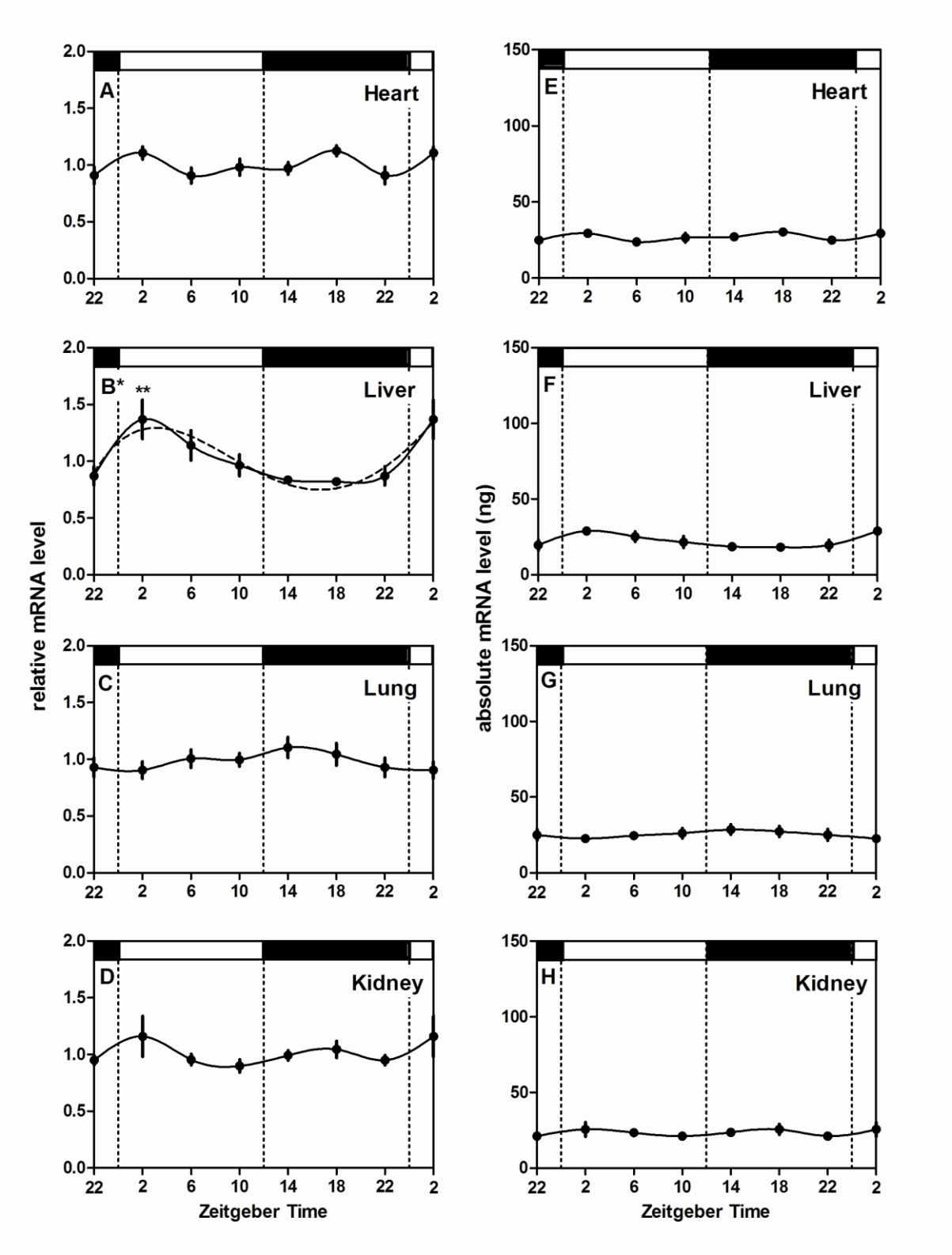
A
Heart
B*
**
Liver
C
Lung
D
Kidney
E
Heart
F
Liver
G
Lung
H
Kidney
relative mRNA level
absolute mRNA level (ng)
Zeitgeber Time
Zeitgeber Time

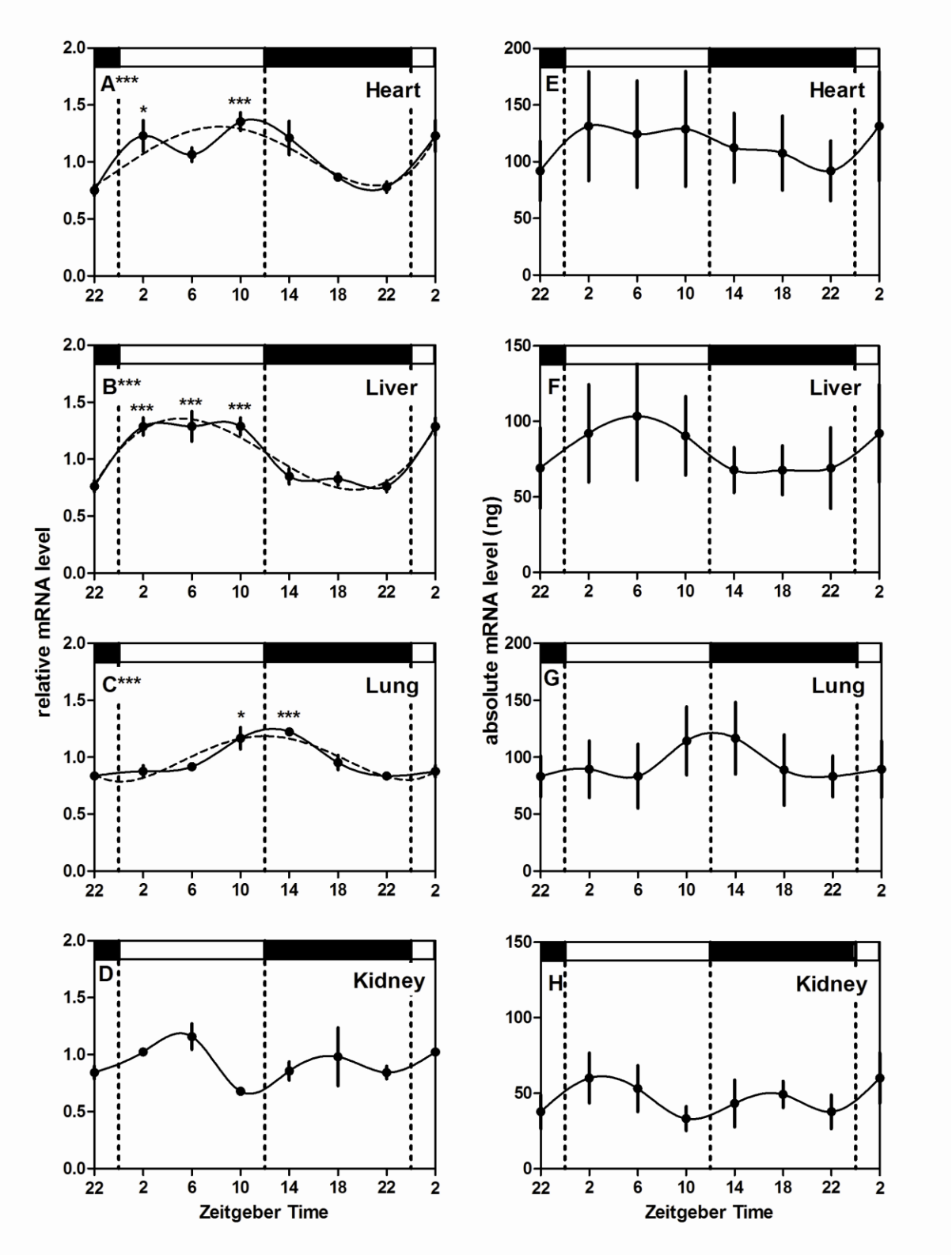
A***
Heart
B***
Liver
C***
Lung
D
Kidney
E
Heart
F
Liver
G
Lung
H
Kidney
relative mRNA level
absolute mRNA level (ng)
Zeitgeber Time
Zeitgeber Time

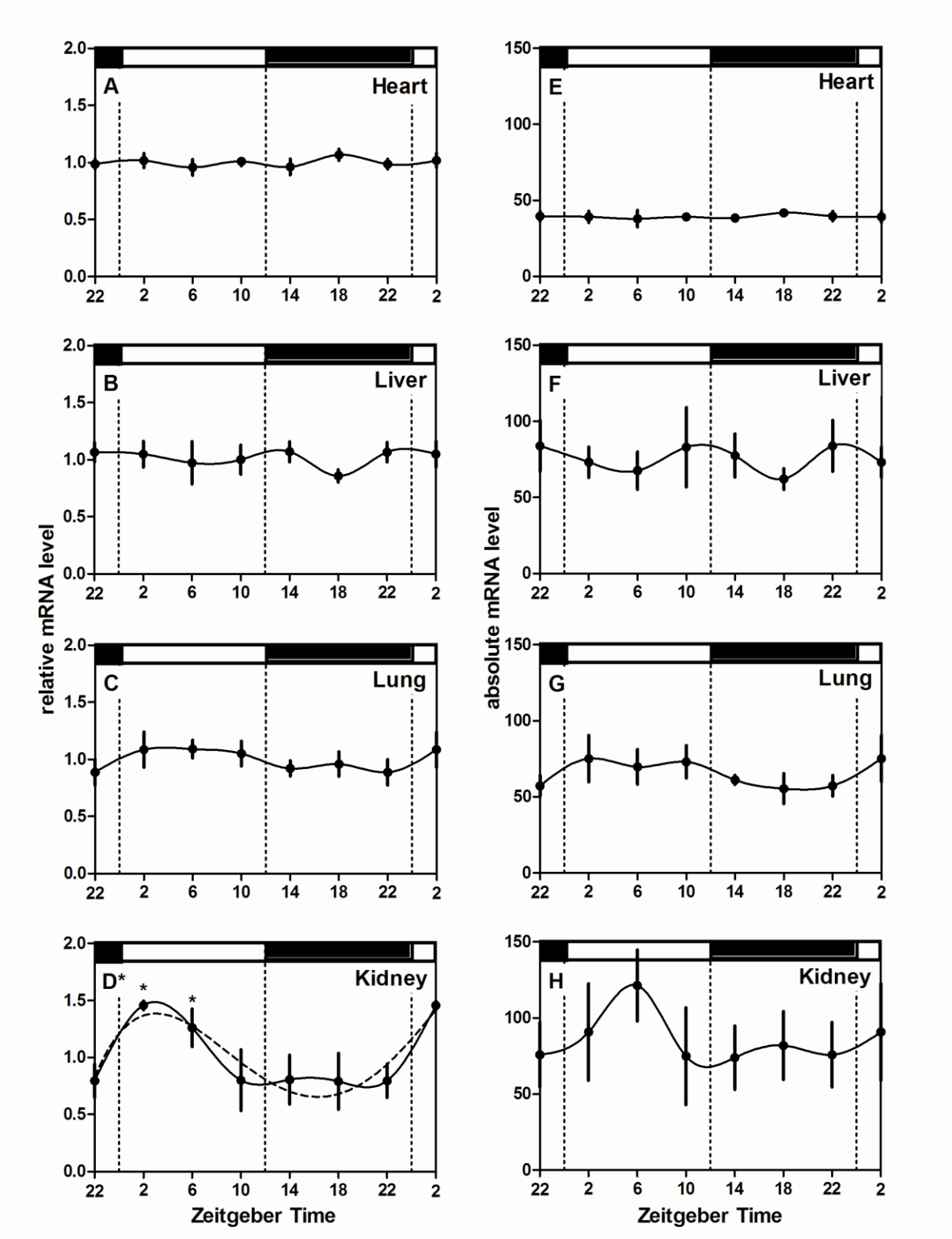
A
Heart
B
Liver
C
Lung
D*
Kidney
E
Heart
F
Liver
G
Lung
H
Kidney
relative mRNA level
absolute mRNA level
Zeitgeber Time
Zeitgeber Time
22 2 6 10 14 18 22 2

Appendix III

Conference contributions

APPENDIX III

Conference contributions

1) **Bioscience graduate research science (BGRS) Symposium Poster session April 2009**
2) **IOC Brazil August 2010**

Title: Avian Circadian Biology: Hypothalamic input and output mechanisms

Catherine Jones and Roland Brandstaetter , School of Biosciences, The University of Birmingham, Edgbaston, Birmingham, B15 2TT, U.K.

Abstract: Circadian rhythms are generated endogenously, but can be entrained by external cues, e.g. light. True circadian rhythms persist when the external cues are removed, for a period of about 24h. Circadian rhythmicity regulates the production of hormones (e.g. melatonin), the organisms' physiology (homeostasis, brain activity, sleep-wake pattern, and cell regeneration) and behaviour (feeding, migration, breeding, etc.) via light-dark entrainment of the day-night cycles. The avian circadian system is more complex than the mammalian system; has the capacity to obtain environmental photic information from the retina, pineal gland, deep encephalic photoreceptors, all of these oscillators have the ability to interact (mutual inhibition) with one another to produce a stable circadian rhythmicity. This study looks at the two input mechanisms and the output mechanisms of the avian hypothalamic oscillator. The inputs are light input during the day and hormone melatonin secreted during the night. Both these inputs can entrain the circadian rhythms to the external environment. The output from the hypothalamic oscillator are neurotransmitters/peptides and hormones, such as arginine-vasotocin, somatostatin, serotonin, vasoactive intestinal peptide, amongst others.

Hypothalamic Circadian Organisation in Birds: Clock input and output mechanisms

Catherine Jones, Gisela Helfer & Roland Brandstaetter
Biological Rhythms Research Group, School of Biosciences, University of Birmingham, Edgbaston, Birmingham, B15 2TT, U.K.

BBSRC

UNIVERSITY OF BIRMINGHAM

Introduction

Circadian rhythms are generated endogenously over a 24hr period, but can be entrained by external cues, e.g. light (Fig. 1). True circadian rhythms persist when the external cues are removed.

Circadian rhythmicity regulates:
- Production of hormones (e.g. melatonin, GnRH)
- Organisms' physiology (homeostasis, brain activity, sleep-wake pattern)
- Cell regeneration and behaviour (feeding, migration, breeding, etc.)

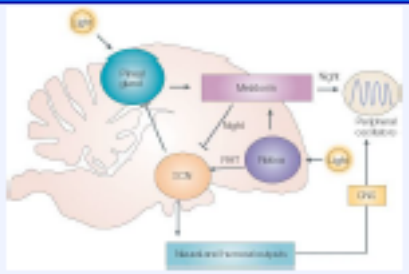

Figure 1. The Avian circadian pacemaker organisation. Bell-Pedersen, et al., (2005).

The two hypothalamic oscillators in birds (Fig. 1 & 4):
- Suprachiasmic nucleus(SCN)
- Lateral Hypothalamic nuclei (LHN) - a dorsal (LHNd) and a ventral (LHNv) part (Brandstaetter & Abraham 2003)

There are two other circadian oscillators in birds (Fig. 1):
- Retina
- Pineal Gland

The oscillators interact with each other to create a stable circadian rhythm.

LIGHT INPUT SIGNALS MELATONIN

- The avian circadian system obtains environmental light information from the:
  - retina
  - pineal gland
  - deep encephalic photoreceptors
- Light inhibits the synthesis and secretion of melatonin from the pineal gland.
- Light input can be detected by looking at c-fos expression using immunohistochemistry. c-fos is involved in the light entrainment pathway and is a member of the *Fos* gene family (Kling & Follet, 1997).
- The Zebra finch will be synchronised to 12hr light:12hr dark cycles. Light pulses will be beamed into the hutches during early 'dark' and late 'dark' to see the effects of light on early gene expression.

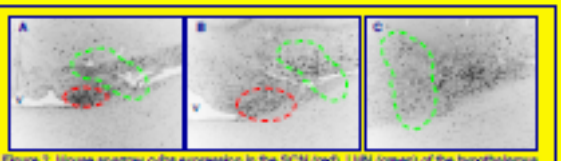

Figure 2. House sparrow c-fos expression in the SCN (red), LHN (green) of the hypothalamus, Rostral (A), Medial (B) and Caudal (C) sections through the hypothalamus. V = third ventricle.

- Melatonin is synthesised in the pineal gland during the night and released into the blood stream, inhibiting activity in the SCN. The synthesis and secretion varies throughout the year.
- There are two known melatonin receptors involved in circadian rhythms in birds, Mel-1A and Mel-1C. These are part of the rhodopsin family of 7 transmembrane receptors.
- I have cloned and sequenced the Mel-1A and Mel-1C genes from Zebra finch. We have shown the expression rhythms of the two genes over a 24hr period in the zebra finch in the brain (Fig. 3).

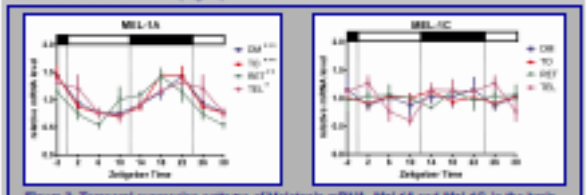

Figure 3. Temporal expression patterns of Melatonin mRNA, Mel-1A and Mel-1C, in the brain tissues of zebra finches kept in LD 12:12. The bar at the top of each graph indicates the light and dark phases. Symbols represent mean (n=6) ± SEM. Each time-point is normalised to TATA box binding protein gene (TBP).

HYPOTHALAMIC OSCILLATORS

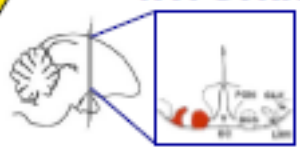

Positive elements:
- Bmal1
- Clock

Negative elements:
- Per2 and Per3
- Cry1 and Cry2

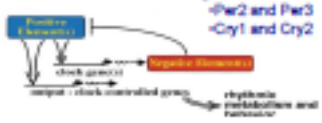

Figure 4. Anatomical features of the avian hypothalamus. Abraham, et al., (2002). Figure 5. Components of the circadian oscillatory loop. Dunlap, (1999).

OUTPUT SIGNALS

There are various hormones, neurotransmitters and neuropeptides involved in the regulation of circadian rhythmicity and behaviour e.g.
- Arginine-Vasotocin (AVT)/Vasopressin(AVP)
- Gonadotropin-releasing hormone (GnRH)
- Neuropeptide Y (NPY)
- Vasoactive intestinal polypeptide (VIP)

I have been looking at the AVT expression in the Zebra finch, Chicken and Japanese quail hypothalamus.

AVT - neurohypophyseal hormone
- maintains fluid homeostasis and regulating blood pressure (Nephew, *et al.*, 2005)
- involved in reproduction function (Seth, et al., 2004)

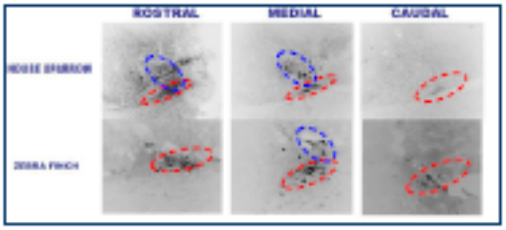

Figure 6. AVT expression differences in the LHNv (red) & LHNd (blue) of the hypothalamus in the House sparrow and the Zebra finch.

Figure 7. Preliminary cell counts of AVT expression through the LHNd in the house sparrow and the zebra finch

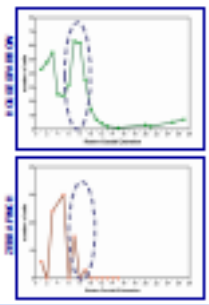

Future work:
- To look at the anatomical expression of the MEL receptors in the SCN, via protein probes and/or RNA *in situ* hybridization.
- To perform and look at the effect of light pulses have on early gene transcription in Zebra finch SCN, by c-fos immunohistochemistry experiment.
- Define output signal, neurotransmitters and peptides in the SCN and LHN of the Zebra finch brain

References: Kling & Follet (1997) J. comp. Physiol. A. 180:541-551. Abraham, *et al.*, (2002) European Journal of Neuroscience, Vol. 16, 429-438. Brandstaetter and Abraham, (2003) Chronobiology International 20(4): 637 - 655. Seth, et al., (2004) J Exp Biol 207: 3025-3033. Bell-Pedersen, *et al.*, (2005) Nat Rev Genet 6: 544 - 556. Nephew, *et al.*, (2005) Hormones and Behavior. 47: 280-289.

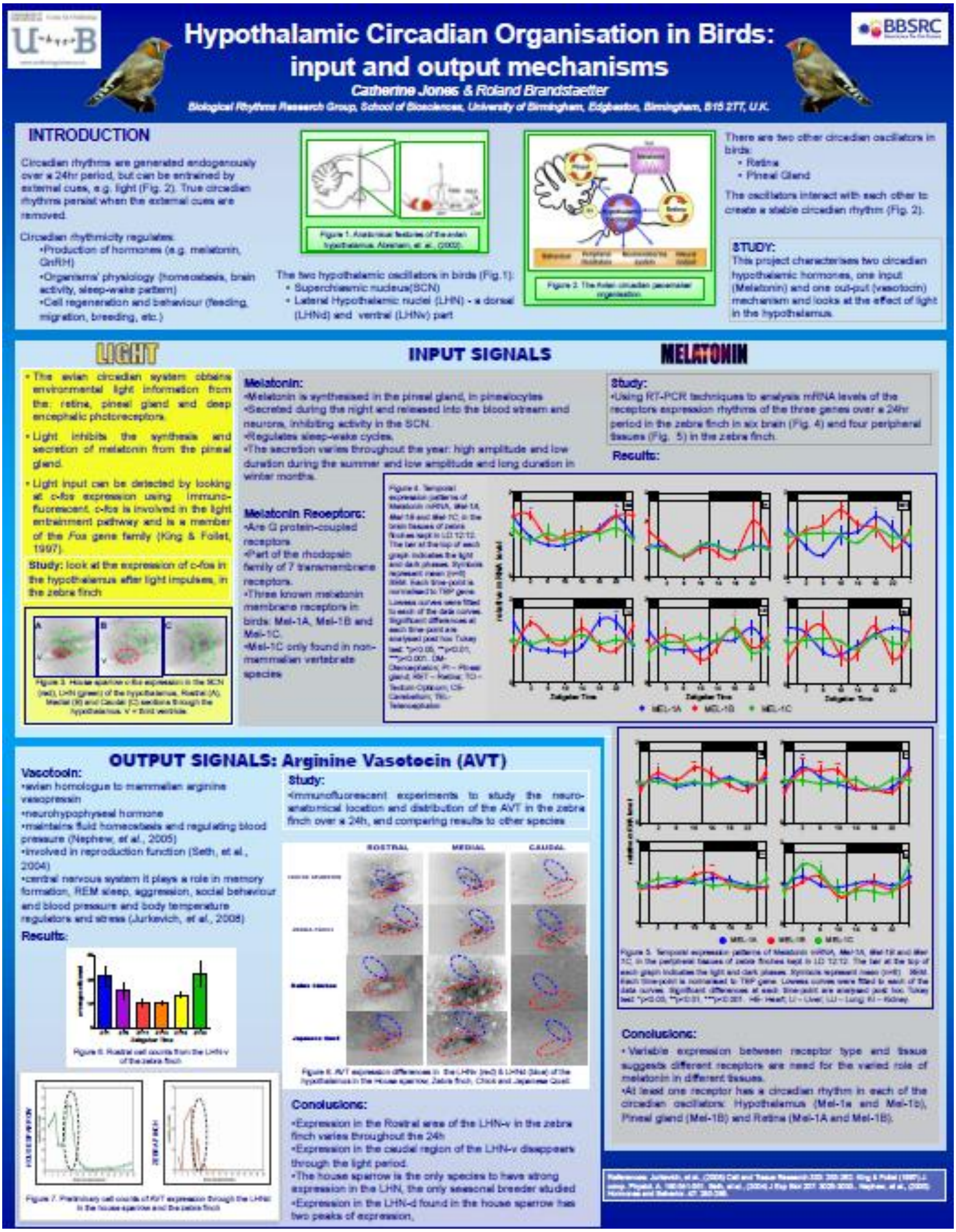
Hypothalamic Circadian Organisation in Birds: input and output mechanisms
Catherine Jones & Roland Brandstaetter
Biological Rhythms Research Group, School of Biosciences, University of Birmingham, Edgbaston, Birmingham, B15 2TT, U.K.
BBSRC
INTRODUCTION
Circadian rhythms are generated endogenously over a 24hr period, but can be entrained by external cues, e.g. light (Fig. 2). True circadian rhythms persist when the external cues are removed.
Circadian rhythmicity regulates:
•Production of hormones (e.g. melatonin, GnRH)
•Organisms' physiology (homeostasis, brain activity, sleep-wake pattern)
•Cell regeneration and behaviour (feeding, migration, breeding, etc.)
Figure 1. Anatomical features of the avian hypothalamus. Abraham, et al., (2002).
The two hypothalamic oscillators in birds (Fig. 1):
• Suprachiasmic nucleus(SCN)
• Lateral Hypothalamic nuclei (LHN) - a dorsal (LHNd) and ventral (LHNv) part
Figure 2. The Avian circadian pacemaker organisation
There are two other circadian oscillators in birds:
• Retina
• Pineal Gland
The oscillators interact with each other to create a stable circadian rhythm (Fig. 2).
STUDY:
This project characterises two circadian hypothalamic hormones, one input (Melatonin) and one out-put (vasotocin) mechanism and looks at the effect of light in the hypothalamus.
LIGHT
INPUT SIGNALS
MELATONIN
• The avian circadian system obtains environmental light information from the: retina, pineal gland and deep encephalic photoreceptors.
• Light inhibits the synthesis and secretion of melatonin from the pineal gland.
• Light input can be detected by looking at c-fos expression using immuno-fluorescent. c-fos is involved in the light entrainment pathway and is a member of the Fos gene family (King & Follet, 1997).
Study: look at the expression of c-fos in the hypothalamus after light impulses, in the zebra finch
Figure 3. House sparrow c-fos expression in the SCN (red), LHN (green) of the hypothalamus. Rostral (A), Medial (B) and Caudal (C) sections through the hypothalamus. V = third ventricle.
Melatonin:
•Melatonin is synthesised in the pineal gland, in pinealocytes
•Secreted during the night and released into the blood stream and neurons, inhibiting activity in the SCN.
•Regulates sleep-wake cycles.
•The secretion varies throughout the year: high amplitude and low duration during the summer and low amplitude and long duration in winter months.
Melatonin Receptors:
•Are G protein-coupled receptors
•Part of the rhodopsin family of 7 transmembrane receptors.
•Three known melatonin membrane receptors in birds: Mel-1A, Mel-1B and Mel-1C.
•Mel-1C only found in non-mammalian vertebrate species
Study:
•Using RT-PCR techniques to analysis mRNA levels of the receptors expression rhythms of the three genes over a 24hr period in the zebra finch in six brain (Fig. 4) and four peripheral tissues (Fig. 5) in the zebra finch.
Results:
Zeitgeber Time
MEL-1A MEL-1B MEL-1C
OUTPUT SIGNALS: Arginine Vasotocin (AVT)
Vasotocin:
•avian homologue to mammalian arginine vasopressin
•neurohypophyseal hormone
•maintains fluid homeostasis and regulating blood pressure (Nephew, et al., 2005)
•involved in reproduction function (Seth, et al., 2004)
•central nervous system it plays a role in memory formation, REM sleep, aggression, social behaviour and blood pressure and body temperature regulators and stress (Jurkevich, et al., 2008)
Results:
Study:
•Immunofluorescent experiments to study the neuro-anatomical location and distribution of the AVT in the zebra finch over a 24h, and comparing results to other species
ROSTRAL MEDIAL CAUDAL
Figure 6. AVT expression differences in the LHNv (red) & LHNd (blue) of the hypothalamus in the House sparrow, Zebra finch, Chick and Japanese Quail.
Conclusions:
•Expression in the Rostral area of the LHN-v in the zebra finch varies throughout the 24h
•Expression in the caudal region of the LHN-v disappears through the light period.
•The house sparrow is the only species to have strong expression in the LHN, the only seasonal breeder studied
•Expression in the LHN-d found in the house sparrow has two peaks of expression.
Conclusions:
• Variable expression between receptor type and tissue suggests different receptors are need for the varied role of melatonin in different tissues.
•At least one receptor has a circadian rhythm in each of the circadian oscillators: Hypothalamus (Mel-1a and Mel-1b), Pineal gland (Mel-1B) and Retina (Mel-1A and Mel-1B).